

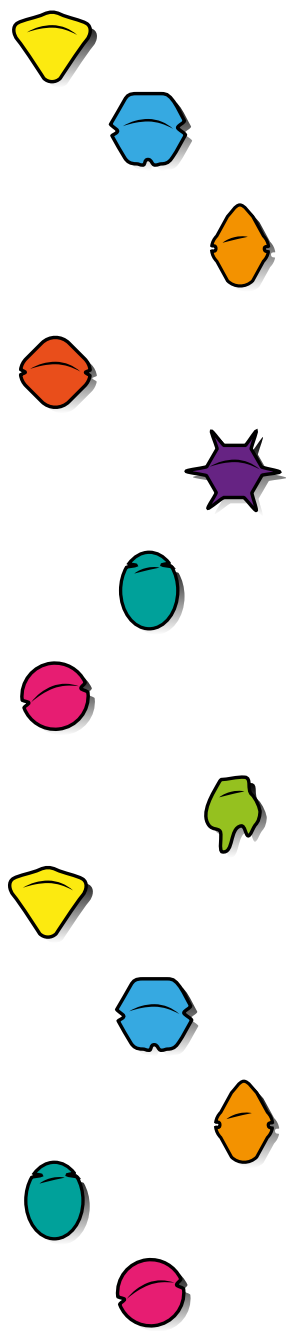
ICHA

19th INTERNATIONAL
CONFERENCE ON
HARMFUL ALGAE
MEXICO 2021 **1**

LA PAZ | baja california sur | october 10-15

www.icha2021.com

PROCEEDINGS



CONVENOR



ORGANIZED BY



**FIRST
VIRTUAL
MEETING**

Proceedings of the 19th International Conference on Harmful Algae

October, 2021. La Paz, B.C.S., Mexico

Editors

Band Schmidt, Christine J.
Rodríguez Gómez, Carlos F.

Reviewers (in alphabetical order)

Aké Castillo, José
Bustillos-Guzmán, José
Doblin, Martina
Durán Riveroll, Lorena
Jenkinson, Ian
Garcés, Esther
Molgó, Jordi
Litaker, Wayne
Murray, Shauna
Ruiz de la Torre, Mary Carmen
Santiago Morales, Ivonne
Trainer, Vera

This document should be cited as:

Band-Schmidt, C.J. and Rodríguez-Gómez, C.F. (Eds.). 2022. Proceedings of the 19th International Conference on Harmful Algae, La Paz, B.C.S., Mexico. International Society for the Study of Harmful Algal Blooms. 365 pp.



INTRODUCTION

The 19th International Conference on Harmful Algae (ICHA 2021) was held in Mexico from 10-15 October, 2021, for the first time in a virtual format. The conference was hosted by the Centro Interdisciplinario de Ciencias Marinas (CICIMAR) from the Instituto Politécnico Nacional (IPN) and the Centro de Investigaciones Biológicas del Noroeste, S.C. (CIBNOR) located in La Paz, Mexico, B.C.S. This conference was postponed for the first time for one year due to the coronavirus disease pandemic. Initially an in-person conference was planned in the beautiful city of La Paz. For a few months in early 2021, we were still optimistic and were planning for a hybrid event, but when we realized that everybody was in a strict lock-down, we had to move to a virtual format. This situation led to the planning of the first-ever virtual ICHA. The local organizing committee worked very closely with the ISSHA Council to make adjustments needed for a successful event.

In spite of the challenges we faced during the planning process, the success of this virtual conference was demonstrated by registration of 804 participants from 51 countries, with a total number of 406 contributions distributed in 9 plenary talks, 247 oral contributions, 40 speed talks and 110 posters. Each abstract was reviewed by three members of the scientific steering committees, whose assistance we greatly appreciate. We had a full scientific program in three parallel rooms divided into 52 oral sessions covering 17 HAB topics. Talks were offered in two time slots to allow participants in most of the world's time zones to listen to the talks during typical working hours. All sessions were chaired by the ISSHA Council as well as local organizers. Thank you to everyone who participated, given the strain of the time differences and some last-minute technical complications. All in all, we did a great job! Presentations were requested to be sent to the organizers one month prior the conference, adding a challenge for many of you. Our community pulled through, and you all send amazing presentations! All presentations, with the exception of the special sessions were pre-recorded. This virtual format allowed us to keep the presentations on the conference website for two months after the conference ended.

The opening ceremony was given by Beatriz Reguera who received the ISSHA Yasumoto Award at the previous ICHA Conference in 2018 in Nantes, France, for her contribution in understanding the biology, population dynamics and sampling strategies for dinoflagellates of the genus *Dinophysis*, producers of diarrhetic toxins. Her talk was titled "Forty years living with *Dinophysis*: myths and realities".

We had eight additional plenary talks that covered different leading HAB topics: "Ciguatera: Current evidence and management options" by Marie-Yasmine Dechraoui Bottein; "A hotter, more uncertain future: Can HAB research meet the environmental challenges of our time, and deliver meaningful outcomes?" by Michele Burford; "Creating large multi-regional community partnerships to monitor Harmful Algal Blooms and shellfish toxins in Alaska" by Chris



Whitehead; “Socializing HABs knowledge, the Mexican Case” by Ernesto García Mendoza; “From genes to ecosystems and back” by Uwe John; “Taxonomy and phylogeny of unarmored dinoflagellates in the Kareniaceae found from Asian Pacific” by Mitsunori Iwataki; “Cell-to-cell interactions in the sea” by Alexandra Z. Worden, and “Chile: Causes, impact and management of a ‘hot spot’ for toxic algal blooms” by Jorge I. Mardones.

We also had five special sessions led by well-known leaders covering timely topics of harmful algae research in both marine and freshwater environments:

- HAB Early Warning Systems Session
- Impacts of HABs on Fish Farms: Addressing Industry and Global Insurance Needs
- Control of Cyanobacterial Blooms
- NHABON-NE, a prototype node for a national HAB sensor network in the United States
- New book!! WHO guidance on cyanotoxins

For this ICHA proceedings we received 49 contributions covering the following topics:

	Number of contributions
Plenary talk	1
HABs in a changing world	3
Harmful algae biology	2
Harmful algae ecology	7
Harmful algae microbiomes	2
Ichthyotoxic HABs	1
Ciguatera and benthic HABs	3
Algal and cyanobacterial toxins	2
Taxonomy and systematics	4
Toxicology	5
Novel HAB technologies	2
HAB prediction	3
Surveillance and management	9
Emerging issues	2

In this ICHA 2021 volume, we have also included eight selected contributions that were presented during the HAB Early Warning Systems Session.

During this virtual conference, we also held the ISSHA General Assembly and two young Investigator Networking meetings. Linda Medlin was the ICHA 2021 Yasumoto Award recipient for her outstanding contributions in molecular biology applied to the study and monitoring of



phytoplankton diversity and HABs species. The ISSHA Gentien Award 2021 was given to Sung Tung Teng, and the Mauren Keller Award for the Best Student presentations were given to Jose Garcia Corona, Steffaney Wood, Taichi Ataka and Teresa Silva. During the ICHA2021 conference, we missed many things we have taken for granted for so many years during our in-person conferences, such as our traditional ISSHA auction, our cultural tours and especially socializing with our favorite ISSHA members. However, a virtual platform for informal meetings was offered with GatherTown, in which participants could walk around a virtual space and meet new people or chat with familiar colleagues.

The ICHA2021 committees would like to thank our generous sponsors, including the Scientific Committee for Ocean Research (SCOR), the National Oceanic and Atmospheric Administration (NOAA), the International Atomic Energy Agency (IAEA), the Food and Agriculture Organization (FAO) and private donations by ISSHA members, which allowed us to cover the registration fees of 78 participants, including students, regular ISSHA members and managers from 13 countries.

Our Chilean colleagues have offered to host the 21st International Conference on Harmful Algae in 2025 in Punta Arenas, Chile. This venue that was accepted by ISSHA members by consensus. However, before going to Chile, we are looking forward to seeing you all again at the 20th ICHA to be held in Hiroshima, Japan in 2023.

Thank you for being an amazing ISSHA community and for supporting this conference during difficult times!

Christine J. Band Schmidt
Chair of ICHA 2021



COMMITTEE

Local Organizing Committee

Dra. Christine J. Band Schmidt

(Centro Interdisciplinario de Ciencias Marinas-IPN)

Dr. José Bustillos Guzmán

(Centro de Investigaciones Biológicas del Noroeste)

Dr. Ignacio Leyva Valencia

(CONACyT, Centro Interdisciplinario de Ciencias Marinas-IPN)

Dr. Francisco Hernández Sandoval

(Centro de Investigaciones Biológicas del Noroeste)

BM Erick Núñez Vázquez

(Centro de Investigaciones Biológicas del Noroeste)

Dr. José L. Peña Manjarrez

(Unidad de Educación Tecnológica Agropecuaria y Ciencias del Mar)

Dr. Ernesto García Mendoza

(Centro de Investigación Científica y de Educación Superior de Ensenada)

Dra. Sonia Quijano Scheggia

(Universidad de Colima)

Dr. Aramis Olivos Ortíz

(Universidad de Colima)

Dr. José Aké Castillo

(Universidad Veracruzana)

Dra. Mary Carmen Ruiz de la Torre

(Universidad Autónoma de Baja California)

Dra. Lorena Durán Riveroll

(CONACyT, Centro de Investigación Científica y de Educación Superior de Ensenada)

Dra. Ivonne Santiago Morales

(Universidad del Mar)

Dr. Oscar Ubisha Hernández Almeida

(Universidad Autónoma de Nayarit)

Dr. David Rivas Camargo

(Centro de Investigación Científica y de Educación Superior de Ensenada)



Regional Scientific Committee

Álvarez, Gonzalo - Chile
Anderson, Clarissa- United States
Astuya Villalón, Allison - Chile
Borbor Córdova, Mercy - Ecuador
Bowers, Holly- United States
Carnicer, Olga- Spain
Deeds, Jonathan - United States
Delgado Ramírez, Claudia- Mexico
Díaz, Patricio - Chile
Doucette, Greg - United States
Fernández Herrera, Leyberth- Mexico
Ferrao Filho, Aloysio- Brazil
Flores Trujillo, Juan G. - Mexico
Frangópulos, Máximo- Chile
Gárate Lizárraga, Ismael- Mexico
Guzmán, Leonardo- Chile
Hambright, David - United States
Helenes, Javier- Mexico
Henrichs, Darren- United States
Mancera Pineda, José E.- Colombia
Mardones, Jorge - Chile
Méndez, Silvia - Uruguay
Mendoza Flores, Armando- Mexico
Mertens, Kenneth- United States
Moore, Stephanie- United States
Nascimento, Silva - Brazil
Nils Müller, Marius - Brazil
Okolodkov, Yuri- Mexico
Pizarro, Gemita- Chile
Poot Delgado, Carlos - Mexico
Pospoleva, Vera- United States
Rodríguez Gómez, Carlos F. - Mexico
Sar, Eugenia- Argentina
Sunesen, Inés - Argentina
Tomlinson, Michelle - United States
Uribe, Eduardo - Chile
Vargas, Maribell - Costa Rica
Vázquez, Gabriela- Mexico



International Advisory Board

Amorim, Ana- Portugal*
Anderson, Donald- United States
Ardura Gutiérrez, Alba- Spain
Band Schmidt, Christine - Mexico*
Bolch, Christopher- Australia
Campbell, Lisa- United States
Cembella, Allan- Germany
Cho, Yuko- Japan
Davidson, Keith- United Kingdom*
Dechraoui Bottein, Marie-Yasmine - France
Enevoldsen, Henrik- Denmark*
Estrada, Marta- Spain*
Fraga, Santiago- Spain
Garcés, Esther- Spain*
Garrido, Esther- Spain
Gernez, Pierre- France
Gobler, Christopher- United States
Hallegraeff, Gustaff- Australia
Hegaret, Helene- France
Hess, Philipp- France*
Imai, Ichiro- Japan*
John, Uwe- Germany
Jenkinson, Ian- China, France*
Krock, Bernd- Germany
Lewis, Jane- United Kingdom*
Li, Aifeng- China
Lim, Po Teen- Malaysia*
Lindehoff, Elin- Sweden*
Litaker, Wayne- United States *
Lundholm, Nina- Denmark*
Mafra, Luiz- Brazil*
Marampouti, Christina- The Netherlands
Molgó, Jordi- France
Murray, Shauna- Australia*
Nagai, Satoshi- Japan
Pitcher, Grant- South Africa
Reguera, Beatriz- Spain
Rengefors, Karen- Sweden
Sassenhagen, Ingrid- France, Germany*
Spyrakos, Evangelos- United Kingdom
Trainer, Vera- United States *
Tubaro, Aurelia- Italy*
Turner, Andrew- United Kingdom
Vale, Paulo- Portugal
van de Waal, Dedmer- The Netherlands*
Verma, Arjun- Australia
Wang, Jiangtao- China
Wohlrab, Silke- Germany
Wood, Steffaney- student representative*

*Members of the ISSHA Council



TABLE OF CONTENTS

Click on any topic to be directed to the corresponding section

PLENARY TALK	001	
HABs IN A CHANGING WORLD	015	
HA BIOLOGY	033	
HA ECOLOGY	045	
HA MICROBIOMES	088	
CYANOBACTERIAL BLOOMS	099	
ICHTHYOTOXIC HABs	118	
CIGUATERA AND BENTHIC HABs	125	
ALGAL AND CYANOBACTERIAL TOXINS	144	
TAXONOMY AND SYSTEMATICS	157	
TOXICOLOGY	180	
NOVEL HAB TECHNOLOGIES	212	
HAB PREDICTION	225	
SURVEILLANCE AND MANAGEMENT	242	
EMERGING ISSUES	294	
EARLY WARNING SYSTEMS FOR HARMFUL ALGAE	308	
AUTHORS INDEX	360	



PLENARY TALK

Yasumoto Awardee

Forty years living with *Dinophysis*: myths and realities

Beatriz Reguera

Centro Oceanográfico de Vigo (IEO-CSIC), Subida a Radio Faro 50, 36390 Vigo, Spain

corresponding author's email: beatriz.reguera@ieo.es

Abstract

Forty years ago, *Dinophysis fortii* was identified as the source of DSP and *Dinophysis* species targeted as potential toxins producers worldwide. Discoveries of their cryptophyte-like pigments, mixotrophic feeding on ciliate prey, and uncertainties about their life cycle made this genus an attractive topic of dinoflagellate biology, phylogeny and ecology. Within the dinoflagellate order, *Dinophysis* species constitute a unique group, the plastidic specialist non constitutive mixotrophs (pSNCM). Only the ciliate *Mesodinium rubrum* fed on *Teleaulax/Plagioselmis/Geminigera* (TPG) clade cryptophytes has been used to grow *Dinophysis*, but alternative prey are being explored. Strains of each *Dinophysis* species exhibit site-specific functional traits in response to environmental change. Progress in modeling the population dynamics of these selective mixotrophs is hindered by the lack of adapted sampling to *Dinophysis* and their potential prey with a common appropriate spatio-temporal resolution. Are *Dinophysis* low density slow-growing dinoflagellates with no sexual life, unrelated to water discolorations and never the dominant component of the microplankton community? Are all members of the *D. acuminata* complex the same species? Can we have an early warning of *Dinophysis* bloom development? Are DSP events increasing in frequency, intensity and geographic distribution? These and emerging issues are discussed here on the light of past mistakes and recent progress in knowledge.

Keywords: *Dinophysis*, morphology, life cycle, mixotrophy, ecology, bloom dynamics

<https://doi.org/10.5281/zenodo.7032546>



Antecedents

Gastrointestinal outbreaks unrelated to bacteria affected 100's of people during shellfish festivals in 1976-77 in Tohoku, Japan and led Prof. Yasumoto *et al.* (1985) to: i) describe a new “Diarrhetic Shellfish Poisoning” (DSP) syndrome; ii) design a mouse bioassay (MBA) to quantify unknown lipophilic toxins (LT) iii) identify *Dinophysis fortii* as the causative organism; iv) elucidate the structure of two groups of toxins: the okadaic acid, OA and its analogs, the dinophysistoxins DTXs (DSP toxins) and the pectenotoxins (PTX), and v) relate *D. fortii* populations ≤ 200 cells L⁻¹ to the two groups of toxins. Other LT producers may co-occur with *Dinophysis*, but analytical techniques were developed to analyze picked-cells (Lee *et al.*, 1989). Nowadays, liquid chromatography coupled with mass spectrometry (LC-MS) (Quilliam *et al.*, 1996) is used to determine LT in picked-cells, net tows, shellfish extracts, and even dissolved toxins in seawater with “solid phase adsorption toxin trackers” (SPATT, MacKenzie *et al.*, 2004).

Toxic *Dinophysis* distribution and impacts

Dinophysis species, ubiquitous for most of the year often go unreported in monitoring programmes because: i) they occur below detection levels (40–100 cells L⁻¹); ii) they form low biomass HABs (10³ cells L⁻¹); iii) symptoms of bacterial gastroenteritis-like DSP go unreported; iv) DSP monitoring is lacking in many countries; and v) routine DSP testing is often interrupted (for economic reasons) when closures are already enforced when more dangerous toxins (e.g. PSP) are present. Social awareness of the risks posed by *Dinophysis* is prompted when mass intoxications of shellfish consumers occur.

Otherwise, DSP monitoring is required for aquaculture exports (Reguera *et al.*, 2014). Under-reporting is obvious when comparing historic distribution of DSP events in Europe, where DSP monitoring started in the late 1980's, with those in the U.S.A. (Fig. 1), with tests prompted after accidental detection of a *D. ovum* bloom in Gulf of Mexico (Campbell *et al.*, 2010), and intoxication of consumers in NW U.S.A. (Pacific) coasts (Trainer *et al.*, 2013).

To date, the presence of OA-related toxins and/or PTXs has been proved by HPLC or LC-MS analysis in picked cells of ten “species” of *Dinophysis* and two of *Phalacroma* as well as toxin production *de novo* in cultures of all *Dinophysis* species except *D. miles*. Field observations support the view that the heterotroph *P. rotundatum* is just a vector of toxins from its ciliate prey (e.g. *Tiarina fusus*) when the latter feeds upon co-occurring *Dinophysis*. There are no reports about cultures of *P. mitra*, which unlike *Dinophysis*, has kleptoplastids of haptophycean origin (Koiike *et al.*, 2005) Information per species tends to be proportional to their worldwide impact. The *D. acuminata* complex (*D. acuminata*, *D. ovum*, *D. sacculus*), together with (from north to south) *D. norvegica*, *D. acuta*, *D. fortii* and *D. caudata*, are the species associated with all DSP events in the world. Information from rare *Dinophysis* or *Phalacroma* species as well as from more strains of the common species is desirable.



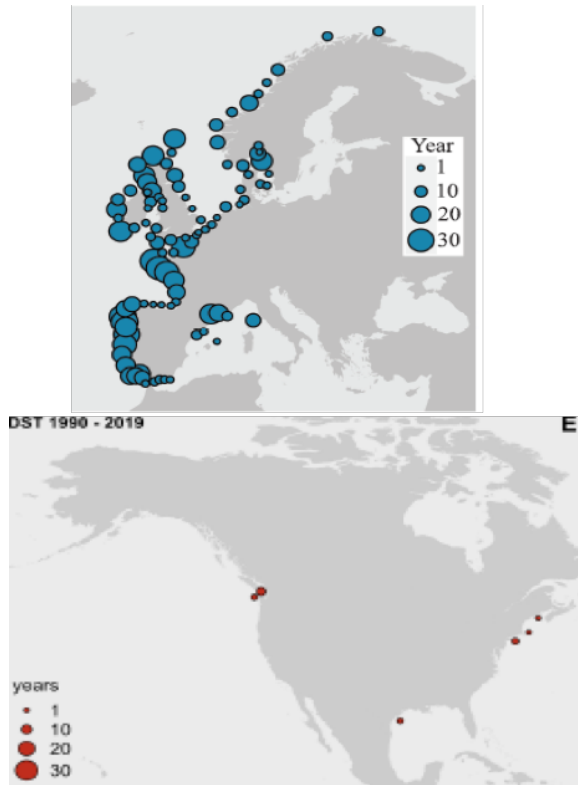


Fig. 1. Reported DSP events in Europe and U.S.A. from 1990 to 2019. IOC HAEDAT database. (in Anderson *et al.*, 2021; Bresnan *et al.*, 2021).

The toxic potential of DSP outbreaks and their impacts are extremely variable and affected by: i) the strain specific toxin profile (OAs : PTXs ratio) and content (cell quota) of the causative organism; ii) interactions of *Dinophysis* blooms and local hydrodynamics, which explain the coexistence of hot spots (retention areas) and “DSP free” areas nearby; iii) the uptake rate and enzymatic transformations by the local commercial species (e.g. mussels accumulate 10 times more toxins than oysters exposed to the same bloom) and iv) the enforced toxin regulations (e.g. PTXs were regulated in Europe until recently; Blanco, 2018).

Historic data need validation in the light of present understanding of the organisms,

their toxins and the strength and weaknesses of past and present analytical procedures. A relevant proportion of *Dinophysis* toxins may be released in the water as “dissolved toxins” (in the filtrate through 0.22 μm) and may be adsorbed by organic aggregates and prevail (detected in net tow samples) weeks after *Dinophysis* cells are no longer observed (Pizarro *et al.*, 2008).

Dinophysis traits I. Size and shape, cell cycle and life cycle

High intraspecific variability affecting size and shape of *Dinophysis* cells is affected by: i) the cell-cycle, with paired cells united by their dorsal margin and recent division (desmoschisis mode) with asymmetric partition of sulcal lists and spines; ii) a polymorphic life cycle, with small gamete-like cells formed from dimorphic paired cells produced by depauperating division; dimorphic mating gametes connected by their ventral margins with a mating tube: engulfment and gamete fusion, and iii) Mixotrophic feeding (myzocytosis mode of phagocytosis) that results in distorted or deformed specimens full of digestive vacuoles. These forms, first seen during exceptional blooms of *Dinophysis* in New Zealand, Portugal and NW Spain in 1989 are best observed during intensive cell cycle sampling at sea and in cultures (Reguera *et al.*, 2012).

A *Dinophysis* life cycle model was proposed in 2001 inspired by field observations and laboratory incubations, and misinterpretations clarified later (Escalera and Reguera, 2008). For example, the small-large (dimorphic) paired cells united by their ventral margin are not undergoing conjugation, i.e., transfer of



nuclear material from a donor to a receptor through a conjugation tube. Instead, a tube from the large cell, similar to the towing peduncle used by heterotrophic protists with their prey, guides the small cell to the cingulum to be engulfed. Some observers interpreted this as an act of cannibalism. Nuclear fusion takes place following engulfment and cellular fusion; planozygotes with two longitudinal flagella can divide without going through a resting cyst stage. It is not known if cells grouped in tetrads result from division of planozygotes or normal vegetative cells. All these forms, plus the first remark about the ciliate *Mesodinium* entangled in mucilage in the bottom of *Dinophysis* culture vessels are well illustrated by Nagai *et al.* (2008). Putative resting cysts turned out to be pellicle cysts of *Fragilidium* after eating *Dinophysis*. A harpoon-like tube has been described for *Dinophysis* to catch prey in addition to a feeding peduncle. How many peduncles do *Dinophysis* species have? After fifteen years with cultures, these and other *Dinophysis* life cycle-related questions have not been resolved.

Controversial “*Dinophysis acuminata complex*”

This complex refers to a group of morphologically similar species of *Dinophysis* difficult to separate when their blooms, with small and intermediate morphotypes co-occur. Sequencing the rDNA-ITS and 5.8S rRNA genes of single cell isolates with a new technique showed a 99% similarity between *D. acuminata* and *D. sacculus*. The apparent success of using the mitochondrial *cox1* gene to discriminate between *D. acuminata* and *D. ovum* (Raho *et al.*, 2008) turned out to be a mistake in the alignment of a *D. acuminata* strain (AM931587). Recently the

impossibility to separate *D. acuminata* from *D. ovum* with the available sequences (SSU rDNA, ITS1, ITS2 and *cox1*) was confirmed (Park *et al.*, 2019). These sequences are the best to group toxigenic species of *Dinophysis* in several clades, such as the *D. acuminata* complex and the *caudata* group (*D. caudata*, *D. tripos*, *D. miles*).

Field samples with dominance of *D. acuminata*, *D. ovum* or *D. sacculus* are well distinguished by monitoring experts in W Europe on the basis of their size and contours. The first two produce only OA, but *D. sacculus* additionally has DTX1 and PTX2 (Riobó *et al.*, 2013). Their distribution shows latitudinal and seasonal differences in Atlantic and Mediterranean coastal waters in Europe as well as in those from Eastern U.S.A. and the Gulf of Mexico (Wolny *et al.*, 2020; Sechet *et al.*, 2021). It would be unfortunate to group them in routine cell counts as “*D. acuminata complex*”, because their life forms are revealing adaptations to environmental conditions, so valuable ecological information would be missed. New portions of the genome or even epigenetic differences should be explored with genomic and transcriptomic tools. In the meantime, we should keep them separated or name them adding the letter *f* (*form*), followed by the epithet (*acuminata*, *ovum*, *sacculus*) that best fits their shape. This is currently done to distinguish morphotypes of *D. caudata* into forms: *abbreviata*, *allieri* and *pedunculata* (Reguera *et al.*, 2007).

***Dinophysis* traits II. Nutritional sources**

From Schnepf and Elbrachter’s (1988) discovery of the orange autofluorescence of cryptophyte-like plastids in *Dinophysis*



until the first culture was established (Park *et al.*, 2006) progress occurred in fits and starts over a period of 20 years. Advances in molecular biology were essential for this progress to be made. Final success had to await the cultivation of the ciliate *Mesodinium rubrum* (*Dinophysis* prey) fed cryptophytes. These cryptophytes were the source of kleptoplastids for the phototrophic ciliate *Mesodinium* (Gustafson *et al.*, 2000). *Dinophysis* was found to be an obligate mixotroph requiring light and nutrients for photosynthesis using kleptoplastids taken from its ciliate prey (e.g. *Mesodinium rubrum*) which in turn keeps most of its cryptophyte prey (of the TPG clade IV *Teleaulax/Plagioselmis/ Geminigera*) as an incomplete endosymbiont (Kim *et al.*, 2012) In the recent reclassification of planktonic mixotrophic protists (Mitra *et al.*, 2016), *Dinophysis* and *Mesodinium* are non-constitutive mixotrophs (NCM), i.e., they lack permanent plastids and need to steal them from their prey. *Dinophysis* eats its prey by piercing it with a feeding peduncle and sucking its content (*myzocytosis*); the eaten prey is dispensed into digestive vacuoles but the plastids are kept as kleptoplastids. Thus, *Dinophysis* is a *plastidic Specialist* NCM (pSNCM), whereas *M. rubrum*, that keeps most of its prey (plastid, nucleus and nucleomorphs) as an incomplete endosymbiont is an *endosymbiont Specialist* NCM (eSNCM). This *Dinophysis-Mesodinium-Teleaulax* three-link food chain is the only one tested so far for *Dinophysis* cultures (Hernández-Urcera *et al.*, 2018). *D. acuminata* prey was estimated to contribute 50% of its daily C intake, but grazing data should be critically reassessed. If the main way *Dinophysis* has to catch *Mesodinium* is with a mucus trap (Nagai *et al.*, 2020) most

Mesodinium losses would be as uneaten specimens disaggregated in the trap.

In addition to live prey, *Dinophysis* needs light and dissolved nutrients to perform photosynthesis. Uptake rates of N¹⁵ labeled compounds during blooms of several HAB species in a coastal upwelling system were measured (Seeyave *et al.*, 2009). *Dinophysis* showed a clear preference for regenerated N sources (ammonium and urea). In contrast with "high uptake velocity strategists" *Pseudo-nitzschia australis* and *Alexandrium catenella*, *D. acuminata*, a "high affinity strategist" succeeded in low N environments that were limiting for the other species. These trends have been confirmed in laboratory incubations of *D. acuminata* which yielded very low uptake rates with nitrate, but rapid assimilation of ammonia and urea (Hattenrath-Lehmann and Gobler, 2015). Similar results were obtained with *D. acuta*, a species 3 times the volume of *D. acuminata* that showed uptake rates 2-3 times higher than those shown by *D. acuminata*. Unlike in autotrophic species, starvation did not boost uptake rates, and indeed they were higher in well fed cultures (García-Portela *et al.*, 2020). Information on NO₃ reductase membrane transporters from 30 dinoflagellate species (Reference Transcriptome database) showed a paucity of these transporters in *D. acuminata* compared to the amount found in the heterotroph *Noctiluca*. New experimental transcriptomic and isotopic data revealed the central role of NH₄⁺ (Hattenrath-Lehmann *et al.*, 2021).

Some authors related increased bloom intensity of *Dinophysis* with eutrophication (Hattenrath-Lehmann *et al.*, 2015). After all the above considerations, it seems very



unlikely that *Dinophysis* could outcompete *Pseudo-nitzschia* and other high velocity strategists in nitrogen-rich environments.

Why is it so difficult to cultivate Dinophysis? *Mesodinium rubrum*, grown in the laboratory with *Teleaulax amphioxeia*, *Plagioselmis prolunga*, *T. gracilis* and *T. minuta*, was considered to be genus-specific about its selected prey (Peltomaa and Johnson, 2017). *P. prolunga*, only 1 bp different from *T. amphioxeia*, was found to be a haploid stage in the life cycle of the latter (Altenburger *et al.*, 2020), so we should change to “TG” the old TPG clade IV. But *Mesodinium* growth rate and yield varied with different prey and optimal results were obtained only if strains of ciliate and its cryptophyte prey had been isolated from the same location (Hernández-Urcera *et al.*, 2019). Likewise, *Dinophysis* growth is not the same with different strains of *Mesodinium*.

Matching of *Dinophysis* and *Mesodinium* field populations (spatial-temporal coincidence of two mixotrophs) with different light and nutrient requirements (or a high predator: prey ratio of good quality prey in the laboratory) is the key factor constraining *Dinophysis* growth. This apparent strain-level selectivity of the cryptophyte prey by *Mesodinium* and strain-level preferences of *Dinophysis* for its ciliate prey would explain the fact that only a few laboratories have been able to grow *Mesodinium* from their own locality. In short, *Dinophysis* fed foreign strains of *Mesodinium* and cryptophyte is growing in suboptimal conditions.

Is Mesodinium rubrum the only possible prey for Dinophysis species?

Mesodinium rubrum is the only species tested

in laboratory cultures, but a coincidence of plastidic sequences in local *Dinophysis* species with those from *M. rubrum* and *M. major* have been found in the Galician Rias (Rial *et al.*, 2015). The latter was the dominant *Mesodinium* species in samples from Argentina and Chile and has recently been established in culture (Drumm *et al.*, 2021). Furthermore, predominance of identical cryptophyte plastid sequences belonging to *Rhodomonas/ Rhinomonas/ Storeatula* (clade V) were found in several species of *Dinophysis*, in ciliates of the genus *Strombidium* and in co-occurring heliozoans in oceanic waters off Los Lagos, Chile (Díaz *et al.*, 2020).

How do Mesodinium and Dinophysis recognize their prey?

One possibility would be a sympatric coevolution of predator and prey similar to that suggested between planktonic parasites and hosts, i.e. a predator genotype-by-prey genotype interaction.

***Dinophysis* Traits III. Specific growth rate μ (d^{-1})**

Dinophysis blooms ($\geq 10^3$ cells L^{-1}) are low biomass HABs; shellfish with DSP toxins above regulatory level (R.L.) have been associated with population densities as low as 200 cells L^{-1} (Yasumoto *et al.*, 1985). Nevertheless, there are notable exceptions of blooms reaching cell numbers 1-2 orders of magnitude above the average annual maximum. In these cases, the key question is if the high numbers are either the result of high intrinsic growth rates, or hydrodynamic forcing or a combination of both (physical-biological interactions). *In situ* division rates of *Dinophysis* populations, regardless



of their cell density, can be estimated with model equations based on the mitotic index approach (Carpenter and Chang, 1988) with intensive (36-48 h) monitoring of two successive “terminal events” or stages formed within a discrete time window. The simplified “maximum frequency approach” of McDuff and Chisholm (1982) may be applied (if the circadian rhythms of the local species are known) for comparative purposes. For example, to see vertical distribution of the specific division rate (μ) at depth (μ_z) to identify the μ_{\max} depth; to follow up division rates throughout the seasonal growth period. We have learned from these cell cycle studies that: i) *Dinophysis* species have phased-cell division, i.e., all mitotic cells divide within a narrow time window and the onset of light cues the division process; ii) *Dinophysis* are not slow-dividing dinoflagellates. Maximal rates of 0.7 d^{-1} (one doubling d^{-1}) have been observed in different species and regions; iii) In optimal conditions, *Dinophysis* may form quasi monospecific thin layers (10^5 - 10^7 cells L^{-1}) and; iv) High apparent net growth may be observed in the absence of cell division due to transport (Pizarro *et al.*, 2008).

***Dinophysis* bloom dynamics and behaviour**

Dinophysis populations follow the common sequence of phases: initiation, exponential growth, maintenance and dissipation or transport (Steidinger, 1975). Bloom dynamics is shaped by the species adaptations and their interaction with the local hydrodynamics affected by geomorphology and climate. Still there are commonalities observed in the same species blooming in different systems with a set of characteristics common to holoplanktonic *Dinophysis*: growth initiation relies on pelagic seeds; development triggered by layering and

matching of the populations with that of their ciliate prey. Different morphospecies of the ubiquitous *D. acuminata* complex and the pair *D. acuminata*/*D. acuta*, with contrasting traits, are the most studied species and their bloom patterns as model organisms will be summarized here.

Dinophysis acuminata: Unlike *D. acuta*, this species has a very long growth season, from spring to autumn and tolerates a wide range of temperature (T), and the light intensity and turbulence conditions found near the surface (Díaz *et al.*, 2016, 2019), i.e., is more stress tolerant and has a wider niche breadth than *D. acuta* (García-Portela *et al.*, 2018, 2019; Baldrich *et al.*, 2021). A conceptual model, based on field observations, was proposed by Velo-Suárez *et al.* (2014) to explain the persistence of *D. acuminata* in an upwelling system (Galician Rías Bajas), leading to up to 9 months of harvesting closures in retention areas: In the model, onset of stratification in spring cues for aggregation of scattered overwintering cells in the pycnocline region. Upwelling pulses enhance stratification and cell entrainment. The growth season starts. Vertical position of the cells is adapted to move offshore with upwelling, inshore with downwelling in a sort of 2D wind-driven conveyor belt. The population boundaries are fixed by the upwelling front. Similar 2D structures are found in other systems where the boundaries are estuarine or tidal fronts and river plumes, and blooms are coupled with the local wind regime.

Dinophysis acuta: has a short growth season, from late summer to early autumn and is more neritic than *D. acuminata*. Blooms of *D. acuta* in SW Ireland (Raine *et al.*, 2018) and Galicia (Escalera *et al.*, 2010) initiated in mid-shelf



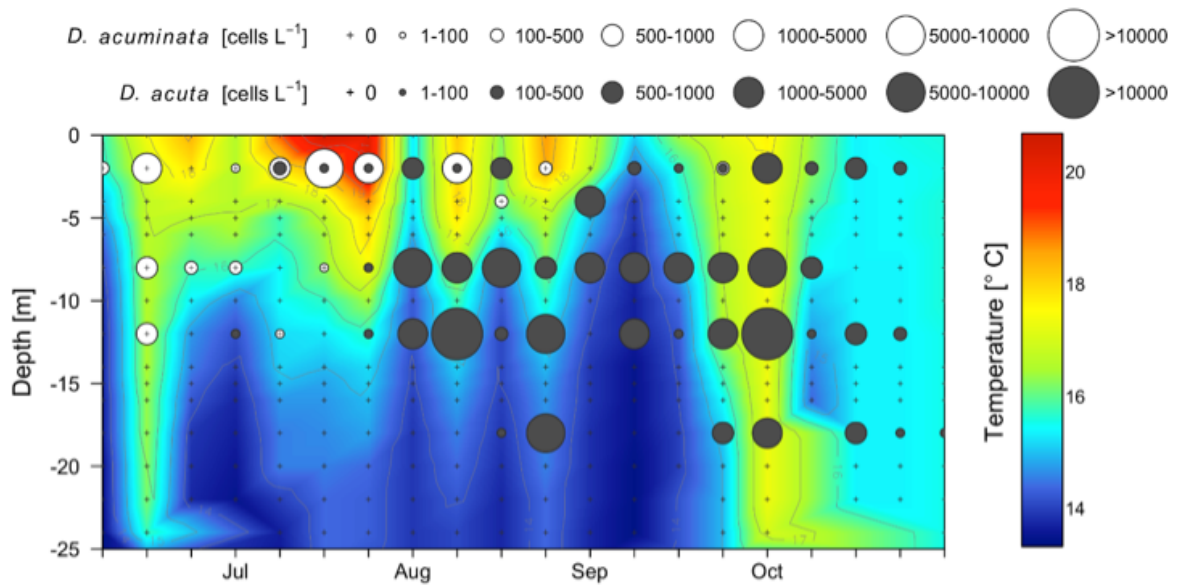


Fig. 2. Vertical segregation of *D. acuminata* and *D. acuta* cell maxima when their blooms co-occur. Ria de Pontevedra, summer-autumn 1990 (modified from Reguera *et al.*, 1993).

waters, share common physical environment requirements: persistent thermal stratification (~2 month) and water column stability met in late summer. Cell maxima and thin layers are formed in the pycnocline region above the *chl*-maximum. A 3D dimension due to long-shore transport (coastal jet in Ireland and Portuguese coastal current in Galicia) adds complexity to bloom forecasting. Wind reversal and transport of shelf population to the aquaculture sites explains high net growth of *D. acuta* in the Scottish lochs (Whyte *et al.*, 2014) and Galician Rías (Escalera *et al.*, 2010).

Aggregation, patchy distribution and thin layering, commonly observed in *Dinophysis* populations are key behavioural traits which interact with physical stratification, and allow for population development (quorum sensing), feeding upon ciliate populations, mating

encounters, allelopathic interactions, etc. Otherwise these low density holoplanktonic mixotrophs would never reach density thresholds required for these processes.

Some hints for *Dinophysis* blooms forecasting

A good starting approach is to analyse conditions associated with exceptional blooms in terms of intensity, distribution and phenological changes, as well as years of absence.

Increased stratification enhanced by climatic anomalies, and unusual wind patterns transporting blooms to exceptional distances are the most frequently reported physical conditions. Simplistic interpretations of bloom densities and T correlations often ignore that sea surface temperature (SST) is



sometimes a proxy for thermal stratification, that temperature salinity (TS) values are signature of water masses and that TS and light intensity co-vary with depth.

Exceptional *D. acuta* blooms have been associated with positive SST anomalies in the Galician Rias, and produced some early conclusions, that it was a stenotherm requiring higher T for optimal growth. But *D. acuta* is a temperate-cold-temperate species. Samplings with adequate vertical resolution showed that when *D. acuminata* and *D. acuta* co-occur, cell maxima of *D. acuta* are in colder deeper water with lower light intensity and higher stability (Fig. 2). Appropriate water column structure must be accompanied by good inoculum for initiation in shelf waters without prey limitation. Strong upwelling dispersal after bloom decay was the hypothesis to explain absence of the population the next year despite growth favourable environmental conditions (Moita *et al.*, 2016). Record densities of *D. acuta* (67×10^4 cells L⁻¹) in a thin layer were found in Puyuhuapi (~41° S), a Chilean fjord with high water residence time, and good connection with oceanic waters, in summer 2017-18. Mesoscale climate anomalies led to extra precipitation and enhanced salinity gradients in the spring preceding summer drought with high positive SST (+2 °C) anomaly (Díaz *et al.*, 2021).

Exceptional densities of *D. acuminata*, two orders of magnitude denser and over two months earlier than the 20 year mean occurred in early spring 2012 in two distant places in what appeared to be a mesoscale event affecting Western Iberia (Galician Rias Bajas) and the Bay of Biscay (Arcachon, France). Anomalous winter wind patterns

and positive anomalies (+2 °C) promoted: in Galicia, upwelling dominance in winter and in the SE Bay of Biscay, reversal of the Gironde River plume bringing increased haline stratification to Arcachon Bay. In both cases, the result was an early diatom spring bloom and stratification preceding *Dinophysis* development (5.3×10^4 cells L⁻¹ in integrated 0-5 m samples in Galicia) (Díaz *et al.*, 2013). Conversely, years of late and poor *D. acuminata* bloom development in the time series (e.g. in 1996) coincided with late onset of the upwelling season. Detection levels of overwintering cells in the rias (after milder autumn conditions) and prediction of the forthcoming upwelling season seem the best tools to predict early spring blooms of *D. acuminata* in NW Iberia.

Another scenario for cell-maxima, in the case of terminal populations of *Dinophysis*, is wind-stress relaxation and downwelling. That was the case with shelf populations in two upwelling systems: *D. fortii* (~ 10^5 cells L⁻¹; Pitcher and Calder, 2006) in the Benguela, South Africa, and *D. acuminata* (~ 10^7 cells L⁻¹; Imarpe, 2017) in the Humboldt, Perú, upwelling system. Longshore transport in buoyant river plumes is another mechanism to advect dense mature populations of *Dinophysis*. The most intense and spread *D. cf ovum* bloom in S Brazil (58×10^4 cells L⁻¹) occurred in autumn-winter 2016. It was associated with exceptionally intense southwesterly winds, which induced an inflow of cold (-4°C anomaly) low salinity buoyant plume from La Plata River up to Paraná, 1100 km north (Proença *et al.*, 2018). The same species had beaten records on the Uruguayan coast, northern margin of La Plata estuary during a hot and dry spring 2015 associated with the warm (> 20°C) saltier (>31



psu) waters of the Brazil Current (Méndez *et al.*, 2018). These conditions probably strengthened the front between the estuarine plume and the Brazil Current, moved the front closer to the coast, and favoured spring phytoplankton growth.

With the exception of a few EU or nationally funded cruises where *Dinophysis* species were the target organism, most information on *Dinophysis* dynamics is based on monitoring data collected within the aquaculture sites. Research on *Dinophysis* species suffers from a lack of information from shelf stations where important processes on initiation and dispersal occur. Recurrent questions about increasing trends in US and other countries cannot be answered until an appropriate multidecadal time series of observations is gathered

Recommendations

- Long term (seasonal and annual) studies on dinoflagellate–ciliate prey relations: rDNA and plastid sequencing of *Dinophysis* and co-occurring endosymbiont-containing ciliates.
- Mesoscale surveys on shelf waters. Data to validate ongoing operational models, in particular transport models; observations in thin layers.
- To monitor *Dinophysis* and potential prey with the same spatio-temporal resolution, explore the poorly studied: neuston and benthic boundary layers.
- Increasing or decreasing trends need decadal time series of data collected with identical methods.

Acknowledgements. I dedicate this review to Takeshi Yasumoto, the brilliant analytical chemist who discovered the role of *Dinophysis* in shellfish poisoning.

This work would not have been possible without the hard work of my great ex PhDs: Laura Escalera, Gemita Pizarro, Lourdes Velo, Patricio Díaz and María García Portela. I learned from them at least as much as they learned from me.

Thanks to most inspiring cruises, discussions and others in the old happy days of the EU HABIT project (2005-2008) with Robin Raine and Patrick Gentien, Sonsoles González, Isa Ramilo and *Dinophysis* talks with colleagues Teresa Moita, Maxi Delgado, Esther Garcés of national and Iberian collaborations. Thanks are also due to my old and current VGOHAB colleagues, in particular the *Dinophysis* freakies (Fran Rodríguez, Pilar Rial and Patri Lourés).

Funded by Spanish project *REMEDIOS* CTM2016-75451-C2-2-R; EU project INTERREG Atlantic Area *PRIMROSE* (EAPA 182/2016) and Grant GRC-VGOHAB IN607A-2019/04 (Xunta de Galicia).

References

- Altenburger, A., Blossom, H.E., Garcia-Cuetos, L. *et al.*, (2020). *Sci. Adv.* 6, eabb1611.
- Anderson, D.M., Fensin, E., Gobler, C.J. *et al.*, (2021). *Harmful Algae* 102, 101975.
- Baldrich, A.M., Pérez-Santos, I., Álvarez, G. *et al.*, (2021). *Harmful Algae* 103, 102010.



- Blanco, J. (2018). *Toxins* 10, 453.
- Bresnan, E., Arévalo, F., Belin, C. *et al.*, (2021). *Harmful Algae* 102, 101976.
- Campbell, L., Olson, R., Sosik, H.M. *et al.*, (2010). *J. Phycol.* 46, 66-75.
- Carpenter, E.J. and Chang, J. (1988). *Mar. Ecol. Prog. Ser.* 43, 105-111.
- Díaz, P.A., Reguera, B., Ruiz-Villarreal, M. *et al.*, (2013). *Mar. Drugs* 11, 2964-2981.
- Díaz, P.A., Ruiz-Villarreal, M., Pazos, Y. *et al.*, (2016). *Harmful Algae* 53, 145-159.
- Díaz, P.A., Ruiz-Villarreal, M., Mouriño-Carballido, B. *et al.*, (2019). *Prog. Oceanogr.* 175, 309-327.
- Díaz, P.A., Fernández-Pena, C., Pérez-Santos, I. *et al.*, (2020). *Harmful Algae* 99, 101907.
- Díaz, P.A., Pérez-Santos, I., Álvarez, G. *et al.*, (2021). *Sci. Total Environ.* 773, 45621.
- Drumm, K., Norlin, A., Kim, M. *et al.*, (2021). *J. Eukar. Microbiol.* 68, e12854.
- Escalera, L. and Reguera, B. (2008). *J. Phycol.* 44, 1425-1436.
- Escalera, L., Reguera, B., Moita, T. *et al.*, (2010). *Harmful Algae* 9, 312-322.
- García-Portela, M., Riobó, P., Reguera, B. *et al.*, (2018). *J. Phycol.* 54, 899-917.
- García-Portela, M., Reguera, B., Ribera d'Alcalá, M. *et al.*, (2019). *Harmful Algae* 89, 101654.
- García-Portela, M., Reguera, B., Gago, J. *et al.*, (2020). *Microorganisms* 8, 187.
- Gustafson, D.E. Jr., Stoecker, D.K., Johnson, M.D. *et al.*, (2000). *Nature* 405, 1049-1052.
- Hattenrath-Lehmann, T. and Gobler, C.J. (2015). *Limnol. Oceanogr.* 60, 1588-1603.
- Hattenrath-Lehmann, T.K., Marcoval, M.A., Middlesdorf, H. *et al.*, (2015). *PLoS ONE* 10, e0124148.
- Hattenrath-Lehmann, T.K., Nanjappa, D., Zhang, H. *et al.*, (2021). *Harmful Algae* 104, 102031.
- Hernández-Urcera, J., Rial, P., García-Portela, M. *et al.*, (2018). *Toxins* 10, 505.
- IMARPE (2017). *Reporte Técnico Floración Algal N° 002- 2017*. Instituto del Mar del Perú.
- Kim, M., Nam, S.W., Shin, W. *et al.*, (2012). *J. Phycol.* 48, 569-579.
- Koike, K., Sekiguchi, H., Kobiyama, A. *et al.*, (2005). *Protist* 156, 225-237.
- Lee, J.S. Igarashi, T., Fraga, S. *et al.*, (1989). *J. Appl. Phycol.* 1, 147-152.
- MacKenzie, L., Beuzenberg, V., Holland, P. *et al.*, (2004). *Toxicon* 44, 901-918.
- McDuff, R. and Chisholm, S. (1982). *Limnol. Oceanogr.* 27, 783-788.
- Mitra, A., Flynn, K. J., Tillmann, U. *et al.*, (2016) *Protist* 16, 106-120.



- Méndez, S., Martínez, A., Fabre, A. (2018). In: Proença, L.A.O. and Hallegraeff, G.M. (Eds.), Proc. 17th ICHA, Florianopolis, Brazil. pp. 22-25.
- Moita, M.T., Pazos, Y., Rocha, C. (2016). Harmful Algae 52, 17-32.
- Nagai, S., Sildever, S., Suzuki, T. *et al.*, (2020). In: Subba Rao, D. (Ed). Dinoflagellates: Classification, Evolution, Physiology and Ecological Significance. Nova Science Publishers, Inc. New York, U.S.A., pp. 129-166.
- Nagai, S., Nitshitani, G., Tomaru, Y. *et al.*, (2008). J. Phycol. 44, 909–922.
- Park, M.G., Kim, S., Kim, H.S. *et al.*, (2006). Aquat. Microb. Ecol. 45, 101-106.
- Park, J.H., Kim, M., Jeong, H.J. *et al.*, (2019). Harmful Algae 88, 101657
- Peltomaa, E. and Johnson, M.D. (2017). Aquat. Microb. Ecol. 78, 147-159.
- Pitcher, G.C. and Calder, D. (2000). S. Afr. J. Mar. Sci. 22, 255-271.
- Pizarro, G., Paz, B., González-Gil, S. *et al.*, (2009) Harmful Algae 8, 926-937.
- Proença, L.A., Schramm, M.A., Alves, T.P., Piola, A.R. (2018). In: Proença, L.A.O. and Hallegraeff, G.M. (Eds.), Proc. 17th ICHA, Florianopolis, Brazil. pp. 42-45.
- Quilliam, M.A., Ishida, N., McLachlan, J.L. *et al.* (1996). UJNR Tech. Rep. 24.
- Raho, N., Pizarro, G., Escalera, L. *et al.*, (2008). Harmful Algae 7, 839 -848.
- Raine, R., Cosgrove, S., Fennell, S. *et al.*, (2018). In: Proença, L.A.O. and Hallegraeff, G.M. (Eds.), Proc. 17th ICHA, Florianopolis, Brazil. pp. 46-49.
- Reguera, B., Bravo, I., Marcaillou-Le Baut, C. *et al.*, (1993). In: Smayda, T.J. and Shimizu, Y. (Eds.), Toxic Phytoplankton Blooms in the Sea. Elsevier, Amsterdam, pp. 553-558.
- Reguera, B., Riobó, P., Rodríguez, F. *et al.*, (2014). Mar. Drugs 12, 394-461.
- Reguera, B., González-Gil, S., Delgado, M. (2007). J. Phycol. 43, 1083-1093.
- Reguera, B., Velo-Suárez, L., Raine, R., Park, M.G. (2012). Harmful Algae 14, 87-106.
- Rial, P., Laza-Martínez, A., Reguera, B. *et al.*, (2015). Aquat. Microb. Ecol., 76, 163.
- Riobó, P., Reguera, B., Franco, J.M., Rodríguez, F. (2013). Toxicon 76, 221-224.
- Schnepf, E. and Elbrächter, M. (1988). Botanica Acta 101, 196-203.
- Sechet, V., Sibat M., Millien, G. (2021). Harmful Algae 107, 101974.
- Seeyave, S., Probyn, T., Pitcher, G. (2009). Mar. Ecol. Prog. Ser. 379, 91-107.
- Steidinger, K.A. (1975) In: V.R. LoCicero (Ed.). Toxic Dinoflagellate Blooms. Me and Technology Foundation, Wakefield, MA. pp. 153-162.



Trainer, V.L., Moore, L., Bill, B. *et al.*, (2013)
Mar. Drugs 11, 1815-1835.

Velo-Suárez, L., González-Gil, S., Pazos, Y
et al., (2014). Deep-Sea Res. II 101, 141-151.

Whyte, C., Swan, S., Davidson, K. (2014).
Harmful Algae 39, 365-373.

Wolny, J.L., Egerton, T.A., Handy, S.M. *et al.*, (2020). J. Phycol 56, 404-424.

Yasumoto, T., Murata, M., Oshima, Y. (1985).
Tetrahedron 41, 1019-1025.





HABs IN A CHANGING WORLD



Plastic-associated harmful phytoplankton assemblages in coastal and off-shore habitats of the Mediterranean Sea

Silvia Casabianca^{1*}, Samuela Capellacci¹, Maria Grazia Giacobbe², Carmela Dell'Aversano³, Luciana Tartaglione³, Fabio Varriale³, Riccardo Narizzano⁴, Rosella Bertolotto⁴, Nicola Ungaro⁵, Arianna Bellingeri⁶, Ilaria Corsi⁶, Antonella Penna¹

¹University of Urbino, 2/4, Via Cà le Suore 61029 Urbino, Italy; ²Istituto per le Risorse Biologiche e le Biotecnologie Marine, Consiglio Nazionale delle Ricerche (IRBIM CNR), Messina, Italy; ³University of Napoli Federico II, Via D. Montesano 49, 80131, Naples, Italy; ⁴Agenzia Regionale per la Protezione dell'Ambiente Ligure (ARPAL), Genova, Italy; ⁵Agenzia Regionale per la Protezione dell'Ambiente Puglia (ARPA Puglia), Bari, Italy; ⁶University of Siena, Earth and Environmental Sciences and INSTM Local Unit, 53100, Siena, Italy.

* corresponding author's email: silvia.casabianca@uniurb.it

Abstract

Plastics (macro, micro and nanoplastics) are durable and persistent pollutants that may alter pelagic and coastal ecosystem functions. Plastics provide a durable substrate that can be colonized by micro and macro-organisms. They support the growth of potential pathogens and HAB species. Further, plastic debris has been considered to play a key role in the dispersal also of biotoxins. The present study aimed to investigate harmful phytoplankton assemblages that colonized numerous samples of micro and macro-plastics collected in the Mediterranean Sea by qPCR assays, and to forecast toxin dispersal by quantifying toxin content onto plastic debris. Further, the impact of polystyrene nanoparticles (PS NPs) to the HA diatom *Skeletonema marinoi* was analyzed. All plastic samples were positive for the presence of Dinophyceae and Bacillariophyceae communities and some plastic samples were colonized by toxic species of dinoflagellate *Alexandrium pacificum*, *Alexandrium minutum*, *Ostreopsis* cf. *ovata* and diatom *Pseudo-nitzschia* spp. Strains of *A. pacificum* isolated from plastic debris and analyzed by LC-HRMS produced PST (paralytic shellfish toxins). The level of potential toxins on plastic samples ranged from 10¹ to 10² ng cm⁻². The interactions between HA diatom and plastic nanoparticles demonstrated an increase of both extracellular and intracellular reactive oxygen species, and significantly reduced colonies length using TEM and SEM techniques. Then, plastics can negatively impact the ecological functioning of oceans. The potential risk of harmful microalgae dispersal associated with plastic pollution was illustrated as well as for chemical compounds to transfer through the trophic chain with implications for human health and marine ecosystem.

Keywords: Assemblages, dispersal, harmful algae, biotoxins, marine plastics, qPCR, ROS, adhesion

<https://doi.org/10.5281/zenodo.7034421>



Introduction

Amounts of 23,150 of the 268,940 tons of plastic particles floating on the surface of the world's oceans are found on the Mediterranean Sea surface. Floating plastics are a durable and persistent substratum for the bio-adhesion of micro- and macro-organisms enabling dispersal from native to new habitats (Eriksen *et al.*, 2014). Plastic debris has been considered to play a role in the dispersal of toxic compounds having implications for humans and marine organisms across the marine food web. In marine ecosystems, biological interactions between plastic debris and biota include biofouling that starts from the adsorption of organic molecules followed by the increased adhesion of bacteria, diatoms and other microorganism communities. Finally, these microorganisms are linked together in a biofilm by extracellular polymeric substances (Flemming and Wingender, 2010). In previous studies, the harmful dinoflagellates *Alexandrium* sp., *Coolia* sp. and *Ostreopsis* sp. were recorded on plastics floating in coastal waters of the Mediterranean Sea (Zettler *et al.*, 2013). Plastic fragmentation, due to degradation of larger plastic waste, down to nanoscale particles (from 1 to 100 nm) was also demonstrated (Corsi *et al.*, 2020) and the effects, such as adhesion, production of reactive oxygen species (ROS) and reduction of photosynthetic yield due to exposure of phytoplankton species to these particles has been documented (Bellingeri *et al.*, 2020). This study aims to characterize and quantify target harmful phytoplankton taxa potentially attached to numerous samples of micro and macro -plastics collected in the coastal waters and offshore of the Mediterranean Sea by the quantitative PCR assay. The levels of potential

toxins transported by plastic samples were determined and the impact of polystyrene nanoparticles (PS NPs) on *Skeletonema marinoi* including ROS production, effects on algal growth and colony length was investigated.

Material and Methods

Environmental plastic sampling and processing

A total of 42 plastic samples were collected in different areas of the Mediterranean Sea from March 2016 to May 2017. Sampling was done by the use of a manta net of 330 µm mesh size, and manually. These macro and micro -plastic samples were analyzed by qPCR for molecular abundance quantification of attached microalgal taxa. Moreover, pellets obtained from ten *A. pacificum* strains isolated from plastic samples were analyzed for PST content by liquid chromatography-high resolution multiple stage mass spectrometry (LC-HRMS). Cultures of the diatom *S. marinoi* CBA4 was used for nanoplastic effects determination.

FTIR spectroscopy

A Nicolet 6700 FT-IR spectrometer (Thermo Fisher, U.S.A.) fitted with a single bounce attenuated total reflectance (ATR) accessory was used to characterize the plastic samples.

DNA extraction and qPCR analyses on environmental marine plastic samples

The genomic DNA was extracted using the DNeasy PowerSoil Kit (Qiagen, Hilden, Germany), according to the manufacturer's instructions. For the quantification of Dinophyceae, Bacillariophyceae, *A.*



minutum, *A. pacificum*, *O. cf. ovata* and *Pseudo-nitzschia* spp. in plastic samples, different standard curves were used (see also Casabianca *et al.*, 2019).

Adhesion rate of harmful algal species to the plastic substrate

Strains of *P. multistriata* CBA174, *Skeletonema marinoi* CBA4, *A. minutum* CBA57, *A. pacificum* CNR-SRA4, *L. polyedrum* LPA0510, *P. reticulatum* PRA0311, *G. spinifera* CBA5 and *O. cf. ovata* CBA1291 were grown in glass bottles together with sterilized plastic sheets. A plastic sheet was harvested every four days from the inoculum and gently scraped in sterile seawater in order to recover the cells adhering to the plastic sheets. Subsamples of 1 mL were collected for cell density estimation by light microscopy. The adhesion rates was determined using the equation: $\mu = \ln(Nt/N0)/\Delta t$, where N is the number of the plastic adherent cells expressed as cells cm⁻² and Δt is the time interval expressed in days.

S. marinoi-PS

NPs interaction and quantification of ROS

S. marinoi cultures were exposed to 1, 10, 50 $\mu\text{g mL}^{-1}$ PS NPs for 15 days and cells growth was investigated. The physical interaction between algal cells and nanoplastics was imaged through ESEM and TEM.

The production of ROS was measured by following the conversion of the non-fluorescent dihydrodichlorofluorescein diacetate (H₂DCF-DA) to the highly fluorescent compound 2', 7',-dichlorofluorescein (DCF) (see Bellingeri *et al.*, 2020).

Results and Discussion

The proportion of sampled microplastics was 64% non-polar (polyethylene and polypropylene) and 36% had a certain level of polarity. All the 42 plastic samples tested positive for the presence of Dinophyceae and Bacillariophyceae and by the qPCR quantification of harmful target microalgal taxa, sixteen plastic samples showed the presence of the toxic and allochthonous *A. pacificum*, nine samples tested positive for the presence of *A. minutum* and *O. cf. ovata* and *Pseudo-nitzschia* spp. was present in almost all plastic samples (n = 31) (Fig. 1). The abundance of the phytoplankton communities found on environmental plastics surface was highly variable with Bacillariophyceae showing the highest abundance of cells, probably because they can the most easily form biofilms on plastics by producing extracellular substances (Reisser *et al.*, 2014). Dinophyceae showed lower abundance than Bacillariophyceae on field marine plastics, but *in vitro* experiments demonstrated that *A. pacificum*, *A. minutum* and *O. cf. ovata* were able to attach to the environmental plastics. Indeed, the dinoflagellate *A. pacificum* appeared to be the species that adhered to the plastics the most rapidly, followed by the diatoms *S. marinoi* and *P. multistriata*. The species that adhered at the slowest rate were *A. minutum* and *O. cf. ovata* (Fig. 2).



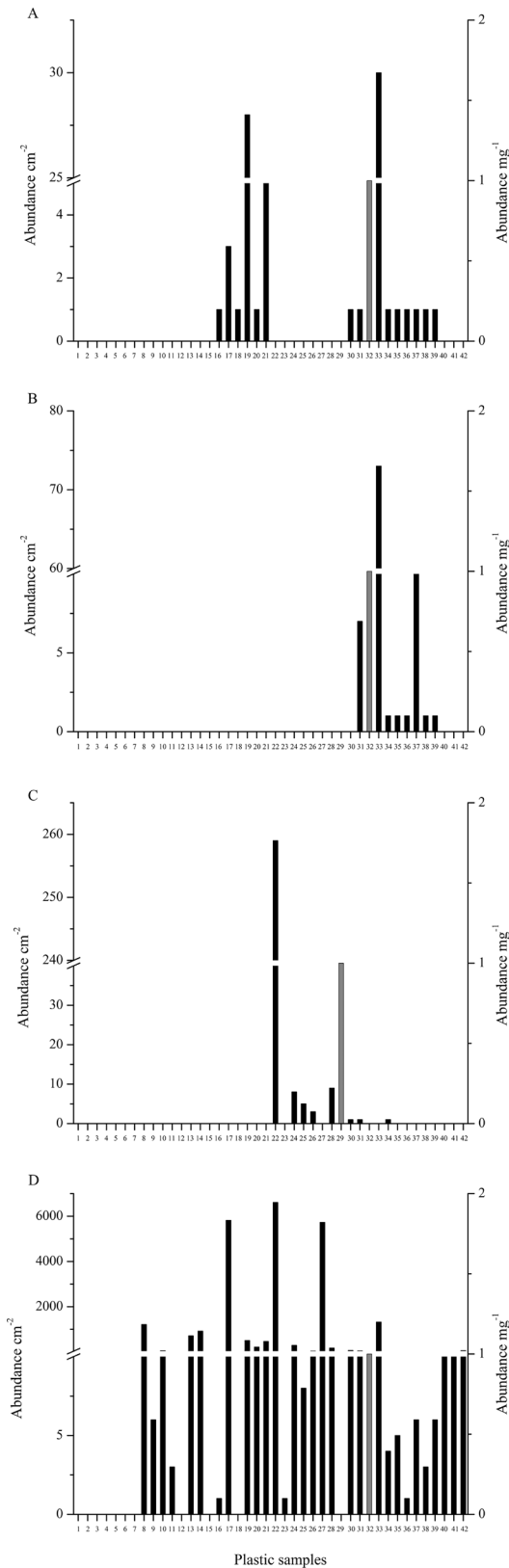


Fig. 1. Molecular quantification of target harmful microalgal species abundance on plastics collected in the Mediterranean Sea by qPCR assay. (A) *Alexandrium pacificum*, (B) *A. minutum*, (C) *Ostreopsis cf. ovata*, (D) *Pseudo-nitzschia* spp.

Thus, from these results and using a qPCR approach we demonstrated that some target HA species adhere tightly to floating plastic debris, which suggests that the selected harmful microalgal species could potentially spread through marine ecosystems and trophic chain, negatively impacting human health and environment.

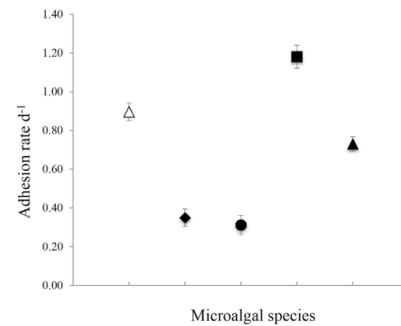


Fig. 2. Adhesion rates of different cultured harmful microalgal strains to the plastic surfaces (means \pm SD, n = 3). *Alexandrium pacificum* (■), *Skeletonema marinoi* (Δ), *Pseudo-nitzschia multistriata* (▲), *Alexandrium minutum* (◆) and *Ostreopsis cf. ovata* (●).

Moreover, all the 10 tested strains of *A. pacificum* produced PST, with total toxin content in the range from 35.14 to 6,032 fg cell⁻¹. From this study, we conclude that the PSP producing species can transport 1-72 pg cm⁻² of PST. Considering the other target species we hypothesized that *Pseudo-nitzschia* can potentially contribute to domoic acid transport with values in the range of 5 and 443 ng cm⁻² on floating plastics based

on the literature values (Trainer *et al.*, 2012). Based on the maximum abundance of 259 cells cm^{-2} of *O. cf. ovata* found on the plastics, we conclude that at least 1-62 ng PLTX compounds cm^{-2} must be accumulated in floating plastics debris (Tartaglione *et al.*, 2017). Marine plastic debris can be linked to a mixture of marine biotoxins, produced by microalgae which can be transferred throughout the trophic chain to higher trophic levels, and thus contaminate seafood for humans (Casabianca *et al.*, 2019).

No effects on diatom growth were observed upon exposure to PS NPs (1, 10 and 50 $\mu\text{g mL}^{-1}$) for 15 days (Kruskal-Wallis Hc = 0.63, p = 0.89). TEM images clearly show nanoplastic aggregates mainly interacting with the terminal fulcportula processes (TFPP) of *S. marinoi* (Figs. 3 a, b). This adhesion affected the length of *S. marinoi* chains.

PS NPs exposed algae showed a high percentage of single cells and 2-cell chains, altogether accounting for 95% and 84% of those exposed to 10 and 50 mg/mL , respectively. Moreover, the occurrence of contact-induced stress, following cell-PS NPs interactions, resulted in enhanced production of both intracellular and extracellular ROS (Fig. 4).

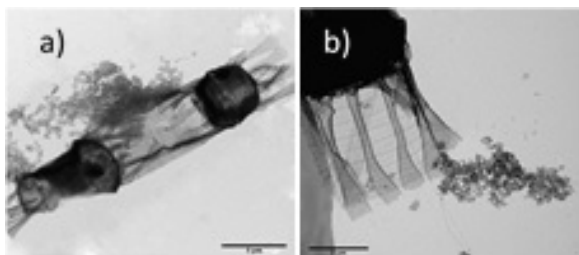


Fig. 3. TEM images of *S. marinoi* exposed to PS NPs.

From these results, new information was obtained regarding the quantities of harmful marine species attached to the plastics floating in the Mediterranean Sea based on qPCR assays. These findings illustrate the potential risk of harmful microorganism dispersal associated with plastic pollution. HA dinoflagellate species abundance was found to be lower than that of diatom communities which include potentially toxic *Pseudo-nitzschia* spp. Moreover, the potential risk of transport of toxins by plastic debris could be likely.

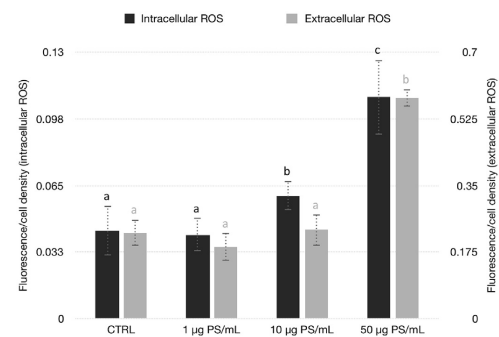


Fig. 4. Intracellular and extracellular ROS levels in *S. marinoi* exposed to PS NPs (1, 10, 50 $\mu\text{g PS mL}^{-1}$) and in controls. Data shown as fluorescence units/cell density (cells mL^{-1}). Data with different letters are statistically different with $p < 0.005$.

By the exposure to plastic nanoparticles, no lethal effect to the marine diatom *S. marinoi* was observed, while an increase in intracellular and extracellular oxidative stress and a reduction of diatom's chain length were observed. These effects could have potential ecological implications such as changes in algal buoyancy as well as the formation and sinking of aggregates potentially affecting marine carbon pump. From the evidence we have shown, measures for preventing and managing plastic pollution are needed



but also further investigation should be carried out to predict the ecological impacts on phytoplankton assemblages involved in primary production.

Acknowledgements. This work was supported by Regione Marche Project Coastal Monitoring n. 49 of 23/12/2013 of Tabella C and EU ENPI CBC-MED M3-HABs Project. We thank people of Wageningen University who kindly provided the PS-COOH nanoparticle batch functionalized with Rhodamine B dye.

References

Bellingeri, A., Casabianca, S., Capellacci, S., Faleri, C., Paccagnini, E., *et al.*, (2020). *Environ. Pollut.* 262, 114268.

Casabianca, S., Capellacci, S., Giacobbe, M.G., Dell'Aversano, C., *et al.*, (2019). *Environ. Pollut.* 244, 617-626.

Corsi, I., Bergami, E., Grassi, G. (2020). *Front. Environ. Sci.* 8, 60.

Eriksen, M., Lebreton, L.C., Carson, H.S., Thiel, M., *et al.*, (2014). *PLoS One* 9, e111913.

Flemming, H.C. and Wingender, J. (2010). *Nat. Rev. Microbiol.* 8, 623-633.

Reisser, J., Shaw, J., Hallegraeff, G., Proietti, M., *et al.*, (2014). *PLoS One* 9, e100289.

Tartaglione, L., Dello Iacovo, E., Mazzeo, A., Casabianca, S., *et al.*, (2017). *Environ. Sci. Technol.* 51, 13920-13928.

Trainer, V.L., Bates, S.S., Lundholm, N., Thessen, A.E., *et al.*, (2012). *Harmful Algae* 14, 271-300.

Zettler, E.R., Mincer, T.J., Amaral-Zettler, L.A. (2013). *Environ. Sci. Technol.* 47, 7137-7146.



New records of intensive blooms of *Alexandrium minutum* (Dinophyceae) in the Jonian Sea, Italy

Rossella Pistocchi^{1*}, Monica Cangini², Franca Guerrini¹, Laura Pezzolesi¹, Silvia Casabianca³, Sonia Dall'Ara², Fiorella Pino², Maria Grazia Aloï⁴, Letteria Settineri⁴, Francesca Pedullà⁴, Margherita Tromba⁴, Stefano Morabito⁴, Antonella Penna³

¹Department of Biological, Geological and Environmental Sciences, Ravenna Campus, Via Sant'Alberto 163, 48123 Ravenna, Italy; ²Fondazione Centro Ricerche Marine, Viale Vespucci 2, 47042 Cesenatico, Italy; ³Department of Biomolecular Sciences, University of Urbino, Campus E. Mattei, 61029 Urbino, Italy; ⁴Dipartimento Provinciale A.R.P.A.Cal., Reggio Calabria, Italy.

* corresponding author's email: rossella.pistocchi@unibo.it

Abstract

In Italy *Alexandrium minutum* is recurrently found at low concentrations in mussel farming areas, such as the Western Adriatic and the Sardinia coasts; mussels positive to PSP toxins have occasionally been detected but rarely exceeded the legal limit for commercial sale. Conversely, in South Italy, the Sicilian coast represents a hot spot of *A. minutum* blooms, repeatedly occurring in high densities. This study shows the presence of extensive blooms detected for the first time on the Jonian coast of Calabria at Roccella Jonica; the first bloom occurred in 2018, followed by a larger event in 2020. Both blooms occurred in March in the harbour dockyard, an area not monitored for toxic algae due to the absence of mussel farms. The blooms caused a yellow/brown water discoloration, but no PSP symptoms were reported. In order to understand if these blooms can cause harmful consequences, five *Alexandrium* strains were isolated from the 2018 event for molecular identification at the species level and analysis of the toxin content and profile. All strains were confirmed to belong to the *A. minutum* group and produce PSP toxins, with four out of five clones displaying higher toxin levels. The toxin profile displayed slight differences among strains, however, GTX 1,4 were the prevalent analogues, as previously observed in the Mediterranean region. Despite *A. minutum* blooms being rare events historically, intensive toxic blooms are increasing, especially on the South Italian coasts. This poses some concerns and highlights the need for better monitoring and management of the new identified spot and of nearby areas.

Keywords: *Alexandrium minutum*, harmful blooms, marine biotoxins, PSP toxins

<https://doi.org/10.5281/zenodo.7034432>



Introduction

Alexandrium minutum Halim, 1960 is a globally distributed dinoflagellate known to produce paralytic shellfish toxins, a family of compounds causing paralytic shellfish poisoning (PSP) in humans. The presence of this species is carefully monitored, thus there is a substantial database to evidence that its blooms are expanding to places where they were not previously observed.

In Europe, *A. minutum* blooms have occurred at different locations, especially in Northern coastal areas (Lewis *et al.*, 2018), but in the Southern Mediterranean region, recurrent blooms have been reported only from few places, in particular on the Catalan coast of Spain (Vila *et al.*, 2005) and, in Italy, in Sardinia (Bazzoni *et al.*, 2020) and in both the Tyrrhenian and Jonian coast of Sicily (Vila *et al.*, 2005; Costa *et al.*, 2021). These blooms usually occur in places characterized by sheltered and stratified waters, with inputs from rivers (Giacobbe *et al.*, 1995; Vila *et al.*, 2005). In different areas, such as the Western Adriatic Sea, *A. minutum* cells are detected every year, especially during spring, in numbers rarely exceeding 4,000 cells L⁻¹ and, even in the presence of higher concentrations, mussels contaminated by PSP toxins have rarely been detected (personal observations). In contrast, on the Sardinian coast (Tyrrhenian Sea), mussels positive to PSP toxins were found since 2002, although not continuously, despite the occurrence of low cell numbers. For example, in 2015, mussels were positive to PSP toxins although only 800 cells L⁻¹ were counted (Bazzoni *et al.*, 2016). It is thus possible to conclude that in Italy, with the exception of Sicily, *A. minutum* blooms can be considered rare events and, accordingly,

episodes of PSP levels exceeding the legal limit for mussel sales have occurred only on few occasions (in the Adriatic Sea, Sardinia and Sicily). The present study is aimed at reporting the occurrence, for the first time, of extensive blooms of *A. minutum* on the Jonian coast of Calabria (Roccella Jonica, province of Reggio Calabria; Fig. 1); results of a study aimed at species confirmation and toxicity evaluation are shown.

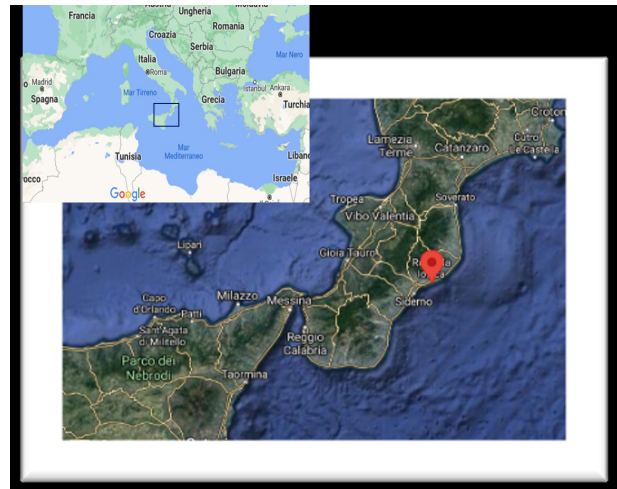


Fig. 1. Roccella Jonica geographic position.

Material and Methods

Seawater sampling

On March 2018 and 2020, water discoloration was noticed by eye; in both years 1 L of seawater was taken with a bottle in the bloom area for preliminary observations, then used for microscope cell identification and counting. An aliquot of the 2018 sample was utilized for cell isolation and culture set up.

Cell cultures

Single cells were isolated under the microscope through glass capillary tube



methods, the cells were allowed to divide in a 24-well plate in f/20 medium and after two weeks five *Alexandrium* spp. strains (C21I, C42I, C53I, C1D and C5D) could successfully be cultured in f/4 medium (f/20 and f/4 were made from Guillard f/2 modified in terms of N and P levels that were both 10- and 2-fold diluted, respectively).

Biovolume measurement

The cell volume of each strain was determined by measuring at least 60 cells in the stationary phase of growth under a light microscope. Cells were considered spherical according to Edler (1979).

DNA extraction and sequencing

Cultures in the exponential growth phase were collected for DNA isolation and analysis. Genomic DNA was extracted using the DNeasy Plant Mini Kit (Qiagen, Hilden, Germany), the ITS - 5.8S region of the rDNA was then amplified (Fig. 3) and sequenced using the universal primer ITSA and ITSB (Adachi *et al.*, 1994).

Toxin analysis

Two liter cultures of each strain were collected by centrifugation and used for toxin analysis performed by means of Liquid Chromatography with Fluorescence Detection (LC-FLD) after derivatization in accordance with AOAC Official Method 2005.06.

Results and Discussion

Events and organism

At Roccella Jonica, the first water discoloration event occurred in March 2018, followed by a second one in the same month of 2020, the latter lasting until the middle of September. They both occurred in the harbour dockyard

where the water appeared intensely yellow/brown coloured from nearly 15 cm from the surface (Fig. 2). Observations under the light microscope pointed to the presence of an *A. minutum* bloom with cell numbers of 79×10^6 cells L^{-1} and 261×10^6 cells L^{-1} , in 2018 and 2020, respectively.

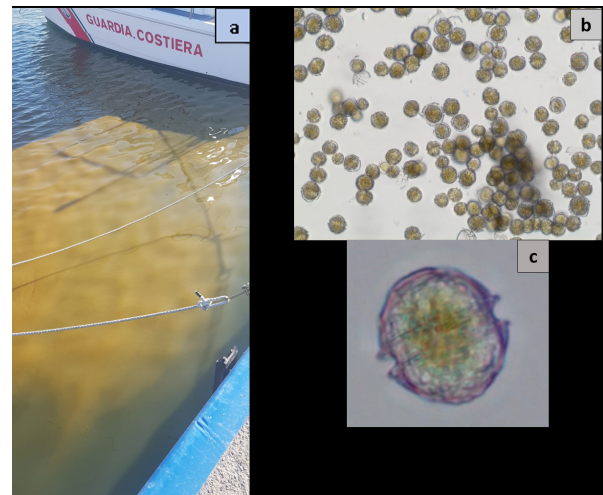


Fig. 2. Bloom of *A. minutum* in the field in 2020 (a) and under the light microscope (b); single cell, mean cell diameter of $20.81 \pm 1.42 \mu m$ (c).

The area is not monitored for toxic algae due to the absence of mussel farms, and during the bloom no one suffered from PSP symptoms. However, a correct identification and evaluation of toxins was undertaken at the first bloom appearance.

The five strains isolated from the 2018 field samples underwent molecular identification. The amplified ITS - 5.8S rDNA was about 550 bp (Fig. 3). All the clone sequences were confirmed to belong to the Mediterranean *A. minutum* species based on 100% rDNA gene sequence similarity using BLAST.



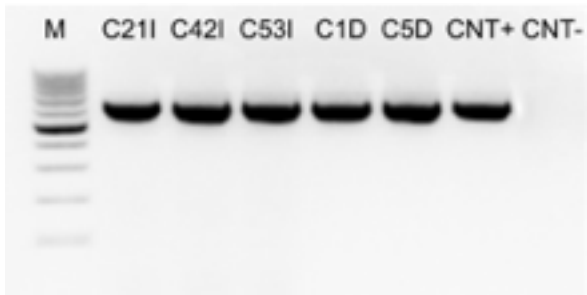


Fig. 3. Amplification of ITS – 5.8S rDNA region of *Alexandrium* spp. C21I, C42I, C53I, C1D and C5D strains. M: 100-bp ladder marker; CNT+: positive control; CNT-: negative control.

All the newly isolated algal strains were determined to be PSP toxin-producers and their toxin profiles were similar (Table 1): GTX 1,4 were the most prevalent analogues (72 - 100%), as previously observed in other strains from the Mediterranean area, whereas minor toxins slightly differed among strains.

Table 1. Toxin profile of the investigated strains.

Strain ID	GTX 2,3	C1,2	GTX 1,4 %	NEO
C53I		27.51	72.49	
C1D			100.00	
C5D	4.62		94.03	1.35
C21I		5.69	94.31	
C42I	4.13	2.84	90.97	2.06

Toxicity levels displayed higher variability but, generally, all the strains appeared to contain a total toxin content in the range of few fg cell⁻¹, with a maximum value of 23.71 fg cell⁻¹ (Table 2). These values are in the range of those measured in different strains from the Adriatic Sea (Perini *et al.*, 2014) and also in strains from other geographical zones (Nascimento *et al.*, 2005), however,

are very low compared to a strain previously analyzed from the Gulf of Trieste (Northern Adriatic Sea) which contained 964 fg cell⁻¹ of total saxitoxins (recalculated from Beani *et al.*, 2000). This difference led us to compare the biovolume of the various strains, all measured in the stationary phase, which resulted in being the same range: the strains from Roccella Jonica had a mean biovolume of 4,606 ± 510 μm³ and the one from the Gulf of Trieste of 6,347 ± 1577 μm³; the latter is slightly higher and accounted for a toxin content, on a biovolume-base, which is 31-fold higher than that of the most toxic strain isolated in Roccella Jonica (0.1519 and 0.0049 fg SXTs fL⁻¹ for Trieste and C5D strain, respectively).

Table 2. Toxicity of the investigated algal strains

Strain ID	Toxin content (fg cell ⁻¹)	Toxicity (fg SXTeq cell ⁻¹)
C53I	1.23	1.21
C1D	7.32	8.28
C5D	23.71	26.60
C21I	4.71	5.05
C42I	9.58	10.50

The reported blooms demonstrate that Roccella Jonica (Calabria Region) may be considered among the Italian Jonian areas which are affected by recurring PSP toxic *A. minutum* blooms, in addition to the Siracusa area (Sicily Region) where the blooms have occurred since 2000 (Vila *et al.*, 2005; Penna *et al.*, 2015; Costa *et al.*, 2019). Blooms detected in Roccella Jonica once more confirm the preference of *A. minutum* for sheltered areas and early spring months, as it was reported for blooms occurring in different areas of South Italy.



The molecular characterization suggests that this population belongs to the Jonian cluster of *A. minutum* in the Mediterranean Sea (Casabianca *et al.*, 2012). In regards to the toxic profile, the Ionic strains belong to cluster 1, which is the one spread throughout Europe, Australia, Taiwan and Malaysia (Lewis *et al.*, 2018). The new isolated strains do not appear highly toxic, however our results confirm the high variability of the toxic potency among strains of similar geographic origin. In view of *A. minutum*'s rapid growth and capacity to reach high cell abundance, its blooms with relatively low toxin per cell but many cells represent a significant source of PSP toxins to the environment.

These results highlight that it is worth increasing the monitoring effort in Roccella Jonica and to perform further investigations on the conditions triggering the blooms.

Acknowledgements. Authors would like to thank the staff of Direzione Marittima di Reggio Calabria, especially the Capitaneria di Porto of Roccella Jonica.

References

- Adachi, M., Sako, Y., Ishida, Y. (1994). *J. Phycol.* 30, 857-863.
- Bazzoni, A.M., Mudadu, A.G., Lorenzoni, G., Arras, I., *et al.*, (2016). *It. J. Food Safety.* 5, 6095.
- Bazzoni, A.M., Cangini, M., Mudadu, A.G., Lorenzoni, G., *et al.*, (2020). *Toxicon* 174, 48-56.
- Casabianca, S., Penna, A., Pecchioli, E., Jordi, A., *et al.*, (2012). *Proc. R. Soc. B.* 279, 129-138.
- Beani, L., Bianchi, C., Guerrini, F., Marani, L., *et al.*, (2000). *Toxicon* 38, 1283-1297.
- Casabianca, S., Penna, A., Pecchioli, E., Jordi, A., *et al.*, (2012). *Proc. R. Soc. B.* 279, 129-138.
- Costa, A., Alio, V., Sciortino, S., Nicastro, L., *et al.*, (2021). *It. J. Food Safety.* 10, 9062.
- Giacobbe, M.G., Oliva, F.D., Maimonea, G. (1995). *Estuar. Coast. Shelf Sci.* 42, 539-549.
- Lewis, A.M., Coates, L.N., Turner, A.D., Percy, L., Lewis, J. (2018). *J. Phycol.* 54, 581-98.
- Nascimento, S.M. Purdie, D.A., Lilly, E.L., Larsen, J., Morris, S. (2005). *J. Phycol.* 41, 343-353.
- Penna, A., Perini, F., Dell'Aversano, C., Capellaci, S., *et al.*, (2015). *Env. Sci. Technol.* 49, 14230-14238.
- Perini, F., Galluzzi, L., Dell'Aversano, C., Dello Iacovo, E., *et al.*, (2014). *Mar. Drugs* 12, 5258-5276.
- Vila, M., Giacobbe, M.G., Masó, M., Gangemi, E., *et al.*, (2005). *Harmful Algae* 4, 673-695.



New species blooms and emergent toxins on the Uruguayan coast

Ana Martínez Goicoechea*, Leonardo Ortega, Silvia Méndez

Dirección Nacional de Recursos Acuáticos (DINARA). Constituyente 1497, Montevideo, Uruguay.

* corresponding author's email: anamart30@gmail.com

Abstract

Climate-driven changes in coastal ocean and ecological systems are, in some cases, exacerbated by localized human activities. These ecosystem alterations can be intensified by changes in circulation and nutrient availability, which affect the distribution of marine populations, including the occurrence of harmful algal blooms (HABs). There is no doubt that the problems caused by HABs are growing worldwide. Certain HABs are expected to increase as sea surface temperature rises, expanding the seasonal bloom opportunity and species distribution range. High temporal resolution monitoring on the oceanic coastal area of Uruguay was used to understand how changes in sea surface temperature may promote the emergence of harmful blooms and new toxins. Using long-term monitoring, two toxic dinoflagellate species were detected for the first time in Uruguayan coastal waters, including *Protoceratium reticulatum*, a yessotoxin producer, and *Dinophysis tripos*, a pectenotoxin producer. The observed warming in the last decade in the southwestern Atlantic coincides with phytoplankton species composition changes. In spring 2017, a huge *P. reticulatum* bloom was found concomitant with detection of a lipophilic toxin. *Dinophysis tripos* has also shown a higher abundance since 2016, but toxins associated with this species have not yet been characterized.

Keywords: HAB, *Dinophysis*, *Protoceratium*, climate change, marine biotoxins

<https://doi.org/10.5281/zenodo.7034438>



Introduction

Climate change is expected to affect the frequency, magnitude, biogeography, phenology, and toxicity of harmful algal blooms (HABs) (Anderson, 2014; Wells *et al.*, 2015, 2020). Increases in water stratification due to warming and increased precipitation favor an increase in the presence of dinoflagellates and cyanobacteria (Thompson *et al.*, 2015; Gobler *et al.*, 2017). The rise in CO₂ may promote the growth of certain harmful algae (Branderburg *et al.*, 2019). Furthermore, species composition is changing (Cloern and Dufford, 2005), associated with alterations in the range of species distribution (Tester *et al.*, 2020; Trainer *et al.*, 2020) at many locations worldwide, including Uruguay (Martínez *et al.*, 2017), due to climate variability. The migration of HABs to new ecosystems may create significant risk to aquatic organisms and humans who inhabit these regions (Gobler, 2020).

Dinophysis tripos is a pectenotoxin (PTX) producing species widely distributed and observed in colder regions, such as the northern Norwegian Sea and sub-Antarctic waters. This species has been found in Buenos Aires province mainly in July (Sars *et al.*, 2010) and has been associated with PTX production in Argentinean waters (Fabro *et al.*, 2015). *Protoceratium reticulatum*, a yessotoxin (YTX) producer has been detected in the region (Brazil, Uruguay, Argentina), generally in low abundances, YTX has been associated with *P. reticulatum* blooms in Argentina (Akselman *et al.*, 2015).

Material and Methods

Samples were collected as part of a weekly HAB monitoring program initiated in 1980 along the Uruguayan Atlantic coast. For the present study, seawater and shellfish samples (more than 550 samples) were collected from five fixed stations along the Uruguayan oceanic coast since 2011 (Fig. 1). The water samples were collected with a plastic bucket and a 250 mL aliquot was fixed with Lugol's solution (Thronsdén, 1978) for phytoplankton analysis. Samples were analyzed using an inverted microscope (Olympus IM) following the Utermöhl method (Utermöhl, 1958). Magnifications from 100 - 1,000x were used (Andersen and Thronsdén 2003) following specific keys and complimentary bibliographies (Hasle and Simps, 1986; Round *et al.*, 1990; Balech, 1988; Tomas, 1997; Gómez *et al.*, 2008; Sunesen *et al.*, 2008; Metzeltin and García-Rodríguez, 2012; Gómez, 2013; Hoppenrath *et al.*, 2013; Nanjappa *et al.*, 2013;) to count at least 100 organisms of the most frequent species (Venrick, 1978).

Biotoxins were detected by mouse bioassay with the modified Yasumoto method (Fernandez *et al.*, 2002) using the whole mollusk bodies. This method detects total toxicity but is unable to distinguish individual lipid toxins such as OA, PTX, and YTX.

The complexity, nonlinearity and nonstationarity of the climate system and HAB requires different statistical analysis to detect relationships between biological and physical forcing. The wavelets coherence analysis of the time series, permits the analysis of two signals along the time and analyses the dependence between them.



It is especially relevant to the analysis of non-stationary systems like both ecological and environmental time series and the relationships between these series, when the temporal evolution has aperiodic and transient signals (Cazelle *et al.*, 2008). This was done using the software R (biwavelet, wmtsa and itsmr packages) (<https://github.com/tgouhier/biwavelet>, <https://rdrr.io/rforge/wmtsa/>, <http://eigenmath.org/itsmr-refman.pdf>).

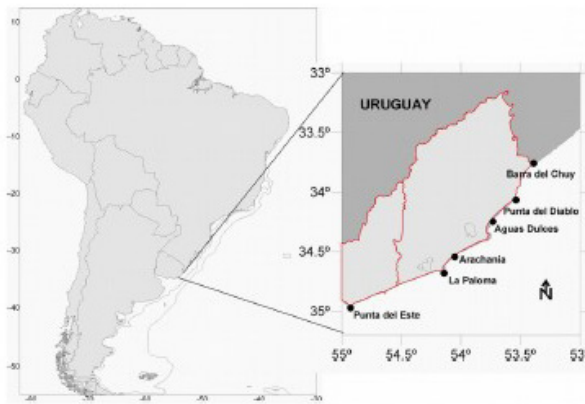


Fig. 1. Map of South America showing the fixed sampling stations along the coast of Uruguay (black dots).

Results and Discussion

Dinophysis tripos blooms were observed only in winter, occurring during low temperature periods, displaying higher salinity affinity and very narrow temperature range (Figs. 2 b, c). This species was observed first in 2013 (ca. week 100, August 2013) but generally in low numbers until 2018 (week 365, August 2018), when a maximum abundance was observed (Figs. 2 a, b).

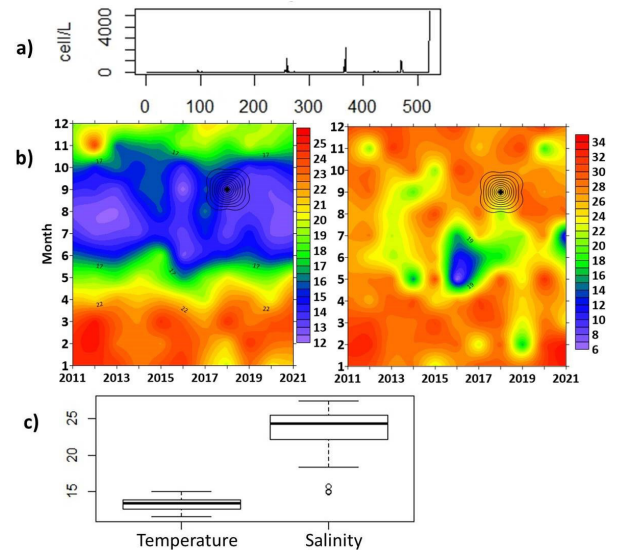


Fig. 2. a) Time series of *Dinophysis tripos* abundance from July 2011 (week 0) to August 2021 (week 522); x-axis (time) is in weeks and y-axis (abundance) is in cell L^{-1} . b) Contour maps for temperature (left) and salinity (right) along the years (x-axis) and month (y-axis) with *D. tripos* abundance shown as black contour lines (maximum during week 365, August 2018). c) Range of temperature and salinity on sampling days when *D. tripos* is detected (from 2011 to 2021), shown as boxplots. The dark line in each box represents the median, with the lower and upper limits at 25 and 75%, respectively. Whiskers represent 10 and 90%, respectively.

Protoceratium reticulatum was present at slightly higher temperatures than *D. tripos* and at high salinity; during spring months, it had generally low abundance, however a huge bloom ($156,300 \text{ cell } L^{-1}$) was detected in 2017 (Fig. 3) with the co-occurrence of lipophilic toxins.

Both species show high significance with temperature, probably related to the El Niño Southern Oscillation (ENSO) cycle,



at 2–7 years on average (Fig. 4). *Dinophysis tripos* shows a negative relationship with temperature ca. five years from the start of sampling (250 weeks; July 2016) (Fig. 4). This species was detected each year, displaying a significant annual occurrence staying from 4 weeks (1 months) to 8 weeks (2 months).

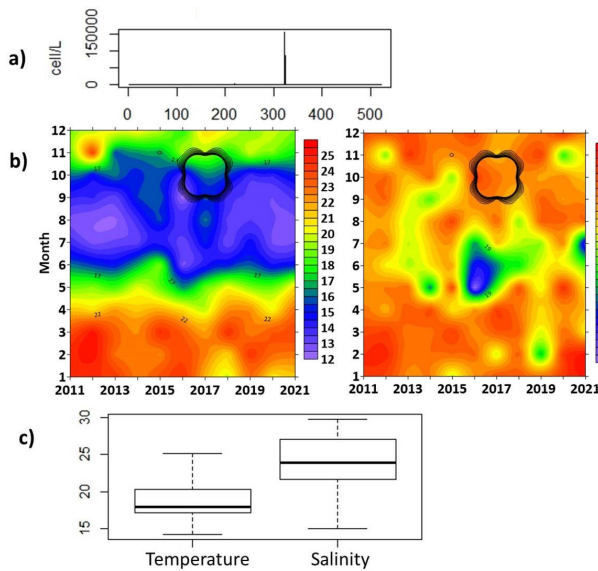


Fig. 3. a) Time series of *Protoceratium reticulatum*, abundance from July 2011 (week 0) to August 2021 (week 522); x-axis (time) is in weeks and y-axis (abundance) is in cell L^{-1} . b) Contour maps for temperature (left) and salinity (right) with *P. reticulatum* abundance shown as black contour lines (maximum during week 322, October 2017), c) Range of temperature and salinity on sampling days when *P. reticulatum* was found (from 2011 to 2021), shown as boxplots. The dark line in each box represents the median, with the lower and upper limits at 25 and 75%, respectively. Whiskers represent 10 and 90%, respectively.

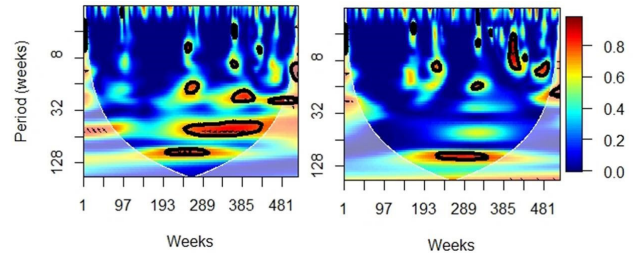


Fig. 4. Wavelet coherence analysis between temperature and abundance of *Dinophysis tripos* (left) and between temperature and abundance of *Protoceratium reticulatum* (right) from July 2011 to August 2021. Colors code from dark blue (low values) to red (high values), as more red is the color higher is the coherence (which can be interpreted as correlation between abundance and temperature) at the location in the time-frequency space. A thick black line surrounds statistically significant periods of coherence.

Prorocentrum reticulatum appeared ca. four years from the start of the sampling (at 190 weeks), showing a positive relationship with temperature. Elevated abundance was detected between eight weeks (2 months) and 12 weeks (3 months) (Fig. 4).

Climate variability produces changes in the species distributions and abundance. In that vein, two toxin producer species were registered for the first time on the Uruguayan coast during the last decade; namely *P. reticulatum* (YTX producer) and *D. tripos* (PTX producer). Neither toxin can be differentiated using bioassay from okadaic acid, the most common lipophilic toxin found on the Uruguayan coast (Turner and Goya, 2015; Martínez *et al.*, 2017), thus toxins produced by each of these species has not yet been confirmed. Both species showed cycles potentially related to the ENSO influence in



the area. The emergence of harmful blooms and potentially new toxins may be promoted by changes in sea surface temperature, even for low-temperature species.

References

- Akselman, R., Krock, B., Alpermann, T. J., Tillmann, U., *et al.*, (2015). *Harmful Algae* 45, 40-52.
- Andersen, P. and Throndsen, J. (2003). UNESCO Publishing, Paris, pp. 99-129.
- Anderson, D. (2014). In: Kim, H.G. (Ed.). *Proc. 15th ICHA*, Changwon Gyeongnam, Korea, 3-17.
- Balech, E. (1988). *Publicación Especial del Instituto Español de Oceanografía*. Madrid, Spain. 310 pp.
- Brandenburg, K. M., Velthuis, M., Van de Waal, D. B. (2019). *Glob. Chang. Biol.* 25, 2607-2618.
- Cazelles, B., Chavez, M., Berteaux, D., Ménard, F., *et al.*, (2008). *Oceanologia* 156, 287-304.
- Cloern, J. and Dufford, R. (2005). *Mar. Ecol. Prog. Ser.* 285, 11-28.
- Fabro, E., Almandoz, G. O., Ferrario, M. E., Hoffmeyer, M. S., *et al.*, (2015). *Harmful Algae* 42, 25-33.
- Fernandez, M.L., Míguez, A., Cacho, E., Martínez, A., *et al.*, 2002. In: Sar, E.A., Ferrario, M.E., Reguera, B. (Eds.), *Instituto Español de Oceanografía*, Madrid, Spain. pp. 77-120
- Gobler, C.J., Doherty, O.M., Griffith, A.W., Hattenrath-Lehmann, T.K., *et al.*, (2017). *Proc. National Academy of Science*, Karl D.M. (Ed.) Honolulu, U.S.A. 114, 4975-4980.
- Gobler, C. J. (2020). *Harmful Algae*. 91, 101731.
- Gómez, F., Claustre, H., Souissi, S. (2008). *Rev. Biol. Mar. Oceanogr.* 43. 25-40.
- Gomez, F. (2013). *CICIMAR Océánides*. 28, 1-22.
- Hasle, G.R. and Sims, P.A. (1986). *Br. Phycol. J.* 21, 97-114.
- Hoppenrath, M., Chomérat, N., Horiguchi, T., Schweikert, M., *et al.*, (2013). *Harmful Algae* 27, 1-28.
- Martínez, A., Méndez, S., Fabre, A. Ortega, L. (2017). *Innotec*. 13, 19-25.
- Metzeltin, D. and García-Rodríguez, F. (2012). *DIRAC Montevideo*, Uruguay. 207 pp.
- Nanjappa, D., W.H.C.F. Kooistra, Zingone, A. (2013). *J. Plankton Res.* 49, 917-936.
- Round, F.E., Crawford, R.M., Mann, D.G. (1990). *Cambridge University Press*, Cambridge, 747 pp.
- Sar, E. A., Sunesen, I., Lavigne, A. S., Goya, A. B. (2010). *Rev. Biol. Mar. Oceanogr.* 45, 451-460.
- Sunesen, I., Hernández-Becerril, D. U., Sar, E. A. (2008). *Rev. Biol. Mar. Oceanogr.* 43, 303-326.



Tester, P., Berdalet, E., Litaker, R.W. (2020). Harmful Algae 91, 101655.

Thompson, P.A., Baird, M.E., Ingleton, T., Doblin, M.A. (2009). Mar. Ecol. Progr. Ser. 394, 1-19.

Thronsdon, J. (1978). UNESCO Monographic Oceanographic Method, 6. pp. 69-74.

Tomas C.R. (1997). Academic Press. U.S.A., 839 pp.

Trainer, V.L., Moore, S.K., Hallegraeff, G., Kudela, R.M., *et al.*, (2020). Harmful Algae 91, 101591.

Turner, A.D. and Goya, A.B. (2015). Toxicon 102, 32-42.

Utermöhl, H., (1958). Mitt Int Ver Limnol. 9, 1-38.

Venrick, E.L. (1978). UNESCO Monographs on Oceanographic Methodology. 6, 167-180.

Wells, M. L., Trainer, V. L., Smayda, T. J., Karlson, B. S. O., *et al.*, (2015). Harmful Algae 49, 68-93.

Wells, M. L., Karlson, B., Wulff, A., Kudela, R., *et al.*, (2020). Harmful Algae 91, 101632.





HA BIOLOGY



Physical factors influencing the production of saxitoxin analogues in *Gymnodinium catenatum* and *Alexandrium pacificum* cultures

Paulo Vale*

IPMA, IP, R. Alfredo Magalhães Ramalho, 6. 1495-165 Algés, Portugal.

* corresponding author's email: pvale@ipma.pt

Abstract

In vitro production of the common saxitoxin analogues C1+2 and B1 in the dinoflagellates *Gymnodinium catenatum* and *Alexandrium pacificum* was determined in relation to several natural physical parameters, such as temperature and oscillations in geomagnetic activity (GMA) or solar activity (SA) derived from the 11-year sunspot cycle, such as the X-ray output. Disulfated C1+2 toxin increased significantly with increasing temperature (from 17 to 28 °C) and X-ray levels (from 0 to 8.5 A-level units) in *G. catenatum*. In *A. pacificum*, C1+2 decreased significantly with X-ray levels. Toxin production did not change with GMA in *G. catenatum*, while in *A. pacificum* a U-shaped hormetic dose response was observed, centred around the 7-20 nT interval. Oxidative stress induced by an extremely weak low-frequency magnetic field or hydrogen peroxide also increased toxin levels. C1+2 toxin increased with natural variations in physical parameters ranged between 120 and 200%, while artificial agents ranged from 110 to 160%. Intracellular concentrations of the bi-sulfated C1+2 were from 9 to 10 times higher than the mono-sulfated B1. The relevance of sulfation observed is in accordance with the general dominance of sulfated analogues in marine dinoflagellates.

Keywords: PST, dinoflagellate, toxin production, geomagnetic activity, magnetic field, oxidative stress

<https://doi.org/10.5281/zenodo.7034496>



Introduction

Gymnodinium catenatum is a marine dinoflagellate that contaminates bivalves with paralytic shellfish poisoning toxins (PSTs) at the Atlantic Iberian coast. Contamination episodes can be absent for several consecutive years. The worst PST episodes on the Portuguese coast between 1986 and 2000 coincided with the last four periods of minimal activity of the 11-year solar cycle (Vale, 2013, 2020a). This has prompted research on the influence of solar activity (SA) and geomagnetic activity (GMA) on cultures of this toxic microalga. Results have revealed differential responses to shock, such as hypo-osmotic shock or addition of oxidising agents (hydrogen peroxide), depending on the occurring SA and/or GMA at the time of the experiments (Vale, 2017; 2018).

The ecological role(s) of PSTs for the producing microorganisms have been hypothesized as pheromones, chromosome structural organization or nitrogen storage (Cusick and Sayler, 2013). The most popular hypothesis is that these function as grazing deterrents (Selander *et al.*, 2015).

This research aimed to determine the variation of PST concentration as a function of several physical factors, such as those derived from naturally occurring SA and/or GMA, temperature or artificial magnetic fields. In addition, the behaviour of a similar warm-temperate, chain-forming and toxin-producing dinoflagellate, *Alexandrium pacificum*, was studied for comparison.

Material and Methods

Gymnodinium catenatum strain AND-A0917 was from Cádiz Gulf, Spain and *A. pacificum* strain EXT-1653 was from Tarragona, Spain. Both were grown at a salinity of 35, enriched with f/2 nutrients, 10^{-7} M selenium, no silica. Culture medium was replenished in one liter GL45 bottles at the end of each week with an approximately 1:1 dilution, maintaining the cultures in a permanent mid-exponential phase. Triplicate 4 mL aliquots were taken for cell counts and fixed with Lugol. Triplicate 30 mL aliquots for PST analyses were centrifuged at 2,500xg and pellets extracted with 2.0 mL of 0.05% acetic acid.

Cultures and experiments were conducted in a dark room without air-conditioning, located at sea-level in a 12:12 h L:D cycle. Two identical LED illumination sets were used, one for controls and another for magnetic tests, when required. Both were mounted on a wood frame attached on top of wooden tables to avoid static magnetic fields derived from ferromagnetic materials. Indoor and outdoor artificial electromagnetic fields were kept to a minimum (detailed at Vale, 2020b). Both were equipped with one overhead LED spot (OSRAM, STAR PAR16 36°, 450 lumens, colour 2700 K, $38 \mu\text{mol m}^{-2} \text{s}^{-1}$ incident PAR at shelf level).

Cells were exposed to natural variations in GMA and SA. The GMA aa Index, obtained from antipodal magnetometers and available in 3 h periods, was retrieved from: www.geomag.bgs.ac.uk/data_service/data/magnetic_indices/aaindex.html. GMA before each experiment was calculated by averaging the six last periods of day (-2) and the eight periods of day (-1) with the 1st and 2nd periods



from day (0). Daily solar X-ray activity was retrieved from ftp.swpc.noaa.gov/pub/indices/old_indices. Most of the X-ray during the experimental period corresponded to A-level, or 10^{-8} W m⁻². X-ray fluxes from day (-2) and day (-1) were averaged.

Cultures were exposed to an extremely-low frequency magnetic (ELFMF) field produced by an alarm clock drive. The frequency of the field was 0.5 Hz; and central amplitude at 1 cm height was 7 μ T (Vale, 2020b). Cells were exposed for 72 h and sampled 8 h after onset of the light phase. Cultures were H₂O₂ exposed to a final concentration of 82 or 163 μ M for *G. catenatum* and, 122 or 245 μ M for *A. pacificum*, respectively, and were sampled 24 h after exposure. For the ELFMF experiments controls were kept at the second shelf (80 cm apart).

Acid extracts were subjected to a double freeze-thaw cycle and a final 15 min in a 100 W ultrasonic bath. Supernatants were analysed for PSTs using H₂O₂ oxidation (detailed in Vale *et al.*, 2021). PSTs were studied once weekly in *G. catenatum* (n = 47) and *A. pacificum* (n = 48) between summer 2018 and winter 2019/2020 (towards solar minima of cycle 24). In this period, X-ray flux varied between 0.0 and 10.8 A-level units, GMA between 2.9 and 63 nT, and temperature between 17.0 and 27.5 °C.

The non-parametric multiple comparison Steel-Dwass Pair-wise comparison test was performed in KyPlot (Kyenslab Inc.). Boxplots denote mean \pm SD, and min-max range. The number of symbols on top of each box denotes increasing significant differences at 0.05, 0.01 and 0.001 level, respectively. When no symbols were presented, no significant differences were found.

Results and Discussion

Both dinoflagellates share several PSTs in common, such as C1+2 and B1. Despite that other PSTs were found, these three were at the highest concentrations with maximal signal/noise ratio and hence provide data of greatest certainty.

In *G. catenatum*, concentration of PSTs was significantly dependent on temperature: average C1+2 concentration above 22.0 °C was 2.0 times higher than at lower temperatures, and B1 was 1.7 times higher (Figs. 1a, d).

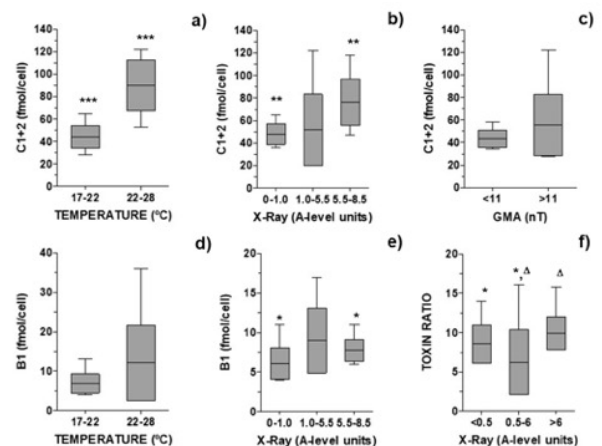


Fig. 1. PSTs in *G. catenatum* influenced by physical parameters: a) and d) temperature (n = 31 when X-ray < 5.0 A-level units), b) and e) X-ray flux (n = 32 when T < 23.0 °C); c) GMA (n = 20; when T < 23 °C and X-ray < 6.0 A-level); f) toxin ratio regarding X-ray flux (n = 32 when T \leq 23.0 °C).

PSTs were studied regarding variations in space weather only below 23.0 °C. Average C1+2 was similar in the intervals from 0.0 to 1.0 and from 1.0 to 5.5 A-level units of X-ray flux, but was 1.8 times higher in the interval from 5.5 to 8.5 A-level units (Fig.

1b). Regarding B1 toxin, it was lowest in the interval from 0 to 1.0 A-level units, and higher in the intervals from 1.0 to 5.5 and 5.5-8.5 A-level units. In the intermediate X-ray interval, B1 was 1.5 times higher than in the lowest X-ray interval (Fig. 1e). For GMA, C1+2 was on average 1.3 times higher above 11 nT than below this threshold (Fig. 1c). For B1, the concentrations were similar below or above 11 nT (data not shown).

In *A. pacificum* the dependence of PSTs with temperature (17.0-27.0 °C) was not evident. SA had to be taken into consideration first, before observing a temperature effect. For temperatures below 23 °C, the average of C1+2 below 2.5 A-level X-ray units was 1.5 times higher than above 2.5 units, while B1 was similar (Figs. 2a, d). For an incoming X-ray flux above 1.0 A-level units, average C1+2 above 22°C was only 1.2 times higher than below, while for B1, these were similar (Figs. 2b, e). PSTs relation with GMA was studied in three intervals (Fig. 2c). B1 concentrations in the outer intervals (3.6-7.5 and 20-35 nT) were 1.9 times higher than in middle interval (7.5-20 nT). For C1+2, concentrations were similar in the three intervals (data not shown).

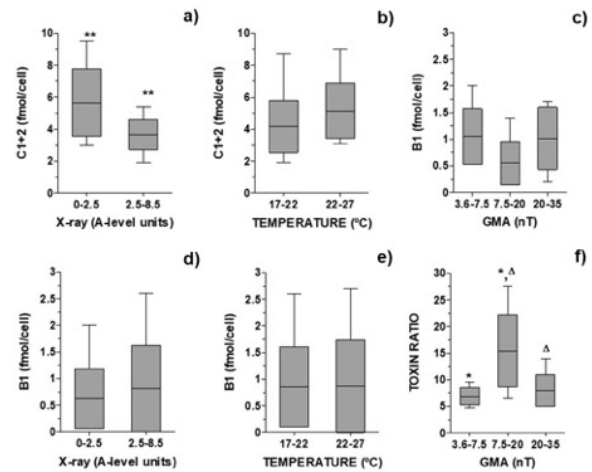


Fig. 2. PSTs in *A. pacificum* influenced by physical parameters: a) and d) X-ray flux (n = 33 when T < 23.0 °C); b) and e) temperature (n = 27 when X-ray > 1.0 A-level units); c) and f) GMA (n = 24; when X-ray < 3.0 A-level units and B1 > 0.15 fmol cell⁻¹).

In *G. catenatum* and *A. pacificum* the disulfated C1+2 was much more abundant than the mono-sulfated B1, with an average ratio of 9:1 and 10:1, respectively. Toxin ratios changed in a tripartite interval, typical of hormetic dose-response, regarding X-flux for *G. catenatum* or GMA for *A. pacificum* (Figs. 1f, 2f). In *G. catenatum*, C1+2 increased faster than B1, as observed by the ratios between 4:1 up to 15:1 or higher (Fig. 3a). In *A. pacificum*, for PSTs below 7 fmol cell⁻¹ there was a high uncertainty in B1 because it was close to the limit of detection. Above 7 fmol cell⁻¹, toxin ratios seemed constant, at approximately 8:1 (Fig. 3b).



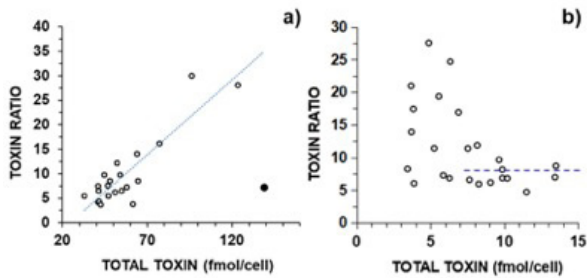


Fig. 3. Relation between C1+2: B1 toxin ratio and total PSTs in: a) *G. catenatum* (n = 22; X-ray < 6.0 A-level units; T < 24 °C); b) *A. pacificum*, when B1 > 0.15 fmol cell⁻¹ (n = 24; X-ray < 3.0 level units). Outliers removed from regression.

An exposure to an ELFMF was aimed at mimicking pulsations observed during GMA storms. PSTs increased +16% in *G. catenatum* and +12% in *A. pacificum*, while average cell concentration reduced to 91% and 98% from control, respectively (Figs. 4a,b). Exposure to H₂O₂, increased average PSTs to 1.5 times or higher than the control in *G. catenatum*, and 1.1 times or higher in *A. pacificum* (Fig. 5). Average cell concentrations reduced to 87 or 69% for *G. catenatum*; and 89 or 74% for *A. pacificum*, for the low and high peroxide concentrations, respectively (data not shown).

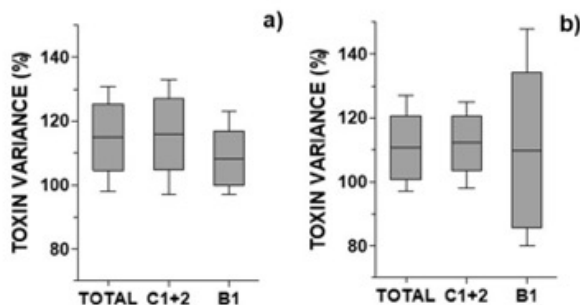


Fig. 4. Variation of PSTs relative to controls after exposure to an ELFMF in: a) *G. catenatum*, b) *A. pacificum* (n = 10).

Toxin content varied with temperature, GMA and SA. The temperature effect in *G. catenatum* might derive directly from enzyme kinetics: O-22 sulfotransferase, an enzyme involved in the sulfation of 11- α,β -hydroxy STX, has an optimal temperature of 35 °C, which could speed up the cascade leading to C1+2 biosynthesis instead of B1 (Yoshida *et al.*, 2002; Oh *et al.*, 2010).

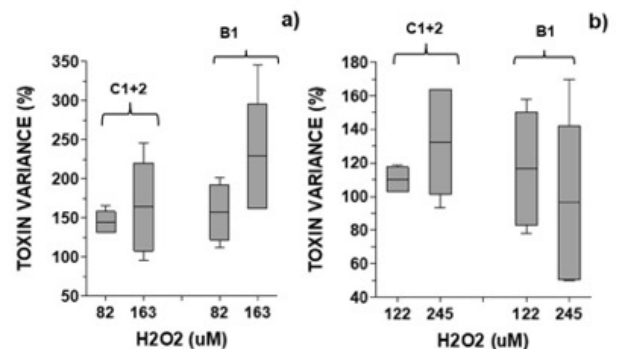


Fig. 5. Variation of PSTs against control after exposure to H₂O₂ in: a) *G. catenatum*, b) *A. pacificum* (n = 5).

The PST decrease with SA in *A. pacificum* might have been conditioned to minimal SA in effect during the study period of 2018-2019. If higher SA had taken place, toxins might have increased. This apparent decrease might correspond to a partial observation resulting from an hormetic dose-response, commonly found when studying S-GMA effects in these dinoflagellates (Vale, 2020a).

ELFMF can alter the radical-pair mechanism (i.e., how a magnetic field can affect reaction kinetics by affecting electron spin dynamics), and concomitantly increase the production of reactive oxygen species (Barnes and Greenebaum, 2015). In this study, a similar moderate increase in PSTs was observed either with external exposure to physical (ELFMF) or chemical (the oxidant H₂O₂)



agents, suggesting that the mechanism of ELFMF might be due to the increase in intracellular free radicals.

Although several abiotic factors have been found to alter toxin production (Oh *et al.*, 2010; Laabir *et al.*, 2013), biotic factors seem to be even more relevant in triggering toxin synthesis, up to 20 times as seen in *Alexandrium* spp. (Selander *et al.*, 2015). The abiotic factors studied here highlight that an increase in PSTs involves the production of highly sulfated molecules – i.e. C1+2 rather than B1. The molar percentages of the disulfated C1+2 have often been found (but not always) above the percentage of the monosulfated B1 either in *G. catenatum* or *A. pacificum* strains from different geographical locations (Oh *et al.*, 2010; Hallegraeff *et al.*, 2012; Laabir *et al.*, 2013).

The role of sulfation remains elusive so far. Detailed data on individual toxicity towards marine predators is still lacking to further understand this relevance, despite sulfated toxins being less toxic to mammalian cells than their respective carbamate analogues (EFSA, 2009).

Acknowledgements. Special thanks to L. Mamán Menéndez (LCCRPP, Andalucía, Spain), M. Tejedor (IRTA, Cataluna, Spain), NOAA's Space Weather Prediction Center, British Geological Survey, IPMA's Laboratório de Biotoxinas Marinhas and Laboratório de zooplâncton. Funding from: 'SNMB-MONITOR II' and 'SNMB-INOV' (FEAMP-2020 projects) is acknowledged.

References

- Barnes, F.S. and Greenebaum, B. (2015). *Bioelectro-magnetics* 36, 45-54.
- Cusick, K.D. and Sayler, G.S. (2013). *Mar. Drugs* 11, 991-1018.
- EFSA, 2009. *The EFSA J.*, 1019, 1-76.
- Hallegraeff, G.M., Blackburn, S.I., Doblin, M.A., *et al.*, (2012). *Harmful Algae* 14, 130-143.
- Laabir, M., Collos, Y., Masseret, E., *et al.*, (2013). *Mar. Drugs* 11, 1583-1601.
- Oh, S.J., Matsuyama, Y., Yoon, Y.H. *et al.*, (2010). *J. Fac. Agric. Kyushu Univ.* 55, 47-54.
- Selander, E., Kubanek, J., Hamberg, M., *et al.*, (2015). *PNAS* 112, 6395-6400.
- Vale, P. (2013). *Biophysics* 58, 554-567.
- Vale, P. (2017). *Gen. Physiol. Biophys.* 36, 7-21.
- Vale, P. (2018). *Photochem. and Photobio.* 94, 95-104.
- Vale, P. (2020a). *Horizons in Earth Science Research*. Vol. 20. Nova Science Pub., Inc., Hauppauge, NY, U.S.A. pp. 153-182.
- Vale, P. (2020b). *Life Sci. Space Res.* 26, 85-96.
- Vale, P., Rodrigues, S.M., Ribeiro, I., 2021. *Food Control* 126, 108081.
- Yoshida, T., Sako, Y., Uchida, A., *et al.* (2002). *Fish. Sci.* 68, 634-642.



Cryoprotectant treatment and cryopreservation of the marine dinoflagellate *Breviolum* sp.

Joseph Kanyi Kihika^{*,1,2}, Susanna A. Wood¹, Lesley Rhodes¹, Kirsty F. Smith^{1,3}, Lucy Thompson¹, Sarah Challenger¹, Ken G. Ryan²

¹Cawthron Institute, Private Bag 2, Nelson 7042, New Zealand; ²School of Biological Sciences, Victoria University of Wellington, PO Box 600, Wellington 6140, New Zealand; ³School of Biological Sciences, University of Auckland, Private Bag 92019, Auckland 1142, New Zealand.

* corresponding author's email: joseph.kihika@vuw.ac.nz

Abstract

Dinoflagellates are among the most ecologically diverse group of microalgae. Dinoflagellate species from the family Symbiodiniaceae form endosymbiotic associations with invertebrates, such as corals, sea anemones, and jellyfish. Strains of dinoflagellates are maintained alive in culture collections worldwide. This is labor-intensive, expensive, and there is a risk of contamination or genetic drift. Cryopreserving these strains will help to maintain long-term viability, molecular integrity and to reduce costs. In this study, we explored the effect of cryoprotectant agents (CPAs) and freezing methods on *Breviolum* sp. A total of 12 CPAs were assessed at concentrations between 5 - 15%, as well as in combination with dimethyl sulfoxide (DMSO) and other non-penetrating CPAs. Two freezing techniques were employed: rapid freezing and controlled-rate freezing. *Breviolum* sp. was successfully cryopreserved using 15% DMSO. For *Breviolum* sp. there was higher cell viability ($45.4 \pm 2.2\%$) when using the controlled-rate freezing compared to the rapid freezing technique ($10.0 \pm 2.8\%$). This optimized cryopreservation protocol will be of benefit for the cryopreservation of other species from the family Symbiodiniaceae.

Keywords: Microalgae, dinoflagellates, Symbiodiniaceae, cryopreservation, cryoprotectant agents, HABs

<https://doi.org/10.5281/zenodo.7034512>



Introduction

Dinoflagellates are motile unicellular algae that are important contributors to primary production in aquatic and marine habitats (Bravo and Figueroa, 2014). Dinoflagellate species from the family Symbiodiniaceae exist in symbiotic relationships with many invertebrates including corals, sea anemones, jellyfish, giant clams, flatworms, and benthic foraminifera (LaJeunesse, 2020; Pochon and LaJeunesse, 2021). They are important for research and studies on the mechanisms of rapid adaptation or acclimatization to environmental changes in corals given the impact of increased sea surface temperatures (Rouzé *et al.*, 2019).

To protect and preserve valuable dinoflagellate species, cryopreservation has been suggested as the most reliable technique to ensure their long-term genetic stability and to reduce storage and regular maintenance costs (Rhodes *et al.*, 2006; Hagedorn and Carter, 2015). However, attempts to have a well-optimized and uniform cryopreservation protocol that can be applied to all microalgae has been unsuccessful (Youn and Hur, 2009). The successful cryopreservation of *Breviolum* sp. would protect its genetic composition, allow easy access for research use, and reduce the risk of contamination during repeated sub-culturing. This study aimed to identify optimal freezing and thawing conditions to enhance the survival of this marine dinoflagellate following cryopreservation.

Materials and Methods

Isolate and culture conditions

The dinoflagellate culture *Breviolum* sp. (CAWD197) was obtained from the

Cawthron Institute Culture Collection of Microalgae (CICCM; <http://cultures.cawthron.org.nz/ciccm/>). Cells were grown in f/2/L1 growth medium (Guillard, 1975; Guillard and Hargraves, 1993) at 25 °C in a 12:12 light: dark cycle under 100 $\mu\text{mol m}^{-2} \text{s}^{-1}$ photosynthetically active radiation (PAR).

Types and combinations of cryoprotectant agents

The cryoprotectant agents (CPAs) used were: DMSO (Purity GC $\geq 99.9\%$, Sigma-Aldrich, Japan), Methanol (MeOH; HPLC grade, $\geq 99.9\%$, Sigma-Aldrich, Germany), Glycerol (Sigma-Aldrich, Malaysia), Propylene glycol (PG; Sigma-Aldrich, Singapore), Diethylene glycol (DEG; Sigma-Aldrich, U.S.A.), Ethylene glycol (EG; spectrophotometric grade, $\geq 99\%$, Sigma-Aldrich, Malaysia), Polyvinylpyrrolidone (PVP; Sigma-Aldrich, U.S.A.) and Polyethylene glycol (PEG; Sigma-Aldrich, Germany). Single CPA solutions were prepared in sterilized growth medium to give final concentrations of 5%, 8%, 10%, 12%, and 15% (v/v or w/v). For combined CPA treatments, DMSO was used at a ratio of 1:1 with the non-penetrating compounds proline (Sigma-Aldrich, U.S.A.), sucrose (BDH, England), sorbitol (Sigma-Aldrich, U.S.A.), and glucose (BDH, England).

CPA treatment experiments

An aliquot (1 mL) of each culture was pipetted into 12-well plates (Costar, China). For each species, 100 μL aliquots of the CPAs were added to the wells with gentle agitation (10 min, Room temperature (RT), 30 $\mu\text{mol m}^{-2} \text{s}^{-1}$ PAR) between each addition until a final 1:1 dilution was obtained. The CPA-



treated cultures were left to equilibrate in complete darkness (30 min, RT). *Breviolum* sp. was maintained at 25 °C, under controlled minimal light (56 $\mu\text{mol m}^{-2} \text{s}^{-1}$ PAR). After incubation for one week with different CPAs, dinoflagellate cells were categorized and enumerated as either healthy, unhealthy, or dead based on changes in the chlorophyll pigmentation as observed using an inverted microscope (Olympus CK X41 Tokyo, Japan).

Freezing techniques

1. *Rapid freezing technique*: The cultures were aspirated into cryopreservation straws (0.5 cc, IMV, France) and the straws were arranged horizontally on a metal rack fitted onto polystyrene floats. The rack (41x 14 x 4 cm, l x w x h) and was placed gently over a liquid nitrogen bath (45 x 30 x 6 cm, l x w x h) to induce rapid freezing of the cells before finally plunging the straws into liquid nitrogen.

2. *Controlled-rate freezing technique*: The cultures were aspirated into cryopreservation straws which were transferred to a controlled-rate freezer (Cryologic Pty, Mt Waverley, Australia). The freezer was programmed to cool from 20 °C to -40 °C at a rate of 1 °C min^{-1} . The straws were held at -40 °C for 10 min before plunging into liquid nitrogen.

The straws were kept frozen under liquid nitrogen for a period of one week.

Thawing procedure

Thawing was carried out by plunging the straws into a water bath (20 °C). Fresh media was added to the thawed cultures which were kept under dark conditions at 20 °C RT for 24 h, followed by 48 h under 27 $\mu\text{mol m}^{-2} \text{s}^{-1}$

of red light (OSRAM L18W/60, Germany) to facilitate the recovering of the cells. Finally, fresh media (40 mL) was added into the plastic vessels (70 mL Labserv, Thermofisher Scientific NZ) and the *Breviolum* sp. cultures were transferred to their normal standard light conditions for growth.

Results and Discussion

In single CPA treatments, at 5% final CPA concentration, DMSO, PVP and EG had >90% of cells surviving. Increasing the CPA concentration to 8%, 83.0 \pm 3.0% of the cells survived in DMSO while in PVP, 97.0 \pm 1.0% of the cells survived and EG had the lowest cell survival at 11.3 \pm 0%. At 10% concentration, DMSO treatment had 13.0 \pm 2.0% of the cells surviving while PVP had 81.0 \pm 2.0% and no cells survived in the EG treatment. At 12% concentration, only PVP treatment had cells surviving (21.7 \pm 1.2%), while one week incubation of the cells at 15% final CPA concentration resulted to no viable cells. During cryopreservation, a range of different single CPAs and different concentrations of combined CPAs commonly used to treat the cells before the freezing experiments (Hubálek, 2003). In this study, *Breviolum* sp. cells were treated with eight different single CPAs with concentrations varying between 5% and 15%. The selected single CPAs for the cryopreservation of *Breviolum* sp. were PVP (final concentrations of 5%, 8% and 10%) followed by EG and DMSO final concentrations of 5% and 8%, respectively. After the CPA treatment and incubation period, the preferred CPAs with the least impact on cells health was DMSO. DMSO was preferred because it penetrates cell membranes easily, can be removed from the cells, and did not support bacterial



contaminations (Taylor and Fletcher, 1999; Stock *et al.*, 2018).

For the combined CPAs, 5% sorbitol + 5% DMSO and 8% sorbitol + 5% DMSO were selected as the preferred combined CPAs for subsequent cryopreservation trials. However, the application of combined CPAs resulted in bacterial overgrowth in initial tests with all the treatments. The CPAs that encouraged bacterial contaminations were glycerol, PEG, PG and PVP. During cryopreservation, presence of high bacterial contaminations following CPA treatment can negatively influence the growth and recovery of cells (Visch *et al.*, 2019).

From the single CPAs selected and tested during the freezing experiments, 15% DMSO gave the best results with high cell viabilities in *Breviolum* sp. after thawing. Very low cell viabilities were observed when 15% EG was used as the CPA during the freezing experiments. The differences in cell viabilities from the two CPAs could be due to the different cryoprotective efficiencies in this species, with DMSO being the more favorable CPA (Hubálek, 2003). The combined CPAs used in this study did not yield any successful results for *Breviolum* sp. This might have been because the 30 minutes pre-incubation period that was used did not allow sufficient time for the combined CPAs to penetrate into the cells and thus, reduce the amount of water forming damaging ice crystals during freezing. Incubating the cells with CPA for a short period may be ineffective and, on the other hand, long exposure to CPAs may lead to toxicity in the cells (Taylor and Fletcher, 1999).

The two freezing techniques used to cryopreserve *Breviolum* sp. were rapid freezing and controlled-rate freezing. During rapid freezing, the cells viability was $10.0 \pm 2.8\%$ in 15% DMSO. When 15% EG was used, the cell viability was $2.0 \pm 0.7\%$ (Fig. 1).

For the controlled-rate freezing technique, *Breviolum* sp. was successfully cryopreserved with the highest cell viability of $45.4 \pm 2.2\%$ in 15% DMSO. When 15% EG was used the cell viability was $17.4 \pm 1.2\%$ (Fig. 2).

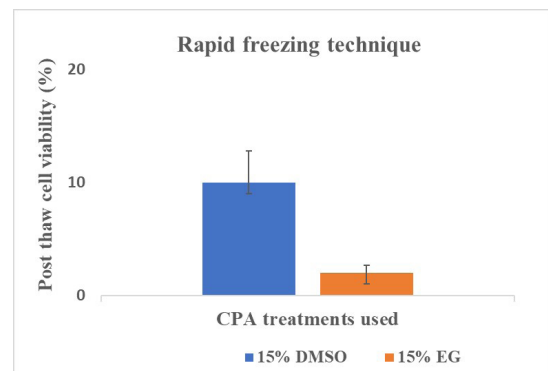


Fig. 1. Cell viabilities of *Breviolum* sp. after rapid freezing technique using dimethyl sulfoxide (DMSO) and ethylene glycol (EG) as cryoprotectant agents (CPAs). The cell viabilities are mean percentages of three replicates with error bars as standard deviation (SD).



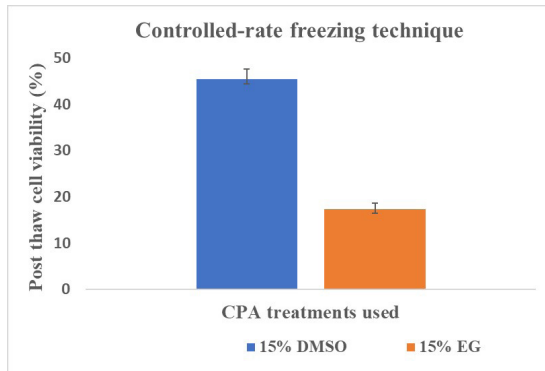


Fig. 2. Cell viabilities of *Breviolum* sp. after controlled-rate freezing using dimethyl sulfoxide (DMSO) and ethylene glycol (EG) as cryoprotectant agents (CPAs). The cell viabilities are the mean percentage of three replicates with error bars as standard deviation (SD).

From the two freezing techniques used in this study, the best cryopreservation technique that had the highest survival rate after thawing *Breviolum* sp. was the controlled-rate freezer using 15% DMSO as the CPA (Fig. 2), and the cells took one week to recover and divide. The optimized cryopreservation protocol described in this study may also enhance the cryopreservation of other species in the family Symbiodiniaceae and this is being investigated. This will protect the genetic integrity of these species for future research aiming to facilitate coral restoration efforts following extensive coral bleaching and habitat destruction.

Acknowledgements. This research was supported by funding from the New Zealand Ministry of Business, Innovation and Employment, Contract number: CAWX0902, and a Cawthron Institute Internal Capability Investment Fund scholarship.

References

- Bravo, I. and Figueroa, R. I. (2014). *Microorganisms* 2, 11-32.
- Guillard, R. R. L. (1975). In: Smith, M.L. and Chanley, M.H. (Eds.), *Culture of Marine Invertebrates Animals*, Plenum Press, New York. pp. 29 - 60.
- Guillard, R. R. L. and Hargraves, P. E. (1993). *Phycologia* 32, 234-236.
- Hagedorn, M. and Carter, V. L. (2015). *PLoS One* 10, 1-16.
- Hubálek, Z. (2003). *Cryobiology* 46, 205-229.
- LaJeunesse, T. C. (2020). *Curr. Biol.* 30, R1110-R1113.
- Pochon, X. and LaJeunesse, T. C. (2021). *J. Eukaryot. Microbiol.* 68, 1-9.
- Rhodes, L., Smith, J., Tervit, R., Roberts, R., *et al.*, (2006). *Cryobiology* 52, 152-156.
- Rouzé, H., Lecellier, G., Pochon, X., Torda, G., Berteaux-Lecellier, V. (2019). *Sci. Rep.* 9, 1-11.
- Stock, W., Pinseel, E., De Decker, S., Seftom, J., *et al.*, (2018). *Sci. Rep.* 8, 1-9.
- Taylor, R. and Fletcher, R.L. (1999). *J. Appl. Phycol.* 10, 481-501.
- Visch, W., Rad-Menendez, C., Nylund, G. M., Pavia, H., *et al.*, (2019). *Biopreserv. and Biobank* 17, 378-386.
- Youn, J.-Y. and Hur, S.-B. (2009). *Algae* 24, 257-265.





HA ECOLOGY



First culture of *Dinophysis acuminata* from southern Chile: Ecophysiology, toxin production and phylogeny

Javier Paredes-Mella¹, Jorge I. Mardones¹, Luis Norambuena¹, Gonzalo Fuenzalida¹, Satoshi Nagai²

¹Instituto de Fomento Pesquero (IFOP). Centro de Estudios de Algas Nocivas (CREAN). Puerto Montt, Chile; ²Fisheries Resources Institute, Japan Fisheries Research and Education Agency, 2-12-4 Fukuura, Kanazawa, Yokohama, Kanagawa, 236-8648, Japan.

* corresponding author's email: javier.paredes@ifop.cl

Abstract

In Chile *Dinophysis acuminata* is a conspicuous mixotrophic dinoflagellate inhabit on Ocean Pacific Coast (OPC) and Patagonian fjords (PF). In this study, for the first time, we evaluated the effects of light and temperature on the growth and the toxin production of the culture strains of *D. acuminata* isolated from southern Chile. The phylogenetic analysis also was carried out using the COI marker. Strains were isolated in 2019-2020 from the OPC and PF and were maintained in culture feeding with *M. rubrum* as prey. Higher growth rates and cell abundances were observed at 45 compared to 90 and 125 $\mu\text{mol photon m}^{-2}\text{s}^{-1}$. However, growth rates were equivalent at both 12°C and 15 °C. Toxins screening revealed the presence of pectenotoxins 2 (PTX2) in six strains isolated from OPC and PF, but okadaic acid and dynophysistoxin were not detected. PTX2 concentration was not affected by temperature and light, showing values ranging from 3.920 to 14.077 pg cell⁻¹. The Chilean *D. acuminata* sequences clustered in the “*Dinophysis acuminata* complex” clade showing among sequences genetic distances ranging from 0.000 and 0.001. Further work is needed to know with major precision the environmental effects on growth and toxin biogeography

Keywords: *Dinophysis acuminata*, ecophysiology, toxins production, culture, Chile, phylogeny

<https://doi.org/10.5281/zenodo.7034888>



Introduction

Dinophysis acuminata is a cosmopolitan species that has been recorded along different coastal zones around the world (Ha Park *et al.*, 2019). This species is responsible for diarrhetic shellfish poisoning (DSP) due to the production of the okadaic acid (OA) and dinophysistoxins (DTXs). Also, some populations can produce pecteno-toxins (PTXs), but there is no evidence that PTXs are toxic to humans. However, due to their toxicity by intraperitoneal injection in mouse bioassays, these toxins are regulated in the European community, Canada and New Zealand.

In Chile, *D. acuminata* is distributed along the Ocean Pacific coast and within the Patagonian fjords where have formed blooms that represent a threat to public health, artisanal fisheries and the aquaculture industry. Despite the years of studying this species and the relevant information obtained, for example from oceanographic studies, cultures of *D. acuminata* not yet been performed.

In this work, for the first time, we established single cell cultures of *D. acuminata* and investigated their taxonomy as well as how environmental conditions effect growth rates and toxin production.

Material and Methods

Strain isolation

Between 2019 and 2020 *Dinophysis acuminata* strains were isolated from plankton samples taken from Patagonian Fjords (FDAM1, FDAM2 and FDAM3) and from Ocean Pacific (PDAM1, PDAM2, and PDAM3) ecosystems (Figure 1). Cells were

deposited in multiple well plate (48 wells), were fed with *Mesodinium rubrum* and this was fed with *Teleaulax amphioxi*. Cells were maintained at 45 $\mu\text{mol photon m}^{-2}\text{s}^{-1}$ light intensity, 12 °C, 16:8 L:D photoperiod, 33 \pm 1 salinity, and (f/2) 1/3 culture medium.

DNA extraction, amplification, sequencing and phylogeny

Dinophysis acuminata culture free-prey were harvested and concentrated by centrifugation at 1500g for 10 min at 4 °C, the supernatant discarded and the cell pellets incubated at 65 °C for one h in 10 μL Proteinase K (10 mg mL^{-1}) and 1 mL cetyltrimethylammonium bromide (CTAB). The Dinocox1F and Dinocox1R primers (in: Ha Park *et al.*, 2019) were used to amplify a segment of the *cox1* gene. Phylogenetic analyses were performed using alignments of 673 bp along with sequences available in GenBank using ClustalW/Geneious Prime 2019.0.3 (Larkin *et al.*, 2007). Then Bayesian analysis was conducted using MrBayes V3.1.2 under the appropriate model (GTR + I) (Ronquist and Huelsenbeck, 2003).

Light microscopy

Two sets of *D. acuminata* cells photography were taken: (1) in the exponential phase of growth and (2) in cultures c.a. three months after prey species was added. Images were taken with a camera implemented in a Zeiss AXIO VERT A1 inverted microscope.

Growth under different light intensity and temperature

Strain PDAM1 was used to evaluate growth under different levels of light intensity and



temperature. The first experiment measured growth rates of *D. acuminata* at 45, 95 and 125 $\mu\text{mol photon m}^{-2}\text{s}^{-1}$. The second experiment evaluated the strain growth at 90 and 45 $\mu\text{mol photon m}^{-2}\text{s}^{-1}$, and temperatures of 12 and 15 °C. In the experiments, strains were maintained using 16:8 L:D photoperiod, 33 ± 1 salinity and (f/2) 1/3 culture medium. The first experiment began with *D. acuminata* abundance of 30 cells mL^{-1} and 5,000 cell mL^{-1} of *M. rubrum*. The second experiment, beginning with 100 cells mL^{-1} of *D. acuminata* 2,000 cell mL^{-1} of *M. rubrum*. Periodically samples were taken (three replicate), fixed with Lugol and counted under inverted microscopy. At the same time, PDAM2, PDAM3, FDAM2 and FDAM3 strains were maintained at 45 $\mu\text{mol photon m}^{-2}\text{s}^{-1}$ light intensity and 15 °C temperature and were fed with 2,000 cells mL^{-1} of *M. rubrum*. After ca. 48 days, strains were filtered for toxin analysis.

Growth rate and maximum cell abundance

The growth rate of *D. acuminata* was determined through a linear regression model $\gamma_i = \alpha + \beta\chi_i$ (Guillard and Hargraves, 1993), where $\gamma_i = \ln$ -transformed cell density (cells mL^{-1}); $\chi_i =$ time (days); $\alpha =$ intercept; and $\beta =$ growth rate (cells div day^{-1}). The maximum cell density at the end of the exponential phase was used as the maximum cell density response (cells mL^{-1}).

Cell toxin production

Cells were filtered through 47 mm diameter glass fiber filters (GF/F Whatman) and the filter was transferred to a 2 mL Eppendorf tube with 1 mL of Methanol 100%. The tubes were placed in a container with ice, sonicated five times for 5 s. After 10 min the solution was filtered using PVDF syringe, filters of 0.22 μm

pore size and 3 mm diameter, and the solution pass-through was deposited in HPLC vials of 1.8 mL. To estimate toxins concentration, selected reaction monitoring (SRM) measurements were performed on a triple quadrupole mass spectrometer (Agilent 6420) equipped with an Electrospray ionization (ESI) source, coupled to 1290 UHPLC system (Agilent, Palo Alto, CA, U.S.A.). The chromatographic separation of Lipophilic Toxins (LTs) and Domoic acid (DA) after injection of 2.5 μl of a sample, was performed by reverse-phase chromatography using a SunShell C18 column (100 x 2.1 mm id, 2.6 μm particle size) at 40°C according to Braña-Magdalena *et al.* (2014). Certified reference standards, of okadaic acid, pectenotoxin-2, dynophysistoxin-1, dynophysistoxin-2, were used, and obtained from the National Research Council of Canada (Halifax, Canada).

Results and Discussion

The phylogenetic analysis of the Chilean COI sequences showed they all fell within the “*Dinophysis acuminata* species complex” clade. This clade was supported by a posterior Bayesian probability of 1.0. The genetic distance among Chilean COI sequences ranged from 0.000 to 0.001. Other species whose COI sequences fell in the same clade as those from the Chilean isolates included *D. sacculus* Stein 1883, and *D. ovum* Schütt, 1895. Previous work indicated COI genes were sufficient to delineate *D. acuminata* complex species. Our results, in contrast, indicated COI gene lacked the ability to distinguish these species.

Both strains showed similar morphological variation along their growth phase. In the exponential phase, length and depth



measurements both strains had greater than after three months of culture without addition of prey cells. In exponential phase, the contour of the largest hypothetical plate was in the major part symmetrical in relation to the longitudinal axis. A small number of asymmetrical forms were also observed. After three months of culture similar forms were observed but asymmetrical form was more evident (Figs. 2, 3). Comparable cells forms have been observed in the strains cultured in the northern hemisphere (Ha Park *et al.*, 2019).

The first experiment revealed low growth at highest light intensity of $125 \mu\text{mol photon m}^{-2}\text{s}^{-1}$ (Fig. 4). In turn, in the second experiment different light levels did effect growth rates, but not temperature over the range investigated (Tables 1 and 2). In the field has been observed the stratification of this species, founding high abundance around the pycnocline (Diaz *et al.*, 2011). Perhaps in the surface, where high light intensity occurs, *D. acuminata* suffer growth inhibition.

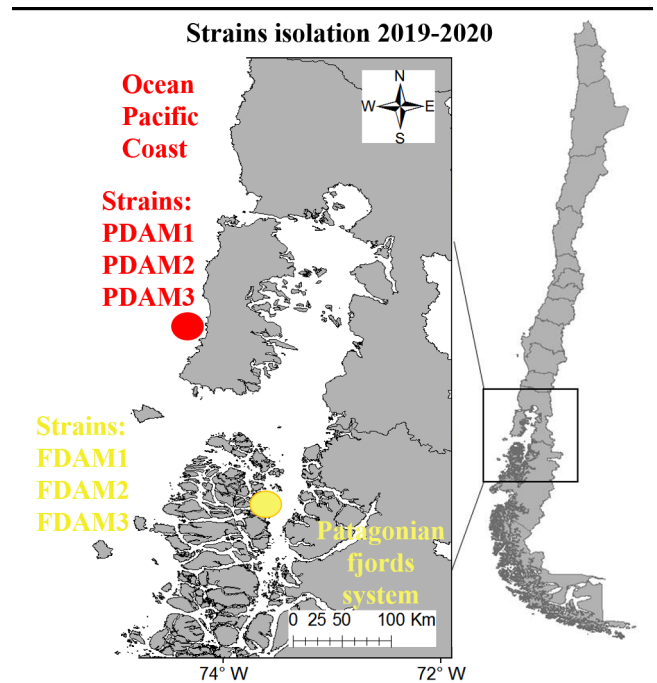


Fig. 1. Zones where strains were isolated, in Los Lagos (red point) and Aysén (Yellow point) regions of Chile.

Toxin production was not affected by either light intensity or temperature (Table 3). PTX2 was the only toxin found in the six strains assessed that were isolated from both Patagonian fjords and Pacific Ocean coast. No OA or DTXs were detected. A similar toxin pattern was reported by Fux *et al.*, (2011) using a strain isolated from the Reloncavi Sound. However, in the extreme south of Chile the presence of the dinophysistoxins was found in shellfish, and the only species recorded at this time in the water column was *D. acuminata*, which was the presumable species implicated in the DSP event (Uribe *et al.*, 2001).

This work presents for the first time the ecophysiology, genetic identification and toxin production of *D. acuminata* strains isolated from contrasting environments in



southern Chile. However, further work using more environmental drivers and levels, and strains isolated along coastal Chile, are needed to know with major precision the environmental effects on growth and toxin biogeography.

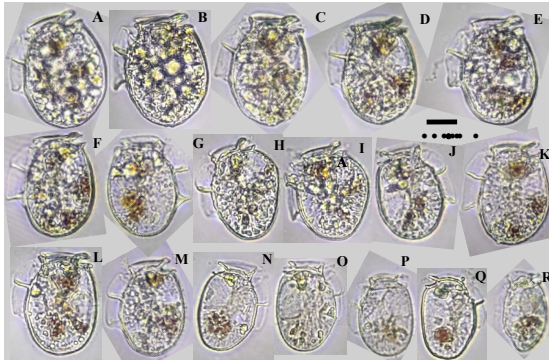


Fig. 2. PDAM1 strain isolated from Ocean Pacific coast. A - F cells in the exponential growth. G - R cells after three months of culture.

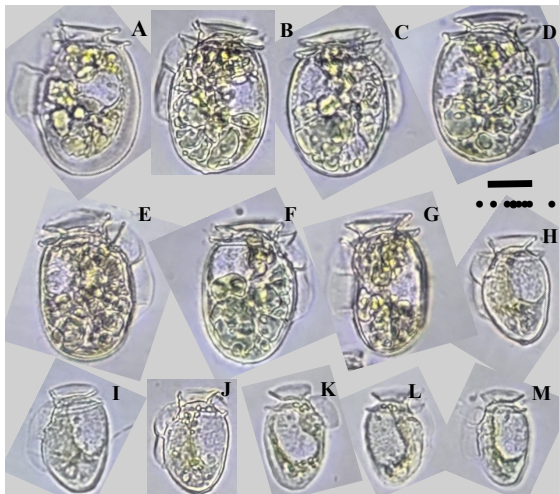


Fig. 3. FDAM1 strain isolated from Patagonian Fjords. A - G cells in the exponential growth. H - M, cells after three months of culture.

Table 1. Growth of PDAM1 strain. GR: growth rate. SE: standard error. Tuk: Tukey HSD posteriority test. MCA: maximum cell density (Cells mL⁻¹).

Light	GR	SE	Tuk.	MCA	SE	Tuk.
45	0.138	0.008	a	829	138	b
95	0.094	0.004	b	453	94	ab
125	0.054	0.005	c	153	11	a

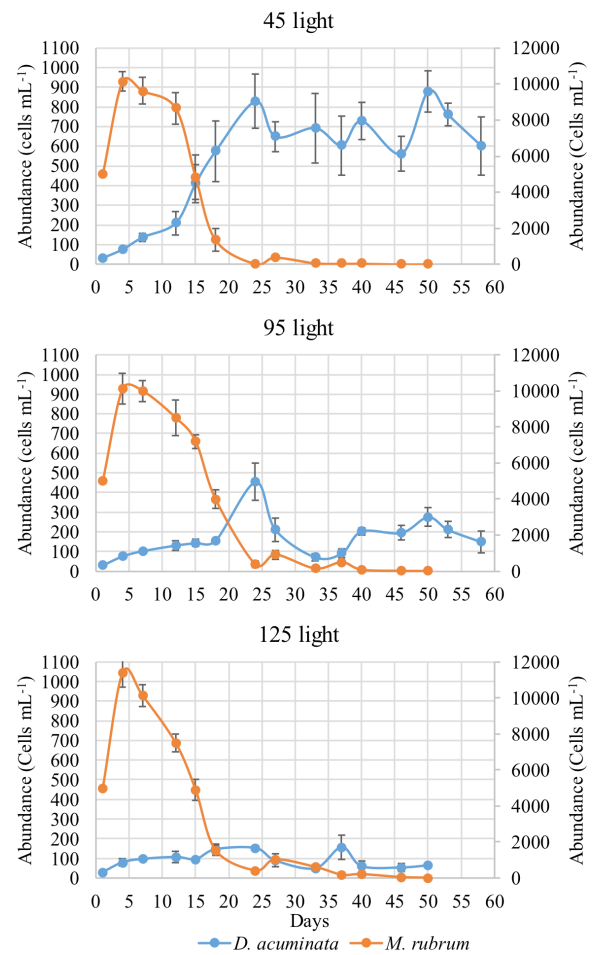


Fig. 4. Growth of PDAM1 strain under different light intensities.

Table 2. Growth of PDAM1. Tem: Temperature. GR: growth rate. SE: standard error. MCA: maximum cell density (Cells mL⁻¹).

Tem.	Light	GR	SE	MCA	SE
12	45	0.052	0.008	700	175
12	95	0.047	0.012	607	115
15	45	0.064	0.007	907	142
15	95	0.027	0.011	407	86

Table 3. Toxin production (pg cell⁻¹) of the strain PDAM1. SE: standard error.

Tem	Light	PTX2	SE
12	45	3.920	0.776
12	95	7.591	3.736
15	45	4.497	1.575
15	95	14.077	8.190

Acknowledgements. This research was supported by the Programa de manejo y monitoreo de floraciones algales nocivas y toxinas marinas en el oceano Pacífico del centro sur de Chile (36° - 44°s), Etapa II, 2019–2020, the Programa de manejo y monitoreo de las mareas rojas en el sistema de fiordos y canales de Chile (XIII Etapa) 2019-2020, and the Subsecretaría de Economía y Empresas de Menor Tamaño (MINECOM, Convenio 2019).

References

- Braña-Magdalena, A., Leão-Martins, J.M., Glauner, T., Gago-Martínez, A., (2014). *J. AOAC Int.* 97, 285-292.
- Díaz, P., Molinet C., Cáceres M., Valle-Levinson A., (2011). *Harmful Algae* 10, 155-164.
- Fux, E., Smith, J.L., Tong, M., Guzmán, L., Anderson, D.M., (2011). *Toxicon* 55, 275-287.
- Larkin, M.A., Blackshields, G., Brown, N.P., Chenna, P.A., *et al.*, (2007). *Bioinformatics* 23, 2947-2948.
- Park, J.H., Kim, M., Jeong, H.J., Park, M.G., (2019). *Harmful Algae* 88, 4-12.
- Ronquist, F. and Huelsenbeck, J.P., (2003). *Bioinformatics* 19, 1572-1574.
- Uribe, C., Garcia, C., Rivas, M., Lagos, N., (2001). *J. Shellfish Res.* 20, 69-74.



Dynamic photo-physiological responses of the dinoflagellate *Karenia brevis* to short-term changes in temperature and nitrogen substrates

So Hyun (Sophia) Ahn^{1*}, Patricia M. Glibert¹, Cynthia A. Heil²

¹ University of Maryland Center for Environmental Science, Horn Point Laboratory, PO Box 775, Cambridge, MD 21613, United States; ² Mote Marine Laboratory, 1600 Ken Thompson Pkwy, Sarasota, FL 34236, United States.

* corresponding author's email: sahn@umces.edu

Abstract

On the West Florida Shelf, annual blooms of the neurotoxin-producing harmful dinoflagellate, *Karenia brevis* (and other *Karenia* species) cause negative effects on the environment, the economy, and on human health. Blooms primarily occur in the fall months and may overwinter into winter and spring, but they rarely persist throughout the hot summer months when water temperatures are above 30°C. During 2020 and 2021, an unusually prolonged (~12 months) *K. brevis* bloom occurred. During the early phase of this bloom (January, 2021) when *K. brevis* were present in low-moderate abundances in southwest Florida, experiments on rates of photosynthesis were conducted on surface samples from two offshore stations within the bloom. Photosynthesis-irradiance responses were examined using PAM fluorometry to assess responses to varying nitrogen conditions and temperatures. Treatments included controls and exposures to temperatures of 15, 20, 25, 30°C with and without 10 µM additions of three nitrogen forms (nitrate, ammonium, urea). Although there were variations between stations, in general decreasing trends of fluorescence parameters with increasing temperature from 15°C to 30°C were observed, suggesting that 30°C might be physiologically stressful for *Karenia*. However, when cells were treated with urea, this reduction was substantially less. These results suggest *K. brevis* dependence on nitrogen form may change with temperature, and availability of chemically-reduced organic forms of nitrogen may be favored at the highest temperatures that *Karenia* may experience.

Keywords: *Karenia brevis*, PAM fluorometry, Fv/Fm, ETR, nitrogen, urea, photosynthesis, temperature

<https://doi.org/10.5281/zenodo.7034896>



Introduction

On the West Florida Shelf (WFS), the toxic dinoflagellate *Karenia brevis* forms red tides almost annually (e.g., Heil *et al.*, 2014a). The location, magnitude, and duration of blooms vary every year and are linked to environmental factors in a complex manner. While both state monitoring and focused research efforts have led to considerable understanding about the ecology and physiology of *K. brevis* (Kusek *et al.*, 1999; Heil *et al.*, 2014b and references therein), many critical questions regarding the physiology of *K. brevis* under different environmental conditions remain unanswered.

Temperature, nutrients, and light are three important environmental factors regulating the physiology of *K. brevis* (Heil *et al.*, 2014a, b). Temperature has long been considered a significant factor affecting *Karenia* bloom dynamics on WFS. Although factors underlying bloom initiation interact in a complicated manner, temperature is considered an important factor in determining whether blooms are likely to occur (Kusek *et al.*, 1999). Blooms rarely persist throughout the summer months, when water temperatures can be above 30°C. Laboratory experiments have shown a temperature optimum of 22-28°C (e.g., Vargo *et al.*, 2009), the lack of summer blooms has been suggested to be due, at least in part, to high temperatures. Temperature not only affects growth, but it also affects the metabolism of different forms of nitrogen (N) differently (e.g., Glibert *et al.*, 2016). These patterns could be species-specific but, in general, the enzyme involved in nitrate (NO₃⁻) metabolism, NO₃⁻ reductase, has an inverse relationship with temperature over the range from 15-30°C (Lomas and

Glibert, 1999a, b). In contrast, the enzymes involved in the assimilation of chemically reduced nitrogen, ammonium (NH₄⁺), glutamine synthetase and glutamate synthase, and of urea, urease, tend to show positive relationships with temperature over this same temperature range (Lomas and Glibert, 1999 a, b; Fan *et al.*, 2003; Glibert *et al.*, 2016). Although it is an obligate autotroph, *K. brevis* can use many different forms of N, including NO₃⁻, NH₄⁺, and urea (Glibert *et al.*, 2009; Bronk *et al.*, 2014). Therefore, multiple N sources available on WFS such as nutrients from freshwater and estuarine flows, and regenerated nutrients from dead fish could support *K. brevis* blooms simultaneously (Heil *et al.*, 2014a). This dinoflagellate can also obtain nutrition via mixotrophy (Glibert *et al.*, 2009).

Blooms of *K. brevis* initiate offshore and may be transported to the WFS via upwelling (Weisberg and He, 2003; Weisberg *et al.*, 2014). Generally, *K. brevis* densities on the WFS start to increase in late summer and can remain high during fall and winter when surface water temperatures can be low as ~15°C. Cell densities tend to decrease during late spring and rarely persist through the hot summer when temperatures are higher than 30°C (Brand and Compton, 2007). Vertical gradients in temperatures of > 5-10°C may also exist throughout the year on WFS (Weisberg and He, 2003; Weisberg *et al.*, 2014). Thus, *K. brevis*, which vertically migrates, can be subject to abrupt changes in temperature and possibly to co-occurring changes in N forms and light conditions. Here, the short-term interactions of temperature, N forms, and light on photosynthetic performance of the



winter *Karenia* community were examined to understand how these responses may relate to the conditions under which the *Karenia* community is found on WFS.

Material and Methods

Bloom sampling and experimental setup

Near-surface water samples were collected from two offshore stations (15S, 26.3896 N, -81.9800 W and 19S, 26.28625 N, -82.34284 W) on January 22nd, 2021. Ambient water temperature was measured using a Seabird 19 plus V2 package. Water was returned to the lab within two h and manipulation experiments were immediately initiated. Water from each station was first transferred to 50 mL polypropylene tubes. Nutrient additions (10 μ M of NO_3^- , NH_4^+ , or urea) were added to four tubes from each station and four unamended tubes from each station served as controls. Subsequently, one set of tubes from each station, including a control, and one each enriched with either NO_3^- , NH_4^+ , or urea, were placed in four different temperature-controlled water baths (15, 20, 25, 30°C) and incubated for one hour under 100 $\mu\text{mol photons m}^{-2} \text{s}^{-1}$.

Chlorophyll a, nutrient and K. brevis cell concentrations

Immediately upon return to the laboratory, water samples were filtered through pre-combusted (450°C, 2-3 h) Whatman GF/F filters for chlorophyll *a* (Chl *a*) determination. The filtrates were frozen in brown bottles for subsequent measurements of NO_3^- + nitrite (NO_2^-), NH_4^+ , urea, and phosphate (PO_4^{3-}) via autoanalyzer at the Mote Marine Laboratory. Additionally, 5 mL of each bloom water was fixed with acidic Lugol's solution and *K.*

brevis concentrations were determined by light microscopy.

Experimental photosynthetic responses

To assess the photosynthetic response of the samples exposed to different nutrient and temperatures, *in vivo* Chl *a* fluorescence was measured using a Phyto-PAM-II multi-excitation wavelength chlorophyll fluorometer (Heinz Walz GmbH, Effeltrich, Germany). With appropriate calibration and deconvolution of fluorescence signals, this instrument can measure the photosynthetic responses of four different major classes of algae, including cyanobacteria, green algae, brown algae, and phycoerythrin -containing cells with a single measurement. The brown algal signal includes both diatoms and dinoflagellates, but microscopic analyses confirmed that the dominant organism present in the samples measured in this category was *K. brevis*.

After one hour of incubation, samples were dark-adapted for 20 min and Rapid Light Curves were conducted using twelve incremental irradiance steps (0, 6, 24, 42, 73, 109, 188, 227, 334, 489, 591, 719 $\mu\text{mol photons m}^{-2} \text{s}^{-1}$). The maximum photochemical efficiency of photosystem II (PS II) was calculated as $F_v/F_m = (F_m - F_o)/F_m$ where F_v is the variable fluorescence, F_o is the minimal fluorescence, and F_m is the maximum fluorescence. The maximum relative electron transport rates ($rETR_{\text{max}}$) were calculated from $rETR$ versus irradiance curves using the Platt *et al.* (1980) equation. Statistical analyses of fluorescence parameters were performed using R.



Results and Discussion

Both stations were characterized by low inorganic nutrient concentrations (Table 1). The Chl *a* concentration was four-fold lower and the phaeophytin/Chl *a* (Phaeo/Chl *a*) ratio was higher at station 19S compared to station 15S (Table 1). Ambient temperature at the time of sampling was 20°C.

Table 1. Concentrations of Chl *a* ($\mu\text{g L}^{-1}$) and nutrients (μM). Urea was not detectable.

	Station 15S	Station 19S
Chl <i>a</i>	10.5	2.4
Phaeo/Chl <i>a</i>	0.23	0.4
$\text{NO}_3^- + \text{NO}_2^-$	< 0.07	< 0.07
NH_4^+	0.23	0.15
PO_4^{3-}	0.20	0.05

Both stations had a mixed phytoplankton community composition, with substantial *K. brevis* abundance. Station 15S was dominated by dinoflagellates (220,000 cell L^{-1}) and 94% of the dinoflagellate population was *K. brevis*. At station 19S, approximately 30% of the algae was dominated by dinoflagellates (20,000 cell L^{-1}) (Fig. 1), of which 75% were *K. brevis*. Neither station had more than a small percentage of diatoms (6%). Therefore, it is reasonable to assume that most of the fluorescence signals of the brown algae originated from *K. brevis* during this study.

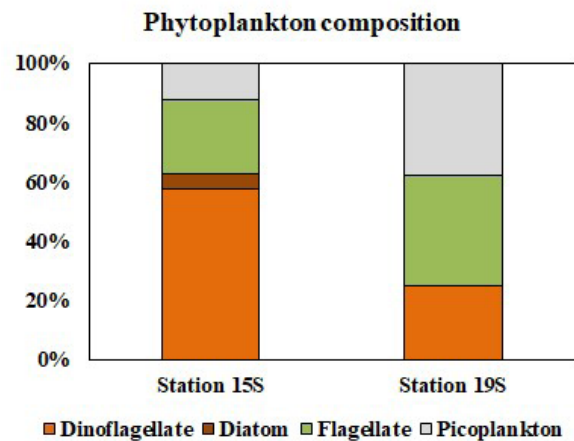


Fig. 1. Phytoplankton composition at two stations during January 22nd, 2021 on WFS.

In general, decreasing trends of the maximum quantum yields of PSII photochemical efficiency, F_v/F_m , were observed in each N treatment as temperature increased from 15°C to 30°C although only the data from station 15S were significantly different (ANOVA, $p < 0.5$) (Figs. 2a, b). However, this trend was less consistent when cells were treated with urea. The $rETR_{max}$ also showed similar trends with F_v/F_m (Figs. 1c, d). Although the differences were less at station 19S, generally $rETR_{max}$ also decreased with increasing temperature except for the urea-treated samples.

In both field and laboratory cultures, *K. brevis* has been observed in the range of 7-33°C, but the optimum temperature range has previously been reported to be relatively narrow, 22-28°C (Kusek *et al.*, 1999). The decline of fluorescence parameters after even one hour exposure to 30°C in this study suggests that this high temperature is stressful for the winter *Karenia* community. However, when bloom water was enriched with urea, fluorescence parameters were



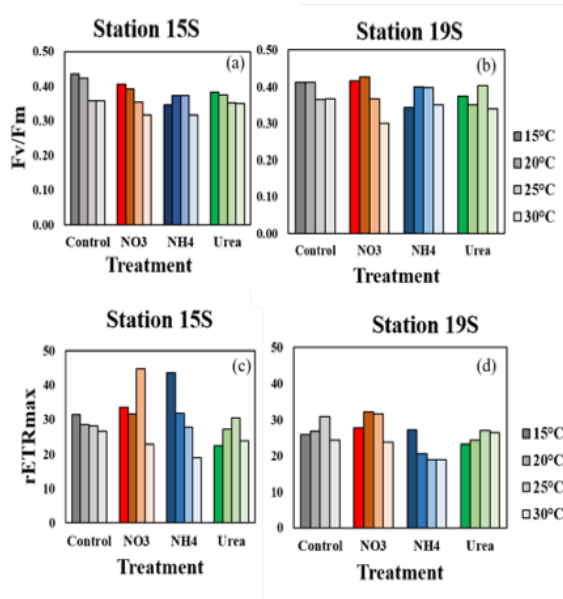


Fig. 2. Fv/Fm and $rETR_{max}$ ($\mu\text{mol electrons m}^{-2} \text{s}^{-1}$) of *K. brevis* exposed to different temperatures (15, 20, 25, 30°C) and nitrogen ($10 \mu\text{M NO}_3^-$; NH_4^+ or urea) additions. The color bars increase in brightness from 15°C to 30°C at each treatment.

reduced to a lesser degree (Fig. 2), implying that urea might induce a photoprotective mechanism. Dinoflagellates have a urea cycle that helps in the reallocation of intracellular carbon (C) and N (Dagenais-Bellefeuille *et al.*, 2013) and in *Karenia mikimotoi*, several enzymes involved in the urea cycle have been identified (Shi *et al.*, 2021). The increased recycling of C and N from catabolism and photorespiration through the urea cycle could enhance overall metabolic flux, thus increasing the demand for chemical energy to run metabolism. To match this demand, a higher proportion of absorbed light energy may be channeled to photochemical reactions, therefore increasing Fv/Fm and rETR. In addition, urease, the enzyme involved in urea metabolism, generally has a positive relationship with temperature (Fan *et al.*,

2003). Therefore, when urea is available at 30°C, high temperature stress might be partly alleviated by balancing light energy demand. At 15°C, which is lower than the optimal temperature range for *K. brevis*, the photosynthetic performance of winter *Karenia* communities was not significantly reduced compared to those temperatures close to, or at, optimal temperatures and some fluorescence parameters (e.g., Fv/Fm) were even higher at this cool temperature (Fig. 2). The winter *Karenia* community, which was adapted to cool ambient water temperatures at the time of sampling, were able to operate their photosynthetic apparatus efficiently at 15°C. Compared to station 15S populations, cells at station 19S did not respond significantly to N pulses, even though ambient N concentration was very low. However, the *K. brevis* cells from this station may have been physiologically less active, as indicated by the higher Phaeo/Chl *a* ratio (Table 1), suggesting that *K. brevis* at station 19S would be less photosynthetic active.

Overall, these results indicate the photosynthetic response of *K. brevis* to changes in N supply may vary with temperature and suggest that the pull of metabolism may buffer the stress of high light, but that the extent of this photoprotection mechanism depends on N form.

Acknowledgements. This study was funded by the NOAA National Centers for Coastal Ocean Science Competitive Research under award NA19NOS4780183. This is Contribution Number 6107 from the University of Maryland Center for Environmental Science and 1010 from the

NOAA ECOHAB Program. The authors acknowledge assistance from Todd Kana (Bay Instruments LLC) and Sarah Klass, Mote Marine Laboratory.

References

- Brand, L.E. and Compton, A. (2007) *Harmful Algae* 6, 232-252.
- Bronk, D., Killberg-Thoreson, L., Sipler, R.E., Mulholland, M.R., *et al.*, (2014). *Harmful Algae* 38, 50-62.
- Dagenais-Bellefeuille, S. and Morse, D. (2013) *Front. Microbiol.* 4, 1-14.
- Fan, C., Glibert, P.M., Alexander, J., Lomas, M.W. (2003). *Mar. Biol.* 142, 949-958.
- Glibert, P.M., Burkholder, J.M., Kana, T.M., Alexander, J., *et al.*, (2009). *Aquat. Microb. Ecol.* 44, 17-30.
- Glibert, P.M., Wilkerson, F.P., Dugdale, R.C., Raven, J.A., *et al.*, (2016). *Limnol. Oceanogr.* 61, 165-197.
- Heil, C.A., Dixon, L.K., Hall, E., Garrett, M., *et al.*, (2014a). *Harmful Algae* 38, 127-140.
- Heil, C.A., Bronk, D.A., Mulholland, M.R., O'Neil, J.M., *et al.*, (2014b). *Harmful Algae* 28, 86-94.
- Kusek, K.M., Vargon, G.A., Steidinger, K. (1999). *Cont. Mar. Sci.* 34, 1-229.
- Lomas, M.W. and Glibert, P.M. (1999a). *Limnol. Oceanogr.* 44, 556-572.
- Lomas, M.W. and Glibert, P.M. (1999b). *Mar. Biol.* 133, 541-551.
- Platt, T., Gallegos, C.L., Harrison, W.G. (1980). *J. Mar. Res.* 38, 687-701.
- Shi, X., Xiao, Y., Liu, L., Xie, Y., *et al.*, (2021). *Harmful Algae* 103, 101977.
- Vargo, G.A. (2009). *Harmful Algae* 8, 573-584.
- Weisberg, R.H. and He, R. (2003). *J. Geophys. Res. Oceans* 108, 3184.
- Weisberg, R.H., Zheng, L., Liu, Y., Lembke, C., *et al.*, (2014). *Harmful Algae* 38, 119-121.



Allelopathic effects of *Margalefidinium polykrikoides* on the growth of *Pyrodinium bahamense* in different nutrient concentrations

Asilah Al-Has¹, Normawaty Mohammad-Noor^{1*}, Sitti Raehanah M. Shaleh², Shuhadah Mustapha³, Deny Susanti Darnis¹, Mohd Nor Azman Ayub⁴, Aimimuliani Adam¹, Ghaffur Rahim Mustakim²

¹Instituto de Fomento Pesquero (IFOP). Centro de Estudios de Algas Nocivas (CREAN). Puerto Montt, Chile; ²Fisheries Resources Institute, Japan Fisheries Research and Education Agency, 2-12-4 Fukuura, Kanazawa, Yokohama, Kanagawa, 236-8648, Japan.

* corresponding author's email: normahwaty@iium.edu.my

Abstract

Co-occurrence of the dinoflagellates *Margalefidinium polykrikoides*, a known fish killer, and the neurotoxic species *Pyrodinium bahamense* is commonly observed in the coastal waters of Sabah, Malaysia. During most of these events, *M. polykrikoides* dominated the bloom, apparently suppressing the growth of *P. bahamense*. To increase our understanding on the nutrient conditions of this phenomenon, a study was conducted to explore the interaction between these species. The specific aim was to document the allelopathic effects, if any, of *M. polykrikoides* on *P. bahamense* when varying ratios of the two species were co-cultured under different nitrogen (N) and phosphorus (P) concentrations. The bioassay experiments started with three cell abundance proportions, which were 5:5 (500 cells mL⁻¹ of each species, *M. polykrikoides*, and *P. bahamense*); 1:5 (100 cells mL⁻¹ of *M. polykrikoides* and 500 cells mL⁻¹ of *P. bahamense*); and 5:1 (500 cells mL⁻¹ of *M. polykrikoides* and 100 cells mL⁻¹ of *P. bahamense*). Additionally, culture filtrates (10, 20 and 50 mL) from the late exponential phase of *M. polykrikoides* were added to 150 mL of *P. bahamense* to determine if cell filtrates were allelopathic. Results indicate that *M. polykrikoides* was allelopathic to *P. bahamense* when nutrients were abundant, but not when nutrients were limiting or N was limiting relative P. The production of allelopathic compounds was supported by abnormal morphological changes in *P. bahamense* when co-cultured with *M. polykrikoides*. This capacity to suppress *P. bahamense* growth, combined with the inherently faster growth rate of *M. polykrikoides* relative to *P. bahamense* can account for why *M. polykrikoides* forms nearly monospecific blooms when nutrients are high. The filtration studies indicated the allelopathic capacity of *M. polykrikoides* required direct cell contact or that the allelopathic compounds degraded rapidly and were inactive when added to *P. bahamense* cultures. These results are important in understanding the bloom mechanisms of these two harmful algal blooms (HABs) species.

Keywords: Allelopathy, bi-algal cultures, *Margalefidinium polykrikoides*, nutrients, *Pyrodinium bahamense*

<https://doi.org/10.5281/zenodo.7034906>



Introduction

Harmful algal blooms (HABs) are natural events where increased phytoplankton biomass can result in adverse impacts on both public and ecosystem health. In recent years, *Margalefidinium* (*Cochlodinium*) *polykrikoides* blooms have gained attention because of their increasing geographical distribution worldwide (Kudela and Gobler, 2012). This species has been reported to produce cysts, is a fast swimmer, mixotrophic, and has Allelopathic properties (Kudela and Gobler, 2012).

Allelopathy is a phenomenon where a species produces chemicals that inhibit the growth of, or kill, other competing species (Hattenrath-Lehmann and Gobler, 2011). Species which have been adversely effected by *M. polykrikoides* include *Gymnodinium catenatum* (Band-Schmidt *et al.*, 2020), *Chattonella subsalsa*, *Isochrysis galbana*, *Heterocapsa rotundata*, *Thalassiosira weissflogii* (Tang and Gobler, 2010) and *Akashiwo sanguinea* (Yamasaki *et al.*, 2007). These studies indicate the allelopathic effects of *M. polykrikoides* are not species-specific. The impacts of other allelopathic species has been shown to be influenced by nutrient limitation, i.e. *Alexandrium tamarensense* (Zhu and Tillmann, 2012) and *Prymnesium parvum* (Uronen *et al.*, 2005). In contrast, the effects of nutrient availability on the allelopathic impacts of *M. polykrikoides* are less studied.

Another HAB species of concern, which often co-occurs with *M. polykrikoides* is *Pyrodinium bahamense*. This species is a saxitoxin producer reported from the Indo-Pacific and Caribbean Sea (Usup *et al.*, 2012). Although the distribution of *P. bahamense* is

more limited compared to *M. polykrikoides*, the species can have devastating impacts where it blooms due to its ability to produce higher intracellular saxitoxin concentrations relative to other saxitoxin producers which cause paralytic shellfish poisoning (PSP) (Usup *et al.*, 2012).

The co-occurrence of *M. polykrikoides* and *P. bahamense* has been monitored by the Sabah Fisheries Department of Malaysia since 1976 (Jipanin *et al.*, 2019). Since 2005, blooms of *M. polykrikoides* have also been observed in the coastal waters adjacent to Kota Kinabalu, the capital city of Sabah (Anton *et al.*, 2008). These later blooms sometimes co-occur with *P. bahamense* (Adam *et al.*, 2011; Chong *et al.*, 2020). Shaleh *et al.* (2010) found that in the laboratory, salinity and pH did not significantly affect interactions between these species. However, field reports indicate elevated nutrient concentrations (N and P) can trigger blooms dominated by *M. polykrikoides* blooms and containing only a small subpopulation of *P. bahamense* (Mohammad-Noor *et al.*, 2014). The present study used bi-species cultures to simulate bloom conditions where either *M. polykrikoides* or *P. bahamense* dominated, or co-dominated the bloom population. These different simulated populations were further allowed to develop under different nutrient conditions. The goal was to quantify how the relative cell densities of *M. polykrikoides* versus *P. bahamense* in conjunction with different nutrient levels might affect the allelopathic interactions between these two species. Also, the effects of cell free filtrates from *M. polykrikoides* on the growth of *P. bahamense* were investigated to evaluate if



direct cell contact was required to achieve any observed allelopathic effects.

Materials and Method

Strains of *M. polykrikoides* and *P. bahamense* were obtained from the Borneo Marine Research Institute (BMRI), University Malaysia Sabah, Malaysia. Strains of *M. polykrikoides* and *P. bahamense* were isolated during blooms in Sepanggar Bay in 2019 and 2013, respectively, and established into unialgal non-axenic cultures in f/2 media. The experiments were conducted by inoculating *M. polykrikoides* into f/2 media containing three nutrient concentrations: (a) f/2 medium, 882 μM $\text{NO}_3\text{-N}$ and 32 μM $\text{PO}_4\text{-P}$, N:P = 27.6 (b) nutrient enriched media (NE), 30 μM $\text{NO}_3\text{-N}$ and 5 μM $\text{PO}_4\text{-P}$, N:P = 6 and (c) cells were added from the late log stock cultures without nutrient addition, low concentration (LC). *Pyrodinium bahamense* was grown in f/2 medium. Trace metals and vitamins were the same as listed in Guillard and Ryther (1962). All media were prepared using autoclaved filtered seawater. The cultures were maintained at 25-26 °C with a 12:12 light–dark cycle illuminated by LED light with an intensity of 100 $\mu\text{mol quanta m}^{-2} \text{ s}^{-1}$.

Cell contact experiments Bi-algal culture experiments were conducted in 250 mL flasks containing 150 mL of f/2 medium which augmented with nutrients as described above. Both species were harvested during their late exponential phase from the unialgal cultures and mixed at three cell abundance ratios, which were 1:5 (100 cells 100 mL⁻¹ of *M. polykrikoides* and 500 cells mL⁻¹ of *P. bahamense*); 5:1 (500 cells mL⁻¹ of *M. polykrikoides* and 100 cells mL⁻¹ of *P.*

bahamense); and 5:5 (500 cells mL⁻¹ of each species). Treatments were run in triplicate.

Culture filtrate experiments Cell-free filtrates of *M. polykrikoides* cultured in different nutrient concentrations (f/2, EN and LC treatments) were harvested at the late exponential phase and filtered through 47 mm GF/F filter (Whatman). Three volumes (10, 20 and 50 mL) of the culture filtrates of *M. polykrikoides* were added to 250 mL Erlenmeyer flasks containing 150 mL of *P. bahamense* containing an initial density of *P. bahamense* was 500 cells mL⁻¹. A three mL aliquot was collected from each experiment daily during seven days for cell enumeration and morphological observations. One milliliter of each sample was counted twice using a Sedgewick Rafter cell under a light microscope (Zeiss, Axiostar). Growth rate (μ) was determined based on the following formula (Guillard and Ryther, 1962).

Results and Discussion

In the f/2 nutrient treatment, *P. bahamense* was able to initially compete well with *M. polykrikoides* when it started with a 5:1 concentration advantage. However, by day four of the experiment, *P. bahamense* began declining relative to the control as *M. polykrikoides* cell concentration began slowly increasing. In the corresponding treatment where *M. polykrikoides* had a 5:1 starting advantage, *M. polykrikoides* increased slowly relative to the control whereas *P. bahamense* failed to increase in the presence of *M. polykrikoides*. Interpretation of these experimental results is complicated because the control culture of *P. bahamense* did not grow well. The treatment starting with the 5:5 (equal concentration of both



species) showed that *M. polykrikoides* cell concentrations steadily increased while the *P. bahamense* cell population steadily declined, with both controls showing steady growth. Cumulatively, these results are consistent with *M. polykrikoides* inhibiting the growth of *P. bahamense* either through allelopathy or an ability to outcompete *P. bahamense* for nutrients. Filtrates from *M. polykrikoides* cultures did not effect the cell morphology or the growth of *P. bahamense*.

Evidence for the production of allelopathic compounds is supported by abnormal changes in the morphology of *P. bahamense* after two more days with direct cell? contact with *M. polykrikoides*. The main changes observed were loss of the thecate plate and cell lysis (Fig. 2). These observations were consistent with allelochemicals increasing the cell membrane penetrability thereby suppressing cell growth (Xue *et al.*, 2018). Future studies where ambient nutrient concentrations are monitored closely are needed to further separate the extent to which the inhibition is related to nutrient competition versus production of allelo-chemical(s).

Interestingly all three experiments showed that *M. polykrikoides* growth in the bi-species cultures was slower than that in the control. This reduced growth rate indicates a cost for competing with *P. bahamense*, but that cost is not likely due to the production of allelochemicals (Zhu and Tillman 2012). Another observation from the control cultures is that *M. polykrikoides* has an inherently faster growth rate than *P. bahamense*. This would give *M. polykrikoides* a growth advantage when nutrient levels are elevated.

The high nutrient treatment corresponds to field conditions where nutrient concentrations are elevated, but there is an excess of P relative to N (N:P = 6). In the treatment where there were five *P. bahamense* relative to one *M. polykrikoides*, the population of *P. bahamense* steadily declined while the *M. polykrikoides* cell counts gradually increased. The 5:1 *M. polykrikoides*: *P. baha-mense* experiment failed after three days and provided no results. In contrast, the 5:5 experiment showed that under the more N-limited conditions, growth of both species in the bi-cultures was very similar to the 1:5 treatment. The only difference from that initial 1:5 treatment is that the control population rapidly increased indicating the media is capable of supporting rapid growth of *M. polykrikoides*. Though these nutrient conditions were not optimal for *P. bahamense* growth, at high enough cell concentration this species inhibited the growth of *M. polykrikoides*. Because *P. bahamense* growth was exceeding slow this inhibition is unlikely due to direct nutrient competition indicating under certain nutrient regimes *P. bahamense* may inhibit *M. polykrikoides*, instead of the reverse situation.

The low nutrient condition, where cells grown in f/2 media, with an N:P ratio closer to the Redfield ratio, and then allowed to become more nutrient limited represents what might happen more toward the end of a bloom. In the 1:5 *M. polykrikoides*: *P. bahamense* treatment the controls grew while the populations in the bi-species cultures steadily declined. In the 5:1 treatment the growth of both species in the controls and the cells in the bi-species cultures were essentially the same (Fig. 1) as was also true for the 5:5 treatment. These results are consistent with cells growth largely



dependent on internally stored nutrient with no indication of any allelopathic interactions.

Cumulatively these results suggest elevated nutrient concentrations favor *M. polykrikoides* over *P. bahamense* because of its inherently higher growth rate. The data are further consistent with high densities of nutrient replete *M. polykrikoides* having the ability to produce allelopathic compounds that impeded the growth of *P. bahamense*. This allelopathic inhibition of *P. bahamense*, however, did not occur at higher nutrient concentrations where the N:P ratio was skewed toward an excess of phosphate or when the cells were nutrient limited (Fig. 1). This may indicate N is a structural component of the allelopathic compound itself. Similarly observed high allelopathic activity of *A. sanguinea*

when nutrient concentrations were high. Tang and Gobler (2010) also demonstrated the allelopathic effect of *M. polykrikoides* was dependent on the initial cell abundance and Band-Schmidt *et al.*, (2020) showed the duration of the inhibition was proportional to cell density.

In summary, *M. polykrikoides* likely dominates over *P. bahamense* when nutrients are high due to its inherently higher growth rate (Kudela and Gobler, 2012). Evidence from this and other studies further support allelopathic suppression of *P. bahamense* when *M. polykrikoides* cell concentration are high. This would account, at least in part, for why there are relatively few *P. bahamense* present when *M. polykrikoides* cell densities are high and nutrients abundant.

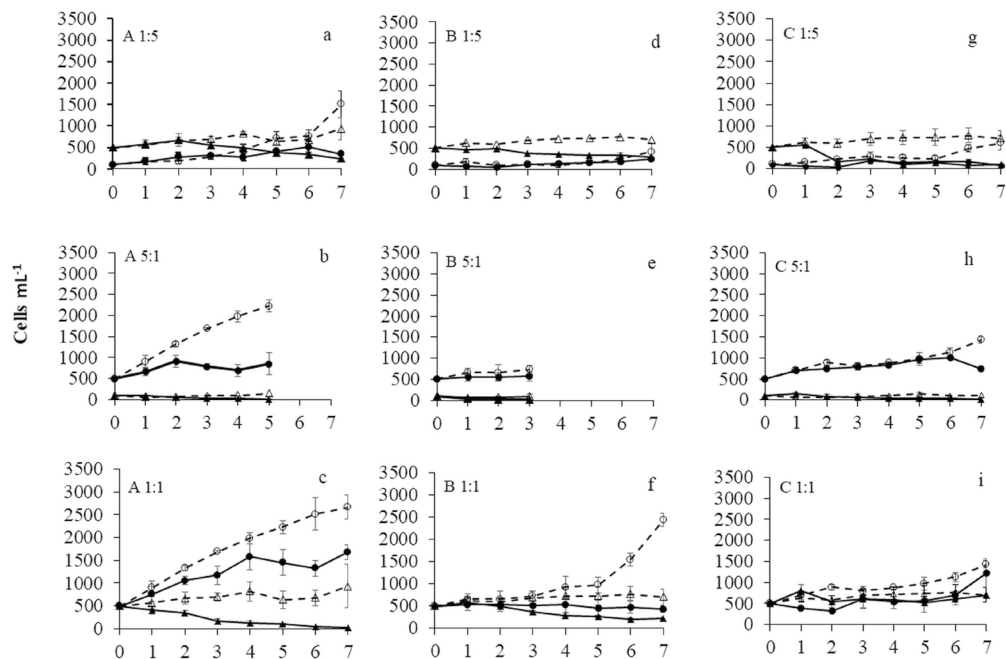


Fig. 1. Cell abundance proportions of *M. polykrikoides* (mean \pm standard deviation) and *P. bahamense* in co-cultured cell contact experiments: (i) 1:5, (ii) 5:1, (iii) 5:5 at different treatments (A) f/2 medium (f/2); (B) nutrient enriched (EN); and (C) low concentration (LC). Closed circles: *M. polykrikoides* in bi-algal culture; open circles: *M. polykrikoides* control; closed triangles: *P. bahamense* in bi-algal culture; open triangles: *P. bahamense* control.



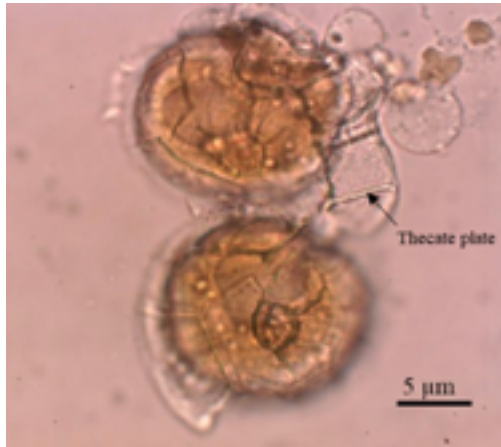


Fig. 2. Detachment of the thecal plate of *P. bahamense* when exposed to *M. polykrikoides*.

References

- Adam, A., Mohammad-Noor, N., Anton, A., Saleh, E., *et al.*, (2011). *Harmful Algae* 10, 495-502.
- Anton, A., Teoh, P.L., Muhamad Shaleh, S.R., Mohammad-Noor, N. (2008). *Harmful Algae* 7, 331-336.
- Band-Schmidt, C.J., Zumaya-Higuera, M.G., López-Cortés, D.J., Leyva-Valencia, I., *et al.*, (2020). *Harmful Algae* 96, 101846.
- Chong, B.W.K., Leong, S.C.Y.L., Kuwahara, V.S., Yoshida, T. (2020). *Reg. Stud. Mar. Sci.* 37, 101326.
- Guillard, R. R. and Ryther, J. H. (1962). *Can. J. Microbiol.* 8, 229-239.
- Hattenrath-Lehmann, T.K. and Gobler, C.J. (2011). *Harmful Algae* 11, 106-116.
- Jipanin, S.J., Muhamad Shaleh, S.R., Lim, P.T., Leaw, C.P., Mustapha, S. (2019). *J. Phys. Conf. Ser.*, 1358, 012014.
- Kudela, R.M. and Gobler, C.J. (2012). *Harmful Algae* 14, 71-86.
- Muhammad-Noor, N., Weliyadi, E., Aung, T., Adam, A., Hanan, D.S.M. (2014). *Sains Malaysiana* 42, 21-29.
- Shaleh, S.S.R., Doinsing, J., Peter, C., Anton, A., *et al.*, (2010). In: Ho, K.-C., Zhou, M.J. and Qi, Y.Z. (Eds.). *Proc. 13th ICHA*, Hong Kong, 95-97.
- Tang, Y.Z. and Gobler, C.J. (2010). *Mar. Ecol. Prog. Ser.* 406, 19-31.
- Uronen, P., Lehtinen, S., Legrand, C., Kuuppo, P., Tamminen, T. (2005). *Mar. Ecol. Prog. Ser.* 299, 137-148.
- Usup, G., Ahmad, A., Matsuoka, K., Teen, P., Pin, C. (2012). *Harmful Algae* 14, 301-312.
- Xue, Q., Wang, R., Xu, W., Wang, J., Tan, L., (2018). *Aquat. Toxicol.* 205, 51-57.
- Yamasaki, Y., Nagasoe, S., Matsubara, T., Shikata, T., *et al.*, (2007). *Mar. Biol.* 152, 157-163.
- Zhu, M. and Tillmann, U. (2012). *Mar. Biol.* 159, 1449-1459.



Termination patterns of *Karenia brevis* blooms in the eastern Gulf of Mexico

Cynthia A. Heil^{1*}, Shady A. Amin², Patricia M. Glibert³, Katherine A. Hubbard⁴, Ming Li³, Joaquín Martínez Martínez⁵, Robert Weisberg⁶, Yonggang Liu⁶, Yunfang Sun⁶

¹Mote Marine Laboratory, 1600 Ken Thompson Pky, Sarasota, Florida 34236, U.S.A.; ²New York University – Abu Dhabi, Experimental Research Building (C1) RL5-20, Abu Dhabi, U.A.E.; ³University of Maryland Center for Environmental Science, Horn Point Laboratory, PO Box 775, Cambridge, MD 21613, U.S.A.; ⁴Florida Fish and Wildlife Conservation Commission, Fish and Wildlife Research Institute, 100 8th St S.E., St. Petersburg, Florida, 33701, U.S.A.; ⁵Bigelow Laboratory for Ocean Sciences, 60 Bigelow Dr., East Boothbay, Maine, 04544, U.S.A.; ⁶College of Marine Science, University of South Florida, 140 7th Ave. S., St. Petersburg, Florida, 33701, U.S.A. <https://doi.org/10.5281/zenodo.7034512>

* corresponding author's email: cheil@mote.org

Abstract

The factors governing the initiation and development of *K. brevis* blooms in the eastern Gulf of Mexico are fairly well understood, however the physical, chemical and biological factors underlying bloom transport and termination are not. The Florida Fish and Wildlife Conservation Commission's HAB Monitoring database was analyzed from 1998 - 2021 for temporal trends in bloom duration, initiation and termination and for repetitive spatial patterns in bloom termination. A unimodal pattern in bloom initiation was observed, with the most frequent initiations in September. Bloom termination was more variable, with the most frequent occurrences in April. Four recurring patterns in bloom termination were identified during this period for southwest Florida *K. brevis* blooms: 1) coastal transport south to the Florida Keys then west into the Gulf of Mexico, 2) transport to the Florida Panhandle with subsequent termination in place, or 3) via coastal transport west to Alabama, and 4) termination in place in southwest Florida. These patterns suggest that consistent physical, chemical and biological drivers underlie the termination stages of *K. brevis* blooms, and that identification of these drivers may provide useful management tools for bloom prediction and monitoring.

Keywords: *Karenia brevis*, Florida Red tide, initiation, termination, Florida HAB Historical Database

<https://doi.org/10.5281/zenodo.7034923>



Introduction

Blooms of the toxic dinoflagellate *Karenia brevis* are an annual feature of the eastern Gulf of Mexico (GoM), resulting in significant environmental, human health and economic impacts (Heil and Muni-Morgan, 2021). Much is known about physical, chemical and biological factors that underlie these blooms' initiation and development stages. Physical drivers and a complex nutrient pathway sometimes involving cyanobacteria (Steidinger, 1975; Lenes *et al.*, 2001; Walsh and Steidinger, 2001) have been shown to be crucial to offshore initiation stages. Offshore upwelling related to Loop Current intrusion plays a complex role in initiation. Some upwelling is required for initiation (Liu *et al.*, 2012; Weisberg *et al.*, 2014), however too much can deliver upwelled NO_3^- to the shelf, potentially favoring other taxa and impeding *Karenia* growth (Heil *et al.*, 2001; Weisberg *et al.*, 2016). Cross-shelf cell transport subsequently occurs via the bottom Ekman layer (Weisberg *et al.*, 2009, 2016), driven by wind-driven and upwelling-related transport. The slow-growing *K. brevis* cells are eventually transported and concentrated toward the shore by winds, frontal systems and longshore currents (Vargo *et al.*, 2001; Weisberg and He, 2003), where these cells may thrive and persist in bloom concentrations for periods of months to years (Steidinger, 2009) and where a variety of nutrient sources of nutrients may support their growth (Heil *et al.*, 2014).

Little is known of the factors influencing bloom termination, however. Physical factors resulting in flow divergence, disrupting bloom integrity (Slobodkin, 1953) or physical transport and dilution of blooms to offshore or

other regions (Steidinger, 2009) are thought to contribute to termination. However nutrient deprivation (Steidinger, 2009; Vargo, 2009) and bacterial and viral interactions (Mayali and Doucette, 2002; Roth *et al.*, 2007; Lenes *et al.*, 2013; Meyer *et al.*, 2014) may also potentially influence termination. As an initial step in the examination of physical, nutrient and biological factors underlying *K. brevis* bloom termination in the eastern GoM, *K. brevis* bloom records from 1998 to 2021 from the Florida Fish and Wildlife Conservation Commission's (FWC) HAB Monitoring Database were examined for repetitive patterns in both spatial and temporal bloom termination.

Material and Methods

Karenia brevis data were obtained from the FWC Database (<https://myfwc.com/research/redtide/monitoring/database/>). This database contains data collected from diverse sources and includes samples collected during research, routine monitoring, and event response sampling of suspected or confirmed *K. brevis* events. This analysis is limited to data post-1998 when routine sampling intensified, but the database contains records dating back to 1953.

Data included geo-referenced *K. brevis* concentrations with the associated date, time, depth, and collecting agencies for all sites within Florida estuarine, coastal and offshore locations during the time period. This time span was chosen for analysis as it includes the start of a regional study for which repetitive monthly shelf sampling was conducted, so ancillary data are available for



future examination of physical, nutrient and biological conditions underlying observed patterns. The month of bloom initiation was defined as a sustained (>1 month) period of *K. brevis* concentrations greater than 2.0×10^3 cells L^{-1} after more than 2 months of background ($<1.0 \times 10^3$ cells L^{-1}) cell concentrations. Bloom termination was defined as a period of > 6 weeks of *K. brevis* cell concentrations at or below background concentrations. Analysis of bloom termination trends from 2000 to 2021 was conducted using FWC's archived status maps (<https://www.flickr.com/photos/myfwc/sets/72157635398013168/>), supplemented with the database for the years 1998 and 1999.

Results and Discussion

No pattern was evident in bloom duration (Fig. 1); blooms lasted from three to 17 months. However, Sobrinho *et al.* (this volume), using the same database, found that freshwater discharge and climate variations as measured by El Niño – Southern Oscillation (ENSO) had direct and indirect roles in timing and magnitude of blooms. The longest bloom durations were observed in the 2004-2005 and 2017-2019 blooms, which extended through the summers into the following years and were associated with significant environmental impacts and economic losses.

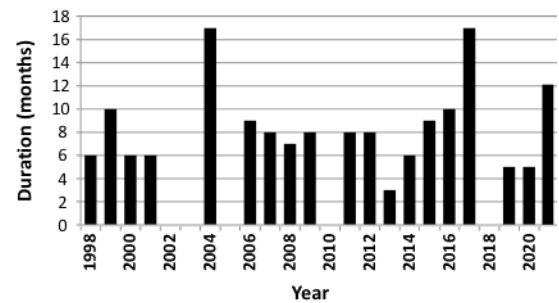


Fig. 1. Duration of *K. brevis* blooms in the GoM as measured from the year the bloom initiated.

Over the 22 years examined, bloom initiation month displayed a unimodal trend, with six blooms initiating in September, four each in August and October and two in July and November (Fig. 2). Bloom termination was observed in all months, from December through June (except January). The maximum number of bloom terminations (six) was observed in April, suggesting that as yet unidentified conditions in April may serve as a 'gate' to potential bloom extension into the summer months. It is of note that in typical years, Florida experiences a shift from the winter dry season to the summer rainy season by mid-May. Delays in the timing of the wet season and related nutrient inputs may be one potential factor influencing bloom duration.

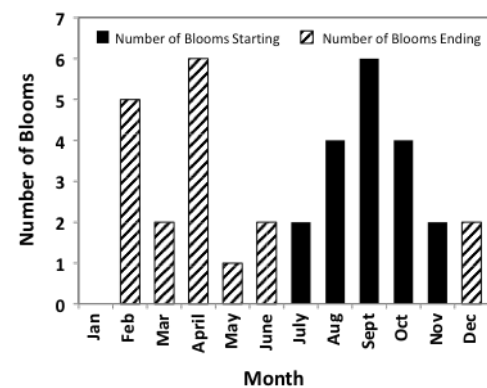


Fig. 2. Monthly distribution of *K. brevis* bloom initiation and termination events from 1998- 2021.



The most common pattern of termination for southwest Florida coastal *K. brevis* blooms (70%) was coastal transport of the bloom south toward the Florida Keys region then west into the GoM (the ‘Everglades Off Ramp’ pattern) as was demonstrated in 2007 and 2008 blooms (Table 1, Fig. 3a). A small percentage of these southwest transported blooms (19%) were transported through the Keys and up the eastern Florida coast (e.g. 2007, 2012 and 2018 blooms; Fig. 3b). However, when this occurred it did not result in termination of the original bloom in the southwest region. The fate of bloom populations transported west into the GoM is unknown.

A smaller percentage (57%) of southwest Florida blooms was displaced to the Panhandle region, where they either terminated in place within two months (e.g., 2013 bloom; Fig. 3c) or were transported west to Alabama (e.g., 2005 and 2018 blooms; Fig. 3d). Blooms in the Panhandle region were preceded by southwest Florida blooms 83% of the time and both termination patterns could occur simultaneously for spatially separated subpopulations of the same Panhandle regional population.

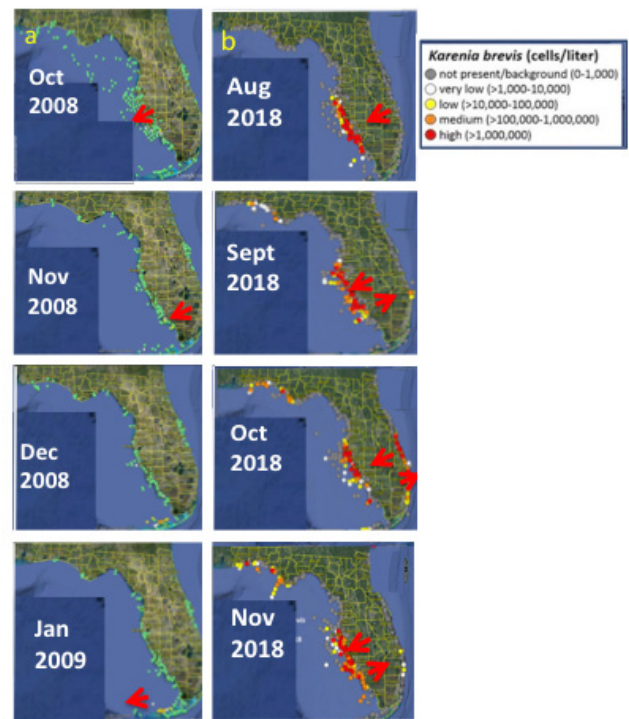


Fig. 3. Examples of the termination patterns described in text. Panels in column a (2008) represent the Everglades off-ramp; panels in column b (2018) represent blooms that were transported through the Keys and up the east coast. Arrows indicate most intense bloom area.



Table 1. Patterns of *K. brevis* bloom termination in the eastern GoM from 1998-2021 expressed as a percentage of southwest Florida blooms.

Pattern	Description	Occurrence
1. Everglades Off Ramp	Southeast coastal transport to Keys, then west into Gulf	70%
2. Panhandle Termination	Transport to Panhandle from SW FL	57%
A. Termination in place	Bloom ends within 1-2 months in place	92%
B. Transport	Bloom transported west to AL from area of 1st appearance	38%
3. Southwest FL Termination	Bloom concentrations reduced in place	20%

In some years, blooms were observed to terminate in place in southwest Florida without coastal transport. As this usually occurred during the late dry season (e.g., May 2013), it is possible that nutrient depletion played a greater role in termination of these blooms.

Offshore expansion of established coastal blooms in the Naples to Cedar Key region was observed during the August-September period of the 2005 bloom and the September through October period of the 2018 bloom (Figs. 3b,d). Both expansion periods were associated with unusual, environmentally destructive (e.g., associated regional anoxia and extensive marine wildlife mortalities) over-summering blooms and neither expansion resulted in bloom termination.



Fig. 3, cont'd. Panels in line c (2013) represent blooms that terminated in place; and panels in line d (2005) represent blooms with offshore expansion. Green dots represent no bloom; yellow, orange, and red dots represent increasing *K. brevis* cell concentrations. Arrows indicate most intense bloom areas.

The patterns identified here suggest that consistent, identifiable physical, nutrient and biological drivers underlie bloom termination stages, and that identification of these drivers may provide useful management tools for bloom prediction and monitoring.

Acknowledgements. This study was supported by NOAA ECOHAB grant NA19NOS4780183, with salary support for C.H. provided by the Economos and Barancik Foundations. We thank FWC's HAB group for the historical data and Flickr maps. This is ECOHAB Publication #1011 and



Contribution #6198 from the University of Maryland Center for Environmental Science.

References

Heil, C.A. and Muni-Morgan, A. (2021). *Front. Ecol. Evol.* 9, 646080.

Heil, C.A., Vargo, G.A., Spence, D., Neely, M.B., *et al.*, (2001). *Harmful Algal Blooms 2000*, pp. 165-168.

Heil, C.A., Dixon, L.K., Hall, E., Garrett, M., *et al.*, (2014). *Harmful Algae* 38, 127-149.

Lenes, J.M., Darrow, B.P., Cattrall, C., Heil, C.A., *et al.*, (2001). *Limnol. Oceanogr.* 46, 1261-1277.

Lenes, J.M., Walsh, J.J., Darrow, B.P. (2013). *Mar. Ecol. Prog. Ser.* 493, 71-81.

Liu, Y., Weisberg, R.H., Vignudelli, S., Roblou, L., *et al.* (2012). *Adv. Space Res.* 50, 1085-1098.

Mayali, X. and Doucette, G.J. (2002). *Harmful Algae* 1, 277-293.

Meyer, K.A., O'Neil, J.M., Hitchcock, G.L., Heil, C.A. (2014). *Harmful Algae* 38, 110-118.

Roth, P.B., Twiner, M.J., Wang, Z., Dechraoui, M.Y.B., Doucette, G.J. (2007). *Toxicon* 50, 1175-1191.

Slobodkin, L.B. (1953). *J. Mar. Res.* 12, 148-155.

Sobrinho, B., Glibert, P.M., Lyubchich, V., Heil, C.A., Li, M. This volume.

Steidinger, K.A. (1975). *Proceedings 1st Intern. Conf. Toxic Dinoflagellate Blooms.* pp. 153-162.

Steidinger, K.A. (2009). *Harmful Algae* 8, 549-561.

Vargo, G.A. (2009). *Harmful Algae* 8, 573-584.

Vargo, G., Heil, C., Spence, D., Neely, M., *et al.*, (2001). *Harmful Algal Blooms 2000*, pp. 157-160.

Walsh, J.J. and Steidinger, K.A. (2001). *J. Geophys. Res. Oceans* 106, 11597-11612.

Weisberg, R.H. and He, R. (2003). *J. Geophys. Res. Oceans* 108, 3184.

Weisberg, R.H., Barth, A., Alvera-Azcárate, A., Zheng, L. (2009). *Harmful Algae* 8, 585-598.

Weisberg, R.H., Zheng, L., Liu, Y., Lembke, C., *et al.*, (2014). *Harmful Algae* 38, 119-216.

Weisberg, R.H., Zheng, L., Liu, Y., Corcoran, A., *et al.*, (2016). *Cont. Shelf Res.* 120, 106-121.



Peridinium quadridentatum (Dinophyceae) is an occasional daily diurnal surface forming algal bloom species in Veracruz, Mexico

José Antolín Aké-Castillo^{1*} and Carlos Francisco Rodríguez-Gómez²

¹Instituto de Ciencias Marinas y Pesquerías, Universidad Veracruzana, Calle Hidalgo 617, Boca del Río, Veracruz, 94290, Mexico; ²Escuela Nacional de Estudios Superiores Unidad Mérida, Universidad Nacional Autónoma de México, Carretera Mérida-Tetiz Km. 4, Ucu, Yucatán, 97357, Mexico.

* corresponding author's email: aake@uv.mx

Abstract

It has been 19 years since the first bloom of the non-toxic dinoflagellate *Peridinium quadridentatum* was recorded in Veracruz, Mexico. Since then, recurrent blooms have occurred in Veracruz central coast, specifically in the port of Veracruz and Boca del Río, the most important cities with an extended urban coastal zone. Prior to the first reported *P. quadridentatum* blooms, the cause of discoloured water in southwestern Gulf of Mexico were recurrent blooms of the toxic dinoflagellate *Karenia brevis*. Though not toxic, *P. quadridentatum* blooms cause hypoxia and significant water discoloration which is unappealing to beachgoers. We analysed the information generated through 13 years of observations of *P. quadridentatum* blooms in different studies in Veracruz including: occurrences, annual dynamics, and diel behaviour of the species. *Peridinium quadridentatum* blooms at the beginning of the rainy season when salinity decreases, with warm water temperature, with cell abundances increasing during the day and under a relatively high Redfield ratio of dissolved nutrient concentrations where N is not limiting. We believe that the benthic-planktonic habitat and the vertical migration of this dinoflagellate is favourable for the daytime blooms. We characterized the blooms of *P. quadridentatum* as an occasional daily diurnal surface (ODDS) forming harmful algal bloom species in Veracruz.

Keywords: benthic microalgae, *Blixaea*, dinotom, Gulf of Mexico, *quinquecorne*

<https://doi.org/10.5281/zenodo.7034930>



Introduction

Peridinium quadridentatum (Stein) Hansen is a thecate dinoflagellate characterized by the possession of four thick spines at the hypotheca (Fig. 1). Specifically, the spines are in pairs on each antapical plate, though a variety exists which exhibits only three spines: one on the first antapical and two on the second antapical plate (Aké-Castillo and Vázquez, 2011). *Peridinium quadridentatum* belongs to the family Kryptoperidiniaceae (Gottschling *et al.*, 2017), whose members utilize a tertiary endosymbiont derived from a diatom to carry out photosynthesis. This species was formerly known as *Heterocapsa quadridentata* Stein, which has been synonymised to *Peridinium quinquecorne* Abé and *Protoperidinium quinquecorne* (Abé) Balech. Recently Gottschling *et al.* (2017) erected the new genus based in the type of *Peridinium quinquecorne* and transferred the species: *Blixaea quinquecornis* (Abé) Gottschling, giving priority to this type over the older *H. quadridentata* type, arguing that the endosymbiont has not been verified in organisms under the name of *P. quadridentatum*.

Peridinium quadridentatum is non-toxic, widely distributed in tropical and subtropical regions (Rodríguez *et al.*, 2021). It is considered a harmful species because it can cause oxygen depletion, increases turbidity, and discolouration of the water creating unaesthetic conditions for visitors at beaches (Okolodkov *et al.*, 2016; Rodríguez-Gómez *et al.*, 2021). *Peridinium quadridentatum* was first recorded forming a bloom in Veracruz, Mexico in 2002 (Barón-Campis *et al.*, 2005). Since then, recurrent blooms have been recorded in at least one location along

the State of Veracruz coast every year (Aké-Castillo *et al.*, 2013; Rodríguez-Gómez *et al.*, 2015; unpublished data). These blooms appear to have replaced the *Karenia brevis* blooms that formerly occurred in the region (Aké-Castillo *et al.*, 2014; Rodríguez-Gómez *et al.*, 2015).

Rodríguez-Gómez *et al.* (2019a) proposed a conceptual model for describing the blooms of *P. quadridentatum* in Veracruz. This model includes the preferential uptake of certain forms of limiting nutrients and general environmental conditions that favor the blooms. Rodríguez-Gómez *et al.* (2019b) further studied the short-term responses of this species to high-frequency environmental fluctuations and demonstrated the bloom population vertically migrates up and down in the water column on a diel basis. The objective of this work was to construct a more complete descriptive model describing the dynamics of the *P. quadridentatum* blooms often observed off Veracruz, Mexico, and along the southwestern Gulf of Mexico generally.

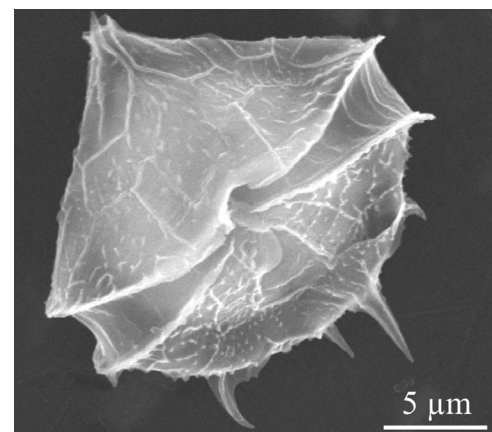


Fig. 1. Microphotograph (SEM) of the dinoflagellate *Peridinium quadridentatum* from Veracruz, Mexico.



Material and Methods

For the conceptual characterization of *P. quadridentatum* blooms in Veracruz, we used the information generated in previous works: Okolodkov *et al.* (2007, 2016); Aké-Castillo *et al.* (2013, 2014); Rodríguez-Gómez *et al.* (2015, 2019a, b).

Results and Discussion

The literature review enabled us to summarise aspects of the ecology of *Peridinium quadridentatum* blooms in Veracruz as follows:

- 1) The species is present all year in some sites along the coast of Veracruz-Boca del Río municipalities.
- 2) Blooms are evident as discoloured (reddish-brown) surface patches that last for short periods of time over the course of the year.
- 3) Blooms occur during the first months of the rainy season (July-August) reaching around 30 thousand cells per millilitre.
- 4) Blooms occur when concentrations of nitrogen (ammonium and nitrates) are high and phosphate (orthophosphate) is limiting, i.e. under relatively high N:P ratios.
- 5) Blooms are most apparent during the daylight hours with cells densities on the surface increasing during the morning, reaching a maximum concentration in the afternoon ($> 3,000 \text{ cell mL}^{-1}$). Surface cell concentrations begin decreasing toward sunset with the lowest concentration observed at night ($< 1,000 \text{ cell mL}^{-1}$). Concomitantly, *P. quadridentatum* abundances in bottom substrates (coral rubble, macroalgae, seaweed, and the seagrass *Thalassia testudinum*)

increase during night and decrease during the day.

6) Blooms occur from one to four days.

7) Surface blooms may occur every year at some locations.

A further breakdown of what is known about the duration and physical location of the bloom is shown in Table 1.

Table 1. *Peridinium quadridentatum* bloom characteristics in Veracruz, Mexico. “Occasional” is defined as blooms occurring one to five times in a year in different locations. “Daily” indicates blooms lasting one to four days. “Diurnal” denotes blooms observed during the day. “Surface” indicates surface blooms that discoloured the water.

Bloom characteristic	References						
	1	2	3	4	5	6	7
Occasional	✓			✓		✓	
Daily		✓	✓		✓		✓
Diurnal		✓	✓	✓	✓	✓	✓
Surface	✓	✓	✓		✓	✓	✓

1) Okolodkov *et al.*, 2007; 2) Okolodkov *et al.*, 2016; 3) Aké-Castillo *et al.*, 2013; 4) Aké-Castillo *et al.*, 2014; 5) Rodríguez-Gómez *et al.*, 2015; 6) Rodríguez-Gómez *et al.*, 2019a; 7) Rodríguez-Gómez *et al.*, 2019b.

Data specifically documenting how the diel vertical migration pattern of *P. quadridentatum* affects surface cell concentrations are shown in Fig. 2. According to this information, we characterized the blooms as an occasional daily diurnal surface harmful algal bloom (ODDS-HAB) (Fig. 2).



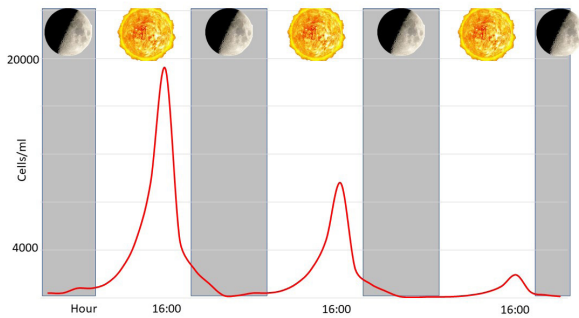


Fig. 2. Diel variation in the surface cell concentrations of *Peridinium quadridentatum*. Red line indicates increase/decrease of cell concentration during a three-day bloom period.

Although the species is present all year in the coasts of Veracruz, it maintains low cell densities most of the months. Contrary to other HAB species around the world, the blooms of *P. quadridentatum* in Veracruz are of short duration (from one to four days). For example, the blooms of *Karenia brevis* (C.C. Davis) Gert Hansen & Moestrup (Tominack *et al.*, 2020) and *Pyrodinium bahamense* Plate (Gárate-Lizárraga *et al.*, 2013), can last several weeks or months. Although ODDS-HAB of *P. quadridentatum* in Veracruz may occur at the beginning of the rainy season, they also can occur occasionally from October to January after the events of cold fronts that affect this region in the Gulf of Mexico.

We believe that large populations of *P. quadridentatum* develop at the bottom, as other blooming benthic dinoflagellates do, such as *Prorocentrum* and *Ostreopsis* (Shears and Ross 2009; Zou *et al.*, 2020). This would occur prior to the rainy season. The initiation of the surface blooms of the species at the beginning of the rainy season may be triggered by the decrease of seawater salinity. The benthic-planktonic condition of the species (Horstmann, 1980; Okolodkov *et al.*, 2016),

is a property that favours the daily dynamics of the blooms, allowing the species to migrate into the water column. If migration by itself is a possible explanation for the blooms, the populations during the rainy seasons would take advantage of the surface condition at daylight hours, for example higher light intensity or availability of a limiting nutrient (Katano *et al.* 2011). This could explain the diurnal changes in water colour and surface vanishing during the night-time.

Other possible explanation is that local hydrodynamics may be concentrating and dispersing blooms in a diurnal cycling. For example, stratification and wind force, maintain surface blooms of *Lingulodinium polyedra* (Ruiz-de la Torre *et al.*, 2013). The ODDS blooms of *P. quadridentatum* in Veracruz have occasionally been observed in elongated patches parallel to the coastal zone between the breakwaters and rarely outside these areas, suggesting cell accumulation due to the presence of convective cells, i.e. Langmuir cells (Evans and Taylor, 1980).

In any case, the end of the surface bloom could be the result of decreasing population, staying some days on the bottom to recover cell density, and blooming again in the following weeks. The clarification of the life history of *P. quadridentatum* and the possible relation with hydrodynamic processes will be a key for understanding its blooms.

The characterization of blooms of *P. quadridentatum* recorded in Veracruz, Mexico (ODDS-HAB), are consistent with reports of blooms of this species in other parts of the world (Horstmann, 1980; Trigueros and Orive, 2000). The conceptual characterization for blooms of *P. quadridentatum* can be



applied in general for the species or other species that behave similarly to synthesize our knowledge of the ecology of this type of bloom dynamics.

Acknowledgements. We would like to thank all the persons that have warned us about the occurrence of the discolouration of water along the Veracruz-Boca del Río coasts that allowed us to record the blooms for some years. CFRG appreciates the postdoctoral scholarship granted by DGAPA-UNAM (Post Doctoral Scholarship Program at UNAM). We appreciate the comments made by reviewers and corrections made in the writing style.

References

- Aké-Castillo, J.A. and Vázquez, G. (2011). *Acta Bot. Mex.* 94, 125-140.
- Aké-Castillo, J.A., Rodríguez-Gómez, C.F., Campos-Bautista, G. (2013). Libro de resúmenes, II Congreso de la Sociedad Mexicana para el Estudio de los Florecimientos Algales Nocivos, p. 23.
- Aké-Castillo, J.A., Okolodkov, Y.B., Rodríguez-Gómez, C.F., Campos-Bautista, G. (2014). Golfo de México. Contaminación e impacto ambiental: diagnóstico y tendencias, 133-146.
- Evans, G.T., Taylor, F.J.R. (1980). *Limnol. Oceanogr.* 25, 840-845.
- Gárate-Lizárraga, I., Pérez-Cruz, B., Díaz-Ortiz, J. A., Alarcón-Tacuba, M.A., *et al.*, (2013). *CICIMAR Oceanides* 28, 37-42.
- Gottschling, M., Calasan, A.Z., Kretschmann, J., Gu, H. (2017). *Phytotaxa* 306, 296-300.
- Horstmann, U. (1980). *J. Phycol.* 16, 481-485.
- Katano, T., Yoshida, M., Yamaguchi, S., Hamada, T., *et al.*, (2011). *Plankton Benthos Res.* 6, 92-100.
- Okolodkov, Y.B., Campos-Bautista, G., Gárate-Lizárraga, I., González-González, J.A.G., *et al.*, (2007). *Aquat. Microb. Ecol.* 47, 223-237.
- Okolodkov, Y.B., Campos-Bautista, G., Gárate-Lizárraga, I. (2016). *Mar. Pollut. Bull.* 108, 289-296.
- Rodríguez-Gómez, C.F., Aké-Castillo, J.A., Campos-Bautista, G., Okolodkov, Y.B. (2015). *E-Bios* 2, 178-191.
- Rodríguez-Gómez, C.F., Vázquez, G., Aké-Castillo, J.A., Band-Schmidt, C.J., Moreno-Casasola, P. (2019a). *Estuar. Coast. Shelf. Sci.* 230, 106412.
- Rodríguez-Gómez, C.F., Aké-Castillo, J.A., Vázquez, G. (2019b). *J. Coast. Res.* SI 92, 22-32.
- Rodríguez-Gómez, C.F., Vázquez, G., Maya-Lastra, C.A., Aké-Castillo, J.A., *et al.*, (2021). *Mar. Biol.* 168, 29.
- Ruiz-de la Torre, M.C., Maske, H., Ochoa, J., Almeda-Jauregui, C.O. (2013). *PLoS ONE* 8, e58958.
- Shears, N.T., Ross, P.M. (2009). *Harmful Algae* 8, 916-925.



Tominack, S.A., Coffey, K.Z., Yoskowitz, D., Sutton, G., Wetz, M.S. (2020). PLoS ONE 15, e0239309.

Trigueros, J.M. and Orive, E. (2000). J. Plank. Res. 22, 969-986.

Zou, J., Li, Q., Lu, S., Dong, Y., *et al.*, (2020). Mar. Pollut. Bull. 158, 111313.



Protoceratium reticulatum bloom in NW Iberia mid-shelf waters

Maria Teresa Moita^{1*}, Paulo B. Oliveira², Ana Santos³, Nuno Zacarias³, Carlos Borges³, Carla Palma³, Ana Amorim^{4,5}

¹CCMAR - Centro de Ciências do Mar, Universidade Algarve, Campus Gambelas, 8005-139 Faro, Portugal; ²IPMA - Instituto Português Mar e Atmosfera, R. Alfredo Magalhães Ramalho 6, 1495-165 Lisbon, Portugal; ³IH- Instituto Hidrográfico, Rua das Trinas 49. 1249-093 Lisbon, Portugal; ⁴Dep. Biologia Vegetal, Faculdade Ciências, Universidade Lisboa, Cpo. Grande, 1749-016 Lisbon, Portugal; ⁵MARE - Centro de Ciências do Mar e Ambiente, Faculdade de Ciências, Universidade Lisboa, Campo Grande, 1749-016 Lisbon, Portugal.

* corresponding author's email: tmoitagarnel@gmail.com

Abstract

The yessotoxin (YTX)-producing dinoflagellate *Protoceratium reticulatum* is a cosmopolitan species occasionally observed in Portuguese coastal waters. In September 2019, and for the first time, a bloom was detected during a cruise carried out offshore F. Foz, Portugal (latitude 40°13' N). We sampled a cross shelf section three times in one week, and the results revealed the bloom was already present at mid-shelf in stratified warm waters and was separated from the coast by coastal upwelling waters. Wind data, sea surface temperature (SST) and chlorophyll *a* (Chl *a*) satellite images indicated that two days prior to the cruise there was a short but strong upwelling event and that, in the leeward side of an upwelling plume rooted at cape Mondego, there was a large patch of Chl *a*. The *P. reticulatum* bloom coincided with the northern side of this patch. It was distributed above the pycnocline, in waters with temperatures from 14° to 17°C, reaching maxima of 2,250 cells L⁻¹ at the surface (17 °C). During the upwelling relaxation conditions observed until the end of the cruise, the bloom approached the coast although being observed in low numbers at the most coastal station. Cysts of *P. reticulatum* were observed in the water column, mainly at the end of the cruise, suggesting encystment was occurring. *P. reticulatum* co-occurred within a dense mixture of diatoms and dinoflagellates, in particular other HAB species such as a *Dinophysis acuta* (22.4 x 10³ cells L⁻¹) and *Pseudo-nitzschia seriata* group (137 x 10³ cells L⁻¹).

Keywords: *Protoceratium reticulatum*, NE Atlantic, Iberian upwelling system, encystment

<https://doi.org/10.5281/zenodo.7034945>



Introduction

Protoceratium reticulatum (Claparède & Lachmann) Bütschli 1885, is a cosmopolitan dinoflagellate with a life cycle that includes planktonic and benthic cyst stages. Strains and isolates of *P. reticulatum* from different regions of the world showed the species comprises at least three ribotypes corresponding to cold, moderate and warm ecotypes, with optimum growth respectively at 15 °C, 20 °C and from 20 to 25 °C (Wang *et al.*, 2019). The species is a yessotoxin-YTX producer (Satake *et al.*, 1997) and blooms have been associated with shellfish diseases and mass mortalities worldwide (Cassis, 2005; King *et al.*, 2021).

On the west coast of Portugal *P. reticulatum* vegetative cells have been reported in plankton samples since the 80's, although seldom observed (Moita and Vilarinho, 1999). The species was also reported more recently in south Iberian Atlantic coastal waters (Paz *et al.*, 2007; Santos *et al.*, 2021). Despite the few references on the presence of this species in the water column, historical cyst records in sediment cores indicate that *P. reticulatum* has been a common species in Atlantic Iberian phytoplankton assemblages in the last two centuries (Amorim and Dale, 2006; Ribeiro *et al.*, 2016; García-Moreiras *et al.*, 2019) with a distribution center around 39°51.0' N, 9°17.0' W, close to major discontinuities in bottom topography (Nazaré Canyon) and coastal morphology (Estremadura Promontory) (Ribeiro *et al.*, 2016). Similar results were obtained in studies based on surface sediments along the W Atlantic Iberian coast. In 1996, a cyst survey covering inshore stations along the coast showed a maximum relative abundance of *P. reticulatum* (24%) at 39°21.1' N (Amorim,

2002). This was also reported by Sprangers *et al.* (2004) from box core surface sediments taken offshore NW Iberia where this species reached the highest relative abundances (> 50%) at the latitude of the Nazaré Canyon (39°35.4' N). In 2019, a surface cyst survey covering the shelf between 40°07' N and 40°49' N (F. Foz and Aveiro) revealed the species maxima were located at mid-shelf, in muddy sediments, reaching 25% of total cysts at 40°12' N (García-Moreiras *et al.*, 2021).

This paper describes the oceanographic conditions associated with the first *P. reticulatum* bloom detected in Portuguese shelf waters during the last 40 years of studies.

Material and Methods

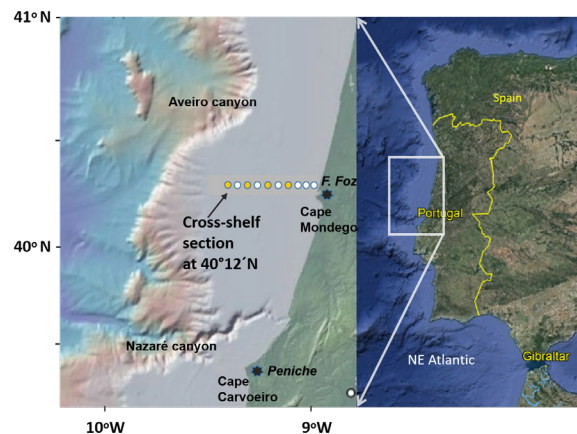


Fig. 1. Map with the location of sampling stations: phytoplankton and nutrients (white circles); CTD casts (yellow and white circles).

Study area

The NW coast of Portugal is part of the north Atlantic Iberian upwelling system, where seasonal upwelling is induced by northerly winds from late spring to early Autumn



(Fiuza *et al.*, 1982). The study was conducted where the NW Portuguese shelf is wider, located between two submarine canyons, and where stratification conditions are enhanced during summer (Fig. 1). Under upwelling conditions, that area can be limited by two major upwelling filaments, rooted at F. Foz (at Cape Mondego) and Aveiro, between which, there is a recurrent lower average summer frontal probability (Relvas *et al.*, 2007). This means that it can be described as a mid/outer shelf stratified pool surrounded by nutrient upwelled enriched waters, that could favour the development of populations of autotrophic dinoflagellates.

Data and methods

Data are from a cruise onboard of the NRP Auriga that covered a cross shelf section, at 40°12' N, three times during the same week (12, 14 and 19 Sept 2019) (Fig. 1). Water column temperature and salinity were profiled with a CTD Ocean Seven 320Plus Woce, Idronaut, coupled with a Seapoint nephelometer. Water samples were collected with Niskin bottles at 5 m, 10 m, 20 m, 30 m, 50 m and 75 m (or near bottom in shallower areas). Phytoplankton water samples were preserved with hexamethylenetetramine buffered formalin and the cells were counted in 50 mL subsamples by the Utermöhl technique (Hasle, 1978). Different cells isolated from water samples were analyzed under a Scanning Electron Microscope (SEM). The identification of *P. reticulatum* was based on the morphologic characteristics of cells isolated from the cruise and observed under SEM (*e.g.* epitheca with six pre-cingular plates) as on the presence of cysts with a characteristic archeopyle and typical hooked processes.

Water samples for nutrient determination were preserved at temperatures below -20 °C and the analyses were performed within 1 month after sampling. Nutrients (nitrate plus nitrite - NO_x, ammonia - NH₄, reactive phosphorus - PO₄, reactive silica - SiO₂) were analysed by UV/vis spectroscopy and using a Skalar SANplus Segmented Flow autoanalyser (see Borges *et al.*, 2019).

To provide information on the regional and large-scale patterns before the surveys, synoptic maps of satellite-derived SST and Chl *a* were produced. The SST data, retrieved from the Sea and Land Surface Temperature Radiometer (SLSTR) at ~1 km resolution, were obtained from EUMETSAT. The Chl *a* data at 300 m resolution were provided by the PML Remote Sensing Group / Natural Environment Research Council (NERC) Earth Observation Data Acquisition and Analysis Service (NEODAAS).

Results and Discussion

Figure 2 shows that three upwelling favourable wind events (black arrows) occurred since the 30th August until the beginning of the cruise, led to a decrease of about 2.5° C (red arrow) in SST. After the first cross shelf section coverage, on Sept 12th, upwelling relaxation conditions prevailed up to the end of the cruise. Those upwelling vs. downwelling conditions are also visible on the satellite SST images (Fig. 3). The spatial distribution of the upwelling filament was complex and quite parallel in NE-SW direction as highlighted by the dashed line on the left top image (SST on Sept 4th). The bottom images in figure 3 show that on the leeward side of those filaments (highlighted by the dashed lines), there is a progressive increase in chl *a* that reached concentrations higher than 5 mg m⁻³.



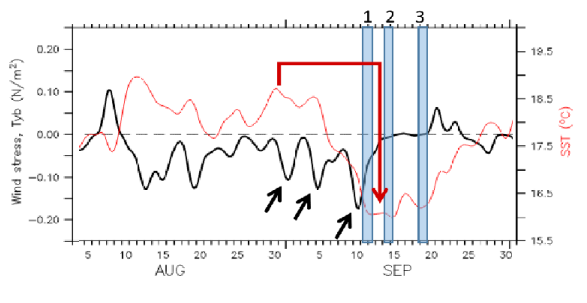


Fig. 2. Daily meridional wind stress anomaly (black) and SeaSurface Temperature (red) during August and September 2019. Blue columns indicate sampling dates.

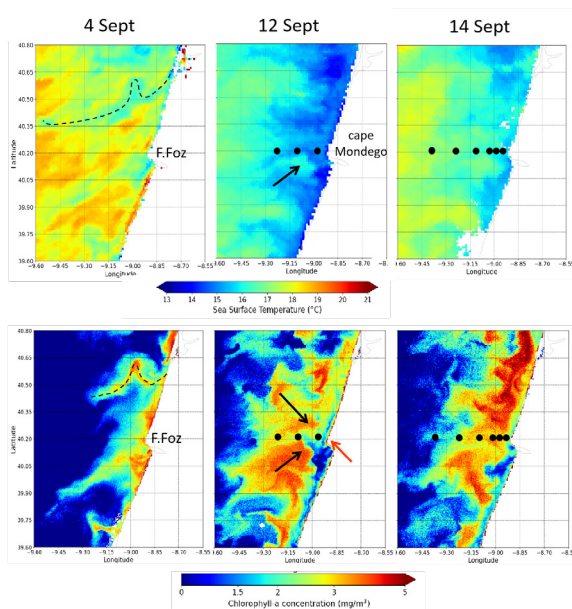


Fig. 3. Maps of satellite SST (°C) (top) and Chl *a* concentration (mg m^{-3}) (bottom), one week before the beginning of the cruise (12th Sept 2019) and two days after (adapted from Nunes, 2021).

On Sept 12th, the sampling section was very close to the cape Mondego filament. To the south of the filament, a pool of warmer water can be observed (black arrow) and the filament seems to interrupt the Chl *a* patch. Another important feature to retain from the images on Sept, 12th and 14th is that, the

main chlorophyll patches are displaced from the coast (red arrow) by the colder coastal upwelled waters. The vertical distribution of water density (σ_T) (Fig. 4A) followed the temperature (see Sept 14th on Fig. 4B), due to a very small variation in salinity (35.75 to 35.9). The water column was stratified with upwelling of colder waters close to the coast on the first two days. On the third day there is clear upwelling relaxation. The distribution of NO_x and PO_4 shows the water column was not nutrient depleted, even at midshelf which is not a common feature at this time of the year above the pycnocline (Moita, 2001).

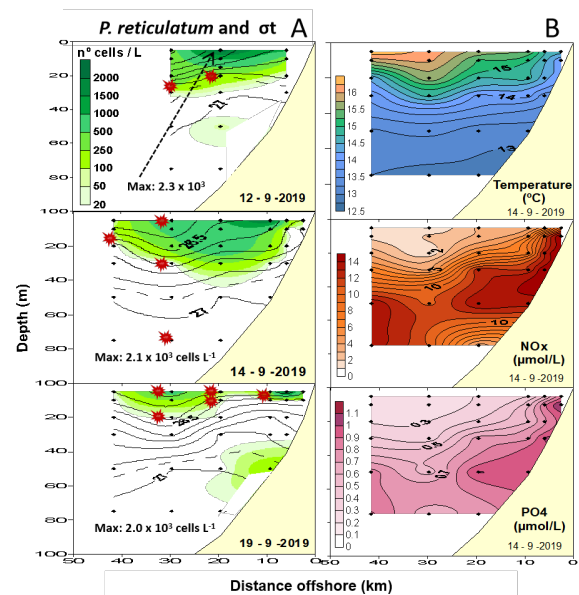


Fig. 4. Cross-shelf distribution of: (A) *P. reticulatum* (green) underlying density anomaly - σ_T (isolines) on Sept 12, 14 and 19th; Red stars indicate *P. reticulatum* cysts presence in the water; (B) Temp., NO_x and PO_4 on Sept 14th.

The *P. reticulatum* bloom was already established at mid-shelf (Fig. 4A) on Sept 12th, in waters with temperatures from 14 °C to 17 °C, and was separated from the coast

by colder upwelled waters more visible on Sept 14th. With the upwelling relaxation, the bloom approached the coast never exceeding 200 cells L⁻¹ at the innermost station. All the observed cysts (red stars in Fig. 4A) had cell contents and were distributed above the pycnocline matching the distribution of the planktonic stages. This suggests that cysts originated from encystment in the water column and not by cyst resuspension from sediments.

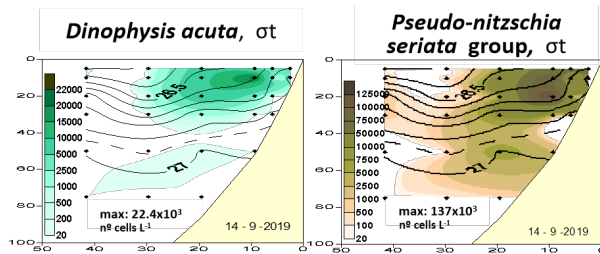


Fig. 5. Cross-shelf distribution of *D. acuta* and *P. seriata* group underlying density anomaly (σ_T).

Protoceratium reticulatum reached its maximum (2.3×10^3 cells L⁻¹) on Sept 12th, at the surface (5 m depth), while other HAB accompanying species such as *D. acuta* and *P. seriata* group had their maxima on Sept 14th and were observed below *P. reticulatum* in the water column. *Dinophysis acuta* reached one of the highest maxima for the region, at lower depths than usually reported (10 m instead of the pycnocline). Despite the bloom approaching the coast on Sept 19th, the HAB monitoring program did not detect *P. reticulatum* cells nor yessotoxins in shellfish, which may reflect the low species concentrations observed at the innermost stations (<https://www.ipma.pt/pt/bivalves/fito/index.jsp>).

This is the first reported *P. reticulatum* bloom on the Portuguese coast, with concentrations

close to those described to cause yessotoxin shellfish contamination in Norway (Aasen *et al.*, 2004). Very little is known on *P. reticulatum* in Iberian waters. Work is now ongoing to investigate its ribotype and yessotoxin profile. This work also describes, for the first time in the study area, at the end of summer and after important upwelling events, that the presence of stratified waters not nutrient depleted at mid-shelf were able to support dense phytoplankton blooms at the surface ($> 5 \text{ mg m}^{-3}$ Chl *a*). These blooms were characterized by a mixture of diatoms with autotrophic and heterotrophic dinoflagellates.

Acknowledgements. We thank the crew of the NRP Auriga for field work support, Vera Veloso for taxonomic advice, and NERC Earth Observational Data Acquisition and Analysis Service for data supply. This study was developed in the frame of HABWAVE project (PTDC/CTA-AMB/31265/2017), LISBOA-01-0145-FEDER-031265, co-funded by EU ERDF funds within PT2020 and Compete 2020. Funding by FCT strategic projects UIDB/04326/2020 and UIDB/04292/2020 is also acknowledged.

References

- Aasen, J., Samdal, I.A., Miles, C.O., Dahld, E., *et al.*, (2005). *Toxicon* 45, 265-272.
- Amorim, A. (2002). Ph. D Thesis, University of Lisbon, Lisbon. Portugal. 161 pp.
- Amorim, A. and Dale, B. (2006). *Afr. J. Mar. Sci.* 28, 193-197.
- Borges, C., Palma, C., da Silva, C.B. (2019). *Anal. Chem.* 91, 5698-5705.



- Cassis, D. (2005). M.S. Thesis, The Faculty of Graduates Studies (Oceanography). The University of British Columbia, Vancouver, p. 73.
- Fiúza, A., Macedo, M.E., Guerreiro, M.R. (1982). *Oceanol. Acta* 5, 31-40.
- García-Moreiras, I., Delgado, C., Martínez-Carreño, N., García-Gil, S., Muñoz Sobrino, C. (2019). *Glob. Planet. Change* 176, 100-122.
- Hasle, G.R. (1978). *In: Sournia A (ed). Phytoplankton Manual. VI. Monographs on Oceanic Methodology. UNESCO, Paris, pp. 191-196.*
- Moita, M.T. and Vilarinho, M.G. (1999). *Portugaliae Acta Biol., Sér. B, Sist.* 18, 5-50.
- Moita, M.T. (2001). Ph. D Thesis, University of Lisbon, Lisbon. Portugal. 272 pp.
- Nunes, P. (2021). MSc Thesis, University of Lisbon, Lisbon. Portugal, 53 pp.
- Paz, B., Riobó, P., Ramilo, I., Franco, J.M. (2007). *Toxicon* 50, 1-17.
- Relvas, P., Barton, E.D., Dubert, J., Oliveira, P.B., *et al.*, (2007). *Prog. Oceanogr.* 74, 149-173.
- Ribeiro, S., Amorim, A., Abrantes, F., Ellegaard, M. (2016). *The Holocene* 26, 874-89
- Santos, M., Moita, M.T., Oliveira, P.B., Amorim, A. (2021). *J. Sea Res.* 167, 101982.
- Satake, M., MacKenzie, L., Yasumoto, T. (1997). *Nat. Toxins* 5, 164-167.
- Sprangers, M., Dammers, N., Brinkhuis, H., van Weering, T.C.E., Lotter, A.F. (2004). *Rev. Palaeobot. Palynol.* 128, 97-106.
- Wang, N., Mertens, K.N., Krock, B., Luo, Z., *et al.*, (2019). *Harmful Algae* 88, 101610.



Harmful phytoplankton species in coastal and deep waters around Cozumel, Mexican Caribbean

Carlos F. Rodríguez-Gómez^{1*}, Vanesa Papiol¹, Ismael Mariño-Tapia¹, Gabriela Vázquez², Cecilia Enriquez¹

¹ UNAM, Escuela Nacional de Estudios Superiores Unidad Mérida, Carr. Mérida-Tetiz, 97357 Mérida, Yucatan, Mexico; ² INECOL A.C., Red de Ecología Funcional, Carr. Antigua a Coatepec, 91073 Xalapa, Veracruz, Mexico.

* corresponding author's email: carlosfco.rodriguez@gmail.com

Abstract

The distribution and abundance of harmful algal blooms (HABs) species is influenced by biotic and abiotic characteristics of the ecosystem. Here, we studied the relationship between harmful bloom forming phytoplankton species and physicochemical and hydrological factors in the Mexican Caribbean. Samplings were performed in oceanic (0 - 200 m depth; daytime) and coastal (0 - 20 m depth; circadian cycles) waters to the east and west of Cozumel Island at different depth layers. The phytoplankton community was dominated by the nitrogen-fixing cyanobacteria *Trichodesmium* spp. In the oceanic region, the highest densities of HABs species *Alexandrium* spp. (2,111 cells L⁻¹), *Phalacroma rotundatum* (56 cells L⁻¹), *Karenia* sp. (333 cells L⁻¹), *Prorocentrum lima* (56 cells L⁻¹), and *Prorocentrum rhathymum* (56 cells L⁻¹) were recorded in the mixed layer: at the surface and the maximum chl *a* fluorescence layer, associated with high temperature, lower salinity, and low nutrient concentrations. In the coastal zone, where reduce depth favors mixing and resuspension processes, the benthic species *Gambierdiscus* sp. was also recorded. The highest densities of the HABs species *Alexandrium* sp. (200 cells L⁻¹), *Gambierdiscus* sp. (40 cells L⁻¹) and *Phalacroma rotundatum* (40 cells L⁻¹) occurred during both day and night; for *Karenia* sp. (60 cells L⁻¹) and *Prorocentrum lima* (60 cells L⁻¹) only during the night, and for *Prorocentrum rhathymum* only during the day, seemingly related to variations in the phosphorous nutrients.

Keywords: phytoplankton ecology, diatoms, dinoflagellates, circadian cycles, stratification

<https://doi.org/10.5281/zenodo.7034953>



Introduction

The frequency of occurrence of harmful algal blooms (HABs) in the Caribbean Sea has increased according to records from 1985 to 2018 (Hallegraeff *et al.*, 2021). Globally, it is one of the regions with the highest recurrence of intoxications associated with toxic phytoplankton due to the presence of ciguatoxins in fish, which when consumed by humans, cause ciguatera illness (Hallegraeff *et al.*, 2021; Sunesen *et al.*, 2021). Besides ciguatera, different types of intoxications have been recorded in the region, such as those produced by paralytic shellfish toxins (PST) and neurotoxic shellfish toxins (NST) (Sunesen *et al.*, 2021).

In the Mexican Caribbean the dinoflagellate *Pyrodinium bahamense* var. *bahamense* stands out as an important HAB species, forming blooms with high densities in coastal lagoons (Gómez-Aguirre, 1998). Recent works have recognized the presence of different bloom-forming species, especially benthic dinoflagellates associated with macroalgae. Among such species, *Gambierdiscus/Fukuyoa*, *Ostreopsis*, *Amphidinium*, *Prorocentrum* and *Coolia* stand out (Almazán-Becerril *et al.*, 2015; Durán-Riveroll *et al.*, 2019; Tarazona-Janampa *et al.*, 2020). However, knowledge of the environmental factors that are associated with HAB-forming species is scarce.

Oceanic and coastal environments are contrasting, mainly due to the bathymetric differences between them. These differences modify the physical and chemical characteristics of the water that regulate the growth and distribution of phytoplankton (Whitney *et al.*, 2005), including harmful

and/or toxic phytoplankton. In oceanic zones, outside the continental shelf, characterized by deep waters, the distribution of planktonic communities is mainly associated with mesoscale physical processes influenced by differences in water density (Mena *et al.*, 2019). In contrast, in the shallow coastal zone, the distribution of phytoplankton communities is associated in the short-term with tidal variation, light and wind intensity.

In this study, we aimed to analyze the relationship between HAB-forming phytoplankton species and physical, chemical, and hydrological factors in the Mexican Caribbean. For this purpose, we used physico-chemical and biological information collected in the oceanic and coastal waters around Cozumel Island.

Material and Methods

Study area

Cozumel Island is located in the east of the Yucatan Peninsula, SE Mexico (Fig. 1). The region has a humid subtropical climate with a rainy season between June and October, a cold front season between November and February, and a warm and dry season between March and May.

The Cozumel Island opens to the Caribbean Sea with depths greater than 1000 m to the east, while to the west, the Island and the Yucatan Peninsula are separated by the narrow (approx. 18 km wide), relatively deep (400 m depth) Cozumel Channel (CC). Cozumel has a semidiurnal micro-tidal regime (range ~0.2 m), and is influenced by a strong western boundary current (Yucatan



current) which flows persistently northward around the island.

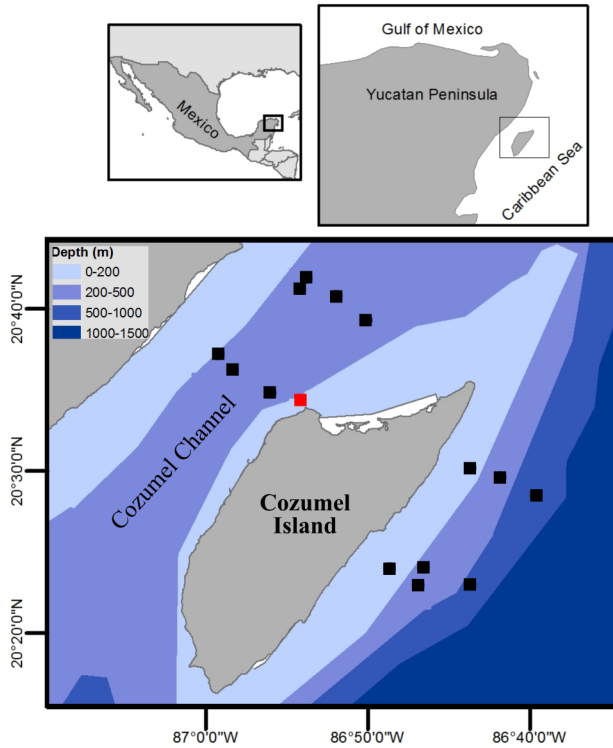


Fig. 1. Study area showing the oceanic stations (black squares) and the coastal sampling point (red square).

Sampling and in situ measurements

Two sampling strategies were used to obtain information on the variation of HAB-forming species and associated environmental factors in the waters around Cozumel Island.

In the oceanic environment, an oceanographic survey on board the R/V Justo Sierra was carried out in April/May 2019 (dry season). Fourteen stations distributed on both sides of Cozumel Island were visited. At each station, three depth strata were sampled: surface (< 10 m), chl *a* fluorescence maximum (62-96 m) and the halocline (96-151 m).

In the coastal zone, a fixed sampling point was established at ~25 m bottom depth, and two 48 h sampling cycles were carried out: one in Sept/Oct 2020 (rainy season) and the other in Apr 2021 (dry season). In each sampling cycle, samples were taken every 4 h at the surface and at 20 m depth.

Water temperature, salinity and density values were recorded *in situ* using a Seabird 9 CTD probe in the oceanic environment, or a SWIFT SVP CTD profiler in the coastal zone. At each sampling depth, both in the oceanic and coastal environment, water samples (250-500 mL) were taken and fixed with Lugols solution to estimate phytoplankton density (Thronsdon, 1978). Water samples (2-3 L) were obtained to estimate the concentration of chl-*a* and nutrients, which were refrigerated until they were transferred to the laboratory.

Phytoplankton, nutrients, and chlorophyll-a
Samples for quantitative analysis of phytoplankton were placed in sedimentation chambers and species composition and abundance were estimated following the Utermöhl method (Hasle, 1978). The refrigerated water samples were filtered through 0.45 µm membranes, which were used to estimate the chl *a* concentration following the trichromatic method (Aminot and Rey, 2000). The filtered water was used to estimate the concentration of dissolved inorganic nitrogen (DIN: ammonium + nitrites + nitrates) and dissolved inorganic phosphorous (DIP) according to colorimetric methods (Strickland and Parsons, 1970).



Results and Discussion

In both the oceanic and coastal zones, the highest phytoplankton densities were of the cyanobacteria *Trichodesmium* spp. Despite this cyanobacterium being the cause of HABs in other parts of the world, in the Caribbean it is considered a resident species and of particular importance in this oligotrophic region, due to the atmospheric nitrogen fixation it performs (Bergman *et al.*, 2013).

In the oceanic region, 70 phytoplankton species were recorded, of which five were HAB-species and occurred at low densities (Table 1). *Alexandrium* sp. was the most abundant taxon, followed by *Karenia*, *Prorocentrum rhathymum*, *Prorocentrum lima* and *Phalacroma rotundatum*. These dinoflagellates were recorded in the surface and Chl *a* fluorescence maximum layer, which had high temperature (26.1-27.8 °C), low salinity (36.2-36.5) and low concentration of nitrogenous and phosphate nutrients. Instead, the halocline layer had the highest nutrient concentrations, but low phytoplankton biomass (Fig. 2). Such results suggest that the stratification in the water column plays some role in defining the vertical distribution of the HAB-forming species.

In the coastal zone, 113 phytoplankton species were recorded, of which six were HAB-forming species: the same taxa as in the oceanic zone, plus the benthic dinoflagellate *Gambierdiscus* sp. (Table 1). Resuspension of this species is likely associated with the greater interaction of water fluxes (e.g. tidal waves, and their associated currents or wind waves, among others) with the seabed in this shallow area. The HABs species *Alexandrium*,

Table 1. Maximum cell abundances of HAB forming species in the oceanic (dry season, 2019) and coastal zone (dry season 2020 and rainy season 2021) of the waters around Cozumel Island (in cells L⁻¹).

Species	Oceanic zone	Coastal zone	MPL
<i>Alexandrium</i> sp.	2111	200	1000
<i>Phalacroma rotundatum</i>	56	40	200*
<i>Karenia</i> sp.	333	60	5000**
<i>Prorocentrum lima</i>	56	60	200
<i>Prorocentrum rhathymum</i>	60	40	200***
<i>Gambierdiscus</i> sp.	-	40	

MPL, maximum permissible limit according to COFEPRIS in Mexico. *Considering the genus *Dinophysis*, ***Karenia brevis* and ****Prorocentrum lima* as a reference.

Gambierdiscus sp., and *P. rotundatum* were recorded during both day and night. *Karenia* sp. and *P. lima* were recorded only during night time, and *P. rhathymum* only during day time, coinciding with the maximum DIP (Fig. 2). HABs species densities at different times of the day suggest a relationship with diel variation in nitrogen and phosphorous nutrients.

The presence in low densities of *P. rotundatum* and *P. lima* in the region suggests a potential risk for diarrheic intoxications (DSP) in the study area.



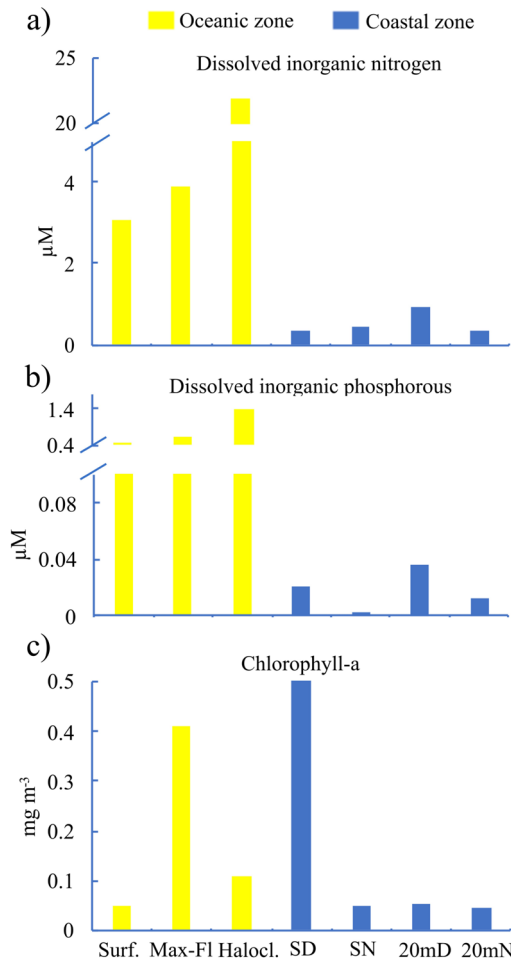


Fig. 2. Average concentration of the dissolved inorganic nitrogen (a), dissolved inorganic phosphorous (b), and Chl *a* (c) in different depths in the oceanic and coastal zone of the waters around Cozumel Island. Surf., surface; Max-FI, maximum of fluorescence; Halocl., halocline; SD, surface daytime; SN, surface nighttime; 20 mD, 20 m depth daytime; 20 mN, 20 m depth nighttime.

Alexandrium was the most abundant bloom-forming dinoflagellate both in the oceanic and the coastal zone. Yet, its density was almost ten times higher in the open sea. According to the guidelines of the Federal Committee for Protection from Sanitary Risks (COFEPRIS, 2016), the maximum

permissible limit in Mexico for the genus *Alexandrium* in seawater is 1,000 cells L⁻¹ (Table 1). Therefore, at least in the oceanic environment, it can be considered that there is a risk for paralytic shellfish poisoning (PSP).

Our results suggest that vertical variation in physical and chemical factors and bathymetric characteristics control the distribution of HAB-forming species at different spatial and temporal scales. Stratification seems to control the vertical distribution of HABs species in the epipelagic zone. In coastal areas, the low water depth and the variations in nutrients availability seem to influence the species composition.

Acknowledgements. The oceanographic survey CEMIE-I was supported by the CEMIE-Oceano project (CONACYT-SENER S0019-2014-06 [0249795]). The coastal surveys were supported under the PAPIIT-UNAM project (IA207120). CFRG appreciates the scholarship granted by the Post Doctoral Scholarship Program at UNAM (DGAPA-UNAM). Authors would like to thank all crew members of the oceanographic vessel Justo Sierra (CEMIE-I cruise) and the coastal surveys for their support during the fieldwork. We are also thankful to A. Martínez, D. Cela, J. Tolome (INECOL A.C.), and K. López Aguiar (PCTY-UNAM) for their help with the nutrients and Chl *a* analysis, and to J. Aragón González (ENES Mérida) for his help with sensors data acquisition and processing.

References

Almazán-Becerril, A., Escobar-Morales, S., Rosiles-González, G., Valadez, F. (2015). Bot. Mar. 58, 115-128.



- Aminot, A. and Rey, F. (2000). International Council for the Exploration of the Sea, 112.
- Bergman, B., Sandh, G., Lin, S., Larsson, J., Carpenter, E.J. (2013). FEMS Microbiol. Rev. 37, 286-302.
- Carrillo, L., Johns, E.M., Smith, R.H., Lamkin, J.T., Largier, J.L. (2016). Cont. Shelf Res. 102, 41-58.
- COFEPRIS. (2016). Lineamiento de trabajo para el muestreo de fitoplancton y detección de biotoxinas marinas. 23 p.
- Durán-Riveroll, L.M, Cembella, A.D., Okolodkov, Y.B. (2019). Front. Mar. Sci. 6, 148.
- Gómez-Aguirre, S. (1998). An. Inst. Biol. Univ. Nac. Autón. Méx., Ser. Zool. 69, 13-22.
- Hallegraeff, G.M., Anderson, D.M., Belin, C., Bottein, M.Y.D., *et al.*, (2021). Commun. Earth Environ. 2, 117.
- Hasle, G.R. (1978). In: Sournia, A. (Ed.) Phytoplankton Manual, 88-96.
- Mena, C., Reglero, P., Hidalgo, M., Sintés, E., *et al.*, (2019). Front. Microbiol. 10, 1698.
- Sunesen, I., Méndez, S.M., Mancera-Pineda, J.E., Bottein, M.Y.D., Enevoldsen, H. (2021). Harmful Algae 102, 101920.
- Strickland, J.D. and Parsons, T.R. (1972). A practical handbook of seawater analysis. 310 p.
- Tarazona-Janampa, U.I., Cembella, A.D., Pelayo-Zárate, M.C., Pajares, S., *et al.*, (2020). Front. Mar. Sci. 7, 569.
- Thronsdon, J. (1978). In: Sournia, A. (Ed.) Phytoplankton Manual, 69-74.
- Whitney, F.A., Crawford, W.R., Harrison, P.J. (2005). Deep Sea Res. Part II Top. Stud. Oceanogr. 52, 681-706.





HA MICROBIOMES



Long-term composition of 16S-based bacterial communities associated with algal bloom events in northern Chile

Andrés Ávila^{*1}, Mariela González-Flores¹, Milko Jorquera², Ignacio Rilling², Carlos Riquelme³, Henry Cameron³, Leonardo Guzmán⁴, Gonzalo Gajardo⁵, Fumito Maruyama⁶, Satoshi Nagai⁷, Shoko Ueki⁸

¹Centro de Excelencia de Modelación y Computación Científica, Universidad de La Frontera, Ave. Francisco Salazar 01145, Temuco, Chile; ²Scientific and Biotechnological Bioresource Nucleus (BIOREN), Universidad de La Frontera, Ave. Francisco Salazar 01145, Temuco, Chile; ³Centro de Bioinnovación de Antofagasta (CBIA), Universidad de Antofagasta, Av. Universidad de Antofagasta s/n, Antofagasta, Chile; ⁴Centro de Estudios de Algas Nocivas (CREAN), Instituto de Fomento Pesquero (IFOP), Padre Harter 547, 5480000 Puerto Montt, Chile; ⁵Laboratorio de Genética, Acuicultura & Biodiversidad, Universidad de Los Lagos, Lord Cochrane 1046, Osorno, Chile; ⁶Center for holobiome and built Environment (CHOBE), Hiroshima University, 1-3-2 Kagamiyama, Higashi-Hiroshima City, Hiroshima 739-8511, Japan; ⁷Japan Fisheries Research and Education Agency, 2-12-4 Fukuura, Kanazawa-ku, Yokohama, Kanagawa 236-8648, Japan; ⁸Institute of Plant Science and Resources, Okayama University, 2-20-1 Chuo, Okayama 710-0046, Japan.

*corresponding author's email: andres.avila@ufrontera.cl

Abstract

There is an increasing interest in how harmful algal blooms affect seawater desalination plants. These plants are critical for supplying municipal drinking water in many arid regions. Blooms can increase the probability of clogging filters, which in turn can disrupt proper plant operations, resulting in temporary shutdowns. Changes in bacterial diversity can be used as predictors of localized algae blooms. In this work, we used high-throughput DNA sequence analyses to study bacterial diversity focused on an event of *Akashiwo sanguinea* bloom in December 2019 on the coast of Antofagasta, Chile, where desalination plants are located. We collected weekly samples of attached-algae bacteria (1.0 µm filter) and free-living bacteria (0.2 µm filter) offshore in Antofagasta city between November 2019 and January 2020. DNA was extracted from the samples and the resulting 16s RNA sequence diversity determined. The resulting data was used to compute alpha diversity indices, Principal coordinate analysis (PCoA), dendrograms, and community composition. We found the relative abundance of attached Cyanobacteria strongly decreased during the bloom whereas Epsilon proteobacteria increased in abundance. Also, relevant functions decreased in blooming in the free-living bacteria.

Keywords: high-throughput DNA, *Akashiwo sanguinea*, algae bloom, bacterial diversity, desalination plants

<https://doi.org/10.5281/zenodo.7034959>



Introduction

There is an increasing interest in harmful algal blooms (HAB) affecting seawater desalination plants. In northern Chile, most plants supply drinking and municipal water. Localized HAB can affect the plant operation, leading to temporary shutdown and changing the HAB holobiome diversity.

Facing the problems of increasing industrial and municipal water demand in arid zones, desalination plants are the main solution. This industry is growing with almost 21,000 projects in over 180 countries (Eke, 2020). These seawater desalination plants can be adversely impacted by harmful algae blooms (HAB) in several ways. For blooms of non-toxin species, the most common issue involves high biomass concentration clogging the desalination membranes. Another major issue is the production of hydrogen sulfide when these blooms decay and the resulting biological oxygen demand reduces oxygen concentrations below 0.5 mg L⁻¹. When hydrogen sulfide rich water is taken into the desalination plant, it readily crosses the processing membranes causing the processed water to have a strong rotten egg smell (Anderson, 2017). When this happens, plant operations have to be suspended until the issue can be resolved, leading to significant hardship for the affected community and increased expenses for plant operations. When toxic blooms occur, toxins released into the water as cells die during the water purification process can also enter the water supply again, leading to a suspension of operations when these toxins are detected. Early detection of both toxic and nontoxic blooms in order to allow desalination plants to take preventive actions (Galán, 2020).

The relation between *A. sanguinea* bloom and bacterial community was recently studied in an indoor environment (Jung, 2021). Changes in bacteria abundance were described in three different groups: during, late, post bloom stages. The Flavobacteria and Gammaproteobacteria are active in the three stages decreasing in late bloom and then increasing in post bloom. Moreover, Alphaproteobacteria is abundant in the bloom phase expecting phototropic genera in the algae riosphere as Rhodobacterias (Li, 2019).

Our main goal is to understand changes in bacterial diversity in a HABs in a coastal scenario comparing attached and free-living bacteria in an *A. sanguinea* bloom in December 2019 in Antofagasta, Chile. This information will help to understand the bacterial diversity before the *A. sanguinea* HAB for keeping water supply and avoid plant clogging.

Material and Methods

Study site

Seawater samples were collected weekly by ship about 100 m offshore south of Antofagasta, Chile (Lat -23.68248, Lon -70.41597), located ~20 km south of the desalination plant.

Sampling

The samples were collected between November 15th, 2019 and January 16th, 2020. The measured parameters included water temperature, salinity, cell concentrations of *A. sanguinea* and Chl *a*. To get the DNA sample, 200 mL of seawater was filtered for 16S-rRNA and 18S-Rrna. In the case of particles, filtering must continue. To separate



free-living and attached bacteria, a tandem filtration is performed with a 1 μm pore-size connected to 0.2 μm pore-sized Sterivex membrane. For 18S-Rna, it uses a single filtration with a 0.2 μm Sterivex membrane (Yarimizu, 2020).

We use high-throughput DNA sequence analyses to study the diversity of alga-associated bacteria (attached and free living) focused on an event of *A. sanguinea* bloom in December 2019 on the coast of Antofagasta, Chile, where desalination plants are located. We considered weekly data from Nov. 2019 to Jan. 2020 in two locations.

Metagenomic data

Each water sample was sequenced in the NGS MiSeq-Illumina 3500 Genetic Analyzer, Applied Biosystems, U.S.A.

Data Analysis

Using QIIME2, we computed alpha diversity indices for previous HAB events (PRE) and during the event (HAB), including Principal Coordinate Analysis (PCoA), and Venn Diagram. Moreover, we search for relevant functions and the dendrogram relating to the samples PRE, HAB, and POST.

Results and Discussion

Taxonomy and bacterial composite

We found that attached *Cyanobacteria* relative abundance changes during the HAB bloom and *Epsilonproteobacteria* increase in abundance. Free bacteria have minor changes in relative abundance with an increase in *Epsilonproteobacteria*.

Relevant functions

From the Faprotax analysis, the attached bacteria relevant functions are chemoheterotrophy, fermentation, and nitrate reduction in the PRE stage, which decrease in the HAB stage. In the case of free-living bacteria, relevant functions are mainly chemoheterotrophy and intracellular parasites followed in a small scale by fermentation, methanol oxidation, methylotrophy, and nitrate reduction. Indeed, chemoheterotrophy and intracellular parasites decrease five weeks before the HAB reaches its minimum, and then increase slowly in the following weeks.

In figure 2, we noticed from the attached bacteria that green samples and yellow samples are close to red samples related to HAB. In the case of the free-living bacteria, we started with yellow samples (PRE) changing to red samples (HAB), and finally the green samples (POST). Check the ordered sample numbering.

Based on our analysis, we detected higher changes in the relative abundances of attached bacteria during PRE and HAB, compared with free-living bacteria. We also found bacterial taxa, which are shared during the long term in analyzed samples. More studies are required to understand the changes and influence of holobiomes in the development of HAB in northern Chile and on its impact on seawater desalination plants.



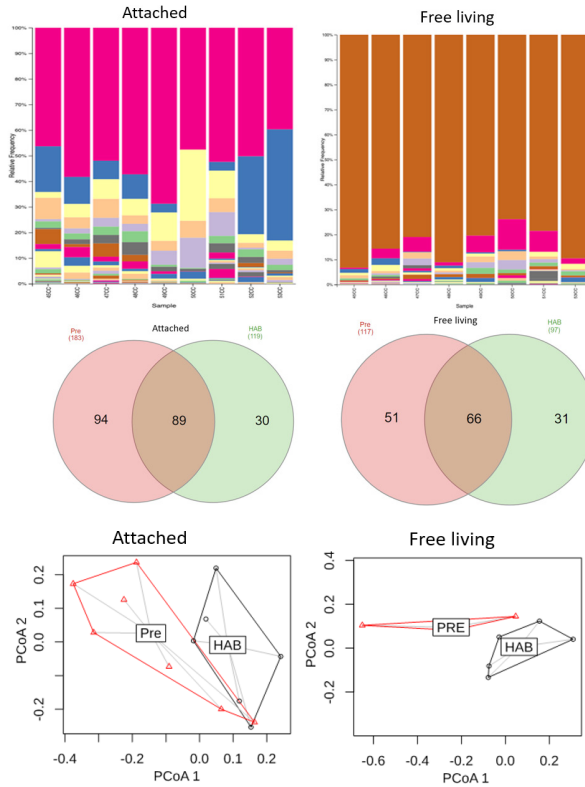


Fig. 1. Relative abundance, Venn plots, and PCoA of PRE and HAB stages for attached and free-living bacteria.

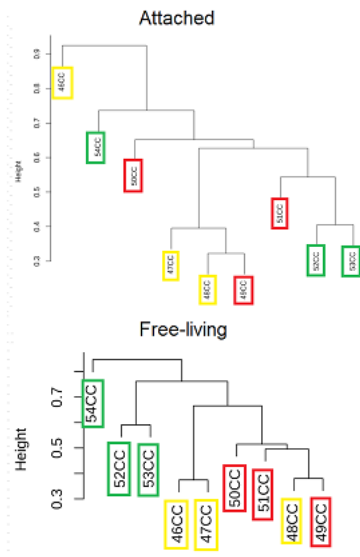


Fig. 2. Dendrograms of attached (up) and free-living (down) bacteria separating by stages: PRE (yellow), HAB (red), POST (green).

Acknowledgements. This research was supported by the SATREPS MACH Project and the supercomputing infrastructure of Soroban at Centro de Modelación y Computación Científica at Universidad de La Frontera.

References

Eke, J., Yusuf, A., Giwa, A., Sodiq, A. (2020). *Desalination* 495, 114633.

Anderson, D. M., Boerlage, S. F., Dixon, M. B. (2017). *Harmful Algal Blooms (HABs) and Desalination: a Guide to Impacts, Monitoring and Management*. 539 pp.

Galán Villegas, L. (2020). *Red tide: characterization, risks and methods for its early detection and reduction of its impact in the operation of desalination plants*. Master thesis, Universidad de Alcalá. Spain, 56 pp.

Li, S., Chen, M., Chen, Y., Tong, J., *et al.*, (2019). *FEMS Microbiol. Ecol.* 95, fiz057.

Jung, S. W., Kang, J., Park, J. S., Joo, H. M., *et al.*, (2021). *Sci. Rep.* 11, 1-11.

Yarimizu, K., Fujiyoshi, S., Kawai, M., Norambuena-Subiabre, *et al.*, (2020). *Int. J. Environ. Res.* 17, 7642.



Comparison of bacterial communities among geographically distinct populations of the benthic dinoflagellate *Prorocentrum lima*

Miguel Martínez-Mercado¹, Clara E. Galindo-Sánchez¹, Edna Sánchez-Castrejón¹, Anaïd Saavedra-Flores¹, Allan D. Cembella², Lorena M. Durán-Riveroll^{3*}

¹Departamento de Biotecnología Marina, Centro de Investigación Científica y de Educación Superior de Ensenada, B. C. Ensenada, Mexico; ²Alfred-Wegener-Institut, Helmholtz-Zentrum für Polar-und Meeresforschung, Bremerhaven, Germany; ³CONACyT-Departamento de Biotecnología Marina, Centro de Investigación Científica y de Educación Superior de Ensenada, B.C. Ensenada, Baja California, Mexico.

* corresponding author's email: lduran@conacyt.mx

Abstract

Members of the *Prorocentrum lima* species complex (PLSC) are most frequently found in high cell abundance in the tropics and sub-tropics and are almost invariably toxigenic. Epiphytic and planktonic bacteria are known to co-occur with such toxigenic *Prorocentrum* but reciprocal allelochemical interactions with the dinoflagellate microbiome have been under-investigated and are poorly understood. The aim of the present study was to identify and compare the bacterial community cultured together with isolates of the PLSC from geographically distant coasts of Mexico. Profiles of bacterial communities associated with dinoflagellate clones were obtained by high-throughput sequencing of 16S V3-V4 amplicons. Our results show that the microbiome of *P. lima* is associated with the location of origin. A similar bacterial diversity was found free-living in culture medium or closely associated with the host dinoflagellate cells. The microbiome comprised a total of fourteen bacterial classes where alpha- and gamma-proteobacteria and Bacteroidia dominated the respective communities. Specifically, members of genera *Labrenzia*, *Roseitalea*, *Cohaesibacter*, *Marivita*, *Muricauda*, *Marinobacter* and *Masilia* were most abundant. Based on known interactions of these genera with other microeukaryotes, they may sustain symbiotic relationships with *P. lima* populations via a variety of allelochemicals and reciprocal nutrient enrichment mechanisms within the phycosphere. Bacterial members identified will improve the study of the toxigenicity, ecology, and biotechnological potential of this benthic dinoflagellate group.

Keywords: Dinoflagellate, *Prorocentrum lima*, microbiome, xenic culture, allelochemicals

<https://doi.org/10.5281/zenodo.7034969>



Introduction

Marine benthic species of the dinoflagellate genus *Prorocentrum* (Ehrenberg) are found around the globe in shallow waters living mainly attached to macroalgae, seagrasses or other benthic substrates (Durán-Riveroll *et al.*, 2019). Epibenthic dinoflagellates are exposed to a microbiome comprising free-living and substrate-attached bacteria and microeukaryotes. Chemical interactions can occur in the extracellular space surrounding the cell, denominated as the phycosphere (Seymour *et al.*, 2017) into which chemicals can diffuse and be exchanged. Chemical interactions within the phycosphere can be either beneficial or detrimental to the epibenthic dinoflagellate, or perhaps mutually beneficial for the microbiome. In the antagonistic case, allelochemicals generated by the dinoflagellate may limit parasitism or reduce competition for inorganic nutrients from the bacterial component, whereas certain bacteria may inhibit growth or survival of the dinoflagellate. In the mutually beneficial case, dissolved or particulate organic matter may be produced by the dinoflagellate, in reciprocal exchange for vitamins or organic macronutrients generated by the bacteria.

The strategic importance of the microbiome in dinoflagellate toxin production and regulation in benthic dinoflagellates is unclear. Associated bacteria within the phycosphere of the benthic dinoflagellate *P. lima* (Ehrenberg) F. Stein influence growth rates and likely also toxin production rate and cell toxin content (Tarazona-Janampa *et al.*, 2020). Elucidation of the microbiome composition is therefore the first step in defining these interactions.

The genus *Prorocentrum* contains more than seventy species, with almost all of the known toxigenic species considered primarily benthic or epibenthic. Some *Prorocentrum* species have not been fully classified and many morphotypes remain provisionally unresolved within various species complexes. Within the *P. lima* species complex (PLSC), molecular methods directed to target sequences of the rRNA gene are required for reliable species classification (Cembella *et al.*, 2021).

We analyzed the microbiome associated with cultures of taxonomically confirmed PLSC isolates from two geographically distant sites on Mexican coasts to evaluate the dependence of the origin on the microbiome structure. The microbiome components were further analyzed to compare the similarity between bacterial communities found free-living in the culture medium and those associated directly to the dinoflagellate cells.

Material and Methods

Prorocentrum lima isolation, culture, and harvest

Prorocentrum lima cells were isolated from macroalgae and seagrasses from Bahía de La Paz, Baja California Sur (Gulf of California, n = 6), and from the Veracruz Reef System (Gulf of Mexico, n = 5). Microscopic examination was performed under a stereodissecting microscope (Discovery.V8, Zeiss). *Prorocentrum lima* single cells were isolated by micropipette into 96-well microplates containing 100 μ L of 50%-strength GSe growth medium modified without soil extract prepared from filtered and autoclaved



seawater at salinity 36. Clonal cultures were maintained on a 12:12 h light:dark cycle at 80 $\mu\text{mol photons m}^{-2} \text{s}^{-1}$ illumination. Where multiple cell divisions were observed, well contents were transferred to 24-well plates with 2 mL of nutrient medium. After observed growth, cells were transferred to 60 x 15 mm Petri plates with modified 50% GSe medium and later maintained as reference cultures at the Department of Marine Biotechnology, CICESE, Ensenada, Mexico.

Dinoflagellate-associated bacterial biomass was generated in 250 mL Erlenmeyer flasks of isolates maintained as xenic reference cultures for approximately two years with monthly transfers (~24 transfers). In late exponential growth phase, dinoflagellate cells and bacteria in the growth medium were separated using UV-sterilized 20 μm mesh sieves under a laminar flow hood. *Prorocentrum lima* cells with their attached or mucus-associated microbiome and free-living bacteria from the growth medium were recovered separately in sterile microtubes by centrifugation (6000 $\times g$ for 3 min). The supernatant was discarded and the cell pellets were frozen at -20 °C until DNA extraction and amplification.

Microbiome sequencing and data analysis

Samples were homogenized in a FastPrep-24 5G instrument (MP Biomedicals) using three cycles of 30 s at 6.0 ms^{-1} with resting incubations of 5 min on ice. Total DNA was extracted with DNeasy Power soil Kit (QIAGEN) according to manufacturer's instructions. The V3-V4 region of the 16S rRNA gene (Klindworth *et al.*, 2013) was amplified to generate Illumina sequencing libraries following the 16S metagenomic sequencing library preparation B protocol. Amplification reactions used

KAPA HiFi HotStart DNA Polymerase (KAPA Biosystems). Amplification products were cleaned with Agencourt AMPure XP beads. Dual indexing was performed with Nextera XT index kit according to the manufacturer's instructions. Libraries were quantified by fluorometry with a Qubit 3.0 (Life Technologies) and sequenced as 250 bp paired-end reads on a MiSeq machine (Illumina).

Sequencing reads were processed in R (v.3.6) with the dada2 v.1.14 general workflow with proper parameter adjustments. Denoised reads were used to form Amplicon Sequence Variants (ASVs) and finally remove chimeras. Taxonomic assignments in dada2 used the SILVA 138.1 database with a confidence threshold of 80. Further analysis of the sequence-count per sample table was conducted in R with functions for phylogenetic and ecological analysis of microbiome data available in the DECIPHER, phangorn, microbiome, phyloseq, and vegan packages. A maximum likelihood tree of ASV sequences was inferred using a GTR+I+G model. Sequence counts per sample were transformed to relative abundances and summarized by respective taxonomic assignment to the class level for visualization of the bacterial community composition. The structure of bacterial communities in the two locations of origin was evaluated by a PERMANOVA analysis (499 permutations) of UniFrac distance matrices, validated by analysis of variance of the groups' dispersions. The first two components of a Principal Coordinates Analysis (PCoA) were used for visualization of the categorical groups.



Results and Discussion

The microbiome of *P. lima* isolates from the Gulf of California was substantially different from that of isolates from the Gulf of Mexico (Fig. 1). A total of 648 ASVs were detected; on average, the samples contained 63 ASVs (min. 45, max. 86). The dinoflagellate cell host- and culture medium-associated bacterial communities of isolates from the two locations of origin were significantly different regarding both UniFrac metrics. This result is likely evidence of the initial differences in the bacteria present at these two locations and thus available for interaction with the dinoflagellate. Once a xenic culture has been established, a diverse microbiome can be sustained through dozens of host-cell generations, an effect also observed for other microalgal species (Jackrel *et al.*, 2020). Nevertheless, the probability of clonal selection in long-term xenic cultures cannot be excluded here.

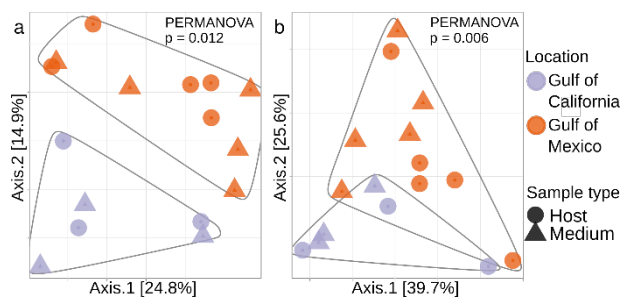


Fig. 1. Bacterial community structure in *Prorocentrum lima* cultures. Principal coordinates analyses of UniFrac distances (a, unweighted; b, weighted) is shown for microbiomes obtained by sequencing of 16S rRNA amplicons of bacteria directly associated with host or free-living in culture medium. Grouping by location of origin was evaluated by PERMANOVA.

The microbiome structure of bacterial samples taken as free-living from the culture medium versus associated to the host dinoflagellate cells did not cluster separately in the ordination. Hence, they cannot be considered as separate groups. One possible explanation for this overlap is that culture conditions – confinement within a small, enclosed, and stable environment – create an artificially expanded “phycosphere” that allows a relatively easy and generalized access to nutrients and potential allelochemicals as secondary metabolites exchanged by molecular diffusion. In natural benthic environments, the phycosphere is more susceptible to disruptive wave action, tidal flux, and wind-driven turbulence that favor molecular dispersion. Under these circumstances, the microbiome must be retained, e.g. within mucus aggregates or biofilms, close to the dinoflagellate cells to facilitate effective interactions for metabolite exchange.

The second objective of this study was to determine the composition of the bacterial community within the microbiome. Similarities at the class level, between paired samples of bacteria from culture medium and host-cells were clear (Fig. 2). At the highly diverse class level, fourteen classes were identified among all sequenced samples. Alphaproteobacteria was the dominant class, occupying > 50%, and up to a maximum 95%, of the ASV composition in each sample. This class has been found commonly associated to planktonic eukaryotic microalgae, such as natural populations of diatoms and other dinoflagellates (Lawson *et al.*, 2018; Maire *et al.*, 2021). Other abundant and widely distributed bacteria belonged to classes Bacteroidia, Gammaproteobacteria, and



Plancto-mycetes. Classes with substantial ASV abundance (> 1%) but present only in some samples were Phycisphaerae and Kapabacteria, mainly in cultured isolates from the Gulf of California (Fig. 2).

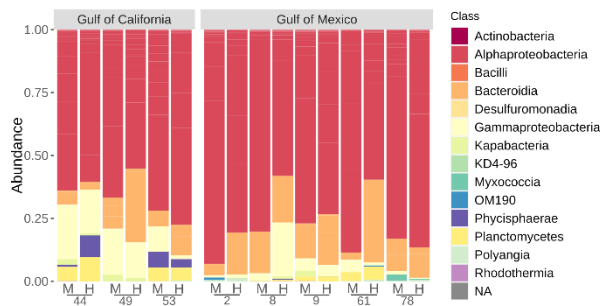


Fig. 2. Bacterial community profiles of *P. lima* xenocultures based on 16S rRNA gene sequence amplicons. Relative abundances at the class level are shown for bacteria associated directly to host dinoflagellate cells (H) cells versus free-living in culture medium (M).

A previous attempt to culture bacteria associated with *P. lima* yielded isolation of bacteria from three classes: Actinobacteria, Alphaproteobacteria and Gammaproteobacteria (Tarazona-Janampa *et al.*, 2020). Our current results confirm the presence of these three classes but add eleven more classes to the diversity profile. The maintenance of such huge bacterial diversity sustained over years in xenocultures may assist in designing optimal culturing conditions to target the other members of the *P. lima* microbiome community for more detailed study.

A closer examination of the members of Alphaproteobacteria reveals the dominance of order Rhizobiales, represented by genus *Labrenzia* as the member present in all isolates with at least 1% abundance. Heterotrophic species in this genus may play a role in the dinoflagellate hosts-stress tolerance due

to dimethylsulfoniopropionate (DMSP) production (Lawson *et al.*, 2018). Other genera identified from Rhizobiales were *Roseitalea* and *Cohaesibacter*, both previously found as core members of endosymbiotic dinoflagellates of Symbiodinaceae (Lawson *et al.*, 2018; Maire *et al.*, 2021). This congruence is rather remarkable given the striking differences in the phycosphere for free-living epibenthic dinoflagellate such as *P. lima*. Finally, the genus *Marivita* (family Rhodobacteraceae) may provide vitamins to the dinoflagellate host contributing to its growth (Park *et al.*, 2017). Representing the Bacteroidia, the genus *Muricauda* (family Flavobacteriaceae) may also help its host by scavenging reactive oxygen species through carotenoids (Maire *et al.*, 2021). *Marinobacter* and *Massilia* represent highly abundant ASVs of Gammaproteobacteria. Some members in these genera can render nutrients such as iron and phosphate biologically accessible for microeukaryotes and presumably other bacteria. In *Massilia*, this bioavailability function was only described in a terrestrial member but this genus has been associated with diatoms in the marine environment (Lupette *et al.*, 2016).

In conclusion, our results show a complex microbiome and suggest potential allelochemical interactions can regulate respective growth and perhaps survival of dinoflagellates and their microbiome members. Despite substantial differences in microbiome structure depending upon the origin of the dinoflagellates, common members of the consortium were found. The specific identity of these bacteria varies by location, but the roles and functions may fill the same specific niches of symbiotic or antagonistic interactions. This study provides



an initial template for elucidation of the role of the microbiome in dinoflagellate toxigenicity and their ecological interactions in natural benthic populations.

Acknowledgements. This work was funded by Cátedras CONACyT Project 1009 and CONACyT Ciencia Básica A1-S-8616. The contribution of Allan Cembella was within Topic 6: Subtopic 6.2-Adaptation of marine life of Alfred-Wegener-Institut, Germany.

References

- Cembella, A.D., Durán-Riveroll, L.M., Tarazona-Janampa, U.I., Okolodkov, Y.B., *et al.*, (2021). *Front. Mar. Sci.* 8, 716669.
- Durán-Riveroll, L.M., Cembella, A.D., Okolodkov, Y.B. (2019). *Front. Mar. Sci.* 6, 148.
- Klindworth, A., Pruesse, E., Schewer, T., Peplies, J., *et al.*, (2013). *Nucl. Acids. Res.* 41-1, e1.
- Jackrel, S.L., Wang, J.W., Schmidt, K.C., Denev V.J. (2020). *ISME J.* 15, 774-788.
- Lawson, C.A., Raina, J.B., Kahlke, T., Seymour, J.R., Suggett, D.J. (2018). *Env. Microb. Rep.* 10, 7-11.
- Lupette, J., Lami, R., Krasovec, M., Grimsley, N., *et al.*, (2016). *Front. Microbiol.* 7, 1414.
- Maire, J., Girvan, S.K., Barkla, S.E., Perez-Gonzalez, A., *et al.*, (2021). *ISME J.* 15, 2028-2042.
- Park, B.S., Guo, R., Lim, W.A., Ki, J.S. (2017). *Mar. Ecol.* 38, e12474.
- Seymour, J.R. Amin, S.A., Raina, J.B., Stocker, R. (2017). *Nat. Micro.* 2, 17065.
- Tarazona-Janampa, U.I., Cembella, A.D., Pelayo-Zarate, M.C., Pajares, S., *et al.*, (2020). *Front. Mar. Sci.* 7, 569.





CYANOBACTERIAL BLOOMS



Macronutrient and B vitamin dynamics of Chowan River (North Carolina, U.S.A.) CyanoHABs

Malcolm A. Barnard^{1*}, Haley E. Plaas¹, Ryan W. Paerl², Colleen M. Karl³, W. Christopher Holland⁴, D. Ransom Hardison⁴, Nathan S. Hall¹, Amy N. Bartenfelder¹, Karen L. Rossignol¹, Jeremy S. Braddy¹, Randolph S. Sloup¹, Hans W. Paerl¹

¹*Institute of Marine Sciences, University of North Carolina at Chapel Hill, Morehead City, 28557 NC, U.S.A.*; ²*Department of Marine, Earth, and Atmospheric Sciences, North Carolina State University, Raleigh, 27695 NC, U.S.A.*; ³*Chowan Edenton Environmental Group, Edenton, 27932 NC, U.S.A.*; ⁴*National Oceanic and Atmospheric Association, NCCOS, Beaufort, 28516 NC, U.S.A.*

*corresponding author's email: malcolm.a.barnard@gmail.com

Abstract

The Chowan River (CR)-Albemarle Sound Estuary, NC has been plagued by a resurgence of toxigenic cyanobacterial harmful algal blooms (CyanoHABs) since 2015. Both N₂-fixing and Non-N₂-fixing cyanobacteria blooms have occurred in the CR blooms and, in summer 2020, potentially harmful N₂-fixing *Dolichospermum* spp. was dominant. To identify the nutritional drivers of the summer 2020 CyanoHAB, we conducted nitrogen (N), phosphorus (P), and B vitamin addition experiments and measured N₂-fixation rates using acetylene reduction assays. Cyanobacteria are generally thought to not require external B vitamins, though the opportunistic use of external vitamins may increase metabolism directly or through stimulation of members of the cyanobacterial 'microbiome'. The CR phytoplankton community exhibited N-limitation with a secondary vitamin limitation in NH₄ addition treatments. B vitamin additions influenced the community composition of the CR CyanoHABs by increasing chlorophyte biomass and reducing cyanobacterial biomass. Furthermore, given the high N₂-fixation rates (240 nmol N L⁻¹ h⁻¹), further research is required to evaluate the budgetary importance of N₂-fixation relative to external N inputs and determine the effectiveness of reducing external N loads in reducing the severity of the blooms. The results demonstrate the importance of N in supporting CR CyanoHABs and the need to better understand multiple nutritional drivers of the recurring blooms.

Keywords: Chowan River, cyanoHABs, nitrogen, phosphorus, B vitamins, N₂-fixation

<https://doi.org/10.5281/zenodo.7034970>



Introduction

As global populations grow, increased agricultural and industrial production, combined with poor sanitation practices, have led to widespread pollution of freshwater bodies, creating an impending crisis of clean water scarcity world-wide. Excessive inputs of nutrients, mainly nitrogen (N) and phosphorus (P) have accelerated eutrophication, increased turbidity, promoted O₂ depletion, and reduced biodiversity (Conley *et al.*, 2009). Anthropogenically-driven nutrient over-enrichment also drives proliferation of toxic algal and cyanobacterial harmful algal blooms (CyanoHABs) (Paerl and Barnard, 2020).

The Chowan River (CR) is a large river system plagued by CyanoHABs draining the coastal plain of north-eastern North Carolina, and a major tributary of the Albemarle-Pamlico Sound. Historically, the CR has suffered from massive CyanoHABs of the N₂-fixing cyanobacteria *Dolichospermum* spp. (Gallucci and Paerl, 1983). These blooms continued until the mid-1980s and then largely disappeared until 2013 when they resurfaced. The current CyanoHABs in the CR shift between *Dolichospermum* spp. and *Microcystis* spp. (NC DEQ 2021). In 2019, blooms dominated by *Microcystis* spp. were highly toxic with hepatotoxic cyanotoxin microcystin concentrations up to 620 µg L⁻¹ (WHO “acceptable” drinking water concentrations are < 1 µg L⁻¹, and recreational contact limit is < 10 µg L⁻¹) (NC DHHS, 2019; Chorus and Welker, 2021). In 2020, the CR CyanoHABs were less toxic (< 1 µg L⁻¹ microcystin) and again dominated by the N₂-fixing *Dolichospermum* spp. At this time, it is still unknown what factors are driving these

newly emerging CyanoHABs. One driver may include availability of B-vitamins, given that many bacterioplankton that co-occur and interact with cyanobacteria are reliant on exogenous B-vitamins (Garcia *et al.*, 2015; Paerl *et al.*, 2018) and some *Microcystis* spp. blooms are rich in populations auxotrophic for at least one B-vitamin (Li *et al.*, 2018). It is crucial to understand whether macronutrient and vitamins are driving the CR CyanoHAB bloom dynamics and associated toxin production.

Material and Methods

Water sampling

We performed experimental manipulations of natural CR (Edenton, NC, U.S.A.) phytoplankton communities that were collected from nearshore docks on the 23rd of August 2020. Water was collected using a bucket integrating the top 0.3 m of the water column, dispensed into pre-cleaned (acid washed then flushed with CR water) 20 L carboys, and transported to the University of North Carolina at Chapel Hill’s Institute of Marine Sciences in Morehead City, NC, U.S.A.

Bioassay methods

We conducted an *in situ* nutrient addition bioassay experimenting using 4 L pre-cleaned polyethylene Cubitainers® to which well mixed natural CR water was added and supplemented using the methodology described in Barnard *et al.* (2021). To evaluate nutrient limitation, triplicated nutrient addition treatments were supplemented with either 100 µM N KNO₃, 100 µM N NH₄Cl, 50 µM urea (50 µM urea to achieve 100 µM N),



20 μM P as KH_2PO_4 or 100 μM N and 20 μM P added as a combined addition of 100 μM KNO_3 and 20 μM KH_2PO_4 (Table 1). To avoid silica or dissolved inorganic carbon limitation in Cubitainers during the incubation period, we added 50 μM Si as Na_2SiO_3 and 83.25 μM dissolved inorganic carbon (DIC) as NaHCO_3 . Vitamin additions were added at f/200 concentrations, which is a 1:100 dilution of f/2 vitamin mix described by Guillard and Ryther (1962). The concentrations of vitamins added in the f/200 vitamin additions were 2.96 nM Vitamin B1, 20.5 pM Vitamin B7, and 3.69 pM Vitamin B12. Incubations were run for 72 h in an outdoor experimental pond at the University of North Carolina's Institute of Marine Sciences.

Pigment analysis

Total phytoplankton biomass was estimated as chlorophyll *a* (Chl *a*) and was collected from each treatment by filtering 50 mL of CR water onto GF/F filters. Filters were frozen at -20°C and subsequently extracted using a tissue grinder in 90% acetone (EPA method 445.0; Arar *et al.*, 1997). Chl *a* in extracts was measured using the non-acidification method of Welschmeyer (1994) on a Turner Designs Trilogy fluorometer calibrated with pure Chl *a* standards (Turner Designs, Sunnyvale, CA, U.S.A.).

Accessory photopigments were used to estimate changes in abundance of various algal groups following experimental treatments. Samples were analyzed by high performance liquid chromatography (HPLC) using a Shimadzu model LC-20AB HPLC equipped with a SIL-20AC autoinjector and a Shimadzu SPD-M20AC photodiode array spectrophotometric detector (Shimadzu, Columbia, MD, U.S.A.). Pigment extraction

Table 1. Experimental additions added to the triplicate mesocosm experiments. All mesocosms received a 50 μM Si and 83.25 μM DIC in addition to the supplements listed in the table.

Nutrient Addition	Control	+f/200 Vitamins
Control	No additions	+Vit
+100 μM KNO_3	+100 μM N	+100 μM N +Vit
+100 μM NH_4Cl	+100 μM N	+100 μM N +Vit
+50 μM Urea	+100 μM N	+100 μM N +Vit
+20 μM KH_2PO_4	+20 μM P	+ 20 μM P +Vit
+100 μM KNO_3 +20 μM KH_2PO_4	+100 μM N +20 μM P	+100 μM N +20 μM P +Vit

Vit – f/200 concentrations of B1, B7, and B12.

and processing techniques were described by Pinckney *et al.* (2001). Absorption spectra were used to identify photopigments using commercial standards (DHI, Denmark). Contributions of the dominant four algal classes (chlorophytes, cryptophytes, cyanobacteria, and diatoms) to total phytoplankton community in response to nutrient manipulations were calculated using Chemtax (Mackey *et al.*, 1996). The input pigment ratio matrix for the four classes was described in Paerl *et al.* (2014).

Nitrogen fixation

N_2 -fixation (nitrogenase activity) rates were estimated using the acetylene reduction (AR) assay, as described by Paerl *et al.* (1981), by dispensing 50 mL of sample into 70 mL stoppered serum vials, and adding 4 mL of acetylene. Triplicate light and dark bottles, as



well as distilled water blanks were incubated with the bioassay for 4 h during midday, after which 3 mL headspace samples were collected in pre-evacuated blood collection tubes (Covidien, LLC). Aliquots of 0.2 mL gas samples were withdrawn for measurements of ethylene production (from acetylene) by flame ionization gas chromatography using a Shimadzu GC9 gas chromatograph (Shimadzu, Columbia, MD, U.S.A.). Acetylene reduction was converted from nmol ethylene L⁻¹ h⁻¹ to the more biologically relevant nmol N L⁻¹ h⁻¹ using the ratio of 4:1 ethylene:ammonia (Paerl *et al.*, 2014).

Results and Discussion

An *in situ* N₂-fixation rate of 240 nmol N L⁻¹ h⁻¹ occurred on the 7th of July 2020 near the beginning of the bloom and was lower, but still relatively high (38 nmol N L⁻¹ h⁻¹) on the 21st of July 2020 during the peak of the bloom. By August, N₂-fixation could not be detected when samples were collected for the bioassay. Despite the lack of measurable N₂-fixation during the experiment, there was clear N-limitation, with NO₃, NH₄, and urea all stimulating phytoplankton biomass in the CR community (Fig. 1). In addition to alleviating N limitation, the NH₄ additions induced a secondary vitamin limitation in the experiment.

While most of the variation in community structure was related to the macronutrient additions (ANOVA: F = 29.69, p < 1 x 10⁻³³, d. f. = 71), B-vitamin additions decreased the biomass (t = -2.715, p = 0.021, n = 6) and the relative community fraction of cyanobacteria (t = -8.073, p = 0.002, n = 6), while increasing the biomass (t = 3.111, p = 0.013, n = 6) and relative community fraction of chlorophytes

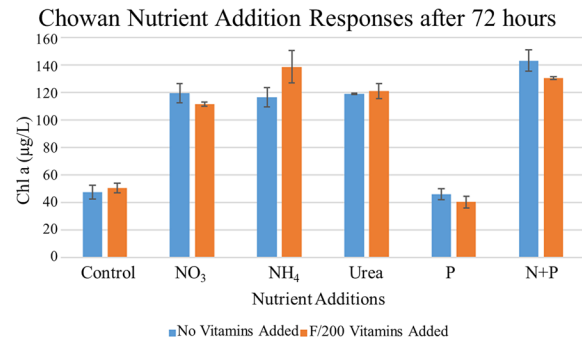


Fig. 1. Chlorophyll *a* response to macronutrient and vitamin additions after 72 h of incubation. Error bars represent standard deviation of replicate values (n = 3).

(t = 4.290, p = 0.004, n = 6). Vitamin additions did not significantly change the biomass or community fraction (Fig. 2) of diatoms (t = 1.350, p = 0.117; t = 1.828, p = 0.064, n = 6) or cryptophytes (t = -1.236, p = 0.136; t = 1.083, p = 0.164, n = 6). These results highlight a potential for a change in external B vitamins to affect the community dynamics of the CR blooms.

In the resurgent CR blooms, P-imitation and N and P co-limitation, observed during the 1970s and 1980s (Kuenzler *et al.*, 1982), have now largely shifted to N-limitation, meaning that N loading reductions may help mitigate the blooms. Despite numerous laboratory culture studies (e.g., Croft *et al.*, 2006), there is very little field evidence supporting the hypothesis that vitamin availability influences freshwater phytoplankton growth at the community level. In the marine environment, B-vitamin additions have been shown to selectively stimulate growth of picophytoplankton (Joglar *et al.*, 2020). This pilot study showed a vitamin addition effect as a decrease in cyanobacterial growth and an increase in chlorophyte growth, but future experiments are needed to verify the effects



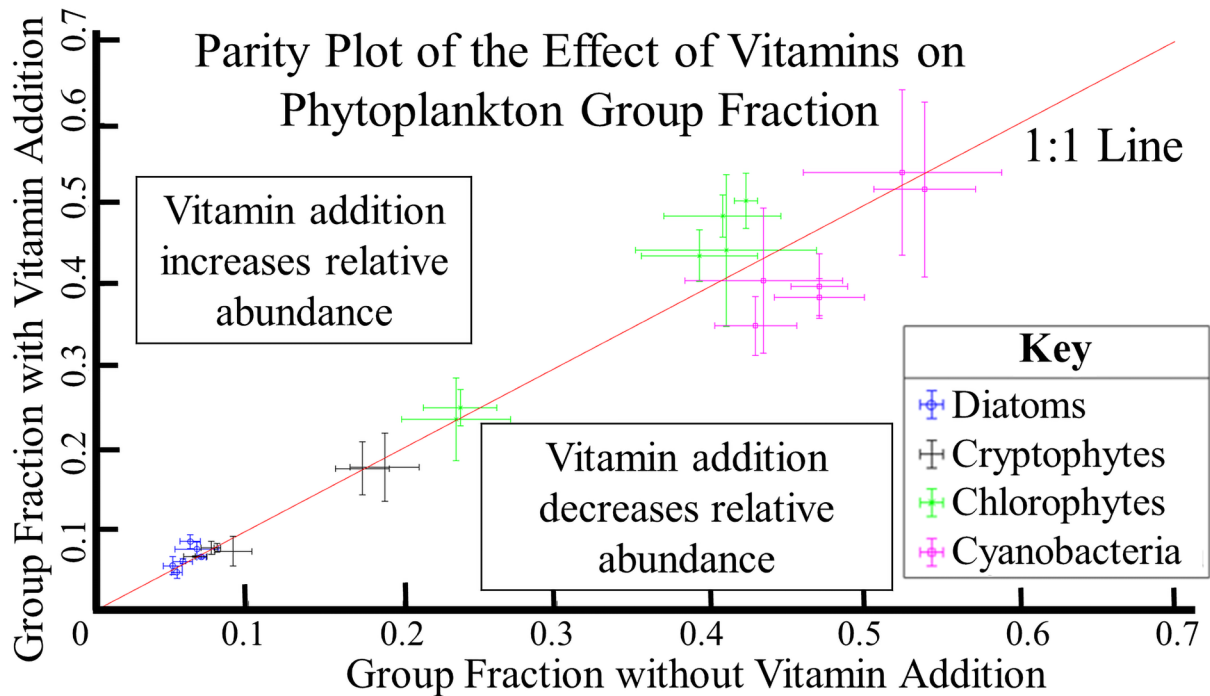


Fig. 2. Parity plot of the effects of vitamin addition of phytoplankton community composition as calculated using HPLC-Chemtax analysis. Error bars are standard deviation (n = 3). Points above the 1:1 line indicate the relative abundance of the phytoplankton group with increasing with vitamin additions and vice versa.

of vitamin additions on community structure, as this is one of the only studies to investigate vitamin effects on community structure in freshwater. We found that with NH_4 additions, vitamins were co-limiting, which have been shown in the ocean for B12 (Browning *et al.*, 2018). Additionally, given the high toxicity of previous CR CyanoHABs, vitamin and macronutrient effects on cyanotoxin production in the CR should be investigated. Many commonly occurring chlorophytes are B-vitamin auxotrophs (Paerl *et al.*, 2017), and are generally considered ‘good’ phytoplankton for food webs and ecosystem health. Our experiment suggests that chlorophytes may compete more effectively with cyanobacteria for DIN once B-vitamin supply is sufficient, and indicates that vitamin additions could be

investigated as a potential treatment for the CR CyanoHABs.

Overall, *in situ* bioassays have demonstrated the potentially important roles of B-vitamins on cyanobacterial bloom dynamics and composition as well as the importance of reducing N to control proliferation of the CR CyanoHABs.

Acknowledgements. This study was carried out with funding from the US National Science Foundation (1831096, 1840715), a Sigma Xi Grant-in-Aid of Research (G201903158412545), an Albemarle Pamlico National Estuary Partnership (APNEP) – NC Sea Grant Graduate Fellowship in Estuarine Research (2019-R/MG-1905 [HEP]), and a



North Carolina Commercial Fishing Resource Fund Grant. The authors also thank the US National HABs Office and NOAA NCCOS for an ICHA 2021 Registration Fee Award [MAB]. The authors would like to thank two anonymous reviewers for their constructive feedback on the manuscript.

References

- Arar, E. and Collins, G. (1997). US EPA Method 445.0.
- Barnard, M., Chaffin, J., Plaas, H., Boyer, G., *et al.*, (2021). *Toxins* 13, 47.
- Browning, T., Rapp, I., Schlosser, C., Gledhill, M., *et al.*, (2018). *Geophys. Res. Lett.* 45, 6150-6159.
- Chorus, I. and Welker, M. (2021). In: Chorus, I. and Welker, M. (Eds.). *Toxic Cyanobacteria in Water*, 2nd edition. Boca Raton, U.S.A., 13-162.
- Conley, D., Paerl, H., Howarth, R., Boesch, D., *et al.*, (2009). *Science* 323, 1014-1015.
- Croft, M., Warren, M., Smith, A. (2006). *Eukaryotic Cell* 5, 1175-1183.
- Gallucci, K. and Paerl, H. (1983). *Appl. and Env. Microbiol.* 45, 557-562.
- Garcia, S., Buck, M., McMahon, K., Grossart, H., *et al.*, (2015). *Mol. Ecol.* 24, 4449-4459.
- Guillard, R. and Ryther, J. (1962). *Can. J. Microbiol.* 8, 229-239.
- Joglar, V., Prieto, A., Barber-Lluch, E., Hernández-Ruiz, M., *et al.*, (2020). *Biogeosci.* 17, 2807-2823.
- Kuenzler, E., Stone, K., Albert, D. (1982). UNC-WRRI Report 82-186.
- Li, Q., Lin, F., Yang, C., Wang, J., *et al.*, (2018). *Front. Microbiol.* 9, 746.
- Mackey, M., Mackey, D., Higgins, H., Wright, S. (1996). *Mar. Ecol. Prog. Ser.* 144, 265-283.
- NC DEQ (2021). [Chowan River Basin Water Resources Plan](#).
- NC DHHS. 16 August 2019. [Press Release](#).
- Paerl, H. and Barnard, M. (2020). *Harmful Algae* 96, 101845.
- Paerl, R., Sundh, J., Tan, D., Svenningsen, S., *et al.*, (2018). *Proc. Natl. Acad. Sci.* 115, E10447-E10456.
- Paerl, R., Bouget, F., Lozano, J., Vergé, V., *et al.*, (2017). *ISME J.* 11, 753-765.
- Paerl, H., Xu, H., Hall, N., Zhu, G., *et al.*, (2014). *PloS one* 9, e113123.
- Paerl, H., Webb, K., Baker, J., Wiebe, W. (1981). In: Broughton, W. (Ed). *The ecology of nitrogen fixation*, Oxford, UK, 193-240.
- Pinckney, J., Richardson, T., Millie, D., Paerl, H. (2001). *Org. Geochem.* 32, 585-595.
- Welschmeyer, N. (1994). *Limnol. Oceanogr.* 39, 1985-1992.



Tracking a novel cyanobacterium bloom in the Indian River Lagoon, Florida, U.S.A., during the summer and fall of 2020

Stephanie Keller Abbe^{1*}, Karen Henschen¹, Laura Markley¹, Célia Villac¹, Eric Muhlbach¹, Charles Tilney¹, Alicia Hoeglund¹, Yida Gao¹, Autumn Biddle¹, Richard Paperno¹, Larry Johnson², Tom Saam², Jim Torpey², Craig Wallace², Tim Moore³, Malcolm McFarland³, Cheryl Swanson⁴, Katherine Hubbard¹

¹Fish and Wildlife Research Institute, Florida Fish and Wildlife Conservation Commission, 100 8th Ave. SE, St. Petersburg, FL, 33701, U.S.A., ²Indian River Lagoon Marine Resource Council, 3275 Dixie Hwy NE, Palm Bay, FL, 32905, U.S.A., ³Harbor Branch Oceanographic Institute, Florida Atlantic University, 777 Glades Road, Boca Raton, FL, 33431, U.S.A., ⁴Florida Department of Environmental Protection, 3900 Commonwealth Blvd., Tallahassee, FL, 32399, U.S.A.

* corresponding author's email: stephanie.kellerabbe@myfwc.com

Abstract

A bloom of an unidentified nano-sized cyanobacterium (~3-4 μm x 5 μm) was observed in the Indian River Lagoon (IRL) system, Florida, U.S.A. from August through December 2020, causing greenish water discoloration. Enumeration by light microscopy revealed concentrations of $> 10^6$ cells mL^{-1} in the northern and central IRL proper, Banana River Lagoon, and Mosquito Lagoon (maximum of 3×10^6 cells mL^{-1}). Bloom concentrations (2×10^5 cells mL^{-1}) were first observed in the northern IRL and Banana River where it persisted longer than in other basins, but cell abundance rapidly declined throughout the system as water temperatures decreased in December. Inspection of archived samples suggested this taxon had been in the system since at least late June. Bloom development and decline was readily observed by satellite imagery (Sentinel-2, Landsat-8). Cells were round to oblong, often with two or more cells aligned in a chain. Live cells had an elongated aerotome that became inconspicuous upon preservation. Flow cytometry indicated that this cyanobacterium had low chlorophyll a and high phycocyanin-like fluorescence. Toxin analysis at five time points between 9/24 and 12/03 returned non-detected concentrations of anatoxin-a and cylindrospermopsin, trace levels of total microcystin-LR in four samples, and saxitoxin in three samples; these positive results are likely unrelated to the cyanobacterium bloom. Direct sequencing followed by PacBio 16S amplicon sequencing revealed a novel cyanobacterial ribotype in bloom samples (i.e., $>75\%$ of 16S amplicons). A complete metagenome assembled genome was retrieved and phylogenetic analysis placed this organism adjacent to *Prochlorothrix hollandica*, although within a clade and tree that encompasses large genetic distances between taxa indicating that specific evolutionary and ecological affinities must be interpreted with caution.

Keywords: coastal lagoon, light microscopy, flow cytometry, remote sensing, cyanotoxins, phylogeny

<https://doi.org/10.5281/zenodo.7034980>



Introduction

The Indian River Lagoon (IRL) is a shallow (in average < 2 m deep) estuarine lagoon system, consisting of multiple basins, extending 250 km parallel to the Atlantic coast of central Florida, U.S.A. In early September 2020, collaborative sampling intensified in the IRL in response to widespread accounts of green water discoloration with incompatible reports of low chlorophyll. Here we discuss the results from efforts focused on following the progression of the event with satellite imagery, cell counts with light microscopy and flow cytometry, toxin analysis, and the determination of the molecular signature of this nano-sized phytoplankton, soon realized to be a novel cyanobacterium.

Material and Methods

Extensive water sampling was implemented from September 2020 through January 2021, comprising 60 sites at a depth of 0.2 - 1 m (Fig. 1a). From these 60 sites, 13 sites were sampled at least five times. Of these 13, the seven most frequented sites were chosen for flow cytometry and three sites were sampled for toxin analyses on select dates (Fig. 1b). In total, 264 live and/or Lugol's preserved samples were analyzed for cell enumeration by the settling technique, using Nunc® chambers and inverted light microscopy, under 630× final magnification (adapted from Edler and Elbrachter, 2010). Level-1 Sentinel-2 satellite images were obtained from the European Space Agency's Copernicus Open Access Hub. These images were processed with the Acolite (Vanhellemont, 2019) to generate true-color images. Flow cytometry samples were preserved in 0.1% glutaraldehyde and analyzed using an

Attune NxT flow cytometer (ThermoFisher, U.S.A.) equipped with lasers and detectors capable of measuring chlorophyll-*a*-like (488 nm excitation, 690/40 nm emission) and phycocyanin-like (637 nm excitation, 670/14 nm emission) autofluorescence signal from phytoplankton cells. Pearson Excel function was applied to test the linear correlation between light microscopy and flow cytometry cell counts. Toxin analyses were performed using EPA method 8321B (EPA, 2007). A sequence initially generated by direct PCR sequencing, followed by PacBio 16S amplicon sequencing, was subjected to BLASTn and SILVA database searches to identify the most closely related taxa (details in Lopez *et al.*, 2021). Subsequently, Oxford Nanopore shotgun sequencing enabled a robust phylogenetic placement using 33 ribosomal proteins.

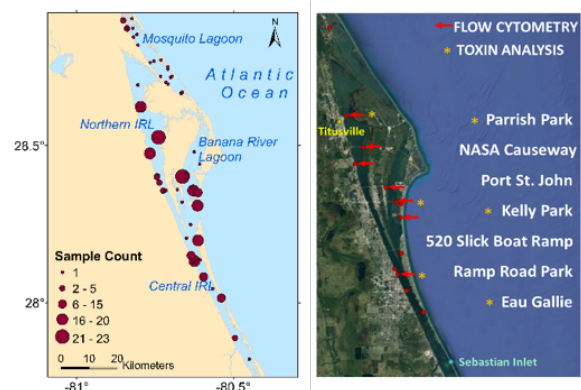


Fig. 1. Sampling coverage from September 2020 through January 2021. (a) The smallest circles indicate sites visited only once; larger circles sites were visited 21 to 23 times during this period. (b) Selected sites for flow cytometry and toxin analysis, including site names.



Results and Discussion

Sentinel-2 imagery tracked the large-scale progression of this event from non-bloom conditions back in March, water discoloration and broad spatial coverage of the bloom in September, and the system approaching bloom decline at the end of December (Fig. 2).



Fig. 2. Sentinel 2 satellite images (<https://www.copernicus.eu/en>) showing peak bloom coverage in September. See text for sequence detail.

The fact that reports of chlorophyll levels in the field were very low to not detected (data not shown) was explained when flow cytometry revealed the dominance of cells with relatively low chlorophyll-*a*-like fluorescence and high phycocyanin-like fluorescence. This result was visually confirmed by epifluorescence microscopy that showed a lack of emission under chlorophyll wavelength excitation (470/27 nm) and cells with a red emission under phycocyanin wavelength excitation (640/30 nm). Based on data from seven sites analyzed at two time points, it was also reassuring to demonstrate early in our monitoring that flow cytometry and light microscopy counts of this

nano-sized alga were within the same order of magnitude and highly correlated (r Pearson = 0.91, $p < 0.001$).

Light microscopy examination revealed an unfamiliar cyanobacterium. Relative to known species, this taxon had unique characteristics based on gross morphology. Cells are round to oblong, approximately 3–4 μm by 5 μm , with a pale translucent green appearance, often seen dividing into chains of two, and up to five, cells (Fig. 3a). Examination of live material indicated the presence of an aerotop, or elongated gas vacuole, that collapsed upon preservation with Lugol's iodine solution; in addition, the cell changed in shape, becoming more capsule-like with more homogenous content (Fig. 3b).

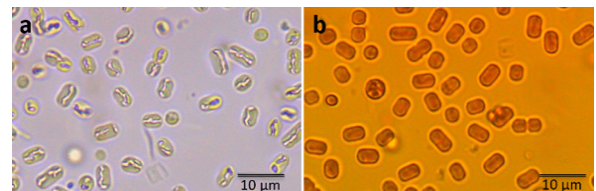


Fig. 3. Unidentified cyanobacterium (a) live and (b) Lugol's preserved material. See text for detailed description.

Bloom concentrations, operationally defined as 2×10^5 cells mL^{-1} , started appearing initially in the Northern IRL and Banana River Lagoon basins with five sites exceeding 1 million cells mL^{-1} . Increased sampling efforts between October and November, with up to 20 samples collected each week, exposed the broadest spatial coverage from the northern Mosquito Lagoon stretching south of Melbourne in the Central IRL, although the highest cell concentrations persisted in the Northern IRL and Banana River basins (Fig. 4). During the last week of December, cell concentrations



dropped to below 10,000 cells mL⁻¹, even in the basins where the bloom had initiated and was sustained in previous weeks.



Fig. 4. Mid-November shows the most expansive spatial coverage and with high cell concentrations throughout.

Light microscopy inspection of available archived samples determined that this taxon had been present since at least June 2020. Bloom levels of this cyanobacterium overlapped with bloom concentrations of a brown tide-forming pelagophyte, *Aureoumbra lagunensis*, at some locations in the Northern IRL and Banana River Lagoon (August and September) and in the Central IRL (late-September to mid-October) (Lopez *et al.*, 2021). The abrupt decline in cell abundance in December 2020 coincided with a decline in water temperature below 20°C (Fig. 5). This indicates that this particular species has a strong affinity for warmer water, a trait shared

with many other cyanobacteria (e.g., Carey *et al.*, 2012).

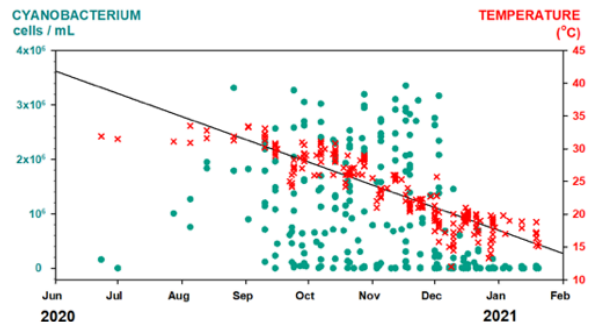


Fig. 5. Bloom distribution over time and associated water temperature with best fit curve.

Toxin analysis at five time points (9/24 - 12/03) returned non-detectable levels of anatoxin-a and cylindrospermopsin and trace levels of total microcystin-LR in four samples, and of saxitoxin in three samples. These positive results for saxitoxin are likely unrelated to the intense cyanobacterium bloom, since the annually occurring summer bloom of the saxitoxin-producing dinoflagellate *Pyrodinium bahamense* was subsiding in the system (Lopez *et al.*, 2021) at the time of sampling.

Direct sequencing with oligonucleotides cya359F and cya781R (b) was successful in a bloom sample from Parrish Park Boat Ramp, and additional direct sequencing with a combination of specific/universal primers yielded a final contig of 2183 bp (GenBank accession number MW816502) covering most of the 16S rRNA gene, the ITS/5S rRNA region, and a partial fragment of the 23S rRNA gene. The closest BLASTn hit was to an uncultured cyanobacterium with percent identity of 96.9% over 65% query coverage (ITS-region missing), and the best hit to a known organism was to *Prochlorothrix*

hollandica, with a percent identity of 93.5% and 74% query coverage. Subsequent shotgun sequencing and metagenome assembly enabled us to align 33 ribosomal proteins to published cyanobacterial genomes and to generate a more robust phylogenetic tree (Fig. 6), which like the 16S rRNA gene data, indicated a placement adjacent to *P. hollandica* and within a clade that also included *Cyanobium*, *Aphanothece*, *Prochlorococcus*, and *Synechococcus*. However, possible evolutionary and ecological affinities between the cyanobacterium from the IRL bloom and *P. hollandica* must be interpreted with caution since this clade, and the entire tree, encompasses large genetic distances. Further studies of thylakoid arrangement and presence of genes associated with the expression of a particular pigment are needed to resolve taxonomic identity and classification. Assessing the genome of this cyanobacterium is expected to shed insight into the physiological capacities and ecological niche of this species and help understand what factors might have contributed to the development of this large and novel bloom.

Acknowledgements. We would like to thank our partners and the field sampling crews: Community Scientists, FL Atlantic University, Marine Resource Council, FL Dep. Agriculture and Consumers Services, FL Dep. Environmental Protection, St. Johns River Water Management District. Special thanks to Cary Lopez, FWRI, for distribution maps in ArcGIS.

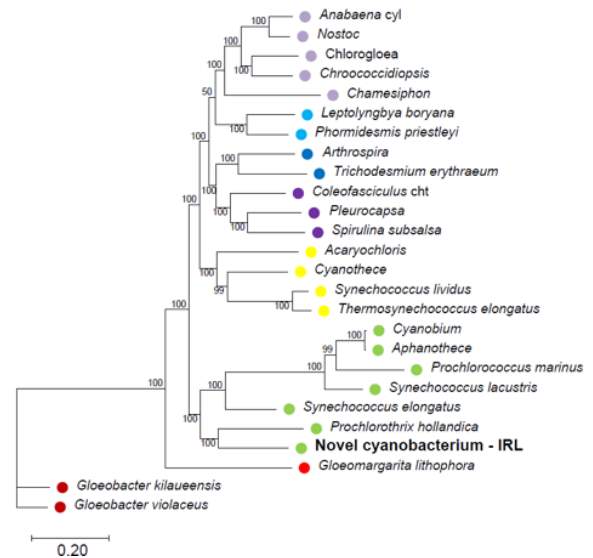


Fig. 6. Phylogenetic placement of the IRL cyanobacterium adjacent to *P. hollandica* based on 33 ribosomal proteins and 3,934 amino acids (PhyML tree, 1000 a-Bayes supports).

References

- Carey, C.C., Ibelings, B.W., Hoffmann, E.P, Hamilton, D.P., Brookes, J.D. (2012). *Water Res.* 46, 1394-1407.
- Edler, L. and Elbrachter, M. (2010). *IOC Manuals and Guides*, no. 55. B. Karlson, C. Cusack, E. Bresnan (Eds). Paris, UNESCO, 13-20.
- EPA (2007). Accessed January 2022. <https://www.epa.gov/sites/default/files/2015-12/documents/8321b.pdf>
- Iteman, I., Rippka, R., Tandeau de Marsac, N., Herdman, M. (2000). *Microbiology* 146, 1275-1286.
- Lopez, C., Tilney, C., Muhlbach, E., Bouchard, J., *et al.*, (2021). *Front. Mar. Sci.* 8, 1737.



Nübel, U., Garcia-Pichel, F., Muyzer, G. (1997). *Appl. Environ. Microb.* 63, 3327-3332.

Rocap, G., Distel, D.L., Waterbury, J.B., Chisholm, S.W. (2002). *Appl. Environ. Microb.* 68, 1180-1191.

Turner, S., Pryer, K.M., Miao, V.P.W., Palmer, J.D. (1999). *J. Eukaryot. Microbiol.* 46, 327-338.

Vanhellemont, Q. (2019). *Rem. Sens. Env.* 225, 175-192.



Blooms of the cyanobacteria *Limnoraphis* cf. *birgei* in a volcanic Lake of El Salvador, Central America

Rebeca Quintanilla*, Oscar Amaya, Jeniffer Guerra

Laboratorio de Toxinas Marinas, Universidad de El Salvador, Final Av. Héroes y Mártires del 30 de julio, zip code 1101 San Salvador, El Salvador.

* corresponding author's email: cesiah.quintanilla@ues.edu.sv

Abstract

In May 2018, the proliferation of a filamentous cyanobacteria was detected for the first time in Lake Coatepeque, a deep, oligotrophic, volcanic lake in western El Salvador, Central America. Since that year, four events of proliferation of this cyanobacteria have been recorded, which had an impact on the inhabitants' activities that depend on the lake's water. Sampling campaigns were conducted both during bloom and non-bloom conditions between in May 2018 and March 2021 in Lake Coatepeque. In these campaigns, surface samples were collected using a sampling bottle at five sites in the lake and physico-chemical data was also registered. Material was characterized by optical microscopy; cell abundance was quantified using a Sedgwick-Rafter camera on an inverted microscope and with the aid of an ocular reticle. In the five blooms events, the causative organism was observed forming uniseriate filaments of 21-24 μm and trichomes 18-22 μm wide, with aerotopes irregularly distributed along the trichome and with a firm yellowish hyaline sheath. According to the morphological characteristics, the species corresponds to the description of *Limnoraphis birgei*, however, molecular and biochemical data is needed to confirm the species identity. Proliferations of *L.* cf. *birgei* generated brown surface agglomerations, which in some cases reached cell concentrations exceeding 900,000 cells mL^{-1} . No human or animal intoxications were reported. This is the first report of occurrence and proliferation of *Limnoraphis* in El Salvador and one of the few cases reported worldwide.

Keywords: cyanobacteria bloom, crater lake, oligotrophic

<https://doi.org/10.5281/zenodo.7034997>



Introduction

The increase in the occurrence of algal blooms is considered as one of the main effects of eutrophication and climate change over aquatic systems (O'Neil *et al.*, 2012; Paerl and Otten, 2013) estuarine, and marine ecosystems. Recent research suggests that eutrophication and climate change are two processes that may promote the proliferation and expansion of cyanobacterial harmful algal blooms. In this review, we specifically examine the relationships between eutrophication, climate change and representative cyanobacterial genera from freshwater (*Microcystis*, *Anabaena*, *Cylindrospermopsis*). In recent years, there has been an increase in the report of harmful algal blooms in freshwater bodies of El Salvador, particularly in the central-western part of the country (Quintanilla *et al.*, 2020). In May 2018, the proliferation of a filamentous cyanobacteria was detected for the first time in Lake Coatepeque (Fig. 1), a deep, oligotrophic, volcanic lake in western El Salvador, Central America.

Until March 2021, five events of proliferation of this cyanobacteria have been recorded, which had an impact on the inhabitants' activities that depend on the lake's water. The study presented here describes the cyanobacterial bloom events in Lake Coatepeque, as well as the taxonomic identification of the causative species by means of light microscopy.



Fig. 1. Mats of cyanobacterial blooms detected in Lake Coatepeque. El Salvador.

Material and Methods

Site description

Lake Coatepeque is a crater lake located in the southwest of El Salvador (13°51' N, 89°32' W), at the altitude of 740 m above sea level (Fig. 2). It has an area of 24.8 km² and is an endorheic water body, thus its drainage is through subsurface infiltration. Maximum depth in the lake is 115 m and the walls that surround it are between 200 m and 300 m. Surface water temperature ranges from 22°C to 31°C along the year. The climate in this area is characterized by a dry season that takes place between November and March, and a warm rainy season between April and October. By 2021, the lake has been classified as oligotrophic, with total phosphorus values ranging from 0.18 mg L⁻¹ to 0.88 mg L⁻¹ (MARN, 2021).

The lake is an important local resource, since it is used for artisanal fishing, recreation, irrigation and, water supply to the surrounding population. It also has a large national significance as a touristic destination, mainly because it regularly changes its color from blue to bright turquoise, which was previously thought to be caused by cyanobacteria (Espinoza *et al.*, 2013).

Sampling and laboratory analysis

Sampling campaigns were conducted both during bloom and non-bloom conditions between May 2018 and March 2021 in Lake Coatepeque. In these campaigns, surface water samples were collected using a sampling bottle in at least five sampling points during each sampling in the lake. Data on water temperature, pH and total dissolved solids (TDS) was recorded *in situ* on each sampling point, using a thermometer, pH meter, and an electrical conductivity meter, respectively.





Fig. 2. A) Location of Lake Coatepeque in El Salvador, and B) Panoramic photo of Lake Coatepeque.

Phytoplankton samples were characterized by optical microscopy. During bloom events, cell abundance was quantified using a Sedgwick-Rafter chamber on an inverted microscope and with the aid of an ocular reticle. During non-bloom conditions, cell abundance was quantified using Utermöhl chambers; cell abundance was calculated as number of cells per milliliter. Length and width of filaments and trichomes were measured using an imaging software.

Results and Discussion

Bloom events took place both during dry season (January, February, and November), as well as during rainy season (May). None of the blooms spread to the entire lake, but rather occurred within specific locations near to the shores. During bloom events, temperature ranged from 22.5 °C to 28.6 °C, pH from 8.3 to 9.3, and TDS from 943 ppm to 1259 ppm.

In the four blooms events, the causative organism was observed forming uniseriate filaments of 21-24 μm wide and trichomes

18-22 μm wide (n = 30), and with a firm yellowish hyaline sheath that surpass trichomes. Cells are shorter than wide and have aerotopes irregularly distributed along the trichome. Trichomes are cylindrical, not constricted at cell walls and with rounded end cells (Fig. 3).

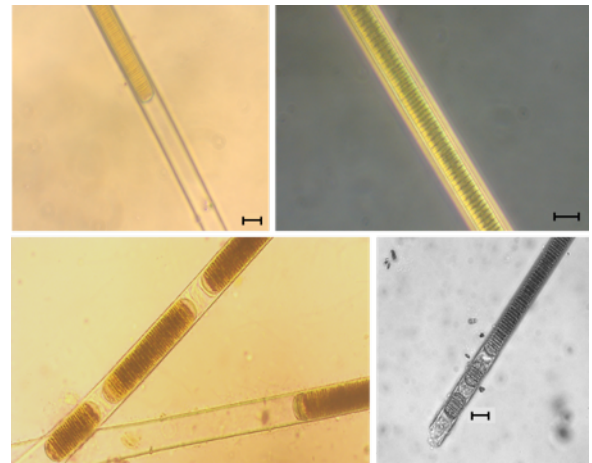


Fig. 3. Filaments of *Limnoraphis cf. birgei*. Scale bar represents 20 μm.

Initially, the causative species of the blooms was identified as belonging to the genera *Lyngbya* (Quintanilla *et al.*, 2020). However, further literature revision and re-examination of samples has allowed to re-identify the causative organism in the genera *Limnoraphis*. Komárek *et al.* (2013) tentatively identified as *Lyngbya robusta*, recently increased in abundance in Lake Atitlán, Guatemala, and since 2008 annual water-blooms occurred. This was one from the first known cases of *L. robusta* water-blooms worldwide. A polyphasic evaluation of *L. robusta* using 16S rRNA gene sequencing, cytomorphological markers, and ecological characteristics was made. This species had several unique features. It produced aerotopes that were irregularly spaced in cells; cyanotoxins were not found, and it fixed nitrogen in spite of the



lack of heterocytes. It contained a high amount of carotenoids, which caused an unusual brown color of the macroscopic scum on the water level. Molecular phylogenetic analyses using the 16S rRNA gene showed that *L. robusta*, together with few other planktic species, formed a clade, separated from typical *Lyngbya* species. The main diacritical markers of this clade were the planktic type of life and formation of gas vesicles in cells. Based upon molecular, morphological and ecological data, a new genus *Limnoraphis* was proposed with four species. © Czech Phycological Society (2013) proposed the separation of planktonic *Lyngbya* species into the new genera *Limnoraphis* based on a polyphasic classification approach. Currently, there are four species identified within this genera: *Limnoraphis birgei* (G. M. Smith) J. Komárek, E. Zapomelová, J. Smarda, J. Kopecký, E. Rejmánková, J. Woodhouse, B. A. Neilan & J. Komárková 2013, *Limnoraphis criptovaginata* (Schkorbatov) J. Komárek, E. Zapomelová, J. Smarda, J. Kopecký, E. Rejmánková, J. Woodhouse, B. A. Neilan & J. Komárková 2013, *Limnoraphis hieronmuysii* (Lemmermann) J. Komárek, E. Zapomelová, J. Smarda, J. Kopecký, E. Rejmánková, J. Woodhouse, B. A. Neilan & J. Komárková 2013, and *Limnoraphis robusta* (Paracutty) J. Komárek, E. Zapomelová, J. Smarda, J. Kopecký, E. Rejmánková, J. Woodhouse, B. A. Neilan & J. Komárková 2013 (Komárek *et al.*, 2013) tentatively identified as *Lyngbya robusta*, recently increased in abundance in Lake Atitlán, Guatemala, and since 2008 annual water-blooms occurred. This was one from the first known cases of *L. robusta* water-blooms worldwide. A polyphasic evaluation of *L. robusta* using 16S rRNA gene sequencing, cytomorphological markers, and ecological characteristics was made.

This species had several unique features. It produced aerotopes that were irregularly spaced in cells; cyanotoxins were not found, and it fixed nitrogen in spite of the lack of heterocytes. It contained a high amount of carotenoids, which caused an unusual brown color of the macroscopic scum on the water level. Molecular phylogenetic analyses using the 16S rRNA gene showed that *L. robusta*, together with few other planktic species, formed a clade, separated from typical *Lyngbya* species. The main diacritical markers of this clade were the planktic type of life and formation of gas vesicles in cells. Based upon molecular, morphological and ecological data, a new genus *Limnoraphis* was proposed with four species. © Czech Phycological Society (2013).

According to the morphological distinction of *Limnoraphis* species made by Komárek *et al.* (2013) tentatively identified as *Lyngbya robusta*, recently increased in abundance in Lake Atitlán, Guatemala, and since 2008 annual water-blooms occurred. This was one from the first known cases of *L. robusta* water-blooms worldwide. A polyphasic evaluation of *L. robusta* using 16S rRNA gene sequencing, cytomorphological markers, and ecological characteristics was made. This species had several unique features. It produced aerotopes that were irregularly spaced in cells; cyanotoxins were not found, and it fixed nitrogen in spite of the lack of heterocytes. It contained a high amount of carotenoids, which caused an unusual brown color of the macroscopic scum on the water level. Molecular phylogenetic analyses using the 16S rRNA gene showed that *L. robusta*, together with few other planktic species, formed a clade, separated from typical *Lyngbya* species. The main diacritical



markers of this clade were the planktic type of life and formation of gas vesicles in cells. Based upon molecular, morphological and ecological data, a new genus *Limnoraphis* was proposed with four species. © Czech Phycological Society (2013, the species found in Lake Coatepeque matches better to the description of *Limnoraphis birgei*; however some feature resemble those of *Limnoraphis robusta*. Filaments' width matches that of *L. birgei* exclusively; however, trichomes width matches with both *L. birgei* and *L. robusta*. It has been identified that *Limnoraphis* trichomes width might decrease during blooms, resembling the morphology of other *Limnoraphis* species (Salazar-Alcaraz *et al.*, 2021), and thus making species identification difficult by means of morphological features alone. As expected, this highlights the need of incorporating molecular and biochemical data in order to confirm the identity of the species found in Lake Coatepeque.

Proliferations of *L. cf. birgei* generated brown surface agglomerations (Fig. 1), which in some cases reached cell concentrations exceeding 900,000 cells mL⁻¹. Bloom events were considered as such when there was a noticeable change in water color due to an increase in cyanobacteria cell abundance. During non-bloom conditions, maximum cell abundance was 62,559 cells mL⁻¹; while during bloom conditions cell abundance ranged between 168,360 and 929,280 cells mL⁻¹ (Fig. 4).

Filaments were also found in samples from 10 m and 20 m depth but in lower abundances. In some blooms, *Limnoraphis* co-occurred with *Microcystis aeruginosa*. *Limnoraphis* blooms have been scarcely reported in freshwater ecosystems. The reported events have taken

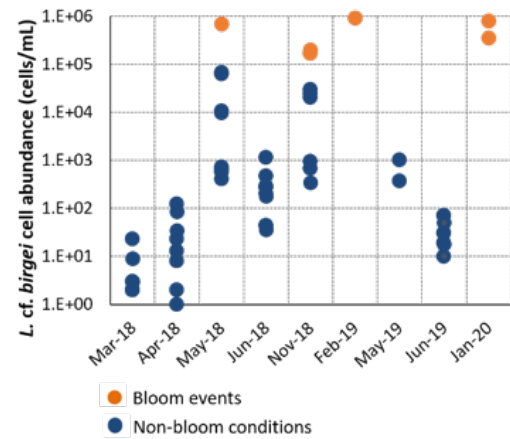


Fig. 4. Cell abundance of *L. cf. birgei* in Lake Coatepeque from May 2018 to December 2020 period.

place at Santa María del Oro crater lake in México (Salazar-Alcaraz *et al.*, 2021), Lake Ontario in Canada (Zastepa and Chemali, 2021), Habanilla reservoir in Cuba (Comas-González *et al.*, 2017), Lake Titicaca in Peru (Komárková *et al.*, 2016), Clear Lake in United States (Kurobe *et al.*, 2013) and Lake Atitlán in Guatemala (Rejmánková *et al.*, 2011).

Blooms of *Limnoraphis* have been related to the upwelling of nutrient rich water (Rejmánková *et al.*, 2011). Particularly, *Limnoraphis robusta* has been reported to occur in oligotrophic to mesotrophic water bodies when phosphorus concentrations increase (Komárek *et al.*, 2013; Salazar-Alcaraz *et al.*, 2021). Additionally, some strains have the ability to fix nitrogen through diazocytes (Rejmánková *et al.*, 2011). Probably this is the case of the *Limnoraphis* strain present in Lake Coatepeque, since it has been confirmed that the lake is oligotrophic.

Further research on the species is needed, both to better understand the potential harm its blooms might represent for the local



inhabitants, as well as to contribute to the morphological and molecular studies of the *Limnorphis* clade.

During blooms events, no human or animal intoxications were reported; however, toxins production needs to be monitored since local population consume the lake's water without any previous treatment, and some species of this genera have been reported to produce trace amounts of cylindrospermopsin and saxitoxins (Rejmánková *et al.*, 2011)

Acknowledgements. We thank Fundación Coatepeque for its support in financing and providing logistical facilities for sampling campaigns, and the project IAEA-RLA7025 for its support in consolidating LABTOX-UES technical capacities and financing participation in ICHA.

References

- Comas-González, A., Labaut-Betancourt, Y., Peraza-Escarrá, R. (2017). *An. Biol.* 39, 1-6.
- Espinoza, J., Amaya, O., Rivera, W., Ruíz, G., Escobar, J. (2013). *Bioma* 4, 43-46.
- Komárek, J., Zapomělová, E., Šmarda, J., Kopecký, J., *et al.*, (2013). *Fottea* 13, 39-52.
- Komárková, J., Montoya, H., Komárek, J. (2016). *Hydrobiologia* 764, 249-258.
- Kurobe, T., Baxa, D. V., Mioni, C.E., Kudela, R.M., *et al.*, (2013). *Springerplus* 2, 1-12.
- MARN, 2021. Evaluación de la calidad del agua del Lago de Coatepeque. San Salvador. 32 p.
- O'Neil, J.M., Davis, T.W., Burford, M.A., Gobler, C.J. (2012). *Harmful Algae* 14, 313-334.
- Paerl, H.W. and Otten, T.G. (2013). *Science* 342, 433-434.
- Quintanilla, R., Amaya, O., Guerra, J. (2020). *Rev. Cuba. Investig. Pesq.* 37, 92-97.
- Rejmánková, E., Komárek, J., Dix, M., Komárková, J., Girón, N. (2011). *Limnologia* 41, 296-302.
- Salazar-Alcaráz, I., Ochoa-Zamora, G.G., Hernández-Almeida, O.U., Palomino-Hermosillo, Y.A., *et al.*, (2021). *Rev. Mex. Biodivers.* 92, e923485.
- Zastepa, A. and Chemali, C. (2021). *Data in Brief* 35, 106800.





ICHTHYOTOXIC HABs



Phylogeny, lipid composition, pigment signature, and growth of the fish-killer *Heterosigma akashiwo* from Chilean Patagonia

Ana Flores-Leñero ^{1*}, Javier Paredes-Mella ¹, Valentina Vargas ¹, Luis Norambuena ¹, Gonzalo Fuenzalida ¹, Kim Lee Chang ², Jorge I. Mardones ^{1,3*}

¹ Centro de Estudios de Algas Nocivas (CREAN), Instituto de Fomento Pesquero (IFOP), Puerto Montt, Chile; ² CSIRO Ocean and Atmosphere, GPO Box 1538, Hobart, TAS, 7001, Australia; ³ Centro de Investigación en Dinámica de Ecosistemas Marinos de Altas Latitudes (IDEAL), Valdivia, Chile.

* corresponding author's emails: ana.flores@ifop.cl ; jorge.mardones@ifop.cl

Abstract

The raphidophyte *Heterosigma akashiwo* is widely distributed in coastal ecosystems where it has caused massive events of fish mortality and shellfish damage. In April 2021, high cell abundances of *H. akashiwo* ($> 70,000$ cells mL⁻¹) killed $> 6,000$ tons of salmon in the Chilean fjords. This study investigated the molecular phylogeny, pigment composition, fatty acid profile, and cell growth of the *H. akashiwo* (strain CREAN_HA03) from Chilean waters. A phylogenetic reconstruction based on the large sub-unit ribosomal nucleotide showed that the Chilean strain belongs to the *H. akashiwo* clade. The genetic distance was 0.00 relative to strains from Japan, Australia, U.S.A., China, and New Zealand. The pigment signature showed that the CREAN_HA03 strain is mainly dominated by fucoxanthin (48.4%), chlorophyll c2 (18.3%), chlorophyll *a* (14.7%), and violaxanthin (9.8%). A factorial T-S growth experiment showed a μ_{\max} of 0.48 d⁻¹ at 17 °C and salinity of 35. The maximum cell abundance of $\sim 50,000$ cells mL⁻¹ was reached at 12°C and a salinity of 25. The fatty acid profile exhibited a high abundance of polyunsaturated fatty acids: 20.94% palmitic acid (16:0), 13.04% EPA (20:5 ω 3), and 10.44% stearidonic acid (18:4 ω 3), which have all been described as highly cytotoxic against fish gill tissue. Further characterization of more Chilean *H. akashiwo* isolates is needed to understand the precise ichthyotoxic mechanisms and environmental drivers that trigger massive bloom events in Chilean Patagonia.

Keywords: Raphidophytes, ichthyotoxins, Chilean fjords, Harmful Algal Blooms (HABs)



Introduction

Heterosigma akashiwo is a small raphidophyte widely distributed in coastal ecosystems. This species produces ichthyotoxic blooms in different parts of the world, responsible for economically devastating fish kill events. This species is a marine phytoflagellate, however, it can be found in estuaries, indicating its ability to tolerate a large range of salinities (Martinez *et al.*, 2010). *Heterosigma akashiwo* has also been previously described its ability to grow at a broad range of temperatures (eurythermal species).

In Chilean waters, the first *H. akashiwo* salmon-killing event was reported in September of 1988, which ignited the phytoplankton monitoring program in Chile (Mardones *et al.*, 2012). After this event, the raphidophyte did not bloom again in high cell densities until April of 2021 in the Comau fjord, Northern Patagonia (42°22.166' S, 72°27.30' W), causing a massive mortality of salmon (> 6,000 tons) (SERNAPESCA, 2021; www.sernapesca.cl).

It has been demonstrated that *H. akashiwo* produces molecules that have a similar toxic effect to brevetoxins, however this molecule is not structurally related to the brevetoxin group. Some authors have proposed that the toxicity is due to high concentrations of lipids like PUFAs (Dorantes-Aranda *et al.*, 2015). However, the cytotoxic compounds produced by *H. akashiwo* are still unknown.

The main objective of this study was to define the phylogenetic position, pigment signature and fatty acid profile of a Chilean *H. akashiwo* strain, as well as the environmental conditions that might promote its growth in southern Chilean waters.

Material and Methods

Microalgae culture conditions

One monoclonal culture of *H. akashiwo* (CREAN_HA03 strain) was isolated from the Comau fjord in 2019 (42° 22.166' S, 72° 27.30' W; Los Lagos Region). The CREAN_HA03 strain was maintained in culture at the CREAN-IFOP algae collection in Puerto Montt, Chile. Non-axenic cultures were grown in L1 medium (Guillard and Ryther, 1962) at 15°C in sterile filtered (0.22 µm), in seawater at a salinity of 33 at 100 µmol photon m⁻² s⁻¹ (cool white fluorescence lamps) under a 18:6 h light:dark cycle.

DNA extraction, amplification, sequencing and phylogeny

A detailed protocol for genetic analyses performed at the CREAN laboratory is described in Mardones *et al.* (2020). Briefly, a culture of *H. akashiwo* was harvested and concentrated to amplify the D1/D2 region of the 28S ribosomal gene using the D1/D2 primers. The PCR products were visualized and then purified using the Illustra GFX PCR DNA and gel band purification kit (GE Healthcare), and sent to MacroGen Sequencing Facility (MacroGen®, South Korea) for ribosomal regions sequencing in both directions. Phylogenetic reconstruction was performed using the sequences published in GenBank using an alignment of 920 bp. For genetic outputs, a maximum likelihood analysis (ML), Likelihood Ratio Test (aLRT), bootstrap analysis (1,000 replicates), and Bayesian analyses were used.

HPLC pigment analysis

For pigment analysis, a detailed protocol is described in Mardones *et al.* (2020). Briefly, 50 mL of the CREAN_HA03 strain



in exponential growth phase were filtered (0.45 μm) and collected cells were extracted in 1 mL acetone after probe sonication (60s) and kept for 24 h at $-20\text{ }^{\circ}\text{C}$. Pigments were quantified using a Shimadzu high-resolution liquid chromatograph (HPLC), and SPD-M20A diode array detector (DAD). Chromatographic separation was carried out by using an ACE C18 PFP column at $40\text{ }^{\circ}\text{C}$. Mobil phase A was prepared with methanol: 225 mM ammonium acetate (82:12 v:v) and mobile phase B with ethanol. The gradient program was set at a flow rate of 1.0 mL min^{-1} . Seven certified reference standards (DHI Laboratory Products, Hoersholm, Denmark) were used for the correct identification of these pigments.

Lipid extraction and analysis

For lipid analysis, a detailed protocol is described in Mardones *et al.* (2020). Briefly, filters containing the CREAN_HA03 strain were extracted using dichloromethane / methanol/ water (1:2:0.8, v/v/v). After phase separation, the extracted lipids were transmethylated for two h at $85\text{ }^{\circ}\text{C}$. After the addition of water, the mixture was extracted three times to obtain fatty acid methyl esters (FAME). Samples were prepared to a known volume with the internal injection standard solution (19:0 FAME) and analysed by gas chromatography. Samples were injected by a split/splitless injector and an Agilent Technologies 7683B Series autosampler in splitless mode at an oven temperature of $120\text{ }^{\circ}\text{C}$. After one min, the oven temperature was increased to $270\text{ }^{\circ}\text{C}$ at $10\text{ }^{\circ}\text{C min}^{-1}$, then to $310\text{ }^{\circ}\text{C}$ at $5\text{ }^{\circ}\text{C min}^{-1}$. FAME were identified by assessment against retention times of laboratory standards. Gas chromatography–mass spectrometry (GC–MS) analyses

were performed for selected samples for confirmation of FAME identification.

Growth of H. akashiwo under different temperatures and salinities

The experiments with *H. akashiwo* (CREAN_HA03 strain) were carried out in triplicate using sterile flasks, each containing 45 mL of L1 culture medium inoculated with 300 cells mL^{-1} . The growth rate and culture yield were studied using a crossed factorial design under six conditions, obtained from combining three salinities (25, 30 and 35) and two temperatures (12 and $17\text{ }^{\circ}\text{C}$). These different salinities and temperature ranges tested are commonly found within the inner Patagonian fjords.

To prevent modifications in the physiological response of *H. akashiwo* due to changes in temperature and salinity, cultures were pre-acclimated to the desired experimental conditions via stepwise transfer over a defined period (> 20 days). The experiment was carried out for 19 days, with samples taken every 2 – 3 days. Cell density was determined immediately after sampling, based on buffered glutaraldehyde fixed cells quantified under an inverted light microscope using a Fuch-Rosenthal chamber. In every sampling date, the mean cell number obtained from the three replicates was used to calculate the growth rate μ (d^{-1}) according to (Guillard and Hargraves, 1993):

$$\mu = \frac{\ln(c_1/c_0)}{t_1 - t_0}$$

were c_0 and c_1 are the cell densities (cells mL^{-1}) at the beginning (t_0) and end (t_1) of the incubation period (days), respectively.



Results and Discussion

Bayesian phylogenetic and Maximum Likelihood analysis of the LSU D1-D2 region showed that the CREAM_HA03 sequence is in a monophyletic clade that comprises only *H. akashiwo* sequences, supported by one probability value (Fig. 1). The monophyletic clade showed that the Chilean sequence of *Heterosigma* has a genetic distance of 0.00 relative to the sequences reported from Japan, Australian, U.S.A., Denmark, China and New Zealand. The genetic distance with other strains from Brazil, Canada, Korea, and New Zealand was 0.001. The distances with *H. minor* were estimated in 0.064. Previous reports have shown that this species has low genetic variability at the intraspecific level among strains of different parts of the world (Bowers *et al.*, 2006), which is in line with the results reported in this study.

The HPLC pigment analysis of the Chilean strain (CREAM_HA03) showed that the most abundant pigment is the carotenoid fucoxanthin, with 48% of the total pigments, followed by violoxanthin with 14% of the sample. Chlorophyll c2 was a significant pigment with 18% of the sample. The carotenoids fucoxanthin and violaxanthin are usually the most abundant secondary pigments among world-wide distributed *H. akashiwo* strains (Martínez *et al.*, 2010), as well as in Chilean strains (this study; Gómez *et al.*, 2021). This chemotaxonomic feature might help for future monitoring of this raphidophyte in Chilean waters using satellite ocean colour data.

The fatty acid profile of *H. akashiwo* strain was dominated by saturated fatty acid (SFA) followed by PUFA (Table 1). Around 20.94%

of the total fatty acid was palmitic acid (16:00, SFA), 13.04% EPA (20:5 ω 3, PUFA), and 10.44% stearidonic acid (18:4 ω 3, PUFA). These lipids have been described as cytotoxic against the RTgill-W1 rainbow trout gill cell line (Dorantes-Aranda *et al.*, 2015; Mardones *et al.*, 2015). This is the first study describing the lipid composition of a Chilean *H. akashiwo* strain. These results may assist in future studies pursuing the understanding of the ichthyotoxic mechanism in *H. akashiwo*, especially their link with the potential production of ROS by this raphidophyte.

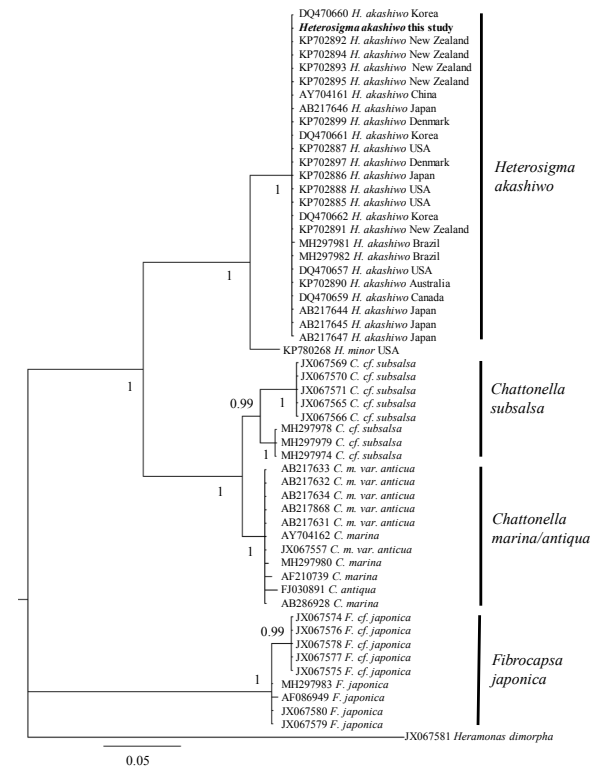


Fig. 1. Phylogeny of the (A) large subunit (LSU rDNA) sequence of the Chilean *H. akashiwo* strain and related species. In bold is the Chilean CREAM_HA03 sequence from this study.



The response of *H. akashiwo* strain CREAN_HA03 to changes in temperature and salinity was significantly different in terms of maximum cell biomass. The maximum cell abundance was $\sim 50,000$ cells mL⁻¹ at 12 °C and salinity of 25 (Fig. 2). However, the growth rate (μ) was not significantly different due to temperature and salinity changes. The highest μ_{\max} (0.48 d⁻¹) was reached at salinity of 35 and at 17 °C, meanwhile the lowest μ_{\max} (0.38 d⁻¹) was reached at a salinity of 25 and at 17 °C.

Table 1. Top three most abundant fatty acids quantified in the Patagonian *H. akashiwo* (strain CREAN_HA03) (as percentage of total fatty acids).

Fatty acids	Mean	SD
SFA		
16:00	20.94	0.14
PUFA		
18:4 ω 3	10.44	0.13
20:5 ω 3	13.04	0.15

Abbreviations: SFA, saturated fatty acids; PUFA, polyunsaturated fatty acids.

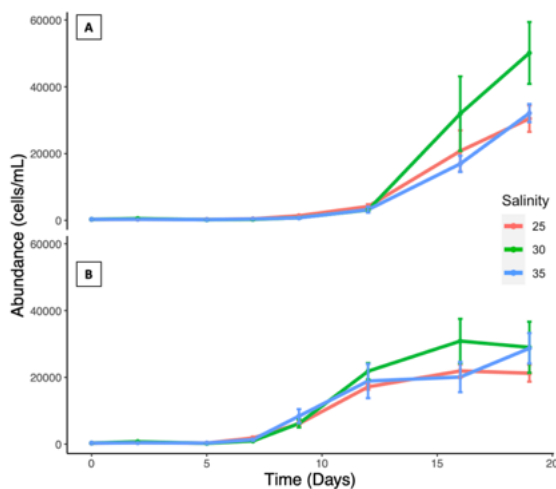


Fig. 2. *In vitro* growth of *H. akashiwo* at (A) 12 °C and (B) 17 °C, and at three different salinities.

These results point to the fact that that Chilean *H. akashiwo* can grow in different conditions of salinity and temperature, euryhaline and eurythermal characteristics that have been described for other world-wide distributed *H. akashiwo* strains (Martínez *et al.*, 2010). These characteristics provide a clear advantage over other microalgae species in highly variable estuarine ecosystems. A pending question is: “why did this species bloom after almost 20 years in the Chilean fjords if it presents such a high phenotypic plasticity?”. It is possible that the undergoing climate change scenario is triggering other important environmental factors such as enhanced water stratification and high-water retention rates that might be contributing to these unexpected HAB events.

This study is the first describing the genetic position and the lipid composition of a Chilean strain of the raphidophyte *H. akashiwo*. Future research should focus on the toxic mechanism of this specie, and how other factors (ie., nutrient concentrations) can affect its growth in a complex environment such as the Patagonian fjords.

Acknowledgements. We thank our colleagues from the CREAN laboratory for microalgae culture support. Funding was provided by the Instituto de Fomento Pesquero (IFOP) and the FIPA 2020-08 grant (SUBPESCA).

References

- Bowers, H. A., Tomas, C., Tengs, T., Kempton, J. W., *et al.*, (2006). *J. Phycol.* 42, 1333-1348.
- Dorantes-Aranda, J. J., Seger, A., Mardones, J. I., Nichols, P. D., Hallegraeff, G. M. (2015). *PLoS One* 10, e0133549.



Gómez, P. I., Inostroza, I., Castro-Varela, P., Silva, J., *et al.*, (2021). *Phycol.* 61, 7-15.

Guillard, R.R.L. and Ryther, J.H. (1962). *Can. J. Microbiol.* 8, 229-239.

Guillard, R.R.L. and Hargraves, P.E. (1993). *Phycol.* 32, 234-236.

Mardones J., Clément A., Rojas X. 2012. *Harmful Algae News* 45, 6-7.

Mardones, J. I., Dorantes-Aranda, J. J., Nichols, P. D., Hallegraeff, G. M. (2015). *Harmful Algae* 49, 40-49.

Mardones, J. I., Norambuena, L., Paredes, J., Fuenzalida, G., *et al.*, (2020). *Harmful Algae* 98, 101892.

Martínez R., Orive E., Laza-Martínez A., Seoane S. 2010. *J. Plank. Res.* 32, 529-538.





CIGUATERA AND BENTHIC HABs



Raising awareness of ciguatera poisoning in Australia: a survey of recreational fishers

Andreas Seger^{1,2}, Natalie Dowsett^{2,3}, Alison Turnbull^{1,2}

¹*Institute for Marine and Antarctic Studies, Fish Health, Biosecurity and Seafood Safety, University of Tasmania, 15-22 Nubeena Crescent, 7053, Taroona, Tasmania, Australia;*

²*Seafood Safety and Market Access Program, SafeFish, GPO Box 397, 5001, Adelaide, Australia;* ³*South Australian Research and Development Institute, Food Sciences, 2B Hartley Grove, 5064, Urrbrae, Australia.*

* corresponding author's email: andreas.seger@utas.edu.au

Abstract

In Australia, recreational fishers are repeatedly associated with ciguatera poisoning. Nevertheless, a myriad of misinformation and “old wives” tales circulate regarding the prevalence of ciguatoxin and how to detect ciguateric fish. As part of the ciguatera awareness campaign run by SafeFish (Australian Seafood Safety and Market Access Program), we conducted an online survey of Australian recreational fishers (recruited through social media and recreational fishing groups) to gauge current awareness levels of this risk and how best to improve them. Answered by 236 respondents, the survey revealed that in this group of voluntary respondents, 90% were aware of ciguatera. These individuals predominantly originated from the ciguatera endemic areas of Queensland and the Northern Territory, as well as New South Wales, which has only started recording ciguatera cases in 2016. Twenty-six percent of the individuals identified as having suffered from ciguatera previously, with 40% not having been diagnosed by a health care worker. In terms of the available information, respondents felt that key information on the fish species at risk of carrying ciguatoxins and ciguatera symptoms was lacking. Based on the survey feedback, a detailed ciguatera fact sheet was prepared and circulated through the identical social media channels used to promote the survey. Efforts to raise ciguatera awareness in Australia are ongoing, with a SafeFish facilitated survey of health care workers on the horizon.

Keywords: ciguatera poisoning, awareness, biotoxin, social media, management

<https://doi.org/10.5281/zenodo.7035010>



Introduction

Ciguatera poisoning accounts for the most frequent seafood safety related illness outbreaks in Australia, making up more than 50% of outbreaks (OzFoodNet data, 2001-2015). Traditionally, these cases have occurred in the tropical and subtropical regions of Australia in the Northern Territory and Queensland. However, since 2014, several cases linked to migratory Spanish Mackerel (*Scomberomorus commerson*) have been reported from further South along the east coast of Australia in New South Wales (Farrell *et al.*, 2017). This number of ciguatera cases is subject to significant underreporting by both health care workers and those affected. It is estimated that less than 20% of the cases are reported in Australia (Lehane and Lewis, 2000). Reasons for underreporting by health professionals include difficulty in reporting (time required to file reports, often remote locations), misdiagnosis (individual experience of health care workers, often complicated with ambiguous symptoms) and lack of awareness of reporting system/requirements. Ciguatera sufferers often do not consult their health care providers due to ambiguous symptoms, the lack of effective treatment options and/or distance to the nearest health care provider (can be hundreds of kilometers in remote Queensland and Northern Territory).

Given the prevalence of ciguatera poisoning in Australia and the potential severity of the illness, ciguatera has been identified as a high research priority by SafeFish, a collaborative program that assists the Australian seafood industry with food safety and market access issues. This led to a multidisciplinary ciguatera poisoning workshop that brought

together Australian regulators, commercial fishers, food authorities and researchers to discuss current knowledge and research directions.

The Australian ciguatera research strategy that was born from this meeting highlights the importance of raising ciguatera awareness amongst the population to improve reporting rates and approach closer to the true incidence of ciguatera in Australia (SafeFish, 2019). Health care workers and recreational fishers were identified as two key demographics at different levels in the reporting hierarchy where immediate improvements could be achieved. We here report the findings from an online ciguatera survey of Australian recreational fishers. The survey aimed to collect data on and raise the awareness of ciguatera poisoning amongst the recreational fishing community and guide the subsequent development of additional awareness materials.

Material and Methods

Survey design

The survey was prepared in an online format (SurveyMonkey) and structured into three different sections:

1. Demographic: state of origin, previous experiences with ciguatera and background awareness.
2. Information and awareness materials: level of satisfaction with existing information on ciguatera, trust in that information and areas for improvement.
3. Citizen science: preparedness of respondents to participate in citizen science-type projects and potential use



of a live ciguatera risk map where fishers can enter details of unlucky catches

Recruitment of participants

Participants were recruited predominantly through social media, focusing on Facebook fishing groups in the ciguatera endemic regions of the Northern Territory and Queensland, as well as New South Wales. Other means of recruitment included direct emails to recreational fishing clubs and Australian fishing associations, as well as distribution through SafeFish seafood industry networks.

Ethics

The survey was conducted under Human Research Ethics approval from the Tasmania Social Sciences Human Research Ethics Committee (23815) and the University of Adelaide (H-2020-234). The highest identifying level of data was state/territory of origin and data pooled across responses. Participants were informed of the intended use of the data upfront in a participant information sheet.

Results and Discussion

Demographic and background information

The survey was answered by 236 respondents, the majority of whom originated from Queensland, the Northern Territory, and New South Wales; the three Australian states where ciguatera is most often reported (OzfoodNet, 2001-2015). Of these respondents, 26% identified as having suffered from ciguatera poisoning before, with less than 64% having their diagnosis confirmed by a health care worker. Where these respondents that have suffered from ciguatera originated from within Australia is identified in figure 1. Poisoning reports from states that do not

border waters known to harbor ciguatoxic fish, such as Tasmania and Victoria, outline the risk that interstate tourist travel and fish trade might pose.

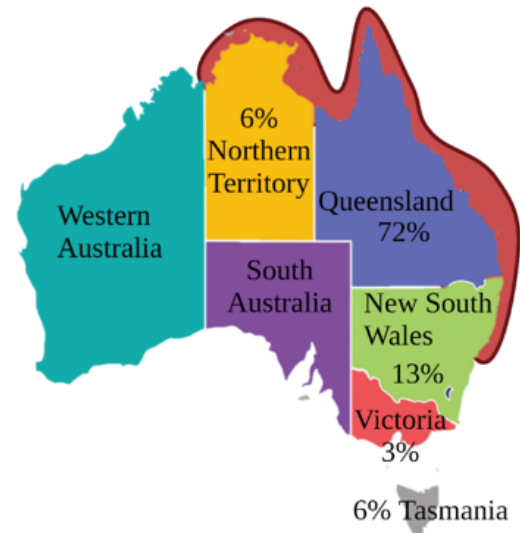


Fig. 1. Map of Australia showing the origin of survey respondents who identified as having suffered from ciguatera in the past (29 out of 236 respondents). The maroon shaded area indicates coastal waters known to harbor ciguatoxic fish.

A prime example is a Maori Wrasse caught in Queensland waters, that was consumed at a Victorian banquet, poisoning 30 diners (Ng and Gregory, 2000). The risk behaviour of the recreational fishers surveyed was dominated by ciguatera conscious individuals that would avoid certain species or sizes of fish (65% of respondents), and those that thought they would be very unlikely to get it (21%). This is comparable to a telephone survey conducted in the Virgin Islands (n = 807), where 62% believe certain fish are poisonous and 50% of respondents indicated avoidance of certain species (Radke *et al.*, 2013).



The majority (90%) of Australian respondents had heard of ciguatera poisoning before, suggesting high levels of awareness. A similar survey on the French Polynesian Island of Moorea indicated that 98% of locals were aware of ciguatera, compared to only 24% awareness among visitors to the island (Morin *et al.*, 2016). Given the high average incidence of ciguatera on Moorea Island (eight cases per 10,000 inhabitants), this high awareness level is not surprising. However, comparably high ciguatera awareness in Australia may be skewed by the survey design. There is no register/licensing requirement for recreational fishers in the Northern Territory or Queensland that would allow for random sampling of fishers. Instead, the survey required voluntary participation, which may have led to an inadvertent selection of individuals with a pre-existing interest in ciguatera. Nevertheless, the survey collected valuable information on currently available and desired awareness materials and raised awareness of ciguatera for members of Facebook fishing groups, irrespective of whether they answered the survey.

Ciguatera awareness materials

The majority of respondents (61%) indicated that currently available information on ciguatera does not meet their needs. When questioned about the quality of that information (availability, content, relevance, level of detail), 34% of the surveyed fishers felt neutral and 20% expressed dissatisfaction, particularly in regard to the level of detail of available information. When asked what data format they would find most engaging, respondents displayed strong interest in fact sheets, written articles and infographics (Fig. 2).

The type of information that recreational fishers were most strongly interested in included a list of fish species that are at risk of carrying ciguatoxins, what symptoms to look for and the available treatment options. Background knowledge of toxin uptake pathways, “survivor” stories and the latest scientific news attracted mild interest, while opportunities to be involved in citizen science type projects were lowest on the priority list. Reflecting current information technology trends, fishers are most likely (71% of respondents) to seek this information through the internet (fishing forums, fisheries, or State Health Department websites), followed by other fishermen, Facebook groups and fishing magazines.

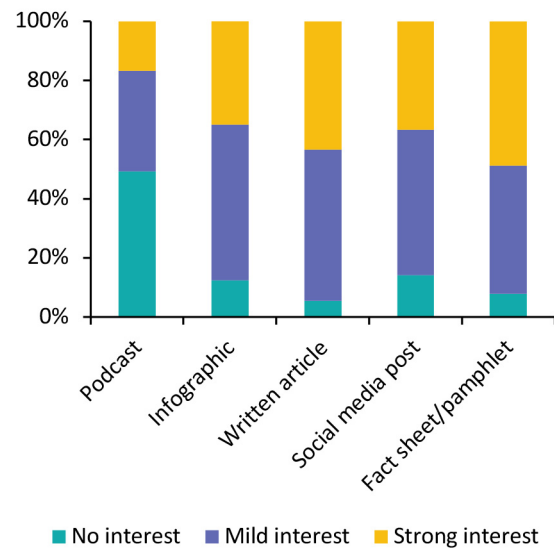


Fig. 2. Ciguatera awareness media format preferences of recreational fishers.

Citizen science

When asked to rate the idea of citizen science-type projects on a scale of 0 (least desirable) to 5 (most desirable), fishers were highly supportive (average rating of 4.1 out of 5). In fact, 30% of respondents had already



participated in citizen science type research. The experiences of these fishers were largely positive (98% had no negative experiences to report regarding the clarity of instructions or project purpose). Communication on past citizen science projects, especially around the outcomes, attracted a few more neutral responses (32% respondents), but experiences were overall positive (56% positive). The idea of an open access platform for recreational fishermen, where they can report the detail of ciguateric fish to warn other fishers of potential risk, was met with strong support (an average rating of 4.2 out of 5). According to the surveyed demographic, such a risk map would ideally be linked to existing navigation or fishing apps (70% of respondents), with 60% of respondents using state government fishing applications.

Conclusion

Raising awareness of ciguatera poisoning is a key step towards improving the reporting rate of individual cases. Our survey of recreational fishers proved to be a valuable tool in this quest, indicating the type, detail, and format of information that fishers felt they required. Based on the information provided in this survey, we developed and distributed a detailed ciguatera Frequently Asked Question (FAQ) fact sheet that is openly available from the SafeFish website SafeFish (2021). While the awareness and ciguatera incident data presented here should be interpreted with care due to the survey likely targeting individuals already interested in ciguatera, sharing the survey through social media in itself has raised awareness among non-respondents. The preparedness of the respondents to participate in citizen science type projects is encouraging and will offer opportunities for both scientists and fishers to benefit, such as a ciguatera risk

map or by providing samples for ciguatoxin analysis (e.g. Kohli *et al.*, 2017). Increasing awareness of ciguatera poisoning is a continuous process and through the SafeFish program we are currently moving to extend our work to a survey aimed at increasing ciguatera awareness among Australian health care workers.

Acknowledgements. This work was facilitated through the [SafeFish Seafood Safety and Market Access](#) partnership of the Australian Fisheries Research and Development Council and the Australian seafood industry through grant numbers 2018-004 and 2021-018. The authors would like to thank Dr. Clémence Gatti for helpful discussion and Dr. Stephen Pahl for reviewing the survey questions. Figure 1 was created using BioRender.com software.

References

- Farrell, H., Murray, S., Zammit, A., Edwards, A. (2017). *Toxins* 9, 367.
- Kohli, G.S., Haslauer, K., Sarowar, C., Kretzschmar, A.L., *et al.*, (2017). *Toxicol. Rep.* 4, 328-334.
- Lehane, L. and Lewis, R.J. (2000). *Int. J. Food Microbiol.* 61, 91-125.
- Morin, E., Gatti, C., Bambridge, T., Chinain, M. (2016). *Harmful Algae* 60, 1-10.
- Ng, S. and Gregory, J. (2000). *Commun. Diss. Intell.* 24, 344-346.



OzfoodNet. (2001-2015). Foodborne disease surveillance network. Australian Department of Health. www1.health.gov.au/internet/main/publishing.nsf/Content/cdna-ozfoodnet.htm. Accessed 10/11/2021.

Radke, E.G., Grattan, L.M., Cook, R.L., Smith, T.B., *et al.*, (2013). Am. J. Trop. Med. Hyg. 88, 908-913.

SafeFish (2019). National ciguatera research strategy: reducing the incidence of ciguatera in Australia through improved risk management. In: Seger, A., Dowsett, N., Turnbull, A. www.safefish.com.au/reports/technical-reports/ciguatera-research-strategy. Accessed 10/11/2021.

SafeFish (2021). Ciguatera (fish) poisoning in Australia - Frequently asked questions. www.safefish.com.au/reports/food-safety-fact-sheets/ciguatera-fish-poisoning-faq. Accessed: 10/11/2021.



Diversity, biogeography, and chemically mediated interactions of toxigenic benthic marine dinoflagellates from Mexican coastal waters

Lorena M. Durán-Riveroll^{1,2*}, Allan D. Cembella², Yuri B. Okolodkov³

¹CONACyT-Departamento de Biotecnología Marina, Centro de Investigación Científica y de Educación Superior de Ensenada, Ensenada, Mexico; ²Alfred-Wegener-Institut, Helmholtz-Zentrum für Polar- und Meeresforschung, Bremerhaven, Germany; ³Instituto de Ciencias Marinas y Pesquerías, Universidad Veracruzana, Boca del Río, Mexico.

*corresponding author's email: lduran@conacyt.mx

Abstract

Many benthic dinoflagellates produce polyketide-derived polyether toxins responsible for diverse seafood poisoning syndromes, such as diarrhetic shellfish poisoning and ciguatera fish poisoning. In Mexico, bHAB events have received recent public health and scientific attention, but many species lack molecular identification, and phylogeographic and toxigenic information remains limited. Our multidisciplinary project on bHAB taxa includes morphological and molecular characterization, phylogeography, and investigation of allelopathic and pharmacological bioactivity, supplemented with bacterial microbiome analysis. We first characterized the phylogeography and diversity of the genus *Prorocentrum* from Mexican coasts and investigated potential allelochemical effects of associated bacteria on growth and toxigenicity of members of the *Prorocentrum lima* species complex. Thus far, we have also completed the first phylogenetic study of benthic *Amphidinium* and registered two species (*A. theodorei* and *A. massartii*) for the first time from Mexico. Preliminary studies on the *in vitro* cytotoxic properties of *A. operculatum* and *Coolia malayensis* are also well advanced, demonstrating pharmacological potential through bioactivity against human cancer cell lines. The focus on functional diversity and species interactions yields valuable insights in evaluating toxin risk in the design and implementation of monitoring systems for bHABs and exploring biotechnological prospects for bioactive secondary metabolites from benthic species.

Keywords: *Amphidinium*, *Coolia*, *Prorocentrum*, phylogeny, *in vitro* cytotoxicity

<https://doi.org/10.5281/zenodo.7035019>



Introduction

Dinoflagellates are essential functional components of benthic food webs and are implicated in species interactions, especially with microeukaryotes and bacteria on epibenthic substrates and the surrounding microbiome (Boisnoir *et al.*, 2018; Richlen and Lobel, 2011). The dinoflagellate genus *Prorocentrum* Ehrenberg is widely distributed in coastal waters of Mexico and throughout Latin America (reviewed in Durán-Riveroll *et al.* (2019). Benthic representatives of *Prorocentrum* are known to produce diarrheagenic toxins, such as okadaic acid and certain dinophysistoxins, plus other polyketide-derived metabolites of uncertain toxicity or bioactivity (Hu *et al.*, 2010). The phylogeographical distribution, cell toxicity, toxin composition, and diversity of benthic *Prorocentrum lima* and *Prorocentrum hoffmannianum* species complexes, PLSC and PHSC, respectively, have been published (Cembella *et al.*, 2021). Nevertheless, such studies are limited to isolates from a few selected sites on the coasts of Mexico and do not represent the complete diversity of the genus at the infraspecific and population levels.

Members of the dinoflagellate genus *Amphidinium* Claparède *et* Lachmann are often abundant in benthic environments, including tropical and subtropical zones in Mexico, frequently attached to macrophytes. Some species have the capacity to synthesize bioactive polyketides, but the structures are poorly characterized in most cases, and studies are limited to a few species (Murray *et al.*, 2012). These polyketide metabolites of *Amphidinium* have shown biological activities worth further investigation as

potential pharmaceuticals or therapeutants (Mejía-Camacho *et al.*, 2021).

Species of the genus *Coolia* Meunier may produce cooliatoxin(s), polyketide analogs of yessotoxin (YTX), but the chemical structures of cooliatoxins have not been fully elucidated. Some members of the genus are known to produce bioactive metabolites in culture against several cancer cell lines (Boente-Juncal *et al.*, 2019) but the active components remain uncharacterized.

Some recent studies have evaluated the cytotoxic, antiproliferative, antibiotic, antifungal, and antidiabetic effects of benthic dinoflagellate metabolites as potential sources for novel drugs (Dewi *et al.*, 2018). The diversity and chemically mediated species interactions of benthic dinoflagellates in Mexican coastal waters are being studied from the morphological and molecular perspective for the species identification, phylogeography, chemical ecology, and production of bioactive metabolites with pharmacological potential. Herein we report preliminary highlights as representative of the emerging state of knowledge on diversity and species interactions.

Material and Methods

Isolation, culture, and harvest of Prorocentrum, Amphidinium, and Coolia species

Benthic dinoflagellate cells were isolated from macroalgae, seagrasses, and inanimate surfaces collected from Bahía de La Paz (Gulf of California), Veracruz (Gulf of Mexico), and Puerto Morelos (Caribbean



Sea). Experimental cultures of *Amphidinium* and *Coolia* were grown in GSe medium without soil extract, prepared from filtered autoclaved seawater at a salinity of 36. Cultures were initiated on a 12:12 h L:D cycle at 24 ± 1 °C with an illumination of $50 \mu\text{mol photons m}^{-2} \text{s}^{-1}$ in 60 x 15 mm Petri plates for microscopic identification and DNA and ethanolic extraction. Subcultures of *Prorocentrum* spp. were transferred to Alfred Wegener Institute, Germany, and grown on K medium at 24 ± 1 °C on a 14:10 L:D cycle under illumination of $86 \mu\text{mol photons m}^{-2} \text{s}^{-1}$. Exponentially growing *Prorocentrum* cultures (*ca.* 10^6 cells) were harvested by centrifugation (10 min, 3,000xg) for DNA sequencing (Cembella *et al.*, 2021) and for toxin analysis (Tarazona-Janampa *et al.* (2020) after esterase inactivation at 100 °C for 5 min.

DNA sequence analysis of Prorocentrum spp. Total DNA was extracted and processed with the Genomic DNA PowerSoil kit (Macherey-Nagel, Düren, Germany), following details in (Cembella *et al.*, 2021). The D1/D2 region of the 28S large subunit (LSU) rDNA and the internal transcribed spacer (ITS) region (including ITS1, 5.8S subunit, and ITS2 sequences) were amplified from each total DNA extract by PCR. Sequencing products were analyzed on an ABI 3130 XL capillary sequencer (Applied Biosystems, Darmstadt, Germany) and the generated sequences were analyzed and assembled with CLC main workbench version 12.0.1.

Phylogenetic analysis included representative sequences of *P. lima sensu lato*, *P. lima*, *P. hoffmannianum*, and *P. belizeanum* from the Americas, Asia, and Europe, retrieved from GenBank2 (n = 68 for LSU and n = 72 for

ITS). Two data sets with 13 species were assembled, one for the LSU locus with 68 sequences, and another for the ITS locus with 72 sequences. Taxonomic sampling within *Prorocentrum* followed Chomérat *et al.* (2019), but with the addition of recently described species (Lim *et al.*, 2019; Luo *et al.*, 2017).

Toxin composition of Prorocentrum spp.

Analysis of DSP toxins, namely okadaic acid (OA) and dinophysistoxins (DTX), was performed as described in Tarazona-Janampa *et al.* (2020) by liquid chromatography coupled with tandem mass spectrometry (LC-MS/MS) following previous protocols (Krock *et al.*, 2008).

Molecular identification of Amphidinium spp. and Coolia spp.

Total DNA extraction of *Amphidinium* isolates AA38, AA60, AA105, and AA112, and *Coolia* isolates CA24, and CA55, was performed by a modified CTAB method according to Jørgensen *et al.* (2004). Approximately 1,450 base pairs (bp) of the D1 and D6 variable domains of LSU rDNA were amplified (Jørgensen *et al.*, 2004; Karafas *et al.*, 2017). PCR products were sequenced by seqXcel Inc. (California, U.S.A.). The NCBI database was accessed through BLASTn for species assignment.

Preparation of ethanolic extracts for cell assays

Amphidinium AA60 and *Coolia* CA24 cultures (13-50 mL) were harvested by centrifugation (35xg for 10 min). Seawater medium supernatants were removed and the pellets frozen at -65 °C. Biomass was extracted with 2 mL 100% ethanol. Complete cell disruption by repeated freeze-thaw cycles



was verified microscopically. The extracted material was centrifuged (6720×g) and the retained supernatant was filtered through a 0.2 μm syringe filter. The ethanolic extracts were lyophilized and later reconstituted for the *in vitro* assays.

Six human cancer cell lines were assayed for effects on growth after exposure to ethanolic extracts: U251 (human glioblastoma), PC-3 (human prostatic adenocarcinoma), K562 (human erythroleukemia), HCT-15 (human colorectal adenocarcinoma), MCF-7 (human mammary adenocarcinoma), and SKLU-1 (human lung adenocarcinoma). All cancer cell lines were obtained from the National Cancer Institute (NCI, Bethesda, MD, U.S.A.). The cell lines were cultured in RPMI-1640 medium supplemented and tested as described in Mejía-Camacho *et al.* (2021).

Results and Discussion

Diversity among Prorocentrum species complexes

Morphotaxonomic and phylogenetic analysis of ITS/5.8S rDNA sequences from *Prorocentrum* isolates from the Gulf of California, Gulf of Mexico and the Caribbean Sea defined five consistent clades with separation of the PLSC and PHSC, with details provided in Cembella *et al.* (2021). This study represents the largest (n = 67 isolates) chemodiversity analysis of polyketide-derived DSP toxins from any benthic dinoflagellate genus. Relative composition of certain analogs distinguished *P. lima* from *P. hoffmannianum sensu lato*, but without clear associations with substrate type or geographical origin within Mexican coastal waters. All *P. lima* and most (one exception) *P. hoffmannianum* isolates were toxicogenic, but

the total cell toxin content was not correlated among strains at the infraspecific level according to biogeographical distribution or origin.

Species identification and molecular diversity of Amphidinium

Cultured *Amphidinium* strains were assigned to species based on molecular criteria as follows: AA38, *A. theodorei*, AA60, *A. operculatum*, AA112, *A. massartii*, and AA105 *A. carterae*. To our knowledge, this is the first report of *A. theodorei* and *A. massartii* in Mexican coastal waters. *Amphidinium* species are notoriously difficult to identify based on morphological criteria alone because cells are fragile and variable in shape with few reliable surface details. The apparent absence of *A. theodorei* and *A. massartii* in records of benthic dinoflagellates from Mexico may be due to the previous lack of molecular studies of this genus in the region. Alignment of the LSU rDNA sequences of the D1-D6 region from *Amphidinium* placed all isolates from Mexican waters within the Operculatum clade, as currently defined, despite the high species diversity among sites (Figs. 1, 2).

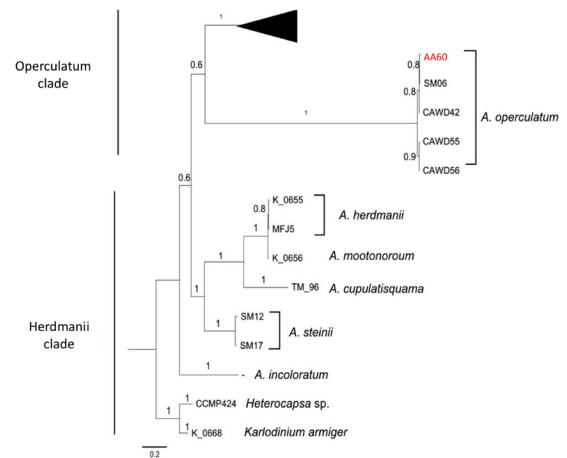


Fig. 1. Phylogenetic tree (Bayesian inference) from LSU rDNA regions D1-D6.

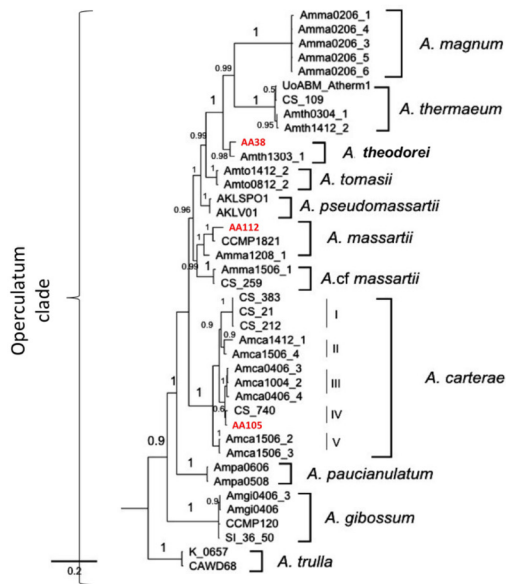


Fig. 2. Phylogenetic tree (Bayesian inference) from LSU rDNA regions D1-D6.

In vitro cell activity of ethanolic extracts of Coolia and Amphidinium

The rRNA sequence analysis of *Coolia* CA24 and CA55 strains confirmed that these strains extracted belonged to *C. malayensis* and *C. monotis*, respectively. *In vitro* cell assays with ethanolic extracts of both *Coolia* strains against human cancer cell lines showed clear bioactive responses only with *C. malayensis* CA24 extracts.

Extracts of *C. malayensis* CA24 exhibited different inhibitory responses against various human cell lines when administered in fixed doses at 25 $\mu\text{g mL}^{-1}$ (equivalent to 5,220 dinoflagellate cells mL^{-1}). The highest growth inhibition was apparent with MCF-7, HCT-15, and SKLU-1 cancer cell lines (Fig. 3).

Extracts of *A. operculatum* AA60 heavily inhibited the growth of MCF-7 and SKLU-1 cell lines (as for *C. malayensis* CA24)

when applied at 25 $\mu\text{g mL}^{-1}$ (equivalent to 5,110 cells mL^{-1}). In contrast, however, all other cell lines were also inhibited to some extent (> 13%) (Fig. 3). Ethanolic extracts of AA60 are generally more potent and with a broader activity spectrum than *Coolia* CA24 at comparable dosages.

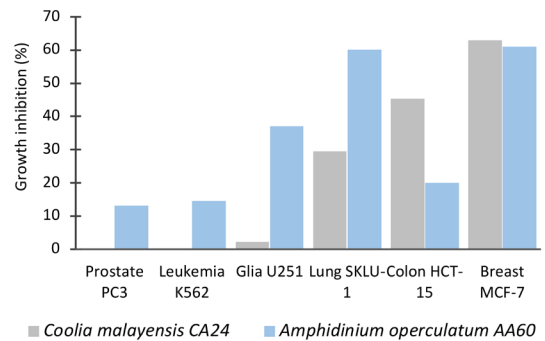


Fig. 3. Growth inhibition of cell lines exposed to ethanolic extracts of *C. malayensis* CA24 and *A. operculatum* AA60 applied at 25 $\mu\text{g mL}^{-1}$.

This preliminary work has demonstrated diversity among benthic *Prorocentrum* from multiple sites on the Gulf of California, the Gulf of Mexico, and the Mexican Caribbean coasts. The next stage is to explore the role of the microbiome on growth and toxigenicity in an ecological context. For other genera such as *Coolia* and *Amphidinium*, the diversity range among species and populations from different regions must first be considered. The high chemodiversity in bioactive secondary metabolites, e.g., toxins and/or allelochemicals produced by the benthic dinoflagellates surveyed herein suggests that it is worthwhile to pursue further bioactivity screening. Biotechnological and pharmaceutical potential can only be critically evaluated by identification of the respective bioactive components and more

detailed screening over a wider range of concentrations. This will also assist in the implementation of rational risk assessment strategies for bHABs.

Acknowledgements. This work was funded by CONACyT A1-S-8616. The participation of AC was within Topic 6: Subtopic 6.2, Adaptation of Marine Life of the Alfred-Wegener-Institut, Helmholtz Zentrum für Polar-und Meeresforschung, Germany. We thank A. Mejía-Camacho, P. García-Santos, A. Nieto-Camacho and M. T. Ramírez-Apán for research contributions.

References

- Boente-Juncal, A., Álvarez, M., Antelo, Á., Rodríguez, I., *et al.*, (2019). *Toxins* 11, 79.
- Boisnoir, A., Pascal, P.-Y., Cordonnier, S., Lemée, R. (2018). *J. Sea Res.* 135, 74-83.
- Cembella, A.D., Durán-Riveroll, L.M., Tarazona-Janampa, U.I., Okolodkov, Y.B., *et al.*, (2021). *Front. Mar. Sci.* 8, 716669.
- Chomérat, N., Bilien, G., Zentz, F. (2019). *Mar. Biodivers.* 49, 1299-1319.
- Dewi, I.C., Falaise, C., Hellio, C., Bourgougnon, N., Mouget, J.-L. (2018). Academic Press, Elsevier.
- Durán-Riveroll, L.D., Cembella, A.D., Okolodkov, Y.B. (2019). *Front. Mar. Sci.* 6, 148.
- Hu, W., Xu, J., Sinkkonen, J., Wu, J. (2010). *Mini Rev. Med. Chem.* 10, 51-61.
- Jørgensen, M.F., Murray, S., Daugbjerg, N. (2004). *J. Phycol.* 40, 351-365.
- Karafas, S., Teng, S.T., Leaw, C.P., Alves-de-Souza, C. (2017). *Harmful Algae* 68, 128-151.
- Krock, B., Tillmann, U., John, U., Cembella, A. (2008). *Anal. Bioanal. Chem.* 392, 797-803.
- Lim, Z.F., Luo, Z., Lee, L.K., Hii, K.S., *et al.*, (2019). *Harmful Algae* 83, 95-108.
- Luo, Z., Zhang, H., Krock, B., Lu, S., *et al.*, (2017). *Algal Res.* 22, 14-30.
- Mejía-Camacho, A.L., Durán-Riveroll, L.M., Cembella, A.D. (2021). *J. Xenobiot.* 11, 33-45.
- Murray, S., Garby, T., Hoppenrath, M., Neilan, B. (2012). *PloS One* 7, e38253.
- Richlen, M.L. and Lobel, P.S. (2011). *Mar. Ecol. Prog. Ser.* 421, 51-66.
- Tarazona-Janampa, U.I., Cembella, A.D., Pelayo-Zárate, M.C., Pajares, S., *et al.*, (2020). *Front. Mar. Sci.* 7, 569.



Benthic harmful algal blooms occurrence in the south coast of Madeira Island, Portugal, from 2018 to 2020

Teresa Silva^{1*}, Ana Amorim^{1,2}, Ana Sousa³, Manfred Kaufmann^{3,4}

¹MARE - Marine and Environmental Sciences Centre, Faculdade de Ciências da Universidade de Lisboa, Campo Grande, 1749-016 Lisboa, Portugal; ²Departamento de Biologia Vegetal, Faculdade de Ciências da Universidade de Lisboa, Campo Grande, 1749-016 Lisboa, Portugal; ³Marine Biology Station of Funchal, Faculdade de Ciências da Vida da Universidade da Madeira, 9000-107 Funchal, Portugal; ⁴CIIMAR - Interdisciplinary Centre of Marine and Environmental Research of the University of Porto, Terminal de Cruzeiros do Porto de Leixões, 4450-208 Matosinhos, Portugal.

* corresponding author's email: teresasilva@fc.ul.pt

Abstract

Ciguatera fish poisoning episodes have been recently reported in the Madeira Archipelago, requiring actions to protect both public health and economic sectors such as tourism and fisheries. Surveys on the occurrence of benthic harmful algal bloom (bHAB) species were performed during three consecutive years (from 2018 to 2020), at Cais do Carvão Bay, Funchal, Madeira. Samples collected on artificial substrates were analyzed for the presence of bHAB species, the seasonal succession of the bHAB community and the effects of abiotic factors on bHAB dynamics. The bHAB community was characterized by the presence of five genera: *Gambierdiscus*, *Ostreopsis*, *Coolia*, *Prorocentrum*, and *Amphidinium*. The abundance of the different genera showed marked differences. *Ostreopsis* displayed cell abundances several orders of magnitude higher than the other genera (841.05×10^3 cells 100 cm^{-2} (September 2018) and was recorded at all sampling dates. The second most abundant genus was *Coolia*, followed by *Prorocentrum* and *Amphidinium*. *Gambierdiscus* always showed the lowest cell densities (max. 0.43×10^3 cells 100 cm^{-2} (September 2018). During summer, *Ostreopsis* abundances exceeded, in several sampling dates the limits of level of concern for respiratory syndrome outbreaks (20×10^3 cells 100 cm^{-2}) as referred to in the literature. *In situ* recorded abiotic data suggests that the increase of *Ostreopsis* densities could be linked to an increase in water temperature during summer. These results confirm Cais do Carvão Bay, as a potential high-risk area for bHAB development, especially concerning the genus *Ostreopsis*.

Keywords: Benthic dinoflagellates, bHAB community, ecology, time-series, Madeira Island

<https://doi.org/10.5281/zenodo.7035055>



Introduction

Ciguatera fish poisoning (CFP) is a syndrome caused by the bioaccumulation of ciguatoxins in fish and their subsequent consumption by humans (Berdalet *et al.*, 2017). These phycotoxins are produced by species of the benthic dinoflagellate genus *Gambierdiscus* and *Fukuyoa*, often associated with the palytoxin-producing genus *Ostreopsis*. Harmful events associated with benthic dinoflagellates, have been reported more frequently over the last decades and are considered a priority for the scientific community and policy-makers, because of bHABs biogeographical expansion from endemic tropical and subtropical areas to temperate areas, namely Macaronesia (Azores, Madeira, Canary Islands, and Cabo Verde) due to natural and anthropogenic causes (GEOHAB, 2012). Both *Gambierdiscus* and *Ostreopsis* genera have been recorded in the Madeira Archipelago (Madeira, Desertas, Porto Santo, and Selvagens islands) and also CFP episodes, affecting several people after ingesting locally caught contaminated fish, were documented in summer 2007 and 2008 from the Selvagens Islands (290 km to SE of Madeira) (Kaufmann and Böhm-Beck, 2013). Thus, actions are required to assess risks and provide baseline information for the implementation of a sustainable monitoring program. The aim of the present study was to characterize the ecology of the bHAB forming species in Madeira Island. This was achieved through: 1) identification of bHAB forming genera in the area, 2) study of the temporal succession of bHABs, and 3) investigating the abiotic factors that could be associated with bHAB dynamics.

Material and Methods

This study was conducted during three consecutive years from 2018 to 2020 at Cais do Carvão Bay, Funchal, south coast of Madeira (Fig. 1). Sampling was performed from June to October in 2018-2019 and from July to December in 2020. Sampling frequency was influenced by sea conditions. Dinoflagellates were collected with an artificial substrate method consisting of the immersion of triplicates of plastic screens in the water column (2-3 m water depth; screens about 20-30 cm above bottom), for 24h (Tester *et al.*, 2014). Data loggers were deployed simultaneously next to screens to record patterns of seawater temperature (ST) and light intensity. Seawater samples (~ 250 mL) for quantification of dissolved inorganic nutrients (nitrate, nitrite, phosphate, and silicate) were also collected. The samples were kept frozen (-20 °C) until analysis. Nutrient concentrations were determined following Grasshoff *et al.* (1999) and measured in a UV/VIS spectrophotometer (UVmini1240, Shimadzu).

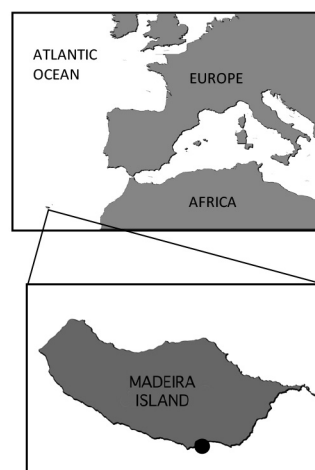


Fig. 1. Sampling site from 2018 to 2020 at the south coast of Madeira Island (black dot), Cais do Carvão Bay.



Screens were retrieved and transferred underwater into plastic bags filled with surrounding seawater and sealed to reduce the chances of losing attached cells. After being transported to the laboratory, plastic bags containing the screens were vigorously shaken for 1 min to detach dinoflagellate cells. Samples were concentrated into a 20 μm sieve and back-washed with pre-filtered seawater into 50 mL tubes. The final volumes (~ 40 mL) were recorded for further quantification. All samples were immediately fixed with neutral Lugol's solution (Edler and Elbrächter, 2010) and 3.7% formaldehyde and stored in the dark until further analyses. Preserved cells were identified under light microscopy. For the quantification of benthic dinoflagellates, specimens were identified at the genus level. Cell counting was carried out in Sedgewick-Rafter chambers and for each concentrated volume (sample), triplicate counting of 1 mL aliquots was performed. Whenever possible, a minimum of 400 cells were counted for statistical consistency. Screen surface area (A_{scr}) was determined according to Tester *et al.* (2014) and cell abundances were expressed as cells 100 cm^{-2} .

Regional mean sea surface temperature (SST) and significant wave height for the study period, except 2019, was obtained from the buoy deployed at 2.5 km from the sampling site (Madeira Port Authority - APRAM). In 2019 the buoy was unavailable for maintenance reasons.

Results and Discussion

From 2018 to 2020 the bHAB forming community, was characterized by the presence of five genera: *Gambierdiscus*, *Ostreopsis*, *Coolia*, *Prorocentrum*, and

Amphidinium. The abundance of the different genera showed marked differences (Fig. 2). *Ostreopsis* displayed cell abundances several orders of magnitude higher than the other genera and was recorded at all sampling dates. The second most abundant genus was *Coolia*, followed by *Prorocentrum* and *Amphidinium*. *Gambierdiscus* always showed the lowest cell densities.

During the study period, maximum cell abundances for all genera were recorded in 2018, except for *Amphidinium* for which maximum abundances were recorded in 2019. *Ostreopsis* presented maximum cell densities of 841.05×10^3 cells 100 cm^{-2} , in September 2018, while *Gambierdiscus*, reached maximum abundances of 4.3×10^2 cells 100 cm^{-2} , also in September 2018. *Coolia* and *Prorocentrum* presented maximum cell densities of 6.49×10^3 cells 100 cm^{-2} in August 2018, and 7.5×10^2 cells 100 cm^{-2} in June 2018, respectively. The highest concentrations of *Amphidinium* (9.9×10^2 cells 100 cm^{-2}) were recorded in June 2019.



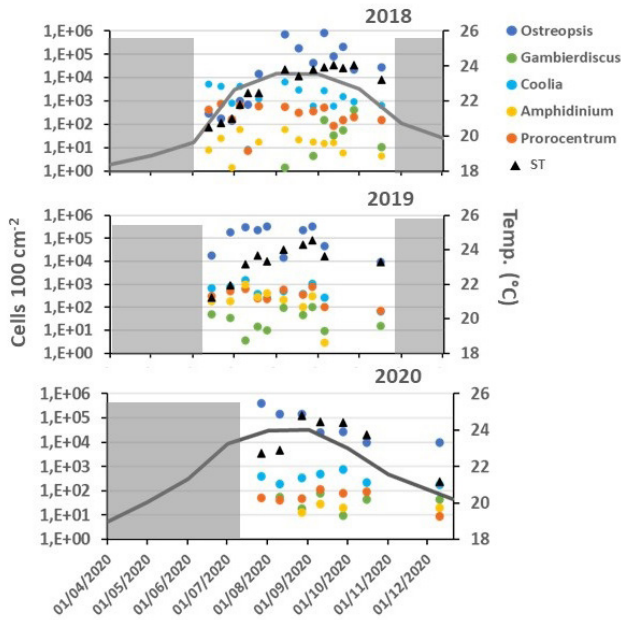


Fig. 2. Distribution of the main bHAB forming genera from 2018-2020 and SST at Cais do Carvão Bay, south Madeira. The grey line represents the mean monthly SST and triangles represent *in situ* ST. Shaded areas, time intervals for which no sampling was performed.

In the three sampled years, *Ostreopsis* abundances increased strongly in July reaching maximum values in August and September (Fig. 2) when higher temperatures (around 24°C) were recorded, suggesting temperature is an important modulator for the development of *Ostreopsis* blooms, while this is not evident for the other genera. Other authors have also found significant positive correlations between *Ostreopsis* spp. densities and temperature (Ciminiello *et al.*, 2006; Ben Gharbia *et al.*, 2019). Furthermore, low waves height seems to be an important factor contributing to bHAB dynamics, particularly for *Ostreopsis* (Fig. 3), in accordance to what has been reported by Santos *et al.* (2019).

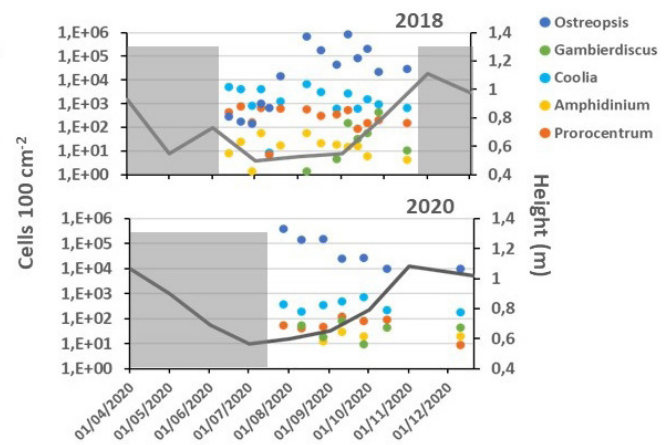


Fig. 3. Distribution of the main bHAB forming genera at Cais do Carvão Bay, south Madeira and significant wave height for 2018 and 2020. Shaded areas, time intervals for which no sampling was performed.

Although 2018 recorded the highest nutrient concentrations and the highest concentrations of *Ostreopsis*, *Gambierdiscus*, *Prorocentrum* and *Coolia*, results indicate that there is no clear relation between bHAB species abundance and nutrients (Figs. 4, 5).

In agreement with what has been described for other Macaronesian islands (Fernández-Zabala *et al.*, 2019), in Madeira *Ostreopsis* is the most abundant bHAB forming genus at shallow depths (from 0.5 to 7 m). *Gambierdiscus* was not detected in high concentrations, however, given the reported occurrence of CFP episodes in other islands of the Madeira Archipelago and in the Canary Islands, the presence of *Gambierdiscus* is a reason of concern. On the other hand, in the summer of all sampled years, *Ostreopsis* abundances exceeded, in several sampling dates the limit of level of concern for respiratory syndrome outbreaks of 20 x



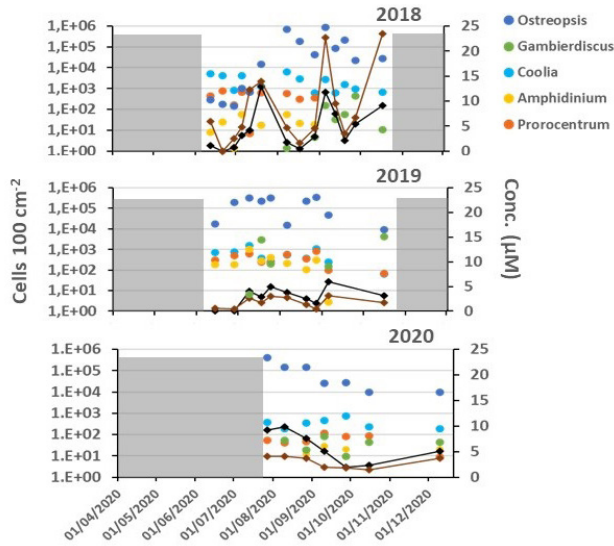


Fig. 4. Distribution of the main bHAB forming genera at Cais do Carvão Bay, south Madeira according to dissolved nutrient concentrations for 2018 and 2020. Black lines represent total dissolved nitrogen ($\text{NO}_3^- + \text{NO}_2^-$); brown line represents silicate (SiO_3^{2-}). Shaded areas, time intervals for which no sampling was performed.

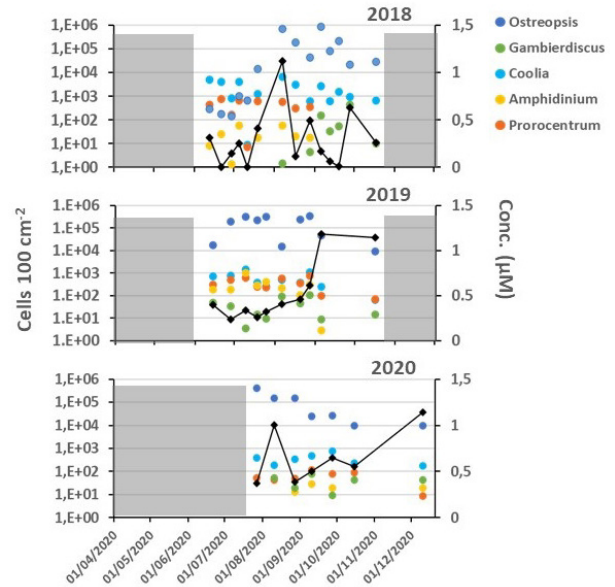


Fig. 5. Distribution of the main bHAB forming genera at Cais do Carvão Bay, south Madeira according to dissolved nutrient concentrations for 2018 and 2020. Black line, total dissolved phosphate (PO_4^{3-}). Shaded areas, time intervals for which no sampling was performed.

10^3 cells 100 cm^{-2} proposed by Tester *et al.* (2014). Overall, these results confirm Madeira (Cais do Carvão Bay), as a potential high-risk area for bHAB development, especially concerning the genus *Ostreopsis*.

Acknowledgements. We are thankful to Madeira Port Authority-APRAM for letting us use temperature and wave height data. We also thank J. Reis (Oceanic Observatory of Madeira) for his support on oceanographic data treatment. This study was supported by a PhD grant (SFRH/BD/ 04292 /2019) to T. Silva funded by ARDITI through the Project M1420-09-5369-FSE-000002 and the Program Madeira 14-20 - Fundo Social. This study was also co-funded by FCT, I.P. under the project UIDB/04292/2020. The activities were developed within the framework of the Interreg MAC 2014-2020 projects; MIMAR (MAC/4.6.d/066) and MIMAR+ (MAC2/4.6d/249).



References

Ben Gharbia, H., Laabir, M., Ben Mhamed, A., Gueroun, S.K.M., *et al.*, (2019). Harmful Algae 90, 101704.

Berdalet, E., Tester, P.A., Chinain, M., Fraga, S., *et al.*, (2017). Oceanography 30, 36-45.

Ciminiello, P., Dell'Aversano, C., Fattorusso, E., Forino, M., *et al.*, (2006). Anal. Chem. 78, 6153-6159.

Edler, L. and Elbrächter, M. (2010). In: Karlson, B., Cusack, C., Bresnan E. (Eds). Microscopic and molecular methods for quantitative phytoplankton analysis. Paris, UNESCO. pp. 13-20.

Fernandez-Zabala, J., Tuya, F., Amorim, A., Soler-Onis, E. (2019). Harmful Algae 86, 101634.

GEOHAB (2012). IOC of UNESCO and SCOR, Paris and Newark.

Grasshoff, K., Kremling, K., Ehrhardt, M. (1999). WILEY-VCH, Weinheim. ISBN: 9783527295890.

Kaufmann, M. and Böhm-Beck, M. (2013). Harmful Algae News 47, 18-19.

Santos, M., Oliveira, P.B., Moita, M.T., David, H., *et al.*, (2019). Harmful Algae 86, 20-36.

Tester, P.A., Kibler, S.R., Holland, W.C., Usup, G., *et al.*, (2014). Harmful Algae 39, 8-25.





ALGAL AND CYANOBACTERIAL TOXINS



Paralytic Shellfish Toxins: a complex group in constant (bio)transformation

Joana F. Leal* and Maria L. S. Cristiano

Centre of Marine Sciences (CCMAR) and Department of Chemistry and Pharmacy, Faculty of Science and Technology – University of Algarve, Campus de Gambelas, 8005-139 Faro, Portugal.

* corresponding author's email: jfleal@ualg.pt

Abstract

Paralytic shellfish toxins (PSTs) are a large group of marine biotoxins (~50 analogues), mainly produced by marine dinoflagellates of the genera *Alexandrium*, *Gymnodinium* and *Pyrodinium*, which are more typical in tropical and temperate climate zones. All members of the toxin group share a common core structure. Still, the combination of different chemical functionalities defines the subgroup of each analogue (e.g., carbamoyl, *N*-sulfo-carbamoyl, decarbamoyl, benzoyl), influencing its toxicological action and determining the level of toxicity of each member. PSTs are prone to biotransformations within living organisms, affording analogues with higher or lower toxicity. Such biotransformations may be mediated by different agents (e.g., enzymes, natural reducing agents, bacteria) in different living organisms undergoing chemical processes, leading to diverse outcomes. This work intends to highlight the main reactions (bioconversions) that occur in living organisms (dinoflagellates, bivalves, and humans) and relate changes in molecular structure, caused by such responses, to toxicity. Additionally, we also present research under development aiming to create chemical solutions for the decontamination of bivalve molluscs, thus helping to minimize this problem's social and economic impacts.

Keywords: marine biotoxins, saxitoxins, bioconversion, humans, bivalves, dinoflagellates

<https://doi.org/10.5281/zenodo.7035065>



Introduction

Harmful algae blooms (HABs) are natural phenomena characterized by the growth of phytoplankton in marine ecosystems, producing highly potent natural toxins, called phycotoxins or marine biotoxins (Egmond, 2004), that cause great social concern and economic losses worldwide. These toxins bioaccumulate in aquatic species, such as bivalves, and may be potentially toxic for humans (through the food chain). Among HABs episodes, paralytic shellfish toxins (PSTs) stand out by their relatively large contribution to the total. Recently published data referring to the period between 1985 and 2018 revealed that the highest percentage (35 %) of the events associated with seafood toxins was attributed to PSTs (Hallegraeff *et al.*, 2021 a, b).

PSTs, also recognized as saxitoxin (STX) and its analogues, or simply saxitoxins (STXs), are a large and diverse group of marine biotoxins responsible for paralytic shellfish poisonings (PSP) (Wiese *et al.*, 2010; Leal and Cristiano, 2022). This group of toxins is of particular concern for its effects on human health, as ingestion of high amounts may lead to death within a few hours. According to a dose-response modelling of PSTs in humans, the lower critical dose with a probability higher than 10% of death is 82.2 μg STX eq kg^{-1} b.w. (Arnich and Thébault, 2018). An antidote or therapy is not known and only some clinical measures are possible at an early stage of intoxication (Montebruno, 1993; Belin and Raffin, 1998; FAO, 2004). 4-aminopyridine seems to reverse sublethal effects of saxitoxin, however no studies in humans have yet been performed (Chang *et al.*, 1997; Nguyen *et al.*, 2021).

Structurally, saxitoxins share a common core, depicted in figure 1, comprising a 3,4-propinoperhydropurine tricyclic system and two guanidine groups, accounting for the hydrophilic and highly polar character of these molecules. The PSTs sub-groups are defined according to their characteristics, based on the substituent group in R4. Most toxins belong to one of the subgroups shown in figure 1, namely the carbamoyl, *N*-sulfocarbamoyl, benzoyl, and decarbamoyl subgroups. Each substituent group affects the binding affinity to the receptor, by steric hindrance, net charge and/or polarity (Leal and Cristiano, 2022). Within each subgroup, the molecules may or may not suffer hydroxylation (R1) at N1, making possible the distinction between hydroxylated and non-hydroxylated toxins. Also, R2 and/or R3 may be replaced by -H, $-\text{OSO}_3^-$ or -OH groups, originating numerous possible combinations. Furthermore, the orientation of the groups at C11 (R2 and R3) defines the stereochemistry of the molecules and may influence their binding affinity to the receptor.

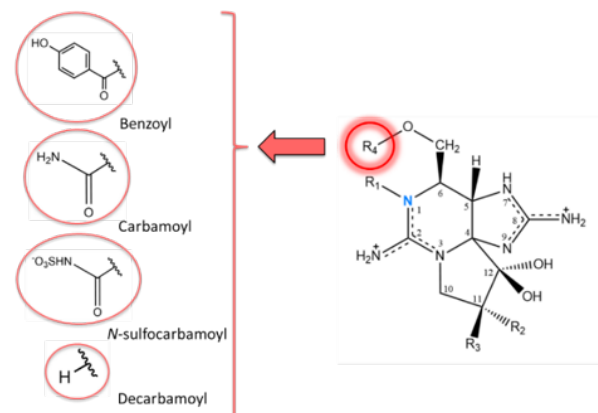


Fig. 1. Core structure of PSTs and identification of the main substituent groups in R4.

Our aim in this study was to highlight the different bioconversion reactions that occur among this group of toxins, discussing the organisms and the conditions in which they predominantly occur, as well as the impacts that those transformations have on their level of toxicity. We also describe our progress in mitigating the socio-economic effects caused by the accumulation of biotoxins in bivalves.

Bioconversions in organisms

The complexity of this group of toxins is due not only to their high number of analogues, but also to their ability to interconvert within organisms, namely, dinoflagellates, bivalves, and humans. There are some common bioconversion reactions to the different organisms. The main ones, compiled in figure 2, are grouped according to the organism where they were observed. Oxidation at N1 is a process common to bivalves, humans, and dinoflagellates. The introduction of a sulfate group (sulfonylation) has been observed in humans and dinoflagellates and may occur in R4 (at N-21) or R2/R3 (at O-22, the oxygen bound to C11) substituent groups. In turn, hydroxylation has been reported to occur in bivalves and dinoflagellates, while reductive cleavage of the *O*-sulfate group has been observed in bivalves and humans. Both reactions were documented to take place at C11. Lastly, hydrolysis of the carbamoyl ester (in R4 substituent group), originating the correspondent decarbamoyl analogues, is frequently reported in bivalves, and in humans. Hydrolysis of the *N*-sulfa group (side chain, in R4) has also been reported in bivalves. In addition to all these reactions, there are others that seem to be more characteristic of a specific organism. For example, as far as we currently know, the reductive elimination

of the *N*-hydroxyl group (at N1), as well as the *O*-desulfonylation (at C11) are reactions only described in bivalves, while in humans a very specific reaction has been proposed: glucuronidation (García *et al.*, 2009, 2010). This reaction occurs at hydroxyl C12 and assumes an important role in accelerating the detoxification process, as it produces more hydrophilic molecules, which favours the excretion of toxins by the body. Most of these reactions in organisms are mediated by enzymes (e.g., carbamoylases, sulfo- or glucuronosyl-transferases, oxidases), but the involvement of natural reducing agents, like glutathione (Sakamoto *et al.*, 2000), and bacteria (Smith *et al.*, 2001) has been reported in some metabolic transformations, namely reductive cleavage (glutathione and bacteria) and reductive elimination (bacterial isolates).

All these reactions may occur naturally and/or may be potentiated by several factors, such as pH, temperature, and even by sample handling procedures prior to analysis (Vale, 2008).

(Bio)conversions may change the toxicological profile in each organism and the overall toxicity. It is difficult to establish “rules” because the same type of reaction may not induce the same consequence in terms of toxicity, mainly if different sub-groups of toxins (based on the R4 classification) are considered. This is due to the introduction of substituent groups that cause a change of the molecular structure, also implying alterations of the physicochemical properties (e.g., pKa, net charge, polarity and/or steric hindrance) of the molecules, which leads to greater or lesser binding affinity with the receptors and, consequently, greater or lesser toxicity.



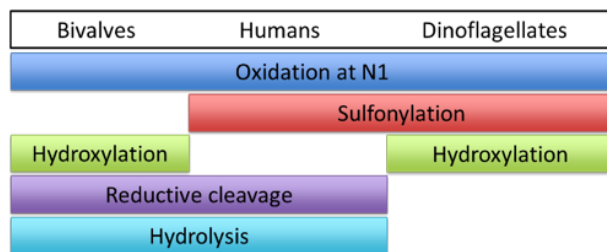


Fig. 2. Common bioconversion reactions reported in bivalves, humans, and dinoflagellates.

Considering the most recent proposal by international entities (FAO/WHO, 2016), based on the toxicity equivalency factor (TEF), the carbamoyl sub-group is the most toxic ($2 \geq \text{TEF} \geq 0.4$), followed by decarbamoyl ($0.5 \geq \text{TEF} \geq 0.2$) and *N*-sulfocarbamoyl ($0.1 \geq \text{TEF} \geq 0.01$) sub-groups. The TEF for toxins belonging to benzoate sub-group are not yet established, but some studies showed these analogues are only slightly less potent than saxitoxin (Llewellyn *et al.*, 2004), whose TEF is equal to one. More recent studies, using a docking simulation approach, seem to corroborate the toxin potency of these analogues (Durán-Riveroll *et al.*, 2016). These authors found some benzoyl analogues bound strongly to the Na_v1.4 channel.

Considering the above relation between the sub-groups and their toxicity, hydrolysis seems to be the most impactful reaction in the toxicity of these molecules. On the one hand, hydrolysis of the carbamoyl ester, converting carbamoyl/*N*-sulfocarbamoyl/benzoyl toxins into decarbamoyl analogues (e.g., STX to dcSTX), decreases the toxicity of the molecule (Leal and Cristiano, 2022). On the other hand, hydrolysis of the *N*-sulfa group (side chain, in R4), converting *N*-sulfocarbamoyl toxins into the correspondent carbamoyl, increases the toxicity of the molecule (e.g., gonyautoxin 5

(GTX5) to STX). Also, sulfonylation at N-21 (side chain, R4) impacts on the toxicity of the molecules. The introduction of a sulfate group at this site, originating *N*-sulfocarbamoyl toxins from carbamoyl toxins (e.g., STX to GTX5), seems to promote a decrease in toxicity. A more detailed and in-depth discussion about this topic may be found in our recent review article (Leal and Cristiano, 2022).

Ongoing work

The presence of marine biotoxins in bivalve molluscs represents a worldwide problem and leads to great economic losses, resulting from the prohibition of their harvesting. For example, data from 2018 indicate that, in southern Portugal (Algarve), the restrictions on harvesting of mussel, cockle and clam due to the presence of marine biotoxins reached an average of 124, 88, and 42 days, respectively (IPMA, 2018). To secure the economic and human health of HAB affected regions, it is critical to develop effective and safe strategies that contribute to solving this problem. The goal of our project, “DEPURATOX”, MAR-01.03.01-FEAMP-0049 (2020-2022) is the development of a product that is capable of decontaminating, *in vivo*, bivalves containing biotoxin levels above the legal limits, in order to avoid the devaluation of this food, either by the death of the bivalves and the consequent need for processing to sale, or by the complete ban on their harvest. The structure and chemical nature of the solutions under development take advantage of the molecular properties and physicochemical characteristics of the toxins, whose structures are known, informing the design to enhance the effectiveness of interventions. Studies have been performed with PSTs, but future studies

with diarrhoeic shellfish toxins (DSTs) are also planned. Updates related to this project may be found on the website (<https://www.researchgate.net/project/DEPURATOX>).

Acknowledgements. This study received funds from the project MAR-01.03.01-FEAMP-0049 co-financed by the Operational Program Mar 2020, Portugal 2020 and the European Union (EU), through the European Maritime Affairs and Fisheries Fund (EMFF), from 2020 to 2022. Authors also acknowledge the financial support of FCT (Foundation for Science and Technology) Portugal, through the project UID/MULTI/04326/2021 (CCMar).

References

- Arnich, N. and Thébault, A. (2018). *Toxins* 10, 141.
- Belin, C. and Raffin, B. (1998). RST.DEL/MP-AO 98-16. 256 pp. //envlit.ifremer.fr/content/download/27379/222288/file/Rephy_84_95.pdf.
- Chang, F.C.T., Spriggs, D.L., Benton, B.J., Keller, S.A., *et al.*, (1997). *Fundam. Appl. Toxicol.* 38, 75-88.
- Durán-Riveroll, L.M., Cembella, A.D., Band-Schmidt, C.J., Bustillos-Guzmán, J.J., *et al.*, (2016). *Toxins* 8, 129.
- Egmond, H.P. van (2004). *Anal. Bioanal. Chem.* 378, 1152-1160.
- FAO (2004). *Marine biotoxins*. Food and Nutrition paper 80. Food and Agriculture Organization of the United Nations, Rome.
- FAO/WHO (2016). *Technical paper on Toxicity Equivalency Factors for Marine Biotoxins Associated with Bivalve Molluscs*. Food and Agriculture Organization of the United Nations (FAO) and World Health Organization (WHO), Rome, 108.
- García, C., Barriga, A., Díaz, J.C., Lagos, M., *et al.*, (2010). *Toxicon* 55, 135-144.
- García, C., Rodriguez-Navarro, A., Díaz, J.C., Torres, R., Lagos, N. (2009). *Toxicon* 53, 206-213.
- Hallegraeff, G.M., Anderson, D.M., Belin, C., Bottein, Marie-Yasmine Bresnan, E., *et al.*, (2021a). *An unprecedented analysis on Global Harmful Algal Blooms launched by IOC*. UNESCO. IOC. //ioc.unesco.org/news/unprecedented-analysis-global-harmful-algal-blooms-launched-ioc.
- Hallegraeff, G.M., Anderson, D.M., Belin, C., Dechraoui Bottein, M.-Y., *et al.*, (2021b). *Commun. Earth Environ.* 2, 1-10.
- IPMA (2018). *Biotoxinas*. //www.ipma.pt/pt/bivalves/biotox.
- Leal, J.F. and Cristiano, M.L.S. (2022). *Nat. Prod. Rep.* 39, 33-57.
- Llewellyn, L., Negri, A., Quilliam, M. (2004). *Toxicon* 43, 101-104.
- Montebruno, D. (1993). *Med. Sci. Law.* 33, 243-246.
- Nguyen, H.V.N., Smith, M.E., Swoboda, H.D. (2021). *Shellfish Toxicity*. StatPearls Publishing, Florida, U.S.A. //europepmc.org/books/NBK470225. Accessed January 27, 2022.



Sakamoto, S., Sato, S., Ogata, T., Kodama, M. (2000). *Fish. Sci.* 66, 136-141.

Smith, E.A., Grant, F., Ferguson, C.M., Gallacher, S. (2001). *Appl. Environ. Microbiol.* 67, 2345-2353.

Vale, P. (2008). *J. Chromatogr. A* 1195, 85-93.

Wiese, M., D'Agostino, P.M., Mihali, T.K., Moffitt, M.C., Neilan, B.A. (2010). *Mar. Drugs* 8, 2185-2211.



Anatoxins in cyanobacterial mat field samples from Atlantic Canada by direct analysis in Real Time–High Resolution Tandem Mass Spectrometry

Daniel G. Beach^{1*}, Janice Lawrence², Meghann Bruce³, Jacob Stillwell², Cheryl Rafuse¹, Pearse McCarron¹

¹ *Biotoxin Metrology, National Research Council Canada, Halifax, Canada;* ² *Department of Biology, University of New Brunswick, Fredericton, Canada;* ³ *Canadian Rivers Institute, Fredericton, Canada.*

*corresponding author's email: daniel.beach@nrc-cnrc.gc.ca

Abstract

Toxic freshwater benthic cyanobacterial mats are increasingly linked to animal fatalities worldwide, often due to the production of high concentrations of anatoxins (ATXs). Considering the high spatial and temporal variability of mat occurrence and concentrations of ATXs, suitable analytical methods are required to enable large-scale field studies in these systems. Here, a rapid, direct analysis in real time–high resolution tandem mass spectrometry (DART–HRMS/MS) method for analysis of anatoxin-a, homoanatoxin-a, and dihydroanatoxin-a including a simple sample preparation procedure and isotope dilution calibration, is investigated to address this challenge. The developed method was applied to three sets of cyanobacterial mat samples collected in Atlantic Canada in the summers of 2018–2020. Samples from all sets showed positive detection of ATXs ranging from $<100 \text{ ng mL}^{-1}$ to $> 70,000 \text{ ng mL}^{-1}$ in mat lysates. One large mat sample collected from the Wolastoq (Saint John River) in New Brunswick, Canada, was used to demonstrate the application of DART–HRMS/MS to study the intra-mat variability of ATXs. This initial work showed the method could be successfully used for the analysis of ATXs in field samples, which will be useful in ongoing studies of this emerging issue in Atlantic Canada and beyond.

Keywords: Cyanotoxins, *Phormidium*, *Microcoleus*, ambient ionization

<https://doi.org/10.5281/zenodo.7035072>



Introduction

Proliferations of freshwater benthic microbial mats dominated by cyanobacteria of the genera *Microcoleus*, *Phormidium*, and *Oscillatoria* are increasingly being reported globally (McAllister *et al.*, 2016; Wood *et al.*, 2020) and are often associated with pet and livestock mortalities (Stevens and Krieger, 1988; Backer *et al.*, 2013; Faassen *et al.*, 2012; Fastner *et al.*, 2018). In the majority of cases, these mortalities can be attributed to poisoning by the potent alkaloid neurotoxin anatoxin-a (ATX) and its structural analogues, collectively referred to as anatoxins (ATXs; Fig. 1).

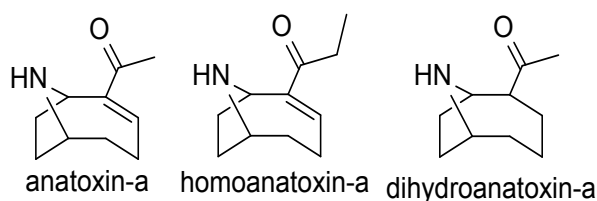


Fig. 1. Chemical structures of anatoxins analyzed in this study.

Challenges associated with studying these proliferations of toxic benthic cyanobacteria include the extremely high spatial and temporal variability in mat occurrence and ATX concentrations within a study area (Wood *et al.*, 2012, 2020). These challenges could be better addressed with analytical methods capable of providing higher throughput analysis as well as improved selectivity and sensitivity over existing approaches.

Direct analysis in real time (DART) is an ambient ionization technique that is capable of vaporizing and ionizing certain analytes for mass spectrometry (MS) detection without the need for a chromatographic separation

(Gross, 2014). This technique is particularly powerful when combined with high-resolution MS (HRMS), which helps improve selectivity in the absence of chromatographic separation. DART-MS has been widely used for the analysis of pesticides, mycotoxins, and drugs of abuse (Busman, 2018; Gross, 2014). Analysis of ATXs by DART was recently demonstrated for screening laboratory cultured cyanobacterial isolates (Beach *et al.*, 2021) but its applicability to more complex field samples has not yet been explored.

Here, we present initial work on a DART-HRMS/MS method for analyzing ATXs in benthic cyanobacterial mat samples. We then demonstrate the utility of the method using cyanobacterial mat samples from Atlantic Canada.

Material and Methods

Chemicals and Reagents

A certified reference material calibration solution for ATX and an in-house calibration solution for homoanatoxin-a (hATX) were obtained from the National Research Council Canada (Halifax, Nova Scotia). Standards of $^{13}\text{C}_4$ -(+)-Anatoxin-a and dihydroanatoxin-a (H_2 -ATX) were obtained from Eurofins Abraxis (Warminster, U.S.A.).

Samples and Sample Preparation

Three cyanobacterial mat samples from three sample sets were collected from Atlantic Canada between 2018 and 2020. Sample set 1 (NS 2019-1 to -3) included suspected cyanobacterial mats collected from brackish waters near Oak Island, Nova Scotia (44.5123° N, 64.2949° W),



in September 2019. Sample sets 2 and 3 consisted of *Microcoleus*-dominated benthic cyanobacterial mats collected along the Wolastoq (Saint John River) near Fredericton, New Brunswick (45.9636° N, 66.6431° W) during the summers. Sample set 2 (NB 2019-1 to -4) was collected in July 2019 following a nearby dog mortality.

Samples were homogenized and stored at -20 °C prior to analysis. Sub-samples of homogenate (~1 mL) were centrifuged at 21,000 × g at 4 °C for 20 min. A sub-sample of supernatant (100 µL) was then mixed with 100 µL of 120 ng mL⁻¹ ¹³C₄-ATX in 90% methanol with 0.015% acetic acid.

DART-HRMS/MS Analysis

A Q Exactive HF Orbitrap mass spectrometer (Thermo, Waltham, MA, U.S.A.) was coupled to a DART-SVP source using a Vapur® interface (Ionsense, Saugus, MA, U.S.A.). Helium was used as the DART gas along with a DART temperature of 350 °C, a capillary temperature of 200 °C and Max IT of 300 ms. Mass spectrometric data were collected simultaneously in full scan over the mass range of 150 to 250 *m/z* and precursor ions of *m/z* 166.1 (ATX), 168.1 (H₂-ATX), 180.1 (hATX), and 170.1 (¹³C₄-ATX) were isolated for tandem mass spectrometry (MS/MS) using the parallel reaction monitoring scan mode with a collision energy of 15 eV, a 0.4 *m/z* isolation window and the 30k resolution setting. Product ions extracted for quantitation were *m/z* 149.0961, 163.1117, 125.0961, and 153.1095, for ATX, hATX, H₂-ATX, and ¹³C₄-ATX, respectively.

Samples were introduced by pipetting five µL of extract onto the tip of a Dip-it sampling rod and manually holding the sample mid-way

between the DART source and the ceramic interface tube for 10 s (Fig. 2). All samples were analyzed in triplicate and a mixed standard (43 ng mL⁻¹ ATX, 46 ng mL⁻¹ hATX, 37 ng mL⁻¹ H₂-ATX and 60 ng mL⁻¹ ¹³C₄-ATX) was run approximately every 10 samples.

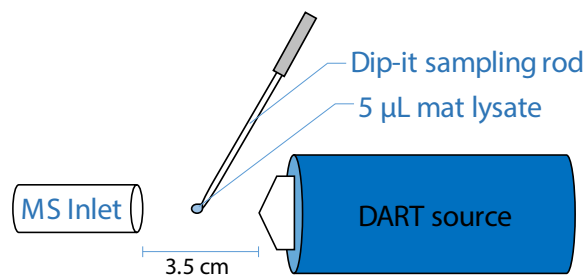


Fig. 2. Graphical representation of manual Dip-it sample introduction used for DART-HRMS/MS.

Results and Discussion

The full scan DART-HRMS method recently presented for the analysis of ATXs in laboratory cultured cyanobacteria (Beach *et al.*, 2021) was not suitably selective for use with more complex benthic cyanobacterial mat field samples. A tandem mass spectrometry (HRMS/MS) method was therefore developed that showed improved selectivity but maintained good sensitivity. Figure 3 shows extracted ion chromatograms from analysis of benthic cyanobacterial mat samples collected in 2019 from the Wolastoq. All samples and the mixed ATX standard were spiked with 60 ng mL⁻¹ ¹³C₄-ATX. Comparing the signal intensity of ¹³C₄-ATX in figure 3 effectively demonstrates the significant and variable degree to which ionization suppression was observed in field samples, up to > 99% suppression. Though significant, this suppression was successfully corrected for by isotope dilution calibration, allowing for quantitation of ATXs by DART-HRMS/MS.



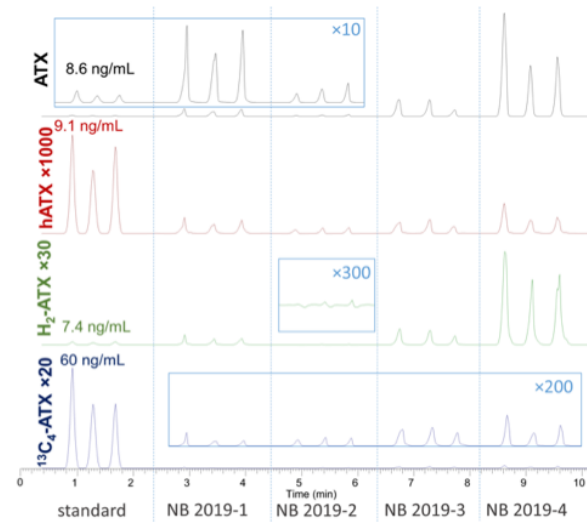


Fig. 3. Extracted ion chromatograms from DART-HRMS/MS showing triplicate analysis of a mixed ATX standard and four benthic cyanobacterial mat samples collected from the Wolastoq in 2019.

Quantitative results from three sets of benthic cyanobacterial mats analyzed by DART-HRMS/MS are shown in Table 1. Sample set 1 consisted of suspected cyanobacterial mats collected from brackish waters near Oak Island, NS in Sept 2019. In this case, low levels of H₂-ATX and hATX were detected in one sample, but the other two were below the limits of detection, which were estimated at 5 ng mL⁻¹ lysate based on 3× the background in control mat extracts. These findings were later confirmed using an LC-HRMS method with a limit of detection of 0.1 ng mL⁻¹ (method as in Beach *et al.* (2021), data not shown).

Light microscopy revealed cyanobacterial cells consistent with the *Microcoleus/Phormidium/Oscillatoria* complex in all three samples (Fig. 4), further supporting the

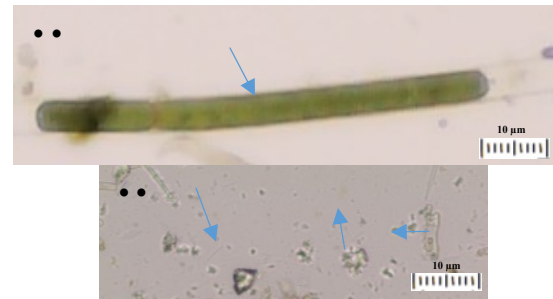


Fig. 4. Light micrographs of two morphotypes of filamentous cyanobacterial cells observed at 400× magnification in samples from Oak Island, Nova Scotia. Panel A) major morphotype, and panel B) minor one.

results of toxin analysis by DART-HRMS/MS. Two morphotypes of cyanobacteria were present. The dominant morphotype (Fig. 4A) was significantly larger in size with a trichome width roughly 1.5× larger than the other morphotype (Fig. 4B) and with thicker cross walls.

Sample set 2 was collected in July 2019 from the shore of the Wolastoq, where an ATX-associated dog death had occurred three days prior. These samples showed variably high concentrations of ATXs consistent with previously reported dog mortalities elsewhere in the world (Backer *et al.*, 2013; Faassen *et al.*, 2012; Fastner *et al.*, 2018). End-point PCR targeting the *anaC* gene, one of the genes involved in anatoxin biosynthesis, confirmed the presence of *anaC* in all samples (method as in Rantala-Ylinen *et al.* (2011), data not shown).



Table 1. Concentrations of ATXs as measured by DART–HRMS in benthic cyanobacterial mat samples from Atlantic Canada.

Sample	ng toxin mL ⁻¹ lysate			
	ATX	hATX	H ₂ -ATX	Total
set 1				
NS 2019-1	87	0	9	96
NS 2019-2	0	0	0	0
NS 2019-3	0	0	0	0
set 2				
NB 2019-1	15060	414	4183	19657
NB 2019-2	2737	128	153	3018
NB 2019-3	9740	121	2569	12431
NB 2019-4	45142	192	15673	61007
set 3				
NB 2018-1	78	4	38	119
NB 2019-5	1111	44	13883	15038
NB 2019-6	30829	181	43430	74440
NB 2019-7	55	6	109	169
NB 2020-1	295	2	320	618
NB 2020-2	107	0	5	113
NB 2020-3	288	2	206	495
NB 2020-4	826	12	42	879

Samples from set 3 were collected from the Wolastoq throughout the summers of 2018–2020 and analyzed to study the broader inter- and intra-mat variability of ATXs in the system. All samples were positive for ATXs, with total ATX concentrations varying by nearly three orders of magnitude.

Sample NB 2018-1 was a large (400 g wet) mat sample that was further sub-sampled in order to demonstrate the capabilities of DART–HRMS in studying small-scale variability of ATXs within a mat (Fig. 5). H₂-ATX concentrations varied by over

an order of magnitude within the sample, however, overall variability was relatively low compared with what has been reported previously (Wood *et al.*, 2012). It should be noted that the sample had been previously frozen, partially thawed, and re-frozen prior to sub-sampling. Considering freeze-thaw is a generally accepted means of cyanobacterial cell lysis, it is expected that the results shown in figure 5 may be an under-estimate of actual intra-mat variability in ATX concentrations.

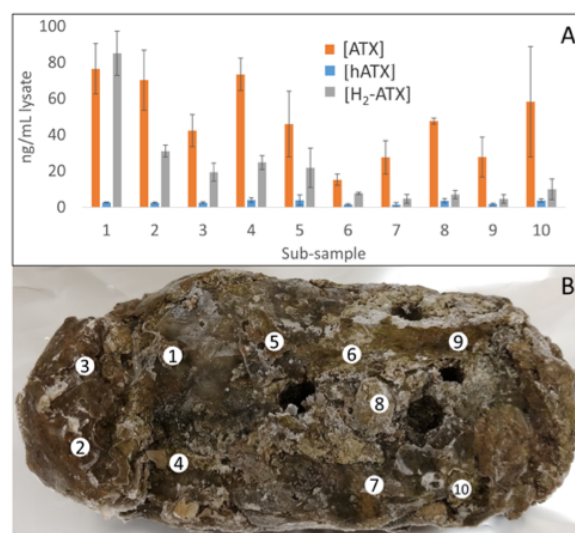


Fig. 5. Concentrations of ATXs measured by DART–HRMS/MS (A) from sub-sampled locations (B) of frozen benthic cyanobacterial mat NB 2018-1.

The work summarized here demonstrates that DART methodology, originally developed for screening culture samples (Beach *et al.*, 2021), could be refined using HRMS/MS detection to be suitable for application to more complex field samples. The method was applied to show the presence of ATXs in samples from Atlantic Canada, with an initial demonstration of the utility of the method for evaluating inter- and intra-mat variability. Work is ongoing to optimize and validate

the DART method parameters for field work and to apply the method in a broader study of cyanobacterial mat and ATX occurrence in the Wolastoq. The method is equally applicable to work in other areas with widespread or suspected proliferations of toxic benthic cyanobacteria. In the future, the throughput of the method could be further improved through automation of sample introduction.

Acknowledgements. Authors acknowledge A. Sinclair from Nova Scotia Environment and Climate Change for provision of field samples, and E. Mudge (NRCC) for review of the manuscript.

References

- Backer, L. C., Landsberg, J. H., Miller, M., Keel K., Taylor T. K. (2013). *Toxins* 5, 1597-1628.
- Beach, D.G., Rafuse, C., Melanson J.E., McCarron, P. (2021). *Rapid Commun. Mass. Spectrom.* 35, e8940.
- Busman, M. (2018). *J AOAC Int.* 101, 643-646.
- Gross, J.H. (2014). *Anal. Bioanal. Chem.* 406, 63-80.
- Faassen, E.J., Harkema, L., Begeman, L., Lurling, M. (2012). *Toxicon* 60, 378-384.
- Fastner, J., Beulker, C., Geiser, B., Hoffmann, A., *et al.*, (2018). *Toxins* 10, 60.
- McAllister, T.G., Wood, S A., Hawes, I. (2016). *Harmful Algae* 55, 282-294.
- Rantala-Ylinen, A., Känä, S., Wang, H., Rouhiainen, L., *et al.*, (2011). *Appl. Environ. Microbiol.* 77, 7271-7278.
- Stevens, D.K. and Krieger R.I. (1988). *J. Anal. Toxicol.* 12, 126-131.
- Wood, S.A., Smith, F.M.J., Heath, M.W., Palfroy, T., *et al.*, (2012). *Toxins* 4, 900-912.
- Wood, S. A., Kelly, L. T., Bouma-Gregson, K., Humbert, J. F., *et al.*, (2020). *Freshw. Biol.* 65, 1824-1842.





TAXONOMY AND SYSTEMATICS



Literature analysis of how well rDNA sequence perform at delineating dinoflagellate species

R. Wayne Litaker^{1*}, Brittany M. Ott^{2*}, William C. Holland³, Charles F. Delwiche⁴

¹CSS, Inc. under Contract to National Oceanic and Atmospheric Administration Beaufort, NC, U.S.A.; ²Joint Institute for Food Safety and Applied Nutrition (JIFSAN), University of Maryland, College Park, MD, U.S.A.; ³National Oceanic and Atmospheric Administration, National Ocean Service, National Centers for Coastal Ocean Science, Beaufort Laboratory, Beaufort, NC, U.S.A.; ⁴Cell Biology and Molecular Genetics, University of Maryland, College Park, MD, U.S.A.

* corresponding author's emails: wayne.r.litaker@noaa.gov, brittany.ott@fda.hhs.gov

Abstract

Dinoflagellate harmful algal bloom species are traditionally defined using morphological characters. Molecular evidence, however, sometimes indicates that morphospecies differ from biological species. This has led to a reliance on molecular characteristics, primarily rDNA-based phylogenies, along with morphology, as a basis for defining new species. This approach assumes that divergence in rDNA or other selected genes consistently parallels speciation events, but this has not been systematically tested. Consequently, this study was undertaken to assess how often rDNA molecular phylogenies succeeded or failed to delineate dinoflagellate species. Specifically, SSU, D1-D3 LSU and ITS/5.8S phylogenies presented in 473 publications were reviewed to determine how well the rDNA phylogenies discriminated dinoflagellate species, including those in known HAB genera. A total of 863 described species representing 232 genera were assessed. Results showed the ITS/5.8S and D1-D3 LSU rDNA phylogenies (~1,850-2,500 bp), in combination, can simultaneously (a) identifying 97% of all dinoflagellate species and (b) provide unique sequences useful for developing species-specific, quantitative molecular assays. Genera where species are well resolved using the ITS/5.8S plus D1-D3 genes include *Alexandrium*, *Ostreopsis* and *Gambierdiscus*. Based on the review of the publications, it was also possible to develop a system for determining how much weight to assign morphological versus molecular characters when describing new species. Utilizing this system can accelerate the description of new dinoflagellate HAB species and the subsequent assessment of their relative toxicities.

Keywords: 5.8S, *Alexandrium*, *Gambierdiscus*, ITS, large and small subunit, ribosomal DNA, *Ostreopsis*, phylogeny

<https://doi.org/10.5281/zenodo.7035075>



Introduction

Significant efforts are underway to identify and describe new species in various dinoflagellate harmful algal bloom (HAB) genera. These efforts have been driven to some extent by the documented co-occurrence of species with nearly identical morphologies but whose toxicity is significantly different. Accurately determining risk in these situations requires that all the co-existing species have been identified, their toxicity evaluated, and molecular or morphological methods developed to accurately determine species composition.

Historically, dinoflagellate species have been described based upon morphological differences in the overall size and shape of the cell, the arrangement, size, and shape of thecal plates covering the cell surface, or internal structural differences (Fensome *et al.*, 1999). Descriptions based solely on morphology, however, have sometimes proven inadequate for identifying species with overlapping morphologies. Consequently, over the past few decades more reliance has been placed on using molecular characters, particularly phylogenetic analyses of rDNA sequences in conjunction with morphology to describe new species. Specifically, the rDNA data are thought to strongly support description of a new species when all the sequences from the putative new species (i.e. obtained from either culture isolates or field-collected cells) included in a phylogenetic analysis fall into a distinct, well-defined clade. How often rDNA sequences, like morphological characters, fail to delineate species, however, has not been systematically examined. To quantify the actual success or failure rate, we reviewed 473 articles containing phylogenies based on

either the SSU, ITS/5.8S or the D1-D3 LSU rDNA domains to determine how well these phylogenies supported currently described species, including those belonging to HAB genera.

Methods and Results

Articles containing relevant rDNA phylogenies were identified using Web of Science, Google searches, or manuscript reference sections. The nomenclatural changes for the various species occurring since those species were first described were determined using AlgaeBase. Tracking these nomenclatural changes was key to resolving instances where sequences ascribed to different species but placed in a single, distinct clade were either (a) actually derived from truly different species (i.e. the rDNA failed to distinguish species) or (b) were sequences from the same species which had different species names depending on when they were entered into GenBank.

The actual determination of whether the rDNA truly delineated (resolved) species was straightforward in most cases, but nuanced in some. Factors complicating this determination included: (a) whether a single sequence or multiple sequences from a given species were included in the phylogeny (more sequences = greater resolution), and (b) whether all the sequences falling into a given clade were properly identified as noted above. Accordingly, species in the various rDNA phylogenies were classified as follows:

- Yes (=Y), cases where two or more sequences originating from a described species form a distinct clade in the rDNA



- phylogeny – i.e. phylogeny completely supports the previously described species.
- Yes provisionally (=YP), same as Y except the species-specific clade is represented by only a single rDNA sequence.
 - Yes, but ambiguous (=YA), indicates two or more sequences attributed to different species form a distinct clade in the rDNA phylogeny and where there is some suggestive, but not definitive, morphological or taxonomic information indicating the sequences are actually from the same rather than different species.
 - No (=N) denotes cases where sequences from different known morphologically distinct species are identical and fall into the same clade – i.e. rDNA phylogenies are incapable of resolving certain morphologically well-defined species.
 - No, but ambiguous (=NA), represents a version of the previous N designation where there is less definitive, but still strong, morphological evidence are indeed distinct species.

Because the species included in the various phylogenies were inconsistent, it was possible for separate phylogenies to indicate a different classification for a given species. For example, a species might be assigned as Y in one study and YP in another, or N versus NA, etc. These differing assignments have to be considered when deciding on how well the rDNA phylogenetic data are able to distinguish species. This was accomplished as follows.

- Species receiving Y, YP or Y/YP designations were assigned to the “resolved” category, i.e. the rDNA phylogeny fully supports the current species description.
- Those with N, NA, N/NA, N/YA, or

N/Y designations were classified as “not resolved”, i.e. the rDNA phylogeny failed to delineate what are clearly distinct species.

- Species with YA, Y/YA or YP/YA designations were classified as “ambiguous”, i.e. the existing data are insufficient to resolve whether the rDNA phylogenies do or do not support the currently described species.

Overall, the SSU and D1-D3 sequences have similar success at delineating > 93% of the dinoflagellate species surveyed, with the ITS/5.8S region capable of resolving > 97% of species (Fig. 1). These data indicate the ITS/5.8S region alone could distinguish most species. However, addition of the D1-D3 further strengthens resolution of the identified species boundaries. Also, the D1-D3 region exhibits a greater sequence variation per base pair compared to the SSU. Consequently, if both the D1-D3 and ITS/5.8S regions are sequenced, it facilitates subsequent identification of unique sequences that can be used to develop quantitative, species-specific molecular assays. In contrast, the SSU region, which would provide equal resolution of species boundaries provides fewer unique site for probe development and is about 600 bp longer to sequence. For this reason, the use of ITS/5.8S in combination with D1-D3 is recommended over ITS/5.8S plus the SSU as the minimum standard for resolving species. If sequencing resources allow, adding the SSU and D8-D10 LSU sequence data to the phylogenies will only further strengthen confidence in the identified species boundaries (Gottschling *et al.*, 2020).

Though successful most of the time, the literature review revealed the divergence in



the rDNA genes for about 3% of the species was insufficient to distinguish species. This includes one or more species in the following genera: *Amphidinium*, *Apocalathium*, *Archaeoperidinium*, *Biecheleria*, *Centrodinium*, *Ceratocorys*, *Dinophysis*,

previously described species, (b) failed to resolve previously described, morphologically well-defined species, or (c) gave ambiguous results due to the data being insufficient to classify the species as either resolved or not resolved. These data represent the summarized results from reviewing phylogenies from the 473 publications reviewed. N = total number of described species found in phylogenies for the particular rDNA gene segment listed in each panel.

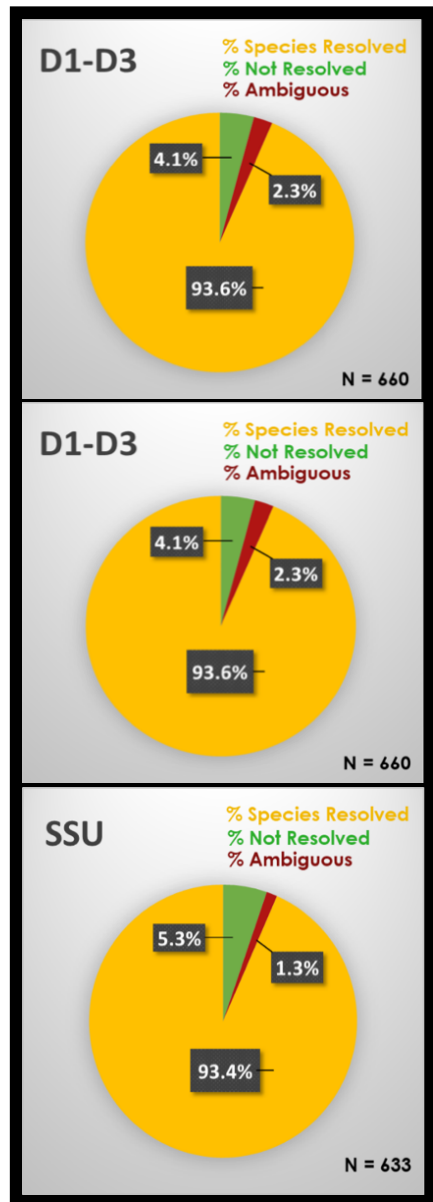


Fig. 1. Pie charts showing the percent of species for which the D1-D3 domains of LSU, SSU, and ITS/5.8S rDNA phylogenies either (a) resolved (confirmed)

Gonyaulax, *Gymnodinium*, *Prorocentrum*, *Scrippsiella*, and *Syltrodinium*. HAB genera where species were consistently resolved include *Alexandrium*, *Gambierdiscus* and *Ostreopsis*.

A more detailed examination of the literature survey results revealed there were five discernible patterns with regard to how well the morphological and molecular data either succeeded or failed to delineate species. The patterns are described below and can be used in helping guide the identification and description of new dinoflagellate species.

Pattern 1 includes those species which are so morphologically distinct they are reliably identified based on morphology alone. In these instances, we advocate the species description also include the corresponding ITS/5.8S and D1-D3 data to help in tracing any future taxonomic changes to assist in distinguishing closely related species that might be discovered in the future, and to facilitate linkage with environmental molecular studies.

Pattern 2 represents instances where the species in question exhibit non-overlapping morphologies consistent with their being distinct species, but whose rDNA sequences are identical. About 3% of the species



examined in the survey fell in this category. These species likely represent recently diverged species whose rDNA sequences have not had sufficient time to diverge (Hickerson *et al.*, 2006), but could also reflect uncharacterized developmental variation. This represents the most difficult case to evaluate. It is recommended that prior to describing such a species, a multigene phylogenetic study be conducted to test the hypothesis that the morphotypes are distinct species. If supporting evidence is found, then the species description would be based on morphology and the multigene phylogeny. If no multigene phylogenetic differences exist, but other compelling data such as one species living exclusively in freshwater habitats and the other in saltwater environments, those data can be used as a basis for the species description (Logares *et al.*, 2007; Čalasan *et al.*, 2019). Such descriptions should include the ITS/ 5.8S and D1-D3 sequence data from the new species along with a detailed description of the other morphologically distinct species sharing the same rDNA ribotype. If no molecular data support the distinction but there is a compelling reason to name a new species, the best available option is to base the species description solely on morphology.

A good example of where morphologically distinct species with identical rDNA sequences occur is in the genus *Dinophysis*. Many of the species such as *D. acuta*, *D. caudata*, *D. dens*, *D. forti* and *D. norvegica* are genetically and morphologically distinct and represent species consistent with pattern 1. In contrast, many of the smaller celled species such as *D. acuminata*, *D. ovum*, *D. okamurai*, *D. pavillardii*, *D. recurva* and *D. sacculus* exhibit indistinguishable ITS and D1-D3

rDNA sequences (Qui *et al.*, 2011; Rodríguez *et al.*, 2012; Wolny *et al.*, 2020). These latter species should be considered valid species until additional definitive morphological or other data prove otherwise.

Pattern 3 includes species such as those in the genus *Gambierdiscus* which are morphologically difficult to distinguish but whose ITS/5.8S and D1-D3 phylogenies clearly show that they are distinct species. In this case, species can be described based solely on the rDNA phylogenetic data. This category also includes cryptic species which are truly morphologically indistinguishable. It can be reasonably claimed that all the species fitting this pattern be described as separate species. We argue, however, that in the case of the cryptic species, it is more prudent to assign each putative species a unique ribotype designation until some toxicological or other function justifies a formal description. This would avoid a proliferation of molecularly distinct, but morphologically identical species whose function is unknown.

Pattern 4 represents a small number of species where the existing morphological and molecular data provide contradictory or difficult to reconcile results such as in the case of *Peridinium cinctum* (López *et al.*, 2018). In these cases, additional morphological or phylogenetic studies are required prior to undertaking species descriptions.

Pattern 5 is included for completeness and represents cases where neither the morphological or molecular data indicate species level differences. Here, any isolates in question would be considered as belonging to the same species.



Finally, and most importantly, it should be noted that all species descriptions must contain a complete, detailed morphological description. No matter how compelling the molecular data, accurate morphological descriptions are indispensable. This is true even for cases such as cryptic species where no morphological distinctions exist. Having these data available is critical if ecologists, toxicologists and other researchers are to accurately assess the species they are working with.

The ITS/5.8S and D1-D3LSU rDNA genes in combination accurately delineate 97% of described dinoflagellate species studied to date, including most HAB species. Following the guidelines provided above, it should be possible to more effectively and systematically utilize combined morphological and molecular data to identify and describe new species. These guidelines include how to recognize and describe those morphologically distinct species, but whose rDNA sequences are indistinguishable.

In the future, multigene approaches will undoubtedly become more streamlined and affordable. The resulting phylogenies will provide an enhanced ability to resolve species boundaries. They will also provide more accurate assessment of the phylogenetic relationships among species than can be achieved with rDNA sequences alone (Leliaert *et al.*, 2014). However, at present, multigene approaches are still relatively expensive, and neither standardized nor (at present) particularly effective at distinguishing morphospecies with indistinguishable rDNAs (Kretzschmar *et al.*, 2019). Until these methods are further refined, results of this study recommend a reliance on the ITS/5.8S

and D1-D3 rDNA sequences as a key basis for defining most dinoflagellate species.

Acknowledgements. This work was supported by NSF Grant #DEB1541529 to CFD and NOAA, National Ocean Service, National Centers for Coastal Ocean Science program funds to WL and CH.

References

- Čalasan, A.Ž., Kretschmann, J., Gottschling M. (2019). *Environ. Microbiol.* 21, 4125-4135.
- Fensome, R., Saldarriaga, J., Taylor, F. (1999). *GRANA* 38, 66-80.
- Gottschling, M., Chacón, J., Žerdoner Čalasan, A., *et al.*, (2020). *Freshw. Biol.* 65, 193-208.
- Hickerson, M., Stahl, E., Lessios H. (2006) *Evolution* 60, 2435-2453.
- Kretzschmar, A.L., Larsson, M.E., Hoppenrath, M., *et al.*, (2019). *Protist* 170, 125699.
- Leliaert, F., Verbruggen, H., Vanormelingen, P., *et al.*, (2014). *Eur. J. Phycol.* 49, 179-196.
- López, A.I., Kretschmann, J., Čalasan, A.Ž., Gottschling, M. (2018). *Eur. J. Phycol.* 53, 156-165.
- Qiu, D., Huang, L., Liu, S. *et al.*, (2011). *PLoS One* 6, e29398.
- Rodríguez, F., Escalera, L., Reguera, B., *et al.*, (2012). *Harmful Algae* 13, 26-33.



Taylor, F.J.R. (1987). The Biology of
Dinoflagellates. 24-91 Blackwell Scientific,
Oxford.



Harmful algal bloom of the dinoflagellate *Blixaea quinquecornis* (Abé) Gottschling in bays of North-Central Peru

Liz Romero^{1*}, Alexis Huamaní², Sonia Sanchez¹, David U. Hernández-Becerril³

¹Phytoplankton and Primary Production Laboratory, Instituto del Mar del Peru (IMARPE). Gamarra y General Valle S/N, Chucuito, Callao, Peru; ²San Luis Gonzales de Ica University. Av. Los Maestros S/N, Ica, Peru; ³Ciencias del Mar y Limnología Institute, Universidad Nacional Autónoma de México (UNAM), Ciudad Universitaria, Coyoacan, 04510, Ciudad de México, México.

* corresponding author's email: lizromero@imarpe.gob.pe

Abstract

Harmful algal blooms of the thecate dinoflagellate, *Blixaea quinquecornis*, generally distributed in tropical, marine, and estuarine areas, are reported in Peru. The identification of this species was done using light, scanning electron microscopy (SEM), and differential interference contrast (DIC) microscopy. This species was found in Miraflores, Paracas and Sechura Bays in 2015 and 2016. The maximum density of *B. quinquecornis* observed in Miraflores bay was 3.2×10^5 cells L⁻¹ in summer of 2016. In Paracas Bay, the maximum cell counts were 2.11×10^5 and 4.11×10^4 cells L⁻¹ in the summer and autumn of 2016, respectively. Low cell densities (160 cells L⁻¹) were observed in Sechura Bay. In Miraflores and Paracas Bays, *B. quinquecornis* was found coincidentally with blooms with the athecate dinoflagellate *Akashiwo sanguinea*. The physicochemical variables associated with blooms of *B. quinquecornis* in Miraflores and Paracas Bays were surface sea temperature ranging from 19.9 to 26.6° C, salinities from 34.7 to 35.3, pH from 7.32 to 8.21, and dissolved oxygen from 2.46 to 7.44 mL L⁻¹.

Keywords: Harmful algal bloom, *Blixaea quinquecornis*, dinoflagellates, Miraflores Bay, Paracas Bay, Peru

<https://doi.org/10.5281/zenodo.7035076>



Introduction

The thecate dinoflagellate *Blixaea quinquecornis* (Abé, 1927) Gottschling, 2017 (s = *Peridinium quinquecorne*) is primarily a marine species. This species blooms in coastal zones worldwide (Okolodkov *et al.*, 2016) and can reach sufficiently high cell densities to cause both seawater discoloration and fish mortalities (Gárate-Lizárraga and Muñeton-Gómez, 2008). There are few records of this species in South America, although conditions in this region are likely ideal for bloom formation (Rodríguez-Gómez *et al.*, 2021). Existing reports are from the Colombian Caribbean (Lozano-Duque *et al.*, 2011), Brazil (Faust *et al.*, 2005) including this study, has shown that these systems contain abundant dinoflagellate species. Consistent with Margalef's prediction, these habitats are protected from wind mixing, show a high degree of stratification, and have restricted water exchange with surrounding oligotrophic waters of the open barrier-reef system. This limited water exchange favors retention of dinoflagellate cells and the trapping of nutrient rich organic material that is rapidly recycled providing a relatively high-nutrient environment. Species-specific blooms are a common feature of these systems. In the study, the ecology and diversity of dinoflagellate species from two nutrient-enriched habitats, Douglas Cay and The Lair at Twin Cay, were examined in detail. A comparison of the species composition from both sites showed that Douglas Cay contained coastal planktonic and offshore oceanic dinoflagellates while The Lair at Twin Cay contained mainly benthic dinoflagellates. A total of 19 bloom-forming species were observed in these systems during three two-week studies. The morphology of eight of

these bloom-forming species is illustrated in Scanning Electron Microscopy (SEM and the Peruvian coasts (Okolodkov *et al.*, 2016).

This study specifically examined the occurrence of *B. quinquecornis* in three bays along the central-north Peruvian coasts. These bays represent a subsection of the Humboldt Current System which impacts the coast of Peru. This system is characterized by a high environmental variability in different spatio-temporal scales, with the presence of temperate-cold waters, strong upwelling, a shallow zone of minimum oxygen (Bertrand *et al.*, 2011), high primary productivity and the occurrence of "El Niño" warm events (Chavez *et al.*, 2008). Harmful algal blooms (HAB) occur frequently in this system. These include recurrent *Akashiwo sanguinea* and *Heterosigma akashiwo* blooms (Sánchez and Delgado, 1996) as well as occasional blooms of *Alexandrium affine* (Vera *et al.*, 1999), *A. minutum* (Baylón *et al.*, 2015), *Pseudo-nitzschia multistriata* (Tenorio *et al.*, 2021), and the non-toxic species, *Azadinium polongum* (Tillmann *et al.*, 2017), among others. In this study, the prevailing environmental conditions associated with observed blooms of *B. quinquecornis* were documented.

Study area

Sechura Bay (Piura) is located north of Peru between 05°12' and 05°50' S, and 80° 50' and 81°12' W. Miraflores Bay (Callao-Lima) is adjacent to Carpayo Beach (fixed station at 12° 04' 09.7" S and 77° 09' 14.4" W), and Paracas Bay (Pisco-Ica) to the south, between 13°47' 2" and 13° 51' 5" S, and 76° 15' 0" - 77° 18' 5" W (Fig. 1).



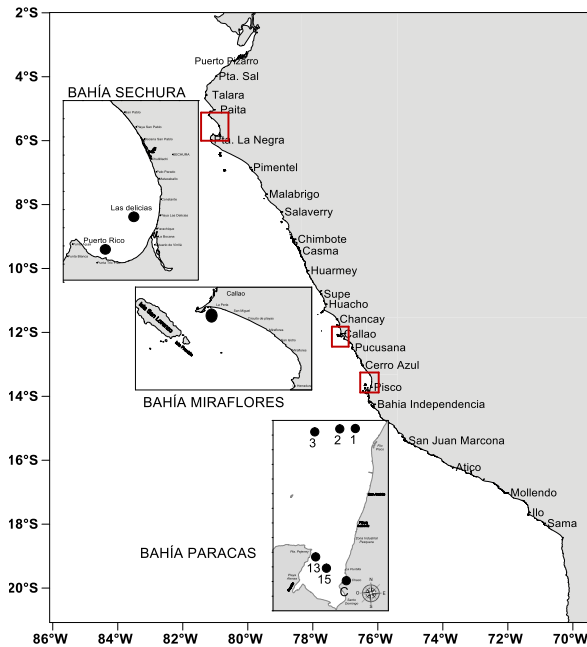


Fig. 1. Study area. Sechura bay in the north, a fixed station in Miraflores bay, and Paracas bay in the south. Methods

Surface water samples were collected from Paracas and Miraflores Bays during blooms three times per week from 2015 to 2016, with a bucket and aliquoted into 80 mL bottles. Samples were fixed *in situ* following Thronsen (1978) in Sournia (1978) and Reguera *et al.* (2011). In Sechura Bay, phytoplankton was sampled with a net (10 μm mesh) according to Reguera *et al.* (2011). Surface sea temperature was measured with an immersion mercury thermometer and water samples (250 mL and 100 mL) were collected for salinity, pH, and dissolved oxygen (O_2) analyses. Salinity was measured in laboratory using a salinometer Portasal 8410A and dissolved oxygen was measured following the Winkler method (Strickland and Parsons, 1972). Phytoplankton community quantification was done with using both Zeiss and Leica DMIL LED inverted microscopes with magnifications of 120x and 320x,

following the Utermöhl method, according to Hasle (1978) in Sournia (1978). Algal bloom samples were analyzed in Sedgwick-Rafter chambers (Reguera *et al.*, 2011).

For the identification of *B. quinquecornis*, plate dissection was done, and micrographs were obtained using epifluorescence and DIC-Nomarski techniques. For the epifluorescence microscopy a Nikon Eclipse Ti-U, equipped with an UV lamp Nikon model Intensilight DS-U3 was used with Calcofluor White SM2 stain (Fritz and Triemer, 1985). Microphotographs were taken at 60X using a Nikon model Digital Sight DS-U3 camera. In order to observe the detailed morphology of *B. quinquecornis* specimens, samples were postfixed with Osmium tetroxide, treated for critical point drying and coated with gold for study with SEM (TESCAN model Vega 3) at the “Electronic Microscopy Laboratory, Pathology Institute” (School of Medicine, Nacional de San Marcos University in Lima, Peru).

Morphometry of 40 individual *B. quinquecornis* specimens from the algal bloom in Paracas Bay was done using a light microscope at 40x, and the digital program NIS Element-D, Nikon. Length was considered from the apical to the antapical extremes, with and without spines, and the transdiameter was also measured.

Results

We identified *B. quinquecornis* as the dinoflagellate causing algal blooms in each of the bays. Solitary cells, various chloroplasts per cell and a characteristic reddish eyespot are typical of the species (Fig. 2a). Cells have a conical epitheca and rounded hypotheca,



with four antapical spines (Figs. 2a, e, f). Originally, the plate formula proposed by Abé (1981) is: pp, 3', 2a, 7'', 5c, 4s, 5''', 2'''''. This arrangement is confirmed in this study. Epithecal plates are formed by three apical plates, two anterior intercalary plates and seven precingular plates. Plate 2a is large and has a heptagonal shape, whereas 1a is small and pentagonal (Figs. 2a, b). Measurements of *B. quinquecornis* specimens from Paracas bay had a length of from 19.29 to 27.84 μm ($23.32 \pm 2.25 \mu\text{m}$) and a width (transdiameter) from 14.74 to 23.9 μm (19.34 ± 2.47).

In June 2015 (autumn), *B. quinquecornis* was found in net samples from Sechura Bay at low density, when prevailing environmental conditions were: water temperature 22.7° C; O₂ 2.42 mL L⁻¹; pH 8.57, and salinity 34.50. Cells were also recorded in February 2016 (summer) at densities of ~160 cells L⁻¹, the environmental conditions were: temperature 26.54 °C; O₂ 2.78 mL L⁻¹; pH 7.29; and salinity 34.175. In Paracas Bay, there was an algal bloom caused by *B. quinquecornis* on 23 Feb 2016, having a brownish color and covering a distance of approximately ~3.5 km², with maximal densities of 2.11 x 10⁵ cells L⁻¹, the environmental conditions were: temperature 24.7 °C; O₂ 2.46 mL L⁻¹; pH 7.95; and salinity 35.08. On 25/26 May 2016, the highest density of *B. quinquecornis* observed was 4.11 x 10⁴ cells L⁻¹ (temperature 19.9 °C; O₂ 7.44 mL L⁻¹; pH 8.18, and salinity 35.21). This bloom co-occurred with *A. sanguinea* (1.93 x 10⁵ cells L⁻¹). On the 26 May 2016, the bloom was associated with an especially foul smell, perhaps coming from compounds released by senescing cells. Despite this odor, there were no reports of fish mortalities or human intoxication associated with the bloom.

By Feb 3rd 2016, in Miraflores Bay, densities of *B. quinquecornis* were low (1.96 x 10³ cells L⁻¹), this was related to water warming, with temperature at 25.7° C, a decrease in salinity (34.83), O₂ at 5.17 mL L⁻¹, and pH of 8.21. Three days later *B. quinquecornis* reached a density of 3.2 x 10⁴ cells L⁻¹, corresponding to a temperature of 24.7° C, salinity 35.12 and pH 5.75. This event was previous to another bloom of *A. sanguinea*, which reached densities up to 7 x 10⁶ cells L⁻¹.

Discussion

The dinoflagellate *B. quinquecornis* was identified as the causative species of the algal blooms in the study area. This was mainly based on the cell morphology, particularly the theca tabulation (Abé, 1981; Gottschling *et al.*, 2017). Usually there are four antapical spines according Abé (1927, 1981) and Horiguchi and Pienaar (1991). There is a variant, *P. quinquecorne* var. *trispiniferum*, which differs in having three rigid antapical spines and two small lateral spines (Aké-Castillo and Vázquez, 2011).

Measurements of *B. quinquecornis* cells from Paracas Bay are similar to those provided in other studies from different locations, such as Maribago Bay, the Philippines, reporting a length from 20 - 35.0 μm and a width from 17.5 - 30.0 μm (Horstmann, 1980). In coastal lagoons of Yemen, cells had a length from 21 to 38 μm and width from 17 - 30 μm (Alkawri *et al.*, 2016). In the coasts of Veracruz, Mexico, cells have been reported with a length from 13.5 - 33.9 μm and a width from 12.2 - 29.3 μm (Barón-Campis *et al.*, 2005), and a length from 17.5 - 28.8 μm ($23.22 \pm 2.37 \mu\text{m}$) and a width from 16.3 - 25.0 μm (20.26 ± 2.46) (Okolodkov *et al.*, 2016).



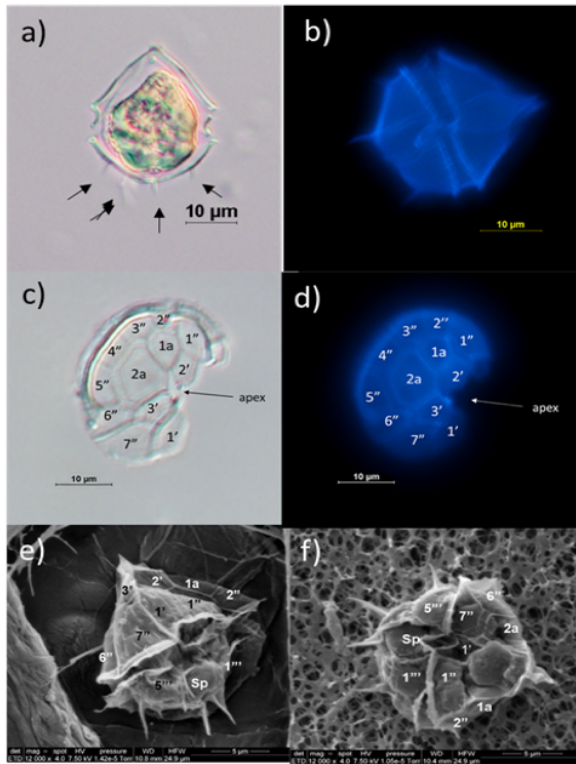


Fig. 2. Morphological details of *Blixaea quinquecornis*, including epithelial plates. a and c) DIC Nomarski technique. b and d). Epifluorescence technique with Calcofluor White. e and f). Ventral view by SEM.

Blixaea quinquecornis is a species related to high temperature. In the Philippines, blooms of this species occur in summer at temperatures between 26 and 28° C and salinities ranging from 35 to 37, although in shallow areas the temperature was 38° C, coinciding with the highest abundance (Horstmann, 1980). Also, in Brazil this species is found at temperatures between 38 and 42° C (Faust *et al.*, 2005), and in Yemen at 33-34° C with a salinity of 36 (Alkawri *et al.*, 2016). The events reported here coincided with an increase of the average temperature (between 19.9 and 24.7° C in Paracas Bay and between 24.7 and 25.7° C in Miraflores Bay), during summer and autumn 2016 when the wind decreased

(Correa *et al.*, 2017), providing favorable conditions for algal bloom formation (Du *et al.*, 2011; Smayda and Trainer, 2010).

Algal blooms caused by *B. quinquecornis* covered relatively small areas in each bay, but cells consistently colored the water dark brown. The highest abundances were found at temperatures between 24.7 and 25.7° C, and salinities between 34.83 and 35.0. The species also occurred in Sechura Bay (bay influenced by tropical currents in summer) and probably in other areas of the Peruvian coast. These findings are important considering the tendency of the temperature to increase as a consequence of climate change, therefore favoring new HAB events and the expansion of niches for invasive species (Gobler *et al.*, 2017) yet the impacts of such changes on harmful algal blooms (HABs).

Acknowledgements. This study was supported by the projects “Integrated Study of the Physical, Chemical and Biological Processes of Coastal Edge Ecosystems” of Phytoplankton and Primary Production Laboratory, IMARPE” and “Strengthening studies of HAB in the Peruvian coastal marine ecosystem” with Fishing Rights PRODUCE funding. We are grateful to staff of the coastal laboratories of Callao, Paita and Pisco, IMARPE. Thanks also to Dr. N. Rojas Morán for the facilities for the SEM and Eng. J. Cabello.

References

- Abé, T.H. (1981). Seto Mar. Biol. Lab. Spec. Publ. Ser. 6, 1-406.
- Aké-Castillo, J. A. and Vázquez, G. (2011). Acta Bot. Mex. 94, 125-140.

- Alkawri, A., Al Areeki, M., Alsharaby, K. (2016). *Plankton Benthos Res.* 11, 75-78.
- Barón-Campis, S.A., Hernández-B., D.U., Juárez-R., N.O., Ramírez-C., C. (2005). *Hidrobiologica* 15, 73-78.
- Baylón, M., Sánchez, S., Bárcena, V., López, J., *et al.*, (2015). *Rev. Per. Biol.* 22, 113-118.
- Chavez, F. P., Bertrand, A., Guevara-Carrasco, R., Soler, P., *et al.*, (2008). *Prog. Oceanogr.* 79, 95-105.
- Correa, D., Vasquez, L., Gutierrez, D. (2017). *Inf. Inst. Mar Perú* 44, 1-5.
- Du, X., Peterson, W., McCulloch, A., Liu, G. (2011). *Harmful Algae* 10, 784-793.
- Faust, M.A., Litaker, R.W., Vandersea, M.W., Kibler, S.R., *et al.*, (2005). *Atoll. Res. Bull.* 534, 103-131.
- Fritz, L. and Triemer, R. E. (1985). *J. Phycol.* 21, 662-664.
- Gárate-Lizárraga, I. and Muñeton-Gómez, M. del S. (2008). *Acta Bot. Mex.*, 47, 33-47.
- Gobler, C. J., Doherty, O. M., Hattenrath-L., T. K., Griffith, A. W., *et al.*, (2017). *PNAS* 114, 4975-4980.
- Gottschling, M., Čalasan, A. Ž., Kretschmann, J., Gu, H. (2017). *Phytotaxa* 306, 296-300.
- Horiguchi, T. and Pienaar, R. N. (1991). *Bot. Mar.* 34, 123-131.
- Horstmann, U. (1980). *J. Phycol.* 16, 481-485.
- Lozano-Duque, Y., Vidal, L. A., Gabriel, R. N. S. (2011). *Bol. Investig. Mar. Cost.* 40, 361-380.
- Okolodkov, Y.B., Campos-B., G., Gárate-L., I. (2016). *Mar. Pollut. Bull.* 108, 289-296.
- Reguera, B., Alonso, R., Moreira, A., Méndez, S. (2011). COI de UNESCO, OIEA, Paris and Viena. *Manuales y Guías de la COI*, 59 (in Spanish).
- Rodríguez-Gómez, C. F., Vázquez, G., Maya-L., C. A., Aké-C., J. A., *et al.*, (2021). *Mar. Biol.* 168, 29.
- Sánchez, S. and Delgado, E. (1996). *Inf. Prog. Inst. Mar Perú, Callao*, 44, 20-37.
- Smayda, T.J. and Trainer, V.L. (2010). *Prog. Oceanogr.* 85, 92-107.
- Sournia, A. (1978). *Monog. Oceanog. Method. UNESCO.* p 337.
- Strickland, J. D. and Parsons, T. R. (1972). In: J. C. Stevenson (Ed). *Fish Res. Board Can. Bull.* 167.
- Tenorio, C., Álvarez, G., Quijano-S., S., Perez-A., M., *et al.*, (2021). *Toxins* 13, 408.
- Tillmann, U., Sánchez-R., S., Krock, B., Bernales-J, A. (2017). *RVMO* 52, 591-610.
- Vera, G., Fraga, S., Franco, J. M., Sánchez, G. (1999). *Inf. Prog. Inst. Mar Perú - Callao*, 105, 1-12.



Molecular identification of *Alexandrium pseudogonyaulax* from Bahía de La Paz, Mexico

Ignacio Leyva-Valencia^{1*}, Christine J. Band-Schmidt², Bernd-Krock³, Delia Irene Rojas-Posadas⁴

¹CONACyT, Instituto Politécnico Nacional-CICIMAR, Av. Instituto Politécnico Nacional s/n, Col. Playa Palo de Santa Rita, 23096, La Paz, B.C.S. Mexico; ²Instituto Politécnico Nacional-CICIMAR, Av. Instituto Politécnico Nacional s/n, Col. Playa Palo de Santa Rita, 23096, La Paz, B.C.S. Mexico; ³Alfred-Wegener-Institut Helmholtz-Zentrum für Polar- und Meeresforschung, Am Handelshafen 12, D-27570 Bremerhaven, Germany; ⁴Centro de Investigaciones Biológicas del Noroeste, Av. Instituto Politécnico Nacional No. 195, Col. Playa Palo de Santa Rita, 23096, La Paz, B.C.S. Mexico.

* corresponding author's email: ileyvav@conacyt.mx

Abstract

The Gulf of California is recognized as an area with a high primary productivity. Dinoflagellate species of the genus *Alexandrium* such as *A. catenella* and *A. ostenfeldii*, that produce hydrophilic and lipophilic toxins inhabit in this region. In April 2019, from a water sample collected in southern Bahía de La Paz individual cells were identified morphologically as *Alexandrium pseudogonyaulax*. To corroborate the identification, monoclonal cell cultures were grown in GSe medium, at 24 ± 1 °C at a salinity of 34, under a 12:12 h L:D cycle at 150 $\mu\text{mol photons m}^{-2} \text{ s}^{-1}$. Molecular identification was performed amplifying rDNA regions: 28S, 18S and 5.8S, with rDNA universal primers. The length of the sequences was 682 bp, 1657 bp, and 493 bp, respectively. Maxima Parsimony, Maximum Likelihood, and Bayesian Inference algorithms were used to perform phylogenetic analyzes. The best substitution model selected for 28S and 5.8S was TrN+G, and GTR+G for 18S sequences. The sequences of BP0419 strain from Bahía de La Paz fell within the *A. pseudogonyaulax* clade. These isolates also produced goniiodomin A ($0.23 \text{ pg cell}^{-1}$), a lipophilic toxin with hemolytic activity, and is the primary reason this species is suspected of being ichthyotoxic. In coastal waters of Mexico *A. pseudogonyaulax* has been reported in the Pacific coast and the Gulf of California, although these previous studies did not confirm the species identification molecularly. The toxicity in animal and cellular models, as well as the allelopathic interactions between this strain and other microorganisms will be determined in future studies.

Keywords: Gulf of California, Molecular taxonomy, phylogeny, rDNA

<https://doi.org/10.5281/zenodo.7035097>



Introduction

Dinoflagellates that produce hydrophilic and lipophilic toxins inhabit in the Gulf of California, an important region for shellfish fisheries in Mexico that supports an extraordinary diversity of marine life, including many species of invertebrates and vertebrates, such as: commercial species of shrimp, sardine and giant squid (Brusca *et al.*, 2005; Okolodkov and Gárate-Lizárraga, 2006; Arreguín-Sánchez *et al.*, 2017).

The genus *Alexandrium* includes more than 30 species, 11 out of which produce saxitoxin and its analogs (paralytic shellfish toxins, PST), also species as *A. ostenfeldii* can produce both PST and spirolides (Cembella *et al.*, 2001; Tomas *et al.*, 2012; Salgado *et al.*, 2015), while *A. monilatum*, *A. hiranoi* and *A. pseudogonyaulax* produce goniiodomin A (GDA), a lipophilic compound with antifungal and hemolytic properties (Murakami *et al.*, 1988; Hsia, 2005).

In recent years the interest in blooms caused by *A. pseudogonyaulax* have increased. Though no adverse in humans have been attributed to this species, it has been shown to be hepatotoxic in animal models (Terao *et al.*, 1898). In Mexico, molecular data of *A. pseudogonyaulax* and toxinology is unknown.

Material and Methods

Sampling and cell isolation

In April of 2019, three water samples were obtained at a depth of 4 m, near Balandra beach (24°19'46" N, 110°20'00" W), an important recreational site in southern Gulf of California. Live phytoplankton cells were collected with a 20 µm phytoplankton net

and transferred to 250 mL flasks. The surface temperature of the water column was 22 °C and the salinity was 35.

In the laboratory, individual cells of *Alexandrium* sp. were isolated by the microcapillary method, “washing” the cells in small drops of GSe medium, modified by the addition of earth worm soil extract (Bustillos-Guzmán *et al.*, 2015). Isolated cells were placed individually in 96-well plates. The isolates were maintained at a salinity of 34, 24 °C ± 1 °C, with a photon flux of 150 µmol m⁻²s⁻¹ and a light dark cycle 12:12. After two weeks cells were transferred to six-well plates, and scaled up to 50 mL glass tubes with 25 mL of GSe medium. Culture of BP0419 was selected for further analysis. When that culture reached 500 cells mL⁻¹, one milliliter was transferred to an Eppendorf tube and centrifuged at 857 rfc (Sorvall Legend XF, ThermoScientific, U.S.A.) at 5 min, 24 °C to obtain a cellular pellet, discarding the supernatant for DNA extraction.

Microscope observations

Live vegetative cells of the strain BP0419 were observed in an inverted microscope AxioVertA1 (Zeiss, Germany). A drop of distilled water was added to induce the cell lysis and view the thecal plates at 40X, giving particular attention to the shape of the 1' precingular plate and the apical pore.

DNA extraction, amplification and sequencing

To obtain genomic DNA from the cellular pellet the Quick DNA™ Miniprep kit (D3024) of ZYMO RESEARCH was used. Extracts of genomic DNA were observed in agarose gel 1.5%, in electrophoresis with TBE 1X buffer.



The amplification of LSU rDNA partial sequences, was performed with the primers D1F (5'ACCCGCTGAATTTAAGCATA3') and D2R (5'CCTTGGTCCGTGTTTCAAGA3') (Scholin *et al.*, 1994); 18F (5'ACCTGGTTGATCCTGC-CAGT3') and 18R (5'TGATCCTTCTGCAG-GTTCAC3'); 5.8F (5'TATGCTTAAATTTCAG-CGGGT3') and (5.8R 5'GTGAACCTGCAGA-AGGATCA3') (Hosoi-Tanabe *et al.*, 2006), the amplicons were verified in agarose gels, finally these samples were sent to Macrogen Inc., Seoul Korea, sequencing service.

Phylogenetic analysis

To obtain a consensus sequence the complementary DNA, forward and reverse strands were edited manually with the software Sequencher 4.1.4 (Gene Codes, Ann Arbor, MI) using default parameters. The sequences were analyzed with Basic Local Alignment Search Tool (BLAST) of the National Center for Biotechnology Information (NCBI), to select sequences of the subgenera: *Alexandrium* and *Gessnerium* for the phylogenetic reconstruction. Sequences were aligned using the software Clustal X v.2.1 and saved in Nexus format. The phylogenetic identity and tree topology were corroborated using three distinct algorithms: maximum parsimony (MP), maximum likelihood (ML) and Bayesian inference (BI). MP and ML tests were executed in PAUP 4.10b (Swofford, 2003), and BI analyses was carried out in MrBayes 3.1.2 (Ronquist and Huelsenbeck, 2003). Node support was assessed via 10 x 10³ bootstrap replicates for MP, and the nucleotidic substitution model for ML and BI was selected using ModelTest v. 3.7 (Posada and Crandall, 1998). A bootstrap of 100 replicates was selected for ML, whereas 3 x 10⁶ generations sampled

every 100 generations and burn-in of 7500 were chosen for BI. Phylogenetic trees were visualized using the program TreeView X 0.5.1 (Page, 1996).

GDA determination

Cells in exponential growth phase were used for toxin analysis at a cell density of 22 x 10³ cells mL⁻¹. A total of 44 x 10³ cells were harvested and lyophilized. The resulting dried pellet was transferred into a 2-mL cryovial and one mL methanol and 0.9 g Lysing Matrix D (Thermo-Savant, Illkirch, France) were added. The sample was homogenized by reciprocal shaking for 45 s at 6.5 m s⁻¹ (FastPrep Instrument, Thermo-Savant) followed by centrifugation for 15 min at 21,130 rfc (5415R, Eppendorf, Hamburg, Germany). The supernatant was transferred into a spin filter (0.45 µm, Millipore Ultrafree, Eschborn, Germany) and centrifuged for 30 s at 10,000 rcf (5415R, Eppendorf). The filtrate was transferred into HPLC vials and analyzed for goniodomins by liquid chromatography coupled to tandem mass spectrometry as detailed in Krock *et al.* (2018).

Results and Discussion

When BP0419 strain was isolated, cell morphology observed under light microscopy suggested that it was similar to *A. pseudogonyaulax*. Figure 1: A) shows a vegetative cell, and B) the apical view showing 1' precingular plate and the apical plate complex, surrounding the apical pore (Po).

Partial sequences of 682 bp, 1,700 bp, and 550 bp of 28S, 18S and 5.8S were analysed (Fig. 2), using as outgroup sequences of *Gymnodinium catenatum*. The best fit substitution model for



28S and 5.8S sequences was TrN+G, while GTR+G model was the best fit substitution model for 18S sequences.

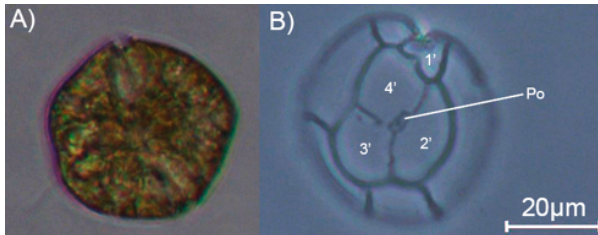


Fig. 1. Light microscopy images at 40x of: A) *A. pseudogonyaulax* BP0419 vegetative cell, and B) apical view showing the shape of the 1' plate and the apical pore (Po).

Sequences of BP0419 strain with each rDNA subunit fell within the *A. pseudogonyaulax* clade. Strains from distant geographic regions, shared the same haplotype.

Although sequences of *A. hiranoi* were not available for the phylogenetic reconstruction with 5.8S sequences, with 28S this species was included within the same clade of *A. pseudogonyaulax*, because only one transversion (adenine in *A. hiranoi* and thymine in *A. pseudogonyaulax*) was observed; whereas 18S sequences showed one transition with adenine in *A. hiranoi* and guanine in *A. pseudogonyaulax*, however the presence the guanine in other species included in the analysis was observed. For this reason, it is necessary to include more sequences of *A. hiranoi* to corroborate that this transition is really a mutation in this species and not a commonly occurring polymorphism.

The close phylogenetic relationship between *A. hiranoi* and *A. pseudogonyaulax* was previously observed by Kim *et al.* (2005), the authors included both species within

group III, were both taxa had few nucleotide differences between them. Authors also indicated that *A. hiranoi* is morphologically similar to *A. pseudogonyaulax*, with slight differences in the cell outline, the shape of the 1' precingular plate, and the position of the ventral pore. Another option to distinguish *A. pseudogonyaulax* from other species is the analysis of cysts paratabulation (Kim *et al.*, 2005).

When BP0419 strain was isolated, the cell morphology observed under light microscopy suggested that was similar to *A. pseudogonyaulax*. The shape of the apical pore and the 1' precingular plate agree with the phylogenetic reconstruction using three molecular markers, corroborating that

BP0419 strain is *A. pseudogonyaulax*. Moreover, toxin analysis revealed the presence of GDA with a cell quota of 0.23 pg cel⁻¹.

We will continue our analysis to obtain images to perform a complete description of this strain. This information will contribute to a better knowledge of the biogeography of *A. pseudogonyaulax* and its toxicity.

Acknowledgements. This study was carried out under the CONACYT projects: A1-S-14968; 1776 and SIP projects: 20195649, 2021-0126. Authors thanks to N. Herrera and L. Fernández for their help during field sampling and for maintain the strain.

References

Arreguín-Sánchez, F., del Monte-Luna, P., Zetina-Rejón, M.J., Albáñez-Lucero, M.O. (2017). *Environ. Dev.* 22, 71-77.



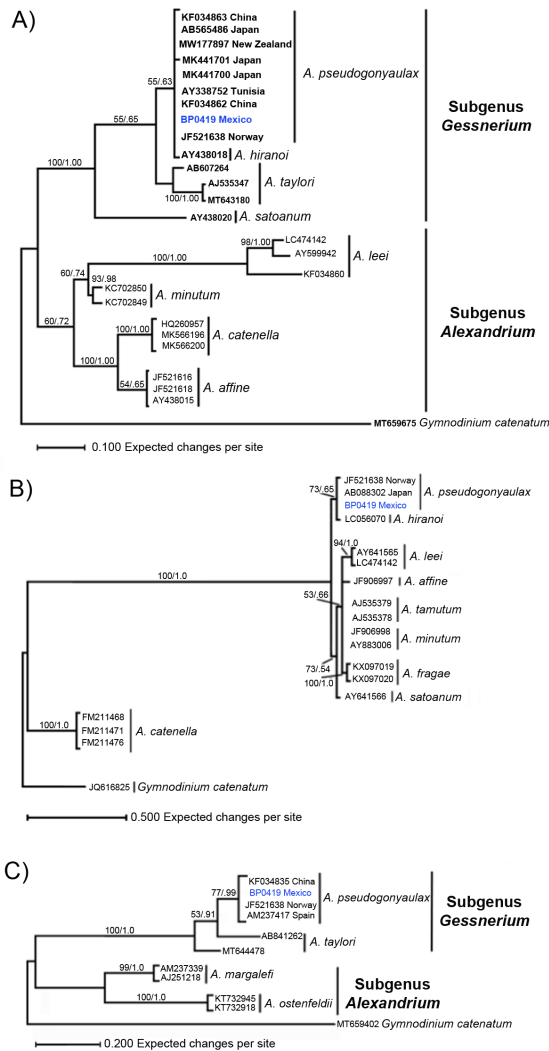


Fig. 2. Phylogenetic trees of rDNA partial sequences of *Gessnerium* and *Alexandrium* species: A) 28S; B) 18S, and C) 5.8S subunits. Values above nodes indicate: ML branch support/BI posterior probability.

Brusca, R.C., Findley, L.T., Hastings, P.A., Hendriks, M.E., *et al.*, (2005). In: Biodiversity, Ecosystems, and Conservation in Northern Mexico. Cartron, J.-L.E., Ceballos, G. (Eds.). Oxford University Press, U.S.A., pp. 179-202.

Bustillos-Guzmán, J.J., Band-Schmidt, C.J., Durán-Riveroll, L.M., Hernández-Sandoval, F.E., *et al.*, (2015). Food Addit. Contam. Part A. 32, 381-394.

Cembella, A.D., Bauder, A.G., Lewis, N.I., Quilliam M.A. (2001). J. Plankton Res. 23, 1413-1419.

Hosoi-Tanabe, S., Otake, I., Sako, Y. (2006). Fish. Sci. 72, 1200-1208.

Hsia, M.H., Morton, S.L., Smith, L.L., Beauchesne, K.R., *et al.*, (2005). Harmful Algae 5, 290-299.

Kim, K.Y., Yoshida, M., Kim, C.H. (2005). Phycologia 44, 361-368.

Krock, B., Tillmann, U., Wen, Y., Hansen, P.J., *et al.*, (2018). Toxicon 155, 51-60.

Murakami, M., Makabe, K., Yamaguchi, K., Konosy, S. (1988). Tetrah. Lett. 10, 1149-1152.

Okolodkov, Y.B. and Gárate-Lizárraga, I. (2006). Acta Bot. Mex. 74, 1-154.

Salgado, P., Riobó, P., Rodríguez, F., Franco, J.M., Bravo, I. (2015). Toxicon 103, 85-98.

Scholin, Ch. A. (1994). J. Phycol. 30, 999-1011.

Terao, K., Ito, E., Murakami, M., Yamaguchi, K. (1989). Toxicon 2, 269-271.

Tomas, C.R., Van Wagoner, R., Tatters, A.O., White, K.D., *et al.*, (2012). Harmful Algae 17, 54-63.



CICCM: new acquisitions and new descriptions of historical cultures

Lesley Rhodes*, Kirsty Smith, Tomohiro Nishimura, Sarah Challenger, Krystyna Ponikla, Juliette Butler, Lucy Thompson, Jacqui Stuart

Cawthron Institute, 98 Halifax Street East, Private Bag 2, Nelson, 7010, Nelson, New Zealand.

*corresponding author's email: lesley.rhodes@cawthron.org.nz

Abstract

The Cawthron Institute Culture Collection of Micro-algae (CICCM) in New Zealand includes more than 600 unique marine and freshwater microalgae and cyanobacteria isolates from tropical, temperate, and polar regions. Half of the collection is cryopreserved, and the other half is regularly sub-cultured. Live cultures, DNA extracts and chemical compounds may be purchased for research purposes, and all have a full description and toxin profile accompanying them (see www.cultures.cawthron.on-line). To date, isolates have enabled the description of new species, the preparation of biotoxin standards to underpin chemical tests, and the carrying out of toxicity studies amongst other research endeavours. For example, extracts of mass cultures of *Alexandrium pacificum* have been supplied to pharmaceutical companies for the preparation of paralytic shellfish toxin standards. Additions to the CICCM since 2019 include 10 dinoflagellate species, 14 diatom species and 11 cyanobacteria species. New descriptions of historic cultures in the collection include *Pavlomulina ranunculiformis* from the newly erected haptophyte class, Rappephyceae.

Keywords: CICCM, Cawthron Institute Culture Collection of Micro-algae, dinoflagellates, haptophytes, cyanobacteria

<https://doi.org/10.5281/zenodo.7035104>



Introduction

The CICCMM includes more than 600 unique marine and freshwater microalgae and cyanobacteria isolates from tropical, temperate, and polar regions. There is a focus on the Pacific region, where increasing sea temperatures are expected to impact microalgal bloom species which will in turn affect marine life, including corals and, in the case of toxic blooms, human health. Live cultures, DNA extracts or chemical compounds may be purchased for research purposes (Fig. 1). Complete strain information is available, including toxin profiles (see www.cultures.cawthron.org.nz). Half the collection comprises cryopreserved cyanobacteria; given they require thawing and on-growing before being dispatched, they may take longer to reach their destination than sub-cultured isolates.

To date, isolates have enabled the description of new species, the preparation of biotoxin standards, the carrying out of toxicity studies and the development of molecular tools. For example, extracts of mass cultures of *Alexandrium pacificum* have been supplied to pharmaceutical companies for the preparation of paralytic shellfish toxin standards. These are essential when toxin tests are carried out to ensure seafood is safe for consumers.

Isolates are also needed to underpin development of molecular detection and quantification assays. To this end, species within the diatom genus *Pseudo-nitzschia*, including four new species records for New Zealand (Nishimura *et al.*, 2021), have enabled the development of new molecular monitoring tools for these domoic acid producing diatoms. The assays will refine and increase the speed of risk alerts of potential amnesic shellfish poisoning for shellfish aquaculture managers.

Additions to the CICCMM since 2019 include 45 dinoflagellate isolates (10 species), 32 diatom isolates (14 species), 49 cyanobacteria isolates (11 species), and one chlorophyte.

Dinoflagellates

Additions to the CICCMM in the last two years include marine species in the genera *Akashiwo*, *Azadinium*, *Biecheleria*, *Bysmatrum*, *Coolia*, *Fukuyoa*, *Gambierdiscus*, *Ostreopsis*, *Prorocentrum* and *Vulcanodinium*.

Nine species of *Gambierdiscus* (28 isolates) are maintained and are being investigated for ciguatera-related compounds (Murray *et al.*, 2021). Strains of *G. cheloniae* (Smith *et al.*, 2016a) from the Cook Islands and *G. honu* from Rangitāhua/Kermadec Islands (Rhodes *et al.*, 2017) provided the data that underpinned these two descriptions.

Twenty-eight strains of *A. pacificum* are held in the CICCMM due to the value of the biotoxins produced. Extracts from mass cultures produced by Cawthron's Natural Compounds group are supplied to pharmaceutical companies for purification for paralytic shellfish toxin standards.

Azaspiracids have been shown to occur, albeit at low concentrations, in some New Zealand shellfish. Isolates of *Azadinium* and *Amphidoma* have helped with the development of molecular identification assays to aid in the determination of the producer of these toxins in New Zealand (Smith *et al.*, 2016b; Balci *et al.*, 2021).



Haptophyta

A haptophyte isolated in 1998 from Tapeka (Northland, New Zealand) was tentatively named *Pavломulina* 'kotuku' and was deposited in the CICCM as CAWP21 (Fig. 2). It is now officially named *P. ranunculiformis* Sym, Pienaar & Kawachi (Kawachi *et al.*, 2021) and belongs to the new haptophyte class Rappephyceae (a sister class to Prymnesiophyceae). The species may be mixotrophic as cells have been observed attaching to oyster larvae and becoming engorged, possibly as they feed (Fig. 2; Rhodes *et al.*, 2011).

The detailed characterisation of *Pavломulina* has allowed for a reconstruction of the ancient evolutionary history of the Haptophyta, one of the most important components of extant marine phytoplankton communities. Thus, the acquisition of novel strains to the collection has facilitated the fundamental science of protistan taxonomy for the benefit of the research community.

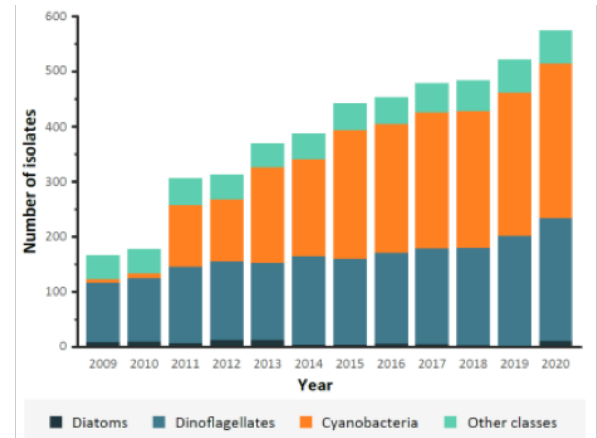
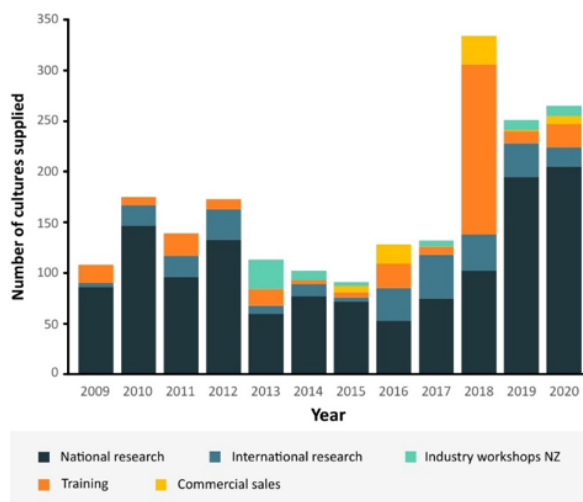


Fig. 1. Cawthron Institute Culture Collection of Micro-algae 2009-2020: Top: cultures supplied to end-users; Bottom: number of isolates of major groups of microalgae available.

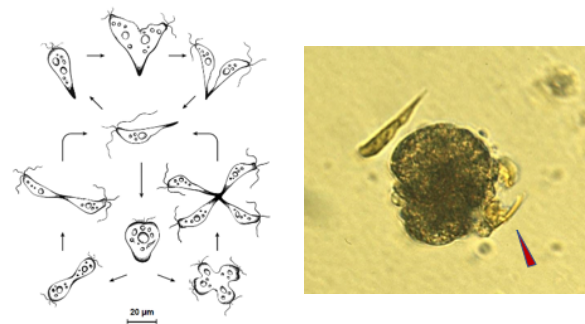


Fig. 2. *Pavломulina ranunculiformis*. Left: details of life cycle (from Othman Bojo's unpublished PhD thesis, 2002, UoOtago, NZ); Right: Cell of *P. ranunculiformis* (CAWP21) attached to a Pacific oyster larva (arrow highlights microalgal cell).

Conclusion

In New Zealand, development of freshwater regulations has in part been supported by research into the cyanobacteria collection and the determination of toxin concentrations for different species. The growing tropical collection has proved a resource for novel compound discovery, as well as a baseline

for tracking climate change impacts in New Zealand (Rhodes *et al.*, 2020).

In conclusion, the CICCM continues to underpin research globally (Fig. 3). The collection continues to grow and support global research, predominantly with new additions from New Zealand's freshwater and marine coastal waters and from the wider Pacific region. Many more cyanobacteria isolates are being investigated for impacts on the environment and on human health and selected strains will be cryopreserved and curated within the CICCM.



Fig. 3. Global distribution of cultures from the CICCM, both purchased as DNA or chemical extracts or provided live for collaborative research programmes. Blue circles: Key collaborators; Red circles: developing contacts.

Acknowledgements. The CICCM is supported by the NZ Ministry of Business, Innovation and Employment, contract: CAWX0902.

References

Balci, M., Rhodes, L.L., Nishimura, T., Murray, J.S., *et al.*, (2021). N. Z. J. Mar. Freshw. Res. 1-16.

Kawachi, M., Nakayama, T., Kayama, M., Nomura, M., *et al.*, (2021). Curr. Biol. 31, 2395-2403.

Murray, J.S., Finch, S.C., Rhodes, L.L., Puddick, J., *et al.*, (2021). Toxins 13, 333.

Nishimura, T., Murray, J.S., Boundy, M.J., Balci, M., *et al.*, (2021). Toxins 13, 637.

Rhodes *et al.* 2011. Phylum Haptophyte. In: Gordon (Ed.), New Zealand Inventory of Biodiversity 3, 312-321.

Rhodes, L., Smith, K.F., Verma, A., Curley, B.G., *et al.*, (2017). Harmful Algae 65, 61-70.

Rhodes, L.L., Smith, K.F., Murray, J.S., Nishimura, T., Finch, S.C. (2020). Toxins 12, 50.

Smith, K.F., Rhodes, L., Harwood, D.T., Adamson, J., *et al.*, (2016b). J. Appl. Phycol. 28, 1125-1132.

Smith, K.F., Rhodes, L., Verma, A., Curley, B.G., *et al.*, (2016a). Harmful Algae 60, 45-56.





TOXICOLOGY



Cytotoxicity of dinoflagellates from the Mexican Pacific Ocean: Inhibition of hNav1.7 by Saxitoxin, a therapeutically relevant sodium ion channel

A. Picones^{1*}, R. Alonso-Rodríguez², L. Morquecho³, M. Matus-Nuñez¹, C.O. Lara-Figueroa¹

¹ *Laboratorio Nacional de Canalopatías. Instituto de Fisiología Celular, UNAM, Mexico.*

² *Unidad Académica Mazatlán. Instituto de Ciencias del Mar y Limnología. UNAM, Mexico.*

³ *Centro de Investigaciones Biológicas del Noreste, S.C. (CIBNOR). La Paz, B.C.S., Mexico.*

* *corresponding author's email: arturopicones@yahoo.com*

Abstract

hNav1.7 is a voltage-gated sodium human channel associated with neuropathic pain. Saxitoxin (STX), a potent neurotoxin, was tested on the functional activity of hNav1.7. In this work STX-Gcat was extracted from strains of the taxonomically identified marine dinoflagellate *Gymnodinium catenatum*, collected from the Mexican Pacific Ocean, cultured and then subjected to: freeze-thaw to induce cell lysis, cleaning with a solid phase extraction cartridge, evaporation for concentration, and separation by chromatographic analysis. Ion currents, recorded by patch-clamp in whole-cell configuration from a cell line heterologously expressing hNav1.7, showed 15% completely reversible inhibition in amplitude by STX at 1 μ M without affecting its kinetics. In addition of its voltage dependence and its rapid kinetics, the unambiguous identification of active functional hNav1.7 channels was confirmed by its 100% blockade by commercially available Tetrodotoxin (TTX) at 100 nM. Using two independent methods of noise analysis (Variance Analysis and Spectral Density Distribution), the biophysical features of the single channel activity were determined. TTX decreased the open probability and the effective number of functional channels, leaving the single channel current and conductance unaffected. Natural toxic metabolites such as STX and TTX, target specific sodium ion channels with great potency and selectivity in cell membranes, affecting marine biota and humans through the consumption of contaminated shellfish, but they also represent an opportunity to apply them therapeutically.

Keywords: Saxitoxin, *G. catenatum*, Nav1.7, patch-clamp, single channel biophysics, noise analysis

<https://doi.org/10.5281/zenodo.7035120>



Introduction

Voltage-gated sodium channels (Nav) are critical in the initiation of electrical signal in a variety of cell types and particularly in excitable membranes where they are responsible of the initial rapid depolarization of the action potential. Notably the malfunction of the nociceptive human Nav1.7 channel has been amply documented in association with neuropathic chronic pain (Young, 2008; Lampert *et al.*, 2010). The search for natural compounds with inhibitory properties might lead to chemical agents with relevant therapeutic potential in this field.

Tetrodotoxin (TTX) and saxitoxin (STX) are well-known positively charged marine guanidinium neurotoxins with specific high-affinity and potent blocking pharmacological activity binding the extracellular mouth of hNav1.7 (Catterall, 1980; Penzotti *et al.*, 1998; Walker *et al.*, 2012).

Here we present an experimental study of the inhibitory action of STX-Gcat and commercial TTX (see next section) on the hNav1.7 channel functionality. In order to propose a molecular mechanism of such inhibition we determined quantitatively the biophysical properties of hNav1.7 single channel activity by Ion Current Fluctuations Analysis (aka Noise Analysis).

Material and Methods

Extraction and isolation of STX samples

STX was extracted from taxonomically identified and scaled up clonal cultures of *Gymnodinium catenatum* (Albinsson *et al.*, 2014) then subjected to freeze-and-thaw to induce cell lysis, cleaning with a solid

phase extraction cartridge, concentrated by evaporation and finally to chromatographic analysis. After lyophilisation, the samples were diluted in physiological solutions for the electrophysiological experiments.

Electrophysiology

Total ionic membrane currents were recorded by the patch-clamp technique in the whole-cell configuration from Chinese Hamster Ovary (CHO) cells heterologously and stably expressing cloned hNav1.7 (donated by Dr. L. Possani, Instituto de Biotecnología, UNAM), utilizing an arrangement as follows: Axopatch 200B/Digidata1550/pCamp10 (amplifier/analog-digital converter/software, all from Molecular Devices). All current recordings were analog filtered at 10 kHz and digitally sampled at 50 kHz. The external solution contained (in mM): 140 NaCl, 3 KCl, 2.4 CaCl₂, 1.3 MgCl₂, 10 HEPES and 10 Glucose (300 mOsm kg⁻¹; pH 7.4 adjusted with NaOH). The internal (pipette) solution contained (in mM): 100 KCl, 40 NaCl, 3 MgCl₂, 5 EGTA and 10 HEPES (300 mOsm kg⁻¹; pH 7.2 adjusted with KOH). TTX was purchased from Alomon Labs.

Data Analysis

Noise analysis of the current recordings was performed using two different and independent methodologies of mathematical modelling: Variance Analysis and Power Spectral Density Distribution (Stevens, 1972; Sigworth, 1980; Neumcke, 1982; Picones and Korenbrot, 1994; Alvarez *et al.*, 2002). In a patch containing N functional ionic channels, each with single-channel current i , the relationship between the mean current amplitude (I) and its variance (s^2) is given by



the parabolic function:

$$\sigma^2 = iI - \frac{I^2}{N} \quad (1)$$

The power spectral density of an ion channel current is described by one or the sum of two Lorentzian functions (Matthews, 1986; Haynes *et al.*, 1986; Picones and Korenbrot, 1994; Picones and Korenbrot, 1995; Picones *et al.*, 2001):

$$S(f) = \frac{S(0)_l}{1 + \left(\frac{f}{f_l}\right)^2} + \frac{S(0)_h}{1 + \left(\frac{f}{f_h}\right)^2} \quad (2)$$

The integral over the positive frequencies of equation 2 gives another independent calculation of the variance of the current fluctuations:

$$\sigma^2 = \frac{\pi}{2} [S(0)_l f_l + S(0)_h f_h] \quad (3)$$

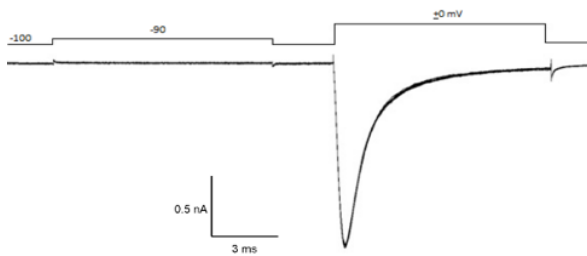


Fig. 1. Voltage protocol (upper trace) and the corresponding ion current (lower trace) for the analysis of membrane current fluctuations (noise) applying the methodologies as described in the text.

Results and Discussion

Figure 2 shows actual total ion current recordings obtained under voltage clamp from two CHO cells. The relationship between the current as a function of voltage (I-V curve) for ten different cells is also shown. The features of the inward going currents, namely their fast kinetics, (of activation and inactivation) and their dependence on membrane voltage correspond to the functional properties of hNav1.7 activity.

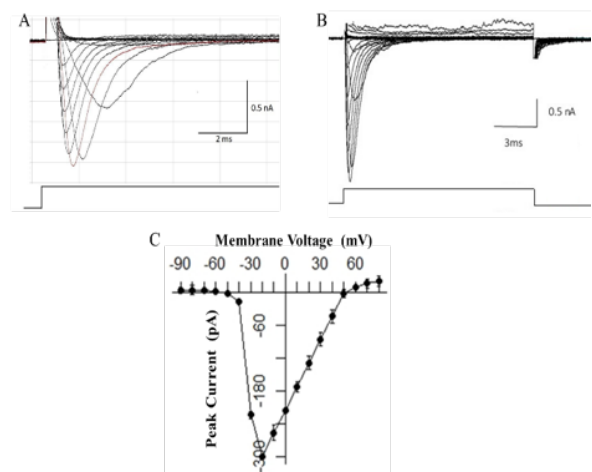


Fig. 2. Functional activity of hNav1.7 heterologously and stably expressed in CHO cells. A and B, two different total membrane current recordings in response to membrane voltage steps (lower traces) from -90 to +80 mV. C, I-V curve for the inward peak amplitude (mean \pm s.e.m.) from 10 different cells.

Figure 3 demonstrates the inhibitory effects of both guanidinium toxins on the inward currents when applied in the external solution. STX-Gcat exerted an inhibition of 15% in a complete reversible manner at a concentration of 1 μ M. Further unambiguous identification of active functional hNav1.7 channels was confirmed by its 100% reversible blockade by Tetrodotoxin (TTX) at 100 nM.

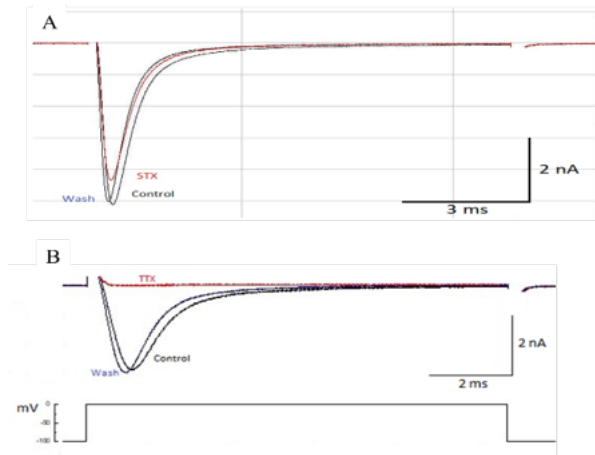


Fig. 3. Inhibitory action of STX 1 μ M (A) and TTX 100 nM (B) on hNav1.7 currents. In all tested cases the current completely recovered to the control condition. Voltage pulse was applied from -100 to 0 mV.

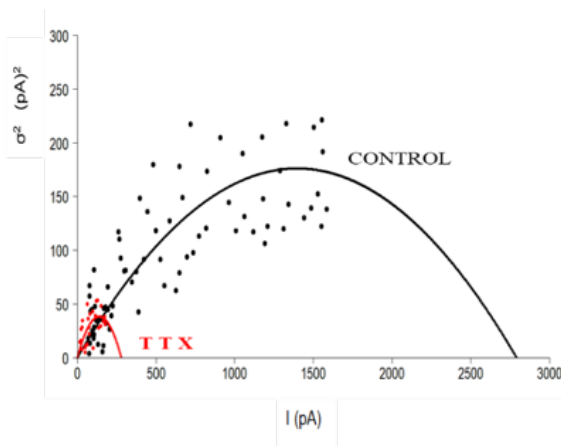


Fig. 4. Analysis of variance (s^2) applied to macroscopic current (I) fluctuations of hNav1.7 activity in control and after the inhibition by TTX at 100 nM in the external solution. Continuous lines are fits of equation 1 to the experimental data points.

Figure 4 shows a representative example of the results obtained by the method of analysis of current variance applied to the electrophysiological activity of hNav1.7 in the control condition and after the presence of 1 nM TTX in the external solution. The

continuous lines are fits of Equation 1 to both experimental conditions. It is clear that the action of TTX modifies the parameters of that mathematical model.

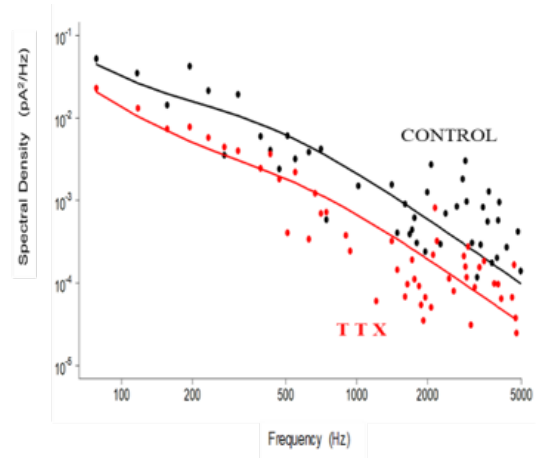


Fig. 5. Power spectral density distribution, $S(f)$, as a function of frequency (f) applied to current fluctuations of hNav1.7 activity in control and after the inhibition of TTX at 100 nM in the external solution. Continuous lines are fits of equation 2 to the experimental data points.

A representative case of the results obtained by applying the power spectral analysis method to the current fluctuations generated by hNav1.7 is illustrated in figure 5. Data points obtained in the control condition and after the addition of TTX to the external solution are both well described by fits of Equation 2 and shows a significant effect on the parameters defining this mathematical formalism. A summary of the numerical parameters which define the biophysical features of the single channel properties of hNav1.7 and their modifications caused by the inhibitory action of TTX is presented in Table 1. The figures in red are the only ones showing a statistical significant change ($p < 0.005$, One-Way ANOVA).

Table 1. Single channel biophysical properties of hNav1.7 activity in normal (control) conditions and their modifications by the inhibition exerted by TTX applied in the external solution (see text).

Method	Parameter	[Units]	Control	TTX (100 nM)
Variance Analysis	i (Single Current)	[pA]	0.47 ± 0.51	0.52 ± 0.22
	N Number of Channels		8718 ± 834	512 ± 170
	P (Open Probability)	[%]	70.90 ± 15	9.28 ± 5.32
	γ (Single Conductance)	[pS]	8.63 ± 0.22	9.4 ± 0.64
Spectral Analysis	i (Single Current)	[pA]	0.35 ± .031	0.31 ± 0.52
	N Number of Channels		88.2 ± 3.3	12.5 ± 10.3
	P (Open Probability)	[%]	9733 ± 1300	1344 ± 1452
	γ (Single Conductance)	[pS]	6.36 ± 3.21	5.63 ± 4.56

Overall the present experimental study and theoretical analysis direct us to the following conclusions:

1. As expected from reports previously published, TTX showed a high potency inhibition of human Nav1.7 current, 100% at 100 nM, in a completely reversible manner.
2. STX isolated from *Gymnodinium catenatum* inhibited hNav1.7 currents only 15%. This inhibition was consistently observed and completely reversible.
3. Results gathered from two different and independent quantitative methods of noise analysis, suggest that the inhibition of hNav1.7 macroscopic current exerted by TTX is due mainly to a clear decrease of the Probability of Opening ($P_o = I / iN$) of the channel.
4. Natural toxic metabolites such as STX and TTX, target sodium ion channels in cell membranes, affecting marine biota and humans through the consumption of contaminated shellfish, but they also represent an opportunity to apply them therapeutically (also see Catterall, *et al.*, 2005).

Acknowledgements. This study was funded by Proyecto de Ciencia Básica CONACYT A1-S-37026.

References

- Albinsson, M.E., Negri, A.P., Blackburn, S.I., Bolch, C.J.S. (2014). PLoS ONE 9, e104623.
- Alvarez, O., Gonzalez, C., Latorre, R. (2002). Adv. Physiol. Educ. 26, 327-341.
- Catterall, W.A. (1980). Ann. Rev. Pharmacol. Toxicol. 20, 15-43.
- Catterall, W.A., Goldin, A.L., Waxman, S.G. (2005). Pharmacol. Rev. 57, 397-409.
- Haynes, L.W., Kay, A.R., Yau, K.-W. (1986). Nature 321, 66-70.
- Lampert, A., O'Reilly, A.O. Reeh, P. Leffer, A. (2010). Pflügers. Arch. 460, 249.263.
- Matthews, G. (1986). J. Neurosci. 6, 2521-2526.
- Neumcke, B. (1982). Int. Rev. Neurobiol. 23, 35-67.
- Penzotti, J.L., Fozzard, H.A., Lipkind, G.M., Dudley, S.C. (1998). Biophys. J. 75, 2647-2657.
- Picones, A. Keung, E. Timpie, L.C. (2001) Biophys. J. 81, 2035-2049.
- Picones, A. and Korenbrot, J.I. (1994). Biophys. J. 66, 360-365.
- Picones, A. and Korenbrot, J.I. (1995). J. Physiol. 485, 699-714.



Sigworth, F.J. (1980). *J. Physiol.* 307, 97-129.

Stevens, C.F. (1972). *Biophys. J.* 12, 1028-1047.

Walker, J.R., Novick, P.A., Parsons, W.H., McGregor, M., Zablocki, J., Pande, V.S., Du Bois, J. (2012). *PNAS* 109, 18102-18107.

Young, F.B.J. (2008). *Clin. Genet.* 73, 31-33.



Negative impacts of lipophilic toxins on zebrafish development, immune system, and tissue regeneration

Javiera F. De La Paz^{1,2,3*}, Nicolás O. Zambrano¹, Patricio Yañez¹, Consuelo Anguita-Salinas^{2,3}, Miguel Miranda^{2,3}, Allisson Astuya-Villalón¹, Miguel L. Allende^{2,3}, Alejandra Llanos-Rivera¹

¹Departamento de Oceanografía, Universidad de Concepción, Barrio Universitario, S/N Concepción, Chile; ²Centro de Regulación del Genoma, Universidad de Chile, Av. Blanco Encalada 2085, Santiago, Chile; ³Danio Biotechnologies, Las Lomas 7844 Santiago, Chile.

*corresponding author's email: jdelapaz@udec.cl

Abstract

The increase in distribution and frequency of Harmful Algal Blooms (HABs) worldwide are cause of social and environmental concern globally. In southern Chile, HAB episodes have caused great losses due to high fish mortalities in salmonid farms and native fauna, affecting biodiversity, local economies, and threatening food safety. The most damaging episodes of HABs in this region of the Pacific Ocean are associated to phytoplankton species producers of paralytic shellfish poison (PSP), but episodes caused by producers of Diarrhetic Shellfish Poison (DSP) and other emergent lipophilic biotoxins have been increasingly detected. Sub-lethal toxic effects on mammals and the mechanisms of action described to date for DSP are diverse, although their impact on fish have been neglected. Using zebrafish (*Danio rerio*) as a model, we tested the effects of four lipophilic biotoxins: Okadaic acid, Dinophysis toxin-1, Dinophysis toxin-2, and Yessotoxin-1. We assessed the effects of sub-lethal concentrations on swim bladder inflation, touch response and locomotor activity on larvae, and the results suggest teratogenic impacts and/or neurotoxicity. Also, using fish expressing fluorescent proteins in a specific cell type and whole-mount staining, we detected changes in the distribution pattern of neutrophils and the amount of Goblet cells, suggesting an activation of the immune response of larvae. Finally, taking advantage of the zebrafish regenerative capacity, we used a tail-fin amputation protocol and detected a negative impact on tissue regeneration. These effects all together can have complex implications for environmental safety, biodiversity conservation and the salmon industry, since small amounts of toxins can probably increase susceptibility to other threats for fish, such as environmental pathogens.

Keywords: Diarrhetic shellfish toxin, lipophilic toxins, zebrafish, bioassays, toxicity

<https://doi.org/10.5281/zenodo.7035130>



Introduction

Aquaculture industry in Chile is one of the main economic activities, and is specially concentrated in the southern macrozone, where the main products are salmonid fishes and mussels. Pacific austral southern macrozone has constant Harmful Algal Bloom (HAB) events, especially on summer, when toxic blooms produce frequently high mortalities in salmon farms. The salmon industry is usually pointed out as responsible for diverse socio-environmental problems in Chile due to water and oceanic floor pollution caused by the excessive use of antibiotics to treat and prevent pathogens and parasites attacks on salmon (Cabello, 2006), the waste from food and metabolism, fish escape effecting ecosystems, and the controversial relationship between aquaculture farms and the increasing occurrence of HABs (Quiñones *et al.*, 2019).

Fishes in salmon farms are submitted to very stressful conditions. High population density and poor water quality, which makes them very susceptible to diverse environmental hazards and pathogens. Considering this, the presence of microalgae producing cytotoxic venoms even in relatively low concentrations, could contribute to worsening the sanitary situation on salmon farms, by producing damage to the skin, affecting the immune system, and/or by reducing wound healing process. Therefore, we wanted to know if marine biotoxins present in Chilean coast can affect the immune response and the regenerative capacity of fishes, and if they can be considered as a risk factor for the transmission of infectious diseases in fish that are related to skin wounds.

To assess this, we studied the impact of four lipophilic biotoxins in zebrafish larvae as a teleost model, exposing them to three toxins from the Okadaic acid group: Okadaic Acid (OA), Dinophysis toxin-1 (DTX-1), Dinophysis toxin-2 (DTX-2), and to Yessotoxin-1 (YTX-1). OA and its derivatives DTX-1 and DTX-2 cause gastrointestinal illness in humans, but in animal models has also been related with cytotoxicity, genotoxicity, neurotoxicity and tumor promotion. While cytotoxic potential on diverse levels (ribotoxic, apoptotic, genotoxic) has also been reported for Yessotoxins (Korsnes and Korsnes., 2017), while at least one report reveals its possible neurotoxic effects (Pérez-Gómez, 2006).

Different studies remark the numerous advantages of using the zebrafish model (*Danio rerio*) for assessing the impacts of marine biotoxins on fishes (Berry *et al.*, 2007). Also, multiple genetic and molecular tools as transgenic reporter lines, vital cell dyes, antibodies, and whole-mount stain techniques are available.

Material and Methods

Toxins and exposure solutions

Certified Reference Material (CRM) from the National Research Council Canada was used. Okadaic Acid (CRM-OA-d), Dinophysistoxin-1 (CRM-DTX1-c), Dinophysistoxin-2 (CRM-DTX2-b), and Yessotoxin (CRM-YTX-c) certified solutions in methanol, were diluted in E3 culture medium (5 mM NaCl, 0.17 mM KCl, 0.33 mM CaCl₂, 0.33 mM MgSO₄, buffered to pH 7.0). Additionally, a solution of methanol



equivalent to concentration in the lowest toxin dilution, was used as solvent control, and a negative control group incubated in E3 medium.

Exposure and fishes

Fifteen zebrafish embryos of 24 to 72 h post fertilization (hpf) were exposed to two concentrations of each toxin on 96-well plates in groups of three embryos with a final volume of 50 μ L (De la Paz *et al.*, 2020) unless otherwise stated, at 26 °C with a daily 14 h light /10 h dark cycle. TAB5 wild type strain was used for general toxic response monitoring, and fin regeneration experiments. Transgenic line Tg(BACmpo:gfp) expressing GFP in the innate immune system neutrophil cells (Renshaw *et al.*, 2006) was used for neutrophil and Goblet cells quantification.

Toxic response monitoring

Survival, edemas and the swim bladder air filling were monitored daily. After 24 h of exposure, locomotor activity was recorded for six hours with three hours period of light and dark, using an automated movement recorder system (WMicrotracker ONE, Phylumtech S.A.), later in the two following days the touch response index was evaluated similarly as previously described (Lefebvre *et al.*, 2004). Shortly, the caudal region was touched using a fine forceps, and reaction scored as following: (3) normal escape reaction, two body length is traveled away from the stimulus, at first touch; (2) delayed response, more than one touch is required for the scape response, (1) reduced response, the animal can't travel the normal distance away from the stimulus, but present a reaction; (0) the animal is totally paralyzed and do not react to the stimulus.

Neutrophil cells quantification

Transgenic Tg(BACmpo:gfp) 24 hpf embryos were exposed for 48 hours, then anesthetized with MS-222, and the number of GFP marked cells were quantified in different regions of the body using a Olympus IX81 epifluorescence microscope.

Goblet cell quantification

After neutrophil quantification, live embryos were incubated again for an additional 30 h (total exposure time 78 h), then transferred to PFA 4% and stained with Alcian Blue 8X (Sigma-Aldrich). Goblet cells in the head and trunk region, were quantified.

Caudal fin regeneration assay

The caudal fin of larvae was amputated, and regeneration area measured as previously described (Morales and Allende, 2019). One hour after amputation groups of six 4 dpf larvae were exposed to E3 medium, 0.5% methanol, AO, DTX-2 and YTX. Three days post amputation the caudal fin area was measured from images captured in an Olympus MVX10 stereomicroscope and analyzed using the ImageJ free software.

Statistical Analysis

For all statistical analysis the Graphpad Prism 9 for macOS software was used. Cell quantification, touch response and caudal fin regeneration data were analyzed with Kruskal Wallis test & Dunn's multiple comparison ($p < 0.05$). For locomotor activity and developmental defects Mann-Whitney test with a multiple comparison with Holm-Sidak method ($p < 0.05$) was used.



Results and Discussion

Neuro-motor response

Locomotor activity in zebrafish larvae raised in a 14 h light/10 h dark photoperiod, decrease its locomotor activity in prolonged dark periods of several hours. When 4 dpf larvae exposed to OA, DTX-1 and YTX for 24 h, were exposed to light changing conditions, the response in the beginning of a dark period was an increase of locomotor activity in toxin treated larvae respect to the control groups in this condition, but statistical analysis revealed a significant only for YTX, that also induce a reduction of touch response in larvae after three days of exposure (data not shown). These results suggests that these lipophilic toxins could have some impact on neuro-motor system in zebrafish larvae.

Survival and acute toxicity

None of the toxins was lethal or induced edemas, but results revealed that exposure to methanol and YTX by immersion can inhibit normal development of the swim bladder (Fig. 1), the flotation organ of larvae that allows buoyancy control, so it is possible that the impact of YTX to fishes on natural environment could affect normal swimming, feeding, and escape capacity on fish larval stages. Therefore, YTX may have an indirect negative impact on fish populations by reduce viability of early stages of fish, and by impeding essential biological functions.

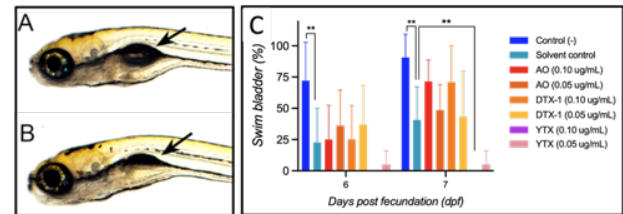


Fig. 1. Yessotoxin and methanol affects development of zebrafish swim bladder. (A) normal zebrafish larva. (B) Treated larva with not inflated swim bladder (arrows). (C) Average and SD of filled swim bladder. (** $p < 0.01$).

Immune cells responses

The first normal response of fishes exposed to noxious chemical or physical agents is the production of skin mucus secreted mainly by epidermal Goblet Cells (Shepard, 1993). Fish skin mucus contains diverse defensive components including glycoproteins, glycosaminoglycans, and several antimicrobial proteins, acting as a first defensive barrier of the innate immune system (Dash *et al.*, 2018)

To resolve if lipophilic biotoxins can affect the defensive barrier of skin and immune system, we assessed the number of skin Goblet cells in the head and trunk of exposed zebrafish larvae. Results shows that even when the solvent control induce a reduction in the number of stained mucus cells, the number is significantly lower when exposed to OA, DTX-1 and DTX-2 (Fig. 2). This shows that these biotoxins induces a response of the mucus producing cells in zebrafish larvae.



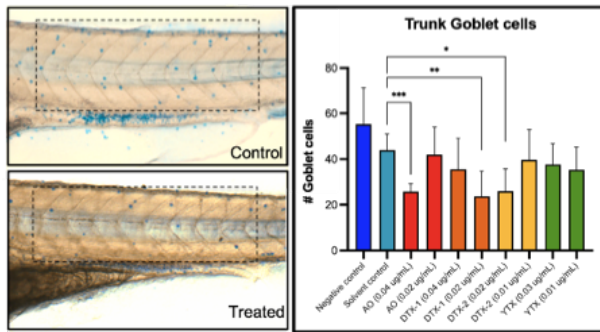


Fig. 2. OA and its derivatives impact skin Goblet cells abundance. Zebrafish larvae exposed to lipophilic toxins present a reduced number of mucus cells (blue dots on left) on the skin of trunk. (* $p < 0.05$; ** $p < 0.01$; *** $p < 0.001$). N 12-13 individuals.

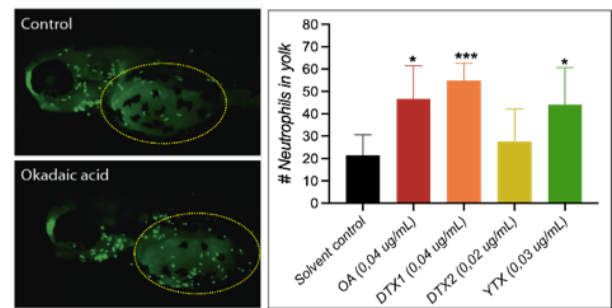


Fig. 3. Lipophilic marine biotoxins induce neutrophil migration to yolk region. Leukocytes in the yolk sac area (yellow oval) of larvae exposed was quantified *in vivo*. Mean and SD (* $p < 0.05$; ** $p < 0.01$; *** $p < 0.001$).

If defensive barriers of mucus and skin are breached, recruitment of neutrophil cells is the first cellular response, and their early activity is necessary not only for pathogen elimination or entry prevention, but also for the subsequent wound regeneration process (Philipson and Kubes, 2019).

Using a transgenic zebrafish strain that expresses the Green Fluorescent Protein (GFP) in neutrophils, we detected that these inflammatory cells migrate specifically to the yolk region of the embryo after being exposed for 48 hours to OA, DTX-1, and YTX (Fig. 3), suggesting a specific cell migration or recruitment to the yolk region that can account for an activation of the innate immune system of the larvae challenged with these biotoxins. Since the relationship between these biotoxins and the fish immune system is practically unknown, the kinetic response for this (and other) cell types should be further studied to make conclusions.

Caudal fin regeneration on zebrafish larvae
To assess possible impacts of YTX and OA and its derivatives on fish tissue regeneration, we executed a caudal fin amputation protocol in the larvae. Results showed that the regeneration process when exposed YTX is affected (Fig. 4).

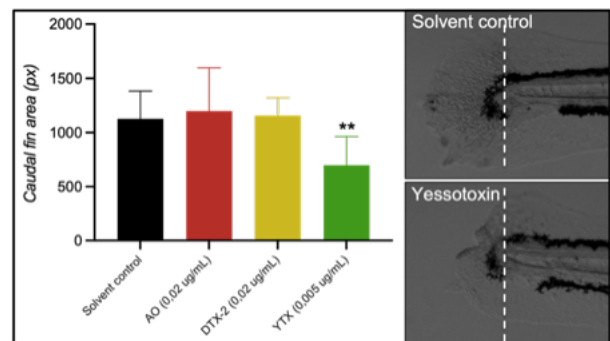


Fig. 4. Yessotoxin affects caudal fin regeneration on zebrafish larvae. Mean and SD for regenerated caudal fin area. Dotted line shows amputation site (** $p < 0.01$).

Our results show that these four lipophilic biotoxins on water can induce a quantifiable response on at least two innate immune cell types: mucus producing Goblet cells (AO,



DTX-1 and DTX-2), and inflammatory neutrophils (AO, DTX-1 and YTX), and can also affect tissue regenerative capacity on zebrafish larvae (YTX).

The possible relationship between these toxins and the innate immune response and regenerative capacity in fishes is not understood to date. This is the first report on this topic, and therefore, more studies are needed to resolve if lipophilic biotoxins can be a risk factor for the transmission of infectious diseases associated to skin wounds in fishes, by impairing mucus physical barrier, cellular innate immune response and/or hindering wound healing and tissue regeneration. More studies are needed to unravel the relationship between the occurrence of HABs, their impacts on general animal health, and on early fish stages. Considering the global warning scenario and the environmental and socio-economic consequences of HABs events in Chile, we consider this a critical matter in zones with high aquaculture activity.

Acknowledgements. To Yariksa Segovia for fish care, and to Ambbar Aballay for technical support.

References

Berry, J. P., Gantar M., Gibbs P. D., Schmale M. C. (2007). *Comp. Biochem. Physiol. C Toxicol. Pharmacol.* 145, 61-72.

Cabello, F. C. (2006). *Environm. Microbiol.* 8, 1137-1144.

Dash, S., Das, S. K., Samal, J., Thatoi, H. N. (2018). *Iran. J. Vet. Res.* 19, 72-81.

De la Paz, J. F., Anguita-Salinas, C., Díaz-Celis, C., Chávez, F. P., Allende, M. L. (2020). *Biomolecules* 10, 1274.

Korsnes, M. S. and Korsnes, R. (2017). *Front. Cell. Dev. Biol. Mar.* 31, 5-30.

Lefebvre, K. A., Trainer, V. L., Scholz, N. L. (2004). *Aquat. Toxicol.* 66, 159-170.

Morales, R. A. and Allende, M. L. (2019). *Front. Immunol.* 10, 253.

Pérez-Gómez A., Ferrero-Gutierrez A., Novelli A., Franco J. M., *et al.*, (2006). *Toxicol. Sci.* 90, 168-77.

Renshaw, S. A., Loynes, C. A., Trushell, D. M., Elworthy, S., *et al.*, (2006). *Blood* 108, 3976-3978.

Shepard, K. L. (1993). *Adv. Drug Deliv. Rev.* 11, 403-417.

Quiñones, R. A., Fuentes, M., Montes, R. M., Soto, D., León-Muñoz, J. (2019). *Rev. Aquacult.* 11, 375-402.



Monitoring and management of paralytic shellfish toxins in Southern Rock Lobster, Tasmania, Australia

Alison Turnbull¹, Andreas Seger¹, Navreet Malhi², Jessica Jolley², Tim Harwood³, Juan Dorantes-Aranda¹, Tom Madigan², Graeme Knowles⁴, Hilary Revill⁵, Quinn Fitzgibbon¹, Gustaaf Hallegraeff¹

¹University of Tasmania, Institute of Marine and Antarctic Studies, Taroona 7052, Tasmania, Australia; ²South Australian Research and Development Institute, Food Sciences, Urrbrae 5064, South Australia, Australia; ³Cawthron Institute, Nelson 7010, New Zealand; ⁴Department of Primary Industry Parks Water and Environment, Animal Health Laboratory, Prospect 7250, Tasmania, Australia; ⁵Department of Primary Industry Parks Water and Environment, Hobart 7001, Tasmania, Australia.

* corresponding author's email: alison.turnbull@utas.edu.au

Abstract

The Tasmanian Southern Rock Lobster (*Jasus edwardsii*) fishery has been challenged by recurrent dinoflagellate blooms of *Alexandrium catenella* since 2012. The initial bloom resulted in the first ever closure of an Australian lobster fishery due to marine biotoxins and exposed several key knowledge gaps for managing food safety and market access risk. To fill these gaps, experimental studies were conducted to determine paralytic shellfish toxin (PST) toxicokinetics. Adult male lobsters fed highly toxic mussels (6 mg STX.2HCl eq kg⁻¹) accumulated PST in the hepatopancreas at an exponential rate of 6% per day, reaching a maximum level of 9 mg STX.2HCl eq kg⁻¹ in three weeks. However, lobsters exposed to toxic algae culture suspensions at 2 x 10⁵ cells L⁻¹ did not accumulate any toxin. Neither accumulation of PST nor exposure to toxic cells resulted in any gross impact on the health of lobsters, as assessed by a comprehensive range of behavioural, immune, nutritional and biochemical indicators. Field studies over a period of eight years confirmed the ability of lobster hepatopancreas to rapidly accumulate and depurate toxins in the wild, with a high degree of variability. Analysis of 496 hepatopancreas samples collected during *A. catenella* blooms identified high risk sites and seasons; demonstrated the usefulness of mussels as sentinel species for indicating PST risk; and enabled quantification of the confidence level associated with current risk management sampling practices. The combined experimental and field results have led to improved risk management for this AUD 97M wild fishery.

Keywords: PST, toxin, lobster, hepatopancreas, non-traditional vector, toxicokinetics, lobster health, *Alexandrium*, risk management

<https://doi.org/10.5281/zenodo.7035135>



Introduction

An extensive dinoflagellate bloom of *Alexandrium catenella* occurred on the east coast of Tasmania in 2012, causing the first ever Australian lobster fishery harvest closure due to marine biotoxins (Campbell *et al.*, 2013). During the bloom, Southern Rock Lobster, *Jasus edwardsii*, accumulated PST to 3.9 mg STX.2HCl equiv kg⁻¹. Since 2012, recurrent blooms of *A. catenella* have occurred during winter and spring months when water temperatures are between 10 and 15°C and coastal waters may stratify (Condie *et al.*, 2019). These blooms have had an ongoing impact on both the commercial lobster fishery in Tasmania, valued at AUD 97 M, and the significant recreational fishing sector. In order to better manage the associated public health and market access risks, a series of experimental and field studies was undertaken. Initial work focused on the risks to human health from PST accumulation in Southern Rock Lobster, looking at the concentration of PST in the hepatopancreas, assessing the fate of PST during cooking, and consumer exposure levels (Madigan *et al.*, 2018a,b; McLeod *et al.*, 2018; Turnbull *et al.*, 2018).

Risk management of PST in lobster in Tasmania has adopted the bivalve PST maximum level (ML) as the regulatory level (DPIPWE, 2020), however, lobster sampling strategies are necessarily different from those for molluscs due to the geographical spread of the wild fishery, the different way the animals are consumed, and the high level of variability among individual animals. Lobsters are keystone marine species, so concern was also raised over potential impacts on lobster health.

Further experimental and field studies were undertaken, seeking knowledge of the toxicokinetics of PST accumulation and depuration; of supply chain risks of exposure to toxic algal cells; impacts on lobster health; and effective methods to monitor PST levels in the field.

Material and Methods

Experimental studies

Two controlled experiments took place in a biosecure facility using adult male lobsters housed in individual tanks in a flow-through aquaculture system (Fig. 1). In the first experiment, lobsters were fed mussels containing 6 mg STX.2HCl equiv kg⁻¹ for 27 days then moved to a non-toxic diet for a further 36 days (Turnbull *et al.*, 2020a). PST in the hepatopancreas was examined at regular intervals during uptake and depuration using LC-MS/MS (Boundy *et al.*, 2015; Turner *et al.*, 2015). Exponential uptake and depuration rates were calculated and changes in the toxin profile noted. At the peak of uptake, PST was also analysed in the hindgut, antennal glands, gills and haemolymph.

In the second experiment, lobsters were exposed to toxic cultures of *A. catenella* at field relevant concentrations of 2 x 10⁵ cells L⁻¹ for three weeks (Turnbull *et al.*, 2021b), replicating potential exposure in the supply chain. PST was measured in the hepatopancreas at three time points.





Fig. 1. Biosecure experimental facility where lobster housed in individual tanks were exposed to PST through either food or toxic algal cultures.

During both experiments, lobster health was assessed at each harvest point via a comprehensive set of behavioural, immune, nutritional and biochemical responses, measured by the same operator in the same order on each harvest day (Turnbull *et al.*, 2020a). Histological analysis of the toxic algae exposed lobsters was conducted using formalin fixed paraffin embedded gill tissues samples cut into three micron thickness and stained with haemotoxylin and eosin.

Field studies

Lobster sampling (n = 496) occurred on a regular basis from 2012 to 2020 in eight lobster biotoxin management zones on the east coast of Tasmania during *A. catenella* blooms (Turnbull *et al.*, 2021a; Fig. 2).

On each sample occasion, lobster hepatopancreas from each site were analysed individually for PST (n = 5 animals). Blue mussels, *Mytilus galloprovincialis*, from adjacent aquaculture farms or specifically installed mussel lines were sampled over the same time period as potential sentinel species. Samples were analysed for PST using either HPLC-FLD (Lawrence *et al.*, 2005) or LC-MS/MS (Boundy *et al.*, 2015; Turner *et al.*, 2015).

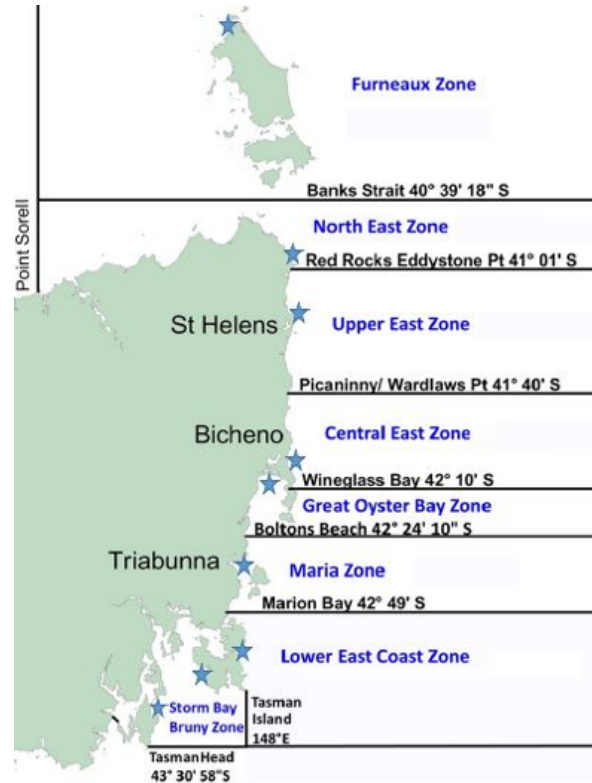


Fig. 2. PST lobster management zones on the east coast of Tasmania, Australia. Sentinel mussel sample locations are indicated with an asterisk. Source: DPIPW, 2020.

Uptake and depuration rates for lobster were calculated for events with four or more consecutive sampling occasions at the same site and compared to concurrent mussel uptake and depuration rates. Data from the start and end of blooms were examined to determine the number of lobsters required to give a 95% confidence that the population is below the bivalve maximum level.

Results and Discussion

When lobsters were fed toxic mussels, PST accumulated rapidly in the hepatopancreas at an exponential rate of 6% per day, reaching



a mean of 6.7 mg STX.2HCl eq kg⁻¹ after 27 days (Turnbull *et al.*, 2020a). The majority of toxins in the hepatopancreas during uptake were GTX2,3 C1,2, and GTX1,4, with the proportion of the latter decreasing as uptake continued (Fig. 3). In comparison the mussel feed contained mostly GTX1,4 and GTX 2,3. The lobsters depurated at a rate of 7% per day once toxic feed was removed. PST was detected in lobster antennal glands and gills (possible excretion routes for PST), however, it was not detected at significant levels in lobster haemolymph. The majority of toxin in the antennal glands and gills were GTX2,3 and dcGTX2,3.

Exposure to PST did not result in mortality nor significant changes in any of the behavioural, health, nutritional and haemolymph biochemical parameters measures suggesting limited gross impact on lobster performance and indicating adult lobster are relatively tolerant to PST (Turnbull *et al.*, 2020b).

Lobsters exposed to highly toxic algal cultures of *A. catenella* did not accumulate PST and no negative impact on lobster health or gill tissue was observed (Turnbull *et al.*, 2021b). The results indicate that PST uptake can only occur through the consumption of toxic prey and hence that there are no food safety or quality risks from exposure to toxic cells during wet storage in boat wells, sea cages or specialized wet storage facilities in the supply chain.

Field studies and regulatory monitoring over the eight year period showed high variability in toxin levels between individuals, sites, months and years. The central Tasmanian coast was identified as the greatest risk site, but confined to the months of July to January

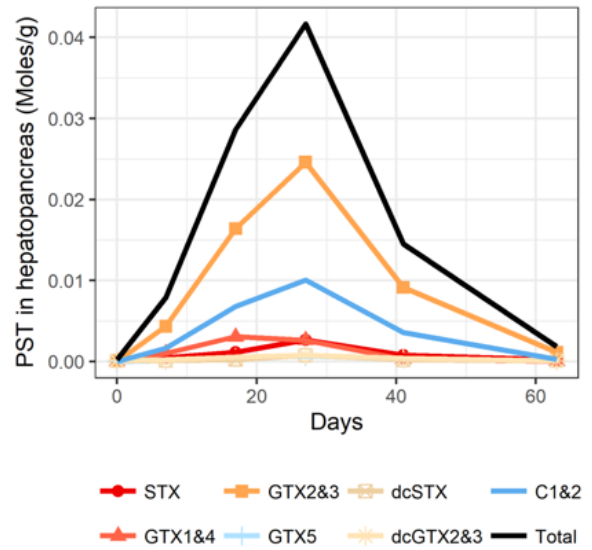


Fig. 3. PST analogue mean molar content in hepatopancreas of exposed *J. edwardsii* during 27 days of uptake and 35 days of depuration.

(Turnbull *et al.*, 2021b; Fig. 4). Relatively high PST uptake rates were observed in lobster hepatopancreas (exponential rate of 2% per day), similar to but consistently less than rates seen in filter-feeding mussels. Lobsters were relatively fast detoxifiers following bloom demise, losing up to 3% PST per day. Mussel sentinel lines were a cost-effective means of indicating PST risk in lobsters, with an annual baseline monitoring cost of <0.1% of the industry value. The current practice of analysing multiple lobster from a site and closing on a conservative trigger level provides a 97.5% confidence level that any lobster from that site would be below the bivalve maximum level of 0.8 mg STX eq kg⁻¹.

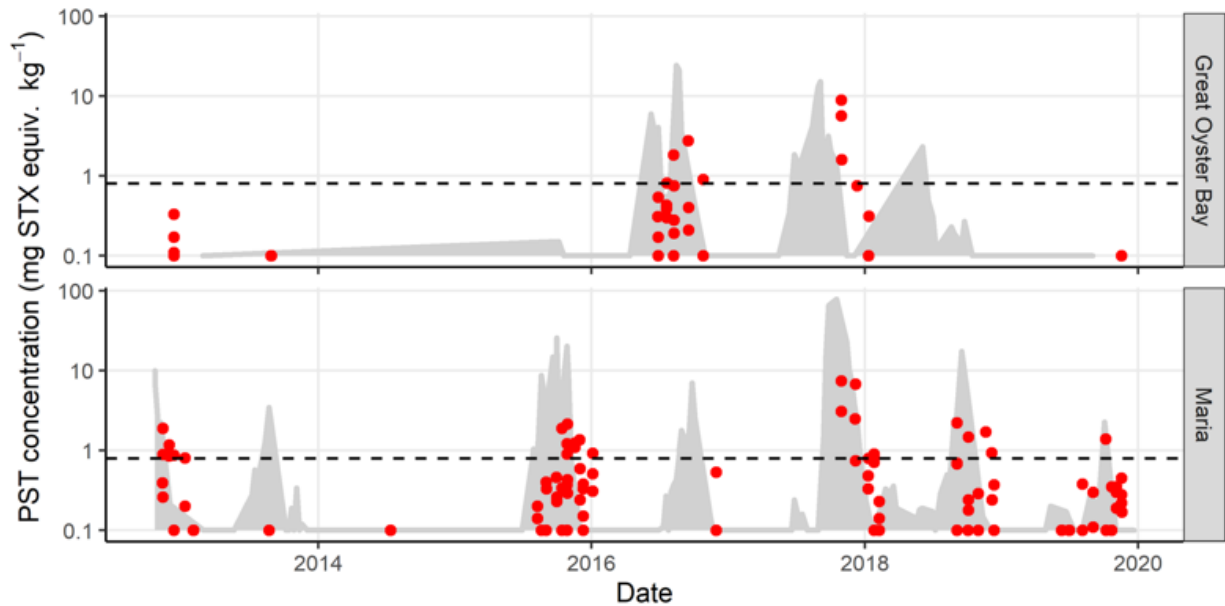


Fig. 4. PST levels in lobster hepatopancreas (red dots) and mussels (grey areas) from the central east coast of Tasmania from 2012 to 2020 inclusive. Modified after Turnbull *et al.* (2021).

Acknowledgements. This study was funded by the Fisheries Research and Development Corporation grants 2013-713, 2014-032, 2017-051 and 2017-086, Southern Rock Lobster Ltd, New Zealand Rock Lobster Industry Council, University of Tasmania, and the South Australian Research and Development Corporation.

References

- Boundy, M.J., Selwood, A.I., Harwood, T.D., McNabb, P.S., Turner, A.D. (2015). *J. Chromatogr. A* 1387, 1-12.
- Campbell, A., Hudson, D., McLeod, C., Nicholls, C., Pointon, A. (2013). FRDC Report 2012/060, SARDI, Australia.
- Condie, S.A., Oliver, E.C.J., Hallegraeff, G.M. (2019). *Harmful Algae* 87, 101628.
- DPIPWE (2020). [//dPIPWE.tas.gov.au/Documents/Rock_Lobster_Biotoxin_Protocols_2020%20final.pdf](https://dPIPWE.tas.gov.au/Documents/Rock_Lobster_Biotoxin_Protocols_2020%20final.pdf)
- Lawrence, J.F., Niedzwiadek, B., Menard, C. (2005). *J. AOAC Int.* 88, 1714-1732.
- Madigan, T., Malhi, N., Tan, J., McLeod, C., *et al.*, (2018a). *Toxicon* 143, 44-50.
- Madigan, T., Turnbull, A., Tan, J., Pearn, R., McLeod, C. (2018b). *Hum. Ecol. Risk Assess. Int. J.* 24, 1565-1578.
- McLeod, C., Kiermeier, A., Stewart, I., Tan, J., *et al.*, (2018). *Hum. Ecol. Risk Assess. Int. J.* 24, 1872.
- Turner, A.D., McNabb, P.S., Harwood, T., Selwood, A.I., Boundy, M.J., (2015). *J. AOAC Int.* 98, 609-621.



Turnbull, A., Malhi, N., Tan, J., Harwood, D.T., Madigan, T. (2018). *J. Food Prot.* 8, 240-245.

Turnbull, A., Malhi, N., Seger, A., Harwood, T., *et al.*, (2020a). *Harmful Algae* 95, 101818.

Turnbull, A., Malhi, N., Seger, A., Jolley, J., *et al.*, (2020b). *Aquat. Toxicol.* 105704. 10.1016/j.aquatox.2020.105704I.

Turnbull, A., Dorantes-Aranda, J.J., Madigan, T., Jolley, J., *et al.*, (2021a). *Mar. Drugs* 19, 5010.

Turnbull, A., Seger, A., Jolley, J., Hallegraeff, G., *et al.*, (2021b). *Toxins* 13, 129.



Gambierol blocks a K⁺ current fraction and affects action potential duration and the firing rate in rat fetal chromaffin cells

Jordi Molgó^{1,2*}, Roland Bournaud², Sébastien Schlumberger², Makoto Sasaki³, Haruhiko Fuwa⁴, Evelyne Benoit^{1,2*}

¹Université Paris-Saclay, CEA, INRAE, Institut des sciences du vivant Frédéric Joliot, Département Médicaments et Technologies pour la Santé, Service d'Ingénierie Moléculaire pour la Santé, Equipe Mixte de Recherche CNRS n° 9004, bâtiment 152, point courrier 24, F-91191 Gif-sur-Yvette, France; ²CNRS, Laboratoire de Neurobiologie Cellulaire et Moléculaire-UPR 9040, F-91198 Gif-sur-Yvette, France; ³Tohoku University, Graduate School of Life Sciences, Sendai, Japan; ⁴Chuo University, Faculty of Science and Engineering, Department of Applied Chemistry, 1-13-27 Kasuga, Bunkyo, Tokyo 112-8551, Japan.

* corresponding authors e-mails: jordi.molgo@cea.fr evelyne.benoit@cea.fr

Abstract

The dinoflagellate genus *Gambierdiscus*, particularly *Gambierdiscus toxicus* is known to produce numerous ladder polycyclic ether compounds, including gambierol, characterized by a transfused octacyclic polyether core, as well as the identified ciguatoxins responsible for ciguatera poisoning. Gambierol inhibits voltage-gated K⁺ (K_v) channels in various mammalian excitable and non-excitable cells, and motor nerve terminals of the neuromuscular junction. In the present study, we investigated the action of gambierol on outward K⁺ currents of cultured rat fetal adrenal medulla chromaffin cells using the whole-cell configuration voltage-clamp method. The pharmacological dissection of the outward K⁺ current, using selective K⁺ channel inhibitors, revealed that gambierol reduced just a small fraction of the total outward current without affecting calcium-activated K⁺ currents that were sensitive to apamin and iberiotoxin, and ATP-sensitive K⁺ currents sensitive to glibenclamide. Cultured fetal chromaffin cells were excitable and generated either evoked (upon direct electric stimulation) or spontaneous action potentials. These action potentials were sensitive to tetrodotoxin that blocks voltage-gated Na⁺ (Na_v) channels. Gambierol neither affected the rising phase nor the overshoot of action potentials but significantly prolonged their repolarizing phase and increased the firing rate of action potentials during sustained current depolarization, as determined using current-clamp recordings. Our results highlight the effects of gambierol on K_v channels and on the electrical properties of rat fetal chromaffin cells. It is likely that gambierol may cross the placental barrier as ciguatoxins do. Further studies are needed to determine whether such actions may have deleterious effects on fetuses.

Keywords: gambierol, marine biotoxin, potassium channels

<https://doi.org/10.5281/zenodo.7035142>



Introduction

Marine dinoflagellates produce bioactive secondary metabolites with unique chemical structures (reviewed in Yasumoto, 2001; Shmukler and Nikishin, 2017). The *Gambierdiscus* genus is known to manufacture a number of ladder cyclic compounds, including the ciguateras, responsible for ciguatera poisoning, and gambierol, which is also suspected to be involved in ciguatera fish poisoning. The chemical syntheses of gambierol (Fuwa *et al.*, 2002; Johnson *et al.*, 2005) and analog compounds (Alonso *et al.*, 2012) have been performed. Consequently, the availability of the polyether toxin allowed the study of its mode of action on ion channels from excitable (i.e. those that can be electrically stimulated) and non-excitable cells. Thus, gambierol inhibits voltage-gated K^+ (K_v) channel subtypes in a range of cells, including mouse taste cells (Ghiaroni *et al.*, 2005), *Xenopus* skeletal myocytes (Schlumberger *et al.*, 2010), rodent cerebellar neurons (Pérez *et al.*, 2012), *Xenopus* oocytes or Chinese hamster ovary (CHO) cells expressing mammalian K_v 1.1- K_v 1.5 subtypes (Cuypers *et al.*, 2008; Konoki *et al.*, 2015), mouse fibroblasts expressing the K_v 3.1 subtype (Kopljar *et al.*, 2009), human T lymphocytes expressing the K_v 3.1 subtype (Rubiolo *et al.*, 2015), and motor nerve terminals of the vertebrate neuromuscular junction (Molgó *et al.*, 2020). The information that some lipid-soluble polyether toxins, like brevetoxin-3, actually cross the rodent maternofetal barrier (Benson *et al.*, 2006), and the fact that fetal chromaffin cells express a diversity of K_v channels (reviewed in Lingle *et al.*, 2018) motivated us to study the effect of gambierol on rat fetal chromaffin cells. In the present work, we performed a pharmacological

dissection of the current components present in the outward K^+ current of cultured rat fetal adrenomedullary chromaffin cells and investigated the action of gambierol on such currents. In addition, we studied whether the time course of spontaneous action potentials was sensitive to the action of gambierol and to the combined action of selective blockers of calcium-activated potassium (K_{Ca}) channels.

Material and Methods

Gambierol (purity >97%) was chemically synthesized, as described previously by Fuwa *et al.* (2002). Stock solutions of gambierol were made in dimethyl sulfoxide (DMSO) and diluted with an external physiological solution. The DMSO concentration was less than 0.1% v/v. Tetrodotoxin, apamin, iberiotoxin, and glibenclamide were obtained from Alomone Labs (Jerusalem, Israel) and Latoxan (Portes-lès-Valence, France). The cell-culture media and all other chemicals were acquired from Sigma-Aldrich (Saint-Quentin-Fallavier, France).

Timed-pregnant Wistar rats were purchased from Elevage Janvier (Le Genest-Saint-Isle, France). Animal care and surgery were performed according to the Directive 305 2010/63/EU of the European Parliament, approved by the French Ministry of Agriculture. The project was submitted to the French Ethics Committee CEEA and obtained the authorization APAFIS #4111-2016021613253432 v5. On day 19-20 of gestation (F19-F20), pregnant rats were euthanized by carbon dioxide gas inhalation, and fetuses were quickly collected and



decapitated with scissors according to the guidance of the European Committee DGXI, regarding animal experimentation.

Adrenal medulla chromaffin cells, removed from adrenal glands of fetuses collected at F19-F20, were used for cell cultures, employing protocols previously described (Bournaud *et al.*, 2007). Membrane currents and potentials were recorded from fetal chromaffin cells using the perforated whole-cell voltage-clamp technique. Patch-glass microelectrodes had a resistance of 2-5 M Ω when filled with the internal solution and were coated with Sticky wax (S.S. White, Gloucester, UK). Under voltage-clamp conditions, the seal resistance was usually 2-10 G Ω , and 75-80% of the series resistance was compensated. Membrane currents (under voltage-clamp conditions) and potentials (under current-clamp conditions in the zero current mode) were monitored with an RK-400 amplifier (Biologic, Claix, France), filtered at 1-3 kHz (Frequency device, MA, U.S.A.), digitized with a DigiData-1200 interface (Axon Instruments, Union City, CA, U.S.A.), and stored on a hard disk. Data acquisition and analyses were performed with the pCLAMP-8.0 software (Axon Instruments). All experiments were performed at constant room temperature (21°C).

The external solution contained (in mM): 135 NaCl, 5 KCl, 2 CaCl₂, 2 MgCl₂, 10 glucose, 10 HEPES [4-(2-hydroxyethyl)-1-piperazine ethane sulfonic acid] (adjusted to pH 7.4, with osmolarity of 300 mOsm). The micropipette solution contained (in mM): 105 K⁺ gluconate, 30 KCl, 0.1 CaCl₂, and 10 HEPES (adjusted to pH 7.2, osmolarity of 290 mOsm) to which amphotericin-B (24 $\mu\text{g mL}^{-1}$) was added. Tetrodotoxin, apamin, iberiotoxin,

glibenclamide, tetraethylammonium chloride (TEA), and 3,4-diamino-pyridine (3,4-DAP) were added to the external solution. The solutions containing these drugs were perfused by a custom-made gravity-fed micro-flow perfusion system positioned close to the recorded cell.

Cells were continuously bathed in a standard physiological solution containing tetrodotoxin (1 μM) to block voltage-gated Na⁺ channels. The involvement of different current components in the total outward K⁺ current was studied using the selective peptide toxins apamin and iberiotoxin, which block respectively the small-conductance and the large-conductance Ca²⁺-activated K⁺ channels (K_{Ca} channels), and glibenclamide that blocks ATP-sensitive K⁺ (K_{ATP}) channels.

Results and Discussion

As shown in a representative recording (Fig. 1A), the perfusion of apamin (400 nM), iberiotoxin (100 nM), and glibenclamide (200 μM) markedly reduced the total outward K⁺ current. The remaining K⁺ current was further reduced by adding gambierol (100 nM) and was completely inhibited by further perfusion of TEA (10 mM) and 3,4-DAP (500 μM) which are well-known organic K⁺ channel inhibitors. Thus, gambierol inhibited only a small fraction of the total K⁺ current when added either before or after K_{Ca} and K_{ATP} blockers. Intriguingly, the percentage of K⁺ current inhibition by apamin, iberiotoxin, and glibenclamide was not significantly different when determined before or after gambierol action, as shown in figure 1B.



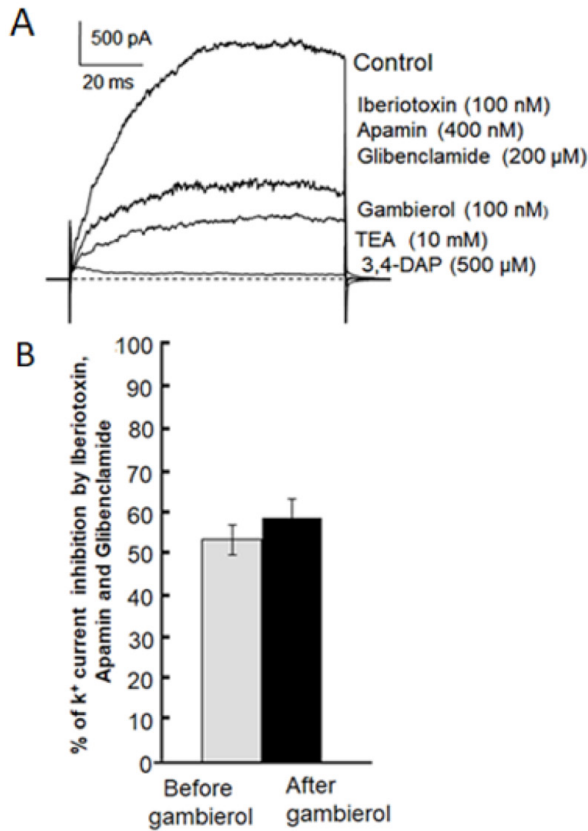


Fig. 1. (A) Superimposed traces of outward K⁺ currents recorded under control conditions and after the simultaneous perfusion of apamin, iberiotoxin, and glibenclamide, and the cumulative perfusion of gambierol, TEA, and 3,4-DAP at the concentrations indicated. The K⁺ current was recorded during 90 ms depolarizing steps from a holding potential of -70 mV to +40 mV. Note that gambierol blocked only a small K⁺ current component. (B) Percentage of K⁺ current inhibition by iberiotoxin, apamin, and glibenclamide before (gray column) and after gambierol addition to the medium (black column) Data in columns represent mean ± SEM, n = 6 different experiments (*p* = 0.848).

To the best of our knowledge, this is the first time that gambierol has been reported to block K_v channels in rat fetal chromaffin cells. These cells express various types of channels that contribute to the total outward K⁺ current. Gambierol inhibited a small component of the total K⁺ current (i.e. 15.86 ± 4.82%, n = 6) when added before or after selective channel blockers, suggesting that the polyether affects neither K_{Ca} nor K_{ATP} channels.

The cultured rat fetal chromaffin cells studied were excitable and generated either induced (in response to electrical stimulation) or spontaneous all-or-none action potentials. Using the current-clamp technique, we investigated the effects of gambierol on the action potentials of fetal chromaffin cells. Under control conditions, the mean membrane resting potential of fetal chromaffin cells was -51.8 ± 3.1 mV (n = 32), with a mean coefficient of variation of 0.32 (standard deviation/mean). The spontaneous spike activity was present in about 2/3 of the cells studied. As shown in a typical recording in figure 2, gambierol (50 nM) had no significant effect on the depolarizing phase and peak amplitude of spontaneous action potentials. Our results strongly suggest that the polyether toxin does not affect Na_v channels in fetal chromaffin cells.



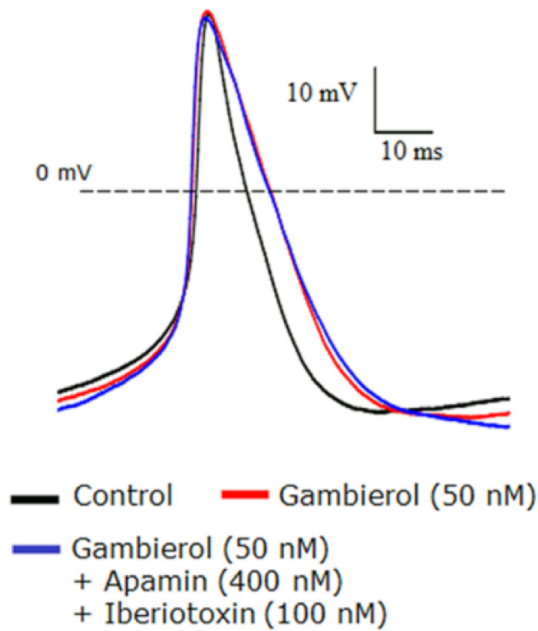


Fig. 2. Superimposed traces of spontaneous action potentials recorded from fetal chromaffin cells under control conditions in standard physiological solution (black trace), during the action of 50 nM gambierol (red trace), and after addition of apamin (400 nM) and iberitoxin (100 nM) to the extracellular medium (blue trace).

Gambierol specifically and significantly prolonged the repolarizing phase of action potentials, measured as the time elapsed from the peak of action potentials to 0 mV membrane potential, by $31.95 \pm 1.62\%$ ($n = 3$; $p < 0.05$; Fig. 2). Interestingly, the subsequent perfusion of apamin (400 nM) and iberitoxin (100 nM) to the physiological solution had no significant effect on the action potential repolarizing phase ($p > 0.05$), indicating that K_{Ca} channels do not participate in the modulation of action potential duration in fetal chromaffin cells. In addition, as shown in Fig. 3, gambierol increased the firing rate of action potentials triggered by depolarizing current pulses of long duration (13 s), when compared to the control, which

exhibited during the sustained depolarizing current a decline in action potential frequency or accommodation. These results suggest that the K^+ current blocked by the polyether is involved in controlling the firing rate of fetal chromaffin cells.

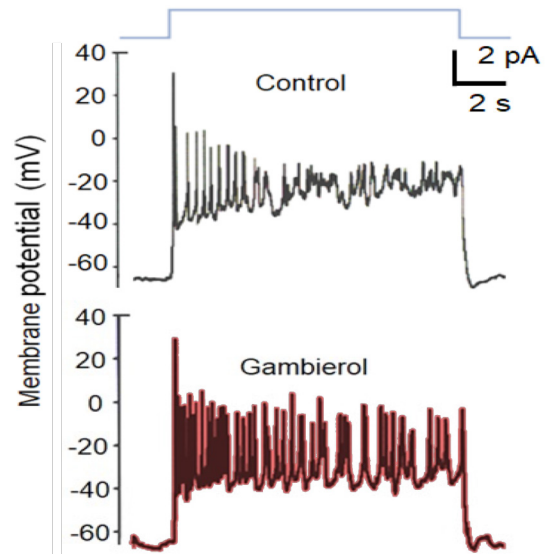


Fig. 3. Current-clamp recordings in a single fetal chromaffin cell under control conditions and during the action of 100 nM gambierol. The upper scheme (in blue) shows the long current pulse depolarization used to trigger the changes in membrane potential (before, in black, and after, in red, gambierol addition).

Overall, our study enhances the knowledge we have on the several types of K^+ channels contributing to the total outward current of rat fetal chromaffin cells and clearly indicates that gambierol affects a small K^+ current component distinct to the K_{Ca} and K_{ATP} currents. In addition, K_V blockade by gambierol prolonged the repolarizing phase and increased the firing rate of action potentials. Further work is needed to determine whether gambierol affects Ca^{2+} -dependent catecholamine secretion, and has harmful effects on fetuses.

Acknowledgments. This study was supported in part by the project ALERTO-X-NET (EAPA_317/2016), funded by the Interreg Atlantic program, and in part by the CNRS.

References

- Alonso, E., Fuwa, H., Vale, C., Suga, Y., *et al.*, (2012). *J. Am. Chem. Soc.* 134, 7467-7479.
- Benson, J.M., Gomez, A.P., Statom, G.L., Tibbetts, B.M., *et al.*, (2006). *Toxicon* 48, 1018-1026.
- Bournaud, R., Hidalgo, J., Yu, H., Girard, E., Shimahara, T. (2007). *Pflügers Arch.* 454, 83-92.
- Cuypers, E., Abdel-Mottaleb, Y., Kopljar, I., Rainier, J.D., *et al.*, (2008). *Toxicon* 51, 974-983.
- Fuwa, H., Kainuma, N., Tachibana, K., Sasaki, M. (2002). *J. Am. Chem. Soc.* 124, 14983-14992.
- Ghiaroni, V., Sasaki, M., Fuwa, H., Rossini, G.P., *et al.*, (2005). *Toxicol. Sci.* 85, 657-665.
- Johnson, H.W., Majumder, U., Rainier, J.D. (2005). *J. Am. Chem. Soc.* 127, 848-849.
- Konoki, K., Suga, Y., Fuwa, H., Yotsu-Yamashita, M., Sasaki, M. (2015). *Bioorg. Med. Chem. Lett.* 25, 514-518.
- Kopljar, I., Labro, A.J., Cuypers, E., Johnson, H.W., *et al.*, (2009). *Proc. Natl. Acad. Sci. U.S.A.* 106, 9896-9901.
- Lingle, C.J., Martinez-Espinosa, P.L., Guarina, L., Carbone, E. (2018). *Pflügers Arch.* 470, 39-52.
- Molgó, J., Schlumberger, S., Sasaki, M., Fuwa, H., *et al.*, (2020). *Neuroscience* 439,106-116.
- Pérez, S., Vale, C., Alonso, E., Fuwa, H., *et al.*, (2012). *Chem. Res. Toxicol.* 25, 1929-1937.
- Rubiolo, J.A., Vale, C., Martín, V., Fuwa, H., Sasaki, M., Botana, LM. (2015). *Arch. Toxicol.* 89, 1119-1134.
- Schlumberger, S., Ouanounou, G., Girard, E., Sasaki, M., *et al.*, (2010). *Toxicon* 56, 785-791.
- Shmukler, Y.B. and Nikishin, D.A. (2017) *Mar. Drugs* 15, 232.
- Yasumoto, T. (2001). *Chem. Rec.* 1, 228-242.



Mode of action of cyclic imine toxins: 20-methyl spirolide-G antagonizes rat neuronal $\alpha 3\beta 2$ nicotinic acetylcholine receptor

Amandine Gaudin¹, Rómulo Aráoz^{1,2*}

¹ Université Paris-Saclay, CEA, Département Médicaments et Technologies pour la Santé, SIMoS ; ² EMR CNRS 9004, F-91191 Gif sur Yvette, France.

*corresponding author's email: romulo.araoz@cea.fr

Abstract

Cyclic imine toxins produced by marine dinoflagellate species move up fast the food chain through shellfish and constitute a potential threat for marine wildlife and public health because of their potent antagonistic activity against nicotinic acetylcholine receptors of muscle and neuronal types. Although not regulated, the lethality of 13-desmethyl spirolide-C does compare the lethality of saxitoxin in mouse bioassay. Besides, cyclic imine toxins are often found in shellfish destined for human consumption. Herein, the unveiling of the mode of action of cyclic imine toxins is reviewed. To illustrate the review, the electrophysiological characterization of the antagonistic capacity of 20-methyl spirolide-G on rat $\alpha 3\beta 2$ nicotinic acetylcholine receptor is described.

Keywords: Cyclic imine toxins, nicotinic acetylcholine receptors, 20-methyl spirolide-G, two-electrodes voltage clamp electrophysiology (TEVC), *Xenopus laevis* oocytes

<https://doi.org/10.5281/zenodo.7035152>



Introduction

Cyclic imines toxins (CiTXs; ~44 members) are marine emergent neurotoxins worldwide distributed among coastal environments. Of dinoflagellate origin, CiTXs move up fast the food chain through shellfish and may constitute a potential threat for public health (Aráoz *et al.*, 2020). CiTXs are potent antagonists of nicotinic acetylcholine receptors (nAChRs). They display a cyclic imine in their structure necessary for interacting with nAChRs (Bourne *et al.*, 2010). Portimines (A-B) produced by *Vulcanodinium rugosum*, display a 5-membered imine ring (Selwood *et al.*, 2013). The following CiTXs display a 6-membered cyclic imine ring: gymnodimines (GYM) (seven congeners), that are produced by *Karenia selliformis* and *Alexandrium peruvianum* (Seki *et al.*, 1995; Van Wagoner *et al.*, 2011), prorocentrolides (six members) produced by *Prorocentrum lima* (Torigoe *et al.*, 1988), spiroprorocentrimine produced by *Prorocentrum* sp. (Lu *et al.*, 2001), and kabirimine produced by *V. rugosum* (Hermawan *et al.*, 2019). Spirolides (SPX) (16 members) produced by *A. ostenfeldii*, reviewed by Gueret and Brimble, 2010, pinnatoxins (PnTX) (A-H) produced by *V. rugosum* (Rhodes *et al.*, 2010) and pteriatoxins (PtTX) (A-C) display a 7-membered cyclic imine ring (Takada *et al.*, 2001).

Mode of action (MOA) of CiTXs

MOA of CiTXs from mouse assay experiments

CiTXs are fast-acting neurotoxic compounds that kill mice by respiratory arrest within minutes after intraperitoneal injection or gavage at lethal toxin doses. The clinical signs preceding mice death induced by CiTXs

were similar to those evoked by curare: the administration of neostigmine, a reversible acetylcholinesterase inhibitor, increases the concentration of acetylcholine (ACh) at the neuromuscular synapse, competitively displacing curare from muscle nAChRs (Leeuwijn *et al.*, 1981). Thus, the administration of two times the LD₅₀ of GYM-A killed all the mice in 3-7 min. However, neostigmine pre-treated rodents survived GYM-A administration at the referred dose (Munday *et al.*, 2012). This was a strong indication that muscle-type nAChR may be a molecular target of GYM-A.

Another key event was the discovery of keto-amine derivatives of SPX-A and -B, namely SPX-E and -F, in the digestive glands of scallops. The cyclic imine rings in SPX-E and -F were open and showed no activity by mouse assay. The hydrolysis of the cyclic imine ring of SPX-A and -B was associated with the presence of one methyl group on the cyclic imine ring. Thus, SPX-C, 13-desmethyl SPX-C and SPX-D were resistant to oxalic acid hydrolysis suggesting that the double methylation of the spiroimine ring confers a better chemical stability to spiroptides (Hu *et al.*, 2001). SPXs (excluding SPX-A and B), PnTXs and PtTXs, have a double methylated cyclic imine ring, reviewed by Gueret and Brimble (2010) and Stivala *et al.* (2015). Further, the amino-keto PnTX-A analogue, bearing an open form of the imine ring, was inactive on muscle and neuronal nAChRs when tested by electrophysiology, confirming that the cyclic imine is critical for CiTX interaction with nAChR (Aráoz *et al.*, 2011).



MOA of CiTXs from electrophysiological research

Electrophysiological recordings using *ex vivo* neuromuscular preparations confirmed that cyclic imine toxins act on nAChRs, reviewed by Molgó *et al.* (2017). Thus, GYM-A produced a concentration- and time-dependent block of twitch responses evoked by nerve stimulation without affecting elicited muscle twitches in isolated mouse phrenic-hemidiaphragm preparations. This suggested that GYM-A blocked muscle nAChR. The reduction of the amplitude of miniature-endsplate resulting from quantal ACh-release and subsequent activation of post-synaptic nAChR, confirmed the blockade of muscle-nAChR by GYM-A (Kharrat *et al.*, 2008). Similar effects on the neuromuscular junction were obtained for 13,19-desmethyl SPX-C and 13-didesmethyl SPX-C (Aráoz *et al.*, 2015; Bourne *et al.*, 2010), 20-methyl SPX-G (Couesnon *et al.*, 2016), PnTX -A, -E, -F and -G (Aráoz *et al.*, 2011; Hellyer *et al.*, 2011), and procontrolide-A (Amar *et al.*, 2018). These findings are consistent with *in vivo* electrophysiological recordings in sedated mice showing that a local injection of PnTX-A or PnTX-G induced the blockade of the maximal compound muscle action potential amplitude, evoked by nerve stimulation (Benoit *et al.*, 2019).

In vitro two-electrodes voltage clamp (TEVC) recordings to determine the mode of action of CiTXs were performed on *Xenopus laevis* oocytes which is a successful electrophysiological model for heterologous *de novo* expression of human ion channels and receptors and for the transplantation of membranes rich in receptors and ion channels for pharmacological studies (Miledi *et al.*, 2004). Binding of ACh to the ligand-

binding sites rapidly (microseconds) shifts the receptor conformation from the resting (closed state) to the open state, initiating the ion flux through the cation-selective pore for ~2 milliseconds, and the receptor channel closes (desensitized state) (Giniatullin *et al.*, 2005). The perfusion of GYM-A, 13-desmethyl SPX-C, 13-19-didesmethyl SPX-C, 20-methyl SPX-G, PnTX-A, -E, -F, and -G or procontrolide does not evoke inward currents on muscle and neuronal nAChRs regardless of subtype composition or toxin concentration. When these CiTXs are co-applied with ACh, the ACh-elicited currents are inhibited in a concentration-dependent manner. The inhibition degree is dependent on the nAChR subtype and on the CiTX tested. The blockade of muscle and neuronal receptors is not voltage-dependent. Indeed, CiTXs are competitive antagonists of muscle and neuronal nAChRs with broad subtype selectivity and high potency. Spirolides showed sub-nanomolar affinities for *Torpedo* ($\alpha 1$)₂ $\beta 1\gamma\delta$ nAChR (Aráoz *et al.*, 2015), while the affinities of GYM-A and PnTX-A and -G were in the nanomolar range (Aráoz *et al.*, 2011; Kharrat *et al.*, 2008). The affinities of the studied CiTXs for human $h\alpha 4\beta 2$ nAChRs are in the nanomolar range (Stivala *et al.*, 2015). Except for PnTX-G, GYM-A, 13-desmethyl SPX-C, 13-19 didesmethyl SPX-C, 20-methyl SPX-G and PnTX-A showed picomolar affinities for $h\alpha 7$ nAChR (Bourne *et al.*, 2015). Portimine-A and procontrolide-A were less active on muscle and neuronal nAChR (Amar *et al.*, 2018; Lamoise *et al.*, 2017). PnTX-A shows the best selectivity profile: the affinity of PnTX-A for $\alpha 7$ nAChR is 50-times higher than its affinity for *Torpedo* ($\alpha 1$)₂ $\beta 1\gamma\delta$ nAChR, and 300-times higher than its affinity for $\alpha 4\beta 2$ nAChR (Aráoz *et al.*, 2011).



CiTXs' target: nicotinic acetylcholine receptor

nAChRs are allosteric transmembrane pentameric proteins belonging to the cysteine-loop ligand-gated ion channel superfamily. Muscle nAChR ensures fast neurotransmission at the neuromuscular junction that is essential for respiration and muscle contraction for daily life, mobility, or escape from predation (Albuquerque *et al.*, 2009). At the central nervous system (CNS), neuronal nAChRs modulate neurotransmitters release, hence participating in fundamental aspects of synaptic plasticity involved in attention, learning, memory, and neurodegenerative disorders. Non-neuronal nAChRs are ubiquitously expressed in the human body from epithelial cells, to primary immune organs such as the bone marrow, thymus and macrophages (Bertrand *et al.*,

2015). Human genomic studies revealed 16 homologous genes coding for nAChR-subunits. The presence of the Cys-pair characterizes α subunits ($\alpha 1$ - $\alpha 10$), and its absence characterize $\beta 1$ - $\beta 4$, γ , δ and ϵ subunits. Muscle-nAChRs can be fetal ($\alpha 1$)₂ $\beta 1\gamma\delta$ or adult ($\alpha 1$)₂ $\beta 1\gamma\epsilon$. Neuronal nAChRs show more variability resulting from the combination of $\alpha 2$ - $\alpha 7$ with $\beta 2$ - $\beta 4$ subunits. The $\alpha 7$ and $\alpha 9$ form monomeric receptors, and $\alpha 8$ subunit was found only in avian tissues. The heteropentameric $\alpha 7\beta 2$ and $\alpha 9\alpha 10$ nAChRs were found in the CNS (Bertrand *et al.*, 2015). Different receptor configurations display distinct pharmacological profiles and receptor distribution patterns across the brain.

MOA of CiTXs from crystallographic studies
GYM-A & 13-desmethyl SPX-C, and PnTX-A & PnTX-G were co-crystalized with the ACh-binding

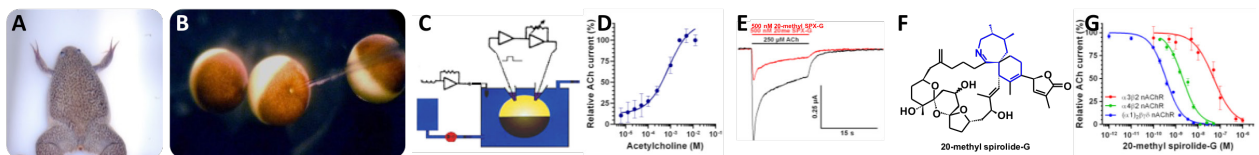


Fig. 1. MOA of 20-methyl SPX-G on $\alpha 3\beta 2$ nAChR. (A) *Xenopus laevis* frog. (B) *Xenopus* oocyte microinjected with mRNA. (C) Schema of TEVC: a *Xenopus* oocyte is impaled with two electrodes. ACh-evoked currents are recorded at a holding potential of -60 mV. (D) ACh dose-response curve on oocytes expressing $\alpha 3\beta 2$ nAChR. (E) Electrophysiological recordings showing ACh-current (black) and the antagonistic effect of 500 nM 20-methyl SPX-G (red). (F) 20-methyl SPX-G. (G) Concentration-dependent inhibition of ACh-evoked currents by 20-methyl SPX-G in *Xenopus* oocytes having incorporated *Torpedo*-($\alpha 1$)₂ $\beta \gamma \delta$ nAChR (blue), or expressing the *ha4* $\beta 2$ (green) (Couesnon *et al.*, 2016), and the $\alpha 3\beta 2$ (red; this work). Amplitudes of the ACh-current peak (mean \pm SEM; 5 oocytes per concentration), were normalized to control currents and fitted to the Hill equation.



protein from *Lymnaea stagnalis* and *Aplysia californica* to define the structural determinants responsible for their with the orthosteric site of $ha7$ nAChR, (Bourne *et al.*, 2010; 2015). These proteins are structural surrogates of the extracellular ligand-binding domain of $ha7$ nAChR. Overall, the co-crystallized CiTXs share a similar binding mode where the conserved loop C envelops the bound toxins buried at the binding interface with high surface complementary. The protonated imine nitrogen of the six- or seven-membered cyclic imines is positioned to hydrogen bond to the backbone carbonyl oxygen of loop C Trp147, a key residue for agonists and antagonists binding. The bis-spiroketal substituent of PnTX-A and PnTX-G binds between the loop C and the complementary side of the subunit interface, as observed for 13-desmethyl SPX-C and for the tetrahydrofuran group of GYM-A. The cyclohexene-butyrolactone of 13-desmethyl SPX-C interacts with Y188 and K143, while in the case of GYM-A, it interacts with Y188 and Q186. In the case of the two latter toxins, very limited interaction is observed with the sequence-variable loop F. On the contrary, the bridged ketal ring specific to PnTXs extends out of the binding pocket underneath loop C to interact with loop F on the negative side of the interface. Specific interactions between the charged carboxylate group of PnTX-A and the vinyl group of PnTX-G, may explain the selectivity towards $ha7$ and *Torpedo*-($\alpha 1$) $_2\beta 1\gamma\delta$ nAChRs (Bourne *et al.*, 2015).

20-methyl SPX-G antagonizes rat $\alpha 3\beta 2$ nAChR

The $\alpha 3$ nAChR subunit was the first to be cloned and the $\alpha 3\beta 2$ nAChR subtype was among the first subtypes to be heterologously expressed in *X. laevis* oocytes for electrophysiology

(Boulter *et al.*, 1987). $\alpha 3\beta 2$ nAChR is expressed in the CNS, the spinal cord and the heart, and as presynaptic receptor in the neuromuscular junction (Young *et al.*, 2008; Fagerlund and Eriksson, 2009). The MOA of 20-methyl SPX-G (CIFGA, Spain) on $\alpha 3\beta 2$ nAChRs determined by TEVC is here shown.

The mRNAs coding for the rat $\alpha 3$ and $\beta 2$ nAChR subtypes were synthesized from the plasmids PKN $\Omega\alpha 3$ and PKN $\Omega\beta 2$ kindly provided by Annette Nicke (LMU, Munich, Germany), and injected into *X. laevis* oocytes (Fig. 1A-B). TEVC electrophysiology was performed as described in (Ar oz *et al.*, 2011) (Fig. 1C). The dose-response curve for ACh gave an EC_{50} of 250 μM ($nH = 0.945 \pm 0.15$; Fig. 1D). The perfusion of 250 μM ACh induced a rapid opening of the $\alpha 3\beta 2$ nAChR's channel (microseconds) followed by a two-phase desensitization pattern: a very fast (milliseconds) after the peak amplitude was reached and a slow desensitization phase (Fig. 1E). The perfusion of a mix containing 250 μM ACh and 20-methyl SPX-G (Figs. 1E, F) at a given concentration in the range of 100 pM – 1 μM induced a competitive blockade of the ACh-evoked currents with an IC_{50} of 50.9 nM ($nH = -0.98 \pm 0.14$ Fig. 1E, 1G), without affecting the desensitization pattern of the receptor. 20-methyl SPX-G is not an agonist of $\alpha 3\beta 2$ nAChR.

20-methyl SPX-G showed picomolar affinities for *Torpedo*-($\alpha 1$) $_2\beta 1\gamma\delta$ nAChR ($IC_{50} = 360$ pM) and for $ha7$ nAChR ($IC_{50} = 480$ pM). Its affinity for the neuronal $ha4\beta 2$ nAChR was 2.1 nM (Fig. 1G) while for rat $\alpha 3\beta 2$ nAChR was 50.9 nM. Unlike *Torpedo*-($\alpha 1$) $_2\beta 1\gamma\delta$ and $ha7$ subtypes, the $\beta 2$ containing $\alpha 4\beta 2$ and $\alpha 3\beta 2$ nAChRs are resistant to α -bungarotoxin, but sensitive to kappa-



bungarotoxin (Boulter *et al.*, 1987). Molecular docking to predict the structural determinants within $h\alpha 3\beta 2$ nAChR and 20-methyl SPX-G were performed (Couesnon *et al.*, 2016). Key amino acids explaining the antagonism of 20-methyl SPX-G towards $h\alpha 3\beta 2$ and $h\alpha 4\beta 2$ nAChRs are conserved in the orthosteric site. The lower affinity of both nAChR subtypes for 20-methyl SPX-G relies on the bulky K77 which provokes steric clashes displacing the spiroketal moiety of the toxin to the $\beta 2$ subunit (Couesnon *et al.*, 2016). Further, the butyrolactone of 20-methyl SPX-G hydrogen bond with R186 of $h\alpha 4\beta 2$ nAChR while it hydrogen bond with K143 of $r\alpha 3\beta 2$ nAChR.

Acknowledgements. We acknowledge the funding from Labex Lermite (Detectneurotox CDE2017-001173-RD91 to RA), NRBC-E (Multitox H35 to RA) and Interreg Atlantic Area (Alertoxnet EAPA_317/2016).

References

Albuquerque, E.X., Pereira, E.F.R., Alkondon, M., Rogers S.W. (2009). *Physiol. Rev.* 89, 73-120.

Amar, M., Araoz, R., Iorga, B.I., *et al.*, (2018). *Toxins (Basel)* 10, 97.

Araoz, R., Barnes, P., Sechet, V., *et al.*, (2020). *Harmful Algae* 98, 101887.

Araoz, R., Ouanounou, G., Iorga, B. I., *et al.*, (2015). *Toxicol Sci.* 147, 156-167.

Araoz, R., Servent, D., Molgó, J., *et al.*, (2011). *J. Am. Chem. Soc.* 133, 10499-10511.

Benoit, E., Couesnon, A., Lindovsky, J., *et al.*, (2019). *Mar. Drugs* 17, Article 306.

Bertrand, D., Lee, C. H., Flood, D., *et al.*, (2015). *Pharmacol. Rev.* 67, 1025-1073.

Boulter, J., Connolly, J., Deneris, E., *et al.*, (1987). *Proc. Natl. Acad. Sci. U.S.A.*, 84, 7763-7767.

Bourne, Y., Radic, Z., Araoz, R., *et al.*, (2010). *Proc. Natl. Acad. Sci. U.S.A.* 107, 6076-6081.

Bourne, Y., Sulzenbacher, G., Radic, Z., *et al.*, (2015). *Structure* 23, 1106-1115.

Couesnon, A., Araoz, R., Iorga, B.I., *et al.*, (2016). *Toxins (Basel)* 8, 249.

Fagerlund, M. J. and Eriksson, L. I. (2009). *Bri. J. Anaesth.* 103, 108-114.

Giniatullin, R., Nistri, A., Yakel, J.L. (2005). *Trends Neurosci.* 28, 371-378.

Gueret, S. M. and Brimble, M. A. (2010). *Nat. Prod. Rep.* 27, 1350-1366.

Hellyer, S.D., Selwood, A. I., Rhodes, L., Kerr, D. S. (2011). *Toxicon* 58, 693-699.

Hermawan, I., Higa, M., Hutabarat, P.U.B., *et al.*, (2019). *Mar. Drugs* 17, Article 353.

Hu, T.M., Burton, I.W., Cembella, A.D., *et al.*, (2001). *J. Nat. Prod.* 64, 308-312.

Kharrat, R., Servent, D., Girard, E., *et al.*, (2008). *J. Neurochem.* 107, 952-963.

Lamoise, C., Gaudin, A., Hess, P., *et al.*, (2017). In: Proenza, L. and Hallegraeff, G.M. (Eds). *Proc. 17th ICHA, Florianopolis, Brazil* 126-129.



Leeuwin, R. S., Veldsemacurrie, R. D., Vanwilgenburg, H., *et al.*, (1981). *Eur. J. Pharmacol.* 69, 165-173.

Lu, C.K., Lee, G.H., Huang, R., Chou, H.N. (2001). *Tetrahedron Lett.* 42, 1713-1716.

Miledi, R., Duenas, Z., Martinez, A., *et al.*, (2004). *Proc. Natl. Acad. Sci. U.S.A.* 101, 1760-1763.

Molgó, J., Marchot, P., Aráoz, R., *et al.*, (2017). *J. Neurochem.* 142, 41-51.

Munday, R., Selwood, A.I., Rhodes, L. (2012). *Toxicon* 60, 995-999.

Rhodes, L., Smith, K., Selwood, A. *et al.*, (2010). *Harmful Algae* 9, 384-389.

Seki, T., Satake, M., Mackenzie, L., *et al.*, (1995). *Tetrahedron Lett.* 36, 7093-7096.

Selwood, A. I., Wilkins, A. L., Munday, R., *et al.*, (2013). *Tetrahedron Lett.* 54, 4705-4707.

Stivala, C.E., Benoit, E., Aráoz, R., *et al.*, (2015). *Nat. Prod. Rep.* 32, 411-435.

Takada, N., Umemura, N., Suenaga, K., Uemura, D. (2001). *Tetrahedron Lett.* 42, 3495-3497.

Torigoe, K., Murata, M., Yasumoto, T., Iwashita, T. (1988). *J.A.C.S.* 110, 7876-7877.

Van Wagoner, R.M., Misner, I., Tomas, C.R., *et al.*, (2011). *Tetrahedron Lett.* 52, 4243-4246.

Young, T., Wittenauer, S., McIntosh, J.M., *et al.*, (2008). *Brain Res.* 1229, 118-124.





NOVEL HAB TECHNOLOGIES



A decade of domoic acid in Monterey Bay -SPATT observations give new insight on toxin variability

Aubrey Trapp*, Kendra Hayashi, Raphael M. Kudela

Department of Ocean Sciences, University of California Santa Cruz, Santa Cruz, U.S.A.

**corresponding author's email: ajtrapp@ucsc.edu*

Abstract

The risk of amnesic shellfish poisoning from *Pseudo-nitzschia* sp. blooms and subsequent domoic acid events has persisted in Monterey Bay on the central California coast for nearly three decades. Over this time, HAB monitoring has experienced rapid advancement in methods and technologies designed to predict toxic blooms and mitigate losses. One such innovation, solid phase adsorption toxin tracking (SPATT), is now widely applied for passive sampling of dissolved toxins, often complementing toxin quantification from shellfish and direct measurements from seawater. Here we show 10 years (2010 - 2020) of domoic acid measured by SPATT in Monterey Bay and investigate trends in relation to key environmental factors. Of the three SPATT resins deployed (HP-20, SP-207, and SP-700) results indicate subtle differences that may affect how well domoic acid from SPATT resembles toxin accumulation in shellfish. In recent years, SPATT samples contained higher levels of domoic acid than might be expected by direct analysis of seawater and extractions from mussels. Analysis of monitoring data from the Santa Cruz Wharf repository revealed complex relationships between passive sampling, cell counts, and direct analysis from seawater, though there was a negative correlation between all toxin parameters and nutrient concentrations. To our knowledge, this is the longest dataset for detecting domoic acid by SPATT. Continued analysis may give insight on future trends and greater understanding of the environmental drivers of dissolved marine biotoxins in Monterey Bay.

Keywords: SPATT, domoic acid, dissolved toxins, harmful algae monitoring

<https://doi.org/10.5281/zenodo.7035160>



Introduction

Monterey Bay, on the central California coast, hosts high productivity and biodiversity. Since 2009, observations from solid phase adsorption toxin tracking (SPATT) have supplemented direct monitoring of domoic acid (DA) at the Santa Cruz Wharf (SCW). The present study revisits an approximately weekly SPATT sampling effort first presented in Lane *et al.* (2010) a neurotoxin produced by some species of the diatom *Pseudo-nitzschia*, can remain undetected in sentinel shellfish stocks during toxic blooms and subsequent marine bird and mammal mass mortality events. Solid Phase Adsorption Toxin Tracking (SPATT) and evaluates relationships between domoic acid observations and key environmental factors. SPATT developed as a passive sampling method for monitoring algal biotoxins and is now widely deployed to monitor a suite of marine and freshwater toxins (MacKenzie *et al.*, 2004; MacKenzie, 2010; Roué *et al.*, 2018) including the low polarity lipophilic compounds such as the pectenotoxins and the okadaic acid complex toxins, are dissolved in the seawater. The results of field trials during *Dinophysis acuminata* and *Protoceratium reticulatum* blooms are presented. These data prove the concept and demonstrate that the technique provides a means of forecasting shellfish contamination events and predicting the net accumulation of polyether toxins by mussels. As an early warning method it has many advantages over current monitoring techniques such as shellfish-flesh testing and phytoplankton monitoring. In contrast to the circumstantial evidence provided by genetic probe technologies and conventional phytoplankton monitoring methods, it directly targets the toxic compounds of interest. The

extracts that are obtained for analysis lack many of the extraneous lipophilic materials in crude shellfish extracts so that many of the matrix problems associated with chemical and biological analysis of these extracts are eliminated. Analyses can confidently target parent compounds only, because analytical and toxicological uncertainties associated with the multiplicity of toxin analogues produced by *in vivo* biotransformation in shellfish tissues are reduced. Time integrated sampling provides a good simulation of biotoxin accumulation in filter feeders and the high sensitivity provides lengthy early warning and conservative estimates of contamination potential. The technique may reduce monitoring costs and provide improved spatial and temporal sampling opportunities. When coupled with appropriate analytical techniques (e.g. LC-MS/MS multi-toxin screens, ELISA assays, receptor binding assays). While passive sampling by SPATT has several advantages over other HAB monitoring methods, including avoiding complications from cell counts and shellfish extractions, its effectiveness for predicting future toxin events in shellfish has shown mixed results (Roué *et al.*, 2018). Here we use a long-term dataset with strong spatial and temporal resolution to compare SPATT observations with direct analysis of domoic acid and *Pseudo-nitzschia* sp. cell counts.

Materials and Methods

Data acquisition

SPATT ring construction and extraction is detailed in Lane *et al.* (2010). Three different SPATT resins are included for comparison of adsorption performance. Environmental



and toxin data was downloaded from CalHABMAP - Santa Cruz Wharf HAB repository (ERDDAP, 2022). Methods for discrete water sampling and analysis are provided in Schulien *et al.* (2017).

Statistics and analysis

Monitoring data included 13 variables with weekly sampling resolution starting the week of December 25th, 2009. SPATT rings were deployed approximately 1 m below mean lower low water level at the Santa Cruz Wharf for two to 29 days with a median and mode of 7 days. SPATT samplers were attached to a weighted rope. Toxin observations were paired with the middle date of each deployment to align multiple variables. A Kolmogorov-Smirnoff test was used to compare the shape of each SPATT timeseries and Spearman's R was used in correlation analyses (R Core Team, 2017).

For comparing multiple variables, time series were linearly interpolated across missing sample dates using weekly mean values, which resulted in a final dataset of 533 consecutive observations. The data were normalized so that each of the 13 variables had mean 0 and variance 1 prior to principal component analysis (PCA) with the factoextra package (Kassambara and Mundt, 2020). The first four principal components were retained as significant based on evaluating the scree plot for eigenvalues greater than one.

Results and Discussion

Domoic acid in SCW sentinel mussels surpassed the regulatory threshold of 20 ppm on at least one occasion annually in five out of 10 years included in the study period. Years 2014 and 2015 had notably high concentrations of

domoic acid resulting from a northeast Pacific warm anomaly (Ryan *et al.*, 2017) during a prolonged oceanic warm anomaly. Caused by diatoms of the genus *Pseudo-nitzschia*, this HAB produced the highest particulate concentrations of the biotoxin domoic acid (DA). Domoic acid spikes in sentinel mussels generally correspond to increases in all other toxin variables (Fig. 1). Two exceptions stand out. First, dissolved domoic acid in 2012 and 2020 did not increase in concert with other variables. Second, observations from SPATT in recent years show relatively high adsorbed domoic acid levels compared to other variables.

Different SPATT resins have different adsorption and extraction efficiencies (Kudela, 2017). In this dataset, domoic acid values from resins HP-20, SP-207, SP-700 were well correlated and statistically different by pairwise Kolmogorov-Smirnov tests (Table 1). Deploying multiple resins can capture different modes of dissolved toxin in the environment. For example, HP-20 has a high percent recovery and is best used to determine background domoic acid over long deployment times. In contrast, resins SP-207 and SP-700 have lower percent recovery, but respond more quickly to episodic toxin events and detect higher concentrations of domoic acid (Kudela, 2017).

The 2014-2015 bloom exhibits this pattern with SP-207 and SP-700 showing higher DA levels than HP-20 (Fig. 1). Overall, resins HP-20 and SP-700 had the best agreement, and resin SP-207 had the best correlation to non-SPATT variables including direct analysis of seawater, sentinel mussels, and cell counts. All three resins were auto-correlated over approximately two months. Resins SP-700



and HP-20 also showed an annual cycle with autocorrelation increasing approximately 52, 104, and 156 weeks after the first sample date.

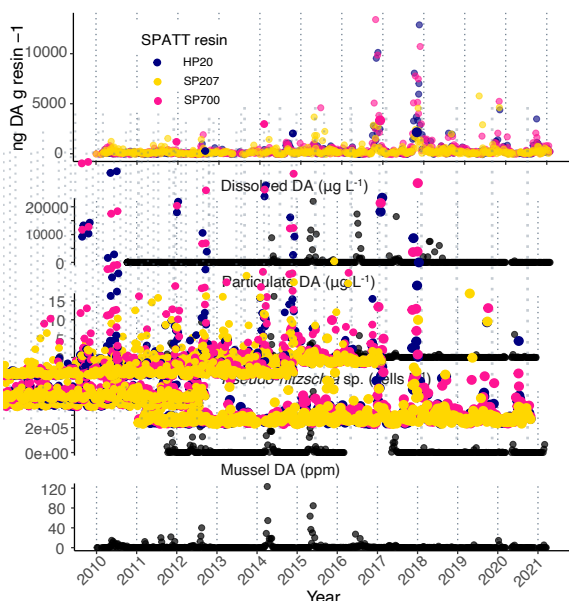


Fig. 1. Ten-year time series of domoic acid variables measured approximately weekly from the Santa Cruz Wharf. (Top) SPATT resin indicated by color. Cell counts for *Pseudo-nitzschia* sp. were unavailable from March, 2016 to May, 2017.

Table 1. Summary statistics for comparing SPATT resins. Spearman's R used for correlation coefficients.

Resin pair	K-S test p-value	Spearman R ($p < 0.05$)
HP-20/SP-700	0.0010	0.75
HP-20/SP-207	0.0003	0.58
SP-207/SP-700	0.0117	0.69

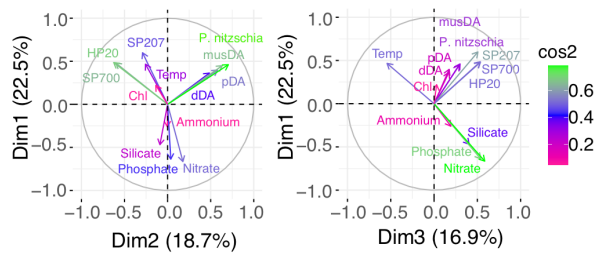
The variability of domoic acid from different sampling methods was explored in broader context by principal component

analysis of 13 variables (Fig. 2). The first two dimensions explain about 41.2% of the variance, and three main clusters emerge 1) SPATT resins and temperature, 2) other toxin variables (*Pseudo-nitzschia* sp. cell counts, dissolved and particulate DA, and DA from sentinel mussels), and 3) nutrient variables (nitrate, phosphate, silicate, and ammonium). In this model, domoic acid from SPATT is not correlated to domoic acid measured by other methods. Resin SP-207 is offset from the close correlation of HP-20 and SP-700 towards the other toxin variables, indicating that results from SP-207 more closely follow direct sampling methods. Negative correlation with nutrient concentrations likely drives the relationship across dimension 1 (Dim 1).

This relationship is also apparent comparing the first and third dimensions. Including dimension 3 explains an additional 16.9% of variance, and SPATT clusters more closely with the other toxin variables. Dimension 2 is most likely influenced by changes over time. Temperature and DA from SPATT show a significant increase over 10 years ($p \ll 0.05$), while domoic acid from direct measurements, cell counts and sentinel mussels peaked mid-decade. Dimension 3 has a negative correlation to temperature, and dimension 4 is strongly influenced by ammonium and chlorophyll. Ammonium and chlorophyll only make a small contribution to the first three dimensions.

SPATT observations of domoic acid at SCW did not show clear links with other HAB and environmental variables over the 10 years. Time series analysis and PCA suggest that SPATT may be more sensitive at detecting dissolved DA than direct measurements, especially in recent years that show





Variable	Dim 1	Dim 2	Dim 3	Dim 4
Ammonium	-0.261	-0.003	0.194	0.771
Silicate	-0.469	-0.089	0.405	-0.255
Phosphate	-0.637	0.037	0.539	-0.008
Nitrate	-0.665	0.178	0.585	0.011
dDA	0.363	0.486	0.172	0.266
pDA	0.398	0.580	0.175	-0.103
musDA	0.448	0.633	0.291	0.010
<i>P. nitzschia</i>	0.460	0.705	0.301	-0.075
SP207	0.599	-0.291	0.506	0.095
SP700	0.480	-0.601	0.535	0.043
HP20	0.485	-0.626	0.534	0.033
Temp	0.466	-0.257	-0.543	0.231
Chl	0.220	-0.137	0.030	-0.653

Fig. 2. (Top) Principal component loading plot of 13 variables measured weekly at SCW. Quality of representation (Cos^2) by each dimension denoted by color and arrow length. (Bottom) Coordinates for first four dimensions.

increasing domoic acid from SPATT. The high sensitivity of SPATT and tendency towards ‘false positive’ results for toxic shellfish has been discussed in other studies as well (Fux *et al.*, 2009; Lane *et al.*, 2010; Pizarro *et al.*, 2013) a neurotoxin produced by some species of the diatom *Pseudo-nitzschia*, can remain undetected in sentinel shellfish stocks during toxic blooms and subsequent marine bird and mammal mass mortality events. Solid Phase Adsorption Toxin Tracking (SPATT. As a passive sampling device, SPATT is

analogous to an average value for dissolved toxin over the last three to seven days. Direct measurements of DA and cell counts are point samples. The offset in sampling timescale could be responsible for differences between the two variable clusters. In addition, SPATT works to concentrate dissolved DA from large volumes of water, which likely contributes to its increased sensitivity relative to point samples. The semi-quantitative nature of SPATT is another challenge in comparing passive samplers and direct measurements, since toxins extracted from SPATT are tied to resin mass and not the true dissolved concentration (Kudela, 2011). Although we were not able to elucidate environmental drivers of SPATT domoic acid in this dataset, results suggest ambient domoic acid levels in Monterey Bay are higher than expected based on direct analysis alone. For this reason, SPATT appears to be a valuable component of biotoxin monitoring, detecting toxins that evade direct sampling methods either through sensitivity and/or time-scale effects.

While there is strong evidence that consuming low-levels of domoic acid has detrimental health effects for marine mammals, birds, and humans, understanding of the effects from chronic exposure to dissolved domoic acid is less developed (Work *et al.*, 1993; Moriarty *et al.*, 2021; Petroff *et al.*, 2021) the causative agent for the human syndrome Amnesic Shellfish Poisoning (ASP. The function of SPATT as an environmental indicator has benefits over direct sampling methods for evaluating ecosystem impacts of dissolved toxins. Results from Bargu *et al.* (2006) showed that dissolved domoic acid significantly reduced the ingestion rate of krill feeding on nontoxic *Pseudo-nitzschia* spp. in lab trials. The study used dissolved



DA concentrations up to 1,000 $\mu\text{g L}^{-1}$, much higher than measured environmental levels at the time but within range of values seen during HAB events from 2014 to 2018. Future work that focuses on the ecosystem effects of persistent dissolved toxins may help advance the impact of SPATT for applied biotoxin monitoring. Finally, this study shows the importance of rigorous, quantitative assessment of domoic acid in Monterey Bay and supports implementation of innovative monitoring methods.

Acknowledgements. Funding was provided by the NOAA Monitoring and Event Response for Harmful Algal Blooms (MERHAB) Award NA04NOS4780239 (Cal-PreEMPT), NOAA Ecology and Oceanography of Harmful Algal Blooms (ECOHAB Grant No. NA11NOS4780030), and NOAA IOOS Award NA16NOS0120021 to the Central and Northern California Ocean Observing System (CeNCOOS). Support for ICHA 2021 registration fees was generously provided by NOAA National Centers for Coastal Ocean Science (NCCOS). We would also like to give special recognition to members of the Kudela Lab for sampling work and helpful feedback throughout the project.

References

Bargu, S., Lefebvre, K., Silver, M. W. (2006). *Mar. Ecol. Prog. Ser.* 312, 169-175.

ERDDAP (2022). Dataset ID: HABs-SantaCruzWharf. [//erddap.sccoos.org/erddap/tabledap/HABs-SantaCruzWharf.html](https://erddap.sccoos.org/erddap/tabledap/HABs-SantaCruzWharf.html)

Fux, E., Bire, R., Hess, P. (2009). *Harmful Algae* 8, 523-537.

Kassambara, A. and Mund, F. (2020). *factoextra: Extract and Visualize the Results of Multivariate Data Analysis*. [//www.sthda.com/english/rpkgs/factoextra](http://www.sthda.com/english/rpkgs/factoextra)

Kudela, R. M. (2011). *Harmful Algae* 11, 117-125.

Kudela, R. M. (2017). *Compr. Anal. Chem.* 78, 379-404.

Lane, J.Q., Roddam, C.M., Langlois, G.W., Kudela, R.M. (2010). *Limnol. Oceanogr. Meth.* 8, 645-660.

MacKenzie, L. A. (2010). *Curr. Opin. Biotechnol.* 21, 326–331.

MacKenzie, L., Beuzenberg, V., Holland, P., McNabb, P., Selwood, A. (2004). *Toxicon* 44, 901-918.

Moriarty, M. E., Tinker, M. T., Miller, M. A., Tomoleoni, J. A., *et al.*, (2021). *Harmful Algae* 102, 101973.

Petroff, R., Hendrix, A., Shum, S., Grant, K. S., *et al.*, (2021). *Pharmacol. Ther.* 227, 107865.

Pizarro, G., Moroño, Á., Paz, B., Franco, J. M., *et al.*, (2013). *Mar. Drugs* 11, 3823-3845.

R Core Team (2017). [//www.R-project.org/](http://www.R-project.org/).

Roué, M., Darius, H. T., Chinain, M. (2018). *Toxins* 10, 1-28.

Ryan, J. P., Kudela, R. M., Birch, J. M., Blum, M., *et al.*, (2017). *Geophys. Res. Lett.* 44, 5571-5579.

Schulien, J. A., Peacock, M. B., Hayashi, K.,



Raimondi, P., Kudela, R. M. (2017). Mar. Ecol. Prog. Ser. 572, 43-56.

Work, T. M., Barr, B., Beale, A. M., Fritz, L., *et al.*, (1993). J. Zoo Wildl. Med. 24, 54-62.



Development and comparison of Imaging FlowCytobot classifiers in coastal California

Anna McGaraghan*, Kendra Hayashi, Patrick Daniel, Raphael M. Kudela

University of California at Santa Cruz, U.S.A.

* corresponding authors email: annamcg@ucsc.edu

Abstract

The Imaging FlowCytobot (IFCB) is emerging as a valuable new tool in phytoplankton ecology and HAB monitoring. Initial development of classifiers is time-consuming and labor intensive, requiring trained taxonomists with knowledge of local phytoplankton. However, after development and testing of a classifier for image identification, an IFCB provides round-the-clock, real-time observation of the phytoplankton community in its deployment location. In this study, IFCBs were deployed at Pier 17 in the San Francisco Bay, and at the Santa Cruz Wharf in Monterey Bay. We investigate how the performance of the classifiers developed in these specific locations compare to one developed in the Gulf of Mexico for identifying common California HAB-forming taxa, including *Pseudo-nitzschia* spp., *Alexandrium* spp., and *Dinophysis* spp. Additionally, data collected from side-by-side IFCB deployments at the Santa Cruz Wharf were used to compare the performance of the instruments to one another. This allowed us to determine how well images from two different instruments represent the phytoplankton community at a single site, and evaluate whether a classifier is inherently tied to the instrument used to build it. Additionally, image classification methodologies were compared and here we present the results of a convolutional neural network (CNN) as an alternative to well-described supervised learning methods. This work provides valuable insight into the development of a HAB-monitoring network of IFCBs along the California coast.

Keywords: harmful algae monitoring, phytoplankton, Imaging FlowCytobot, machine learning, convolutional neural network, image classifier

<https://doi.org/10.5281/zenodo.7036182>



Introduction

Phytoplankton play a vital role in the marine environment, and serve as indicators of ocean health. However, many species of phytoplankton produce potent toxins that can negatively impact marine life and human health. As the phytoplankton community shifts and changes regularly and rapidly in both time and space, close monitoring of phytoplankton genera is necessary. In coastal California, harmful algal bloom-producing (HAB) genera monitored by the California Department of Public Health and/or California Harmful Algal Bloom Monitoring and Alert Program (HABMAP) are *Akashiwo*, *Alexandrium*, *Ceratium*, *Dinophysis*, *Lingulodinium*, *Margalefidinium*, *Prorocentrum*, and *Pseudo-nitzschia*.

In addition to traditional phytoplankton monitoring methods, many organizations in California are embracing a new monitoring technology, the Imaging FlowCytobot (IFCB). An IFCB is an in-situ automated submersible flow cytometer that uses a combination of flow cytometric and video technology to capture high resolution images of suspended particles. Coupled with a machine learning algorithm, an IFCB can capture and identify up to 30,000 high-resolution images of phytoplankton per hour.

There are several methods commonly used to build image recognition algorithms (classifiers), and in this study we compare a variety of classifiers developed with different methods and in different locations. These data can be used to best determine allocation of resources as IFCB use becomes more common in California.

Material and Methods

IFCB deployment

In this study, the IFCBS IFCB104 and IFCB113 were used to collect data for analysis. IFCB104 was deployed beneath the Santa Cruz Wharf in Monterey Bay, and IFCB113 was deployed at Pier 17 in San Francisco Bay. At both locations, the IFCBs were positioned on the pier above the water, with water pumped to the instrument as described in Fischer *et al.* (2020).

During May and June 2020, both instruments were temporarily deployed together at the Santa Cruz Wharf for four weeks. During this simultaneous deployment the photomultiplier tube (PMT) settings for each instrument were initially the same, which resulted in a dramatic discrepancy in total cell concentration seen in the data (Fig. 1). After adjustment of IFCB113's PMT settings, total cell concentration seen by each instrument became comparable (McLane, 2018).

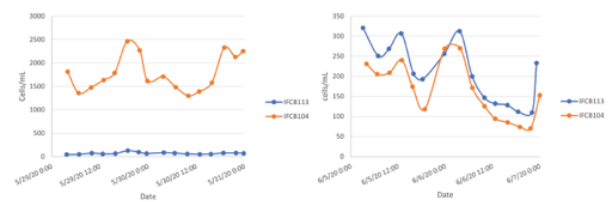


Fig. 1. Total cell counts between the instruments at the beginning of deployment with identical PMT settings (left), and after adjusting IFCB113's PMT settings to better represent the cell sizes present in Monterey Bay (right).

Random Forest classifier development

To develop the location-specific random forest classifiers, data from each location were manually classified and processed following the instructions from the IFCB



Wiki page (<https://github.com/hsosik/ifcb-analysis/wiki>). The Monterey Bay classifier (MBRF_24) was built with data collected from 2016-2019 and identifies 24 classes of phytoplankton (Fischer *et al.*, 2020). The San Francisco Bay classifier (SFBRF_32) was built with data collected from 2018-2020, and has 32 phytoplankton classes. We also tested a classifier developed by the TOAST lab at Texas A&M (Henrichs *et al.*, 2021), TOAST_RF_54, with 54 phytoplankton classes.

Convolutional Neural Network classifier development

Images from the Santa Cruz Wharf were classified using an Xception architecture depth-wise convolutional neural network (CNN) (Chollet, 2016). The model was trained using ~82,000 manually classified images from 50 distinct classes collected at the Santa Cruz Wharf. Training results indicate a validation accuracy of 0.98. Using the trained model, images from the year 2020 were classified and the highest probability class was assigned to the image. Cell concentrations were calculated as the sum of images in a given class per sample divided by the sample volume. The mean daily cell concentration for each class was subsequently calculated as the average of all daily samples.

Phytoplankton analysis with whole cell probes

Weekly water quality samples have been collected at the Santa Cruz Wharf since 2006. These data include whole cell probe (WCP) analysis for *Alexandrium catenella*, *Pseudo-nitzschia australis*, and *Pseudo-nitzschia multiseriata* (Scholin *et al.*, 1994; Miller and Scholin, 2000). These toxigenic HAB species are routinely monitored by the California Department of Public Health (<https://www.cdph.ca.gov/Programs/CEH/DRSEM/Pages/EMB/Shellfish/Phytoplankton-Monitoring-Program.aspx>).

Dinophysis spp. cell concentrations were estimated using autofluorescence (Ex 470 nm, Em 515 nm) and are a potential problem in Monterey Bay (Shultz *et al.*, 2009).

Results and Discussion

The initial performance of the newly developed random forest classifier SFBRF_32 is equivalent to MBRF_24, with 99.1% overall accuracy when run against the training set of images. During the side-by-side deployment at the Santa Cruz Wharf, SFBRF_32 performed similarly to MBRF_24 on data acquired from both instruments, with accuracies ranging from 94-96%. This indicates that the instrument being used for data collection is not a major factor in how a classifier performs. Additionally, it appears that SFBRF_32 and MBRF_24 yield equivalent identifications in this small subset of data.

To further explore the cross-application of classifiers, we compared the community composition of major phytoplankton groups (HABMAP HAB genera, diatoms, dinoflagellates, and other) as interpreted by the four classifiers over an 8-month time series in 2020 (Fig. 2). A paired t-test on log transformed data showed the HABMAP HAB group from SCW_CNN_50 was statistically similar to MBRF_24, while the other pairings were not. However, Pearson's r correlation revealed that the HABMAP HAB groups for SFBRF_32, SCW_CNN_50, and TOAST_RF_54 were all correlated well with the results produced by MBRF_24. These findings point to the need for regionally tuned classifiers



when trying to assess community structure and ecology, but still show some potential for non-optimized classifiers for evaluating HAB genera.

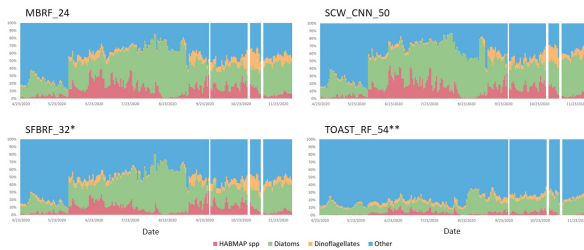


Fig. 2. Percent community composition in 2020 at the SCW based on daily averaged cell concentrations for four classifiers. Classes were grouped by CalHABMAP genera (*Akashiwo*, *Alexandrium*, *Ceratium*, *Dinophysis*, *Lingulodinium*, *Margalefidinium*, *Prorocentrum*, and *Pseudo-nitzschia*), diatoms, dinoflagellates, and other (includes unclassified).

The Pearson's r correlation confirmed MBRF_24 had strong relationships with the other classifiers for *Alexandrium*, *Dinophysis*, and *Pseudo-nitzschia*, but like the HABMAP HAB species group data, the classifiers were statistically different for these three genera (paired t-test, $p < 0.05$). HABs are generally defined by a cell concentration threshold and the IFCB and WCP cell concentration data were categorized as “bloom” or “not bloom” based on the threshold for each genus (Fig. 3). The bubble plots and a chi-square test confirm ($p < 0.05$) that binarized concentrations from all four classifiers are similar to the WCP data for *Dinophysis* and *Pseudo-nitzschia*. The binarized *Alexandrium* data from the classifiers are statistically different from the WCP results, but the three classifiers are statistically similar to each other. Indicating that, while not perfect or ideal, a non-tuned classifier can still provide useful information to managers about HABs.

Interestingly, the bubble plots reveal *Alexandrium* and *Dinophysis* cell concentrations were above the bloom threshold for most of 2020 at the SCW. While not surprising, as SCW was re-entering the “age of dinoflagellates” in 2018 (Fisher *et al.*, 2020), it may indicate a need to re-evaluate the bloom thresholds for data collected from IFCBs.

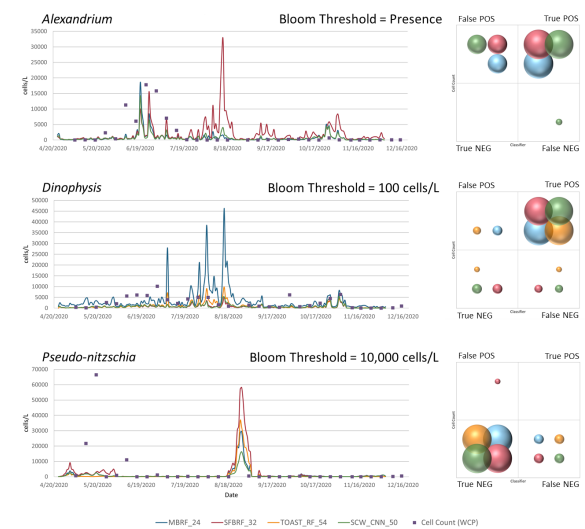


Fig. 3. Time series and quadrat plots for the three toxigenic CA HAB genera. Colors (lines and bubbles) represent the four classifiers. Cell counts are weekly using whole cell probes (WCP). Quadrat plots compare daily averaged classifier results to real-time WCP counts based on regulatory bloom thresholds for each genus. Bubble size represents the number of instances (bloom or no bloom) in each category. No bubble = no occurrence.

The *Pseudo-nitzschia* bubble plot alarmingly implies that classifiers and IFCBs are not able to identify *Pseudo-nitzschia* blooms. However, the *Pseudo-nitzschia* cell concentrations represented by the IFCB images are generally an underestimate, as each image of *Pseudo-nitzschia* is at least



two cells (end to end chains are a diagnostic characteristic). Given the wealth of data an IFCB provides, it may be worth evaluating standard bloom threshold values which were originally based on point samples.

In the next year the State of California will have 10 IFCBs deployed along its coastline. Only two of those sites have classifiers tuned to their region (Monterey Bay and San Francisco Bay) and 1 additional site has an image library large enough to build (or tune) a classifier (San Diego). The results from this study show that “tuned” IFCBs will collect equivalent data sets that can be comparable across sites. Results also indicate that a region-specific random forest classifier is as powerful as its equivalently-trained CNN counterpart. As these regional models are being applied to other locations, validation becomes an important step to ensuring any algorithm is providing accurate phytoplankton community structure data.

Acknowledgements. The IFCBs were purchased as part of the NOAA Technology Transition program under NOAA award NA14NOS0120148. Operations and maintenance were supported by NOAA awards 305053-00001 (PCMHAB) and NA16NOS0120021 (Central and Northern California Ocean Observing System). We would like to thank Jamie Walton for consolidating the 2020 time series, Jesse Lopez for providing guidance and code for developing the CNN, and Corinne Gible for her statistical analysis recommendations.

References

- Chollet, F. (2016). *IEEE Xplore* 7, 1251-1258.
- Fischer, A., Hayashi, K., McGaraghan, A., Kudela, R.M. (2020). *Limnol. Oceanogr.* 65, 2125-2141
- Henrichs, D., Angles, S., Gaonkar, C., Campbell, L. (2021). *Environ. Sci. Pollut. Res.* 28, 28544-28555.
- McLane Research Laboratories (2018). *Imaging FlowCytobot User Manual, Rev 18.F.01.*
- Miller, P.E. and Scholin, C.A. (2000). *J. Phycol.* 36: 238-250.
- Scholin, C.A, Herzog, M., Sogin, M., Anderson, D.M. (1994). *J. Phycol.* 30, 999-1011
- Shultz, D., Campbell, L., Kudela, R.M. (2019). *Harmful Algae* 88, 101641.
- Sosik, H.M. and Olson, R.J. (2007). *Limnol. Oceanogr. Meth.* 5, 204-216.
- TOAST: <https://sites.google.com/tamu.edu/phytolab/toast>





HAB PREDICTION



Application of a quantitative molecular methods to characterize abundance and distribution of *Alexandrium* cysts for NOAA's HAB Forecasting

Cheryl Greengrove^{1*}, Steve Kibler², Julie Masura¹, Julie Matweyou³, Courtney Hart⁴

¹University of Washington Tacoma, 1900 Commerce Street, Tacoma WA 98402, U.S.A.;

²NOAA Beaufort Laboratory, 101 Pivers Island Rd, Beaufort, NC 28516, U.S.A.; ³Julie Matweyou – University of Alaska Fairbanks - Alaska Sea Grant, 118 Trident Way, Kodiak AK 99615, U.S.A.; ⁴Courtney Hart – University of Alaska Fairbanks - Juneau Center, 17101 Point Lena Loop Road Juneau, AK 99801, U.S.A.

* corresponding author's email: cgreen@uw.edu

Abstract

The toxic dinoflagellate *Alexandrium catenella* overwinters as a benthic resting cyst and germinates into the water column in the spring, making cells available for filter feeding by shellfish. Previous studies have mapped winter distribution of *A. catenella* cysts in Gulf of Maine and Puget Sound sediments to provide shellfish growers/harvesters with an early warning system of potential hotspots for blooms. However, the current protocol for cyst enumeration by fluorescent microscopy is time consuming and requires highly specific training. This MERHAB project is to develop a new qPCR assay for *A. catenella* cysts for evaluation against the standard microscopy protocol to produce more rapid and accurate cyst abundance data. 2019 and 2020 sediment samples were collected in the Gulf of Maine, Puget Sound and Alaska for cyst mapping, interlaboratory comparison, and qPCR development. Interlaboratory comparisons of cyst enumeration using the standard microscopy method show no significant differences. qPCR development is underway and preliminary results are presented here.

Keywords: *Alexandrium catenella*, cysts, qPCR, forecasting, Gulf of Maine, Puget Sound, Alaska

<https://doi.org/10.5281/zenodo.7036215>



Introduction

NOAA is developing *Alexandrium catenella* bloom forecast products through the harmful algal bloom (HAB) Operational Forecasting System (HABOFS) to mitigate human health risks and economic effects of shellfish closures during seasonal blooms of the toxic dinoflagellate *A. catenella* in U.S. Atlantic northeast and Pacific northwest states (<https://coastalscience.noaa.gov/research/stressor-impacts-mitigation/hab-forecasts/>). This species overwinters as a benthic resting cyst and germinates in the spring (Anderson, 2014), making saxitoxin-laden vegetative cells available for filter feeding by shellfish (Cusick and Sayler, 2013). Ingestion of shellfish containing saxitoxin by humans can result in Paralytic Shellfish Poisoning (PSP) (Price *et al.*, 1991; Lefebvre *et al.*, 2016). Forecasting efforts hinge on determination of *A. catenella* cyst wintertime abundance at bloom locations.

Previous studies have mapped winter distribution of *A. catenella* cysts in Gulf of Maine (GoME; Anderson *et al.*, 2014) and Puget Sound (PS; Horner *et al.*, 2011; Greengrove *et al.*, 2015) sediments to provide shellfish growers with an early warning of potential hotspots for blooms. In addition, sediment cyst surveys in SE Alaska (Tobin *et al.*, 2017) and the Bering and Chukchi Seas (Natsuike *et al.*, 2013; Anderson *et al.*, 2021) indicate high concentrations of *A. catenella* cysts where there are limited monitoring and forecasting capabilities. The current protocol for cyst enumeration by fluorescent microscopy (Yamaguchi *et al.*, 1995) is laborious, time consuming and requires highly specific training. There is a need to streamline cyst quantification to shorten the

turnaround time in advance of the spring bloom season and make the quantification methods consistent across regions.

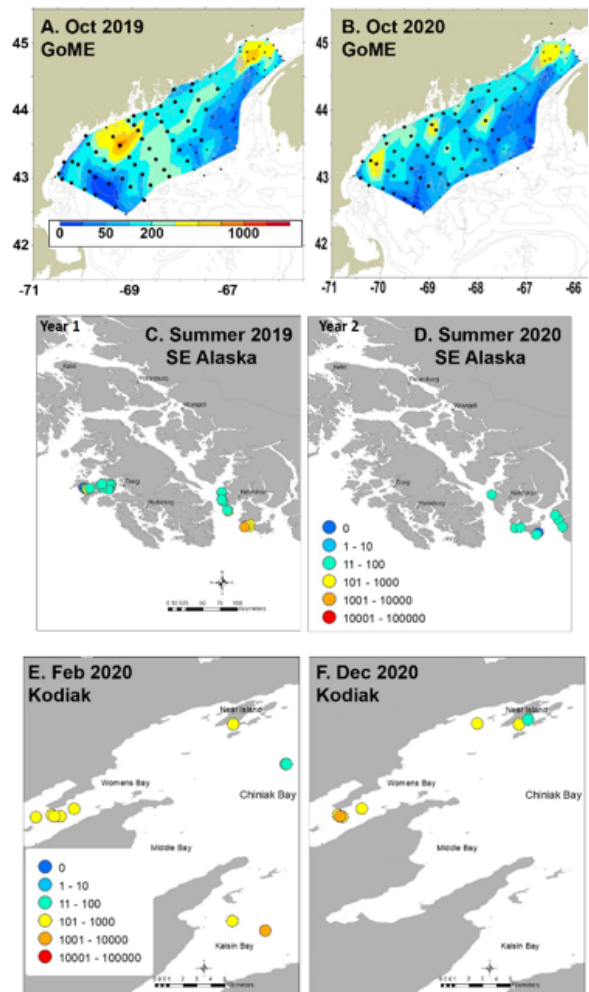


Fig. 1. Contour maps of *A. catenella* cyst distribution (cysts cm^{-3}) in the GoME in A) Oct 2019 and B) Oct 2020; in SE Alaska in C) summer 2019 and D) summer 2020; and in Chiniak Bay, Kodiak in E) Feb 2020, and F) Dec 2020.

Using sediment samples from the GoME, PS and AK, this project funded by NOAA's MERHAB program is to map regional *A. catenella* cyst abundances, conduct



interlaboratory comparison of the standard microscopy method for cyst enumeration to check for consistency of counts, and compare microscopy-derived abundances with those using qPCR. The same sediment samples are being used to develop and evaluate a qPCR assay for *A. catenella* cysts. This molecular work builds on prior species-specific molecular methods developed over the last two decades (Anderson *et al.*, 1999; Hosoi-Tanabe and Sako, 2005, 2006; Erdner *et al.*, 2010; Vandersea *et al.*, 2017). If successful, the new tool will provide cyst abundance data to HABOFS and other regional marine resource management systems more quickly and consistently than is currently possible with microscopy-based methods.

Material and Methods

Surface sediment samples were collected by Craib corer or Van Veen grab sampler at 54 GoME stations in Oct 2019 (Y1) and 53 stations in Oct 2020 (Y2); at 47 PS stations in Jan-Feb 2020 (Y1); at 24 stations in SE Alaska in summer 2019 (Y1) and 8 stations in 2020 (Y2); and at 12 Kodiak, Alaska stations in Feb 2020 (Y1) and Dec 2020 (Y2). Craib cores were sliced into 0-1 cm (surface) and 1-3 cm segments and retained for processing. The grab samples were sampled from the upper 2 cm of sediment with a plastic scoop. Prior to processing, the sediment samples from GoME and Alaska were split and subsamples were sent to University of Washington Tacoma (UWT) for duplicate counting as part of the interlaboratory comparison. Samples from PS and Alaska were split and subsamples were sent to the NOAA Beaufort Lab for qPCR development. The 0-1 cm GoME samples and all samples from PS and Alaska were processed and enumerated

at each investigator's lab using the standard microscopy method (Yamaguchi *et al.*, 1995). Cyst abundances were mapped using ArcGIS and microscopy-based cyst enumeration results were compared among labs using a t-test (normal data) or Wilcoxon Signed Rank Test (non-normal).

Sediment samples for cyst counting and qPCR were homogenized, and a 5 cm³ subsample collected for processing. Subsamples were sonicated and sieved to isolate the 20-100 µm cyst fraction after (Anderson *et al.*, 2005). The cyst fraction was concentrated onto a 47 mm, 8 µm NucleoporeTM polycarbonate filter and DNA was extracted using the Nucleospin Soil DNA extraction Kit (Takara Bio U.S.A., Inc., San Jose, CA) with lysis buffer SL1 after the manufacturer's protocol. A FastPrep-24 ClassicTM bead beater (MP Biomedicals, Santa Ana, CA) was used to disrupt cysts in each sample at a speed of 6.0 m s⁻¹ for 1 min. The DNA was eluted in 50 µL and qPCR amplified with a BIO RAD CFX ConnectTM real time system (BIO RAD, Hercules, CA) (Vandersea *et al.*, 2017). The qPCR reaction mix contained SYBR green QuantiNova Probe PCR Master Mix (Qiagen, Germantown, MD) and 1 µL of each DNA extract using a quantification cycle (Cq) after Bustin *et al.* (2009). A melting curve analysis was performed following thermal cycling to check the specificity of the PCR reactions.

Cyst-based qPCR standard curves were constructed using microscopy-based counts. A cyst concentrate was first created by processing multiple aliquots of sediment with the method above, and using density gradient centrifugation (Richlen *et al.*, 2016) to concentrate the cysts and remove contaminating particulates. Aliquots of the



cyst concentrate (1-1,000 cysts) were then extracted for qPCR with identical aliquots for cyst counts. Standard curves were constructed by plotting the Cq values vs log transformed cyst concentrations, and linear regression analysis was used to calculate the slope.

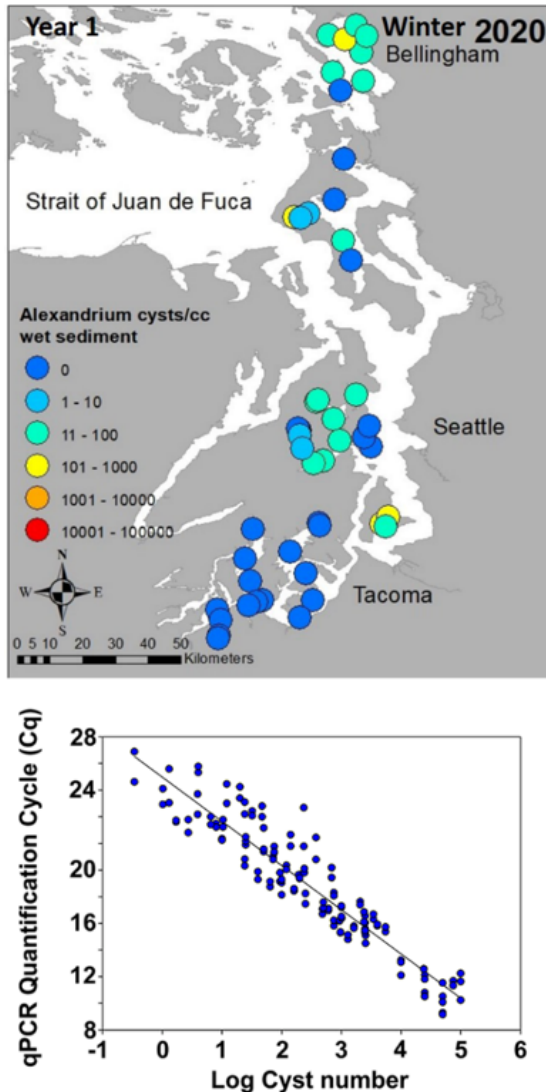


Fig. 2. A) *Alexandrium catenella* cyst distribution (cysts cm^{-3}) in PS during Feb 2020. B) Draft qPCR standard curve for cysts.

Results and Discussion

Cyst distribution maps for GoME, PS, SE Alaska and Kodiak are shown in figures 1-4. Note that no Y2 data were collected for PS due to sampling constraints associated with the COVID pandemic. Y1 cyst abundances in the GoME were highest offshore between Casco Bay and Penobscot Bay and NE of Grand Manan Island near the mouth of the Bay of Fundy (Anderson *et al.*, 2014). Y2 cyst abundances were lower overall with lower abundances. In PS during Y1, cyst abundances were generally lower than prior studies (Horner *et al.*, 2011; Greengrove *et al.*, 2015), but with high cyst abundances in Quartermaster Harbor, Bellingham Bay, and bays in the western Main Basin of PS. One area of increased cyst abundance is Penn Cove, which has historically been a site with PSP toxin occurrences (Trainer *et al.*, 2003). In SE Alaska, high Y1 cyst abundances were found on the west coasts of Prince of Wales Is. (near Craig) and Gravina Is. (near Ketchikan); and between Annette and Duke Is. in Sealed Passage. Only the Ketchikan area was sampled in Y2 with less cysts overall compared to the prior year. Kodiak had high cyst abundances throughout Chiniak Bay in both years and Womens Bay had even higher cyst abundances in Y2 than Y1. Overall, cysts were present in all three areas (GoME, PS and coastal Alaska), but Alaska cyst abundances were the highest of all three regions (2019 and 2020).

Cyst enumeration results from the NOAA Beaufort Lab and the UWTLab were compared for not found to be statistically different ($p = 0.906$). Also, no statistical differences were found when comparing University Alaska Fairbanks (UAF) - Juneau Lab and the UWT

Lab cyst counts for both years ($p = 0.057$). A comparison between the UAF – Kodiak Lab and UWT is still pending. The results thus far indicate that with proper cross-lab training, *A. catenella* cyst enumeration can be consistent.

Method development of the cyst qPCR assay is proceeding. The draft qPCR standard curve (Fig. 5) indicates the qPCR cyst assay is linear over six orders of magnitude ($y = 26.2 - 3.2x$, $r^2 = 0.94$, $p < 0.05$), and can be used to estimate cyst abundance in the GoME, PS and Alaska. This assay is an improvement over a previous qPCR assay by Erdner *et al.* (2010) because we use a cyst-based standard curve (instead of an amplicon) with a greater dynamic range (six orders of magnitude). Further testing is underway before assay validation with microscopy- and qPCR-derived abundances over multiple seasons. Pending favorable validation results, the assay will be used to map cyst distribution, and will be integrated into HABOFS forecast results.

Acknowledgements. This project is funded by NOAA National Centers for Coastal Ocean Science (NCCOS) MERHAB grant number NA19NOS4780188.

References

Anderson, D.M., Fachon, E., Pickart, R.S., Lin, P., *et al.* (2021). PNAS 118, e2107387118.

Anderson, D.M., Keafer, B.A., Kleindinst, J.L., McGillicuddy Jr., *et al.* (2014). Deep-Sea Res. II 103, 6-26.

Anderson, D.M., Kulis, D.M., Keafer, B.A., Berdalet, E. (1999). J. Phycol. 35, 870-883.

Anderson, D.M., Stock, C.A. Keafer, B.A.,

Bronzino, A., *et al.* (2005). Deep Sea Res. II 52, 2522-2542.

Bustin S.A., Benes V., Garson J.A., Hellemans J., *et al.* 2009. Clin. Chem. 55, 611-622.

Cusick, K.D. and Sayler, G.S. (2013). Mar. Drugs 11, 991-1018.

Erdner, D.L., Percy, L., Keafer, B., Lewis, J., Anderson, D.M. (2010). Deep-Sea Res. II 57, 279-287.

Greengrove, C.L., Masura, J.E., Moore, S.K., Bill, B.D., *et al.* (2015). In: MacKenzie, A.L. (Ed.) Proc. 16th ICHA. Wellington, New Zealand. 163-166.

Horner, R.A., Greengrove, C.L., Davies-Vollum, K.S., Gawel, J.E., Postel, J.R., Cox, A. (2011). Harmful Algae 11, 96-105.

Hosoi-Tanabe, S. and Sako, Y. (2005). Harmful Algae 4, 319-328.

Hosoi-Tanabe, S. and Sako, Y. (2006). Fish. Sci. 72, 77-82.

Lefebvre, K.A., Quakenbush, L., Frame, E., Burek Huntington, K., *et al.* (2016). Harmful Algae 55, 13-24.

Natsuike, M., Nagai, S., Matsuno, K., Saito, R., Tsukazaki, C., *et al.*, (2013). Harmful Algae 27, 52-59.

Price, D.W., Kizer, K.W., Hansgen, K.H. (1991). J. Shellfish Res. 10, 119-145.

Richlen, M.L., Zielinski, O., Holinde, L., Tillman, U., *et al.*, (2016). Mar. Ecol. Progr. Ser. 547, 33-46.



Tobin, E., Eckert, G., Whitehead, C., Sullivan, K. (2017). Alaska Marine Science Symposium, Anchorage, Alaska.

Trainer, V.L., Eberhart, B.-T.L., Wekell, J.C., Adams, N.G., *et al.*, (2003). J. Shellfish Res. 22, 213-223.

Vandersea M.W., Kibler S.R., Van Sant S.B., Tester P.A., *et al.* (2017). Phycologia 56, 303-320.

Yamaguchi, M., Itakura, S., Imai, I., Ishida, Y. (1995). Phycologia 34, 207-214.



Time series analysis of the *Karenia brevis* blooms on the West Florida Shelf: relationships with El Niño – Southern Oscillation (ENSO) and its rate of change

Bruna Sobrinho¹, Patricia M. Glibert¹, Vyacheslav Lyubchich², Cynthia A. Heil³, Ming Li¹

¹University of Maryland Center for Environmental Science, Horn Point Laboratory, PO Box 775, Cambridge, MD 21613, U.S.A.; ²University of Maryland Center for Environmental Science, Chesapeake Biological Laboratory, PO Box 38, Solomons, MD 20688, U.S.A.; ³Mote Marine Laboratory, 1600 Ken Thompson Parkway Sarasota, Florida 23236, U.S.A.

* corresponding author's email: bsobrinho@umces.edu

Abstract

Blooms of the toxigenic dinoflagellate *Karenia brevis* occur regularly in the Gulf of Mexico, especially along the coast of western Florida, U.S.A. Here, time-series data from 1998 to 2020 were used to examine relationships between *K. brevis* abundance and the El Niño – Southern Oscillation (ENSO) and its rate of change, as well as temperature, precipitation, river flow, and salinity. This time series includes periods of substantial blooms ($\sim 1.4 \times 10^6$ cells L⁻¹) and times characterized by background cell concentrations ($\sim 1.0 \times 10^3$ cells L⁻¹). El Niño brings wet and cool weather to South Florida, including a greater frequency of storms, while La Niña brings dry and warm weather. However, mild La Niña and periods of ENSO transitions bring a higher frequency of hurricanes that directly impact Florida. Excluding the large bloom of 2020–2021 (not included herein), the highest *K. brevis* abundances observed were associated with blooms in 2004–2005 and 2017–2018, both of which occurred when hurricanes followed drought periods. High correspondences between cell concentrations, Peace River discharge and ENSO index indicated that freshwater flow, and climate oscillations may play important roles—both direct and indirect—on *K. brevis* blooms on the West Florida Shelf. These time-series analyses will help to inform new models of bloom formation and termination in western Florida waters and may help to guide nutrient reduction targets from river discharge.

Keywords: *Karenia brevis*, West Florida Shelf, ENSO, time series analysis

<https://doi.org/10.5281/zenodo.7036227>



Introduction

Blooms of the toxigenic dinoflagellate *Karenia brevis* occur annually in the eastern Gulf of Mexico (Steidinger, 2009). Bloom duration can vary from months to years, and blooms can extend up to 1000 km along the coastline. Blooms initiate offshore (20–65 km) and the transportation of the cells nearshore occurs via the bottom Ekman layer driven by wind-driven and upwelling-related transport (Steidinger, 1975; Weisberg *et al.*, 2016). Both physical drivers and nutrient supply are important to the initiation, development, and maintenance of *K. brevis* blooms (reviewed in Heil and Muni-Morgan, 2021; Li *et al.*, 2021).

Oscillations of El Niño and La Niña, the El Niño - Southern Oscillation (ENSO), affect southwest Florida in complex ways. El Niño brings wet and cool weather to South Florida, including a greater frequency of storms, while La Niña brings dry and warm weather. However, both mild La Niña periods and transitions in ENSO periods may bring a higher frequency of hurricanes, which increase both freshwater flows and associated nutrient delivery to coasts. This study investigated the relationship between environmental conditions (temperature, salinity, river discharge and the ENSO) and the *K. brevis* concentration along the southwestern coast of Florida, using available long-term data.

Materials and Methods

Overview of Florida HAB database

Geo-referenced *K. brevis* surface cell concentration data (cells L⁻¹) with associated temperature (°C), and salinity data for southwest Florida from 1998 to 2020 were

obtained by request from the Florida Fish and Wildlife Research Institute (FWRI). This *K. brevis* cell concentration database (the Florida HAB Historical Database) contains data collected by state and county agencies, private research institutions and university researchers and represents samples collected during research, routine monitoring, and event response sampling of suspected or confirmed *K. brevis* events. This analysis is limited to data post-1998 when routine sampling intensified, but the database contains records dating back to 1953. This analysis also does not include the large bloom that began in late 2020.

Monthly ENSO status was derived from the US National Oceanic and Atmospheric Administration (NOAA; <https://ggweather.com/enso/oni.htm>). These data are reported as running three-month averages. Precipitation data (mm) and the discharge of the Peace and Caloosahatchee Rivers (cubic feet s⁻¹) data were from the United States Geological Survey (sites USGS 2296750 and USGS 2292000, respectively; <https://waterdata.usgs.gov/nwis>). The Peace River is one of the largest rivers in Florida with a natural flow. The Caloosahatchee River is significantly larger; however, its flow is actively managed and thus does not necessarily parallel precipitation trends.

Statistical analysis

Monthly *K. brevis* cell concentration averages were calculated for the whole southwest Florida to compare all variables during the study period of 22 years. To determine relationships, correlations were estimated using Pearson's correlations between these



monthly averaged *K. brevis* (log-transformed) abundances and environmental variables were calculated. As there is a possibility of a lag response in *K. brevis* concentration in relation to environmental conditions (Dixon and Steidinger, 2004), cross-correlation analysis with lags from 0 to 12 months was performed. Multi-co-linearity was assessed before estimating a model with a combination of predictors. A generalized additive mixed model (GAMM) representing the relationship between Peace River discharge and environmental parameters (ENSO index and precipitation) was also developed. In both approaches, normality, variance homogeneity, and uncorrelatedness of model residuals were assessed using residual time series and Q–Q plots, Shapiro–Wilk normality tests, and plots of the autocorrelation function. As the residuals of the models presented non-normal distribution, the sieve bootstrap approach was used to obtain sample distributions of the model coefficients and assess their statistical significance. All analyses were performed using R language (R Core Team, 2021).

Results and Discussion

Blooms of *K. brevis* typically originate in late summer, following the wet season (e.g., Lenos and Heil, 2010). However, annual variations in bloom duration and intensity are large. In years of substantial La Niña, when dry conditions develop, blooms are typically short lived, as exemplified by the 2000 bloom (Fig. 1a). The spring accumulations of *K. brevis* during 2000 represented the prolonged bloom that was initiated the previous year. In contrast, during El Niño years (e.g., 2015), blooms may be sustained at high cell abundances for a longer period throughout the fall months, following the more significant

flows of the summer wet season (Fig. 1b). The annual timing of blooms implies that nutrients delivered during the summer wet season help to sustain nearshore blooms into the fall months and may help to regulate the magnitude of blooms that develop.

Extreme bloom conditions are witnessed only occasionally, as exemplified in 2005, when high cell abundances were observed throughout the year (Fig. 1c), including throughout the summer months. That blooms can be sustained throughout the summer months, at least during some years, implies that higher summer temperatures are not an obstacle to sustaining blooms. While summer temperatures may exceed the temperature optimum for growth (Steidinger, 2009; Vargo, 2009), they are not necessarily inhibiting for growth, especially if sufficient nutrients are available. In 2005, when the bloom was sustained through the summer months, flow from the Caloosahatchee River was three times its long-term average during the months of April and May, thus potentially delivering above average nutrient loads early in that year.

Positive significant correlations between Peace River discharge, ENSO, and *K. brevis* were observed with zero lag (Table 1). Dixon and Steidinger (2004) observed a similar relationship between *K. brevis* concentration and Peace River flows for the 1953-1998 period. Moreover, the GAMM indicated a statistically significant relationship between the Peace River discharge and ENSO at both lag 0 and 1 month. Although cross-correlation analysis showed a lag response of two months between ENSO and *K. brevis*, it was not statistically significant in the model. Also, significant negative relationships were



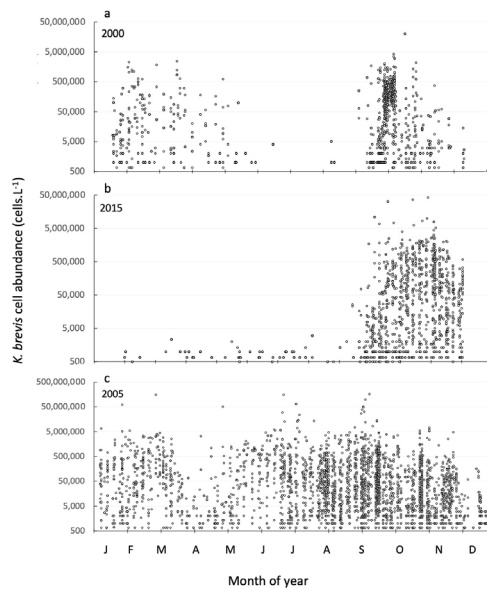


Fig. 1. Examples of the variation in annual *K. brevis* bloom intensity and timing. The year 2000 was a year of La Niña, 2015 was a year of substantial El Niño, and 2005 was a year of transition from El Niño to La Niña. Note difference in scales between years.

observed between precipitation, salinity, temperature, and *K. brevis* (Table 1). No significant relationships were observed with flow from the Caloosahatchee River, as was observed by Dixon and Steidinger (2004) for 1953-1998. While overall flows from the Caloosahatchee River are higher than those of the Peace River, flows are more irregular, as they are actively managed to avoid inland flooding, which leads to a lack of long-term correlations across years.

Blooms in 2000, 2010 and 2020, were associated with intensive La Niña conditions (ENSO <1), while bloom years such as 2015 had intensive El Niño conditions (ENSO >1). More common, however, are bloom years that are neutral with respect to La Niña or El Niño (i.e. mild ENSO conditions). Intensive La

Table 1. Statistically significant cross-correlation between time series of log-transformed *K. brevis* abundance and the environmental variables with lags ranging from 0 to 12 months. P-values are in parentheses.

Variables	Lag	Correlation (p-value)
ENSO	0	0.15 (0.01)
Peace River discharge	0	0.14 (0.01)
Precipitation	0	-0.13 (0.02)
Salinity	0	-0.13 (0.03)
Temperature	0	-0.15 (0.01)

Niña years bring drought and few hurricanes, but milder La Niña conditions and ENSO transition periods can yield hurricanes that directly impact the Florida coast (Fig. 2). Excluding the large bloom that is currently ongoing (2020–2021), the highest annual abundances of *K. brevis* observed in this study were during the 2004–2005 and 2017–2018 blooms, which occurred when hurricane events followed drought periods (Fig. 2). When combining these data, the periods of largest blooms occurred during transition periods in the ENSO index (Fig. 2).

Nutrient loads were not directly addressed herein, however Li *et al.* (2021) demonstrated that the probability of *K. brevis* increased with increasing river flows across all discharge levels, suggesting that the composition of nutrients discharged by different rivers impacts localized coastal *K. brevis* blooms. Medina *et al.* (2020) observed NO_{3+2} levels at lock S79 upriver of the Caloosahatchee River mouth were related to localized *K. brevis* concentrations at the river mouth from 2012–2018, although it was unclear if this effect was the result of river or estuarine nutrient sources. Effects of nutrient loads on HABs associated



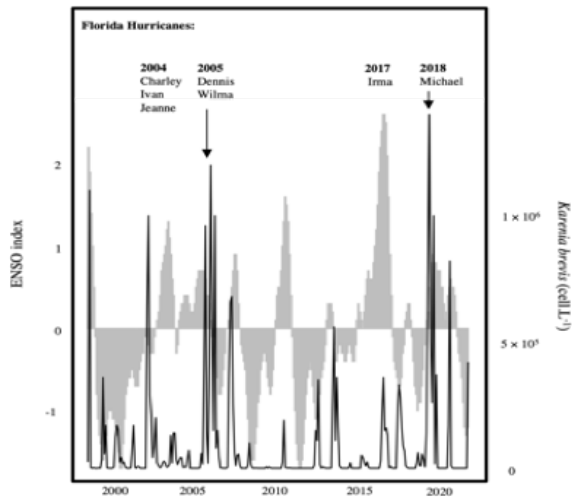


Fig. 2. ENSO index and *K. brevis* abundance (cells L^{-1}) between the years 1998 and 2020 in West Florida Shelf.

with hurricanes and ENSO have also been documented for Lake Okeechobee, the Indian River Lagoon and Florida Bay (Phlips *et al.*, 2020; Glibert *et al.*, 2021). A study using a three-dimensional ocean-biogeochemical model has also identified ENSO as the main driver of the variability of plankton biomass in the northern Gulf of Mexico during winter and spring (Gomez *et al.*, 2019).

In summary, as the river drainages impacting the West Florida Shelf are large, changes in precipitation can translate to large changes in discharges and associated nutrients. Changes in discharge arising from ENSO oscillations as well as active management have the potential to affect *K. brevis* bloom timing, duration, and intensity through changes in nutrient delivery and salinity and temperature. These relationships may also help to inform potential nutrient reduction strategies to mitigate blooms.

Acknowledgements. This study was funded by the NOAA National Centers for Coastal Ocean Science Competitive Research under award NA19NOS4780183. This is Contribution Number 6106 from the University of Maryland Center for Environmental Science and 1012 from the NOAA ECOHAB Program.

References

- Dixon, L.K. and Steidinger K.A. (2004). In: Steidinger, K.A., Landsberg, J.H., Tomas, C.R., Vargo, G.A. (Eds.), *Harmful Algae*, UNESCO, 29-31.
- Glibert, P.M., Heil, C.A., Madden, S.J., Kelly, S.P. (2021). *Biogeochem.* 1-27.
- Gomez, F.A., Lee, S.K., Hernandez, F.J., Chiaverano, L.M., *et al.*, (2019). *Sci. Rep.* 9, 1-10.
- Heil, C. A. and Muni-Morgan, A. L. (2021). *Front. Ecol. Evol.* 9, 1-38.
- Lenes, J.M. and Heil, C.A (2010). *J. Plankton Res.* 32, 1421-1431.
- Li, M.F., Glibert, P.M., Lyubchich, V. (2021). *J. Mar. Sci. Engin.* 9, 1-21.
- Medina, M., Huffaker, R., Jawitz, J.W. Munoz-Capena, R. (2020). *Harmful Algae* 98, 101900.
- Phlips, E.J., Badylak, S., Nelson, N.G., Havens, K.E. (2020). *Sci. Rep.* 10, 1-12.
- R Core Team. *A Language and Environment for Statistical Computing*. 2021. Available online: [//www.R-project.org/](http://www.R-project.org/)



Steidinger, K.A. (1975). Environ. Lett. 9, 129-139.

Steidinger, K.A. (2009). Harmful Algae 8, 549-561.

Vargo, G.A. (2009). Harmful Algae 8, 573-584.

Weisberg, R.H., Zheng, L., Liu, Y., Corcoran, A.A., *et al.*, (2016). Cont. Shelf Res. 120, 106-121.



Assessing the accuracy of Visible Infrared Imaging Radiometer (VIIRS) and MultiUltra-high Resolution (MUR) Sea-Surface Temperature products for inclusion of a model to forecast blooms of *Alexandrium catenella* in south-central Alaska

Timothy T. Wynne¹, Steven R. Kibler², Alexandria Sabo^{2,3}, Kaytee Pokrzywinski²

¹National Ocean and Atmosphere Administration, National Centers for Coastal Ocean Sciences, HAB Forecasting Branch, 1305 East-West Highway, Silver Spring, MD 20910, U.S.A.; ²National Ocean and Atmosphere Administration, National Centers for Coastal Ocean Sciences, HAB Forecasting Branch, 101 Pivers Island Rd., Beaufort, NC, U.S.A.; ³CSS, Inc., 101 Pivers Island Rd., Beaufort, NC, U.S.A.

* corresponding author's email: timothy.wynne@noaa.gov

Abstract

The toxic harmful algal bloom species *Alexandrium catenella* has been observed to bloom in Alaskan coastal waters when sea surface temperatures (SST) exceed approximately 8°C. Consequently, acquiring, fine scale SST data for Alaskan coastal waters represents a critical first step in developing ecological models capable of predicting the occurrence of toxic *Alexandrium* blooms in this region. Remotely sensed satellite SST records represent the most comprehensive SST data set, but before those data can be used, the satellite data require validation which was the goal of this study. Specifically, we compare a remotely sensed monthly sea surface climatological data set produced by NASA's Jet Propulsion Laboratory with seven meteorological buoys provided by the National Ocean and Atmosphere Administration (NOAA) National Data Buoy Center (NDBC). The comparisons were done on a point-to-pixel basis as well as an aerial estimation method. The selected study area, the Kodiak Archipelago in Alaska (U.S.A.), is characterized as possessing a varied coastline, filled with a number of coves and embayments. Three of the NDBC buoys are located in embayments and an additional one is in the ~40 km wide Shelikof Strait, with the remaining three offshore. The remotely sensed and in situ measurements were highly correlated providing the basis for the extraction fine scale SST data for the Alaska region over the past 10+ years which can be subsequently incorporated into bloom prediction models.

Keywords: water temperature, sea surface temperature, Alaska, *Alexandrium catenella*, forecasting

<https://doi.org/10.5281/zenodo.7036236>



Introduction

Sea-Surface Temperature (SST) is one of the most easily quantifiable environmental parameters in the marine environment, and one of the most used in biophysical modeling exercises. Many biological properties are influenced by SST, including phytoplankton growth rates and nutrient uptake kinetics (Lomas and Glibert, 1999). Work by Vandersea *et al.* (2017) found temperature was the factor best predicting when toxic *Alexandrium catenella* blooms occur in Alaskan coastal waters. If accurate models predicting the likelihood of *Alexandrium* blooms are to be developed, it is imperative to have reliable and detailed estimates of SST for this region. Synoptic remote sensing represents the most robust way to quantify this parameter. Consequently, an intensive validation for satellite sensed Alaskan sea surface temperatures was undertaken as the first key step in developing predictive models for *A. catenella* bloom occurrence.

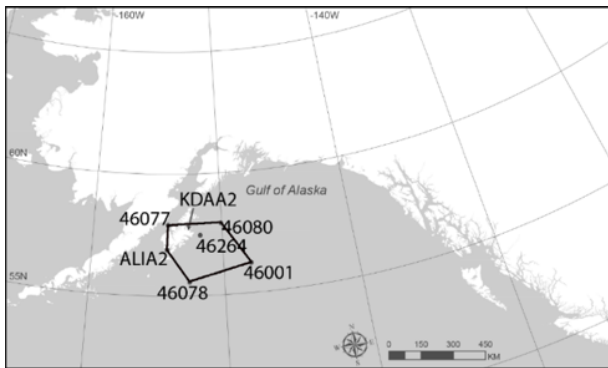


Fig. 1. Locations of the NDBC buoys used in this manuscript. The polygon shown is what was used to extract the data from the MUR imagery for the comparison shown in figure 3.

Material and Methods

Water Temperature Data

The water temperature (WTMP) data were acquired from the National Data Buoy Center (NDBC, 2021). These data are collected as frequently as every quarter of an hour. Daily and monthly means were calculated with missing data values discarded. Seven stations were considered that are in the vicinity of the Kodiak Archipelago (Fig. 1).

Sea Surface Temperature Data

Monthly SST data were acquired from NOAA PolarWatch (2021), from NASA Jet Propulsion Laboratory (JPL) Multi-scale Ultra-high Resolution (MUR) SST product. This is a global product combining an array of data, including microwave data, and mapped to a 0.01° spatial resolution (JPL, 2021). It should be noted that part of the data stream into the MUR modelled SST product was from the NDBC buoys (Chin *et al.*, 2017). Daily Sea Surface Temperature (SST) was acquired from the NOAA Coastwatch program from the Visible Infrared Imaging Radiometer (VIIRS) at a spatial resolution of 750 m (Coastwatch, 2021).

Comparison Methods

The MUR monthly data were compared to the NDBC water temperatures in two ways. The first was a traditional point-to-pixel matchup. A 3 x 3 box of pixels was extracted from each monthly image and the median of this 3 x 3 box was calculated and compared directly with the monthly median water temperature from the NDBC data.

The second method was adopted by Wynne *et al.* (2021) where a polygon was drawn around the seven buoys in figure 1 and then all of the



included data were extracted and averaged. This polygon is shown in figure 1. In this manner, each month had a single point. This average was compared to the mean of the seven different NDBC stations. This process was termed the integrated method by Wynne *et al.* (2021).

The mean daily water temperature was calculated from the NDBC data. A 3 x 3 box around the point of interest was extracted from the daily VIIRS SST. The median was calculated from the extracted points. A daily matchup was achieved if a single point from the 3 x 3 matchup was available.

Results and Discussion

A least squares regression from the point-to-pixel match-ups was used to assess differences in monthly MUR data (Fig. 2). The regression line fit well, indicating relatively low error and bias.

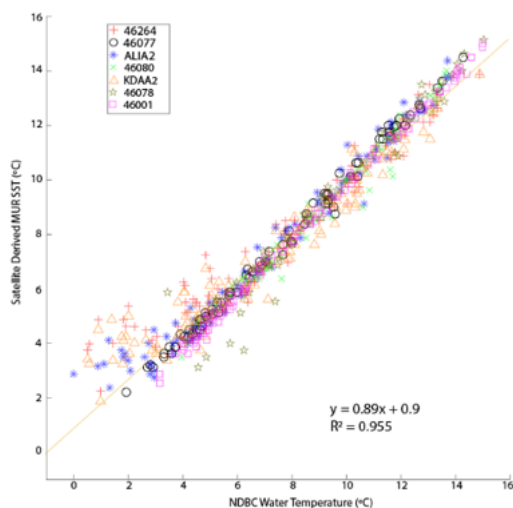


Fig. 2. Regression between the monthly NDBC water temperatures and the combined monthly MUR SST for the stations in figure 1 based on a point-to-pixel matchup technique and the monthly MUR data water temperatures.

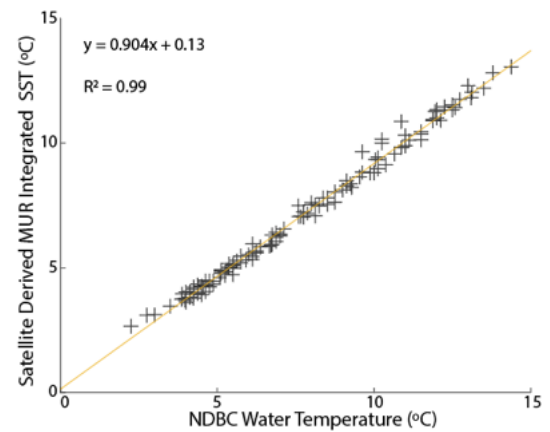


Fig. 3. Relationship between the monthly NDBC water temperature and the monthly MUR SST from the integrated technique (orange line). Each month is reduced to a single point.

Using this method, the monthly mean NDBC water temperature data and the monthly MUR SST data were also compared using a least-squares regression analysis for the integrated technique (Fig. 3).

The daily water temperature and from the NDBC and the daily VIIRS regression is shown in figure 4.

The slopes from the monthly point-to-pixel matchup (Fig. 2) and the monthly integrated matchup (Fig. 3) vary by less than 2%. This indicates that the integrated method produces a reliable representation of water temperatures around the Kodiak Archipelago. This could have important ramifications for subsequent HAB forecasting work in that datasets with a coarse spatial resolution may be sufficient for forecasting across southern Alaska.



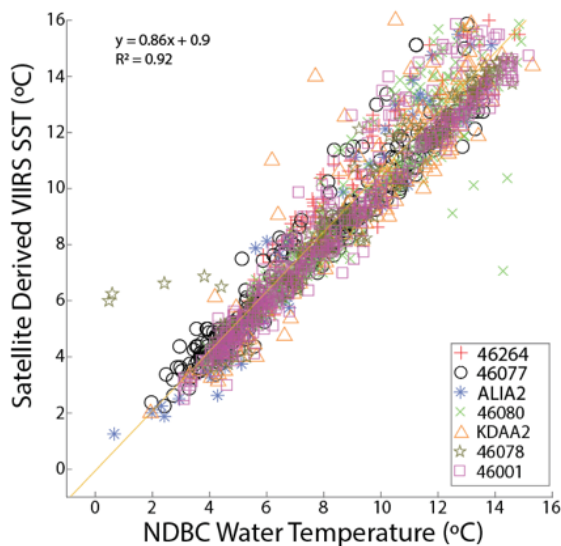


Fig. 4. Correlation between the daily NDBC water temperature and the daily VIIRS SST for the stations in figure 1 based on a point-to-pixel matchup technique.

The slopes between the regression lines of the VIIRS daily imagery and the MUR monthly imagery using the point-to-pixel matchup are also within good agreement varying by ~3%.

It appears that the two different SST products both underestimate the water temperatures by approximately 10%. This bias can be corrected relatively easily, by dividing the SST by the slope of the regression line. The results here indicate that the VIIRS daily product, with high spatial resolution (750 m pixel vs 1 km for MUR) shows good agreement with field water temperatures around the Kodiak Archipelago. Similarly, the MUR monthly SST product shows good agreement with NDBC water temperature, and with the high spatial resolution VIIRS data. The results of this analysis indicate ability to provide gap filled coverage would be a good choice for a monthly SST product in the Gulf of Alaska for any potential biophysical model to predict the occurrence of *Alexandrium* blooms.

Acknowledgements. Bryan Eder provided support to create figure 1. Jennifer Sveadijian from Coastwatch helped obtain and process the MUR and VIIRS datasets.

References

- Chin, T.M., Vazquez-Cuervo, J., Armstrong, E.M. (2017). *Remote Sens. of Environ.* 200, 154-169.
- Coastwatch (2021). [//coastwatch.noaa.gov/cw/satellite-data-products/sea-surface-temperature/noaa-coastwatch-cogridded.html](https://coastwatch.noaa.gov/cw/satellite-data-products/sea-surface-temperature/noaa-coastwatch-cogridded.html). Accessed November 11th, 2021.
- Lomas, M.W. and Gilbert, P.M. (1999). *Limnol. Oceanogr.* 44, 556-572.
- NDBC, National Data Buoy Center (2021). [//www.ndbc.noaa.gov](http://www.ndbc.noaa.gov). Accessed September 9th, 2021.
- Vandersea, M.W., Kibler, S.R., Van Sant, S.B., Tester, P.A., *et al.*, (2017). *Phycol.* 58, 303-320.
- Wynne, T.T., Mishra, S., Meredith, A., Litaker, R.W., Stumpf, R.P. (2021). *Remote Sens.* 13, 2305.





SURVEILLANCE AND MANAGEMENT



History of Harmful Algal Blooms (HABs) in Indonesia: Factors involved in outbreaks in Lampung Bay

Mariana DB Intan^{1,2*}; Muawanah Muawanah³; Hikmah Thoha²; Martina A. Doblin¹

¹Climate Change Cluster, University of Technology Sydney, P.O. Box 123 Broadway, Sydney, NSW 2007, Australia; ²Research Center for Oceanography (RCO), National Research and Innovation Agency (BRIN), Jl. Pasir Putih No. 1, Ancol Timur, Jakarta 14430, Indonesia; ³Main Center for Marine Aquaculture of Lampung (BBPBL), Jl. Yos Sudarso, Desa Hanura Kec. Padang Cermin, Pesawaran-Lampung 35454, Indonesia

*corresponding author's email: marianadestilabayu.intan@student.uts.edu.au; mari015@brin.go.id

Abstract

In Indonesia, the world's largest island nation, HABs have been observed since the 1970s, where blooms often occur in eutrophic waters surrounding large population centres (e.g., Ambon Bay, Jakarta Bay, and Lampung Bay). Lampung Bay, in particular, has undergone extensive development and is a major economic hub, hosting a large port and a significant aquaculture industry. *Margalefidinium polykrikoides* blooms have been recorded in the inner-middle bay and Legundi Island, in the southern part of the bay. Here, we analyse the monitoring data of *M. polykrikoides* blooms in Lampung Bay from 2012 to 2020 using multivariate analysis (distance-based redundancy analysis). Outbreaks have caused mortality of caged fish including cobia (*Rachycentron canadum*; at low bloom density; from 10^3 to 10^4 cells L^{-1}), pomfret (*Trachinotus blochii*; moderate bloom; 10^5 cells L^{-1}), and grouper (*Cromileptes altivelis*, *Epinephelus fuscoguttatus*, and *E. lanceolatus*; dense bloom; $>10^5$ cells L^{-1}). Bloom density was strongly correlated with salinity and phosphate (DIP) concentration ($P < 0.05$), where dense blooms (from 1.68×10^7 to 4.70×10^7 cells L^{-1}) were associated with high DIP (7 - 12 μM) and moderate to high blooms (from 4.34×10^5 to 4.81×10^6 cells L^{-1}) associated with higher salinity (31.8 - 32). In addition, low (from 1.45×10^3 to 2.81×10^4 cells L^{-1}) and moderate (from 3.1×10^4 to 9.5×10^4 cells L^{-1}) bloom density may be influenced by high nitrate, DO, pH, and temperature ($P < 0.05$). At moderate salinity (31.3 - 31.6), the blooms showed that nitrate and DIP are the dominant macronutrient that limits overall *M. polykrikoides* density in the bay. This study suggests that *M. polykrikoides* blooms in Lampung Bay under wide environmental conditions but that cell densities may be regulated by nutrient availability.

Keywords: *Margalefidinium polykrikoides*, ichthyotoxic, eutrophication, aquaculture, distance-based redundancy analysis (db-RDA)

<https://doi.org/10.5281/zenodo.7032802>



Introduction

Harmful algal blooms (HABs) have been observed in Indonesia since the 1970s. Blooms often occur in waters surrounding large population centres that have experienced eutrophication (e.g., Ambon Bay, Jakarta Bay, and Lampung Bay). Eutrophication is one of several factors (besides hydrodynamics and weather conditions) that leads to more frequent and extensive HABs globally (Anderson *et al.*, 2002, 2012; Damar *et al.*, 2021) including those considered toxic or harmful, can be natural phenomena, the nature of the global problem of harmful algal blooms (HABs).

Margalefidinium polykrikoides outbreaks have exclusively been observed in Lampung Bay. Anthropogenic activities, such as waste water discharge, shipping, and aquaculture, has led to the accumulation of nutrients in Lampung Bay (Damar *et al.*, 2012) that have coincided with more extensive outbreaks of *M. polykrikoides* (expanding to Legundi Island, the southern part of the bay in 2020; Muawanah and Garbono, 2020). Blooms have caused a decline in aquaculture enterprises from 150 farms in 2010 to 26 in 2018 (Muawanah *et al.*, 2018). In this study, we assess monitoring data of *M. polykrikoides* outbreaks in Lampung Bay to investigate the regulation of bloom density by nutrient availability.

Material and Methods

Study Area

Lampung Bay (5° 26' S - 5° 50' S, 105° 10' E - 105° 35' E; Fig. 1), is a shallow water bay (17.6 m mean depth) located in south-

eastern Sumatra (Wiryawan *et al.*, 1999). The tidal pattern is semi-diurnal, influenced by the water mass from the Indian Ocean that is transported through the Sunda strait (Helfinalis, 2000; Wiryawan *et al.*, 1999). The nutrient load in Lampung Bay is 5002.8 t DIN y⁻¹, 1095.56 t PO₄-P y⁻¹ and 14731.5 t SiO₄ y⁻¹ with a relatively long water residence time of 15 days, in comparison to Jakarta that has a shorter water residence time (five days; Damar *et al.*, 2012).

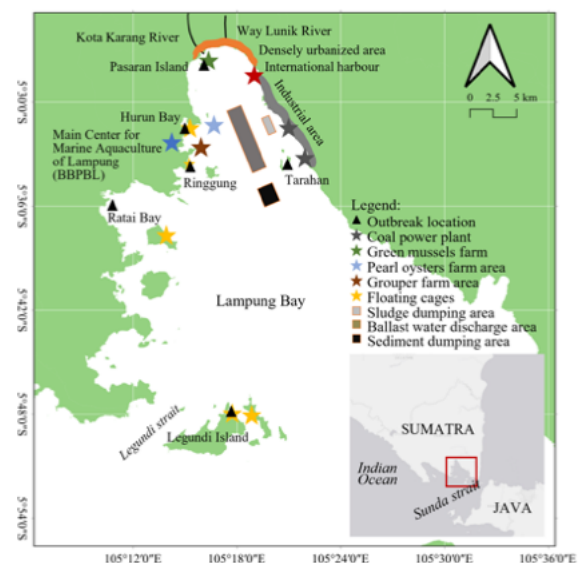


Fig. 1. *Margalefidinium polykrikoides* bloom locations from 2012 to 2020 and main anthropogenic activities in Lampung Bay (modified from Thoha *et al.*, 2019)

In addition to land runoff and anthropogenic activities, nutrient input to Lampung Bay is influenced by oceanographic circulation patterns. During the Northwest monsoon (rainy season) nutrient levels in the mouth of the Kota Karang and Way Lunik rivers and the inner part of the bay are elevated. In



contrast, during the Southeast (SE) monsoon (dry season), the nutrients in the middle and outer part of the bay show a high value due to nutrient-enriched water masses from Java Island that come through the Sunda Strait into the Bay (Damar *et al.*, 2014, 2012).

These nutrient inputs support high primary productivity in Lampung Bay with an annual primary production ranging from 31 to 196 g C m⁻² y⁻¹ (Damar *et al.*, 2014, 2012), which is suitable for aquaculture. However, the bay is susceptible to HABs. Outbreaks of *Alexandrium* sp., *Ceratium furca*, *Chaetoceros socialis*, *Dynophysis caudata*, *Gymnodinium* sp., *M. polykrikoides*, *Noctiluca scintillans*, *Ostreopsis* sp., *Prorocentrum* sp., *Protoperidinium* sp., *Pseudo-nitzschia*, *Pyrodinium bahamense*, and *Trichodesmium* sp. have been reported to occur in Lampung Bay since 2012 (Muawanah unpublished data, 2020).

Monitoring activity

Water quality monitoring has been conducted frequently since 2012 based on reports of blooms in aquaculture areas. Monitoring involved measuring the surface water (turbidity, dissolved oxygen, temperature, and salinity), dissolved nutrients (ammonium, nitrate, nitrite, total DIN, phosphate (DIP)), and phytoplankton density. Dominant phytoplankton found in surface water preserved in Lugol solution (Edler and Elbrächter, 2010) were identified and enumerated under a light microscope (Zeiss, Germany).

Data Analysis

Blooms of *M. polykrikoides* recorded in six locations (Pasaran Island, Hurun Bay, Ringgung, Ratai Bay, Tarahan, and Legundi

Island; figure 1) during 2012-2020 were analysed. To determine the association between environmental parameters and *M. polykrikoides* bloom density, distance-based redundancy analysis (db-RDA) was undertaken. Blooms with incomplete water quality data were excluded from the analysis, leaving 27 samples from five locations (excluding Legundi Island) in the dataset. Kruskal-Wallis statistical tests (significance level $P < 0.05$) were used to assess whether the variation between stations and seasons was significant. Species data were square-root transformed, and all the explanatory variables (environmental parameters) were standardised. The db-RDA reduced model was obtained by subjecting the db-RDA full model to *posthoc* analysis by a variance inflation factor (VIF) to detect multicollinearity within explanatory variables. Explanatory variables with a VIF value > 10 (showing collinearity with other variables) were removed in the reduced db-RDA model, and Monte-Carlo permutations were run to test the model's significance. The most significant explanatory variables in db-RDA best model were observed by obtaining stepwise selection of environmental variables. The db-RDA and its *posthoc* analysis were performed using the “vegan” package in R (Zuur *et al.*, 2007; Borcard *et al.*, 2011).

Results and Discussion

A total of 63 *M. polykrikoides* outbreaks were recorded in Lampung Bay from 2012 to 2020. Blooms were frequently observed in the northern inner bay waters within Hurun Bay (38 events) and Pasaran Island (13 events). However, there was no distinct variation (Kruskal Wallis, $P > 0.05$) in bloom occurrence, mean bloom density, and mean



bloom duration across spatial and temporal scales, meaning *M. polykrikoides* outbreaks arise throughout Lampung Bay and may occur throughout the year.

Table 1. Summary of *Margalefidinium polykrikoides* bloom conditions in Lampung Bay

Variable	Min	Max	Average ± SD	Limit*
Bloom density (cells L ⁻¹)	1.45 x 10 ³	4.70 x 10 ⁷	4.40 x 10 ⁶ ± 1.27 x 10 ⁷	-
Bloom duration (weeks)	1.0	3.7	1.7 ± 1.0	-
Temperature (°C)	28.45	31.38	29.90 ± 0.70	-
Salinity (ppt)	28.50	33.00	31.37 ± 0.90	30 - 34
Nitrate (µM)	0.98	42.20	14.62 ± 8.82	0.13
Ammonium (µM)	0.47	52.28	10.72 ± 10.89	8.81
Phosphate (µM)	0.15	40.72	3.65 ± 7.54	0.12

*Threshold of water quality defined by Minister of Environment and Forestry in Ministerial Decree (No. 51, 2004, Indonesia).

Overall, nutrient concentrations during outbreaks were higher than the regulated threshold (Table 1). The outbreaks often occurred in the afternoon after one day of heavy rains, which were marked by brownish water discolorations and fish mortality (Muawanah *et al.*, 2015). In addition, caged fish killed during mortality events included cobia (*Rachycentron canadum*) at low-density blooms (10³-10⁴ cells L⁻¹), pomfret (*Trachinotus blochii*) during moderate-blooms (10⁵ cells L⁻¹) and grouper (*Cromileptes altivelis*, *Epinephelus fuscoguttatus* and *E. lanceolatus*) during dense blooms (>10⁵ cells L⁻¹), all with excessive mucus on their gills (Muawanah *et al.*, 2013).

Based on the db-RDA best model (P < 0.05; data not shown), salinity and phosphate (DIP) were the two most significant explanatory variables (with an r-square value of 22%) that appeared to influence the distribution of *M. polykrikoides* bloom density in Lampung Bay. Moreover, the db-RDA reduced model (P < 0.05; Fig. 2) showed the inclusion of other environmental parameters (ammonium, nitrate, DO, pH, and temperature) increased the r-square value to 42%.

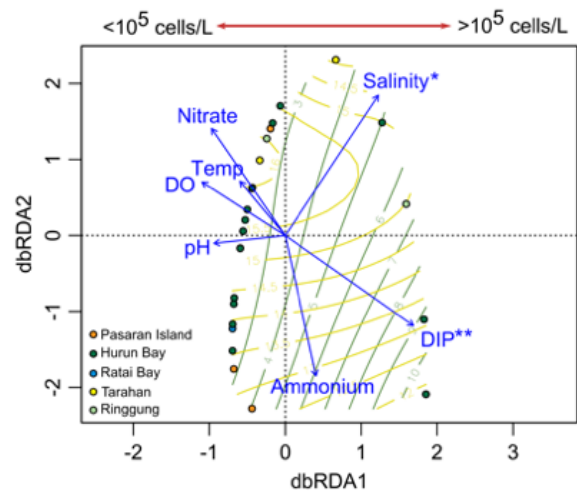


Fig. 2. Ordination of reduced db-RDA model (P < 0.05) on *M. polykrikoides* bloom abundance in Lampung Bay using only explanatory variables with VIF value < 10. Green lines show phosphate (DIP) distributions; Yellow lines show nitrate distribution; ** 0.05; * 0.01.

Thus, the ordination indicates that dense blooms (1.68 x 10⁷ - 4.70 x 10⁷ cells L⁻¹) in Q4 correlates with high DIP (7-12 µM; Fig. 2) and moderate to high blooms (4.34 x 10⁵ - 4.81 x 10⁶ cells L⁻¹) in Q3 correlates with high salinity (31.8-32; Fig. 2). In addition, low (1.45 x 10³ - 2.81 x 10⁴ cells L⁻¹) and moderate (3.1 x 10⁴ - 9.5 x 10⁴ cells L⁻¹) bloom density observed in Q1 and Q2, respectively, may



be influenced by high nitrate, DO, pH, and temperature.

Interestingly, in Q2 and Q4, where the salinity was moderate (ranging from 31.3-31.6 (data not shown), indicative of freshwater runoff), the bloom density seemed to be driven by different factors, high nitrate (15.5-16 μM) in Q2 and high DIP (7-12 μM) in Q4, with the bloom density tending to be lower in Q2 than in Q4. This suggests that nitrate and DIP are the dominant macronutrients that limit overall *M. polykrikoides* density in the bay.

Although our statistical analysis showed no significant difference across location and season, most of the bloom outbreaks under high nitrate (Q2) occurred during the dry season (Southeast (SE) monsoon), with the nutrient source likely being nutrient-enriched water masses that are transported through the Sunda Strait into the Bay, as well as the aquaculture activities observed in this location (Sachoemar *et al.*, 2005; Damar *et al.*, 2012, 2014). Conversely, blooms under high DIP (Q4) were observed during the rainy season (Northwest (NW) monsoon) with nutrients sourced from the Kota Karang and Way Lunik rivers.

Apart from nutrients however, there are other factors (e.g., ecological interactions such as grazing) that were not measured in this study that may help to explain bloom variance. For example, the relative abundance of HAB species within a phytoplankton community is an important context for the competitive success of HABs (Wells *et al.*, 2020). Thus, *M. polykrikoides* abundance as a proportion of the overall phytoplankton biomass may potentially influence the timing and progression of blooms. Furthermore, the

high density of *M. polykrikoides* cysts in the sediment collected at Hurun Bay and Pasaran Island (166.1 and 645.6 cysts g^{-1} dw, respectively; Thoha *et al.*, 2019) may also contribute to inducing high bloom occurrence in these locations (Anderson, 1998).

Given the detrimental consequences of *M. polykrikoides* blooms on caged fish, nutrient management is essential for the sustainability of food production in Lampung Bay. Further studies should involve phytoplankton community and toxicity assessment and ecological processes during bloom and non-bloom periods.

Acknowledgements. The authors are grateful to the Main Center for Marine Aquaculture of Lampung (BBPBL) for providing data for this study. We also thank ISSHA and SCOR for supporting the registration fee for MDBI to attend the virtual ICHA 2021, Mexico.

References

- Anderson, D., Glibert, P.M., Burkholder, J.M. (2002). *Estuaries* 25, 704-726.
- Anderson, D. M. (1998). *NATO ASI Series Vol. G41*, 29-48.
- Anderson, D.M., Cembella, A.D., Hallegraeff, G.M. (2012). *Ann. Rev. Mar. Sci.* 4, 143-176.
- Borcard, D., Gillet, F., Legendre, P. (2011). *Numerical ecology with R (Vol. 2, p. 688)*. New York, Springer.
- Damar, A., Colijin, F., Hesse, K.-J.J., Wardiatno, Y. (2012). *J. Trop. Biol. Conserv.* 9, 61-81.



- Damar, A., Colijn, F., Hesse, K. (2014). *J. Trop. Biol. Conserv.* 11, 63-85.
- Damar, A., Ervinia, A., Kurniawan, F., Rudianto, B.Y. (2021). *IOP Conference Series: Earth and Environmental Science.* 744, 012010.
- Decree of the State Minister of Environmental Affairs No. 51, 2004 (Indonesia), 1-10.
- Edler, L. and Elbrächter, M. (2010). *Microsc. Mol. Methods Quant. Phytoplankt. Anal.* 110, 13-20.
- Helfinalis (2000). *Pesisir dan Pantai Indonesia [Indonesian Coastal and Beach] IV*, 31-37.
- Muawanah, Kurniastuty, K., Haryono, T., Widiatmoko, W. (2013). *Buletin Bududaya Laut [Marine Aquaculture Newsletter] No. 34*, 1-10.
- Muawanah, Haryono, T., Widiatmoko, W., Purnomowati, R. (2015). *Buletin Bududaya Laut [Marine Aquaculture Newsletter] No. 39*, 1-15.
- Muawanah, Purnowati, R., Rosiah. (2018). *Buletin Bududaya Laut [Marine Aquaculture Newsletter] No.45*, 1-13.
- Muawanah and Garbono, A. (2020). Unpublished. Monitoring Report. Main Center for Marine Aquaculture of Lampung (BBPBL). Directorate General of Aquaculture (KKP), 1-10.
- Muawanah (2020). [Unpublished data]. Main Center for Marine Aquaculture of Lampung (BBPBL). Directorate General of Aquaculture (KKP).
- Sachoemar, S.I., Muawanah, Yanagi, T. (2005). *Bay. Coast. Mar. Sci.* 30, 1-6.
- Toha, H., Muawanah, Bayu Intan, M.D., Rachman, A., *et al.*, (2019). *Front. Microbiol.* 10, 1-12.
- Wells, M.L., Karlson, B., Wulff, A., Kudela, R., *et al.*, (2020). *Harmful Algae* 91, 101632.
- Wiryanah, B., Marsden, B., Susanto, H.A., Mahi, A.K., Ahmad, M., Poespitasasri, H. (Eds.). (1999). *Lampung Coastal Resources Atlas. Bandar Lampung: Coastal Resources Center, University of Rhode Island and Centre for Coastal and Marine Resources Studies, Bogor Agricultural University.*
- Zuur, A. F., Ieno, E. N., Smith, G. M. (2007). *Analysing ecological data (Vol. 680)*. New York: Springer.



Harmful algal blooms along central Guatemalan Pacific coast

Paz-Cordón, Karla Evelyn^{1*}, Okolodkov, Yuri B.², Cobo-Gradín, Fernando³, Ortíz-Aldana, José Roberto¹, Martínez-Dubón, Rebecca Magali¹

¹Instituto de Investigaciones Hidrobiológicas, Centro de Estudios del Mar y Acuicultura, Universidad de San Carlos de Guatemala, Ciudad de Guatemala, Guatemala; ²Instituto de Ciencias Marinas y Pesquerías, Universidad Veracruzana, Boca del Río, Veracruz, Mexico; ³Universidad de Santiago de Compostela, Pontevedra, Galicia, Spain.

*corresponding author's email: kevelynpaz@gmail.com

Abstract

Along the Guatemalan Pacific coast, sporadic studies on harmful algal blooms (HAB) date back to 1987 when 193 human intoxications (including 22 deaths) caused by the dinoflagellate *Pyrodinium bahamense* were reported. In recent years, HAB in the study zone have been caused by *Margalefidinium polykrikoides* and *P. bahamense*; however, the reports do not mention accompanying species. To fill this gap, studies on phytoplankton and its spatial-temporal changes in relation to physical-chemical variables were initiated. In November 2019, *P. bahamense* reached an abundance of 1.00×10^4 cells L⁻¹. In September 2020, *M. polykrikoides* vegetative cells reached 1.24×10^6 cells L⁻¹ and its cysts 1.53×10^6 cells L⁻¹. *Noctiluca scintillans* bloomed in November 2020 and March 2021 (up to 1.20×10^6 cells L⁻¹). Since January 2021, monthly monitoring has been launched at three sampling stations with site depths from 1.5 to 5 m at 3-5 km from the coastline. In March 2021, a *M. polykrikoides* bloom was detected (1.20×10^6 cells L⁻¹). Yearly monitoring allowed us to follow seasonal changes in both harmful species and the entire phytoplankton community; this is recommended for considering when studying a bloom event.

Keywords: Guatemala, harmful algal blooms, *Margalefidinium*, Pacific, *Pyrodinium*

<https://doi.org/10.5281/zenodo.7032902>



Introduction

Plankton studies in Guatemala are associated with the history of algal blooms due to poisoning problems in humans that occurred in August 1987, when 193 intoxications due to shellfish consumption were reported on the Pacific coast of Guatemala, of which 22 cases were fatal (Rosales *et al.*, 1989). *Pyrodinium bahamense* var. *compressum* was the causative agent that produced a paralytic toxin. The species was reported again as blooming in November 2019 in coastal waters of Guatemala's Pacific (Paz-Cordón, 1997). The main objective of this study was to contribute to the knowledge of phytoplankton diversity, distribution and abundance and its relationship with the physico-chemical variables in Guatemala's Pacific.

Material and Methods

The sampling zone was located at Puerto Quetzal, in the area of the submarine San José Canyon, which cuts the continental slope perpendicularly and runs into the Mesoamerican Trench, near the sediment plumes of the Achiguate and María Linda rivers (Fig. 1).

Monthly monitoring was performed from January to May 2021 in the morning between 8:00 and 12:00. Phytoplankton was collected from three sites (at the Texaco, Entre Morros and Recalada navigation buoys) from 1.5 m and 5 m depths using a 6.4 L Van Dorn water bottle. Additionally, horizontal surface tows were taken for 5 min at each station with a hand net of 25 μ m mesh size. The samples were fixed with acid Lugol solution and stored in 500 mL Kimax-Kimble glass bottles in a cooler. Transparency was measured with

a Secchi disk. Surface water temperature, dissolved oxygen, conductivity and salinity were measured and recorded using a HANNA HI-98194 multiparameter meter.



Fig. 1. Phytoplankton sampling sites at three navigation buoys from January to May 2021.

In the laboratory, total dissolved solids (TDS), phosphorus, ammonium, total nitrogen, sulphates and chlorophyll-*a* were measured by the absorbance technique using prepared solutions and calibration curves. Phytoplankton cells were counted under an Olympus CKX41 inverted microscope using the Utermöhl technique after sedimentation in 50 mL cylinders. To determine the differences in abundance between months and sampling site, a non-parametric Kruskal-Wallis test and a one-way ANOVA analysis were applied. To elaborate the species-accumulation curve the program EstimateS (version 9.1.0) and non-parametric estimators Chao 1 and ACE (Abundance-based Coverage Estimator) were used.

In addition, from October to November 2019, bivalves were collected for saxitoxin determination using a mouse bioassay at the National Laboratory of Health in cooperation



with the Directorate of Normativity of Fishery and Aquaculture of the Ministry of Agriculture, Livestock and Food (MAGA in Spanish) of Guatemala. These bloom events were observed by the Guatemala National Commission of Red Tide Studies. Saxitoxin concentration was determined by the AOAC official method 959.08.16.

Results and Discussion

The site depths varied between 20 m and 30 m, and bottom sediments were limesand (Entre Morros and Recalada buoys) or sand (Texaco buoy). During the study period the mean surface water temperature was 28.79 °C (ranging from 27.77 to 30.72), the mean salinity was 33.67 (ranging from 33.15 to 33.76) and the mean transparency was 23.37 m (from 5 to 35 m).

Cyanobacteria contributed up to 46% in terms of abundance, mainly due to *Trichodesmium erythraeum*. From January to February it was one of the dominant species in net samples. Dinoflagellates were the most abundant (71%) during the study period, followed by diatoms (23%). Among other major taxonomic groups, cyanobacteria were most important, contributing about half in terms of abundance, mainly represented by the filamentous colonial *T. erythraeum*. Among dinoflagellates, at the level of order, the Gymnodiniales predominated in abundance (56%), mainly due to *Akashiwo sanguinea* and *Margalefidinium polykrikoides* (both vegetative cells and cysts), followed by the Gonyaulacales (33%), Peridiniales (6%), Prorocentrales (3%), Dinophysiales and Noctilucales (1% each). The diatoms from the order Thalassiosirales were the most abundant (Table 1), mainly represented by

Lauderia annulata, *Planktoniella sol* and *Skeletonema tropicum*.

Table 1. Mean abundances of planktonic diatoms at the order level in the central Guatemalan Pacific from January to May 2021.

Order	Mean abundance (cells L ⁻¹)
Bacillariales	19.47
Biddulphiales	2.72
Briggerales	1.96
Chaetocerotales	11.33
Coscinodiscales	8.07
Eupodiscales	2.52
Hemiaulales	0.47
Lithodesmiales	0.56
Melosirales	1.40
Naviculales	7.14
Rhaphoneidales	1.40
Rhizosoleniales	9.44
Stephanopyxales	1.87
Thalassionematales	2.24
Thalassiosirales	30.20

No significant differences in phytoplankton abundances occurred between sampling sites or between the two sampling depths at each site (Kruskal-Wallis test, $p = 0.6742$); however, there were significant differences between months ($p = 0.004$). No significant differences in species richness between sampling sites or months were observed (ANOVA, $p = 0.3056$).

In March 2021, high phytoplankton abundances occurred at Entre Morros and Recalada buoys at the entrance to Port



Quetzal. It is a hydrodynamically active area influenced by currents produced by ships that also resuspend bottom sediments forming sand banks.

In general, both the highest species richness and abundance were found at 1.5 m depth. The Simpson index varied inversely with heterogeneity: the index values decrease or increase according to the increase or decrease in diversity, respectively. The index of dominance overestimates the role of the most abundant species at each sampling site, which allowed us to observe a very close relationship (in terms of physico-chemical variables, species richness and cell abundance) between Entre Morros and Recalada buoys. Pielou's equitability index was highest at the Texaco buoy at 1.5 m depth, where *Pseudo-nitzschia* sp., *S. tropicum* and *M. polykrikoides* cysts dominated. This sampling site is located closer to the Achiguat River and further from the port operations than other sites. River runoff increased during the study period under the influence of the El Niño-Southern Oscillation phenomenon; this may have resulted from the above average rainfall.

The Bray-Curtis dissimilarity in cell abundance between sampling sites and sampled depths (in total, six) revealed two groups (Fig. 2): (1) the Entre Morros and Recalada buoys, and (2) the Texaco buoy.

Hitherto, the species richness from the three sampling sites reached 111; however, after five monthly surveys it has not reached an asymptote although the database includes 8,784 species records.

During October and November 2019, blooming planktonic microalgae were

sampled at the Entre Morros and Recalada buoys and counted in a 1 mL Sedgwick-Rafter chamber. In October 2019, *Pyrodinium bahamense* var. *compressum* reached 3.90×10^4 cells L^{-1} , and saxitoxin concentration reached 3,275 MU 100 g^{-1} . Cell abundances and saxitoxin concentrations were 3,037 MU 100 g^{-1} and 1.01×10^4 cells L^{-1} on November 7, and 5,200 MU 100 g^{-1} and 3.90×10^4 cells L^{-1} on November 22, respectively (saxitoxin concentration is given in mouse units per 100 g of bivalve mollusc flesh). Historically, *M. polykrikoides* vegetative cells and cysts and *P. bahamense* var. *compressum* have caused blooms in the central Guatemalan Pacific. In November 2020, a *Noctiluca scintillans* bloom was reported in the marina of the Port of Quetzal, and for the first time for the study area the abundance of this species was estimated; *N. scintillans* was observed again in March 2021.

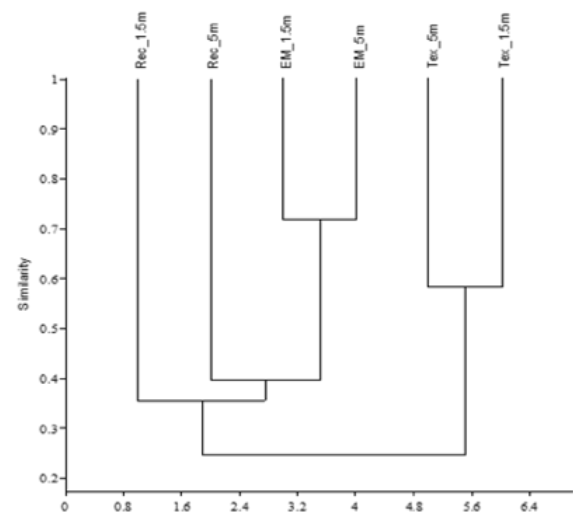


Fig. 2. Bray-Curtis dissimilarity in cell abundance between sampling sites (three) and sampled depths (two per site: 1.5 m and 5 m); Rec: Recalada, EM: Entre Morros, Tex: Texaco.



Although the monitoring of harmful phytoplanktonic species has been focused on a few critical species, it should be continued in the framework of phytoplankton monitoring in general to trace any blooms caused by other species. Inter-institutional collaboration continues to be an important way to obtain meaningful results.

Acknowledgements. The monitoring was performed within the framework of the project “Strengthening capacities in marine and coastal environments using nuclear and isotopic techniques” (RLA 7025; financed by the International Atomic Energy Agency through the Network of Studies on Marine-Coastal Stressors of the Latin America and Caribbean (REMARCO in Spanish); local coordinator on a harmful algal stressor: KEPC). The study was possible due to the collaboration between CEMA-USAC, the Department of Observation and Marine Research (OBIMAR in Spanish) of the Quetzal Port Company and the Pacific Naval Command of Guatemala

References

Paz-Cordón, K.E. (1997). Tesis de licenciatura. Universidad de San Carlos de Guatemala, Centro de Estudios del Mar y Acuicultura, Ciudad de Guatemala, Guatemala. 127 pp.

Rosales-Loessener, F.M.W. (1989). In: Okaichi, T., Anderson, D.M., Nemoto, T. (Eds). Red tides: Biology, environmental science and toxicology, pp. 113-116. Elsevier Science Publishing, Amsterdam, The Netherlands.



Human poisonings by neurotoxic phycotoxins related to the consumption of shellfish: study of cases registered by the French Poison Control Centres from 2012 to 2019

Sandra Sinno-Tellier¹, Eric Abadie², Luc de Haro³, Nathalie Paret⁴, Jérôme Langrand⁵, Gaël Le Roux⁶, Magali Labadie⁷, Juliette Bloch¹, Nicolas Delcourt⁸

¹French Agency for Food, Environmental and Occupational Health & Safety, Maisons-Alfort, France; ²French Research Institute for Exploitation of the Sea, Sète, France; ³Poison Control Centre, Marseille University hospital, Marseille, France; ⁴Poison Control Centre, Lyon University hospital, Lyon, France; ⁵Poison Control Centre, Paris University hospital, Paris, France; ⁶Poison Control Centre, Angers University hospital, Angers, France; ⁷Poison Control Centre, Bordeaux University hospital, Bordeaux, France; ⁸Poison Control Centre, Toulouse University hospital, Toulouse, France.

*corresponding author's email: sandra.sinno-tellier@anses.fr

Abstract

In June 2019, a paralytic shellfish poisoning case related to the consumption of mussels contaminated by saxitoxin at a concentration below the regulatory threshold alerted the health authorities to probable undetected human cases of poisoning by neurotoxic phycotoxins. ANSES, PCCs and Ifremer conducted a retrospective study of poisoning cases by bivalve shellfish recorded by the French PCC from 2012 to 2019. Cases that could be related to neurotoxic phycotoxins were identified. Diagnosis was based on symptoms compatible with ingestion of contaminated shellfish and on contamination data for the shellfish production area, or notifications to the European Rapid Alert System for Food and Feed. Among the 619 shellfish poisoning cases recorded in the national PCCs database (SICAP) during the study period, 134 (22%) had at least one neurological symptom. Review of all medical records and environmental data led to suspicion of 14 cases of paralytic shellfish poisoning and one case of amnesic shellfish poisoning. Five patients experienced persistent neurological symptoms. Marine toxins were not tested in the blood or urine of these patients. This study led ANSES, PCCs and Ifremer to develop a prospective questionnaire and to recommend actions to take when neurological symptoms related to shellfish consumption are reported to a PCC. Daily monitoring of shellfish poisoning cases registered in the SICAP was also implemented in order to rapidly detect any cases suspected of being related to neurotoxic phycotoxins, alert the competent authorities, and warn the general population.

Keywords: domoic acid, saxitoxin, poison control centre, phycotoxins, shellfish

<https://doi.org/10.5281/zenodo.7032934>



Introduction

In June 2019, the Rapid Alert System for Feed and Food (RASFF) informed the competent European authorities of two batches of mussels imported from Italy that were contaminated by saxitoxin. During the same period, a Poison Control Centre (PCC) reported the case of a person who had developed neurological signs potentially associated with the consumption of contaminated mussels to the French National Agency for Food, Environmental and Occupational Health and Safety (ANSES), responsible for coordinating toxicovigilance in France (Delcourt *et al.*, 2021). The symptoms and the time to onset were consistent with paralytic shellfish poisoning (PSP) according to the US Centers for Disease Control definition of PSP (McLaughlin *et al.*, 2011). However, confirmation of this assumption met with two difficulties: the saxitoxin concentrations measured in the mussels from the implicated batch (313 $\mu\text{g eq STX kg}^{-1}$ mussel flesh) were below the regulatory threshold (800 $\mu\text{g eq STX kg}^{-1}$ shellfish flesh); no biological samples (blood, urine, etc.) had been collected to test for saxitoxin. The link between the symptoms and exposure to paralytic toxins was established based on the report received by the RASFF from the product distributor, which was not mandatory since the measured concentrations were below the regulatory limit. This alert highlights the probable under-diagnosis of human poisoning cases with neurotoxic phycotoxins, since the link between shellfish consumption and neurological signs is, depending on the situation, neither routinely sought nor established.

In this context, ANSES carried out a review of bivalve shellfish poisoning cases recorded by the French PCCs, looking for a link with environmental monitoring data when possible, specifically in order to identify those cases presenting neurological signs compatible with neurotoxic phycotoxins.

Material and Methods

Study design

This retrospective descriptive study was based on symptomatic poisoning cases related to the consumption of shellfish recorded by all of the French PCCs between the 1st of January 2012 and the 31st of December 2019.

Case definition

Cases were defined as symptomatic human poisoning in relation to bivalve mollusc consumption in France, regardless of symptomatology, registered by the PCCs. Cases of poisoning that occurred abroad, or with no causality between the suspected exposure agent and the symptoms, or without symptoms, were excluded from the study.

Data were extracted from the French PCC national database (SICAP), where all PCC cases, corresponding to “patients”, are collected in medical records, corresponding to “events”, each event (or shellfish meal in this study) containing either a single case or collective cases related to the same exposure. Among included cases, those with neurological symptoms were selected. A toxicologist reviewed all the medical records in which at least one neurological symptom was reported to specifically search for and describe cases that could be related to



neurotoxic phycotoxins, taking into account the type of symptoms and their time of onset after shellfish consumption. Cases with symptoms suggestive of an allergic reaction were excluded. The diagnosis was made retrospectively based on the clinical signs recorded, as well as, when the origin of the shellfish was known, co-occurrence with shellfish contamination reported in the monitored production areas (based on REPHYTOX database) or RASFF notification of imported products.

The REPHYTOX network, whose data are analysed by the French Research Institute for Exploitation of the Sea (Ifremer), under the authority of the Ministry of Agriculture and Food, collects samples from several hundred shellfish sites. This is sufficient to provide the authorities in charge of public health safety with information to make decisions on bans in harvesting areas.

Results and Discussion

Among the 727 cases coded as shellfish poisoning extracted from the SICAP during the study period, we included 619 patients, all types of symptoms combined, distributed in 452 events. In 19.5% of events, the number of patients per event was between two and eight. We excluded 108 cases unrelated to shellfish consumption, or with no causal link, or for which shellfish was consumed abroad. Fifty percent of the 452 included meals involved oysters, 33% mussels, 11% scallops, 2% mussels and oysters, and other shellfish for the remainder (4%).

Temporal distributions

As shown in figure 1, the annual trend of events (shellfish meals) remained steady from 2012 to 2017 and ranged from 58 to 42

during this period. The trend then increased gradually from 2018 to 2019, when 68 and 82 events were observed. The annual distribution of cases followed the same trend with more pronounced variations in numbers, since some events involved up to eight patients.

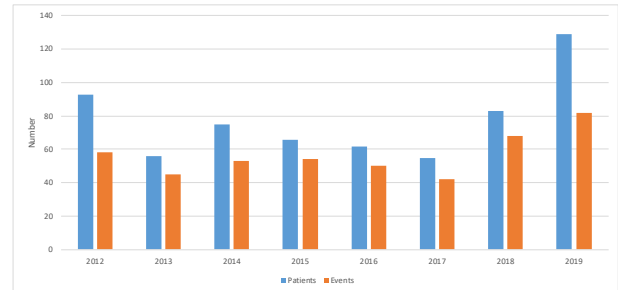


Fig. 1. Annual distribution of intoxicated patients and related events (shellfish meals). Data from January 2012 to December 2019. Source: SICAP.

We observed yearly seasonality in shellfish poisoning. Oyster poisoning showed winter seasonality, with a peak in December (representing 42% of patients and 37% of events) (Fig. 2). The seasonality of mussel poisoning was less pronounced, with poisoning occurring year-round.

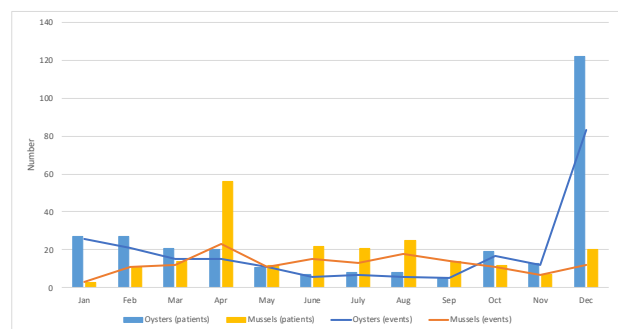


Fig. 2. Cumulative monthly distribution of intoxicated patients and related events (shellfish meals) with oysters and mussels. Data from January 2012 to December 2019. Source: SICAP.



Case description

Age of cases ranged from eight months to 93 years, with a mean age of 45.7 years \pm 20.3 and a median age of 45 years (missing age for 8% of the 619 patients included). The sex ratio M/F was 0.7 (240/330).

While, as expected, 88% of the patients developed one or more digestive symptoms (vomiting for 61%, diarrhoea for 47%, and nausea for 27%), 22% (134 patients) experienced at least one neurological symptom (headache 10%, dizziness 4%, paraesthesia 3%), alone or combined with other symptoms. Three quarters of the patients who presented at least one neurological symptom also reported a digestive symptom, which helped identify the possible food origin of the symptoms.

Cases related to neurotoxic phycotoxins

Review of medical records for the 134 patients in whom a neurological sign was mentioned led to the *a posteriori* identification of 15 patients related to the consumption of bivalves contaminated by a neurotoxin phycotoxin. PSP was suspected for 14 patients and amnesic shellfish poisoning (ASP) for one patient. No poisoning with other marine neurotoxins (pinnatoxins, tetrodotoxins, or brevetoxins) was suspected based on the available information. Marine toxins (saxitoxin, domoic acid) were not tested for in the blood or urine of any of these patients.

The 14 patients with PSP had consumed 11 meals; 10 of them had eaten mussels, while the others had eaten oysters, scallops or clams. Six patients had developed paraesthesia, affecting their hands and/or their feet in four cases and the mouth in two cases; five patients had experienced muscle pain or cramps, two of these had also developed paraesthesia.

Neurological symptoms occurred within 2 h and 30 min for half of the patients, and from 5 min to 72 h for all of them.

While the severity of the reported symptoms was mild (PSS1; Persson *et al.*, 1998) in 10 cases, four patients experienced more severe or persistent neurological symptoms (PSS2): bilateral paraesthesia of the hands and/or the feet, ascending paraesthesia from the hand to the arm, and associated muscle stiffness. The symptoms spontaneously regressed within 12 h in the 11 patients where the clinical outcome was known.

The origin of the consumed shellfish was available in the medical record regarding six meals (eight cases). A specific episode of shellfish contamination in the harbour of the city of Brest, Brittany in 2012 was linked to one probable case of PSP. Similarly, other recurrent episodes of shellfish contamination in the Étang de Thau (lagoon on the Mediterranean coast) could have caused five cases of PSP from 2015 to 2016. Two other meals could be linked to the June 2019 RASFF alert notification concerning mussels imported from Italy.

Lastly, the 15th patient developed memory disorders and severe mental confusion (PSS3) following the consumption of dog cockles and whelks. As the origin of the shellfish was known, the REPHYTOX data from the same period showed concentrations of domoic acid above the regulatory threshold, suggesting ASP. The patient, who had been admitted to an intensive care unit, made a full recovery.

To our knowledge, this is the first time that human poisoning, recorded by the French PCCs, can be linked to contamination of



shellfish production areas, since the first recording of saxitoxin in shellfish production areas in France in 1988 and domoic acid in 1999.

However, the data should be interpreted with caution given that the cases collected by the PCCs are not exhaustive, and their representativeness remains unknown. People who present symptoms after a shellfish meal may consult a doctor or a pharmacist, go to the emergency department of a hospital, or choose self-medication, without calling a PCC.

Our 14 cases of PSP demonstrated the common findings of neurologic and gastrointestinal symptoms related to saxitoxin poisoning (Etheridge, 2010; Hurley *et al.*, 2014). While four cases of PSP reported persistent neurological symptoms, no life-threatening cases or deaths occurred. Monitoring programs of shellfish poisoning by marine biotoxins have probably minimized the risk of severe human cases.

As toxicological assays of neurotoxins in human matrices (serum, urine) are currently not routinely performed by medical analysis laboratories, determination of the type and origin of the shellfish is essential in order to seek information on toxin concentrations detected by REPHYTOX or in RASFF notifications when shellfish have been imported.

ANSES, PCCs and Ifremer developed a specific guide to collect information when a person reports neurological signs after shellfish consumption and to recommend actions to take for further investigations. The patients should keep and freeze any

meal leftovers for subsequent analyses. Measurement of toxin concentrations in unconsumed shellfish are key, especially when poisoning is associated with shellfish harvested from uncontrolled areas.

The suspected cases should be referred to the emergency department of a hospital, for collection of biological samples that may be frozen (in particular for *a posteriori* testing for marine toxins, even those not yet regulated in European countries such as pinnatoxins and brevetoxins). These samples will help to confirm the poisoning.

Daily automatic monitoring of cases of shellfish poisoning recorded in the PCC national database was also set up to detect any suspected case the day following the call to the PCC. The aims are to launch appropriate investigations, alert the competent authorities, and inform the population as soon as possible.

Acknowledgements. The authors would like to thank all the members of the French Poison Control Centers.

References

- Delcourt, N., Arnich, N., Sinno-Tellier, S., Franchitto, N. (2021). *Clin. Toxicol.* 59, 7677.
- Etheridge, S. M. (2021). *Toxicol.* 56, 10822.
- Hurley, W., Wolterstorff, C., MacDonald, R., Schultz, D. (2014). *West. J. Emerg. Med.* 15, 37881.
- McLaughlin, J.B., Fearey, D.A., Esposito T.A., Porter, K.A. (2011). *Morbidity and Mortality Weekly Report (MMWR)*, 18 November 2011, sect. 60 (45).



Persson, H. E., Sjöberg, G.K, Haines, J.A,
Pronczuk de Garbino, J. (1998). J. Toxicol.
Clin. Toxicol. 36, 20513.



A multi-year study on the detection and distribution of domoic acid contamination of shellfish in production areas from Los Lagos Region, Chile (2000-2021)

Benjamín A. Suárez-Isla*, Fernanda Barrera, Juliana Calbuyahue, Daniel Carrasco, Américo López-Rivera, Ignacio Rubilar, Carolina Tamayo

Laboratory of Marine Toxins, Institute of Biomedical Sciences, Faculty of Medicine, University of Chile. Santiago and Castro, Chile.

*corresponding author's email: bsuarez@u.uchile.cl

Abstract

Domoic acid, a marine neurotoxin causative of Amnesic Shellfish Poisoning (ASP) was first detected in Chilean shellfish in January 1997. The presence of domoic acid (DA) in shellfish extracts was determined by reverse-phase HPLC-UV. Domoic acid concentrations exceeded in some instances the maximum permitted level (MPL) of 20 mg kg⁻¹ of tissue. The highest levels were found in mussels (*Mytilus chilensis*) and its presence was associated with diatom blooms of the genus *Pseudo-nitzschia*. Since the diatoms *P. cf. australis* and *P. cf. pseudodelicatissima* are frequent phytoplankton components with a wide distribution in Chilean coastal waters, a permanent ASP monitoring program was implemented by the National Fisheries Service (Sernapesca) in 2000. Analyses of live shellfish samples collected from production areas from Los Lagos Region (41°30' to 42°30' S) are reported from January 1999 to May 2021. A total of 94 from 57,882 samples (0.16%) were found to contain DA above 20 mg kg⁻¹. Another 1,360 samples (2.35%) contained DA below MPL (0.01 to < 20 mg kg⁻¹). Diatom blooms and domoic acid were detected every year. However, toxicity levels above MPL were observed only in nine of the 22 years of continuous monitoring. Regular increases in toxicity were observed mainly during the transition from spring to summer (October to March) with peaks during December and January. High detoxification rates of DA from mussels ($T_{1/2} < 4 \pm 1$ days) allowed the development of contingency plans during the blooms that minimized harvest closures. Despite its recurrent nature, the risk observed to date has been low, with no reported cases of poisoning in humans, marine mammals, or birds.

Keywords: *Pseudo-nitzschia* diatoms, domoic acid, management, monitoring, mussels

<https://doi.org/10.5281/zenodo.7032974>



Introduction

Marine biotoxins of the paralytic and diarrhetic type have caused severe public health and economic impacts in southern Chile (41° - 55° SL) and are produced mainly by toxigenic dinoflagellates, such as *Alexandrium catenella* since 1972, and *Dinophysis acuta* since 1994, respectively (Díaz *et al.*, 2019; Sunesen *et al.*, 2021). In addition, blooms of the potentially toxic pennate diatoms of the genus *Pseudo-nitzschia* are common and distribute over large coastal areas of Chile (18° to 54° SL) (Suárez-Isla *et al.*, 2002; Alvarez *et al.*, 2009; Pizarro *et al.*, 2017; Díaz *et al.*, 2019).

An early paper by Rivera (1985) reported the presence of several *Pseudo-nitzschia* species in Chile (*P. australis*, *P. calliantha*, *P. cuspidata*, *P. delicatissima*, *P. pungens* and *P. fraudulenta*). The species *Pseudo-nitzschia pseudodelicatissima* and *P. fraudulenta* were described by Espinoza-González *et al.* (2016) and *P. seriata* by Pizarro *et al.* (2017) and Pinto-Torres *et al.* (2018 a, b). Only four toxigenic *Pseudo-nitzschia* species were associated with the production of domoic acid (DA), which was detected in cultures and samples: *P. australis* (Suárez-Isla *et al.*, 2002), *P. calliantha* (Alvarez *et al.*, 2009), *P. seriata* and *P. delicatissima* in the Magallanes region by Pizarro *et al.* (2017), Pinto-Torres *et al.* (2018b) and Díaz *et al.* (2019).

Previous studies have found significant accumulation of DA in mussels, scallops, and a tunicate, well above the regulatory limit of 20 mg kg⁻¹. In November 1999, maximum levels of 330 mg kg⁻¹ were detected in mussels from Chiloé following a bloom with high dominance of *P. australis* (Suarez-Isla *et al.*, 2002). In scallops from Northern

Chile, levels of 103 mg kg⁻¹ were detected during a *P. australis* bloom. (Alvarez *et al.*, 2009). Domoic acid was found in lower concentrations in edible tissues in native sea squirts (*Pyura chilensis* Molina, 1782) (8.7 to 15.5 mg kg⁻¹), showing the complex impact of these blooms on the marine food chain (López-Rivera *et al.*, 2009).

Los Lagos Region (41°30' to 42°30' S) includes the Chiloé archipelago and the Chiloe Inner Sea (Fig. 1). This is a unique ecosystem and an important shellfish aquaculture area (Seguel and Sfeir, 2010). Mussel aquaculture has grown steadily at an annual rate of 12% since 2002. In 2020, more than 495,000 tons were landed, with more than 90% of this production destined for export. This production had a value of more than US\$250 million, and 400,304 tons were accounted for by *Mytilus chilensis* only, while other species were harvested for export and domestic consumption

Annual blooms of *Pseudo-nitzschia* diatoms and the presence of domoic acid in shellfish have affected the local economy within the Los Lagos Region since 1999 (Figs. 1, 2). We report here the detection and distribution of DA in extracts from Chilean shellfish tissues collected from commercially relevant aquaculture sites and natural beds as part of a national shellfish sanitation program. Domoic acid concentrations exceeded the regulatory level of 20 mg kg⁻¹ of tissue in a few cases. The presence of the toxin was associated with blooms in which pennate diatoms of the genus *Pseudo-nitzschia* were highly dominant (> 90%). These blooms have not been associated to date with confirmed cases



of human Amnesic Shellfish Poisoning (ASP) intoxications, but pose a serious potential public health threat. Because diatoms *P. cf. australis* and *P. cf. pseudodelicatissima* (and others) are common phytoplankton constituents that are widely distributed in Chilean coastal waters, a permanent ASP monitoring program was implemented by the Servicio Nacional de Pesca (Sernapesca) as part of a Chilean National Shellfish Sanitation Program (NSSP, 2021). The NSSP includes over 150 sampling stations throughout Los Lagos Regions (Fig. 1). Weekly samples of live shellfish, phytoplankton, and abiotic parameters were collected by certified samplers. The frequency of sampling was increased during contingencies when causative toxic species and/or toxins were detected. This program also includes analyses of chemical contaminants (pesticides and heavy metals: Hg, Cd and Pb) and microbiological pathogens (*Escherichia coli*, *Salmonella*, and *Vibrio parahaemolyticus*) from lower frequency samples. The data sets are integrated into an on-line early warning system (mr-SAT) for local health authorities responsible for setting precautionary closures.

Materials and Methods

Shellfish samples and analysis

Statutory analyses were performed at the Laboratory of Marine Toxins on live shellfish samples provided by the NSSP. Domoic acid was determined by reverse-phase HPLC analysis with UV detection (after Quilliam *et al.*, 1995; López-Rivera *et al.*, 2005). For each analysis, a sample of 200 g wet weight of shellfish containing between 12 to 18 individuals was used. The method was in-house validated and accredited according to ISO 17025:2017 (LOD = 0.01 mg kg⁻¹).

Certified reference materials were provided by NRCC, (Canada).

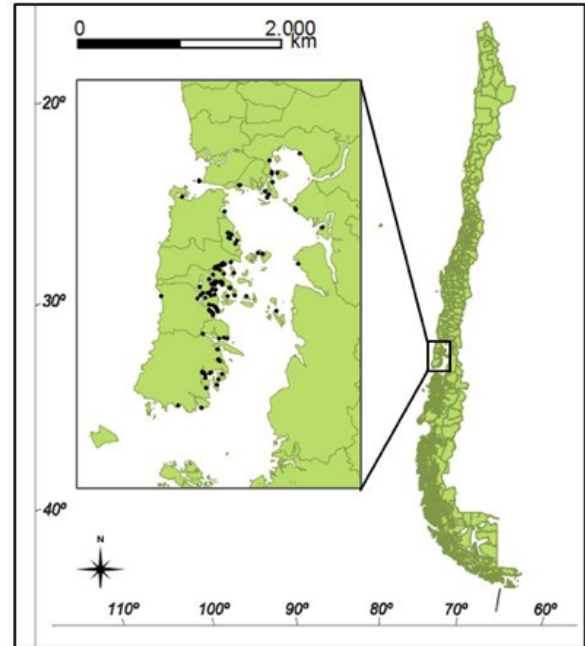


Fig. 1. Map of Chile indicating the location of Los Lagos Region. Black circles, sampling stations.

Data sets

Analyses of live shellfish samples collected from production areas from Chiloé archipelago, Los Lagos Region from January 1999 to May 2021 are reported. Shellfish samples (mussels 90%, clams 9%, 1% other) were collected weekly from 102 NSSP sampling sites (Fig. 1). Phytoplankton cell densities were retrieved from data sets from 18 stations from the Institute for Fisheries Research (IFOP) regional monitoring program reports, which include 10 monthly surveys per year (IFOP 2016). Phytoplankton net samples are collected monthly following IFOP methodology (IFOP 2016) and in the areas identified in figure 2. Microscopic identification and concentrations of cells

per liter are obtained from cell counts on Uttermohl chambers. IFOP has been providing time series of phytoplankton distribution and toxin levels along with environmental and oceanographic parameters from the three southernmost regions since 2006.

Results and Discussion

A total of 94 from 57,882 samples (0.16%) were found to contain DA above 20 mg kg⁻¹. Another 1,360 samples (2.35%) contained DA below the MPL (0.01 to < 20 mg kg⁻¹). These results provide the first detailed long-term study of the occurrence and distribution of DA in the Inner Sea of Chiloé (Fig. 2). Diatom blooms and domoic acid were detected every year. However, toxicity levels above MPL were observed in only nine of the 22 years of continuous monitoring.

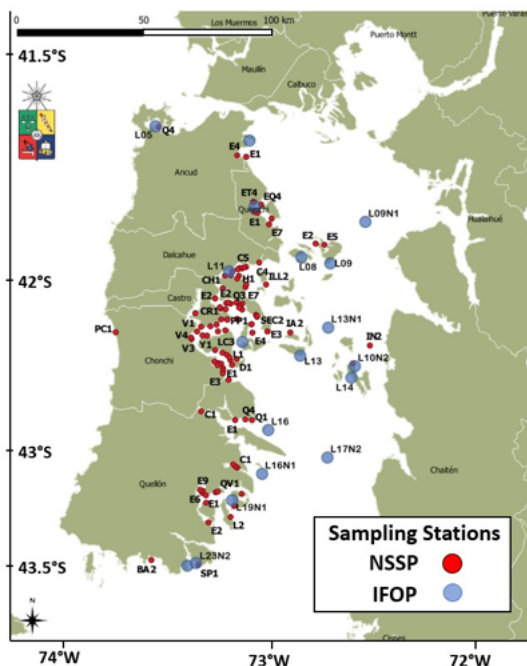


Fig. 2. Distribution of NSSP sampling stations (in red) and IFOP stations (in blue).

In the Southern hemisphere, the transition from spring to summer occurs in December. To account for the seasonality of the blooms, figure 3 depicts data for the second semester of a given year, followed by the first half of the following year. Toxin detections per sampling station are reported as:

$$\text{Detection rates} = \frac{\text{N}^\circ \text{ of detections} * 100}{\text{total N}^\circ \text{ of analysis per yearly period}}$$

The solid line represents the total number of samples per yearly period. From 2006 to 2021, the average of annual samples was 3,209 ± 302 (9.41% variability).

Regular increases in toxicity were observed mainly during transition periods from spring to summer (October to March), with peaks in December and January.

As shown in figure 4, high DA detoxification rates from mussels ($T_{1/2} < 4 \pm 1$ days) allowed the development of contingency plans during the bloom period that minimized the risk to human health and allowed for short harvest closures.

The seasonal evolution of toxicities of domoic acid in shellfish is indeed related to blooms of *Pseudo-nitzschia* species in the Chiloé Inner Sea. Domoic acid concentrations in shellfish could be related to the densities of *Pseudo-nitzschia* species in some cases.

As reported by others (Bates *et al.*, 2018), the relationship between *Pseudo-nitzschia* species densities and the evolution of shellfish toxicity is a complex issue. The literature is inconclusive regarding toxicity levels of *P. cf. australis* and/or *P. cf. delicatissima* or other species that may be present.

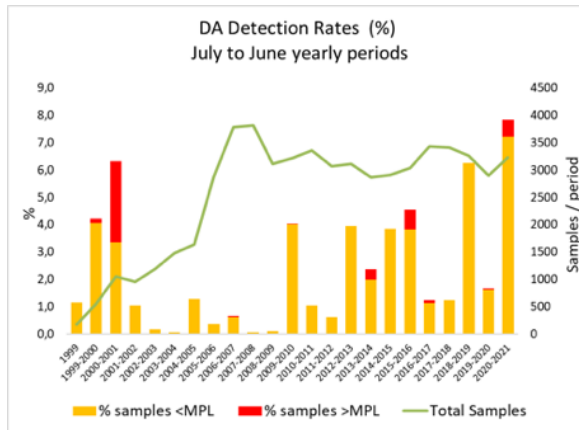


Fig. 3. Detection rates of domoic acid in shellfish samples. Percentage of all assays > LOD from July to June of consecutive years (1999-2021). The red segments correspond to the percentage of samples above the MPL.

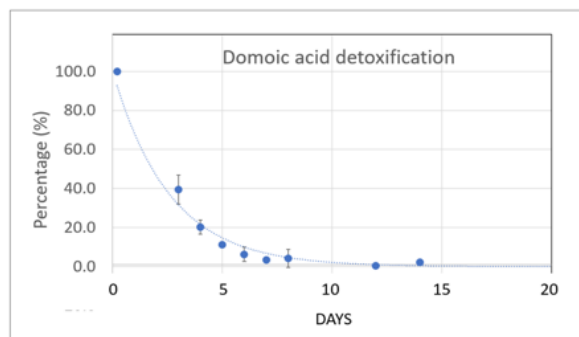


Fig. 4. Detoxification of DA in mussels. A single exponential function was fitted to data (mean \pm SD) from seven sampling stations (Sigmaplot 14.5).

The risk of DA intoxications remains low and under control. This is an important result of the NSSP managed by Sernapesca, the regional surveillance programs of the Ministry of Health and the collaborative network of authorized laboratories.

Despite the annual *Pseudo-nitzschia* blooms and seasonal detections of domoic acid, there have been no confirmed cases of poisoning in humans, marine mammals, or

birds. There have been no reported cases of toxic or subtoxic lots being marketed in the last 22 years. The spatial and temporal distribution can be used as a risk map to support management decisions and guide policy decisions by health authorities.

Acknowledgements. This study was carried out as part of statutory work for the National Shellfish Sanitation Programme. The support by the National Fisheries and Aquaculture Service (Sernapesca) is gratefully acknowledged.

References

- Álvarez, G., Uribe, E., Quijano-Scheggia, S., López-Rivera, A., *et al.*, (2009). Harmful Algae 8, 938-945.
- Bates, S.S., Katherine A. Hubbard, K.A., Lundholm, N., *et al.*, (2018). Harmful Algae 79, 3-43.
- Díaz, P.A., Álvarez, G., Varela, D., Pérez-Santos, I. *et al.*, (2019). *Perspect. Phycol.* 6, 39-50.
- Guzmán, L. and Campodónico, I. (1975). Publ. Instituto de La Patagonia. Ser. Mon. 9, 44.
- IFOP (2016). Informe final, Programa Manejo y Monitoreo de las mareas rojas en las regiones de Los Lagos, Aysén y Magallanes. IX etapa, 2015-2016. Tomos I y II. Subsecretaría de Economía y EMT. (<http://www.ifop.cl/busqueda-de-informes/>) (Accessed 12 Nov 2021).
- López-Rivera, A., Suárez-Isla, B.A., Eilers, P.P., Beaudry, C.G. *et al.*, (2005). *Anal. Bioanal. Chem.* 381, 1540-1545.

NSSP (2021). National Shellfish Sanitation Program (Sernapesca) (Accessed 12 Nov 2021).

[//www.sernapesca.cl/sites/default/files/parte_ii_seccion_i_control_en_origen_20211105.pdf](http://www.sernapesca.cl/sites/default/files/parte_ii_seccion_i_control_en_origen_20211105.pdf)

Pinto-Torres, M.A., Frangópulos, M., Pizarro, G., York, R., Iriarte, J.L. (2018a). In: 18th ICHA. Nantes, France. Abstract Book, 389.

Pinto-Torres, M., Pizarro, G., Frangópulos, M., York, B. *et al.*, (2018b). In: 18th ICHA. Nantes, France. Abstract Book, 293.

Quilliam, M.A., Xie, M., Hardstaff, W.R. (1995). *J. AOAC International*. 78, 543-554.

Rivera, P. (1985). *Gayana Botanica* 42, 9-38.

Seguel M. and Sfeir A. (2010). *Cienc. Tecnol.* 33, 43-55.

Suarez-Isla, B.A., López-Rivera, A., Hernández, C., Clement, A., Guzmán, L. (2002) Cap. 12: In: Sar, E.A., Ferrario, M.E., Reguera, B. (Eds.), *Floraciones Algales Nocivas en el Cono Sur Americano*. Instituto Español de Oceanografía, pp. 257-267.

Sunesen, I., Méndez, S.M., Mancera-Pineda, J.E., Dechraoui Bottein, M.-Y., Enevoldsen, H. (2021). *Harmful Algae* 102, 101920.

Pizarro, G., Frangópulos, M., Krock, B., Zamora, C. *et al.*, (2017). In: Proença, L.A.O. and Hallegraeff, G.M. (Eds.). *Proc.17th ICHA*, Florianopolis, Brazil. pp. 30.



An extraordinary 2021 *Heterosigma akashiwo* (Raphidophyte) bloom in Chile: large-scale farmed salmon mortality associated with unusual environmental conditions

Marco Pinto-Torres^{1,2,3*}, Maximiliano J. Vergara-Jara¹, Javier Paredes-Mella¹, Ana Flores-Leñero¹, Osvaldo Artal⁴, Elías Pinilla⁴, Andrea Corredor², Jorge I. Mardones^{1,2*}

¹Centro de Estudios de Algas Nocivas (CREAN), Instituto de Fomento Pesquero (IFOP), Puerto Montt, Chile; ²Centro de Investigación en Dinámica de Ecosistemas Marinos de Altas Latitudes (IDEAL), Valdivia, Chile; ³Escuela de Graduados Programa de Doctorado en Ciencias de la Acuicultura, Universidad Austral de Chile, Puerto Montt, Chile; ⁴Centro Tecnológico Para la Acuicultura (CTPA)-Putemún, Instituto de Fomento Pesquero (IFOP), Castro, Chile.

* corresponding author's email: marcoapintot@gmail.com, jorge.mardones@ifop.cl

Abstract

During early Austral Autumn, the Comau fjord (42° S) experienced an extraordinary HAB event that led to losses of more than 6,000 tons of farmed salmon during an extremely low rain – high solar radiation period. Field sampling and monitoring activities were carried out at the bloom site in the vicinity of farming cages close to the Lloncochaigua river mouth (Los Lagos Region). CTD data from the fjord transect, where some of the highest mortalities occurred, showed a pronounced stratification with high chlorophyll (70 mg L⁻¹), low salinity (~ 24), high temperature (~17 °C), high dissolved oxygen values at the surface (> 10 mg L⁻¹), and a shallow pycnocline (mostly in the upper 10 m of the water column). At the surface, cell abundances of *H. akashiwo* reached to ~70,000 cells mL⁻¹ and significantly lower abundances along with increasing depth. Hydrodynamic modeled particulate dispersion (Party - MOSA) showed high retention times in the Comau fjord, suggesting that this physical driver might have an important role in enhancing cell aggregation processes (patchiness) at the very surface layer of the water column. Finally, the end of the bloom was associated with cloudy - rainy weather. These observations highlight the need for differentiated strategies to tackle fast developing HAB events in Chilean Patagonia.

Keywords: Raphidophyte, cell abundances, water column, fish mortality, Chilean Patagonia

<https://doi.org/10.5281/zenodo.7032991>



Introduction

The Raphidophyte *Heterosigma akashiwo* is a small (from 10 to 20 μm in length) golden-brown phytoflagellate, which has been implicated in massive fish kill events worldwide. *Heterosigma akashiwo* can be considered as an eurythermic and euryhaline species, due to its distribution in different coastal ecosystems such as estuaries and bays where it colonizes effectively due to the rapid rates of cell division (up to five or six per day), which are associated with the characteristics of the water column, that allow its rapid cell growth (Smayda, 2007). This is due to the plasticity it presents to changes in salinity (between 5 and 35) and temperature (from 12° to 21 °C) (Martínez *et al.*, 2010). Associated with its high colonizing capacity in highly stratified systems, which turns seawater into an oxidized brown color (Honjo, 1993).

Blooms can be transient or remain for months if water column stratification persists (Taylor *et al.*, 1994). Even in nearby locations within the same general area, some blooms may be highly lethal as described in China, Japan, New Zealand, Canada and the United States (Kempton *et al.*, 2008; Rensel *et al.*, 2010), while others are relatively benign. Physical or biological conditions that affect toxicity have not been identified and may differ considerably from those conducive to bloom formation.

The toxicological mechanisms responsible for the ichthyotoxic properties of *H. akashiwo* are currently under debate. For raphidophytes, three main mechanisms have been proposed: i) production of neurotoxins (*e.g.* brevetoxins), ii) high content of free fatty acids, and iii) production of reactive oxygen species (ROS).

ROS generated during harmful algal blooms have been linked to lesions of gill tissue in fish, including epithelial uplift, cell necrosis, and disruption of chloride cells. These wounds, in turn, produce massive mucus secretion from the gills and physiological responses such as hypoxia, suffocation, and subsequent death (Astuya *et al.*, 2018; Mardones *et al.*, 2021).

In the case of the southern fjord system of Chile (41° S), historical events of harmful algal blooms (HAB) have been reported affecting the salmon farming industry since 1982 to date. Fish mortality has often been associated with the rapid growth of HAB-forming species, but the harmful effect can also be associated with any species of phytoplankton that rapidly increases their biomass, which can have negative effects on the ecosystem. In this study, we report an extraordinary HAB event produced by *H. akashiwo* due to unusual environmental conditions during 2021 in southern Chile, generating more than 6,000 tons in salmon mortality (report salmon farming).

Material and Methods

An unusual HAB produced by *H. akashiwo* was recorded during March and April 2021 in the Comau fjord (42° S, Los Lagos region; Fig. 1). During this event, four sampling stations were selected in a transect defined from East to West and fluorescence, salinity, temperature and dissolved oxygen (DO) profiled using a SAIV A/S CTD-F/O model SD204. All stations were sampled for phytoplankton collection at discrete depths (0, 5, 10, 15 and 20 m) using a 2.5 L Niskin bottle. Cell counts were carried out immediately after sampling



using an inverted microscope. To estimate the water circulation within the fjord, the dispersion of particles was modeled using the Parti-MOSA platform every 6 h for 12 days (from March 25 to April 7) at a depth of 5 m, and with a dispersion radius of 250 m.

Results and Discussion

Heterosigma akashiwo was the dominant species in the Comau fjord during the outbreak (more than 90% of the phytoplankton assemblage). Most of the algal biomass was detected in the water surface producing dense cell aggregations (Fig. 2).

The cell concentrations quantified *in situ* reached a range over 70,000 cells mL⁻¹ (Fig. 3), which were maintained for weeks, independent of the weather characteristics (rain and wind).

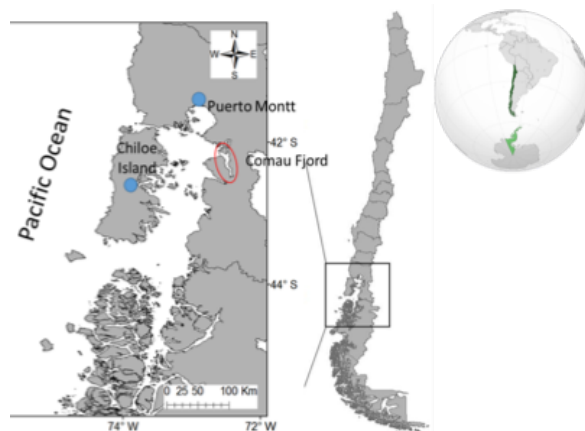


Fig. 1. Map of Chile. Red circle showing the Comau Fjord in 42° S, Los Lagos region.

The hydrological characteristics of the water column showed a highly stratified two-layer system, with salinities between 25 to 29 for the surface layer and > 31 for the subsurface layer (below 10 m). The thermocline showed

variations with a range between 11 and 16 °C, from the surface to 30 m (Figs. 4A, B).

The maximum fluorescence was detected on the surface with a value of 75 ug L⁻¹, decreasing steadily up to 4 m (Fig. 4C) corresponding with maximum cell abundances and the structure of the pycnocline. The DO measurements showed a maximum of 10 mg L⁻¹ at the water surface, abruptly decreasing at 4 m, and maintained a sustained load of 4 mg L⁻¹ until 30 m depth (Fig. 4D). Our results differ from those described by Silva *et al.* (2002) and Iriarte *et al.* (2014), for the Comau fjord and adjacent fjords, in which differences were found in oxygen concentrations with the range between 10 to 20 mg L⁻¹, and with fluorescence ranges between 5 and 75 ug L⁻¹, for the surface layer (0 – 10 m).

This system is highly stratified due to the interaction between Subantarctic Waters (SAAW), with high nutrient content at the bottom layer and the influence of different freshwater systems (high Si) present in the study area, resulting in a strong salinity gradient (Iriarte *et al.*, 2012).



Fig. 2. Aerial picture of the *H. akashiwo* bloom in the Comau Fjord in April 2021. Photo: Huinay Foundation.

Events with similar characteristics have been reported in the inland sea of Chiloé since the



beginning of the salmon farming. The first reported *H. akashiwo* bloom event occurred in 1988 in the Quintupeu fjord (at the vicinity of the Comau fjord) (Clément and Lembeye, 1993). A new event with high cell biomass was reported in 2000 and later in 2002 (Fuica *et al.*, 2007; Mardones *et al.*, 2012). These reports clearly identify *H. akashiwo* as a common species within the phytoplankton assemblage, even though massive outbreaks are quite sporadic.

An open question that remains is related to the mechanisms involved in the massive fish kills observed during the 2021 event. According to Barnes *et al.* (2011), 4 mg L⁻¹ is a critical oxygen threshold for the survival of *Salmo salar*. Based on our results, it is clear that low DO concentration (approx. 4 mg L⁻¹) measured below 5 m depth may have produced an important physiological stress on fish during the outbreak.

Under this scenario, cultured fish were trapped during days between the oxygenated surface layer containing potential ichthyotoxins produced by *H. akashiwo* and the low DO-bottom layer.

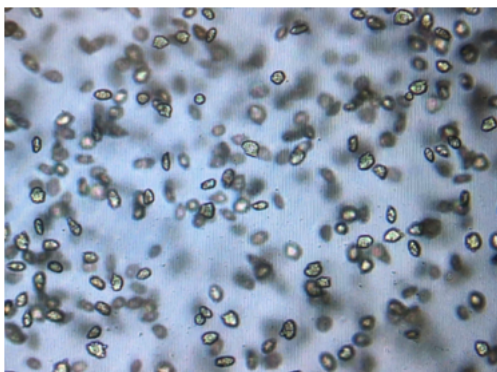


Fig. 3. *In situ* cells of *H. akashiwo* under a light microscope.

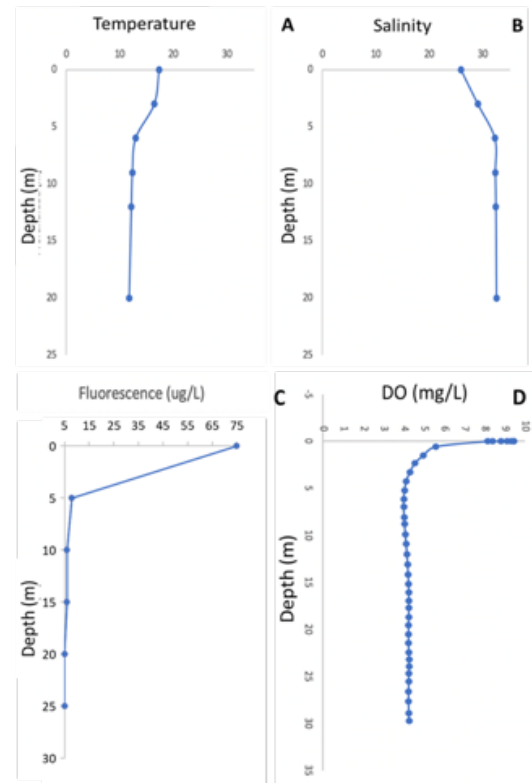


Fig. 4 A-D.: Vertical profiles of the water column in Comau fjord with CTD-O SeaBird 19.

Faced with the new global scenarios and extreme environmental conditions, the negative effects on high latitude systems (e.g., ENSO - Niño, global warming, acidification, etc.) are increasingly evident, which show a greater frequency and recurrence of HAB events. In the case of this study, *H. akashiwo* responds to the intrusion of freshwater from the ice fields of Patagonia, which generates a stratification system in the Comau fjord, which led to the proliferation of *H. akashiwo* in the surface layer, followed by a decrease in DO below 5 m, triggered physiological stress in large-scale cultured fish, generating high mortalities.

Acknowledgements. The authors thank colleagues from the CREAN group for



laboratory and fieldwork. Funding was provided by the FIPA2020-08 grant (SUBPESCA) and the Instituto de Fomento Pesquero (IFOP) (Projects 656-139 and 656-147).

References

- Astuya, A., Rivera, A., Vega-Drake, K., Aburto, C., *et al.*, (2018). PLoS One 13, e0201438.
- Barnes, R., King, H., Carter, C.G. (2011). Aquaculture 318, 397-401.
- Clément, A. and Lembeye, G. (1993). In: Smayda, T.J. and Shimizu, Y. (Eds.). Toxic Phytoplankton Blooms in the Sea. Elsevier, Amsterdam, pp. 223-228.
- Fuica, N., Rojas, X., Fuica, A., Bittner, V., Silva, M., Uribe, C. (2007). Salmocencia 2, 61-71.
- Honjo, T. (1993). In: Smayda, T. J. and Shimizu, Y. (Eds.). Toxic Phytoplankton Blooms in the Sea, Elsevier, Amsterdam, pp. 33-41.
- Iriarte, J. L., Pantoja, S., González, H. E., Silva, G., *et al.*, (2012). Environ. Monit. Assess. 185, 5055-5070.
- Iriarte, J. L., Ardelan, M. V., Cuevas, L. A., González, H. E., *et al.*, (2014). Phycol. Res. 62, 136-146.
- Kempton, J., Keppler C., Lewitus, A., Shuler, A., Wilde, S. (2008). Harmful Algae 7, 235-240.
- Mardones, J., Clément, A., Rojas, X. (2012). Harmful Algae News 45, 6-7.
- Mardones, J., Paredes, J., Godoy, M., Suarez, R., *et al.*, (2021). Sci. Total Environm. 766, 144383.
- Martínez, R., Orive, E., Laza-Martínez, A., Seoane, S. (2010). J. Plankton Res. 32, 529-538.
- Rensel J.E.J., Haigh N., Tynan T.J. (2010). Harmful Algae 10, 98-115.
- Silva, N. and Palma, S. (2006). In: Silva, N. and Palma, S. (Eds.). Comité Oceanográfico Nacional-Pontificia Universidad Católica de Valparaíso, Valparaíso, Chile. 37-43.
- Smayda, T. (2007). Harmful Algae 6, 601-622.
- Taylor, F. J. R., Haigh, R., Sutherland, T. F. (1994). Mar. Ecol. Prog. Ser. 103, 1-2.



Toxic marine microalgae and associated phycotoxins in shellfish: 14 years of data from the Italian coasts

Accoroni Stefano^{1,2,*}, Cangini Monica³, Angeletti Roberto⁴, Arcangeli Giuseppe⁴, Bacchiocchi Simone², Barile Nadia⁵, Contiero Lidia⁴, Costa Antonella⁶, Di Taranto Aurelia⁷, Escalera Laura⁸, Fedrizzi Giorgio⁹, Garzia Angela¹, Longo Francesca¹⁰, Macaluso Andrea⁶, Melchiorre Nunzia¹¹, Milandri Anna³, Milandri Stefania⁵, Montesor Marina⁸, Neri Bruno¹⁰, Neri Francesca¹, Gallo Pasquale¹², Piersanti Arianna², Rubini Silva¹³, Scortichini Giampiero¹⁴, Suraci Chiara¹⁵, Susini Francesca¹⁰, Vadrucci Maria Rosaria¹⁶, Verniani Daniela¹⁷, Virgilio Sebastiano¹⁸, Vivaldi Barbara¹⁹, Vodret Bruna¹⁸, Totti Cecilia¹, Zingone Adriana⁸

¹DiSVA, Università Politecnica delle Marche, Ancona, Italy; ²IZS Umbria e Marche, Ancona, Italy; ³National Reference Laboratory for Marine Biotoxins, CRM, Cesenatico (FC), Italy; ⁴IZS delle Venezie, Legnaro (PD), Italy; ⁵IZS dell'Abruzzo e del Molise, Termoli (CB), Italy; ⁶IZS della Sicilia, Palermo, Italy; ⁷IZS della Puglia e della Basilicata, Foggia, Italy; ⁸Stazione Zoologica Anton Dohrn, Napoli, Italy; ⁹IZS della Lombardia e dell'Emilia-Romagna, Bologna, Italy; ¹⁰IZS del Lazio e della Toscana, Roma, Italy; ¹¹ARPAL, La Spezia, Italy; ¹²IZS del Mezzogiorno, Portici (NA), Italy; ¹³IZS della Lombardia e dell'Emilia-Romagna, Ferrara, Italy; ¹⁴IZS dell'Abruzzo e del Molise, Teramo, Italy; ¹⁵ARPA Friuli Venezia Giulia, Trieste, Italy; ¹⁶ARPA Puglia, Bari, Italy; ¹⁷ARPAT, Firenze, Italy; ¹⁸IZS della Sardegna, Sassari, Italy; ¹⁹IZS del Piemonte, Liguria e Valle d'Aosta, Genova, Italy.

*corresponding author's email: s.accoroni@univpm.it

Abstract

Along the Italian coasts, toxins of algal origin in wild and cultivated shellfish have been reported since the 1970s. In this study, we used data gathered by the Veterinary Public Health Institutes and the Italian Environmental Health Protection Agencies from 2006 to 2019 to investigate toxicity events and relate them to the distribution of toxic species. Among detected toxins (OA and analogs, YTXs, PTXs, STXs, DAs, AZAs), OA and YTX were those most frequently reported in cases of seafood contamination. Levels of those toxins exceeding regulatory limits for OA were associated with high abundances of *Dinophysis* spp. and for YTX with blooms of *Gonyaulax spinifera*, *Lingulodinium polyedra*, and *Protoceratium reticulatum*. Seasonal blooms of *Pseudo-nitzschia* spp. occurred all along the Italian coast, but DA was only occasionally found in shellfish, at concentrations consistently below the regulatory limit. *Alexandrium* was recorded in many more areas than STXs, which only rarely exceeded the regulatory limit. *Azadinium* was sporadically recorded, and AZAs were sometimes detected in low quantities. Among the emerging toxins, PLTX-like toxins often accumulated in wild mussels and sea urchins due to the occurrences of *Ostreopsis* cf. *ovata*. Overall, Italian coastal waters harbour numerous potentially toxic species, with a few HAB hotspots related to DSP toxins. Still, rare cases of intoxications have occurred so far, reflecting the whole Mediterranean Sea conditions.

Keywords: domoic acid, emerging toxins, marine lipophilic toxins, paralytic shellfish toxins, toxic algae

<https://doi.org/10.5281/zenodo.7033020>



Introduction

The European legislation limits the commercialization of seafood for human consumption when contaminated by phycotoxins, setting a threshold level for each toxin (European Council, 2004) processing and distribution of food and to exports, and without any prejudice to more specific requirements relating to food hygiene. The following principles are taken into special account: The recent finding of toxins never detected before in European coasts led the European Food Safety Authority (EFSA) to express a series of scientific opinions concerning these emerging biotoxins, for which regulatory limits are not established yet.

Observations of HABs in Italy date from the 1970s (Pistocchi *et al.*, 2012) which is highly exploited for mollusk farming, the first occurrence of human intoxication due to shellfish consumption occurred in 1989, nearly 10 years later than other countries in Europe and worldwide that had faced similar problems. Until 1997, Adriatic mollusks had been found to be contaminated mostly by diarrhetic shellfish poisoning toxins (i.e., okadaic acid and dinophysistoxins. However, it was not until 1989 that the first shellfish contamination by okadaic acid (OA) was reported in the northern Adriatic Sea, in concomitance with the presence of *Dinophysis fortii* in the water column (Fattorusso *et al.*, 1992). Since then, toxic outbreaks due to harmful algal blooms (HABs) have also been observed in the Tyrrhenian and Ionian Seas, encompassing the entire Italian coastline.

In this study, we analyzed the data gathered from 2006 to 2019 by the Italian Veterinary

Public Health Institutes and the Environmental Health Protection Agencies, which are the authorities responsible for the monitoring of biotoxins in cultivated and wild seafood and of toxic phytoplankton. Our aim was to investigate toxicity events along the Italian coasts and relate them to the distribution of potentially toxic species.

Material and Methods

Shellfish samples (mainly mussel *Mytilus galloprovincialis*) were collected from 2006 to 2019 in fortnightly frequency from aquaculture farms located along the coasts of Abruzzo, Apulia, Campania, Emilia-Romagna, Friuli-Venezia Giulia, Lazio, Liguria, Marche, Molise, Sardinia, Sicily, Tuscany, and Veneto regions. For toxin analysis, shellfish were opened, deprived of the shell, and washed with running water to remove any residues. Then, each sample was homogenized with a blender and stored at $-20\text{ }^{\circ}\text{C}$ until the analysis. The lipophilic toxins (Okadaic Acid (OA) and analogs, Pectenotoxins (PTXs), Yessotoxins (YTXs), Azaspiracids (AZAs)), Saxitoxins (STXs) and Domoic Acid (DA) were analyzed at the Veterinary Public Health Institutes following the methods provided for by the European legislation (Commission Regulation (EC) 2074/2005).

Shellfish samples were considered positive when contaminated by phycotoxin levels above the thresholds indicated by the European Council (EC) Regulation No. 853/2004 and subsequent amendments: $160\text{ }\mu\text{g kg}^{-1}$ for OA and analogs, PTXs, and AZAs, 20 mg kg^{-1} for DA, 0.8 mg kg^{-1} for STXs, and 3.75 mg kg^{-1} for YTXs.



Seawater samples for phytoplankton analysis were collected in the same areas with both 20 µm mesh nets and bottles following the Intergovernmental Oceanographic Commission guide (Reguera *et al.*, 2016). Samples were preserved by adding acid or neutral Lugol solution. Toxic or potentially toxic species were counted following the Utermöhl method (European Standard, 2006).

Results and Discussion

Shellfish collected along the Italian coastal waters were found to accumulate most of the major known algal toxins. Okadaic acid and analogs, YTXs, PTXs, STXs, DAs, AZAs, were recorded in shellfish tissues in several regions over the sampling period (Fig. 1).

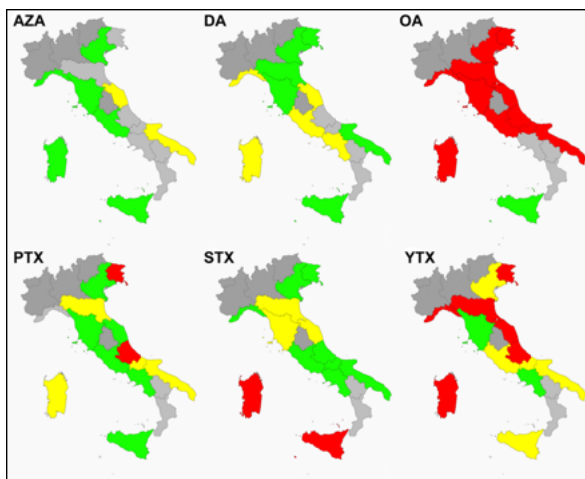


Fig. 1. Microalgal toxins (AZA = Azaspiracid; DA = Domoic Acid; OAs = Okadaic Acid and analogs, PTX = Pectenotoxin, STX = Saxitoxins, YTX = Yessotoxin) in shellfish tissues along the Italian coasts (2006-2019). Red and yellow: toxin concentrations at least once above and below the EU limits, respectively. Green: no toxins recorded. Grey: data not available.

Okadaic acid and analogs and YTXs were the most frequently reported toxins in

seafood in Italy, as also reported for the rest of the Mediterranean Sea (Zingone *et al.*, 2020)HABs. Their concentrations were often above the legal limits and caused the closure of shellfish farms as well as a few cases of DSP diagnoses in humans (Lugliè *et al.*, 2011; Pistocchi *et al.*, 2012) which is highly exploited for mollusk farming, the first occurrence of human intoxication due to shellfish consumption occurred in 1989, nearly 10 years later than other countries in Europe and worldwide that had faced similar problems. Until 1997, Adriatic mollusks had been found to be contaminated mostly by diarrhetic shellfish poisoning toxins (i.e., okadaic acid and dinophysistoxins. Azaspiracids and DAs never exceeded the EU limits, while STXs values above the EU limit were found in Sardinia and Sicily.

Several potentially toxic species were recorded during the study period (Table 1). A relationship between potentially toxic algae abundances and toxin levels in seafood was only found in some regions and was related to the presence of OA and YTX.

Dinophysis (mainly *D. acuminata* complex, *D. caudata*, *D. tripos* and *D. fortii*) were frequently reported in those regions affected by mussel contamination by OA above the EU limits. Their maximum abundances usually did not exceed 10^2 cells L^{-1} , with some exceptions reaching the maximum of 7,700 cells L^{-1} in 2012 (*D. acuminata* complex), exceeding the previous maximum Mediterranean record of $\sim 2,000$ cells L^{-1} from Slovenian waters (Francé *et al.*, 2018).



Table 1. Potentially toxic species identified in light microscopy along the Italian coasts from 2006 to 2019 and associated types of toxins.

<i>Bacillariophyceae</i>	Toxins
<i>Halamphora coffeiformis</i>	DA
<i>Pseudo-nitzschia australis</i>	DA
<i>Pseudo-nitzschia cf. delicatissima</i>	DA
<i>Pseudo-nitzschia cf. fraudulenta</i>	DA
<i>Pseudo-nitzschia cf. pseudodelicatissima</i>	DA
<i>Pseudo-nitzschia galaxiae</i>	DA
<i>Pseudo-nitzschia multiseriis</i>	DA
<i>Pseudo-nitzschia multistriata</i>	DA
<i>Pseudo-nitzschia pungens</i>	DA
<i>Pseudo-nitzschia subpacificica</i>	DA
<i>Dinophyceae</i>	
<i>Alexandrium minutum</i>	STX
<i>Alexandrium ostenfeldii</i>	STX, CIs
<i>Alexandrium pacificum</i>	STX
<i>Alexandrium pseudogonyaulax</i>	GDA
<i>Alexandrium tamarense</i>	STX
<i>Alexandrium taylorii</i>	STX, GDA
<i>Azadinium dexteroporum</i>	AZA
<i>Azadinium poporum</i>	AZA
<i>Dinophysis acuminata</i>	OA
<i>Dinophysis acuta</i>	OA
<i>Dinophysis caudata</i>	OA
<i>Dinophysis fortii</i>	OA
<i>Dinophysis ovum</i>	OA
<i>Dinophysis sacculus</i>	OA
<i>Dinophysis tripos</i>	OA
<i>Gonyaulax spinifera</i>	YTX
<i>Gymnodinium catenatum</i>	STX
<i>Lingulodinium polyedra</i>	YTX
<i>Ostreopsis cf. ovata</i>	PLTX-like
<i>Phalacroma mitra</i>	OA
<i>Phalacroma rotundatum</i>	OA
<i>Prorocentrum lima</i>	OA, CIs
<i>Prorocentrum rhathymum/mexicanum</i>	OA
<i>Protoceratium reticulatum</i>	YTX

Gonyaulax spinifera, *Protoceratium reticulatum* and *Lingulodinium polyedra* were frequently reported in those regions affected by YTX mussel contamination above the EU limits.

Seasonal blooms of *Pseudo-nitzschia* spp. often attained 10^6 cells L^{-1} , but DA was only occasionally detected and never above regulatory limit (Rossi *et al.*, 2016). The low DA levels in seafood even in bloom conditions could be explained considering that (i) cryptic species (some toxic and some non-toxic) can co-occur, and (ii) toxicity may vary within individual species (Giulietti *et al.*, 2021).

Azadinium spp. were sporadically recorded, while AZAs have been occasionally detected but always under the regulatory limits. This could be explained by the low toxicity of those *Azadinium* species (Giuliani *et al.*, 2019) novel AZAs produced by the Mediterranean dinoflagellate *Azadinium dexteroporum* were discovered (AZA-54, AZA-55, 3-epi-AZA-7, AZA-56, AZA-57 and AZA-58 which, in addition, never reached high abundances throughout the years.

Alexandrium minutum, *A. tamarense* and *A. pacificum* were recorded in many more areas than STXs and exceeded 10^5 cells L^{-1} in Sicily and Sardinia when STXs exceeded the regulatory limit. In other regions, *Alexandrium* species were commonly recorded but with low abundances (generally 10^2 cells L^{-1}), while the co-occurrence of both toxic and non-toxic species (or species producing other toxins, e.g. spirolides for *A. ostenfeldii*, Ciminiello *et al.*, 2006) might explain the lack of limit-exceeding STX levels in seafood samples.



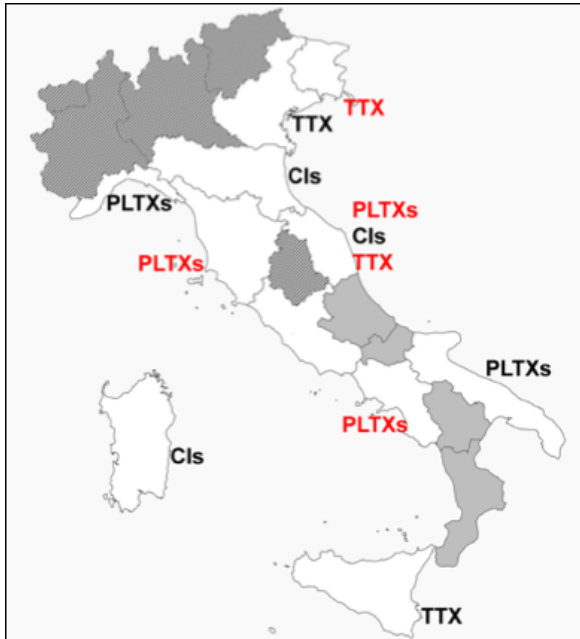


Fig. 2. PLTXs (Palytoxin-like compounds), CIs (Cyclic imines) and TTXs (tetrodotoxins) recorded in seafood along the Italian coast. Red colour indicates toxin concentration above EFSA opinion. Grey: not available.

Among the emerging toxins, one of the most important classes in the Mediterranean Sea are the PLTX-like compounds produced by several *Ostreopsis* species, benthic dinoflagellates whose blooms (up to 10^6 cells g^{-1} of macroalgal fresh weight) have become regular phenomena in summer and autumn along all the Italian coasts in the last decades (Emilia-Romagna and Veneto are the only exceptions). PLTX-like toxins have often accumulated in seafood during *Ostreopsis* cf. *ovata* blooms, often with concentrations exceeding the EFSA threshold (EFSA, 2009).

Cyclic imines (spirolides and gymnodimines, related to *Alexandrium ostenfeldii*) and tetrodotoxins (related to bacteria) were recorded in seafood often with concentrations

exceeding the EFSA threshold (EFSA 2017) (Fig. 2). Recently, also *Prorocentrum cordatum* was related to TTX-like compounds' production when associated to specific bacteria (Rodríguez *et al.*, 2017).

Overall, the Italian coastal waters support numerous potentially toxic species, but the cases of intoxication are relatively rare and impacts on aquaculture are limited to a few hot spots in the northern Adriatic Sea, where DSP is the main concern. A variety of toxins have been detected in several instances in microalgae strains from these waters (Pistocchi *et al.*, 2012), while seafood toxicity, when detected, has commonly remained below the safety limits. Therefore, no clear trends in occurrence nor expansions emerge for either toxic microalgae or seafood contamination in Italian coasts, in line with what has been observed in the rest of Mediterranean Sea (Zingone *et al.*, 2020) HABs.

Acknowledgements. This research was partially funded by the Italian Ministry of Health (Ricerca Finalizzata 2016), grant number GR-2016-02363211.

References

- Ciminiello, P., Dell'Aversano, C., Fattorusso, E., Magno, S., *et al.*, (2006). *Toxicon* 47, 597-604.
- Commission Regulation (EC) 2074/2005. *Off. J. Eur. Union*. L338/27.
- EFSA (2009). *EFSA J.* 7, 1393.
- EFSA (2017). *EFSA J.* 15, 65.



European Council (2004). Regulation (EC) No 853/2004 of the European Parliament and of the Council of 29 April 2004 laying down specific hygiene rules for food of animal origin.

European Standard (2006). EN 15204.

Fattorusso, E., Ciminiello, P., Costantino, V., Magno, S., *et al.*, (1992). *Mar. Pollut. Bull.* 24, 234-237.

Francé, J., Petelin, B., Mozetič, P. (2018). Abstract book, 4th International Symposium of The Effects of Climate Change on the World's Oceans, 179.

Giuliani, M.E., Accoroni, S., Mezzelani, M., Lugarini, F., *et al.*, (2019). *Mar. Drugs* 17, 595.

Giulietti, S., Romagnoli, T., Siracusa, M., Bacchiocchi, S., *et al.*, (2021). *Phycologia* 60, 247-264.

Lugliè, A., Satta, C., Pulina, S., Bazzoni, A., *et al.*, (2011). *Biol. Mar. Mediterr.* 18, 2-9.

Pistocchi, R., Guerrini, F., Pezolesi, L., Riccardi, M., *et al.*, (2012). *Mar. Drugs* 10, 140-162.

Reguera, B., Alonso, R., Moreira, Á., Méndez, S., Dechraoui Bottein, M.Y. (2016). *IOC Manuals and Guides*, 77.

Rodríguez, I., Alfonso, A., Alonso, E., Rubiolo, J.A., *et al.*, (2017). *Sci. Rep.* 7, 40880.

Rossi, R., Arace, O., Buonomo, M.G., Capozzo, D., *et al.*, (2016). *Ital. J. Food Saf.* 5, 5706.

Zingone, A., Escalera, L., Aligizaki, K., Fernández-Tejedor, M., *et al.*, (2020). *Harmful Algae* 101843.



Rapid, portable, multiplexed detection of harmful algal toxins in freshwater

Sarah Bickman^{1*}, George Bullerjahn², Gregory Boyer³, Gregory Lewis¹, Cassandra Petrou¹, Brooks Macdonald¹, Seth Buchholz², Katelyn Barker², Jack Roser¹, Michael Lochhead¹

¹LightDeck Diagnostics, 5603 Arapahoe Ave, Boulder, CO 80303, U.S.A.; ²Bowling Green State University, 1001 E Wooster Street, 230 Life Sciences Building, Bowling Green, OH 43403, U.S.A.; ³SUNY College of Environmental Science and Forestry, 320 Jahn Laboratory Syracuse, NY 13210, U.S.A.

*corresponding author's email: sarah.bickman@lightdeckdx.com

Abstract

Harmful algal blooms are a significant threat to fresh waters necessitating routine testing to protect humans from exposure to contaminated drinking and recreational waters and for forecasting and modelling. Since toxin profiles change spatially and temporally there is significant need for rapid tests that can provide real-time, local answers. Currently, the four classes of toxins that are typically monitored in freshwater are microcystins (MC), cylindrospermopsins (CYN), saxitoxins (STX) and anatoxin-a (ATX-a). There is currently no method of measuring STX in freshwaters in the field and only a semi-quantitative test strip for ATX-a. A rapid, portable multiplexed test would reduce the time and cost associated with collecting critical data while improving human safety by ensuring that all four toxin classes are always monitored. The LightDeck technology enables portable, multiplexed detection of toxins and has been demonstrated in a duplex MC/CYN panel and is being expanded to include STX and ATX toxin classes.

Keywords: microcystin, cylindrospermopsin, saxitoxin, anatoxin-a, HAB, sensor, paralytic shellfish toxin

<https://doi.org/10.5281/zenodo.7033098>



Introduction

Harmful algal blooms (HABs) are a significant and growing problem threatening fresh waters globally. Cyanobacterial HABs contribute to more than \$2 billion in annual U.S. economic losses and the estimated annual cost of cyanobacterial HABs (CHABs) in western Lake Erie (WLE) alone exceeds \$65 million, which does not include the millions of dollars lost due to events like the Toledo water crisis. CHABs necessitate routine testing to protect humans from exposure to contaminated drinking and recreational waters and for forecasting and modelling. Since toxin profiles change spatially and temporally, there is significant need for rapid tests that can provide real-time, local answers (John *et al.*, 2019).

Currently, the four toxins that are most frequently monitored in freshwater are microcystins (MC), cylindrospermopsins (CYN), saxitoxin (STX), and anatoxin-a (ATX-a). STX causes paralytic shellfish poisoning (PSP) and ATX-a is also known as Very Fast Death Factor (VFDF). Currently available rapid tests for these toxins are semi-quantitative. STX has been documented in freshwater sources in the United States and worldwide (Wiese *et al.*, 2010; Savela *et al.*, 2015) and the frequency and distribution of STX-producing cyanobacterial blooms have been on the rise (Pearson *et al.*, 2016). In the United States, the 2007 National Lakes Assessment (NLA) revealed that 7% percent of U.S. lakes were impacted by STX (Loftin *et al.*, 2106). This is consistent with a recent California survey, which detected STX in 7% of wadable streams (Fetscher *et al.*, 2015) and in New York where STX toxins were detected in 15% of the blooms collected from inland



Fig 1. The LightDeck HAB Toxin MC + CYN System is shown along with a disposable multiplexed cartridge.

lakes (Smith *et al.*, 2019). A previous study from Lake Erie detected the *sxtA* gene, a gene involved in the synthesis of STX, in 12 of 18 samples from a *Dolichospermum* bloom in the central basin of Lake Erie in July of 2016 and 2017 (Chaffin *et al.*, 2019). In an ECOHAB-funded 2019 basin-wide survey of western Lake Erie (172 samples total), the *sxtA* gene has been detected in all of the 46 samples that have currently been analysed and it is expected that this number will increase as the remaining samples are analysed (Davis, 2019). In addition to widespread *sxtA* detections across the western and central basins of Lake Erie, saxitoxin was detected in surface scums in July 2017 at concentrations of 0.022 and 0.026 $\mu\text{g L}^{-1}$ (Chaffin *et al.*, 2019). *Microseira* (basinonym *Lyngbya*) *wollei* mats are common in shallow zones of WLE (Bridgeman *et al.*, 2010) and this species has been shown to produce multiple variants of STX (Boyer, 2019; Smith *et al.*, 2019). Furthermore, detection of ATX-a is also on the rise across the USA with reports from diverse locations such as California (Howard *et al.*, 2016; Bouma-Gregson *et al.*, 2018; Kelly *et al.*, 2019), New York (Boyer, 2007; Smith *et al.*, 2019), Washington (Hobbs



et al., 2019), Utah (Utah 2018), and WLE (Bouma-Gregson *et al.*, 2018; Smith *et al.*, 2019). Globally, ATX-a has been detected in countries such as Australia (John *et al.*, 2019), New Zealand (McAllister *et al.*, 2018), France (Gugger *et al.*, 2005), and Germany (Ballot *et al.*, 2010) to name a few.

While these toxins have been detected throughout the Great Lakes, currently the only way to collect quantitative data for STX and ATX-a is to have samples collected, processed in a lab and analysed by individual ELISA tests or shipped to laboratories that can perform LC-MS/MS analysis. The delay of laboratory analysis can unnecessarily expose people to toxins while testing is being conducted. Furthermore, performing multiple separate tests is time consuming, expensive, and occasionally necessitates decisions that limit the amount of testing. A rapid, portable, multiplexed test would reduce the time and cost associated with collecting critical data while improving human safety by ensuring that all four toxins are always monitored.

This tool will be an asset to water managers and community-based monitoring networks as they will have the ability to rapidly quantify the aforementioned cyanotoxins using this user-friendly platform. Furthermore, this tool will be incorporated into routine monitoring programs and experiments by academic, state and federal researchers to improve scientific understanding of HABs. Improved spatial and temporal understanding of HABs will allow for better models and improved predictive capabilities. In short, this technology is an improved scientific tool for management of freshwater sources, and is of particular relevance to the Great Lakes, where algal blooms are of significant concern.

This technology can be used to protect public safety by allowing for on-the-spot decisions about beach closures or whether a particular source of water should be used as the intake for a public water utility.

Here, we describe development of STX and ATX-a assays that will be integrated into a multiplexed assay with the existing LightDeck MC+CYN test (Fig. 1).

Material and Methods

The LightDeck platform uses planar waveguides illuminated by solid-state diode lasers that reproducibly couple light into the waveguide (Devlin *et al.*, 2013; Meneely *et al.*, 2013; McNamee *et al.*, 2014; Murphy *et al.*, 2015; Reverté *et al.*, 2017; Bickman *et al.*, 2018). Detection of all toxins uses competitive immunoassays where toxin-protein conjugates are printed on the waveguides using microarray technology and fluorophore-labelled antibodies bind to the printed spots as shown in figure 2.

Results and Discussion

The LightDeck MC and CYN assays were previously developed and were tested with natural water samples with expected correlations.

Preliminary development of an assay for saxitoxins (paralytic shellfish toxins) has demonstrated a sensitive assay with congener coverage that correlated well with the toxicity of the congeners. The 50% inhibition concentration is $1.2 \mu\text{g L}^{-1}$ and the assay range is from 0.6 to $2.7 \mu\text{g L}^{-1}$ based on the 20% and 80% inhibition concentrations. In the quantitative range, the assay percent



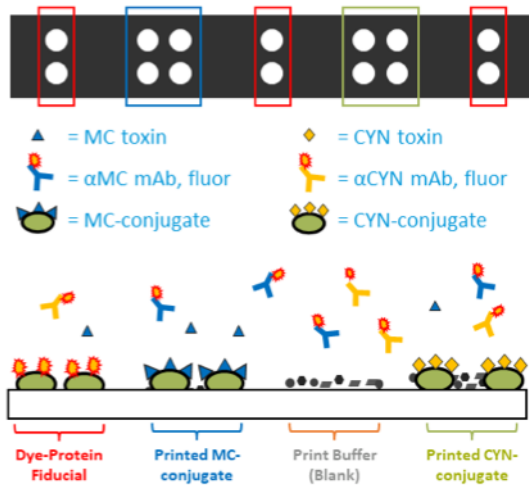


Fig. 2. Top) A microarray image where spots in red are dye-protein fiducials, spots in blue detect MC, spots in green detect CYN, and blank spots are print buffer blanks. Bottom) Schematic of the competitive immunoassays to detect toxins. Toxin-protein conjugates are immobilized on the waveguide surface. The sample is mixed with detection reagents containing fluorophore-labeled antibodies, which will bind to the microarray spot when no toxin is present and bind to toxin in the sample when toxin is present.

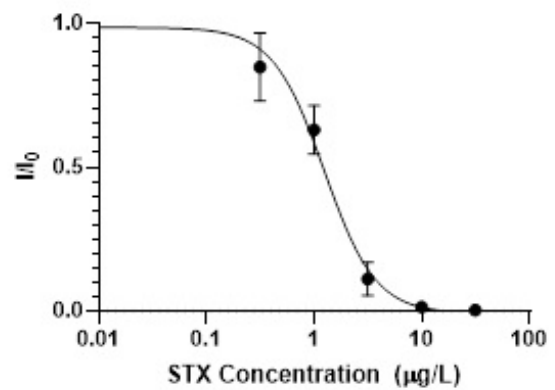
coefficient of variation based on 6 replicates is 13%. Congener cross reactivity is calculated as the 50% inhibition concentration of STX divided by the 50% inhibition concentration of the congener (see Fig. 3). All results are preliminary and will be repeated when the assay is fully optimized.

Immunogen production for ATX-a is underway and will be used to create an antibody to be used in a competitive immunoassay.

In summary, a 4-plex assay for the simultaneous detection of the most common toxins in freshwater is underway. A rapid, quantitative, multiplexed test such as the one

described here will allow water managers to make faster, more informed decisions about water treatment.

Acknowledgements. This work was supported by the U.S. National Oceanic and Atmospheric Association/National Centers for Coastal Ocean Science under awards NA19NOS4780190, NA20NOS4780186, and NA20NOS4780181 and by the US Department of Agriculture/National Institute of Food and Agriculture award 2019-33610-30177.



Congener	Toxicity (%)	LightDeck Cross Reactivity (%)
STX	100%	100%
C1&2	1%, 10%	18%
dcGTX2&3	15%, 38%	4%
dcNEO	Not known	25%
dcSTX	51%	16%
GTX1&4	99%, 73%	98%
GTX2&3	36%, 64%	66%
GTX5	6%	50%
GTX6	Not known	69%
LyngbiaWoller	Not known	25%
NEO	92%	189%

Fig. 3. Top) A standard curve measured for STX. Data is an average of three replicates ± one standard deviation. Bottom) Preliminary congener cross-reactivity for saxitoxin.

References

- Ballot, A. Fastern, J., Lentz, M., Weidner, C. (2010). *Toxicon* 56, 964-971.
- Bickman, S., Campbell, K., Elliott, C., Murphy, C., *et al.*, (2018). *Environ. Sci. Technol.* 52, 11691-11698.
- Bouma-Gregson, K., Kudela, R. M., Power, M.E. (2018). *PLoS One* 13, e0197669.
- Boyer, G.L. (2007). *Lake Reserv. Manag.* 23, 153-160.
- Bridgeman, T. B. and Penamon, W. A. (2010). *J. Great Lakes Res.* 36, 167-171.
- Chaffin, J.D., Mishra, S., Kane, D., Bade, D., *et al.*, (2019). *J. Great Lakes Res.* 45, 277-289.
- Devlin, S., Meneeley, J., Greer, B., Greef, C., *et al.*, (2013). *Anal. Chim. Acta* 769, 108-113.
- Fetscher, A.E., Howard, M., Stancheva, R., Kudela, R., *et al.*, (2015). *Harmful Algae* 49, 105-116.
- Gugger, M., Lenoir, S., Berger, C., Ledreux, A., *et al.*, (2005). *Toxicon* 45, 919-928.
- Kelly, L.T., Bouma-Gregson, K., Puddick, J., Fadness, R., *et al.*, (2019). *PLoS One* 14, e0220422.
- Hobbs, W. and Wong, S. (2019). *The Prevalence of Cyanobacteria: A historical Perspective from Lake Sediment*, Department of Ecology State of Washington (Ed.)
- Howard, M., Fetscher, B., Nagoda, C. (2016). *The Prevalence of Cyanotoxins in Southern California Waterbodies Based on Screening Assessments and Regional Monitoring Programs*, C.W.S.W.A.M. Programanat, Editor.
- John, N., Baker, L., Ansell, B., Newham, S., Crosbie, N., Jex, A. (2019). *Sci. Rep.* 9, 10894.
- Loftin, K. A., Graham, J., Hilborn, E., Lehmann, S., *et al.*, (2016). *Harmful Algae* 56, 77-90.
- McAllister, T.G., Wood, S. A., Hawes, I. (2016). *Harmful Algae* 55, 282-294.
- McNamee, S., Elliott, C., Greer, B., Lochhead, M., Campbell, K. (2014). *Environ. Sci. Technol.* 48, 13340-13349.
- Meneely, J., Campbell, K., Greef, C., Lochhead, M., Elliott, C. (2013). *Biosens. Bioelect.* 41, 691-697.
- Murphy, C., Stack, E., Krivelo, S., McPartlin, D., *et al.*, (2015). *Biosens. Bioelectron.* 67, 708-714.
- National Science and Technology Council Committee on Environmental and Natural Resources. *National Assessment of Harmful Algal Blooms in US Waters* (2000). Available from: www.coastalscience.noaa.gov/publications/handler.aspx?key=172.
- Pearson, L.A., Dittmann, E., Mazmouz, R., Ongley, S., *et al.*, (2016). *Harmful Algae* 54, 98-111.



Reverté, L., Campas, M., Yakes, B., Deeds, J., *et al.*, (2017). *Sens. Actuators B: Chemical* 253 (Suppl. C), 967-976.

Savela, H., Spoof, L., Perala, N., Preede, M., *et al.*, (2015). *Harmful Algae* 46, 1-10.

Smith, Z.J., (2019). Occurrence and Methods for Freshwater Paralytic Shellfish Poisoning Toxins and other Cyanobacterial Neurotoxins in New York Lakes, in *Environmental Science and Forestry*. State University of New York: Syracuse, New York.

Smith, Z.J., Martin, R., Wei, B., Wilhelm, S., Boyer, G. (2019). *Toxins (Basel)* 11, 44.

Utah Department of Health (2018), *Utah Health Status Update: Harmful Algal Bloom Cyanotoxins*.

Wiese, M., D'Agostino, P., Mihali, T., Moffitt, M., Neilan, B. (2010). *Mar. Drugs* 8, 2185-2211.



Humorous content effectiveness in marine biotoxins' risk communication through social media

Panagiota Katikou^{1,2*}, Gideon Mekonnen Jonathan², Brian Kloss³

¹Directorate of Research, Innovation and Education, Ministry of Rural Development and Food, 54626 Thessaloniki, Greece; ²Department of Computer and Systems Sciences (DSV), Stockholm University, Postbox 7003, SE-16407 Kista, Sweden; ³SUNY Upstate Medical University, 550 East Genesee Street, Syracuse, NY 13202, U.S.A.

*corresponding author's email: pkatikou@otenet.gr

Abstract

Social media are largely integrated into citizens' daily routines and constitute powerful communication tools, often exploited by regulatory authorities as information distribution channels for risk communication purposes. Food safety issues frequently raise public concern, requiring management through trustworthy information provision, ideally disseminated by digital means. Risk communication strategies entailing the use of humor in social media are increasingly becoming popular, aiming to raise public awareness and induce risk perception. The objective of this work was to assess the effectiveness of humor-mediated risk communication strategies regarding the food safety hazard of marine biotoxins in a multinational audience. A multinational survey targeting adult English-speaking social media users was conducted, also involving participants with food safety and marine biotoxin expertise, by means of an online questionnaire that included: (a) demographical data, educational/professional background, food safety-related attitude and social media usage; and (b) respondents' perception on various effectiveness parameters, examining three groups of materials relevant to marine biotoxins (conventional, humorous and combination), as risk communication scenarios. The majority of the 218 participants indicated humorous materials as of lower effectiveness than conventional ones; however, the former were scored as more "likeable" or sharable, especially by those more familiar with food safety and/or marine biotoxins. Interestingly, participants perceived materials combining both humorous and conventional elements as comparably effective to those purely conventional. In conclusion, materials combining both informative and humorous elements, may constitute potentially valuable tools in food safety/marine biotoxins' risk communication through social media, by further content optimization.

Keywords: humor, marine biotoxins, risk communication, social media, user perception

<https://doi.org/10.5281/zenodo.7033103>



Introduction

Social media (SM) are popular and easily accessible communication tools, globally constituting a part in peoples' daily routines, due to their low usage costs and user friendliness (Charlebois and Summan, 2015). Exploitation of SM covers a wide range of purposes, from plain entertainment and social networking, to distance education, scientific information dissemination, risk communication (RC) and professional interactions (Kuttschreuter *et al.*, 2014). As such, regulatory bodies and public administration organizations pursue an active presence in multiple SM, with official accounts serving as valuable distribution channels for information of both utmost significance and simple interest to citizens/consumers (Charlebois and Summan, 2015; Ruzza *et al.*, 2020). Of particular importance are RC activities related to food safety (FS), public health and environment/climate change, nowadays comprising popular topics of citizen/consumer concern, frequently generating online debates (Rutsaert *et al.*, 2013; Mou and Lin, 2014; Kuttschreuter *et al.*, 2014; Overbey *et al.*, 2017; Skurka *et al.*, 2018; Meadows *et al.*, 2019; Topp *et al.*, 2019).

Strategies involving SM networks entail dissemination of messages specifically tailored to evoke emotions, such as amusement, fear, concern, and frustration, aiming at capitalizing the audiences' appeal to induce risk perception. Emotional responses may influence individuals' potential towards undertaking preventive actions, or even evoke crises' escalation. Humorous/sarcastic messages in SM seem to be the most popular with high like-and-share rates (Mou and Lin, 2014; Overbey *et al.*, 2017; Skurka *et al.*,

2018; Meadows *et al.*, 2019). In this context, RC-responsible agencies progressively use humorous material to induce positive emotions, such as amusement and relief, even in severe public health crises (Chew and Eysenbach, 2010; Fraustino and Ma, 2015; Meadows *et al.*, 2019; Karmegam and Mapillairaju, 2020).

Marine biotoxins (MBs) were chosen as a food-safety theme for the humorous content, being tightly connected with both public health (as causes of human illness), and environmental/ climate change influences (as products of toxic microalgae during proliferations known as harmful algal blooms) (Morabito *et al.*, 2017), thus fitting within all major thematic areas considered in the literature comprising the study's theoretical framework. As such, the aim of this study was to explore the effectiveness of humor-mediated risk communication strategies considering the food safety hazard of marine biotoxins, at a multinational level. To serve this aim, the following research questions (RQ) were formed: RQ1: To what extent is humorous content on social media perceived as effective in communicating risks related to marine biotoxins? RQ2: To what extent is this perceived effectiveness associated with participants' demographic characteristics, level of previous familiarization/expert knowledge, and personal attitudes on FS issues?

Material and Methods

Research strategy and data collection method
A survey strategy was chosen to obtain primary, factual empirical data, delivered by



an adequately large sample of the targeted population. Addressing a diverse multinational audience at a specific time-point by means of quantifiable rigid questions, in a low-cost way, indicated “questionnaire” as the optimal data collection method (Denscombe, 2010).

A web-based questionnaire qualified as an ideal choice, taking into account time and resources constraints, design attractiveness (graphics and audio-visual material), and user-friendliness of web-hosted applications, dissemination easiness and automated transfer of responses to specifically generated spreadsheets (Denscombe, 2010; Johannesson and Perjons, 2014).

Questionnaire properties and content

The questionnaire accommodated the literacy level of adult English-speaking participants without any prior experience on either FS or MB risks, with technical jargon kept to a minimum. All questions were of closed or 5-point Likert-scale type to facilitate quick answering. Three MB scenarios were created (Type-A: conventional, B: humorous, and C: combination), comparable to analogous studies on climate change (Skurka *et al.*, 2018; Topp *et al.*, 2020), but closely fitting our conceptual framework and RQs. The questionnaire was divided into three sections: a) introduction (context, purpose, structure, participation requirements and information on confidentiality and anonymity within the survey; b) main part containing the questions and c) final part (“tick box” statements, in lieu of an ‘informed consent form’). The main part contained 18 questions (Q): Q1-4 enquired on demographics (countries of birth and residence, age and gender), Q5-9 referred to participants’ academic and professional backgrounds and affinity with the FS and

MB sectors; Q10-11 explored respondents’ personal attitudes towards FS issues and Q12-18 examined the participants’ SM use and perception on specific types of MB-related SM contents in fictional cases related to RC purposes. The questionnaire was created using “Google Forms” (Google LLC, Mountain View, CA, U.S.A.).

Sampling – survey participants

Purposive, snowball and convenience sampling (Denscombe, 2010) were combined to attract the widest possible audience at multinational level (both MB and FS experts and general public). The targeted survey participants were English-speaking adults being regular SM users of any professional/educational background.

Data analysis methods

Our study entailed exclusively quantitative data; all variables were discrete, belonging to the nominal or ordinal type. Initially, raw data were cleansed, grouped, and encoded and non-numerical values were replaced by positive integers. Finally, cleansed data were analyzed by the “Statistical Package for Social Sciences” (SPSS) v.27 software, using nonparametric descriptive statistics (median, frequency distribution), graphical exploratory analysis, Kruskal-Wallis H-test, Pearson’s chi-square test, and Spearman’s correlation, at the 95% significance level ($p < 0.05$).

Results and Discussion

A total of 218 responses were collected, corresponding to a calculated error of margin 6.64% at a 95% confidence level, assuming a population from 500 to 700 million English-speaking adult SM users.



1. Demographics – Academic/Professional background. Participants originated from and resided in 34 and 32 different countries/territories, respectively. Different age groups contributed from 1.4% (75 years or older) to 30.7% (45-54 years). Out of 218 responders, 126 (57.8%) were females, whereas 95 of the participants (43.6%) had completed doctorate studies. More than half of the responders were employed in the public sector (119, 54.6%), whereas 62 (28.5%) were private-sector employees or freelancers and 25 (11.5%) were full-time students. People with medical or applied sciences background constituted 63.7% of the sample, with the remaining divided between ICT/Social Sciences (17.0%) and other disciplines (19.3%). Familiarization/experience concerning food safety issues ranged between 11.0 - 31.7%. As regards familiarization with the term “marine biotoxins”, respondents were rather evenly distributed among the five levels, from people who had never encountered the term to field experts, with percentages ranging from 14.2% to 24.8%.

2. Personal attitudes towards food safety and social media use. The majority of participants were generally well aware and interested in FS issues at a proportion of at least 74.3%. Similarly, 62.4% of the respondents expressed concern about the possibility of being affected by a FS incident or crisis. On the other hand, those not interested or aware and those non-concerned about FS constituted minorities of 8.2% and 11%, respectively, indicating a generally positive attitude of participants towards FS importance.

Most responders were multiple SM users; the most popular was Facebook (180 cases, 82.6%), followed by YouTube (165 cases,

75.7%). More than half of the participants also used WhatsApp (56.0%), LinkedIn (52.3%), and Instagram (51.4%), while TikTok showed the lowest penetration with only 6.0% (Fig. 1).

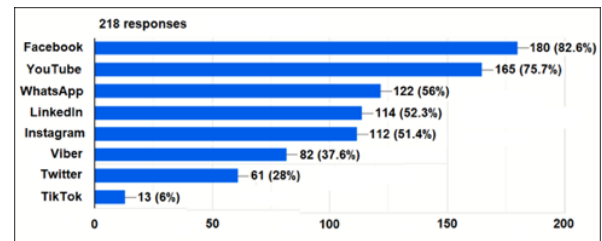


Fig. 1. Social media used by survey participants.

3. Participants' evaluation of different SM content types. Type-A content (conventional) was perceived by participants as the most informative, credible and alerting (87.1%, 78.4% and 56.9%, respectively), compared to Type-B (humorous; 66.5%, 39.0% and 51.8%, respectively) and Type-C (combination; 77.1%, 64.3% and 55.1%, respectively). On the other hand, 47.2% of the participants considered Type B content as the most amusing/relieving, in contrast to 15.6% and 35.8% for Type-A and C, respectively. Type-C was regarded as the most motivating/creating an intention for action (50.9%), followed by Type-B (47.3%) and Type-A (42.2%) contents.

Concerning the three content types' acceptability, answers exhibiting a positive attitude (Likert scale 4 and 5) cumulatively showed that Type-A and C contents were equally likely to be “liked” (56.0%), with this likelihood being slightly lower for Type-B content (52.3%). Sharing/retweeting likelihood was the highest for Type-A content (58.3%); Types B and C followed closely, with almost half of the participants (49.6% and 50.0%, respectively) also indicating



sharing as possible. Overall though, Type-A content was perceived as the most effective RC means by 78.0% of the participants, with Types C and B accounting for 71.1% and 65.6%, respectively.

Kruskal-Wallis H-testing indicated a significant difference ($p < 0.05$) between distributions of the three content types regarding their potential for creating awareness, trust, and sense of relief, as well as their perceived effectiveness. Pair-wise comparisons showed that humorous content (Type-B) was considered as significantly less informative and trustworthy compared to Types A and C, whereas conventional content (Type-A) was overall perceived as significantly more effective than Type-B. Type-C (combination) content was considered as equally humorous to Type-B, but also equally informative and effective compared to Type-A content (Fig. 2).

4. Associations between variables. The most prominent associations revealed by chi-square testing included: (a) concern about FS issues with Type-B content considered as informative; (b) age group with sharing likelihood of Type-C content; (c) level of familiarization on FS and MBs issues with likelihood of “liking” and sharing some or all three content types; (d) highest level of studies and academic/professional discipline, with “liking” of Type-A and C contents.

Post hoc tests examined the exact sources of dependencies. Regarding the association of “FS issues concern” with Type-B content (humorous) considered as awareness-raising, highly-concerned people strongly agreed on this content’s informative nature, whereas those declaring limited FS concern disagreed

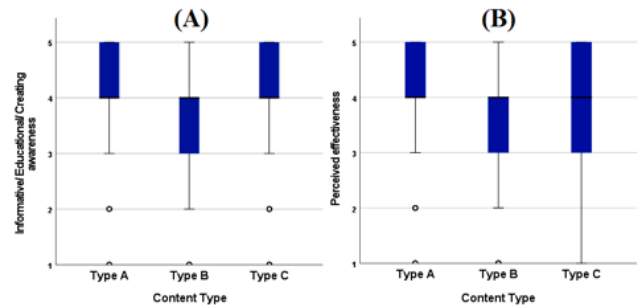


Fig. 2. Kruskal-Wallis H-test of effectiveness-related variables across content types: (A) Informative/Educational/Creating awareness; (B) Perceived effectiveness.

with this characterization. MBs experts were significantly more likely to “like” Type-A and B contents and share all three types, compared to less FS-familiarized participants who were very unlikely to “like” or share Type-A or C contents, while significantly less of the MB-unfamiliarized people would share any of all three content types on SM. Respondents of an Environment/Fisheries background were significantly more likely to “like” Type-A content, while Type-C content was significantly more “likeable” by participants within Veterinary Medicine and Chemistry/Pharmacology sectors. By contrast, people of ICT/Social sciences’ backgrounds were greatly unlikely to “like” Type-A and C contents compared to other disciplines.

Overall, it was concluded that the majority of the participants perceived SM materials entailing humorous elements (Type B) as less effective than conventional, purely informative posts, although the former were more likely to be “liked” or shared by SM-users affiliated or familiarized with the FS and MB fields. In addition, combination content comprising humorous MB-related images supplemented by scientific explanatory text



in a video format (Type C), was not perceived as significantly less effective compared to conventional. Finally, considering the drawback that humor use in RC is frequently criticized for trivializing risks' importance, the above evidence favors the potential usability of combined content types for RC purposes through SM in FS/MB, and possibly in other closely-related sectors.

Acknowledgements. This research was conducted within the “Scientific Communication and Research Methodology (FMVEK) course, in partial fulfilment of the requirements of the Master’s programme in “Open eGovernment” organized by the Department of Computer Science, Stockholm University, Sweden, where PK is studying. Humorous material used in the scenarios was provided by BK and is available on the Kloss & Bruce website (<http://klossandbruce.com>) and YouTube channel (https://www.youtube.com/channel/UctJewaUfT7eyFNUxNYLTg_g).

References

- Charlebois, S. and Summan, A. (2015). *Trends Food Sci. Technol.* 45, 153-165.
- Chew, C. and Eysenbach, G. (2010). *PLoS One* 5, e14118.
- Denscombe, M. (2010). *The good research guide: for small-scale social research projects*, 4th edition. McGraw-Hill Education, Open Univ. Press, Berkshire, UK. 373 p.
- Fraustino, J.D. and Ma, L. (2015). *J. Appl. Commun. Res.* 43, 222-241.
- Johannesson, P. and Perjons, E. (2014). *An introduction to design science*. Springer International Publishing, Cham, 197 p.
- Karmegam, D. and Mapillairaju, B. (2020). *BMJ Health Care Inform.* 27, e100133.
- Kuttschreuter, M., Rutsaert, P., Hilverda, F., Regan, Á., *et al.*, (2014). *Food Qual. Prefer.* 37, 10-18.
- Meadows, C.W., Meadows, C.Z., Tang, L., Liu, W. (2019). *Commun. Stud.* 70, 453-469.
- Morabito, S., Silvestro, S., Faggio, C. (2017). *Nat. Prod. Res.* 32, 621-631.
- Mou, Y. and Lin, C.A. (2014). *Sci. Commun.* 36, 593-616.
- Overbey, K.N., Jaykus, L.A., Chapman, B.J. (2017). *J. Food Prot.* 80, 1537-1549.
- Rutsaert, P., Regan, Á., Pieniak, Z., McConnon, Á., *et al.*, (2013). *Trends Food Sci. Technol.* 30, 84-91.
- Ruzza, M., Tiozzo, B., Rizzoli, V., Giaretta, M., *et al.*, (2020). *Risk Anal.* 40, 2071-2092.
- Skurka, C., Niederdeppe, J., Romero-Canyas, R., Acup, D. (2018). *J. Commun.* 68, 169-193.
- Topp, K., Thai, M., Hryciw, D.H. (2019). *Environ. Educ. Res.* 25, 691-700.



Toxigenic microalgae and co-occurrence of toxins in Patagonian Gulfs of Argentina

Leilén Luciana Gracia Villalobos^{1*}, Norma Herminia Santinelli², Alicia Viviana Sastre², Noelia Mariel Uyua², Soledad Díaz Ovejero², Emiliano Agustín Crippa², Bernd Krock³

¹Laboratorio de Química Ambiental y Ecotoxicología (LAQUIAE), Centro para el Estudio de Sistemas Marinos (CESIMAR) – CONICET, Boulevard Brown 2915, (9120) Puerto Madryn, Chubut, Argentina; ²Instituto de Investigación de Hidrobiología, FCNyCS, UNPSJB, Gales 48, (9100) Trelew, Chubut, Argentina; ³Alfred Wegener Institut-Helmholtz Zentrum für Polar- und Meeresforschung, Chemische Ökologie, Am Handelshafen 12, 27570 Bremerhaven, Germany.

*corresponding author's email: gracia@cenpat-conicet.gob.ar

Abstract

In the coastal waters of Chubut Province in Argentina, several species of toxigenic microalgae have been recorded. Among those, the dinoflagellate *Alexandrium catenella* has caused poisonings and human deaths since 1980, resulting in closures of mollusk fisheries due to the presence of paralytic shellfish toxins (PST). In recent years, in addition to PST outbreaks, fishery closures have also been imposed due to lipophilic toxins above regulatory limits in shellfish. Phytoplankton analyses were performed during 2018 at six sites located in the North Patagonian gulfs (San Matías, San José, and Nuevo). Between February and June, the presence of toxins and toxic species was assessed. Domoic acid (DA) was detected in 47% of the samples, while the pectentoxins (PTX) PTX-2 and/or PTX-2sa were detected in 79% of the samples. The co-occurrence of both toxins was observed during all months except March. The diatoms *Pseudo-nitzschia pungens*, *P. fraudulenta*, and *P. calliantha* were identified as the potential DA producers, while the dinoflagellates *Dinophysis tripos* and *D. acuminata* were identified as the potential producers of PTX. This study expands the knowledge on the simultaneous presence of multiple phycotoxins in the North Patagonian gulfs and raises questions about the possible impacts of such occurrences on public health. This study was carried out in the frame of the Provincial Plan for Prevention and Control of Red Tides.

Keywords: Southwest Atlantic, bioaccumulation, phycotoxins, harmful algal blooms, monitoring

<https://doi.org/10.5281/zenodo.7033115>



Introduction

Several toxigenic microalgae species have been recorded along the coast of the Chubut Province (Argentina) since 1980 (Carreto *et al.*, 1981), and they have caused many harmful algal bloom (HAB) events. The most frequent toxin-producing species are: *Alexandrium catenella*, paralytic shellfish toxin (PST)-producing species; *Dinophysis tripos*, *D. acuminata*, *D. caudata*, *D. fortii*, *D. acuta*, *Phalacroma rotundata*, and *Prorocentrum lima*, lipophilic shellfish toxin (LST)-producing species; and *Pseudo-nitzschia australis*, *P. multiseries*, *P. pungens*, *P. fraudulenta*, and *P. calliantha*, amnesic shellfish toxin (AST)-producing species (Sastre *et al.*, 2018). The species *A. catenella* and members of the genus *Dinophysis* cause toxin-related harmful events, including direct impact on human health or natural resources

or indirect impact to the aquaculture industry. It should be considered that recent studies in different areas of the Argentine Sea have indicated the presence of new groups of phycotoxins in samples of phytoplankton and mollusks. These phycotoxins are produced by various genera of dinoflagellates, such as yessotoxins, spirolides, and azaspiracids (Almandoz *et al.*, 2014, 2019; Akselman *et al.*, 2015; Krock *et al.*, 2015; Turner and Goya, 2015; Tillmann *et al.*, 2016; Fabro *et al.*, 2017, 2019; Guinder *et al.*, 2018; Montoya *et al.*, 2021). Likewise, the list of toxigenic species in the Argentine Sea continues to increase, as is the case with the recent detection of *Prorocentrum texanum* off the coast of the Province of Buenos Aires (Sunesen *et al.*, 2020).

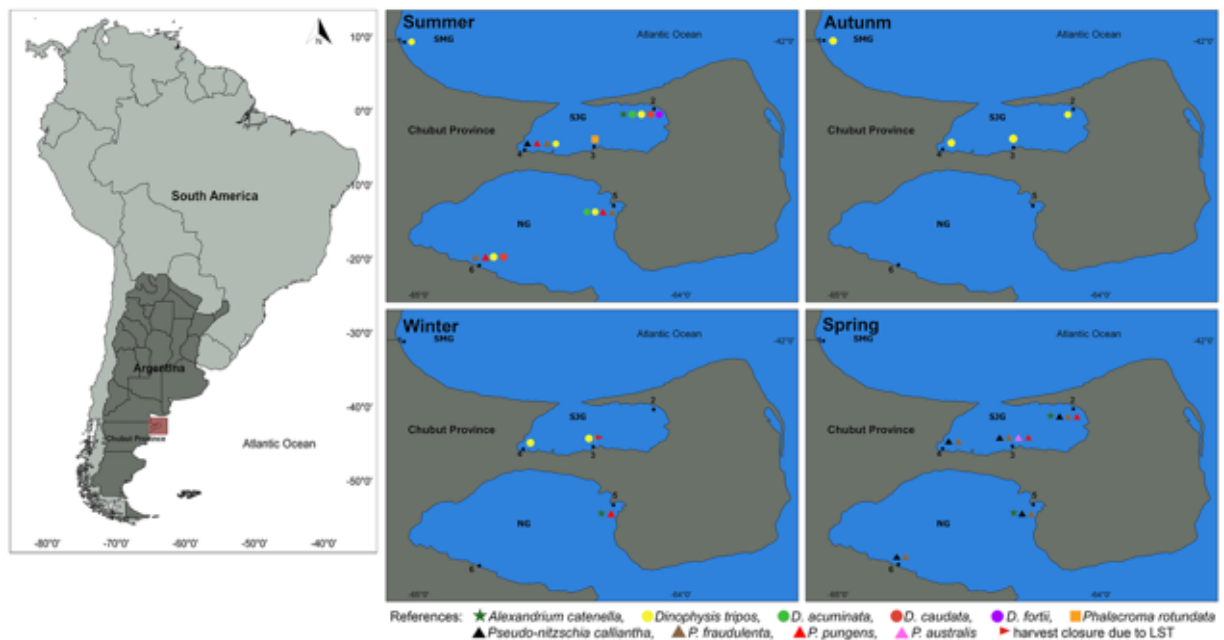


Fig. 1. Distribution of harmful microalgae and shellfish harvest closure due to LST in the North Patagonian gulfs San Matias (SMG), San José (SJG) and Nuevo (NG). Sampling stations: 1 = Puerto Lobos, 2 = Bengoa, 3 = Larralde, 4 = Riacho, 5 = Pardelas, 6 = Playa Paran



The primary aim of this study was to analyze the spatiotemporal distribution of toxigenic microalgae and co-occurrence of toxins present in the Northern Patagonian gulfs.

Material and Methods

Phytoplankton sampling was carried out during 2018 in the North Patagonian gulfs (between 41° and 43° S) San Matías, San José and Nuevo. These are located on the North-eastern coast of the Chubut Province, in Argentina. Samples were collected monthly at the stations Puerto Lobos (San Matías Gulf), Bengoa, Larralde and Riacho (San José Gulf), and Playa Paraná, and Pardelas (Nuevo Gulf), in the frame of the monitoring program.

Water samples for quantitative phytoplankton analyses were collected using a sampling tube with 80 cm of length and 11 cm of diameter. The 250 mL samples were preserved with Lugol's acid solution and stored in the dark. Qualitative phytoplankton samples were taken using a 25 µm mesh net through oblique tows and fixed with formaldehyde at a final concentration of 4%.

A sampling survey to collect phytoplankton for toxin analysis was carried out between February and June in the study area. Phytoplankton samples were collected by oblique net tows from 5 m depth to the surface with a 25 µm mesh net. Ten-milliliter aliquots of the captured material were preserved in Lugol's solution for microscopic observation and used to calculate cell concentrations. The rest of each sample was filtered through Whatman GF/F filters and frozen (-20 °C) until further analysis. Phytoplanktonic species were morphologically identified and counted in a phase-contrast inverted microscope

(Leica DMIL, Wetzlar, Germany). Scanning electron microscopy (SEM) observations of the samples were done with a JSM-6360 LV (Jeol, Tokyo, Japan) at the Facultad de Ciencias Naturales y Museo, Universidad Nacional de La Plata, to identify *Pseudo-nitzschia* species.

Toxin analyses were performed by liquid chromatography coupled to a tandem mass spectrometer (LC-MS/MS), as described in Krock *et al.* (2008).

Results and Discussion

Distribution spatial-temporal of harmful microalgae: relative abundance and cell density

During the summer (January), resting cysts of *A. catenella* were observed in the San José Gulf, and in late winter (August) and spring (October and November), the motile form in Nuevo and San José gulfs. However, no PSTs were recorded in mollusk samples.

Dinophysis tripos was observed from January and presented a maximum concentration of 6,720 cells L⁻¹ in March. In autumn (May-June), lipophilic toxins were recorded in mollusk samples through mouse bioassays in the San Matías and San José (Bengoa and Larralde) gulfs. *Dinophysis acuminata*, *D. fortii*, and *D. caudata* were observed only in net samples with low relative abundances.

During spring and summer, *P. pungens*, *P. fraudulenta*, and *P. calliantha* were present in gulf San José and Nuevo. *P. calliantha* was the most abundant, with maximum values of around 10⁵ cells L⁻¹, contributing to more than 80% of the total phytoplankton (Fig. 1).



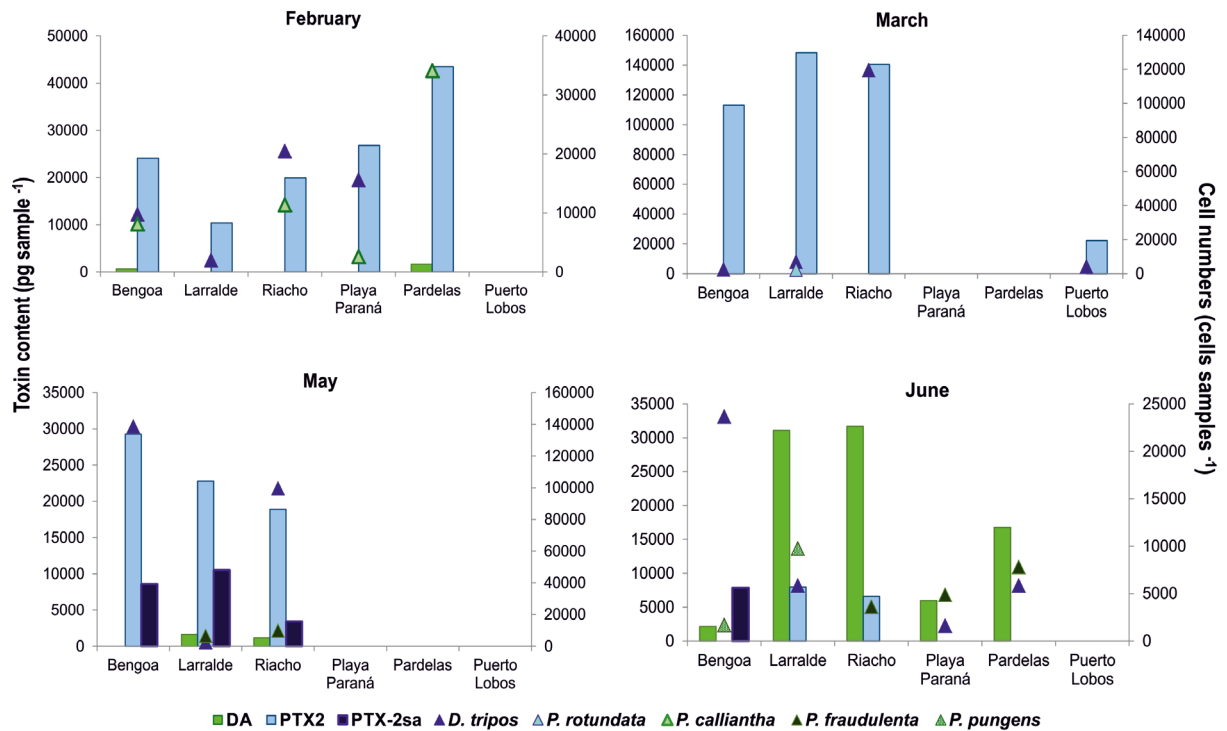


Fig. 2. Cell abundances of toxigenic microalgae in phytoplankton samples and amount of lipophilic and amnesic toxins.

Toxin analyses and species distribution

Qualitative plankton samples from different locations were taken, and *Dinophysis* and *Pseudo-nitzschia* cells were enumerated, and lipophilic and amnesic toxins were determined. Of the LST-producing species, only *D. tripos* and *Phalacrocoma rotundata* were detected, although the latter was recorded in very low density and only in one sample. Of the amnesic shellfish toxin-producing species, *P. fraudulenta*, *P. calliantha*, and *P. pungens* were detected.

The lipophilic toxin profiles in all samples consisted mainly of pectenotoxins PTX-2 followed by PTX-2sa, which were detected in 79% of them. Domoic acid (DA) was detected in 47% of the samples (Fig. 2).

Toxigenic phytoplankton species were recorded throughout 2018 in the North Patagonian gulfs. Although these species have been previously reported for this region (Santinelli *et al.*, 2002; Gracia Villalobos *et al.*, 2015; Sastre *et al.*, 2018), the co-occurrence of toxigenic species of different genera during the greater part of the year has not been reported before. The presence of lipophilic toxin profiles in plankton samples is in accordance with previous reports by Gracia Villalobos *et al.* (2015). In addition, the detection of DA was previously recorded in plankton samples from Nuevo Gulf by Sastre *et al.* (2007). However, this is the first time that simultaneous presence of lipophilic toxins and DA has been reported in plankton samples.

These results highlight the need to permanently update the monitoring programs to mitigate the adverse effects of HAB events on human health, shellfish fisheries, aquaculture, and tourism. In addition, they contribute to know the importance of the transfer and accumulation of phycotoxins to higher levels in the food web in the North Patagonian gulfs.

Acknowledgements. This study was supported by Project PI 1548 of the Universidad Nacional de la Patagonia San Juan Bosco. We are grateful to the Provincial Plan for Prevention and Control of Red Tide (Chubut Province).

References

- Akselman, R., Krock, B., Alpermann, T., Tillmann, U., *et al.*, (2015). *Harmful Algae* 45, 40-52.
- Almandoz, G., Montoya, N., Hernando, M., Benavides, H., *et al.*, (2014). *Harmful Algae* 37, 100-109.
- Almandoz, G., Cefarelli, A., Diodato, S., Montoya, N., *et al.*, (2019). *Mar. Pollut. Bull.* 145, 105-117.
- Carreto, J., Lasta, M., Negri, R., Benavides, H., 1981. Instituto Nacional de Investigación y Desarrollo Pesquero (INIDEP), Mar del Plata, p. 55. Contribución N° 399.
- Fabro, E., Almandoz, G., Ferrario, M., Jon, U., *et al.*, (2017). *J. Phycol.* 53, 1206-1222.
- Fabro, E., Almandoz, G., Krock, B., Tillmann, U. (2019). *Mar. Freshwater Res.* 71, 832-843.
- Gracia Villalobos, L., Santinelli, N., Sastre, V., Krock, B., Esteves, J.L. (2015). *J. Shellfish Res.* 34, 1141-1149.
- Guinder, V.A., Tillmann, U., Krock, B., Delgado, A., *et al.*, (2018). *Front. Mar. Sci.* 5, 394.
- Krock, B., Tillmann, U., John, U., Cembella, A.D. (2008). *Anal. Bioanal. Chem.* 392, 797-803.
- Krock, B., Borel, C.M., Barrera, F., Tillmann, U., *et al.*, (2015). *J. Mar. Syst.* 148, 86-100.
- Montoya, N.G., Carignan, M.O., Mattera, M.B. (2020). *Acta Toxicol. Argent.* 28, 21-30.
- Santinelli, N., Sastre, V., Esteves, J.L. (2002). In: Sar, E.A., Ferrario, M.E., Reguera, B. (Eds.). Instituto Español de Oceanografía, Madrid, pp. 197-208.
- Sastre, V., Santinelli, N., Marino, G., Solís, M., *et al.*, (2007). *Harmful Algae News* 34, 12-14.
- Sastre, A.V., Santinelli, N.H., Solís, M.E., Pérez, L.B., *et al.*, (2018). In: Hoffmeyer, M.S., Sabatini, M., Brandini, F.P., Calliari, D.L., Santinelli, N.H. (Eds.). Springer, pp. 495-515.
- Sunesen, I., Rodríguez Hernández, F., Aguiar Juárez, D., Tardivo Kubis, J.A., *et al.*, (2020). *Phycologia* 59, 634-650.
- Turner, A.D. and Goya, A.B. (2015). *Toxicon* 102, 32-42.
- Tillmann, U., Borel, C., Barrera, F., Lara, R., *et al.*, (2016). *Harmful Algae* 51, 40-55.





EMERGING ISSUES



Inclusive partnerships for forecasting and managing HAB risk in Washington State coastal communities

Vera L. Trainer^{1*}, Ervin Joe Schumacker², Usha Varanasi³

¹ National Oceanic and Atmospheric Administration (NOAA), Seattle, WA 98112, U.S.A.;

² Department of Fisheries, Quinault Indian Nation, Taholah, WA 98587, U.S.A.; ³ School of Aquatic and Fishery Sciences, College of the Environment, University of Washington, Seattle, WA 98195, U.S.A.

* corresponding author: vera.l.trainer@noaa.gov

Abstract

Current health and climate crises will require a proactive approach, focused on establishing and fostering partnerships to identify and eliminate primary causes of the disconnect between humans and nature. In the northeast Pacific Ocean and the adjacent coastal areas, lessons focused on human respect for nature have been learned through unique scientific partnerships that blend current-day technology with observational knowledge of Indigenous communities, such as the study of harmful algal blooms (HABs). Explicit examples of proactive strategies used to address environmental problems include projects focused on understanding and mitigating HAB impacts in coastal Washington State. These projects are based upon mutual respect of Indigenous and non-Indigenous scientists and include: 1) establishment of the Olympic Region Harmful Algal Bloom (ORHAB) partnership, 2) sharing of science knowledge in tribal youth camps; 3) development of a forecasting system for HABs to alert resource managers of the risk they pose to shellfish harvests and community health. These collaborative projects teach all participants the value of reciprocity, demonstrating how the bounty of the ocean and its protection can promote our well-being. Programs that give equal respect to all voices promote proactive strategies that foster both human and ocean health.

Keywords: HAB, climate change, Indigenous partnerships, sato-umi, health, Washington State

<https://doi.org/10.5281/zenodo.7033133>



Introduction

The growing movement calling for *reciprocal* healing of nature and people (Kimmerer, 2015; Hayden, 2019; Fleischner and Sewall, 2020; Varanasi, 2020; Myers and Frumkin, 2021) considers Indigenous knowledge about conservation and resource management with increasing regard (Kimmerer, 2015; Polfus *et al.* 2016; Ban *et al.*, 2018; Atlas *et al.*, 2020), especially realizing that Indigenous people effectively manage over 40% of the world's ecosystems (Garnett *et al.*, 2018). Given that biodiversity is among the highest on lands managed by Indigenous communities, the protection of these lands and respect for the voices of their inhabitants are critical in the survival of the entire human species (Schuster *et al.*, 2019). Indigenous traditional ecological knowledge has recently been recognized to be a critical component of decision-making, contributing to scientific, technical, social, and economic advancements of the United States and to our collective understanding of the natural world (Memorandum, 2021). By bringing together experts of all backgrounds, Indigenous and non-Indigenous scientists alike, solutions are created that promote the harmonious co-existence of people and nature.

The linkage of human and ocean health

Humans are an integral part of the natural world who often take advantage of the healing properties of nature –by walking on the seashore or hiking in the forest. But it is time to shift the focus from nature *for* health to nature *and* health, allowing human and ecological health to be joint goals (Varanasi, 2020; Varanasi *et al.*, 2021). In fact, the Japanese term “Sato-umi”, meaning village-seas, was created to describe the dependency

of human and nature interactions to achieve productive and diverse ocean ecosystems (Makino, 2011). This centuries-old goal of living harmoniously with nature is shared by Indigenous communities in many parts of the world.

Community based partnerships

The Sato-umi principles (Table 1) have provided lessons for collaborative studies of HABs that have passed the test of time – and that are still ongoing today in Washington State, USA. The

Table 1. The Sato-umi principles

- | |
|--|
| • Share knowledge, including local knowledge |
| • Listen |
| • Foster collaborative and equitable relationships from the inception of an idea |
| • Conduct science as a collective action |
| • Cultivate mutual respect |

Olympic Region HAB ([ORHAB](#)) partnership was established in response to a coastal survey that highlighted HABs as the largest coastal issue. This grassroots idea came from the communities to scientists, not the other way around, and has lasted the test of time as a partnership of Indigenous scientists, managers, and community members with State and Federal scientists (Fig. 1). ORHAB empowers tribal and state managers to make scientifically-based decisions about managing and mitigating HAB impacts on coastal fishery resources. ORHAB is the only HAB project of its kind that has been transferred from federal to state and tribal government



support, funded by tribal governments and a tax paid by recreational shellfish harvesters when they purchase a state shellfishing license (Trainer and Suddleson, 2005). Thus, ORHAB is funded and operated by the community that it serves. This community-driven science partnership has formed the basis of successful programs in Puget Sound, WA (the SoundToxins partnership), Oregon, and Alaska (the SEATOR program) as well other parts of the world, including Guatemala and Indonesia (Trick *et al.*, 2012; Trainer *et al.*, 2016). These partnerships demonstrate that local people are an indispensable part of ecosystem studies (Makino, 2011) and show the critical need to *foster collaborative and equitable relationships from the inception of an idea* – by including the people who live on the coast in the design and implementation of scientific studies.

The success of community-driven programs (such as ORHAB) has been highlighted by Elinor Ostrom, the only woman to receive a Nobel Prize in Economic Sciences. She states in her work that projects established by resource users - by communities, not governments - achieve the greatest sustainability (Ostrom, 1990). Cooperation is maintained by establishment of trust. ORHAB is an example of this established trust in a science partnership. Ostrom's work emphasizes the need to implement community-driven approaches in dealing with global environmental problems, including HABs and climate change.

Our initial meetings with tribal elders were held two decades ago, in which we asked for their ideas to sustain the ORHAB partnership. We spoke about all the great work we wished to do on their coastal beaches and the adjacent

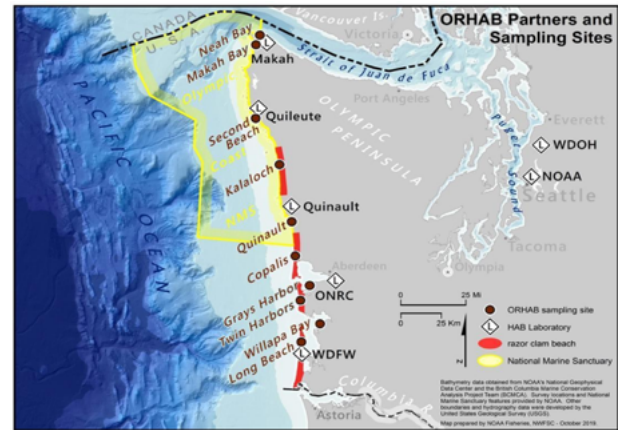


Fig. 1. ORHAB sites on the Washington State, U.S.A. coast for phytoplankton sampling (•), toxin analysis (L), and razor clam harvest (see legend; Trainer and Suddleson, 2005). Partners include NOAA, the Washington State Department of Health (WDOH), the Washington Department of Fish and Wildlife (WDFW), the University of Washington Olympic Natural Resources Center (ONRC), the Quinault Indian Nation (Quinault), the Makah Tribe (Makah), and Quileute Tribe (Quileute). Reprinted from Varanasi *et al.* (2021).

seas by building HAB monitoring programs and establishing labs where tribes could do their own testing. The elders listened but sat silently until we talked about our plans to teach their children. As we *listened* to them, the importance of *conducting our science as a collective action*, by not only working with adults, but by teaching the children, the next generation, was established as a need within their community. The partnership was strengthened by including all voices – children and adults, western and Indigenous scientists. This led to the establishment of a summer camp curriculum that included lectures on HABs, introduction to phytoplankton identification by microscopy, and rapid toxin testing. The summer camp teachers included tribal elders who spoke about bioluminescent waters that



warned of toxic shellfish, demonstrating to the children the value of their traditional knowledge of HABs.

Knowledge sharing

These summer camps were held on the coast of the Pacific Northwest of the USA, first inhabited by Indigenous people with the present-day names, Quinault Indian Nation and Quileute, Hoh, and Makah Tribes. These tribes have taught us respect for the sea by their saying “when the tide is out, the table is set”, referring to the historical abundance of shellfish during low tides. During our first meetings with Makah tribal elders, they spoke about a highly productive region off the coast of WA where seas “were quite heavy with halibut” and whales could be found. During several research cruises over the last several years, we found that what the Makah called the Big Prairie, also named the Juan de Fuca eddy, was indeed a productive region and an initiation site for *Pseudo-nitzschia* HABs that impact crabbing and clamming. By *sharing this knowledge*, an early warning system for these HAB was co-designed with Indigenous scientists to promote seafood safety for all coastal people. This knowledge and our research together have led to the development of the Pacific Northwest HAB Bulletin, a synthesis of data from ORHAB monitoring, weather reports, models, and more, known to be important in forecasting HABs. This early warning Bulletin, provided to State and tribal co-managers of razor clams during harvesting season, enabled them to respond quickly to impending HABs by permitting selective harvest at safe locations or enabling pre-emptive increases in harvest limits when

HABs are lurking offshore. The Bulletin allowed for safe harvest only through a collaborative effort made possible through *mutual respect* that has been cultivated over many years. Matt Hunter, an Oregon State shellfish manager, commented that the Pacific Northwest (PNW) HAB Bulletin allowed a safe, pre-emptive increase in the clam harvest limit after months of closures due to domoic-acid in clams. He stated, “*The Long Beach, Washington razor clam opening and increased bag limit was a boon for Oregon north coast economies as well. A lot of people were hungry for clams*”.

Science advancement through collaboration

The establishment of mutual respect has allowed our scientific goals to be expanded into areas that we could only dream about two decades ago when our joint work began. With the Makah, Quileute, Quinault tribes and other partners, joint funding was received in 2020 for a project to deploy the Ocean Aero Triton, an autonomous unmanned submersible vehicle (AUSV), to sample HAB organisms and toxins off the coast of Washington State. Because rough seas and bad weather often prevent sampling of these dynamic ocean regions using small boats, the AUSV is a safe and effective alternative to in-person sampling. The samples collected by the Triton will be analyzed at tribal labs and used to improve the forecast provided by the PNW HAB Bulletin. Seawater samples from HAB “hotspots” or initiation sites provide an early warning of toxins that can affect coastal shellfish (crabs and clams) harvest.





Fig. 2. The Triton AUSV off the coast of Washington State. Credit: Bill Burns/Ocean Aero.

Conclusions

To summarize the Sato-umi approach: 1) humans are a part of nature; 2) community-driven science is the longest lasting approach to collaborative projects; 3) coastal residents need to be an integral part of our science. Our relationship with nature is not just a sense of “being close to nature to heal ourselves” but includes a reverence for nature to address issues such as the increasing intensity and changing global distribution of HABs. This closeness to nature is achieved by working with community members to conduct our joint scientific inquiries – by being inclusive from the inception of a scientific idea. As the Indigenous scholar Robin Kimmerer says “the relationship between the self and the world is reciprocal. It is not a question of first getting enlightened or saved and then acting. As we work to heal the earth, the earth heals us (Kimmerer, 2015).”

Whether fishing together, collecting clams from a windy beach, or conducting collaborative science, each person’s attention to protective, sustained engagement with nature can create a ripple effect for

conservation and build communities with a sense of solidarity, sharing, and a collective mission to care for each other and the planet. Ocean researchers, lawmakers, industries, managers of natural resources, and the general public committed to envisioning “the science we need for the ocean we want” are coming together during the 2021-2030 [UN Decade of Ocean Science for Sustainable Development](#) to design ocean solutions to combat climate change, environmental degradation, and societal problems like HABs. This initiative stems from the paradigm that both oceans and people will benefit from conservation practices and advocacy for balanced approaches to science and solutions that serve society. Indeed, oceans and humans are undeniably linked: our approach to resource use on land, sea, and in the air affect ocean health and in turn the health of the oceans influences us (e.g., Fleming *et al.*, 2019; Franke *et al.*, 2020).

Acknowledgements. We thank Professor Mitsutaku Makino for his review of this manuscript and insights on the Sato-umi approach. We acknowledge the helpful comments of an anonymous reviewer. We are grateful for funding from NOAA’s U.S. Integrated Ocean Observing System Office for the Triton AUSV project and NOAA National Centers for Coastal Ocean Science (NCCOS) for ORHAB. This is NCCOS Monitoring and Event Response to HAB (MERHAB) publication #242. The ideas in this paper are discussed in more detail in Varanasi *et al.* (2021).

References

Atlas, W.I., Ban, N.C., Moore, J.W., Tuohy, A.M. *et al.*, (2020). *BioScience* 71, 186-204.



- Ban, N.C., Frid, A., Reid, M., Edgar, B., *et al.*, (2018). *Nat. Ecol. Evol.* 2, 1680-1683.
- Fleischner, T.L. and Sewall, L. (2020). *Ecopsychology* 12, 159-161.
- Fleming, L.E., Maycock, B., White, M.P., Depledge, M.H. (2019). *People and Nature* 1, 276-283.
- Franke, A., Blenckner, T., Duarte, C.M., Ott, K., *et al.* (2020). *One Earth* 2, 557-565.
- Garnett, S.T., Burgess, N.D., Fa, J.E., Fernández-Llamazares, Á., *et al.* (2018). *Nat. Sustain.* 1, 369-374.
- Hayden, W. (2019). *A Sense of Wonder Towards Nature: Healing the Planet through Belonging*; Routledge, Taylor and Francis, pp. 213.
- Kimmerer, R.W. (2015). *Braiding Sweetgrass: Indigenous Wisdom, Scientific Knowledge, and the Teachings of Plants*; Milkweed Ed., pp. 391.
- Makino, M. (2011). *Fisheries Management in Japan*. Springer, Dordrecht, 200 pp.
- Memorandum on Indigenous Traditional Ecological Knowledge and Federal Decision Making (Nov 15, 2021).
- Myers, S. and Frumkin, H. (2020). *Planetary Health: Protecting Nature to Protect Ourselves*; Island Press, pp. 536.
- Ostrom, E. (1990). *Governing the Commons: The Evolution of Institutions for Collective Action*. Cambridge University Press, New York.
- Polfus, J.L., Manseau, M., Simmons, D., Neyelle, M., *et al.*, (2016). *Ecol. Soc.* 21, 18.
- Schuster, R., Germain, R.R., Bennett, J.R., Reo, N.J., Arcese, P. (2019). Vertebrate biodiversity on indigenous-managed lands in Australia, Brazil, and Canada equals that in protected areas. *Environ. Sci. & Pol.* 101, 1-6.
- Trainer, V.L., Trick, C.G., Cochlan, W.P. (2016). *PICES Press* 24, 2.
- Trainer, V.L. and Suddleson, M. (2005). *Oceanogr.* 18, 228-237.
- Trick, C.G., Trainer, V.L., Wells, M.L., Cochlan, W.P. (2012). *PICES Press*. 20, 2.
- Varanasi, U. (2020). *Ecopsychology* 12, 188-194.
- Varanasi, U., Trainer, V.L., Schumacker, E.J. (2021). *Int. J. Environ. Res. Public Health.* 18, 2662.



Harmful or beneficial algae? How organic matter secreted by plankton and neuston algae, including that in the surface microlayer and in sea foam, may be participating in climate regulation: a review

Ian R. Jenkinson^{1,2*}, Elisa Berdalet³, Wei-Chun Chin⁴, Michel Denis⁵, Haibing Ding^{6,7}, Jizhou Duan⁸, Florence Elias⁹, Igor Emri¹⁰, Santosh K. Karn^{11,12}, Zhuo Li^{13,14}, Alenka Malej¹⁵, Xavier Mari^{16,17}, Laurent Seuront¹⁸, Jun Sun¹⁹, Tim Wyatt²⁰, Wuchang Zhang²¹, Oliver Wurl²²

¹Chinese Academy of Sciences Institute of Oceanology, CAS Key Laboratory of Marine Ecology and Environmental Sciences, Qingdao 266071, China; ²Agency for Consultation and Research in Oceanography, 19320 La Roche Canillac, France; ³Institute of Marine Sciences (ICM-CSIC), E-08003, Barcelona, Catalonia, Spain; ⁴University of California, Dept. of Bioengineering, Merced, CA, U.S.A.; ⁵Aix Marseille University, Université de Toulon, CNRS/INSU, IRD, Institut Méditerranéen d'Océanologie (MIO), Case 901, 13288 Marseille cedex 09, France; ⁶Ocean University of China, Key Laboratory of Marine Chemistry Theory and Technology, Qingdao, China; ⁷Chinese Academy of Sciences Qingdao Science and Education Park, West Coast New Area of Qingdao 266400, China; ⁸Key Laboratory of Environmental Corrosion and Biofouling, Institute of Oceanology, Chinese Academy of Sciences, Qingdao, 266071, China; ⁹Laboratoire Systèmes et University Matières complexes, Université Paris Diderot, CNRS UMR 7075, Paris, France; ¹⁰University of Ljubljana, Dept. of Mechanics, Polymers and Composites, Centre for Experimental Mechanics, Ljubljana, Slovenia; ¹¹Sardar Bhagwan Singh University, Dept. of Biochemistry and Biotechnology, Balawala, Dehradun, 248161, Uttarakhand, India; ¹²Key Laboratory of Environmental Corrosion and Biofouling, Institute of Oceanology, Chinese Academy of Sciences, Qingdao, 266071, China; ¹³State Key Laboratory of Pollution Control and Resource Reuse, Tongji University, Shanghai 200092, China; ¹⁴Shanghai Institute of Pollution Control and Ecological Security, Shanghai, China; ¹⁵National Institute of Biology, Marine Biology Station, Piran, Slovenia; ¹⁶Aix-Marseille Université, CNRS/INSU, Université de Toulon, IRD, Mediterranean Institute of Oceanography (MIO) UM 110, Marseille, France; ¹⁷University of Science and Technology of Hanoi (USTH), Vietnam Academy of Science and Technology (VAST), Hanoi, Vietnam; ¹⁸CNRS UMR 8187, Laboratoire d'Océanologie et de Géoscience, Wimereux, France; ¹⁹College of Marine Science and Technology, China University of Geosciences (Wuhan), Wuhan 430074, China; ²⁰Barrio A Tomada, Borreiros, Gondomar, 36378 Pontevedra, Spain; ²¹CAS Key Laboratory of Marine Ecology and Environmental Sciences, Institute of Oceanology, Chinese Academy of Sciences, Qingdao 266071, China; ²²Carl von Ossietzky Universität Oldenburg, Institute for Chemistry and Biology of the Marine Environment, 26382 Wilhelmshaven, Germany.

*corresponding author's e-mail: ian.jenkinson@ocean-expert.org

<https://doi.org/10.5281/zenodo.7033151>



Abstract

While phytoplankton has been shown to influence climate in diverse ways, this review treats just two aspects: reduction of sea-air fluxes, and increase in ocean foam coverage. Plankton and neuston algae produce dissolved organic matter (DOM), which tends to concentrate in the sea-surface microlayer (SML). Fluxes of matter and energy exchange across the sea-air surface and are important in regulating weather and climate. Freshly produced DOM shows marked surface and rheological activity, and it reduces these fluxes. Foam covers part of the ocean surface, largely produced by breaking and spilling waves. Its longevity is increased in areas subject to high biological productivity, and particularly during blooms of some species of harmful algae and may involve specific DOM molecules and the algal genes that produce them. Ocean foam is generally white and reflects about 50% of incident solar radiation, while the foam-free ocean surface reflects only about 5%. Thus, algal DOM helps to cool the planet by increasing foam coverage. Unpredictable changes in abundance and taxonomic composition of phytoplankton and phytoneuston may be adding uncertainty to modelling global and local climate. Further research on the roles of the ocean in climate regulation should thus pay more attention to algal communities, their specific genes and the physical and chemical characteristics of the DOM they produce.

Keywords: climate; plankton; neuston; dissolved organic matter; rheology; sea surface microlayer

Introduction

Oceans cover about 70% of the Earth's surface. At the top, there is a sharp interface between the atmosphere and the ocean, underlain by a surface microlayer (SML), 50 to 100 μm thick. Between the SML is an intermediate layer of near-surface underlying water (ULW) extending down to very roughly 1 m, below which deeper ULW extends to near the sea bottom (Fig. 1). The SML incorporates strong gradients in temperature, salinity, nutrient concentrations, pH and viscosity (η). While the ULW also shows gradients of these and (other biological) parameters, they tend to be much less sharp than in the SML (Zhang *et al.*, 2003a,b,c; Wurl *et al.*, 2017). In addition, measurements made by Zhang *et al.* (2003b) over 24 h in samples from both the SML and from the ULW at 25 cm depth showed η values consistently higher in the SML.

In 25 cm-deep ULW (Zhang *et al.*, 2003b) both layers they showed a diurnal rhythm; they showed noticeably higher η values during daylight than at night, suggesting that short-lived (< 1 day) dissolved organic matter (DOM) excreted largely because of primary production by phytoneuston and phytoplankton increased the viscosity η . This is consistent with the positive relationship found by Jenkinson and Biddanda (1995) between η and chlorophyll content, as well as with the findings of higher 2D compression-dilatation viscosity and elasticity in the SML than in the ULW at 10 cm depth (Williams *et al.*, 1986).

Tumminello *et al.* (2021) investigated sea-spray aerosols derived by wind and bubble-bursting from the SML over the course of a



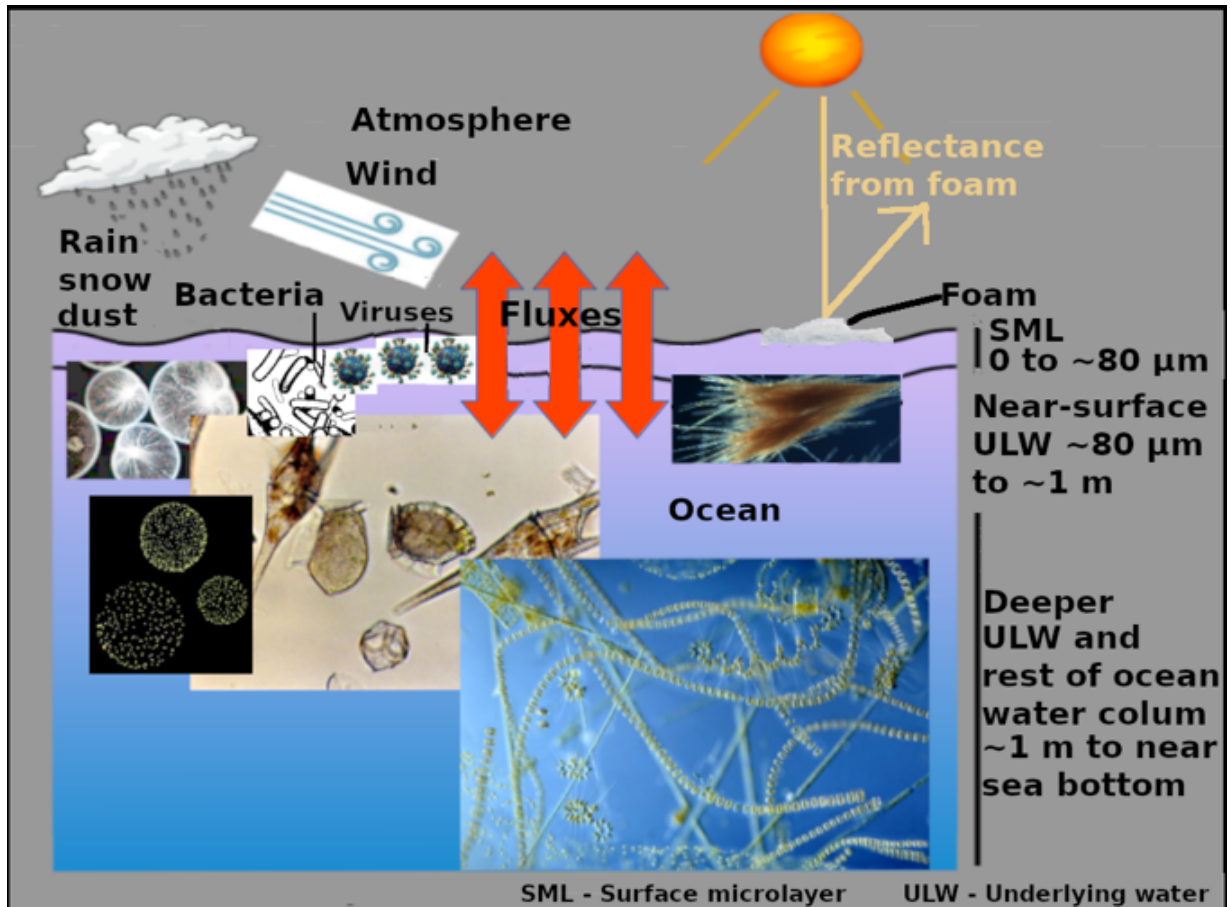


Fig. 1. A schema of the ocean and the atmosphere, emphasizing the aspects treated in this presentation. Inserts within the ocean, from left to right: micrographs of the dinoflagellate *Noctiluca* sp.; the colonial prymnesiophyte *Phaeocystis globosa*; other dinoflagellates (*Ceratium* sp., *Dinophysis* spp.); bacteria; viruses; diatoms; filamentous cyanobacteria. Dissolved organic matter, more or less colloidal and aggregated, is present throughout the oceans, but tends to concentrate in the surface microlayer.

phytoplankton bloom in an experimental tank. Viscosity in the aerosol droplets (calculated from “bounce factor”) increased up to 1000-fold relative to organics-free seawater, with a strong relationship to the amounts and types of organic matter (including carbohydrates, proteins and lipids) and to chlorophyll *a*.

Values of η in both seawater and algal cultures are composed of a Newtonian component η_w due to water and salt, plus a non-Newtonian excess component η_e due to polymeric DOM

(Jenkinson and Sun, 2010). The SML also is most often, but not always, enriched in dissolved organic matter (DOM) relative to the ULW (Jenkinson *et al.*, 2021), where it is present sometimes even as a gel phase (Wurl *et al.*, 2016).

Ocean DOM is composed of two main fractions: firstly “old” (years to millennia) and refractory, with little surfactant or rheological activity, and secondly “young” or “fresh” (hours to days) biologically and



chemically labile, that are characterized by strong surfactant and rheological activity (Shen and Benner, 2019; Barthelmeß *et al.*, 2021). Likely, it was the second fraction that produced (i) the diurnal viscosity variations reported in Zhang *et al.* (2003b), and (ii) the increased viscosity and foam formation and duration of Kesaulya *et al.* (2008) and of Callaghan *et al.* (2012), as well as the widespread surface gels reported by Wurl *et al.* (2016), and the more exceptional, often light-coloured, floating organic material reported by Flander-Putrelle and Malej (2008) in the North Adriatic and by Balkis-Özdelice *et al.* (2021) in the Sea of Marmara.

In this context, we aim to review the effects of DOM produced by plankton and neuston algae on two important in determining climate. These two processes are ocean-atmosphere fluxes and reflexion of solar radiant energy by sea foam, including whitecaps. Figure 1 shows a schema of the ocean and the atmosphere, emphasizing the aspects treated here.

Algal DOM and ocean-air fluxes

Near-surface and SML-associated DOM reduces sea-air exchange of gases, as well as salts, humidity, aerosols, heat and mechanical energy (Calleja *et al.*, 2009; Mustafa *et al.*, 2020; Adenaya *et al.*, 2021), all of which are important regulators of climate, including storm formation (Veron, 2015). For example, Mustafa *et al.* (2020) reported that SML DOM reduces global CO₂ fluxes by ~19%, and that sea-surface slicks exhibit the strongest suppression.

The specific chemical composition of different types of DOM may modulate these

processes differently. Future studies need to investigate the molecular mass and the tertiary polymeric structure of such DOM, as well as its rheological properties and surface activity in relation to the different algal taxa and the expressed genes that produce it.

DOM-enhanced ocean foam increases planetary ocean albedo

Waves spilling or breaking on a water–air interface entrain air bubbles into the water. These bubbles tend to rise and accumulate at the surface, producing patches of foam (whitecaps).

The decay of these foams proceeds by the coalescence of bubbles as the inter-bubble water drains, allowing the surfaces of adjoining bubbles to touch and burst (Cantat *et al.*, 2013). Draining is retarded and foam lifetime becomes longer if the liquid is a surfactant that binds to the surfaces or if it is more viscous. Relative to their duration in waters of low phytoplankton biomass (PB) or low primary production (PP), ocean foam duration is increased in waters of high PP or high PB (Callaghan *et al.*, 2012), particularly in the presence of certain specific taxa. Blooms that produce a lot of foam are caused by taxa including dinoflagellates *Karenia brevis* (in North Atlantic and Asian coasts Pierce *et al.*, 2003) and *Margalefidinium polykrikoides* (= *C. polykrikoides*) (Vargas-Montero *et al.*, 2006), as well as the prymnesiophyte *Phaeocystis* spp. (North Sea, Kesaulya *et al.*, 2008).

The fraction of incident radiant energy that is reflected is known as albedo. Foam-free ocean surface has a typical albedo of only ~0.05, but foam is white and albedo is ~0.5. Therefore,



when foam is more stabilized by algal DOM the oceans reflect more solar energy back into space, reducing solar heating of the Earth (Stabeno and Monahan, 1986; Evans *et al.*, 2010).

Discussion and conclusions

Different types of “young”, biologically and chemically labile DOM are formed mainly by PP by phytoplankton and phytoneuston. This young DOM is rheologically active and surfactant. It affects sea-air exchange of matter and energy, and it slows the decay of reflectant whitecaps and other ocean foam. Unpredictable changes in abundance and taxonomic composition of phytoplankton and phytoneuston may be adding hitherto unmodelled uncertainty to global and local climate.

To understand their impacts better, and whether they are harmful or beneficial, the tertiary chemical structures of this “young” DOM in the SML should be characterized in relation to their surface and rheological properties, as well as to the taxa and genomes of the plankton and neuston that produce them.

Acknowledgements and funding. We thank two anonymous reviewers for greatly improving this review. Chinese Academy of Science Research Fellowship for Senior International Scientists (2009S1-36 to I.R.J.); National Natural Science Foundation of China grant (41876134 to J.S.); Changjiang Scholar Program of Chinese Ministry of Education.

References

- Adenaya, A., Haack, M., Stolle, C., Wurl, O., Ribas-Ribas, M. (2021). *Oceans* 2, 752-771.
- Balkis-Özdelice, N., Durmuş, T., Balci, M. (2021). *Int. J. Env. Geoinformatics* 8, 414-422.
- Barthelmeß, T., Schütte, F., Engel, A. (2021). *Front. Mar. Sci.* 8, 718384.
- Bianchi, T.S., Engelhaupt, E., Westman, P., Andren, T., *et al.*, (2000). *Limnol. Oceanogr.* 45, 716-726.
- Callaghan, A.H., Deane, G.B., Stokes, M.D., Ward, B. (2012). *J. Geophys. Res. Oceans* 117, C09015.
- Calleja, M.L., Duarte, C.M., Prairie, Y.T., Agustí, S., Herndl, G.J. (2009). *Biogeosciences* 6, 1105-1114.
- Cantat, I., Cohen-Addad, S., Elias, F., Graner, F., *et al.*, (2013). *Foams*, Oxford Univ. Press, Oxford.
- Evans, J.R.G., Stride, E.P.J., Edirisinghe, M.J., Andrews, D.J., Simon, R.R. (2010). *Clim. Res.* 42, 155-160.
- Flander,-Putrle, V. and Malej, A. (2008). *Harmful Algae* 7, 752-761.
- Jenkinson, I.R. and Biddanda, B.A. (1995). *J. Plankton Res.* 17, 2251-2274.
- Jenkinson, I.R. and Sun, J. (2010). *J. Mar. Sys.* 83, 287-297.



- Jenkinson, I.R., Berdalet, E., Chin, W.-C., Denis, M., *et al.*, (2021). *J. Plankton Res.* 43, 801-821.
- Kesaulya, I., Leterme, S.C., Mitchell, J.G., Seuront, L. (2008). *Oceanologia* 50, 67-182.
- Mustaffa, N.I.H., Ribas-Ribas, M., Banko-Kubis, H.M., Wurl, O. (2020). *Proc. Roy. Soc. A* 476, 20190763.
- Pierce, R.H., Henry, M.S., Blum, P.C., Lyons, J., *et al.*, (2003). *Bull. Env. Contam. Toxicol.* 70, 161-165.
- Shen, Y. and Benner, R. (2019). *Limnol. Oceanogr.* 65, 1061-1071.
- Tumminello, P.R., James, R. C., Kruse, S., Kawasaki, A., *et al.*, (2021). *Earth Space Chem.* 5, 2995-3007.
- Stabeno, P.J. and Monahan, E.C. (1986). *In* Monahan, E.C., Mac Niocaill, G. (Eds.), *Oceanographic Sciences Library*. Springer, Netherlands, pp. 261-266.
- Vargas-Montero, M., Freer, E., Jiménez-Montealegre, R., Guzmán, J. C. (2006). *Afr. J. Mar. Sci.* 28, 215-217.
- Veron, F. (2015). *Ann. Rev. Fluid Mech.* 47, 507-538.
- Williams, P.M., Carlucci, A.F., Henrichs, S.M., Van Vleet, E.S., *et al.*, (1986). *Mar. Chem.* 19, 17-98.
- Wurl, O., Stolle, C., Thuoc, C.V., Thu, P.T., Mari, X. (2016). *Prog. Oceanogr.* 144, 15-24.
- Wurl, O., Ekau, W., Landing, W.M., Zappa, C J. (2017). *Elem. Sci. Anth.* 5, 31.
- Zhang, Z., Liu, L., Liu, C., Cai, W. (2003a). *J. Coll. Interf. Sci.* 264, 148-159.
- Zhang, Z., Zhang, A., Liu, L., Liu, C., *et al.*, (2003b). *Chin. J. Oceanol. Limnol.* 21, 351-357.
- Zhang, Z.B., Cai, W.J., Liu, L.S., Liu, C.Y., *et al.*, (2003c). *Sci. in China (Ser. B)* 46, 339-351.





EARLY WARNING SYSTEMS FOR HARMFUL ALGAE

FAO, IOC and IAEA
EIGHT CASE STUDIES

19th International Conference on Harmful Algae, October 2021.
La Paz, B.C.S., Mexico.

Editors

Mary Carmen Ruiz de la Torre
Dulce V. Ramírez Rodríguez



INTRODUCTION

During the 19th ICHA a side-event on Early Warning Systems (EWS) was organized jointly with FAO, IOC and IAEA on the 14th of October 2021. The EWS virtual session registered around 60 participants. During the EWS side-event relevant talks on EWS with an emphasis on food security and food safety were addressed. Herein, we present eight case studies of field exercises at different locations, focused on different target species, and the application of new tools and approaches for the early detection of HABs. The first case describes an EWS for benthic dinoflagellate genera, such as *Ostreopsis* in Mediterranean beaches. The second case describes *Gambierdiscus* sampling challenges in coastal Spanish waters. The third case presents an international agreement RAMOGE (www.ramoge.org) to monitor *Ostreopsis* blooms in summer by Mediterranean countries. The fourth case discusses Ciguatera fish poisoning and presents a standardized sampling and species-specific cell identification in field samples, *in situ* toxicity monitoring using Solid Phase Adsorption Toxin Tracking (SPATT) samplers and toxicity determination in wild samples/clonal cultures to fully understand the scope of a *Gambierdiscus* event that affected human health in French Polynesia. Citizen science is an important component of HAB studies: it has become essential to share information in different ways, such as academia with society and *vice versa*; this fifth case applies a fast and easy tool for sharing information about HABs in Sabah, Malaysia, location impacted by the presence of *Pyrodinium bahamense* var. *compressum* and *Margalefidinium polykrikoides*. WebApps contain useful information to the users, such as the causative agent, recent and previous HAB cases, as well as providing a platform for sharing and exchanging information. An Ireland case study (sixth) discusses the successfully operating system on a weekly basis to all stakeholders and the public since 2013, the weekly published bulletin that contains several data products obtained from historical and current biotoxin and phytoplankton profiles, along with oceanographic *in situ* satellite and modelled data products, which has helped to develop a short-term forecast prediction (3-5 days) in Irish coastal waters. The seventh case is based on studies of the forecasting of *Karenia brevis* blooms in the Gulf of Mexico; focusing on the monitoring challenges due to the impact variations in the distribution of brevetoxin aerosol, that depend on bloom patchiness, wind speed and wind direction. The improvement of nowcast timeliness with an automated capability to combine new resources allows generation of risk models and significantly improves intensification forecasting. The enhancement of new tools is critical for HAB monitoring and prediction: our last case study presents different algorithms coupled to an intelligent ASVs based on Artificial Intelligent aLERT (AILERT-HAB) system, a novel approach for deciding where and how to take measurements for building models that predict HAB evolution and for alerting authorities. EWS for HAB's goals focused on consumer protection and environmental monitoring. All cases presented here highlight the relevance of new approaches for monitoring HABs, considering that not all countries and institutions can implement the same level of EWS. A relevant contribution recognizes the importance of early involvement of stakeholders for development of EWS for HABs, thus enabling better outcomes.



Developing an *Ostreopsis* Early Warning System: the joint engagement of scientists, environmental agencies, and community science

Magda Vila^{1*}, Laia Viure¹, Rodolphe Lemée², Elisa Berdalet¹

¹Institut de Ciències del Mar (CSIC), Pg. Marítim de la Barceloneta 37-49, 08003 Barcelona, Catalonia-Spain; ²Sorbonne Université, CNRS, Laboratoire d'Océanographie de Villefranche, 06234 Villefranche-sur-Mer, France.

*corresponding author's email: magda@icm.csic.es

Abstract

In the last twenty years blooms of the harmful benthic dinoflagellate *Ostreopsis*, affecting human and environmental health, have become a common seasonal phenomenon in many temperate areas. Therefore, implementing an Early Warning System (EWS) of benthic harmful algal blooms (BHABs) is needed. While most routine monitoring programs are focused on plankton, collecting benthic samples is important in order to evaluate the stock of toxic microalgae. In the Mediterranean, several administrations have been conducting BHABs monitoring using scientific approaches in coordination with research centres. For an EWS to be effective, samples should be collected and processed soon and the results quickly communicated to the users. In the frame of the CoCliME project, an easy and reliable BHAB-sampling protocol was co-designed and implemented by scientists and stakeholders. Scientists produced and provided sampling kits and training sessions. Results (*Ostreopsis* abundance and risk level) were shared on coordinated online platforms between scientists and public agencies. This protocol has been successfully tested in Catalonia and France during the summers 2020 and 2021. It was proven to be an effective EWS for authorities to quickly raise recommendations on the health risks associated with *Ostreopsis* blooms in Mediterranean beaches. The protocol also contributes to build time series for elucidating climate change effects on *Ostreopsis* blooms.

Keywords: Early Warning System (EWS), Benthic Harmful Algal Blooms (BHABs), benthic microalgae, *Ostreopsis* blooms, community science, Mediterranean

<https://doi.org/10.5281/zenodo.7033157>



Introduction

The genus *Ostreopsis* was first described in tropical waters but in the last 25 years its biogeographic distribution has increased towards temperate latitudes where recurrent blooms are documented, in particular in the Mediterranean Sea (Vila *et al.*, 2001; Mangialajo *et al.*, 2011; Tester *et al.*, 2020).

Ostreopsis life history includes a plankton phase but it preferentially attaches to benthic substrates, such as macroalgae, other organisms, rocks, pebbles or sand, forming a mucilaginous matrix that covers the bottom. This benthic phase constitutes the reservoir of the *Ostreopsis* population which, in some circumstances can attain high cell numbers. Due to a combination of physical (wind, currents) and biological factors (migration), cells are released from the benthos to the plankton and also accumulates at surface. During huge blooms, the water colour turns brownish and floating foaming aggregates become visible at naked eye (known as “water flowers”).

Ostreopsis blooms have been linked to mortality of benthic fauna of scarce mobility (sea urchins, sea stars, crabs, etc.) (Shears and Ross, 2009; Illoul *et al.*, 2012) and it was linked (but not proven yet) to rare seafood poisonings fatalities in tropical areas (Randall, 2005). Luckily, such foodborne poisonings have never been reported in the Mediterranean (Kermarec *et al.*, 2008) where *Ostreopsis* blooms have been related with mild respiratory problems in people that stay near the seashore and inhale marine aerosol for several hours (Gallitelli *et al.*, 2005), experiencing symptoms such as rhinorrhea, pharyngeal pain, cough, general

malaise, headache, eye irritation and, and in occasions, fever ($\geq 38^{\circ}\text{C}$) (Vila *et al.*, 2016, and references there in). The concern of these blooms is reflected in the increased number of papers dealing about these BHAB species.

Harmful Algal Blooms (HABs) are a recurrent problem. In particular, *Ostreopsis* blooms have received special attention because, in addition to the just mentioned environmental and human health risks, they decrease the water quality of the Mediterranean beaches and can have an economic impact (Lemée *et al.*, 2012). However, the control of benthic harmful microalgae, such as the genus *Ostreopsis*, is not included in most routine monitoring programs in the world. The aim of this work is to present the Early Warning System (EWS) of benthic harmful algal blooms (BHABs) developed and tested in some beaches of Catalonia and France during the 2020 and 2021 summers to manage the risk posed by *Ostreopsis* blooms.

Material and Methods

For the EWS to be effective in providing information related to the bloom, three main aspects were considered: 1) reducing the time between sampling and results delivery, 2) training people to conduct the sampling (e.g., environmental agencies in Catalonia, Surfrider Foundation NGO in France) and 3) establishing a network of citizen/community contributors at stations where blooms are known to be recurrent.

A simplified protocol, adapted from the one used by scientists (e.g. as described in Moreira and Tester, 2016), was designed to



be applied by non-scientific people with the aim to quantify *Ostreopsis* abundance and to determine the associated health risks for humans exposed to aerosols and/or in direct contact with the seawater. Thus, previous knowledge on the *Ostreopsis* dynamics in the two study areas was used to define the period of study (from mid-June to the end of August or september) and to choose the number, location and frequency of sampling stations. The stations, selected based on previous information of *Ostreopsis* blooms occurrence plus people attendance to the beach, were monitored in the summers 2020 and 2021 with a variable frequency, every one or two weeks in Catalonia and from once a week (twice a week during blooms) to twice a month in France.

Sampling protocol

Macroalgae were collected by carefully picking them up by their base, placed in a flask with *in situ* seawater, shaken for a minute to detach their epiphytic cells and sieved through 200 microns mesh net. A picture of the seawater containing the released cells were taken at that time: it constituted a first indication of the presence and abundance of *Ostreopsis* in the sample. Immediately, microalgal cell samples were fixed with lugol. Macroalgae were slightly dried, extended on a white tissue paper, photographed, and stored in a fridge. Lugol fixed seawater and macroalgae were sent to the research institute. There, cell counts were conducted, and macroalgae were weighted. Cell counts were referred to grams fresh weight macroalga (g FW).

Scientists, samplers, and public agencies shared on the cloud the sampling protocol, a macroalgae identification guide, data

of the sampling day (meteorology, water temperature, salinity, sampled macroalgae, water volume of resuspension, pictures, etc.) and the results of *Ostreopsis* monitoring.

Cell counts were conducted at the research centres, but can also be done by trained personnel e.g. Surfrider NGO. The cell abundances were classified with colors, with a “Fire Light Scale” indicative of the thresholds and range values potentially related to health risks (Table 1), based on the experience in the area and in the literature (e.g., Funari *et al.*, 2015; Giussani *et al.*, 2017; Mangialajo *et al.*, 2017).

Results and Discussion

Management of BHABs requires established reference warning and alarm values. Five categories were established (Table 1): 1) not detected (blue); 2) presence ($\leq 2 \cdot 10^4$ cells g^{-1} FW; green); 3) moderate abundances ($2 \cdot 10^4$ to $2 \cdot 10^5$ cells g^{-1} FW; yellow); 4) high abundances ($\geq 2 \cdot 10^5$ cells g^{-1} FW; light brown), well established bloom, alert threshold; 5) abundances above $5 \cdot 10^5$ cells g^{-1} FW (red), alarm threshold for human health risk of *Ostreopsis*-related symptomatology. These colors were also consistent with the pictures taken by the samplers *in situ*. Thus, the first inspection of the sample when collected contributes to have an initial idea of the *Ostreopsis* abundance.

In Catalonia, in 2020, 44% of the samples collected in 13 stations exceeded the alert threshold, and the risk threshold was reached at least once in the 38% of the sampled stations (not shown).



In 2021, the risk threshold was attained in the 60% of the 20 sampled stations, although, symptoms were reported only in one station (not shown). To compare the two years, the mean, maximum and minimum cells concentrations were calculated for the same 10 stations sampled in both summers (Table 1). The alert (brown) or risk (red) thresholds were surpassed in six stations in 2020 and seven stations in 2021. Based on this, the intensity of the blooms in 2020 and 2021 were similar.

Station	2020				2021			
	n	Mean	Max	Min	n	Mean	Max	Min
Canyelles Petites	3	329.326	716.664	28.698	4	1.076.824	3.055.970	250.608
Sa Tarnardia	3	91.904	180.449	5.806	4	1.264.531	3.398.738	78.629
Mar Menuda	3	864.571	733.747	558.099	3	655.985	1.318.240	205.212
Pins Mar	7	1.850.663	3.413.467	498.321	6	866.761	2.595.445	47.493
Ponent	2	4.336	8.010	662	5	249.411	538.539	570
Ocata	2	1.007.228	2.014.455	0	3	794	1.737	124
Sant Miquel	3	215.591	357.564	2.203	4	206.727	357.541	1.492
Mota Sant Pere	3	246.494	499.569	263	5	141.073	205.687	17.121
La Mora	3	34.651	98.302	17	3	53.336	132.948	664
Cavet	3	125.803	313.834	5.151	6	619.1791	1.258.936	212.688

Abundance
 Benthic *Ostreopsis* sp. (cells /g FW)
 ● > 500 000 Risk level: very high concentration. Symptoms possible to occur
 ● > 200 000 Alert level: high concentration
 ● 20 000 - 200 000
 ● < 20 000
 ● Not detected

Table 1. *Ostreopsis* abundances (mean, maximum and minimum) in the 10 stations along the Catalan coast sampled in the 2020 and 2021 summers. The colors in the table correspond to the criteria shown below combining cell abundance and risk of experiencing *Ostreopsis*-related symptoms.

In Villefranche (France), in summer 2020, the *Ostreopsis* abundances surpassed three times the alert threshold and once the risk threshold (Fig. 1). The risk level in France was reached mainly in July, whereas in Catalonia it was reached in July, August and September.

The results on the abundance of *Ostreopsis* and the potential risk were communicated to the respective environmental or health administrations within a few days after samples were collected. Data were transferred

to the regional administration, the Catalan Water Agency in Catalonia and the Health Regional Agency in France, and also via RAMOGE, see further. If necessary, rapid contact was established with environmental technicians in the municipalities and / or regional Health Agencies, and warnings were given on the information panels of the affected beaches (Catalonia). In some stations, where the bloom is recurrent, an incipient net of community science contributors (including beach users, workers, and front-line residents) provided information to scientists when they observed the bloom or detected symptoms that could be related with *Ostreopsis* blooms.

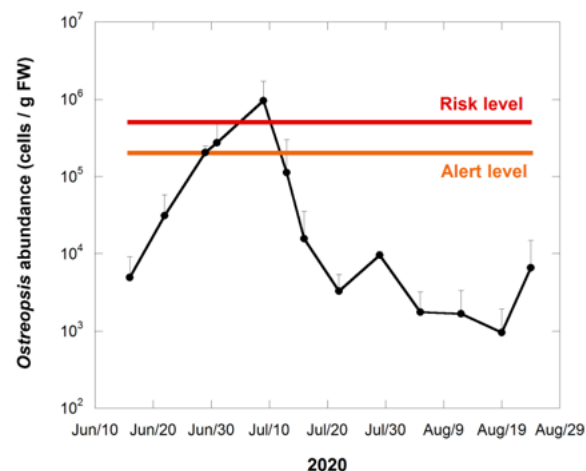


Fig 1. Time plot of *Ostreopsis* in Rochambeau (Villefranche Bay, France) in summer 2020.

This surveillance is also structured with some coordination meetings among the different entities (Fig. 2). On one hand, the Water Catalan Agency organizes three meetings during the summer with environmental technicians in coastal city halls and scientists involved in the environmental programs, to identify the environmental status of the beaches. Analogous coordination exists in France among the LOV, the Surfrider NGO,



the Centre Antipoison de Marseille and the Health Regional Agency (ARS). The overall results and strategies are shared during regular RAMOGE *Ostreopsis* Working group (<http://www.ramoge.org>) with the participation of Italy and Monaco entities that conduct intensive and consolidated monitoring and research on *Ostreopsis* blooms.

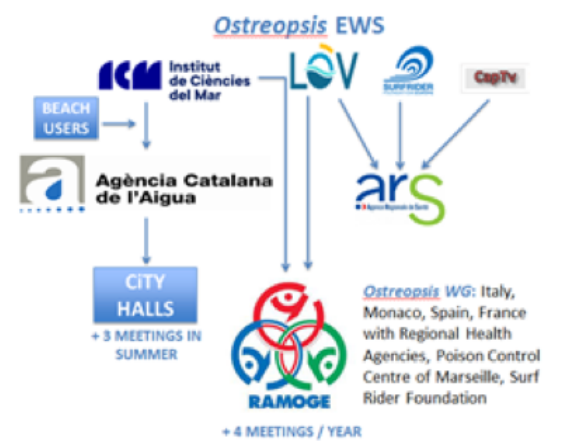


Fig. 2. Diagram showing the flux of information between the different members involved in the EWS of *Ostreopsis*. LOV: Laboratoire d'Océanographie de Villefranche; CapTv: Poison Control Center of Marseille, France; ARS: regional Health Agencies, France.

This EWS has been successfully tested in Catalonia and France during the summers 2020 and 2021. It was proven to be an effective EWS for authorities to quickly raise recommendations on the health risks associated to *Ostreopsis* blooms in Mediterranean beaches. It also contributes to elaborate time series for elucidation of climate change effects on *Ostreopsis* blooms. This initiative is an example of the implementation of Responsible Research and Innovation (RRI) where researchers play a relevant role in the relationship between science and society.

Acknowledgements. This study was supported by the Spain funded project OstreoRisk (CTM2014-53818-R), CoCliME (part of ERA4CS, an ERA-NET initiated by JPI Climate, and funded by EPA -Ireland-, ANR -France-, BMBF -Germany-, UEFISCDI -Romania-, RCN -Norway- and FORMAS -Sweden-, with co-funding by the European Union; Grant 6904462), the contract between Catalan Water Agency (ACA-Generalitat de Catalunya and ICM-CSIC; CTN2000526 and CTN2100434), and the French ANR project OCEAN 2015. French authors are part of the national French GDR PHYCOTOX (CNRS and Ifremer). We thank the whole sampler teams, citizen collaborators and the RAMOGE consortium without whom this Early Warning System would not have been possible.

References

- Funari, E., Manganelli, M., Testai, E. (2015). Harmful Algae 50, 45-56.
- Gallitelli, M., Ungaro, N., Addante, L.M., Procacci, V., *et al.*, (2005). JAMA Lett. 239, 2595-2600.
- Giussani, V., Asnaghi, V., Pedroncini, A., Chiantore, M. (2017). Harmful Algae 68, 97-104.
- Illoul, H., Rodríguez, F., Vila, M., Adjias, N., *et al.*, (2012). Cryptogam. Algol. 33, 209-216.
- Kermarec, F., Dor, F., Armengaud, A., Charlet, F., *et al.*, (2008). Environm. Risques. et St. 7, 357-363.
- Lemée, R., Mangialajo, L., Cohu, S., *et al.*, (2012). Cryptogam. Algol. 33, 137-142.



Mangialajo, L., Ganzin, N., Accoroni, S., Asnaghi, V., *et al.*, (2011). *Toxicon* 57, 408-420.

Mangialajo, L., Fricke, A., Perez-Gutierrez, G., Catania, D., *et al.*, (2017). *Harmful Algae* 64, 1-9.

Moreira, A. and Tester, P. (2016). *IOC Manuals and Guides* 59, 19-29.

Randall, J.E. (2005). *Pac. Sci.* 59, 73-77.

Shears, N.T. and Ross, P.M. (2009). *Harmful Algae* 8, 916-925.

Tester, P.A., Litaker, W., Berdalet, E. (2020). *Harmful Algae* 91, 101655.

Vila, M., Garcés, E., Masó, M. (2001). *Aquat. Microb. Ecol.* 26, 51-60.

Vila, M., Abós-Herràndiz, R., Isern-Fontanet, J., Àlvarez, J., *et al.*, (2016). *Sci. Mar.* 80, 107-115.



Early Warning Systems for *Gambierdiscus* and other benthic harmful algae: sampling challenges

Patricia A. Tester^{1*}, Elisa Berdalet², Mireille Chinain³, Marie-Yasmine Dechraoui Bottein⁴, Juan Fernández-Zabala⁵, Esther Garrido Gamarro⁶, R. Wayne Litaker⁷, Emilio Soler-Onís⁵

¹*Ocean Tester, LLC, Beaufort, North Carolina, U.S.A.*; ²*Institute of Marine Sciences, Barcelona, Catalonia, Spain*; ³*Institut Louis Malardé, Papeete-Tahiti, French Polynesia*; ⁴*Université Côte d'Azur, CNRS, UMR 7035 ECOSEAS, Nice, France*; ⁵*Observatorio Canario de HABs, Universidad de Las Palmas de Gran Canaria, Canary Islands, Spain*; ⁶*Food and Agriculture Organization of the United Nations, Rome, Italy*; ⁷*CSS, Inc. under Contract to National Oceanic and Atmospheric Administration.*

*corresponding author's email: Ocean.Tester@gmail.com

Abstract

Ciguatera poisoning (CP) is a long-neglected foodborne disease affecting tropical regions of the Pacific and Indian Oceans and the Caribbean Sea. CP was raised by the Pacific Nations at the 32nd Session of the FAO Committee on Fisheries in 2016. In 2017, it was an agenda item at the 11th Session of the Codex Committee on Contaminants in Foods. The committee requested scientific advice from FAO and WHO, so late 2018 a group of experts met to develop the Joint FAO-WHO Report of the Expert Meeting on Ciguatera Poisoning that provided risk management options for CP. In parallel with this, an interagency global ciguatera strategy was developed among FAO, IOC, IAEA and WHO. Building on these initiatives, these three UN Agencies convened an expert meeting to develop Joint FAO, IOC, IAEA Technical guidance for the implementation of Early Warning Systems (EWSs) for harmful algal blooms (HABs). The EWS approach includes monitoring protocols for sampling benthic genera like *Gambierdiscus* and *Fukuyoa* that produce toxins responsible for CP. Advances in *Gambierdiscus* and *Fukuyoa* taxonomy, better understanding of their global distribution and toxicity and species-specific molecular identification and enumeration methods help make this possible.

Keywords: Artificial substrate, cell-based early warning system, *Ostreopsis*, *Prorocentrum*

<https://doi.org/10.5281/zenodo.7033165>



Introduction

Key to standardizing a protocol for cell based EWS for *Gambierdiscus* is how, when, and where to sample. Unlike planktonic species, there is no agreed upon, sampling method for harmful, benthic microalgal species (BHABs). We fully appreciate that pelagic phytoplankton sampling techniques have been refined over a century and it is completely accepted that planktonic phytoplankton cells are normalized to the volume of water collected.

Traditionally, benthic epiphytic cells abundances are normalized to grams wet weight of the macrophytes that serve as substrates. There are myriad arguments against this collection technique, including ignoring the use of more accurate, surface-area normalized cell densities and habitat destruction. Artificial substrates, rather than macrophytes, are proposed as sampling platforms so cell abundances can be normalized to surface areas rather than biomass. We hope to open a dialog among interested colleagues and invite them to develop proof of concept projects comparing traditional macrophyte sampling methods with artificial substrates.

Historically, the mismatch between normalizing BHAB cell abundance to wet weight (biomass) or to host surface area was recognized. Lobel *et al.* (1988) observed a nearly four-fold difference in the ratio of wet weight to surface area between the two macrophytes, *Dictyota* and *Galaxaura*, despite having equivalent mass to volume ratios (1.05 and 0.96, respectively). Estimates of *Gambierdiscus* cell densities from these macroalgae varied greatly depending on

whether they were normalized to mass or surface area (Lobel *et al.*, agreed with Bomber *et al.* (1985);

“Analysis of these data demonstrate the misleading nature of dinoflagellate abundance expressed per gram of host alga and provides a good argument for yet another change to common enumeration methodologies – namely the normalization of dinoflagellate abundance to host surface area rather than biomass “

While normalization of cell abundance to macrophyte surface area was the correct way to sample, very few researchers have taken the time to make the tedious measurements of macrophyte surface area. Such measurements are incredibly time consuming and not feasible for use in monitoring programs.

Another complication, an unstated assumption, associated with macrophyte based sampling is that *Gambierdiscus* and other BHABs, prefer to settle on specific macrophyte species. The available field data, however, do not support this (Fig. 1). Data from 60 published studies show no consistency in the same macrophyte groups harboring the highest *Gambierdiscus* cell densities, these macrophytes, as well as other substrates such as turf algae, do have in common a greater surface area per gram of tissue compared to the other macrophytes sampled in the various studies. In many habitats, high density species are the foliose macrophytes, but these species are not always present (Lee *et al.*, 2020).

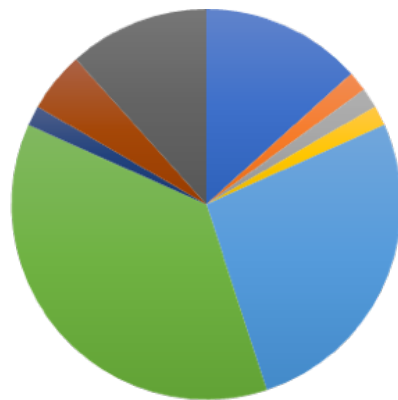
The reason the cell concentration in seawater to cell density per surface area relationship



exists is the frequent movement of BHAB cells into the water column and their settlement on new surfaces. The larger the population of BHAB species, the greater the proportion of cells that detach from their substrate. Where these cells will land is highly stochastic, but on average, the predominant macrophytes with the highest surface area per gram will recruit the greater number of cells, simply by chance. In this case, when abundances are expressed as cells g^{-1} wet weight algae, the higher surface area species will, on average, harbor more cells. The higher density is not due to active “preference” but due to stochastically landing on substrates having the highest surface area per unit biomass.

et al. (2018) sampled different habitat types and found that *Gambierdiscus* was most abundant on turf algae, a carpet of different species covering the surface of rocks or other hardsubstrates. The second highest cell abundances were found on hard coral and the third most abundant counts were from habitats with fleshy or foliose algae. Clearly, a less habitat dependent method is required for collecting BHABs for quantification of toxic cell for early warning systems.

To develop a sound monitoring program, a standardized, universal, and unbiased sampling protocol is needed. The method also should allow comparisons of data across different habitats, locations, time periods (seasons) and bloom phases. To address this need, we propose an artificial substrate sampling method, where cells are recruited from the surrounding substrates and cell abundance can be normalized to surface, notto biomass. This approach allows samples to be taken in the different habitats using a statistically robust sampling method which is key to any effective monitoring program.



- Chlorophyta ■ Dead Corals ■ Hydroid
- Mangrove detritus ■ Ochrophyta ■ Rhodophyta
- Sand patch ■ Seagrass ■ Turf algae

Fig. 1. Classes of macrophytes, turf algae and coral reported to support the highest *Gambierdiscus* densities. Data are from 60 journal articles published between 1970 and 2021.

Methods and Results

Many artificial substrates could be used but we selected window screen mesh. It is readily available, inert, light weight and inexpensive enough to be disposable so there is no possibility for cells to be carried over to cause contamination. A carefully measured piece of window screen is suspended between a weight and a float on a shortline, so the entire sampling device is sub surfacet to avoid any disturbance from waves and swells (Fig. 2).

A further complication of sampling macrophytes is that high abundances of *Gambierdiscus* and other BHAB species can occur in habitats lacking macrophytes. Lee



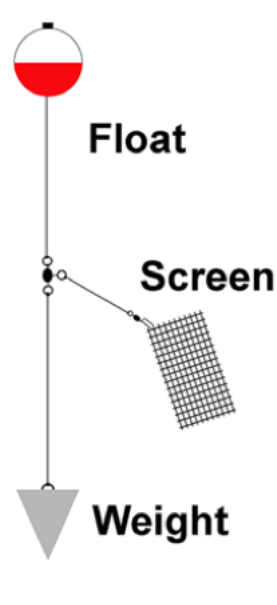


Fig. 2. Artificial substrate sampling device with window screen mesh suspended between a weight and a subsurface float to keep the screen suspended approximately 5 cm off the bottom

It is important to calculate the surface area of the mesh fibers, not just the overall dimensions of the piece of screen (Tester *et al.*, 2014). For sampling high concentrations of *Ostreopsis* a frame has been added to help support the screen and in high energy areas it is useful to keep the mesh screen from folding back on itself (Jauzein *et al.*, 2018; Fernández-Zabala *et al.*, 2019). Screens are retrieved after 24 h, and the cells dislodged for counting. Cell abundances are reported in cells cm^{-2} .

For *Gambierdiscus* 24 h is the optimal sampling or loading time for the mesh screens. From 6 h through 24 h cells recruit to the screens. This observation is consistent with the BHAB species moving around and colonizing free space in proportion to the overall abundance of cells in the surrounding environment. The concentration of cells

on the screens does not increase after 24 h (Tester *et al.*, 2014; Fernández-Zabala *et al.*, 2019). This loading pattern suggests a diel rhythm for the cells to release from substrates, swim and be transported in the water column and then resettle (Fernández-Zabala *et al.*, 2019; Fig. 3) This same pattern was observed for *Ostreopsis* loading on three replicate screens over a 24-h period (Jauzein *et al.*, 2018). Given the success of a frame to support sampling screens, we recommend its use.

When cells g^{-1} wet weight of macrophyte host are plotted against cells cm^{-2} , there is a reasonable correspondence in the data from *Gambierdiscus* (Fig. 3) and *Ostreopsis* (Jauzein *et al.*, 2018). In each of the *Gambierdiscus* studies below five or more replicates were used (Fig. 3).

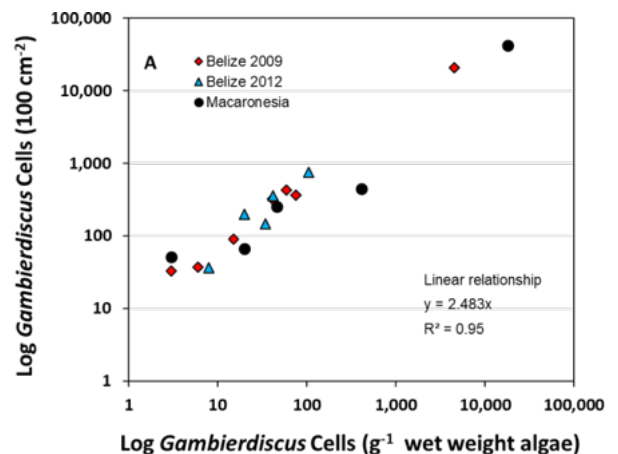


Fig. 3. *Gambierdiscus* abundance comparison using macrophyte hosts (cells g^{-1} wet weight) and artificial substrate (cells cm^{-2}). Data from Tester *et al.* (2014) and Fernández-Zabala *et al.* (2019).

These data suggest screens samplers are as capable of estimating cell densities in habitats dominated by macrophytes as directly

sampling the macrophytes themselves. This is further support for using screen sampling for monitoring programs. It should be noted this is a log-log plot and though the relationship of cell densities estimated using both methods are relatively good, the highly patchy distribution of BHAB cells means that, regardless of the sampling method, variability around mean cell estimates will be high. This leads us to a discussion of the importance of replicate samples.

With patchy distributions of BHAB cells, how many replicate samples are required to achieve cell estimates with standard errors of the mean less than 100%? The lower the cell abundance, the more replicates are needed to achieve the lowest possible coefficient of variation (CV, %). A power analysis is needed to determine the adequate number of replicates (Lobel *et al.*, 1988; Tester *et al.*, 2014). For example, with low numbers of cells a minimum of 10 replicates or more are needed. If cell abundance is high, (more than 100 cells cm⁻²) five replicates would be expected to produce a CV of 50% of the mean (Tester *et al.*, 2014). To reduce the CV, it is imperative to sample adequate numbers of replicates, or the data will not be meaningful. In contrast, for very high numbers (e.g. > 50,000 *Ostreopsis* or *Prorocentrum* cells cm⁻²) three replicates could be sufficient.

The need to wait for 24 h to ensure a representative collection of cells in the screens, constitutes a drawback of this method. However, samples are cleaner for cell counting, toxin determination and molecular identification.

Advantages and Recommendations

Artificial substrates allow cell counts to be normalized to surface area and supports randomized sampling regimes that are less biased than depending on specific macrophytes whose density and location can change over time. The screen samples, in the water for 24 h, integrate cells originating from multiple sources so they provide a better estimate of cell densities in structurally complex habitats where it is not possible to sample different substrate types equally well.

It is necessary for any monitoring program to determine the BHAB species present as well. Species composition matters because *Gambierdiscus* species-specific toxicities can vary by more than 1,000-fold with intraspecific toxicities varying 100-fold and seasonal toxicity changes are possible as well (Chinain *et al.*, 2010; Litaker *et al.*, 2017; Rossignoli *et al.*, 2020). Studies from each part of the globe inform us about the difference in species toxicity. By making a preliminary survey on the major toxin producing species in the monitoring area (Smith *et al.*, 2017), molecular techniques can be used to quickly identify increased abundance of target species.

Because toxic and nontoxic BHAB species are often quite difficult to identify using light microscopy, species-specific qPCR represents an alternative for quantifying cell densities. These assays are easier to perform using screen samples because they are less susceptible to interference from debris which is a major problem when using cells from macrophytes. The qPCR assays are also easy to scale up for large numbers of samples. The combination of clean samples collected



from screens followed by species- specific qPCR is the backbone of a Cell Based Early Warning System for Benthic HABs.

References

Bomber, J.W., Norris, D.R., Mitchell, L.E. (1985). Toxic Dinoflagellates, Elsevier, New York. 45-50 p.

Chinain, M., Darius, H.T., Ung, A., Cruchet, P., *et al.*, (2010). *Toxicon* 56, 739-750.

Fernández-Zabala, J., Tuya, F., Amorim, A., Soler-Onís, E. (2019). *Harmful Algae* 87, 1-11.

Jauzein, C., Açaf, L., Accoroni, S., Asnaghi, V., *et al.*, (2018). *Ecol. Indic.* 91, 116-127.

Lee, L.K., Lim, Z.F., Gu, H., Chan, L.L., Litaker, R.W., *et al.*, (2020). *Sci. Rep.* 10, 11251.

Litaker, R.W., Holland, W.C., Hardison, D.R., Pisapia, F., *et al.*, (2017). *PLoS One* 12, 10: e0185776.

Lobel, P.S., Anderson, D.M., Durand-Clement, M. (1988). *Bio. Bull.* 175, 94-101.

Rossignoli, A.E., Tudó, A., Bravo, I., Diaz, P.A., Diogène, J., *et al.*, (2020). *Toxins* 12, 134.

Smith, K.R., Biessy, L, Argyle, P.A., Trnski, T., Halafihi, T., *et al.*, (2017). *Mar. Drugs* 15, 243.

Tester, P.A., Kibler, S.R., Holland, W.C., Usup, G., *et al.*, (2014). *Harmful Algae* 39, 8-25.



Case study of harmful benthic events caused by *Ostreopsis*

Elisa Berdalet^{1*}, Mireille Chinain², Marie-Yasmine Dechraoui Bottein³, Esther Garrido Gamarro⁴, Rodolphe Lemée⁵, Patricia A. Tester⁶

¹*Institut de Ciències del Mar, ICM-CSIC, Barcelona, Catalonia, Spain;* ²*Institut Louis Malardé - UMR EIO, Papeete-Tahiti, French Polynesia;* ³*Université Côte d'Azur, CNRS, UMR 7035 ECOSEAS, Nice, France; former Food and Agriculture Organization of the United Nations;* ⁴*Food and Agriculture Organization (FAO) of the United Nations, Rome, Italy;* ⁵*Sorbonne Université, CNRS, Laboratoire d'Océanographie de Villefranche (UMR 7093), Villefranche-sur-Mer, France;* ⁶*Ocean Tester, LLC, Beaufort, North Carolina, U.S.A.*

*[corresponding author's email: berdalet@icm.csic.es](mailto:berdalet@icm.csic.es)

Abstract

Blooms of the benthic genus *Ostreopsis* are increasing from tropical to temperate latitudes, becoming recurrent in some beaches (especially in the Mediterranean coasts) and appearing in new zones. The main threats posed by *Ostreopsis* blooms on human health include respiratory and other problems associated with the aerosolization of toxic compounds produced by *Ostreopsis*, and potential (not clarified yet) food borne poisoning. To prevent the impacts on human health, scientists, stakeholders, and public authorities have been coordinating efforts in different Mediterranean countries via the International Agreement RAMOGE to monitor *Ostreopsis* blooms in summer periods. The gained knowledge and successful experience constitute an Early Warning System that can be translated to other BHAB cases.

Keywords: benthic harmful algal bloom, dinoflagellate, early warning system, *Ostreopsis*, palytoxin analogues

<https://doi.org/10.5281/zenodo.7033169>



Introduction

The biogeographic distribution of the *Ostreopsis* species as well as their blooms have expanded from 28°S - 28°N to 45°S to 45°N since 1995. It is not known whether the species were present in the past in temperate latitudes or whether their blooms have increased in these areas due to natural and anthropogenic factors (e.g., Tester *et al.*, 2021).

The main threats posed by *Ostreopsis* blooms on human health include: i) the respiratory and other health problems associated with the aerosolization of unknown toxic compounds produced by *Ostreopsis* and ii) the risk of food borne poisoning due to the potential food web transfer (not proven yet) of palytoxins analogues (ovatoxins, ostreocins) produced by the microalga. Some *Ostreopsis* spp. blooms have also been linked to massive benthic fauna mortalities. *Ostreopsis* related respiratory cases reported in several Mediterranean beaches prompted intense scientific research and monitoring in the last two decades. Valuable information about *Ostreopsis* species taxonomy, toxin production, impacts on human health and ecosystems, driving bloom factors, biogeographic distribution, and potential impacts of climate change on their occurrence (reviewed e.g., by Pavaux *et al.*, 2020; Tester *et al.*, 2020; Zingone *et al.*, 2021) is now available. Despite *Ostreopsis* is not a priority case concerning foodborne diseases by now, given the biogeographic expansion of the genus, the blooming recurrence in some beaches, the high biomass detected in new areas (see for instance the recently documented blooms in the coast of Senegal, Brehmer *et al.* (2021)) and new massive human health outbreaks (such as

the summer event in beaches of the Bay of Biscay -Atlantic and Spanish French coasts-, with more than 700 persons impacted; pers. comm. by the French Regional Health Agency and A. Laza -EHU-) we summarize here the information about monitoring tools and strategies successfully implemented in the Mediterranean, which can be eventually used in the design of Early Warning Systems (EWSs) in other areas and other benthic harmful algal blooms (BHABs).

Case study – *Ostreopsis*

1. Description of the problem (what type of HABs)

The genus *Ostreopsis* grows in shallow and well illuminated waters, mainly attached (by a self-produced mucilage) to biotic (macroalgae, corals, bryozoans) and abiotic surfaces (rocks, sands). Cells may also detach from the substrates and become part of the plankton, forming dense aggregates of *Ostreopsis* cells at sea surface during the blooms.

The palytoxin analogues produced by some *Ostreopsis* species are high molecular weight compounds. They are determined by LC-MS/MS, although standards for the different toxins are lacking. Ovatoxins and isobaric PLTX were reported in mussels, sea urchins or fish collected in the Mediterranean coasts (reviewed by Pavaux *et al.*, 2020) at concentrations exceeding the safety alert threshold of 30 µg of PLTX-equivalent per kg of fresh flesh recommended by the European Food Safety Authority (EFSA, 2009) but, luckily, related seafood poisonings have not been reported in the Mediterranean region yet.



Nowadays, *Ostreopsis* related toxins are not regulated in Europe and thus, not monitored in marine food products. The monitoring is focused on the detection of *Ostreopsis* cells and blooms in beaches to prevent respiratory, otorhinolaryngology and cutaneous impacts on users. The toxicity effects are diverse, and not clearly associated to a particular species.

2. Information about stakeholders - Who was impacted? Were needs identified?

Ostreopsis blooms pose a main risk on beach users. In the Mediterranean, the summer vacation season coincides with the period of *Ostreopsis* blooms (in general), with potential economic cost in the touristic zones due to beach closures. Since the first health outbreaks potentially attributed to *Ostreopsis* blooms that occurred in Italy, France, Spain and Algeria, scientists were aware that an emerging HAB problem was a common threat in the Mediterranean basin. Luckily, national, and international funds for research facilitated not only scientific activities at local level, but also fostered the coordination of the research among scientists of different Mediterranean countries. Examples of such projects were MediOs in France, Ebitox in Spain and the Interreg Med coordinated project M3-HABs.

A general framework was established to structure an efficient preventive strategy, with particularities in each country (Funari *et al.*, 2015; Lemée *et al.*, 2012; Vila *et al.*, 2012; Meroni *et al.*, 2018). Fluid communication was established between scientists and the Environmental Agencies, to establish the *Ostreopsis* Monitoring program. Information about the health symptoms was also provided and determined by Public Health Authorities, and special attention was given to train related professionals in Primary Health Care

centers and hospitals, and first aid support (Red Cross and lifeguards in the beaches). Local authorities of the affected beaches were informed about the evolution of *Ostreopsis* blooms in the beach and alert signs were installed when necessary (Fig. 1) to inform the general public about the presence of the microalga, the potential symptoms, what to do and when necessary, the beach was closed. Informative brochures were elaborated by scientists with the essential information as well. Communication between scientists and the public was established through common citizen science mechanisms.



Fig. 1. Warning signs in multiple languages about the presence of *Ostreopsis* bloom with information about health symptoms for beachgoers on two Mediterranean beaches.

The international RAMOGE Agreement (www.ramoge.org) between France, Monaco and Italy, with Spain as invited participant, is facilitating the coordination among scientists of these countries, including medical professionals. Every year, prior to the summer season, virtual meetings are organized to inform about the monitoring strategies that are going to be followed in each country. After the summer period, a new meeting is held to exchange information about the balance of the season in terms of *Ostreopsis* bloom events and impacts on human health and the environment. A common database



is being elaborated with the data provided by the different institutions. The collected information during more than 10 years can allow evaluating key questions concerning risk assessment, including the sampling method as well as the alert threshold values for health symptoms, which still differ among countries. The coordination structure developed under the RAMOGE umbrella constitutes the foundation of a solid approach for the *Ostreopsis* EWS in the Mediterranean.

3. What was the development status of the country or region in terms of monitoring?

Regular monitoring of *Ostreopsis* blooms is conducted in some areas where nearly annual blooms are known to occur. Until now, most monitoring programs conduct traditional plankton samplings assuming that cells present in the water column are preferentially related to the cutaneous and respiratory impacts reported. However, the *Ostreopsis* benthic populations constitute the pool or reservoir of cells that determine the duration and maintenance of the blooms. Planktonic cells and floating aggregates transported by currents facilitate the dispersion of the bloom and the colonization of new sites. For this reason, sampling of macroalgae to estimate the *Ostreopsis* benthic population has been introduced progressively in Italy, Monaco, France, and Spain (Catalonia) as well.

4. What approach and what technology were used to solve the problem?

The most common sampling method for benthic populations is the collection of the dominant macroalgae in the area that appear covered by the mucilaginous biofilm containing *Ostreopsis* cells as described by Moreira and Tester (2016). Cell abundance is referred to as cells per gram of macroalgae

fresh weight. Plankton samples in the same area are also collected. Scientists working in the Mediterranean were soon aware that a major challenge was to find a consistent collection method to standardize cell abundances from benthic substrates. The BEDI protocol is a proposed integrative approach to estimate the cell concentration in the benthic populations and the surrounding water (Mangialajo *et al.*, 2017) while providing a direct measure of the risk associated with inhalation of aerosols. Also, the artificial substrate by Tester *et al.* (2014) has been examined and adapted in the Mediterranean and the Atlantic coast of France for *Ostreopsis* collection by Jauzein *et al.* (2018) and in the Pacific by Lee *et al.* (2020). The artificial substrate is deployed during 24 h, which integrates the diurnal variability of the cell concentrations of the benthic and planktonic *Ostreopsis* populations as recently studied in detail by Pavaux *et al.* (2021).

5. Describe EWS put in place (communication, interaction with stakeholders)

For the design of an EWS, the selection of the sampling method should be discussed, and the best strategy selected, taking into consideration logistic, technical, and human resources available in the area.

Recently, in the frame of the CoCliME project (www.coclimate.eu), an easy and reliable protocol was co-designed and implemented by scientists and stakeholders. Scientists elaborated and distributed a benthic sampling kit and provided simple training sessions on sampling. Results (*Ostreopsis* abundance) were shared between scientists and public agencies using coordinated online platforms. Microscopy cell counts were conducted at the research centres but can also be done by trained personnel and citizens provided with



microscopes (e.g., Surfrider Foundation; <https://surfrider.eu/en/>). This protocol has been successfully tested in Catalonia and France during the summers 2019 and 2020 and is described by Vila *et al.* (2022).

6. What were the forecast operation results?

The available data from some Mediterranean countries suggest that human health effects may occur at thresholds values of 2×10^5 cells g^{-1} wet weight of macroalgae and/or 3×10^4 cells L^{-1} of seawater (Lemée *et al.*, 2012; Funari *et al.*, 2015; Mangialajo *et al.*, 2017). Symptoms may not occur along the whole duration of the bloom but during certain periods (Vila *et al.*, 2016; Berdalet *et al.*, 2021). Environmental effects depend on the duration and extension of the bloom event. In the field, massive mortalities have been observed at 1.4×10^6 cells g^{-1} fresh weight of macroalgae in New Zealand (e.g., Shears and Ross, 2009) and from 250×10^6 to 3×10^9 cells L^{-1} of seawater in Italy (Sansoni *et al.*, 2003). Data on threshold cell abundances having toxic effects on different organisms have been mainly obtained from experimental ecotoxicity tests (e.g., Giussani *et al.*, 2015, 2016). The responses are variable, depending on experimental conditions and the tested organism. Overall, this information helps the authorities to provide information to the public, and to decide about the necessity to close the access to beaches.

7. What consequences did the EWS have on stakeholders' needs?

The EWS based on benthic sampling conducted by trained personnel (described in Vila *et al.*, 2021) was proven to be an effective EWS for authorities to quickly make recommendations on the health risks associated to *Ostreopsis* blooms in

Mediterranean beaches. The monitoring data protocol also contributes to the joint effort to build a time series dataset for elucidation of climate change effects on *Ostreopsis* blooms.

Conclusions

Ostreopsis is becoming an emerging issue in new (not yet monitored) areas. The problems posed by *Ostreopsis* blooms have, for now, a smaller relevance compared to *Gambierdiscus* and *Fukuyoa* blooms and Ciguatera Poisoning in the tropical regions of the world. For *Ostreopsis*, uncertainties include identification of the toxic compounds and harmful mechanisms involved in human and environmental health problems, and the future trends of the blooms under a general warming scenario. Meanwhile, the benthic nature of *Ostreopsis* and their blooms in temperate latitudes and different habitats offer the possibility to approach the challenges of addressing other potential benthic HABs and providing a template for establishing EWSs.

Acknowledgements. Scientific projects in the Mediterranean countries addressed to understand the *Ostreopsis* bloom dynamics, MediOs, Ebitox, OstreoRisk, CoClima, M3HABs, ShareMed, the Acord RAMOGE, and many others.

References

- Berdalet, E., Pavaux, A.S., Abós-Herràndiz, R., *et al.*, (2021). Abstract book ICHA19, La Paz, B.C.S. Mexico.
- Brehmeer, P., Ndiaye, W., Mbaye, A., *et al.*, (2021). Note Politique AWA, CSRP-IRD, Dakar, 13 p.



- EFSA Panel on Contaminants in the Food Chain (CONTAM); Scientific Opinion on marine biotoxins in shellfish – Palytoxin group. EFSA J. (2009), 1393.
- Funari, E., Manganelli, M., Testai, E. (2015). Harmful Algae 50, 45-56.
- Giussani, V., Sbrana, F., Asnaghi, V., *et al.*, (2015). Harmful Algae 44, 46-53.
- Giussani, V., Costa, E., Pecorino, D., *et al.*, (2016). Harmful Algae 57, 49-58.
- Jauzein, C., Fricke, A., Mangialajo, L., *et al.*, (2017). Mar. Pollut. Bull. 107, 300-304.
- Lee, L.K., Lim, Z.F., Gu, H., *et al.*, (2020). Sci. Rep. 10, 11251.
- Lemée, R., Mangialajo, L., Cohu, S., *et al.*, (2012). Cryptogam. Algol. 33, 137-142.
- Mangialajo, L., Fricke, A., Perez-Gutierrez, G., *et al.*, (2017). Harmful Algae 64, 1-10.
- Meroni, L., Chiantore, M., Petrillo, M., Asnaghi, V. (2018). Harmful Algae 80, 64-71.
- Moreira, A. and Tester, P. (2016). IOC Manuals and Guides 59.
- Pavaux, A.S., Berdalet, E., Lemée, R. (2020). Front. Mar. Sci. 7, 498.
- Pavaux, A.-S., Velasquez-Carvajal, D., Drouet, K., *et al.*, (2021). Harmful Algae 110, 102144.
- Sansoni, G., Borghini, B., Camici, G., *et al.*, (2003). Biol. Ambient. 17, 17-23.
- Shears, N.T. and Ross, P.M. (2009). Harmful Algae 8, 916-925.
- Tester, P.A., Kibler, S.R., Holland, W.C., *et al.* (2014). Harmful Algae 39, 8-25.
- Tester, P.A., Litaker, W., Berdalet, E. (2020). Harmful Algae 91, 101655.
- Vila, M., Abós-Herrándiz, R., Isern-Fontanet, J., *et al.*, (2016). Sci. Mar. 80, 107-115.
- Vila, M., Viure, L., Lemée, R., *et al.*, (2021). Abstract book ICHA19, La Paz, B.C.S. Mexico.
- Zingone, A., Escalera, L., Aligizaki, K., *et al.*, (2021). Harmful Algae 102, 101843.



Case study of a harmful benthic event caused by *Gambierdiscus*

Mireille Chinain^{1*}, Elisa Berdalet², Marie-Yasmine Dechraoui Bottein³, Esther Garrido Gamarro⁴, Patricia A. Tester⁵

¹*Institut Louis Malardé - UMR EIO, Papeete-Tahiti, French Polynesia;* ²*Institute of Marine Sciences, ICM-CSIC, Barcelona, Catalonia, Spain;* ³*Université Côte d'Azur, CNRS, UMR 7035 ECOSEAS, Nice, France;* *former Food and Agriculture Organization of the United Nations;* ⁴*Food and Agriculture Organization of the United Nations, Rome, Italy;* ⁵*Ocean Tester, LLC, Beaufort, North Carolina, U.S.A.*

*corresponding author's email: mchinain@ilm.pf

Abstract

The increased numbers of adverse incidents associated with benthic harmful algae blooms (BHABs) has generated strong research interests in the last decade and calls for early warning system that provide warnings and reduce risk to human health. The complex habitats of BHABs make many detection methods difficult or unfeasible so case studies of bloom management, like the one we present here, are especially helpful.

Keywords: benthic harmful algal bloom, ciguatera, ciguatoxin, dinoflagellate, Early Warning System

<https://doi.org/10.5281/zenodo.7033174>



Introduction

Ciguatera poisoning (CP) has a long history with reports dating to the sixteenth century and affects 50,000 to 100,000 consumers of seafood annually. It is a poisoning caused by the ingestion of fish or shellfish from tropical and subtropical regions when lipid-soluble ciguatoxins (CTXs) produced by dinoflagellates of the benthic genera *Gambierdiscus* and *Fukuyoa* bioaccumulate in marine food webs. Renewed interest has spurred active research on these benthic organisms causing harmful blooms (BHABs) in the last two decades, producing much valuable information. However, there are some needs that require urgent attention (FAO and WHO, 2020). Sampling methods need to be standardized so cell abundances can be compared within and across regions. Too, there is a clear mandate for risk management plans to provide effective outreach programs and define protocols to avoid the risk of consuming tainted seafood. To provide sufficient lead-time for management activities an effective early warning system (EWS) must be in place.

Currently a Technical Guidance document for the Implementation of Early Warning Systems for Harmful Algal Blooms is being drafted jointly by the Food and Agriculture Organization of the United Nations (FAO), the International Oceanographic Commission of UNESCO (IOC-UNESCO) and the International Atomic Energy Agency (IAEA) for publication after pilot testing planned for 2022. Some of the most useful information in this document comes from case studies of harmful algal blooms (HABs) including the benthic ones (BHABs) like *Gambierdiscus* and *Fukuyoa*. Here we describe a case study

for *Gambierdiscus* and a nascent Early Warning System (EWS) for CP-causing dinoflagellates.

Ideally, an EWS should include the early detection of the presence of the harmful organism before it reaches threshold abundance values related to noxious impacts on the health of people (and/or the environment) and the determination of the involved toxic compounds specially in seafood. In regions with only sporadic BHAB events or areas without resources to test for toxins, EWS are generally based on detection of seasonal changes in cell abundances. Yet, Chinain *et al.* (1999) conducted a long-term survey in French Polynesia from February 1993 to December 1997 that included both *Gambierdiscus* cell abundances and toxicity and they concluded:

Toxicity screening revealed that toxin production was maximum from October 1994 through december 1996. No correlation was found between toxicity of these blooms and their biomass nor the seasonal pattern of temperatures. It has been suggested, that the toxicity of naturally-occurring blooms of *Gambierdiscus* spp. and, consequently, the severity of ciguatera incidents in a given area, is mainly dependent on the clonal nature of cells which coexist within local populations of this dinoflagellate.

Gambierdiscus and *Fukuyoa* cell abundances are not sufficient to support an EWS based on cell counts alone. Sampling the marine food web for CTXs is the most direct way to determine toxicity but it is both difficult and costly. To assist in sampling



environmental CTXs, passive sampling solid phase adsorption toxin tracking (SPATT) technology has been developed as a tool to monitor algal toxins (MacKenzie *et al.*, 2004; Roué *et al.*, 2018).

A number of *in vitro* and field studies have shown the use of the technique to trace an array of algal or cyanobacterial toxins in algal cultures or marine and coastal environments, including hydrophilic toxins such as saxitoxins and domoic acid, and lipophilic toxins, such as azaspiracids, brevetoxins, CTXs, okadaic acid and microcystins (Shea *et al.*, 2006; Stobo *et al.*, 2008; Fux *et al.*, 2009; Lane *et al.*, 2010; Kudela, 2011; Caillaud *et al.*, 2011). For example, Zendong *et al.* (2014) used passive samplers to capture toxins from both pelagic and benthic or epiphytic microalgae. Pinnatoxin-G and dinophysistoxin-1 were accumulated in significant amounts, indicating the presence of both *Vulcanodinium rugosum* and *Prorocentrum lima* in the study site.

Table 1. Species-specific relative cell abundance in three bays on Nuku Hiva Island in the Marquesas archipelago (French Polynesia), site of a ciguatera poisoning event in July 2014 that affected nine people who ate gastropods (*Tectus niloticus*) found to contain ciguatoxins. Data from Darius *et al.* (2018).

<i>Gambierdiscus</i> Species	Location		
	Anaho Bay	Taipivai	Taiohae
<i>G. caribaeus</i>	<1%	<1%	<1%
<i>G. carpenteri</i>	17%	90%	88%
<i>G. pacificus</i>	<1%	<1%	<1%
<i>G. polynesiensis</i>	82%	10%	10%
<i>G. toxicus</i>	<1%	<1%	<1%
Total cells	~2,900	~415	~420

Case study – Ciguatera Poisoning

EWSs based on field studies targeted at *Gambierdiscus* currently exist in several regions of the world. For example, the case study of Nuku Hiva Island in the Marquesas archipelago in French Polynesia is a good illustration of the benefits of an EWS approach that reduce the risk of exposure of local populations to ciguatera toxins in CP-prone areas.

In June 2014, a mass-poisoning outbreak involving nine tourists in Nuku Hiva Island following the consumption of a gastropod, *Tectus niloticus*, was reported in the frame of the country-wide epidemiological surveillance network established since 2007 in French Polynesia. All patients exhibited clinical symptoms typical of CP (Gatti *et al.*, 2018). The implication of this novel gastropod vector of high value for local populations in a CP incident prompted a two-years field survey involving the monitoring of *Gambierdiscus* species distribution and environmental toxins by means of passive samplers, the toxicity screening of *in vitro* cultures of *Gambierdiscus* spp. established from wild material, as well as a follow-up survey of the toxicity in *T. niloticus* specimens in three distinct fishing sites of Nuku Hiva Island, Anaho Bay, Taipivai Bay and Taiohae Bay.

The qPCR assays carried out on artificial substrate (window screen) devices (Tester *et al.*, 2014) to survey for *Gambierdiscus* relative cell abundance and species distribution showed a high species biodiversity in Nuku Hiva study site since up to five distinct species



were detected, with *G. polynesiensis* as the dominant species in Anaho Bay (~82%) vs *G. carpenteri* in Taipivai Bay and Taiohae Bay (90% and 88%, respectively) (Table 1).

The CBA-N2a and LC-MS/MS toxicity analyses conducted periodically on *T. niloticus* showed that only specimens collected from Anaho Bay were toxic (Fig. 1). Despite a progressive 19-fold decrease in CTX contents over time, the residual toxicity monitored in *T. niloticus* remained well above the safety limit recommended for human consumption even 28 months after the poisoning event (Fig. 1) (Darius *et al.*, 2018).

In parallel, several *Gambierdiscus* spp. cultures were also successfully established in the laboratory, although the culturing approach gave a highly biased representation of the community species composition in the three study sites as assessed by the artificial substrate method. It confirmed only one strain, a *G. polynesiensis* isolate, out of the 17 clonal strains examined produced CTXs at levels around 1.20 ± 0.14 pg P-CTX-3C equiv./cell. Conversely, none of the *G. carpenteri* isolates showed toxicity *in vitro*.

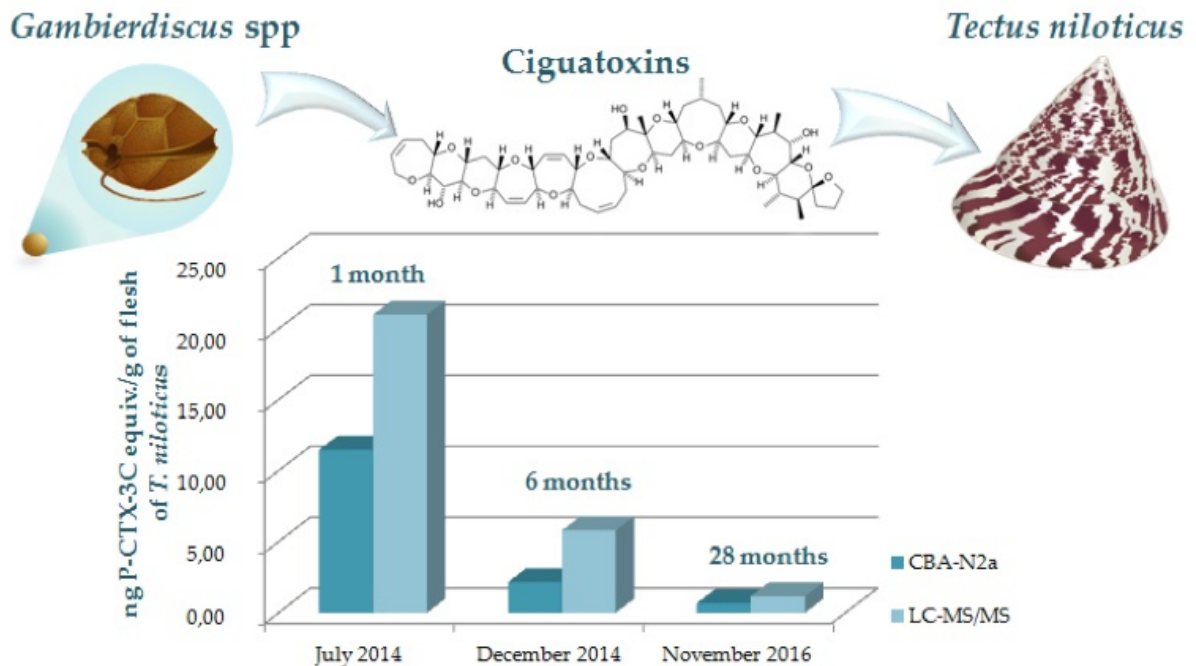


Fig. 1. Ciguatoxins in specimens of the gastropod *Tectus niloticus* sampled from Anaho Bay in Nuku Hiva Island (Marquesas, French Polynesia) over a 28-month period, as measured by a cell-based assay (CBA-N2a) and chemical analysis (LC-MS/MS). After Darius *et al.* (2018).



Based on LC-MS/MS data, four distinct P-CTX analogs were detected in toxic *T. niloticus* tissues, namely CTX3B, -3C, -4A and -4B, with CTX3B as the major congener. Since these four analogs are consistently found in *G. polynesiensis* culture extracts (Longo *et al.*, 2020), it can be concluded that *G. polynesiensis* populations, which predominate in Anaho Bay benthic assemblages, are the primary source of the CTX analogs detected in neighboring *T. niloticus*. Interestingly, these findings are consistent with the results of the field survey conducted in this same area by means of SPATT technology, which also showed evidence of the presence of CTX3B and -3C in the environment (Roué *et al.*, 2020). Of note, in addition to CTXs, okadaic acid and DTX-1 were also detected in SPATT extracts using a LC MS/MS-based multi toxin screening approach, thus, highlighting the usefulness of passive samplers in the routine surveillance of CP and other phycotoxin-related risks in ciguatera-prone regions.

Conclusions

Gambierdiscus live in complex benthic habitats and only rarely proliferate in the sense of a phytoplankton bloom, so an EWS based on remote-sensing information is not feasible. A combination of standardized sampling and species-specific cell identification of field samples, *in situ* toxicity monitoring using SPATT samplers and toxicity determination of wild samples/clonal cultures are necessary to fully understand the scope of a *Gambierdiscus* event that affects human health. Detailed case studies help guide future efforts to anticipate events in endemic CP areas and effectively mitigate CP events in new or unexpected places.

Acknowledgements. The field study conducted in Nuku-Hiva Island was supported by funds from the countries of France (Arrêté No. HC/491/DIE/BPT of 30 March 2016) and French Polynesia (No. 7937/MSR/REC of 4 December 2015), in the frame of the CARISTO-Pf research program.

References

- Food and Agriculture Organization of the United Nations and World Health Organization. (2020). Report of the expert meeting on ciguatera poisoning: Rome, 19-23 Nov. 2018. WHO. <https://apps.who.int/iris/handle/10665/332640>.
- Chinain, M., Germain, M., Deparis, X., Pauillac, S. *et al.*, (1999). *Mar. Biol.*, 135, 259-267.
- Caillaud, A., de la Iglesia, P., Barber, E., Eixarch, H., *et al.*, (2011). *Harmful Algae* 10, 433-446.
- Darius, H.T., Roué, M., Sibat, M. Viallon, J., *et al.*, (2018). *Tectus niloticus* (Tegulidae, Gastropod), as a novel vector of ciguatera poisoning. Detection of Pacific ciguatoxins in toxic samples from Nuku Hiva Island (French Polynesia). *Toxins* 10, 2.
- Fux, E., Bire, R., Hess, P. (2009). *Harmful Algae* 8, 523-537.
- Gatti, C.M., Lonati, D., Darius, H.T., Zancan, A., Roué, M., *et al.* (2018). *Toxins* 10, 102.
- Kudela, R.M. 2011. *Harmful Algae* 11, 117-125.



Lane, J.Q., Roddam, C.M., Langlois, G.W., Kudela, R.M. (2010). *Limnol. Oceanogr. Meth.* 8, 645-660.

Longo, S., Sibat, M., Darius, H.T., Hess, P. *et al.*, (2020). *Toxins* 12, 767.

MacKenzie, L., Beuzenberg, V., Holland, P., McNabb, P., *et al.*, (2004). *Toxicon* 44, 901-918.

Roué, M., Darius, H.T., Chinain, M. 2018. *Toxins* 10, 167.

Roué, M., Smith, K., Sibat, M., Viallon, J., *et al.*, (2020). *Toxins* 13, 321.

Shea, D., Tester, P., Cohen, J., Kibler, S., *et al.*, (2006). *Afr. J. Mar. Sci.* 28, 379-381.

Stobo, L.A., Lacaze, J.P.C.L., Scott, A.C., Petrie, J., *et al.*, (2008). *Toxicon* 51, 635-648.
Tester, P.A., Kibler, S.R., Holland, W.C., Usup, G., *et al.*, (2014). *Harmful Algae* 39, 8-25.

Zendong, Z., Herrenknecht, C., Abadie, E., Brissard, C., *et al.*, (2014). *Toxicon* 91, 57-68.



'MyRedTides' a fast and easy tool for sharing harmful algal bloom information in Sabah, Malaysia

Normawaty Mohammad-Noor^{1*}, Zuhairi Ahmad¹, Shuhadah Mustapha², Ahemad Sade³

¹Department of Marine Science, Kulliyah of Science, International Islamic University Malaysia, Jalan Sultan Ahmad Shah, Bandar Indera Mahkota, 25200 Kuantan, Pahang, Malaysia; ²Sabah Fisheries Biosecurity Office, Fisheries Complex, 88400 Kota Kinabalu, Sabah, Malaysia; ³Department of Fisheries, Head Quarter Office, Level 4, Block B Wisam Pertanian Sabah, Jalan Tasik Luyang, 88624, Kota Kinabalu, Sabah, Malaysia.

*corresponding author's email: normahwaty@iium.edu.my

Abstract

The coastal waters of the Malaysian state of Sabah are frequently affected by harmful algal blooms (HABs) mainly caused by *Pyrodinium bahamense* var. *compressum* and *Margalefidinium polykrikoides*, that have negative impacts on the aquaculture industry and human health. The project aims to develop a Public Information Map using ArcGIS to increase the effectiveness of sharing and communication of HAB information among relevant stakeholders and the community. The Department of Fisheries Sabah (DOFS) also participated in the project and knowledge transfer was done through a two-day on-line training. The output of the project are WebApps called MyRedTides. Altogether, two WebApps were developed: 1) cell density of *P. bahamense* and *M. polykrikoides* and 2) paralytic shellfish poisoning (PSP), i.e., toxin concentration of various coastal locations in Sabah. The developed WebApps contain useful information to the users such as the species responsible, recent, and previous HAB cases, as well as providing a platform for the sharing and exchange of information. Nevertheless, the use of this online WebApps as an early warning system is still at the preliminary stage because the acceptance and reaction of the stakeholders and local communities need to be evaluated. This is important to ensure that the HAB information is handled in the most effective manner.

Keywords: Early warning system, red tide, ArcGIS, knowledge transfer, MyRedTides

<https://doi.org/10.5281/zenodo.7033184>



Introduction

Harmful algal blooms (HABs) have been reported in Sabah coastal waters since 1976. Initially, the first HAB species identified to cause the problem was a toxic *Pyrodinium bahamense* var. *compressum* that causes paralytic shellfish poisoning (PSP) (Roy, 1977, Adam *et al.*, 2011; Mohammad-Noor *et al.*, 2018). Since then, many reports of human illnesses including death have been reported. In 2005, another HAB species that is a fish killer was also identified in the area, namely *Margalefidinium polykrikoides* (Anton *et al.*, 2008; Adam *et al.*, 2011; Mohammad-Noor *et al.*, 2014). The algal blooms have caused mass mortality of caged fish, with losses estimated in the millions of Malaysian Ringgits. Till today, both species continue to have devastating impacts in the Sabah coastal waters. Furthermore, with the rapid development of Kota Kinabalu, the capital of Sabah which is located near to the coastal area and climate change, there is positive sign that more HAB problem will occur in the future.

To decrease the impacts of these HAB species to human health and the aquaculture industry, the Department of Fisheries Sabah (DOFS) has carried out monitoring since 1976 (Jipanin *et al.*, 2019). The monitoring covers 13 districts in Sabah with a total of 69 sampling stations. Samples collected at each district are sent to the Sabah Biosecurity Fisheries Division for analysis of cell density and toxin concentration. If PSP is detected, it will take 3 days before the result in Microsoft Word format can be released to the district officers, village heads, village community Chairmen and District Health offices (Jipanin *et al.*, 2019). Therefore, it is imperative to improve the HAB data management and presentation

to emphasize important results while making it easy and interesting to understand and disseminate.

The Public Information Map, which is based on the WebApps responsive web design (RWD) and developed with ArcGIS, is a current technique for the dissemination and sharing of information. Online information, such as HAB data, can be made available to the public in website form, RWD and sharing-based social media links. Therefore, this platform can be used to increase the effectiveness of sharing and communication of HAB information to relevant stakeholders and the public. By adopting this approach, this project aims to develop WebApps to share HAB results i.e., cell density and PSP concentration (STX) in scale format, collected from Sabah coastal waters with the stakeholders (Department of Fisheries and Ministry of Health), fishermen and local community. Through this sharing platform, hopefully, the impact of HAB can be minimized and provide valuable information for those who are directly or indirectly involved with HAB.

Material and Methods

Public information map

The WebApps application is a recent technology developed by ArcGIS (Esri, California, U.S.A.) that can be used to disseminate and share information via an online public information system. It can be used to retrieve survey locations, update HABs information and provide a warning system. The online information can be made available to the public in various forms and platforms.



The numerical forecasting results can also be viewed and explored in the WebApps. By selecting a variable and a date in the widgets, the spatial distribution of the variable will be visualized in the map viewer. The system provides a web-based environment to monitor and forecast HABs by leveraging layers of external data and information from various fields. The system allows end users to view the *in situ* observations, remote sensing maps and numerical model forecasts in a geospatial context (Olson, 2019). By leveraging WebApps technologies, the web portal of the system provides a single map-based interface, in which data of different types (point time series, vector, and raster) can be visualized and analyzed through interactive tools (Yong and Mutao, 2019).

Knowledge transfer to Sabah Fisheries staff

A workshop was carried out in July 2021 to train the DOFS staff on the development of the WebApps for HABs in Sabah's coastal waters. The two-day workshop was done virtually with the participation of 15 DOFS personnel. During the workshop, the participants were given a step-by-step guidance on how to develop the WebApps. During the first day, the participants were introduced to the ArcGIS Online WebApps which includes the registration of an online ArcGIS account and explanations about the licensing, development of the database and group authorizations of data. In the second day, participants were requested to use their HAB data to develop their own WebApps. This is to ensure that the participants have a full understanding on how to create and handle the WebApps.

Development of Web App for HAB, Sabah

The cell densities of *P. bahamense* var

compressum and *M. polykrikoides*, and toxin concentrations collected from 13 Sabah districts were used to build the WebApps separately. The data, together with the latitude and longitude were arranged in a text file and imported into the ArcGIS. The monthly data was presented in a range, and each was added as a layer to the WebApps database. Information about the HAB species, actions that should be taken if a HAB is spotted or the occurrence of PSP symptoms were added in detail. Other important information added were the phone number and email address of the person to be contacted to lodge a complaint or to make a suggestion. A link was produced for each WebApps and can be shared through many platforms, including WhatsApp, Instagram and Facebook.

Data collection for WebApps development

Samples were collected once per month or twice per month from 13 Sabah districts. At each sampling station, the sample was collected using a Van Dorn water sampler at 1 m depth. Samples were brought to the laboratory of the Sabah Biosecurity Fisheries Division for enumeration. For toxin concentration, shellfish were collected from breeders, purchased from wet markets and shellfish collectors. Samples were kept at < 9°C and transported to the laboratory to analyze for saxitoxin using ELISA.

Results and Discussion

Based on the training conducted, WebApps were successfully developed for cell densities of *P. bahamense* var. *compressum* and *M. polykrikoides* (Fig. 1), and for PSP i.e., toxin concentration (Fig. 2) by DOFS staff. The developed WebApps are known as MyRedTides. This name was chosen due to



two reasons: 1) the term ‘Red Tides’ has been used colloquially since the first bloom was recorded, 2) the local community in Sabah is familiar with it and understand clearly the meaning of Red Tides. The developed WebApps are very informative because they contain basic and important information on HABs, especially for local communities. For example, users can access information on the HAB cell density or level of PSP for a specific month, understand the occurrence pattern which will give an indication on the potential occurrence of HABs. This will allow them to take the necessary actions to safeguard human health and the aquaculture industry. This can be done by avoiding the risky areas or to develop adaptive strategies (Guillotreau *et al.*, 2021). This is because the shellfish closure or ban on collecting shellfish can cause huge economic losses to aquaculture farmers and fish mongers. In addition, the ban can cause loss of confidence among the public thus led to drop in fish price and sale. Although, the DOFS has already started to educate the public on HABs (Jipanin *et al.*, 2019), this application can further enhance their work by being a more efficient way to disseminate information. Through this user-friendly application, the community can share their experiences or report HAB occurrences to the DOFS through platform provided within the WebApps.

The developed WebApps are useful to the DOFS because the collected HAB data can be shared faster in a more meaningful and interesting way. Furthermore, the DOFS can control the data input, data sharing and data to be shown. This will ensure the security of the HAB data is at its optimum level, as this data is confidential to a certain extent. Nevertheless, the usage of WebApps is at the preliminary

stage because the acceptance and the reaction of stakeholders and local communities have yet to be evaluated. Access to the WebApps is currently restricted to the DOFS staff and selected stakeholders. Through this practice, the WebApps can be further improved to produce a better application.

Overall, the developed WebApps are useful, though they need further fine tuning to suit the local situations and needs. The applications provide a better way to present data, whereby HAB information can be displayed on a map, frequently updated and shared online, as well as to be employed as an early warning system.

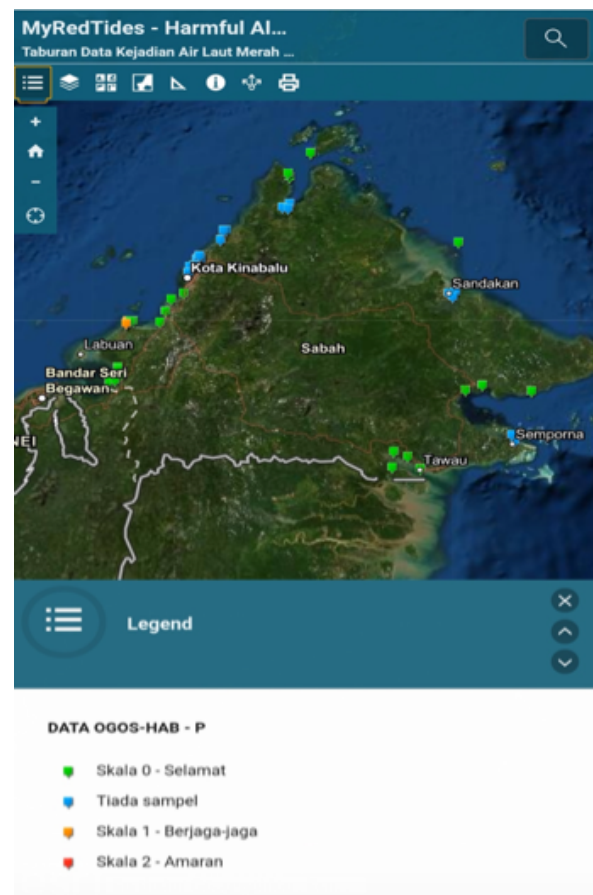


Fig. 1. WebApp for cell densities of *P. bahamense* var. *compressum* and *M. polykrikoides*. Legend showing the level of HAB alert based on colors: green – safe, blue – no sample, orange – attention, red – warning.



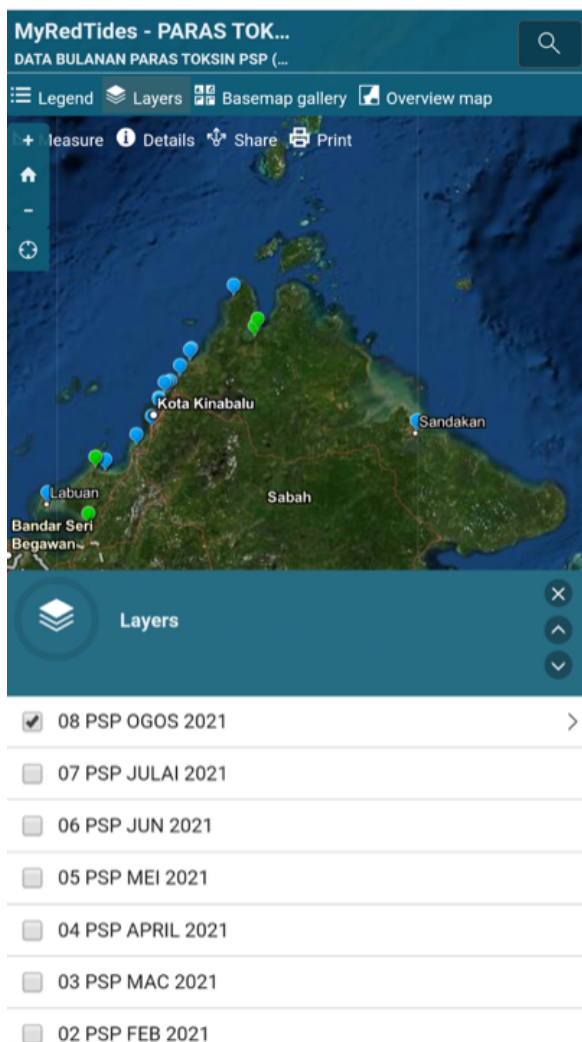


Fig. 2. WebApp for toxin concentration of PSP. Layers showing month selected (tick) for toxin concentration. The user can select a specific month to see the toxin concentration.

Acknowledgements. This study was carried out under the Memorandum of Understanding between the International Islamic University Malaysia (IIUM) and the Department of Fisheries Sabah (DOFS), Malaysia. The authors would like to thank all the members of the Kulliyah of Science and the DOFS for their help and advice during this study.

References

- Adam, A., Mohammad-Noor, N., Anton, A., Ejria, S., *et al.*, (2011). Harmful Algae 10, 495-502.
- Anton, A., Teoh, P.L., Sitti Raehanah, M.S., Mohammad-Noor, N. (2008). Harmful Algae 7, 331-336.
- Guillotreau, P., Le Bihan, V., Morineau, B., Pardo, S. (2021). Harmful Algae 101, 101968.
- Jipanin, S.J., Muhamad Shaleh, S.R., Lim, P.T., Leaw, C.P., Mustapha, S. (2019). J. Phys. Conf. Ser. 1358, 012014.
- Mohammad-Noor, N., Weliyadi, E.A., Than, A., Adam, A., *et al.*, (2014). Sains Malays. 43, 21-29.
- Mohammad-Noor, N., Øjvind, M., Leaw, C.P., Lim, P.T, *et al.*, (2018). Harmful Algae of Malaysia. IIUM Press. International Islamic University Malaysia.
- Olson, S.J., Barnas, K.A., Williams, M.R., Wheaton, C., *et al.*, (2019). <https://www.pnamp.org/document/15001>
- Roy, R.N. (1977). Med. J. Malay. 31, 247-251.
- Yong, T. and Mutao, H. (2019). J. Mar. Sci. Eng. 7, 314.



Establishment and maintenance of an Early Warning System in Ireland: A case study

Dave Clarke

Marine Institute, Rinville, Oranmore, Co. Galway, Ireland.

corresponding author's email: dave.clarke@marine.ie

Abstract

Harmful Algal Bloom events can result in multiple effects and impacts on aquaculture and fishing operations, often resulting in socioeconomic losses, either through mortalities or temporary bans on the harvesting of product in aquaculture production areas. Many of these events give rise to food safety concerns, where marine biotoxins can accumulate within the tissues of filter feeding bi-valve molluscs above regulatory levels causing a variety of serious human illnesses if consumed. Many countries operate routine monitoring programmes for the detection of these events, where in recent years some countries have further expanded on these programmes to develop and establish Early Warning Systems to provide short term forecasting and prediction of the onset and duration of these events. From a stakeholder perspective, this leads to improved regulation, food safety and risk-based management decisions taken by the operator and regulator to minimise the economic and supply losses which are usually incurred of these events and ensuring the protection of the consumer. Ireland has been successfully operating such a system on a weekly frequency to all stakeholders and the public since 2013, by publishing a weekly bulletin which contain several collated data products from historical and current biotoxin and phytoplankton profiles, along with oceanographic in-situ satellite and modelled data products. These products and generated datasets are combined, where an expert evaluator reviews the data and provides a short-term forecast prediction (3-5 days).

Keywords: Early Warning Systems, Harmful Algal Blooms, prediction, forecasting, aquaculture
<https://doi.org/10.5281/zenodo.7033201>



Introduction

The Marine Institute, Ireland has been providing a weekly bulletin report to all stakeholders and the public since 2013. Ireland has a complex biotoxin profile in shellfish, multiple known toxigenic and ichthyotoxic phytoplankton species in its coastal waters and is often subject to large blooms resulting in water discolouration, foaming and mass mortalities of finfish, shellfish, and benthic invertebrates.

Large scale HAB events which occurred in Ireland during 2005-2007, resulting in multiple and prolonged closures in shellfish aquaculture production areas, and large-scale mass mortalities of finfish, prompted requests from stakeholders, in particular the aquaculture industry for the provision of an Early Warning System (EWS) to be implemented. Through the ASIMUTH project (Applied simulations and Integrated modelling for the understanding of toxic and harmful algal blooms) this allowed for the approach, stakeholder consultation process, design, and development of a prototype EWS to be implemented. Through successive funding projects, Ireland's EWS has been further enhanced over the years, and is detailed in this case study.

Early Warning System Case Study–Ireland's Experience

Through rigorous, robust, and intensive monitoring programmes over a 40-year period, we have identified the presence and regular occurrence of four main marine biotoxin groups in Ireland; Diarrhetic Shellfish Toxins (DST); Amnesic Shellfish Toxins (AST); Azaspiracids (AZA) and Paralytic

Shellfish Toxins (PST). The occurrence of causative toxigenic plankton species in the water column and their associated Harmful Algal Bloom (HAB) events are a regular occurrence, often resulting in long periods of closure for harvesting in production areas, and occasionally responsible for the mortalities of farmed finfish and wild fish, shellfish, and benthic invertebrates.

Information about the stakeholders—who was impacted and were needs identified?

From the mid to late 1990's, there were a number of reported illnesses following the consumption of shellfish exported from Ireland. The development and expansion of the aquaculture industry was constrained by the multiple and long periods of closures prohibiting harvesting and product recalls. This contributed to a review and overhaul of the monitoring programme by affected stakeholders. The main stakeholders who were and continue to still be impacted HAB events can be categorised into the following four main groups; Industry; Regulators; Health and Society. The identified requirements and needs of these four groups of an EWS system overlap with each other.

Industry—commercial Food Business Operators (FBO) of shellfish and finfish licensed aquaculture operations in classified production areas. Fishermen and fishing vessels for pelagic and demersal fishing, and the dredging of shellfish i.e., scallop (*Pectinidae*) and razor clam (*Ensis*) species from offshore areas. Identified needs of an EWS for this group included the early notification and predictive forecasting of the probability of a HAB event occurring (short



term 3–5-day forecast) with the forecast to be presented in a visual, understandable, and interpretable format accessed through a user-friendly platform.

Regulatory–Competent Authorities including enforcement; licensing; movement of products, and legislative agencies. National reference laboratories and approved monitoring laboratories. Other national agencies include those with a remit covering natural resources (i.e., water), and food security. Identified needs of an EWS for this group included the predictive forecasting of the onset and duration of a HAB event and its spatial extent, and to support and supplement the scientific advice presented to regulatory agencies and authorities.

Health–Public and private health bodies, and agencies with a remit in the management of water quality and food security. Identified needs of an EWS for this group include the communication of alerts and data on toxin concentrations from HAB events and their associated potential impacts on human health and related illnesses.

The society (individuals and communities), particularly regarding prevention and protection of public health. Identified needs of an EWS for this group included the publication and dissemination of alerts of HAB events and blooms occurring in recreational settings, i.e., beaches and water bodies used for water sports, diving, and swimming.

Developmental and monitoring status in Ireland

Ireland established routine phytoplankton monitoring in the 1980s for the identification and enumeration of toxigenic species

known to cause human illnesses through the consumption of toxin contaminated shellfish. This was the first important step to compile and understand the complexity of the biotoxin profile in Irish coastal waters. This monitoring expanded with the growth of the aquaculture industry to include shellfish monitoring in the 1990's for the presence/absence of biotoxins by bioassay, whilst in the 2000's chemical monitoring for the discrimination and quantification of biotoxin compounds was implemented.

Presently, Ireland has a widely distributed and varied aquaculture industry, with approximately 100 classified production areas harvesting blue mussel (*Mytilus edulis*), pacific oyster (*Crassostrea gigas*), native oyster (*Ostrea edulis*), clam (*Ruditapes*, *Venerupis*, *Ensis* species), common cockle (*Cerastoderma edule*) and King scallop (*Pecten maximus*).

The routine phytoplankton monitoring programme includes full community analysis (species identification and enumeration) on a weekly frequency from all actively harvesting production areas. The biotoxin monitoring programmes analyse all shellfish species from active production areas, where the frequency is weekly for *Mytilus edulis*, fortnightly for *Pecten maximus* and monthly for all other species. The frequency is increased accordingly if a potential risk is observed, including time of year, toxicity in adjacent areas or in other shellfish species and the presence/increase of the toxigenic phytoplankton species.

In 2020, the total value of the Irish Seafood sector was €526 million (m) with a total volume of 290,400 tonnes (t). This breaks



down to €346m (252,400t) of sea-caught fish; €129m (14,000t) of farmed finfish and €51m (24,000t) of farmed shellfish (BIM, 2021).

Due to the frequent occurrence of HAB events impacting on harvesting regimes and commercial operations, a requirement was identified by stakeholders for an early warning system (EWS) to forecast the onset of HAB events to assist risk management decision making at industry/FBO/regulator level.

Approaches and technologies adopted in implementing an EWS

The Irish EWS comprises of Weekly HAB report/bulletin, which is compiled and published by the Irish Marine Institute as an assistance information tool to industry. These weekly 12-page bulletins contain a number of collated data products from historical and current biotoxin and phytoplankton profiles, along with oceanographic in-situ and modelled data products used as a predictive forecasting tool. An expert evaluator reviews the data and provides a short term 3–5 day forecast prediction (Fig. 1.).

The generation and publication of the weekly HABs Bulletin is an eight-step process (Fig. 2.).

1. *In situ* HAB and Biotoxin Data Products– collates the current and historical results from the phytoplankton and biotoxin monitoring programmes from the Marine Institutes SQL server database, HABs2, presented as spatio-temporal scatter and donut plots
2. Phytoplankton Data Products– generates a report of the top five most abundant phytoplankton taxa in cells L⁻¹ per coastal region for the week previous.
3. Satellite– generates daily maps which present large spatial scale information on surface phytoplankton blooms (Chl *a*) and sea surface temperature.
4. Calculate Chlorophyll and Sea Surface Temperature Anomalies–generates a series of daily images of the current weekly conditions of chlorophyll and sea surface temperatures.
5. *In-situ* weather buoys– data collated by the Irish weather buoy network used to create a ten-year SST for the week in analysis.
6. Modelled Data Products– generates particle tracking imagery at three depths and three-day predictive hydrodynamics (estimated water flows at the mouth and mid-bay sections) for three bays of interest.
7. Data Evaluation and Prediction– text prediction with rationale, based on interpretation of all available data by an expert evaluator, is presented. The rationale is based on available scientific data, potential driving factors and experience.

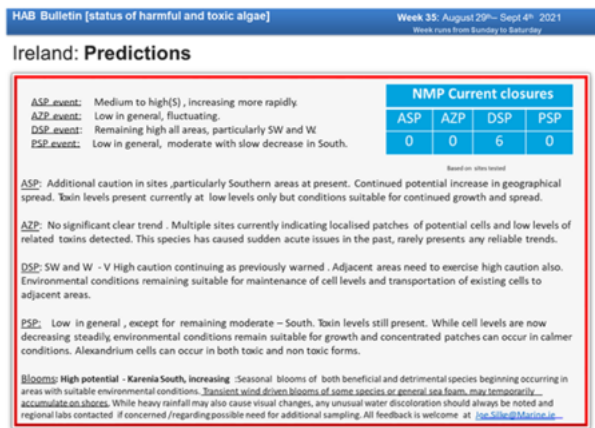


Fig. 1. Example of the front page of the Irish weekly bulletin detailing the short-term predictions and risk for the week. *AHAB bulletin*



- Publication—a .pdf of the current bulletin is uploaded to the Marine Institute’s HABs website <https://webapps.marine.ie/habs>

Description of EWS implemented and the communications and interactions with stakeholders

Ireland’s EWS provides valuable information to assist and inform its stakeholders. The focus is to provide information to facilitate rapid decision making prior to the onset of a HAB event. These decisions can include increased

harvesting prior to closures in affected areas, movement, and transfer of caged finfish away from high biomass blooms, and other measures to mitigate or minimise losses. Interactions and feedback from stakeholders are requested on a regular basis. Ideas and novel technologies are often explored to provide additional information and further accuracy to prediction and forecasting. Stakeholder feedback has also been sought through surveys and questionnaires since its implementation in 2013 to continuously assess the EWS is fit for purpose.

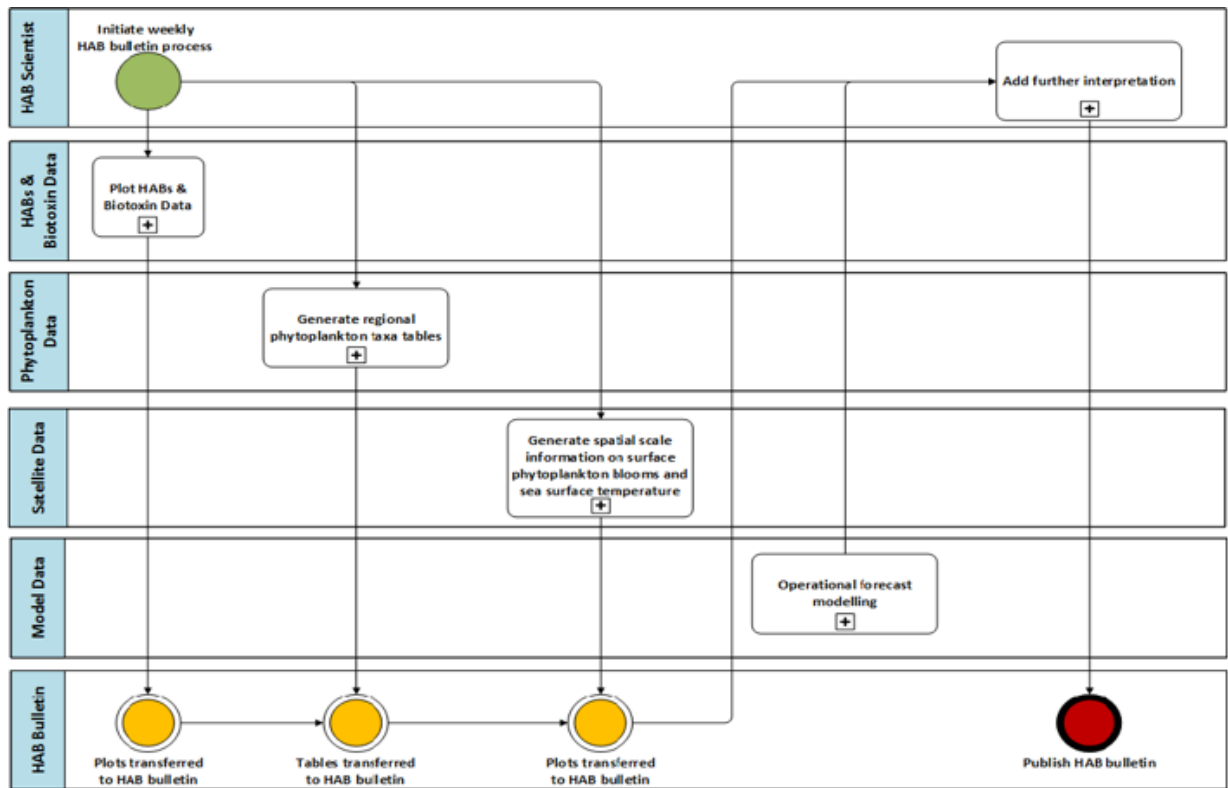


Fig. 2. An overview of the process to generate and publish a weekly HAB bulletin (Leadbeatter *et al.*, 2018).



Results in terms of forecast operations

To measure how accurate and successful the forecast bulletins are in their weekly predictions and alerts, two separate evaluation exercises were conducted. During the ASIMUTH project (Applied simulations and Integrated modelling for the understanding of toxic and harmful algal blooms) the estimation of success was through assessing an assigned score if the toxin concentrations observed were above or below regulatory levels during a 16-week period for each biotoxin group. Overall, the success of prediction was calculated at approximately 80% (Maguire *et al.*, 2016)

Through the PRIMROSE project (Predicting the impact of regional scale events on the aquaculture sector). A different method was applied to calculate the success rate of forecasting prediction and accuracy, by comparing the published prediction of a current week and if the predicted area was closed the following week due to biotoxin concentrations above regulatory levels. An overall success rate of 87.25% was calculated for a 17-week period during 2020, where it was observed that incorrect predictions were always due to overestimating the risk of a HAB event occurrence. Therefore, all HAB event occurrences over this period were predicted.

Consequences of EWS on stakeholder requirements

The EWS products which have been developed fulfil the requirements of the four identified groups of stakeholders; Industry; Regulators; Health and Society. These developed end products include *in-situ* HAB and biotoxin products, remote sensing satellite products, regional oceanic modelling systems detailing

the hydrodynamic processes into and out of specific bays including particle tracking at the mouth and mid-sections of water bodies. These products when combined are designed to meet the requirements and is achieved by the outputs of industry—reduce mortalities, minimise against financial loss and improve supply demand logistical chains. The output here is for profitability, expansion, and production of safe seafood products.

Regulators—ensuring food safety and the protection of the consumer is enforced by taking the necessary actions, development of strategies minimising economic losses and impacts on the environment. The main output is that monitoring and prediction through EWSs ensures safe seafood on the market.

Health—protecting human health ensuring only safe product is on the market for human consumption and ensuring water quality is to a high standard. This translates into the output of reducing the number of human illnesses occurring and reported from HAB events.

Society—forecasting of blooms which may impact on leisure activities, water sports and swimming. The output for this group also results in reducing the number of human illnesses occurring and reported from HAB events and reducing environmental impacts.

Lessons learned

When establishing and implementing an EWS in Ireland there has been several valuable lessons learned and actioned in a bid to continually improve the service:

- a. It is critically important to have an in-depth knowledge and understanding of the country/region toxicity profile, which can



- vary from region to region.
- b. With this understanding, the designed monitoring programmes should be fit for purpose so all HAB events of all types can be captured by in-situ observations, modelling and remote sensing monitoring programmes and tools.
 - c. For the generation of fluid weekly bulletins without delays, it is vital that all datasets used in the compilation and generation of the bulletin are reliable (quality control checks to ensure integrity) and available.
 - d. That all aspects of the bulletin generation and publication are continuously reviewed and evaluated to ensure they continue to be fit for purpose and of relevance to the stakeholders.
 - e. As part of the above review and evaluation, it is necessary to continue to liaise, listen and work with stakeholders ensuring their requirements are continuously met and delivered.
 - f. Data disruption due to downtimes are minimised and mitigated against, and that detailed procedures are in place to cover hardware and software upgrades, backup, and disaster recovery.
 - g. Financial support, in addition to having the appropriate human and technical resources, is critical for the ongoing maintenance and improvements of established working EWSs.
 - h. Ongoing stakeholder support and commitment is continuously required for EWS success, especially from end users and those who make risk based operational decisions on the forecast predictions, particularly industry and regulators.

The success of any implemented EWS in a region is due to a combination of the above, and to the system's capacity and ability to

evolve and improve over time to incorporate new technologies, data streams, modelling and in-situ monitoring. The established EWS should not be a static process, but a system which can evolve and keep pace with stakeholder requirements.

Acknowledgements. This work received support and funding from; The BOHAB project (Biological Oceanography of Harmful Algal Blooms off the west coast of Ireland) through the National Development Plan 2000 – 2006 with the support of the Marine Institute and the Marine RTDI (Research, Technology, Development, and Innovation) Measure, Productive Sector Operational Programme, Grant-aid Agreement No. ST/02/01. The ASIMUTH project (Applied simulations and Integrated modelling for the understanding of toxic and harmful algal blooms) through the European Research Council under the European Union's Seventh Framework Programme (FP7/2007-2013) for Research and Technological Development - EC FP7 Programme, Space Theme, Grant Agreement No. 261860. The MyOcean 2 project through the EC FP7 Programme, Space Theme, Grant Agreement No. 283367. The AtlantOS project through the European Union's Horizon 2020 research and innovation programme, Grant Agreement No. 633211. The PRIMROSE (Predicting the impact of regional scale events on the aquaculture sector) project, co-financed by the European Regional Development Fund through the Interreg Atlantic Area Programme, EAPA_182/2016. The CoCliME (Co-development of climate services for adaptation to changing marine ecosystems) project is part of the European Research Area for Climate Services (ERA4CS), an ERA-NET initiated by JPI Climate, and funded by EPA (IE), ANR (FR), BMBF (DE),



UEFISCDI (RO), RCN (NO) and FORMAS (SE), with co-funding by the European Union (Grant Agreement No. 690462).

The author would like to thank all the Marine Institute staff involved from the biotoxin and phytoplankton teams in the routine monitoring programmes and to those within the oceanographic and data management teams. Tara Chamberlain, Marine Institute, for the weekly generation and publication of the HAB bulletins.

References

BIM Bord Iasc Mhara (2021). The Business of Seafood 2020, a Snapshot of Ireland's Seafood Sector.

Leadbetter, A., Silke, J., Cusack, C. (2018). Creating a weekly Harmful Algal Bloom bulletin. Marine Institute, Galway, Ireland.

Maguire J., Cusack, C., Ruiz-Villarreal M., Silke J., McElligott D., Davidson K. (2016). Harmful Algae 53, 160-166.



Improving forecasts for *Karenia brevis* in the Gulf of Mexico

Richard P. Stumpf^{1*}, Barbara Kirkpatrick², Katherine Collins³, Robert Currier², Michelle C. Tomlinson¹, Katherine A. Hubbard⁴, Alicia Hoeglund⁴, Grant Craig², Tony Reisinger⁵, Andrew Meredith³, D. Ransom Hardison⁶, and William C. Holland⁶

¹National Oceanic and Atmospheric Administration, National Ocean Service, National Centers for Coastal Ocean Science 1305 East-West Highway, Silver Spring, MD 20910, U.S.A.; ²Gulf of Mexico Coastal Ocean Observing System Regional Association, Department of Oceanography, 3146 TAMU, College Station, TX, 77843, U.S.A.; ³CSS Inc. Under Contract to National Oceanic and Atmospheric Administration, National Ocean Service, National Centers for Coastal Ocean Science 1305 East-West Highway, Silver Spring, MD 20910, U.S.A.; ⁴Fish and Wildlife Research Institute, Florida Fish and Wildlife Conservation Commission, 100 8th Ave SE, St. Petersburg, FL 33701, U.S.A.; ⁵Texas A&M AgriLife Extension Service / Texas Sea Grant at Texas A&M University, 1390 West Expressway 83, San Benito, TX 78586, U.S.A.; ⁶National Oceanic and Atmospheric Administration, National Ocean Service, National Centers for Coastal Ocean Science, 101 Pivers Island Rd, Beaufort, NC 28516, U.S.A.

*corresponding author's email: richard.stumpf@noaa.gov

Abstract

Brevetoxins produced by *Karenia brevis* can be aerosolized and lead to severe respiratory irritation, with documented health risks for people with asthma. Economic impacts also occur as even healthy people avoid beach businesses when a “red tide” is reported to be in a region. However, the distribution of brevetoxin aerosol impact varies greatly, depending on patchiness of blooms and wind speed and direction. Locating and forecasting the blooms and respiratory risk are then necessary to reduce health and economic impacts. Previously, manual and qualitative evaluation determined the location and respiratory risk of these blooms at coarse resolutions (daily and county scale). The forecast has substantially been improved for nowcast timeliness with an automated capability that combines new resources and models. These include a chlorophyll-a fluorescence algorithm applied to Sentinel-3 satellite products, the HABscope (a microscope deployed by volunteers with digital video analysis), existing water sampling networks, improved weather forecasts, respiratory irritation risk models, and a bloom intensification forecast.

Keywords: brevetoxins, aerosols, asthma, forecast, HABscope, *Karenia brevis*

<https://doi.org/10.5281/zenodo.7033205>



Introduction

Karenia brevis toxic aerosols have significant human health impacts, particularly in people with asthma (Fleming *et al.*, 2005a, 2005b, 2007, 2009, 2011; Kirkpatrick *et al.*, 2006, 2011). These aerosols also lead to significant economic impacts resulting from the cost of associated medical visits and from reductions in tourism when people avoid beaches (Hoagland *et al.*, 2009). With insufficient information and notification on respiratory risk, the potential for health issues increases. Although *Karenia brevis* blooms, which are locally termed “red tides”, can extend significant distances along and offshore of coastal regions, respiratory irritation is often quite variable from day to day and beach to beach. This variability is caused by a combination of patchiness in the cell density combined with shifts in wind from onshore to offshore (Stumpf *et al.*, 2009). Fig.1 illustrates the variability of winds between morning and afternoon. In 2004, a twice weekly Gulf of Mexico Harmful Algal Bloom (HAB) forecast was launched by NOAA to provide more warning of bloom impacts at county beaches. A validation study found that the forecast of respiratory irritation somewhere in the county was correct over 70% of the days (for example, if a forecast of high risk of irritation was made, it did occur somewhere in the county), however, when applied to individual beaches, the forecast was correct only 20% of the time (Stumpf *et al.*, 2009). With lack of detailed information, there is exposure risk to those with chronic respiratory illness. They may visit a beach when toxins are present. Also, those who have experienced even minimal “red tide” symptoms are likely to assume that all beaches are not safe and avoid them and coastal businesses. Our goal is to

provide sufficient resolution to protect the health and economy of the community.

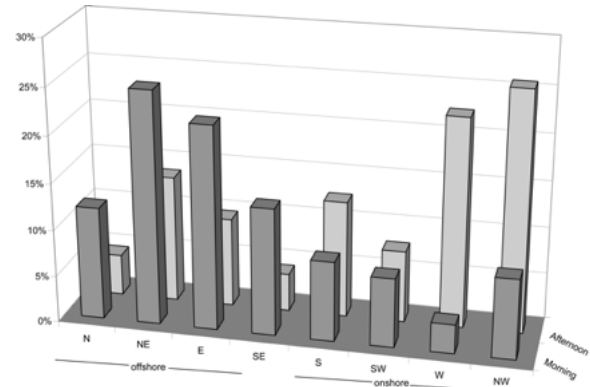


Fig. 1. Difference in frequency of offshore (left) and onshore (right) winds between morning (dark in front) and afternoon (light in back) (Stumpf *et al.*, 2009).

The goal of this project is to provide beach level forecasts in 3-hour time intervals with updates that are fully automated like a weather report. Providing frequent updates due to changing conditions allows beach goers to make informed decisions regarding their exposure to toxic *K. brevis* aerosols.

Material and Methods

To achieve these goals, we employed a combination of 21st century technologies.

Improved satellite data

We use the Sentinel-3, Ocean Land Colour Instrument (OLCI), launched in 2016 by the Copernicus program. OLCI has a 300 m pixel resolution and provides six images per week. Previous satellites (Terra and Aqua) offered 1 km pixels, an order of magnitude lower areal resolution, and no information within about 2 km (pixels) of the shore. OLCI allows a better ‘snapshot’ of the bloom that can aid



decision making on where water sampling efforts should occur. An example of the improved detail is shown in Fig. 2.

HABscope

To improve the spatial and temporal resolution of water samples and cell counts, we developed the HABscope. This instrument employs an easy-to-use microscope combined with an iPod touch tablet computer (Fig. 3). The iPod is set on the microscope using a 3D printed mount. In lieu of the traditional method of manually counting cells, a short video of the water sample is captured, and uploaded to a GCOOS (Gulf of Mexico Coastal Ocean Observing System) portal where an image analysis algorithm automatically identifies, tracks, and counts the live cells (Hardison *et al.*, 2019). The ease of use of the HABscope has allowed a citizen science network to be established to provide a substantial increase in the frequency and spatial extent of monitoring for *K. brevis* abundance. The forecast ingests cellular abundance from both HABscope and traditional monitoring.

Higher resolution weather models and forecasts

Our third step in this improved forecast involves the use of higher resolution wind forecasts (available through the National Digital Forecast Database, NDFD, at digital.weather.gov) and determines the beach orientation relative to the wind forecast. NDFD has hourly 2.5 km resolution, which became operational in 2014. Fig. 4 illustrates a graphical display of wind orientation against the shoreline in the vicinity of Tampa Bay. The combination of wind direction with cell counts is used in a model of respiratory forecast risk (Stumpf *et al.*, 2009)

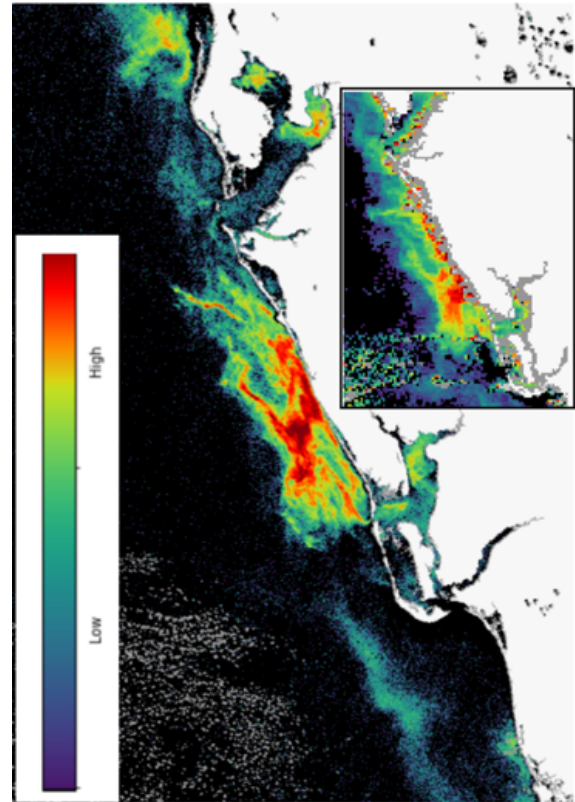


Fig. 2. Example imagery from Sentinel-3 OLCI of a *Karenia brevis* bloom along southwest Florida, U.S.A., 19 Aug 2021. The inset shows the lower resolution data from Terra satellite, which was previously used. Note lack of data (gray) in Terra.



Fig. 3. HABscope.



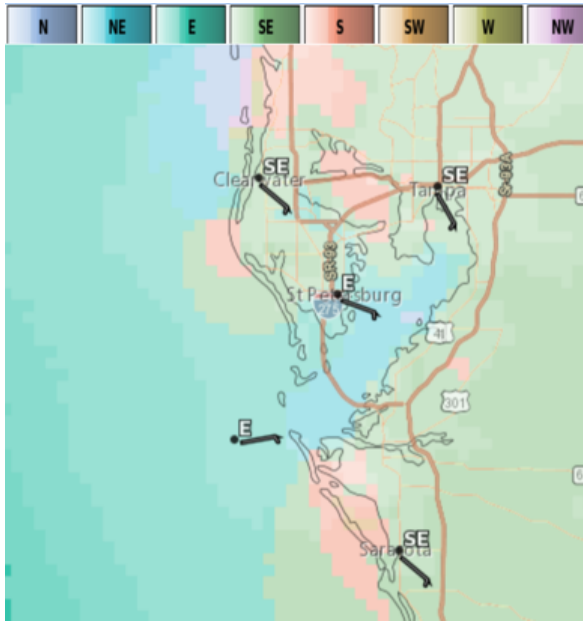


Fig. 4: Example NDFD wind direction.

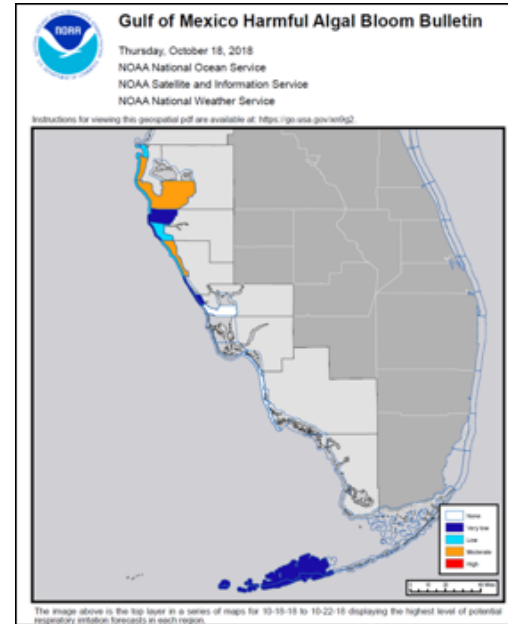


Fig. 5. Previous Gulf of Mexico HAB Bulletin.

Results and Discussion

The results of these efforts are a significant improvement in the resolution compared to the 2004 Gulf of Mexico HAB Bulletin. Instead of a general statement of daily risk across all county beaches, individual beaches are forecasted at 3-hour intervals throughout the day. Beachgoers then select the location and/or the time of their beach visit, allowing them to minimize their risk of exposure to the toxic *Karenia* aerosols. Fig. 5 shows a forecast map from the previous HAB Bulletin. Only the county that is impacted is highlighted. In Figs. 6 (4 pm) and 7 (10 pm), we show the new forecast which demonstrates the spatial variability from beach to beach and the temporal variability from 3-hour windows within the same day.

The respiratory forecast, hosted by GCOOS, and the improved remote sensing products, produced by NOAA, is a demonstration of the improved HAB products that can be produced through multi-partner projects. The forecasts will expand to the Texas coast as needed. To date, we have had over 200,000 visits to the site, primarily from the US but also a large number from Canada and Europe. We believe these products will allow residents and visitors to make informed decisions regarding their beach visits during *K. brevis* blooms.



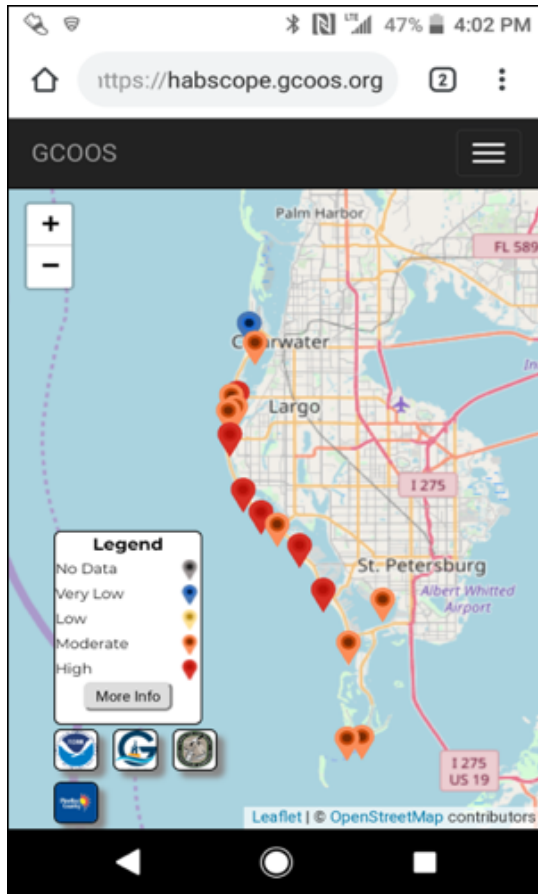


Fig. 6. New GoMex HAB Respiratory Forecast, 4 pm forecast.

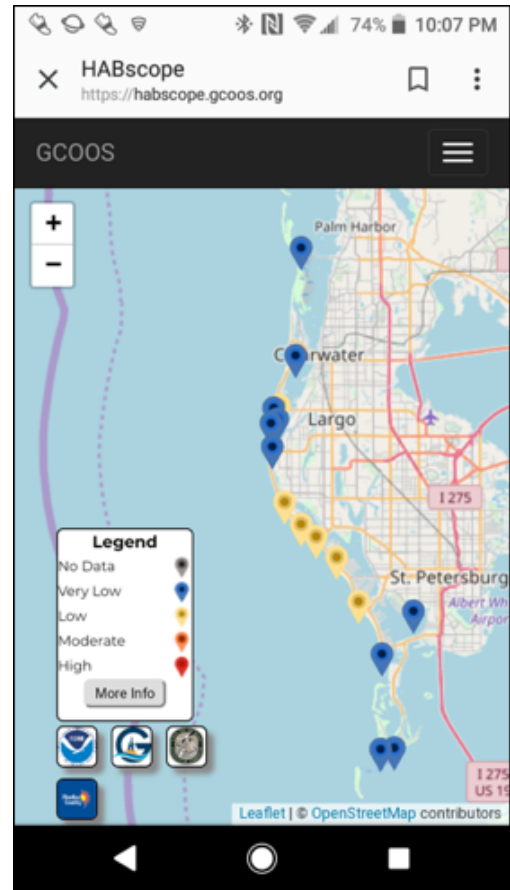


Fig. 7. New GoMex HAB Respiratory Forecast, 10 pm the same day as Fig. 6.

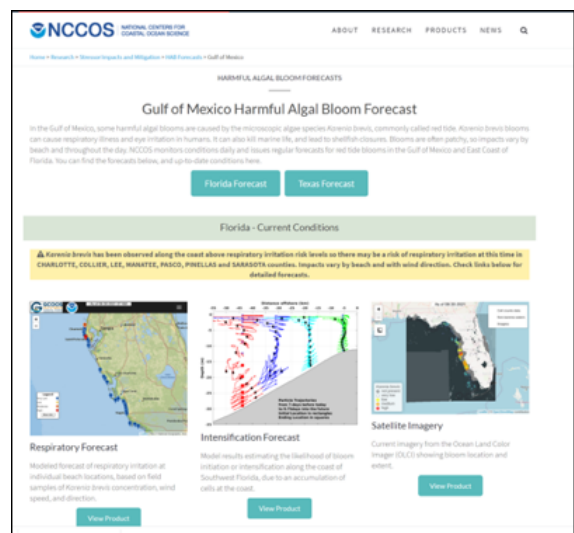


Fig. 8. New Gulf of Mexico HAB Forecast site.



Acknowledgements. We want to acknowledge and thank the enormous sampling effort by our dedicated HABscope community partners and volunteers who have made this project possible. This work was supported by NOAA Internal funding, NOAA NCCOS MERHAB NA20NOS4780194, the US Integrated Ocean Observing Program (US IOOS) and NASA Applied Sciences Health and Air Quality, ROSES NN13ZDA001. Reference to any specific commercial product does not constitute or imply endorsement or recommendation by the United States Government.

References

- Fleming, L.E., Backer, L.C., Baden, D.G. (2005a). *Environ. Health Perspect.* 113, 618-620.
- Fleming, L.E., Bean, J.A., Kirkpatrick, B., Cheng, Y.S., *et al.*, (2009). *Environ. Health Perspect.* 117, 1095-1100.
- Fleming, L.E., Kirkpatrick, B., Backer, L.C., Bean, J.A., *et al.*, (2007). *Chest.* 131, 187-194.
- Fleming, L.E., Kirkpatrick, B., Backer, L.C., Bean, J.A., *et al.*, (2005b). *Environ. Health Perspect.* 113, 650-657.
- Fleming, L.E., Kirkpatrick, B., Backer, L.C., Walsh, C.J., *et al.*, (2011). *Harmful Algae* 10, 224-233.
- Hardison, R, Holland, C.W., Currier, R.D., Kirkpatrick, B., *et al.*, (2019). *PLoS One* 14, e0218489.
- Hoagland, P., Jin, D., Polansky, L.Y., Kirkpatrick, B., *et al.*, (2009). *Environ. Health Perspect.* 117, 1239-1243.
- Kirkpatrick, B., Fleming, L.E., Backer, L.C., Bean, J.A., *et al.*, (2006). *Harmful Algae* 5, 526-533.
- Kirkpatrick, B., Fleming, L.E., Bean, J.A., Nierenberg, K., *et al.*, (2011). *Harmful Algae.* 10,138-143.
- Stumpf, R.P., Tomlinson, M.C., Calkins, J.A., Kirkpatrick, B., *et al.*, (2009). *J. Marine Syst.* 76, 151-161.



Intelligent ASVs to explore water bodies and support HABs detection, prediction and early warning

José María Girón-Sierra*, Eva Besada Portas, Gonzalo Carazo-Barbero, Juan Francisco Jiménez, José Luis Risco Martín, José Antonio Lopez-Orozco

Dep. Arquitectura de Computadores y Automática, Universidad Complutense de Madrid, Spain.

*corresponding author's email: gironsi@ucm.es

Abstract

Harmful Algae Blooms (HABs) are dynamic biological processes that occur inside many water bodies and become visible as they expand into the water surface. They should be anticipated/detected as soon as possible, to warn the authorities about dangerous situations. Early warning systems in use today, are not enough to capture HAB temporal-space evolution, because their probes, placed at fixed locations, cannot provide the quantity and distributed data required to understand what is happening. Autonomous Surface Vehicles (ASVs, a kind of robotized boats) can be used instead as mobile sensor platforms to take measurements of the variables of interest at different locations and depths of the water body. Our research goes one step beyond and aims to develop an Artificial Intelligent aLERT (AILERT-HAB) system based on intelligent ASVs capable of deciding where and how to take measurements for building models that predict HABs evolution and alert the authorities about them. Our ASVs are equipped with on-board computers and software designed for mixed-initiative work, which lets human operators intervene when desired, while ASVs usually function autonomously as a fleet, performing coordinated exploration tasks supported by different principles. For instance, these tasks can be achieved from a systematic water covering/monitoring perspective, by pre-planning the ASV and probe trajectories using the information provided by the simulations and/or the probability distribution of the HABs, or with data-driven controllers that adapt the ASVs displacements to the information extracted in real-time from the measurements taken by its on-board probes. During this paper, we will provide an overall view of our system, with details of the already-developed elements.

Keywords: HAB early warning, Autonomous Surface Vehicles, water exploration algorithms

<https://doi.org/10.5281/zenodo.7033213>



Introduction

Every year, Harmful Algae Blooms (HABs) develop on inland waters, and some of them (e.g., cyanobacteria blooms) generate toxins. Moreover, the evolution of algae population and their physiological state in reservoirs, lakes, and rivers, follows a spatio-temporal process, difficult to monitor and predict. Hence, it is urgent to devise early warning systems that incorporate new means to localize and understand better the biological phenomena that originate the HABs.

In Spain, where there are about 350 reservoirs (some of them among the ten largest in Europe) and convenient weather conditions for the HABs, they are a noteworthy problem. Here, data acquisition stations are being used to monitor the water conditions from fixed locations, with limited results. Besides, people on board floating vehicles are sent for sampling and measuring sporadically or when suspicious HABs activity has been detected. Both solutions provide scarce information, not enough to predict new HABs.

Our proposal is to use Autonomous Surface Vehicles (ASVs, a kind of robotized boats) for automatic data acquisition. They should operate in an intelligent manner to get to the regions of interest at proper times, to maximize the probability of getting relevant measurements (or samples). This is not straightforward, since HABs can move horizontally, as well as up and down, according to the wind, currents, diffusion, and thermal stratification.

This proposal is being explored in two research projects. The key idea of the first, named AMPBAS (Automatic Monitoring

of Pollutants in dammed waters using Biosensors and ASVs), is to provide simulation support, complemented with intelligent historical data analysis, for guiding the navigation decisions taken by the ASVs, to improve the chances of collecting successfully located measurements. The idea has already been developed and tested under simulations and remains to be experimentally evaluated in real-world scenarios. The second project, named IA-GES-BLOOM-CM (towards a comprehensive system for the alert and management of cyanobacteria blooms in inland waters), is in preliminary steps and involves the synergic collaboration of biologists, and experts in robotics and automation. Its purpose is to develop an early warning system, that involves fleets of intelligent ASVs, which act as nodes of an Internet of Things (IoT) infrastructure, to help water managers to anticipate cyanobacteria blooms. Interest in the results of both projects comes from companies and institutions with responsibilities in drinking water supply, and authorities linked to large (national) parks, wild-life support, and recreational facilities.

Material and Methods

Autonomous Surface Vehicles (ASVs)

A typical example of ASV would be a boat with an on-board electronic control system, which governs the boat motion, according with algorithms and some specifications of the desired boat behaviour. Besides, their onboard sensors, including cameras for instance, can be used for taking measurements about its surroundings. Finally, usual designs of the boat come in the form of catamarans, trimarans, or mono hulls.



Our experience on ASVs development and automation starts in 1997. Since then, different ASVs have been built in our facilities for several purposes: including boom towing, harbour surveillance, or research on ASVs swarms. Our ASVs use electric propulsion to move fast, or slow, depending on application. Their size also depends on the research targets, ranging from small (around 60 cm long) to moderate size (1.5m) and larger (4m long).

Our ASVs carry on-board control systems that we develop and build. Currently, they are based on a powerful-enough digital processor with convenient inputs and outputs for robotic control application. We also develop the control software to be free to select the functional endowment of the ASV, for present and future applications. At present, we have programmed a mixed initiative for the ASV control, to let ASVs decide autonomously where to move (or which actions to execute) and to let human operators take the ASV control from distance when required. Lastly, each ASV has a digital radio link for interaction with a supervision station, and a standard radio control channel for direct human intervention.

For AMPBAS and IA-GES-BLOOM-CM, moderate-size ASVs have been selected, easy to transport and deploy on the field, cheap-enough for many types of water bodies, straightforward to be used without a high-level expertise.

Two types of ASVs, as the ones presented in figures 1 and 2, are under development and testing. Both can navigate on shallow waters. One carries sensors for measurements near the epilimnion. The other has a sort of crane,

to handle up and down, for a depth of several meters, a multi-parameter probe. Both types of ASVs are medium size (around 120 cm long; less than 30 kg weight) to facilitate its transportation and deployment on places difficult to reach (e.g., the shore can be rocky, without flat access). It is also worth noting that at present, the ASVs use LiPo batteries. In the future, its power system will incorporate solar panels and a battery management intelligent system to increment the ASV autonomy.



Fig. 1. ASV with camera and sensors.



Fig. 2. ASV with crane for multiparameter probe.



Besides, the ASVs motion specification-scripting framework is being incrementally developed and tested. Several types of waypoints can be established, allowing for the ASV to move from waypoint to waypoint. Each waypoint has an attached behaviour, for example the ASV can stop on them for taking measurements or to explore around them. In addition, some typical exploratory operations, such as a lawn-mow trajectory in a rectangular area, can be concisely specified (e.g., by just setting the corners of the rectangle). Moreover, the ASVs behaviour can be guided by more complex algorithms, such as those summarized in the following sections. Finally, note that all this functional flexibility represents an original contribution of our research, compared with existing commercial ASVs.

Simulation-based ASVs path planning

In certain cases, no information on suspicious biological activity is available in each water body, and a systematic exploration is in order (such as the zig-zag trajectory presented in Fig. 3).



Fig. 3. Systematic exploration of a reservoir.

However, completely blind explorations could be avoided by means of exploiting the local history of previous events or the clues provided by simulations. In other words,

we can send the ASVs toward the places of interest, according to available information, and ensure that they are reached at the appropriate times.

We have developed a simulation prototype for demonstrating how this could be useful for planning the path of the ASV, by combining the predictions of a HAB simulator and an effective optimization of different aspects of the mission.

Supposing that a certain population of algae is initially located at a region of the water body, our simulator determines the evolution of the 3D distribution and concentration of this population, in function of biological growth, light intensity at different depths, and water currents. To do it, we first simulate the water currents and next the dispersion and growth of a bloom represented by a set of particles. For illustrating this process, on one hand, figure 4 shows, using warmer colors for higher values, the speeds only at the surface of a water body (with a surface area of $3.17 \times 10^5 \text{ m}^2$ and a maximum depth of 100 m) that is under a certain water inflow and outflow. On the other one, figure 5 summarizes the evolution of the algae population, whose initial location (at $t = 0$) is represented by the set of red particles displayed at the image in the left-hand side and whose final situation (including population growth), after 56 h, is displayed at the image in the right hand.

Once the simulation is accomplished, we optimize, using evolutionary algorithms, a 3D trajectory for the ASV and its probe depth, to ensure that it can get as many useful measurements as possible, while minimizing the mission duration and trajectory length. Figure 6 shows in black the optimized



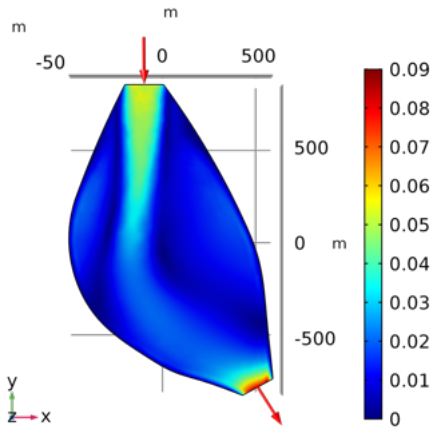


Fig. 4. Surface speeds of the flow simulation of a particular water body with inflow and outflow.

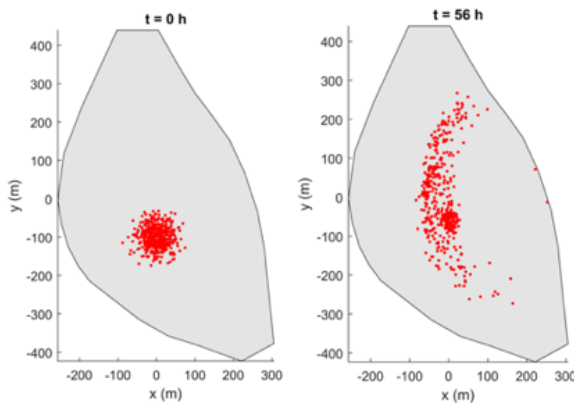


Fig. 5. Algae population evolution after 56 hours.

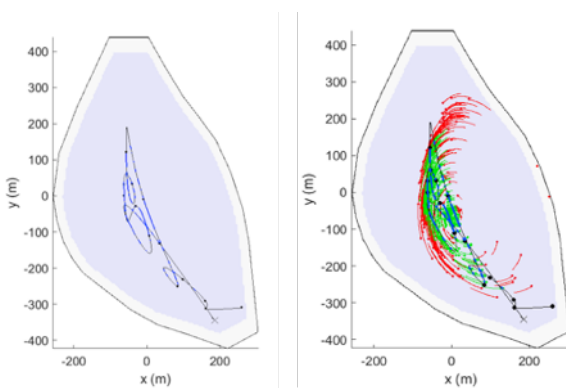


Fig. 6. ASV trajectory optimization for getting useful data while the HAB evolves and move.

trajectory of the ASV. On its right hand, the traces of the HAB area sensed by the ASV, after having travelled the whole trajectory, are highlighted in green. See (Carazo-Barbero *et al.*, 2021) for more details.

Sensor-driven ASV control

In practice, when no other information is available, it could be useful for the ASVs to use their sensors for detecting the algae, and move towards locations of maximum concentration, or follow a contour of the algae bloom. To illustrate this idea, figure 7 showed a bloom on the sea, where we have marked a contour with a yellow-ellipse a maximum with a red-dot.

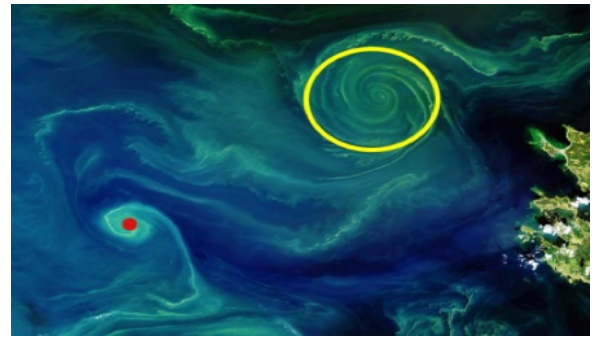


Fig. 7. A bloom on the sea; we marked a contour.

For driving towards a maximum, we successfully tried the Nelder-Mead SIMPLEX algorithm, which is used in numerical optimization of 2D functions. The algorithm departs from three points forming a triangle. A systematic procedure is followed to substitute the worst vertex for a new one, selected among four possible cases. A series of triangles is obtained, with the triangles moving towards the maximum, expanding towards better areas, encircling the maximum, and shrinking around it.



To obtain the maximum, we translate each vertex to a waypoint for ASV motion on water. The value at the vertex is the measurement that the ASV takes at the waypoint. Therefore, the ASV will move according to the algorithm while gathering measurements that will be used to decide the next movement. Figure 8 shows, in red, the trajectory followed by the ASV in simulation, considering a bivariate Gaussian distribution of the algae population. The colours in the legend of figure 8 can be used to identify each of the triangles created by the SIMPLEX algorithm.

To determine the contour, we use the PAT algorithm, which is even simpler. Basically, it builds a triangular grid around the contour, considering only if the measurements taken at the two last visited vertexes of the grid are both inside, both outside or one inside and the other outside of the contour level. Figure 9 shows the result of a simulation with this approach.

Results and Discussion

Although part of this research is in a preliminary stage, good results in simulation have been obtained. We have also made experiments with one of the ASVs, on a river, for functional study in the presence of potential users. See (Besada-Portas *et al.*, 2021) for more details

Acknowledgments. The AMPBAS project (RTI2018-098962-B-C21) of University Complutense of Madrid (UCM) is funded by the Spanish Societal Challenges program. The IA-GES-BLOOM-CM project (Y2020/TCS-6420) and Universidad Autónoma of Madrid is funded by the Synergic program of the Madrid Region.

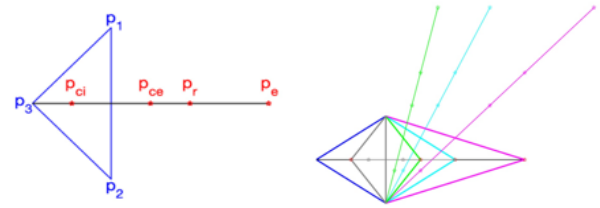


Fig. 8. Basic concept of the SIMPLEX algorithm.

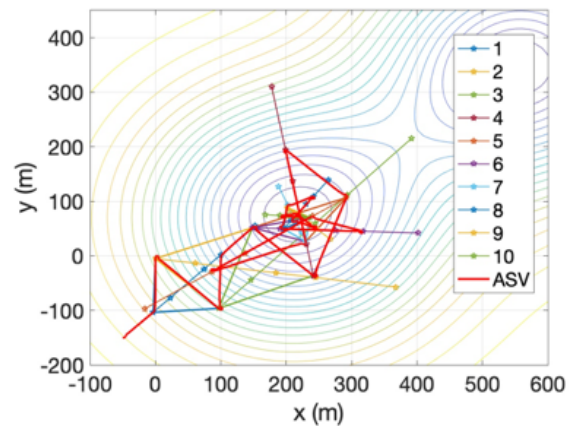


Fig. 9. ASV locating the maximum guided by the SIMPLEX algorithm.

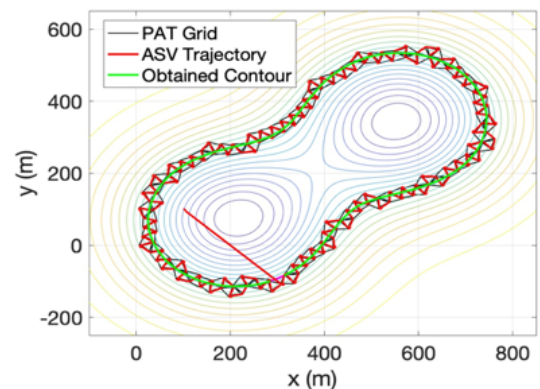


Fig. 10. ASV determining a contour guided by the PAT algorithm.



References

Besada-Portas, E., Girón-Sierra, J.M., Jimenez, J. Lopez-Orozco, J.A. (2021). Winter Sim Conf. Phoenix Arizona, December 13-17.

Carazo-Barbero, G., Besada-Portas, E., Girón-Sierra, J.M., Lopez-Orozco, J.A. (2021). EvoApplications 2021, 812-824.



AUTHORS INDEX



Abadie E.	254	Calbuyahue J.	260
Accoroni S.	271	Cameron H.	89
Adam A.	58	Cangini M.	22, 271
Ahmad Z.	334	Capellacci S.	16
Ahn S. H.	52	Carazo-Barbero G.	353
Aké-Castillo J. A.	70	Carrasco D.	260
Al-Has A.	58	Casabianca S.	16, 22
Allende M. L.	187	Cembella A.D.	93, 132
Aloi M. G.	22	Challenger S.	40, 176
Alonso-Rodríguez R.	181	Chin W.-C.	301
Amaya O.	112	Chinain M.	316, 322, 328
Amin S. A.	64	Clarke D.	339
Amorim A.	76, 138	Cobo-Gradín F.	249
Angeletti R.	271	Collins K.	347
Anguita-Salinas C.	187	Contiero L.	271
Aráoz R.	205	Corredor A.	266
Arcangeli G.	271	Corsi I.	16
Artal O.	266	Costa A.	271
Astuya-Villalón A.	187	Craig G.	347
Ávila A.	89	Crippa E.A.	289
Azman Ayub M. N.	58	Cristiano M. L. S.	145
Bacchiocchi S.	271	Currier R.	347
Band-Schmidt C.J.	171	Dall'Ara S.	72
Barile N.	271	Daniel P.	220
Barker K.	277	de Haro L.	254
Barnard M. A.	100	de La Paz J. F.	187
Barrera F.	260	Dechraoui Bottein M.-Y.	316, 322, 328
Bartenfelder A.N.	100	Delcourt N.	254
Bayu Intan M. D.	243	Dell'Aversano C.	16
Beach D.G.	151	Delwiche C. F.	158
Bellingeri A.	16	Denis M.	301
Benoit E.	199	Di Taranto A.	271
Berdalet E.	301, 310, 316, 322, 328	Díaz Ovejero S.	289
Bertolotto R.	16	Ding H.	301
Besada Portas E.	353	Doblin M. A.	243
Bickman S.	277	Dorantes-Aranda J.	193
Biddle A.	106	Dowsett N.	126
Bloch J.	254	Duan J.	301
Borges C.	76	Durán-Riveroll L. M.	93, 132
Bournaud R.	199	Elias F.	301
Boyer G.	277	Emri I.	301
Braddy J. S.	100	Enriquez C.	82
Bruce M.	151	Escalera L.	271
Buchholz S.	277	Fedrizzi G.	271
Bullerjahn G.	277	Fernández-Zabala J.	316
Butler J.	176	Fitzgibbon Q.	193



Flores-Leñero A.	119, 266	Kloss B.	283
Fuenzalida G.	46, 119	Knowles G.	193
Fuwa H.	199	Krock B.	171, 289
Gajardo G.	89	Kudela R. M.	213, 220
Galindo-Sánchez C.E.	93	Labadie M.	254
Gallo P.	271	Langrand J.	254
Gao Y.	106	Lara-Figueroa C. O.	181
Garrido Gamarro E.	316, 322, 328	Lawrence J.	151
Garzia A.	271	Le Roux G.	254
Gaudin A.	205	Leal J.F.	145
Giacobbe M. G.	16	Lee Chang K.	119
Gideon Mekonnen J.	283	Lemée R.	310, 322
Girón-Sierra J. M.	353	Lewis G.	277
Glibert P. M.	52, 64, 232	Leyva-Valencia I.	171
González-Flores M.	89	Li M.	64
Gracia Villalobos L. L.	289	Li Z.	301
Greengrove C.	226	Litaker R. W.	158, 316
Guerra J.	112	Liu Y.	64
Guerrini F.	22	Llanos-Rivera A.	187
Guzmán L.	89	Lochhead M.	277
Hall N. S.	100	Longo F.	271
Hallegraeff G.	193	Lopez-Orozco J. A.	353
Hardison R. D.	100, 347	López-Rivera A.	260
Hart C.	226	Lyubchich V.	232
Harwood T.	193	Macaluso A.	271
Hayashi K.	213, 220	Macdonald B.	277
Heil C. A.	52, 64, 232	Madigan T.	193
Henschen K.	106	Malej A.	301
Hernández-Becerril D.U.	165	Malhi N.	193
Hoeglund A.	106, 347	Mardones J. I.	46, 119, 266
Holland W. C.	100, 158, 347	Mari X.	301
Huamaní A.	165	Mariño-Tapia I.	82
Hubbard K. A.	64, 106, 347	Markley L.	106
Jenkinson I. R.	301	Martínez Goicoechea A.	27
Jiménez J. F.	353	Martínez Martínez J.	64
Johnson L.	106	Martínez-Dubón R. M.	249
Jolley J.	193	Martinez-Mercado M.	93
Jorquera M.	89	Maruyama F.	89
Karl C. M.	100	Masura J.	226
Karn S. K.	301	Matus-Nuñez M.	181
Katikou P.	283	Matweyou J.	226
Kaufmann M.	138	McCarron P.	151
Keller S. A.	106	McFarland M.	106
Kibler S. R.	226, 238	McGaraghan A.	220
Kihika J. K.	40	Melchiorre N.	271
Kirkpatrick B.	347	Méndez S.	27



Meredith A.	347	Quintanilla R.	112
Milandri A.	271	Rafuse C.	151
Milandri S.	271	Rahim Mustakim G.	58
Miranda M.	187	Reguera B.	2
Mohammad-Noor N.	58, 334	Reisinger T.	347
Moita M. T.	76	Revill H.	193
Molgó J.	199	Rhodes L.	40, 176
Montresor M.	271	Rilling I.	89
Moore T.	106	Riquelme C.	89
Morabito S.	22	Risco Martín J. L.	353
Morquecho L.	181	Rodríguez-Gómez C. F.	70, 82
Muawanah M.	243	Rojas-Posadas D. I.	171
Muhlbach E.	106	Romero L.	165
Mustapha S.	58, 334	Roser J.	277
Nagai S.	46, 89	Rossignol K. L.	100
Narizzano R.	16	Rubilar I.	260
Neri B.	271	Rubini S.	271
Neri F.	271	Ryan K. G.	40
Nishimura T.	176	Saam T.	106
Norambuena L.	46, 119	Saavedra-Flores A.	93
Okolodkov Y. B.	132, 249	Sabo A.	238
Oliveira P. B.	76	Sade A.	334
Ortega L.	27	Sanchez S.	165
Ortiz-Aldana J. R.	249	Sánchez-Castrejón E.	93
Ott B. M.	158	Santinelli N. H.	289
Paerl H. W.	100	Santos A.	76
Paerl R. W.	100	Sasaki M.	199
Palma C.	76	Sastre A. V.	289
Paperno R.	106	Schlumberger S.	199
Papiol V.	82	Schumacker E. J.	295
Paredes-Mella J.	46, 119, 266	Scortichini G.	271
Paret N.	254	Seger A.	126, 193
Paz-Cordón K. E.	249	Settineri L.	22
Pedullà F.	22	Seuront L.	301
Penna A.	16, 22	Silva T.	138
Petrou C.	277	Sinno-Tellier S.	254
Pezzolesi L.	22	Sitti Raehanah M. S.	58
Picones A.	181	Sloup R. S.	100
Piersanti A.	271	Smith K. F.	40, 176
Pinilla E.	266	Sobrinho B.	232
Pino F.	22	Soler-Onís E.	316
Pinto-Torres M.	266	Sousa A.	138
Pistocchi R.	22	Stillwell J.	151
Plaas H. E.	100	Stuart J.	176
Pokrzywinski K.	238	Stumpf R. P.	347
Ponikla K.	176	Suárez-Isla B.A.	260



Sun J.	64	Varanasi U.	295
Sun Y.	301	Vargas V.	119
Suraci C.	271	Varriale F.	16
Susanti Darnis D.	58	Vázquez G.	82
Susini F.	271	Vergara-Jara M. J.	266
Swanson C.	106	Verniani D.	271
Tamayo C.	260	Vila M.	310
Tartaglione L.	16	Villac C.	106
Tester P. A.	316, 322, 328	Virgilio S.	271
Thoha H.	243	Viure L.	310
Thompson L.	40, 176	Vivaldi B.	271
Tilney C.	106	Vodret B.	271
Tomlinson M. C.	347	Wallace C.	106
Torpey J.	106	Weisberg R.	64
Totti C.	271	Wood S. A.	40
Trainer V. L.	295	Wurl O.	301
Trapp A.	213	Wyatt T.	301
Tromba M.	22	Wynne T. T.	238
Turnbull A.	126, 193	Yañez P.	187
Ueki S.	89	Zacarias N.	76
Ungaro N.	16	Zambrano N. O.	187
Uyua N. M.	289	Zhang W.	301
Vadrucci M. R.	271	Zingone A.	271
Vale P.	34		



CONVENOR



ORGANIZED BY



SPONSORS

